Synthesis and polymerization of thioester containing compounds

under Supervision of Dr. C. Remzi Becer

PhD Thesis

Suzan Aksakal

Submitted in partial fulfilment of the requirements of the Degree of Doctor of Philosophy

School of Engineering and Materials Science
Queen Mary, University of London
November 2018

Statement of Originality

I, Suzan Aksakal, confirm that the research included within this thesis is my own work or that where it has been carried out in collaboration with, or supported by others, that this is duly acknowledged below and my contribution indicated. Previously published material is also acknowledged below.

I attest that I have exercised reasonable care to ensure that the work is original, and does not to the best of my knowledge break any UK law, infringe any third party's copyright or other Intellectual Property Right, or contain any confidential material.

I accept that the College has the right to use plagiarism detection software to check the electronic version of the thesis.

I confirm that this thesis has not been previously submitted for the award of a degree by this or any other university.

London, 15.11.2018
Suzan Aksakal

This work was supported by the H2020 program of the European Union (project Euro-Sequences, H2020-MSCA-ITN2014, grant agreement 642083).

Details of collaboration and publications:

Parts of this work has been carried out in close collaboration with J. O. Holloway and F. E. Du Prez at Ghent University, Belgium.

Parts of this thesis have been published:

S. Aksakal and C. Remzi Becer, *Polym. Chem*., 2016, **7**, 7011-7018.

J. O. Holloway, S. Aksakal, F. E. Du Prez and C. R. Becer, *Macromol. Rapid. Comm*., 2017, **38**, 1700500

Aksakal, S.; Aksakal, R.; Becer, C. R. *Polym. Chem*., 2018, **9**, 4507

Acknowledgement

It will not be possible to mention everyone of course, but whoever helped me, whoever positively influenced me, criticised me harshly, motivated, inspired me and more importantly encouraged me, helped me in a way to do better, I would like to thank you. Let's start with my inspirational supervisor Dr. Remzi Becer. I would like to thank you for the chance to work in the world's greatest polymer team, as well as for allowing me to be part of EuroSequences and to pursue my PhD in your group. Remzi always motivated his students to perform better, to work harder and not to lose our motivation and to keep our focus. You have been a group leader, mentor, friend, judge and therapist in defeats. He has taught me, that up and downs are normal during the PhD and that it is so much more important to stand up quickly after a failure and to see even bad results as results that can lead to potential innovations. I will never forget the moments where my supervisor was more excited than me, almost jumping out of his chair, when discussing new results and when something finally worked out. :)

My work was supported by the H2020 program of the European Union, EuroSequences and I would like to thank the EU for funding my PhD and giving me the opportunity to be involved in this programme with so many outstanding scientists. My funding made it possible for me to travel to conferences and to see so many great scientists and speak to them in person. I will never forget when I met Graeme Moad and Dave Haddleton and had the chance to present them my poster. How exciting it was to discuss thioacrylates with Nikos Hadjichristidis and Patrick Theato. How cool it was to chat with David Leigh at the EUROSEQUENCES meetings and with Yusuf Yagci and Mitsuo Sawamato during conferences. Furthermore, I would like to thank Professor Filip Du Prez for allowing me to join his great group for two months at the University of Ghent. I will never forget the useful and sometimes funny kitchen-egg meetings. I gained a lot of experience under his guidance and I learned a lot from his amazing group. Special thanks to Professor Jean-François Lutz for his useful comments during the ITN-meetings, especially on my presentation slides. Thanks to my examiners, Professor Sébastien Perrier and Doctor Theoni Georgiou for an interesting and enjoyable viva.

My family, my sisters and parents. Baba ich danke dir für alles was du mir und meinen Schwestern ermöglichst hast. Du bist mir damals wie heute ein sehr grosses Vorbild.

Ich liebe dich. Wer aber jemals gedacht hat, dass Eltern den Platz als Familenoberhaupt einnehmen, der hat nie eine grosse Schwester gehabt. Danke Tülay, du bist meine Heldin. Super-Mutti Filiz, für alles was mich ausmacht. Du bist immer an meiner Seite gewesen, vor allem während meiner Zeit in Düsseldorf. Jasmin, danke für deine ehrliche und sehr verrückte Art. Mama, ich danke dir für all den Mut den du mir so viele Jahre zugesprochen hast. Selbst wenn es schlechte Ergebnisse waren du hast mich immer wieder ermutigt. Du warst immer auf meiner Seite, selbst dann wenn kein anderer es war. Du hast mir gezeigt, dass viel Arbeit sich irgendwann auszahlt, dass man Geduld haben muss. Dieser Moment ist dank dir so nah. Alles was hier geschrieben steht habe ich dir zu verdanken ich liebe dich so sehr und danke dir mit der Widmung meiner Doktorarbeit. Dr. Dr. Ruprecht Vondran and Jutta Vondran, for guiding me in the right direction. The time I spent with you in Benrath are so priceless to me. My dear friend Dennis Mo, my very best friend since the first weeks of my bachelors degree in chemistry, thank you for being so caring. Of course I need to mention Artem as well. Thanks for all the good memories of our time at the HHU and in countless irish pubs. We three have been the perfect trio. Nathalie, the funny girl I met during my time at the research center in Jülich, you are such an incredible and motivating person, I just love you.

Next I would like to thank my team at QMUL. The crazy Ed Malins for introducing me to the world of RAFT and all the fun times with you. Ben Gridley for helping us with the organisation of the lab and much more. Gökhan my dearest friend, I will never forget how much we enjoyed teasing each other, I missed it very much in my last year, thanks a lot for all the good memories, I will never forget when we had our first menemen together. Now, moving to Manuel, I would like to say thank you for all advice, science as well as personal wise. I could always ask him any question any time, thanks for this and all the nice evenings we had. Valentine, I cannot describe you in words, maybe the guy I was arguing most with in the lab, the person I loved to annoy with Helene Fischer songs until I started to really like her songs. The guy with a garden full of vegetables in the summer and who liked to share them with me, atemlos und schwindelfrei wie in einer Achterbahn! His good humour and great mood made my early mornings so much better. Thank you Valli. The nice and best dressed guy Tian, Martin for helping me endless times with coating my plates for WCA measurements. Dom, thanks a lot for your good taste in music, your knowledge on sugars and just the

nice talks. The guy I enjoyed a lot to sing with in the late lab-evenings, it was a pleasure Luca. A very important and inspirational woman, Laily you have always been so nice and caring for others, I will miss our talks during our coffee breaks a lot. The next person I like to thank, is one of the most kindhearted, friendly, respectful and funny person I have met in my entire life. There are so many things I have learned from you even though you are much younger. Jacky did not leave my side in the first weeks at QMUL, as I always got lost on campus, but also in good and bad times where I needed a good friend. He stayed with me in the lab in the late evenings and made sure I am OK and everything is fine. Thank you my friend for the last years and all the flowers haha. I thank Ale for the last year, where I finally was not the only girl in the lab anymore and could finally have some funny girl talks. I also like to thank Ben for all the help, I could always ask you for advice and time you spent in explaining the microwave and helping me with changing the cylinders. Thank you all, it is one thing to work in a field you are passionate about, but it is another to be surrounded by nice people and makes it definitely much easier and better. I remember how many times we celebrated someone's good result and joking about bad results or whoever had the worse PDI (Was it Valli or Manu?). Muchun I thank you for all the delicious snacks you offered my daily in the office and much more for your help to get this thesis printed. Now, the moment of truth, I sincerely apologise for all the bad thiol smell in the lab. I will leave the lab, however the smell in the rotavap will stay as well as the thiols I have ordered in the last three years (we have kilos of them now in the lab, especially my favourite thiophenol). Enjoy them but always be prepared with litres of bleach!! I like to thank Josh a lot, we had so much fun during our collaboration and I have learned so much about solid phase. Don't forget the wobbly fridge! However, some of his very british phrases and jokes I still do not understand (don't really want to anyway). I thank you and Hannes for your help with sorting out things in Belgium, thank you guys. Steven, I guess he is at his desk with his head in thousands of books and covered in papers. I have never met a person working harder than him, he inspired and motivated me a lot. Adrian thank you for helping me with every chemistry related issue, you always helped even though you were busy. The other Manchester guy, Javier I really enjoyed the time we three spent together. Markus, the person with the biggest chemistry knowledge of all PhDs I know so far, thank you! Sofia thank you for all the help within the network. Two very inspirational woman I look up to, my

favourite dancing partner Roza Szweda and Nezha Badi, which I met during my time at UGent.

Special thanks to Ayse and Turgut Aksakal, supporting me, especially during my time in London and giving me the very best present ever ;). Last but not least, Resat, my best friend, my travel partner, my mentor, my husband and my colleague. You have been my greatest support and I cannot describe how much you have contributed in so many good things in the last seven years (or eight??). You have been so supportive during my Bachelor, my Master and mostly during my PhD. You helped me to never lose my focus, you cheered me up every time (remember, who was the first person who polymerised …???), my life is better and complete with you and I know we can accomplish so much more together. You are priceless to me.

Table of Contents

List of Figures

List of Schemes

List of Tables

Abstract

The objective of this thesis was to investigate the controlled radical polymerisation of thioester compounds and explore their potential with the goal to use the functional group for post-polymerisation modifications.

The thesis describes the utilisation of thioester containing monomers in CRP. Firstly, the synthesis and RAFT polymerisation of various thio (meth)acrylates are presented. Investigation of polymerisation parameters affecting the apparent rate constant (*e.g.* temperature, initiator concentration and different degree of polymerisation), thermal properties and hydrophobicity are elaborated. Furthermore, examples to obtain well-defined poly(thioacrylates) are given by exploring possible reaction conditions for NMP. In addition, modification reactions on poly(ethyl thioacrylate) with primary amines and alcohols were investigated. As well as the copolymerisation with a second functional monomer (PFS).

In order to investigate polymerisation conditions for Cu-mediated RDRP, polymerisation parameters were systematically varied and optimised. Ideal reaction conditions were found to utilise a bimetallic system of iron and copper.

Chain extension with acrylate and subsequent modification led to a copolymer containing all three types of acrylic monomers. The utilisation of a 4-arm star initiator has also proven to be compatible. Finally, analogues ester, amide and thioester based ATRP initiators have been synthesised and their kinetics were compared to the homopolymerisation of EA. The 4-arm thioester based initiator allowed a rapid and direct access to a thioester based star shaped polymer, whereby the post modification with a protected amino acid resulted in its disassembly to linear polymers.

Furthermore, the bifunctional property of ETA monomers has been shown in an aza-*Michael* addition on the double bond and a catalysed reaction on the thioester moiety, to mimic an amide functionality. In a combination with thiolactone chemistry, a range of sequence-defined oligomers have been obtained on solid phase.

Abbreviations

CoA	Coenzyme A
AcSEMA	2-(acetylthio)ethyl methacrylate
AIBN	Azobisisobutyronitrile
Am	Acrylamide
AMP	Adenosine monophosphate
ATP	Adenosine 5-triphosphate
ATRP	Atom transfer radical polymerisation
AuNP	Gold nanoparticles
BDTMP	Butyl 2-(((dodecylthio)carbonothioyl)thio)2-methylpropanoate
BPO	Benzoyl peroxide
BEA	Bromoethyl acrylate
BuA	Butylacrylate
BuTA	Butyl thioacrylate
BzAm	Benzylacrylamide
$CDCl_3$	Deuterated chloroform
CLRP	Controlled living radical polymerisation
COSY	Correlation spectroscopy
CRP	Controlled radical polymerisations
CTA	Chain transfer agent
DA	Degree of amidation
DBAm	Di(Boc)-acrylamide
DBTL	Dibutyltin dilaurate
DCC	N,N′-Dicyclohexylcarbodiimide

DCM	Dichloromethane
DCTB	trans-2-[3-(4-tert-Butylphenyl)-2-methyl-2-propenylidene]malononitrile
DEPT	Distortionless enhancement by polarisation transfer
DMA	Dimethylacrylamide
DMAP	4-(Dimethylamino)pyridine
DMF	Dimethylformamide
DMPP	Dimethylphenylphosphine
DMSO	Dimethylsulphoxide
DNA	Deoxyribonucleic acid
DP	Degree of polymerisation
DRI	Differential refractive index
DSC	Differntial scanning calorimetry
EA	Ethylacrylate
EBiB	Ethyl-2-bromoisobutyrate
eq.	Equivalents
eROP	Enzymatic catalysed ROP
ESI-MS	Electrospray ionisation mass spectroscopy
ETA	Ethyl thioacrylate
ETMA	Ethyl thiomethacrylate
f	Initiator efficiency
FID	Flame ionisation detector
FRP	Free radical polymerisation
FTIR	Fourier-transform infrared spectroscopy
GC	Gas chromatography

GPC	Gel permeation chromatography
h	Hour(s)
HMBC	Heteronuclear multiple bond correlation
HPLC	High pressure liquid chromatography
HRMS	High resolution mass spectroscopy
HSQC	Heteronuclear single quantum coherence spectroscopy
I	Initiator
[I]	Initiator concentration
J	Coupling constant
k_{act}	Rate constant of activation
k_i	Rate constant of initiation
k_p	Rate constant of propagation
k_p^{app}	Apparent propagation rates
k_t	Rate constant of termination
k_{tc}	Rate constant of termination by recombination
k_{td}	Rate constant of termination by disproportionation
L	Ligand
LCMS	Liquid Chromatography Mass Spectroscopy
LRP	Living radical polymerisation
M	Monomer
$[M]_0$	Concentration of monomer at t = 0
MA	Methyl acrylate
MALDI	Matrix assisted laser desorption ionisation
Me_6TREN	N,N,N’,N’,N’’,N’’-Hexamethyl-[tris(aminoethyl)amine]
M_n	Molecular weight

MS	Mass spectroscopy
Mt^m	Transition metal species in oxidation state m
N/A	Not available
NCL	Native chemical ligation
NHS	N-Hydroxysuccinimide
NEt_3	triethylamine
NIPAM	N-Isopropylacrylamide
NMP	Nitroxide mediated polymerisation
NMR	Nuclear magnetic resonance
Nu	Nucleophile
OEGMA	Oligo(ethylene glycol) metyhyl ether methacrylate
PDI	Poly dispersity index
PFP	pentafluorophenyl
PFP4VP	vinylbenzoates
PFPA	pentafluorophenyl ester-based acrylates
PFPMA	pentafluorophenyl ester-based methacrylates
PFS	2,3,4,5,6-Pentafluorostyrene
PPM	post polymerisation modification
ppm	Parts per million
R	Radical
R_i	Rate of initiation
R_p	Rate of propagation
RAFT	Reversible addition-fragmentation chain transfer
rt	Room temperature
RDRP	Reversible-deactivation radical polymerisation

ROMP	Ring opening metathesis polymerisation
ROP	Ring opening polymersation
SFRP	Stable free radical polymerisation
s	Seconds
SAMs	Self-assembled monolayers
SG1-MAMA	N (tert-butyl)-N-(1-diethylphosphono-2,2-dimethylpropyl)-O-(2 carboxylprop-2-yl) hydroxylamine
TA	Thioacrylate
T	Temperature
TBD	1,5,7-triazabicyclo[4.4.0]undec-5-ene
T_d	Decomposition temperature
TEMPO	2,2,6,6-tetramethyl-1-piperidinoxyl
TFA	Trifluoroacetic acid
T_g	Glass transition temperature
TGA	Thermogravimetric analysis
THF	Tetrahydrofuran
Tla	Thiolactone
ToF	Time of flight

Chapter 1

1 Thioester containing polymers – an introduction

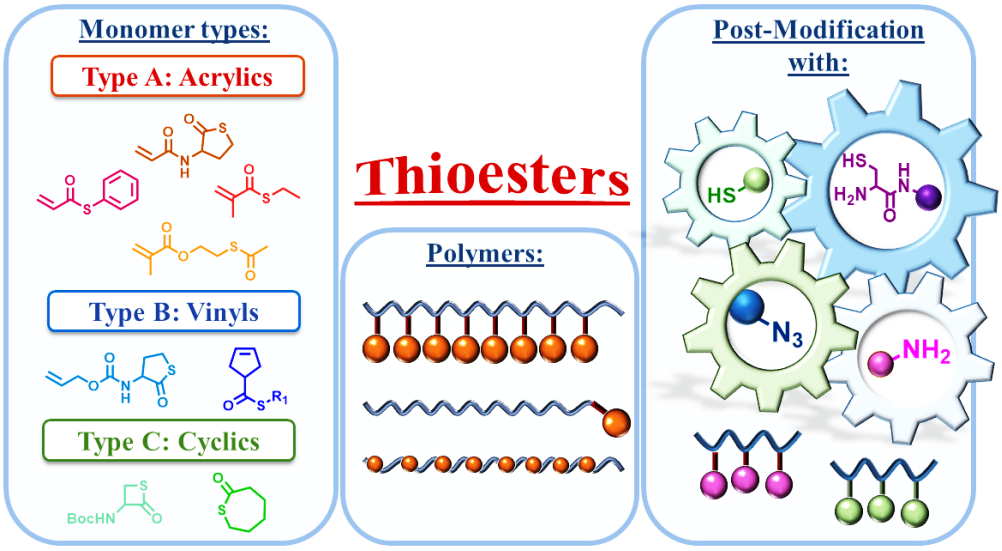

Inspired by the uniqueness and ubiquity of thioesters in nature, much attention has been paid to thioester functionalised materials, yielding applications ranging from responsive polymers to bioconjugates and (bio)degradable polymers. This chapter focuses on various applications of thioesters in polymer science, covering the synthesis and polymerisation of thioester containing monomers, thioester generation via polymerisation processes or the presence of thioesters in chain ends, such as initiators or chain transfer agents. Examples of post-polymerisation modifications with various compounds (e.g. thiols, azides, amines and cysteine containing peptides) to enable modification via pathways such as ligation, amidation or exchange reactions are also presented.

Parts of this chapter have been published;

S. Aksakal, R. Aksakal and C.R. Becer, *Polym. Chem.*, 2018, **9**, 4507-4516

1.1 Introduction

The word “polymer” was introduced by the Swedish chemist *J. J. Berzelius* in 1833, derived from “poly” meaning many and “meros” meaning part.[1] He described polymers as compounds with the same empirical formula but difference in molecular weight, in which he names ethylene and butene as polymers. His definition was not consistent with the current idea of high molecular weight long polymer chains and therefore underwent later a modification to its modern meaning in 1920 by *H. Staudinger*. The idea of “macromolecules” as large molecules, connected by covalent bonds between the monomers in the backbone was coined in his publication on rubber hydrogenation.[2] In 1996, the international union of pure and applied chemistry (IUPAC) has redefined the terms of macromolecule to “a molecule of high relative molecular mass, the structure of which essentially comprises the multiple repetition of units derived, actually or conceptually, from molecules of low relative molecular mass”.[3]

The polymers we encounter in our daily life are either natural polymers such as important components of a living cell (polysaccharides, proteins and peptides) or synthetic polymers. Synthetic polymers have been tailored to suit the different purposes of our life in a (soft) material word, starting from the surfactants in toothpaste, to the flexible bristles of our toothbrush to more complex, smarter and functional polymers as for biotechnology and medicine approaches. Consequently it is not surprising that more and more families of polymeric materials have been designed to serve the wide range of needs of mankind.

1.1.1 Functional Polymers by Polymerisation

Properties of the polymers can be tuned by a combination of composition, topology and functionality. The composition of a polymer is defined by the distribution of monomers, combination of the same monomer as in homopolymers, statistically, blocky structures by incorporation of at least two different block segments, periodically as in repeated sequences or composition with a gradient.

Topologies are based on the combination of polymer chains and include linear, cyclic, branched, graft (comb and brushes) as well as structures that resemble stars. A functional polymer is a polymer that contains a functional group such as amines, hydroxyl or carboxyl groups. Functional polymers have increased attention due to their interesting and specifically designed properties and also due to reactions on the functional moiety with other groups.[4]

Functionality can be brought into a polymer along the chain (pendant-functionalised) or placed at specific positions (end-functionalised), such as in telechelic polymers, resulting in various compositions or topologies **(Figure 1.1)**.

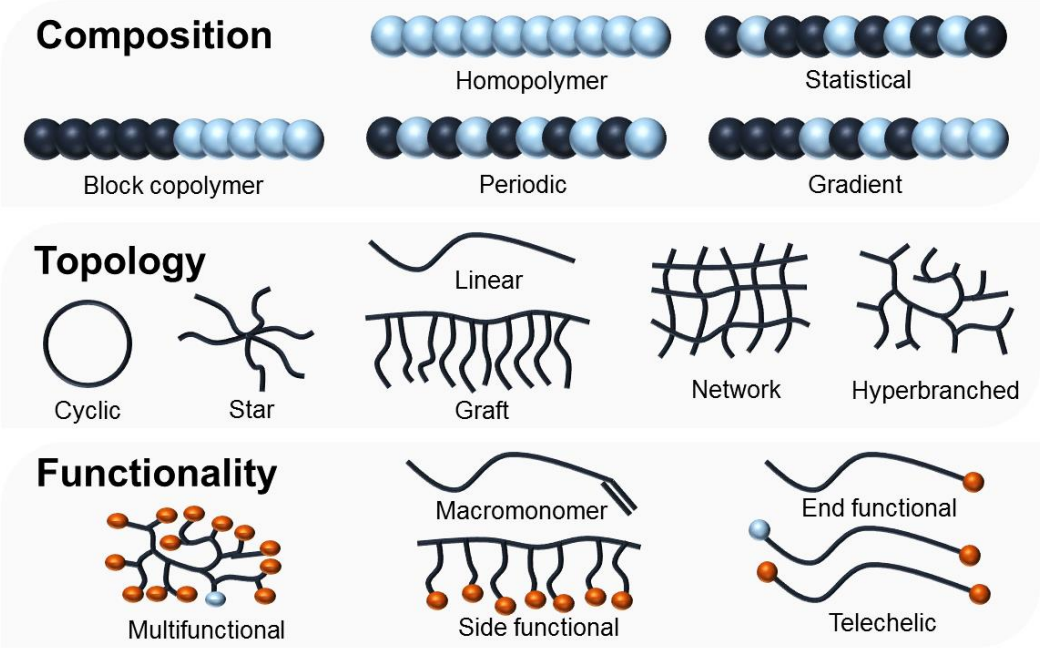

Figure 1.1: Macromolecular architecture guide. The three main aspects of polymer architecture: composition, topology and function. Adapted from Ref.[5]

Practically, a variety range of functional groups can be brought into a polymer to allow further modification to new macromolecules with a higher degree of chemical functionality and application. The current challenge is to combine multiple architectural components –composition, topology, in the hope offering new complex macromolecules, such as multifunctional (miktoarm) polymers (μ-Stars).[6]

1.1.1.1 Free radical polymerisation (FRP)

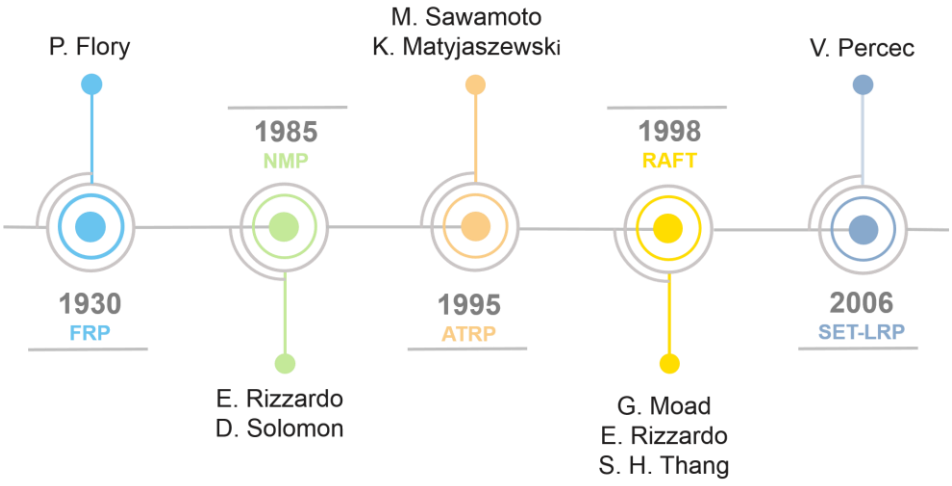

Figure 1.2 Timeline of polymerisation techniques.

In 1930, *Flory* introduced the free radical polymerisation (FRP)[7], which is the most commonly used method for the generation of polymers (*e.g.* Styrene). From an industrial viewpoint, FRP is much more tolerant to protic solvents (such as alcohols and water) and impurities such as oxygen or stabilisers and the wide range of commercially available and cost effective monomers with a wide range of groups (*e.g.* amino, hydroxyl)[8]. Although it is possible to polymerise styrene by anionic, cationic or metal catalysed polymerisation, it is economically more affordable to polymerise styrene *via* FRP in industry.[9] Nevertheless, the radical process is governed by termination or transfer due to the high reactivity of radicals. As a result, those polymers suffer from broad dispersity and poor control over chain architecture and end group and can lead to deactivation or branching of the growing polymer.

1.1.1.1.1 Sequence of events

FRP consist of three steps; *initiation*, *propagation*, and *termination*. The initiation step of the polymerisation involves two reactions, where the first reaction describes the generation of free radicals. Homolytic cleavage of the covalent bonds of the initiator (I) is caused by either increase of temperature or radiation and a pair of radicals is formed (2R·). The newly formed radical can react with a non-radical, the monomer to produce the chain-initiating radical (M·), described as the second part of the initiation **(Eq. 1.2)**.

$$\mathrm{I} \xrightarrow{k_d} 2\mathrm{R}\cdot \qquad \textbf{(1.1)}$$

$$\mathrm{R}\cdot + \mathrm{M} \xrightarrow{k_i} \mathrm{M}\cdot \qquad \textbf{(1.2)}$$

The initiation-step is then followed by propagation, where the chain-initiating radical chain grows into a longer chain by sequential addition of more monomers (M).

The successive addition is described in **Eq. 1.3 – 1.5,** where k_p is the rate constant for propagation. This term can be generalised in **Eq. 1.6**. Although it can vary, typical k_p values for most monomers varies between 10^2–10^4 L·mol^{-1}·s^{-1} in radical polymerisations, a much larger rate constant compared to those we usually find in step polymerisations.

$$M_1\cdot + M \xrightarrow{k_p} M_2\cdot \quad \textbf{(1.3)}$$

$$M_2\cdot + M \xrightarrow{k_p} M_3\cdot \quad \textbf{(1.4)}$$

$$M_3\cdot + M \xrightarrow{k_p} M_4\cdot \quad \textbf{(1.5)}$$

In general terms

$$M_n\cdot + M \xrightarrow{k_p} M_{n+1}\cdot \quad \textbf{(1.6)}$$

At a certain point, the propagating polymer chain stops growing further and terminates. Termination reactions can occur by *recombination* of two radical growing chains to a neutral chain with higher molecular weight **(Eq. 1.7)**. More rarely, termination can also be induced by an abstraction from the *β*-hydrogen atom of the radical growing chain by a disproportionation process to another radical center. This mode of termination is called *disproportionation* **(Eq. 1.8)**. This termination reaction will yield two neutral polymer chains, one consist of one saturated end and an unsaturated end (double bond on chain end).

Combination:

$$M_n\cdot + M_m\cdot \xrightarrow{k_{tc}} M_{n+m} \quad \textbf{(1.7)}$$

Disproportionation:

$$M_n\cdot + M_m\cdot \xrightarrow{k_{td}} M_{n-1} = M_n \quad + \quad M_{m-1}M \quad \textbf{(1.8)}$$

The rate constants of terminations by recombination and disproportionation (k_{tc} and k_{td}) can be expressed by **Eq. 1.9**.

$$M_n\cdot + M_m\cdot \xrightarrow{k_t} \text{dead polymer} \quad \textbf{(1.9)}$$

The rate constants of the two possible termination reactions (k_{tc} and k_{td}) can be combined and simplified to a unspecified term represented in **Eq. 1.10**. Fractions of termination by coupling is represented by a, where (1-a) represents the fractions of termination by disproportionation.

$$k_t = \mathrm{a}k_{tc} + (1 - \mathrm{a})k_{td} \quad \textbf{(1.10)}$$

Typical k_t values lie in the range of 10^6-10^8 L·mol^{-1}·s^{-1} or even orders of magnitudes greater than k_p, the propagation rate constant during the polymerisation process. The greater value of k_t compared to k_p does not prevent propagation, as the radical species present is in very low concentration and as the polymerisation rate depends on the one-half power of k_t only.

1.1.1.1.2 Rate Expression

To obtain a kinetic expression for the *rate of polymerisation*, assumption of the independence of k_p and k_t on the size of the radical species has to be made. Radicals with small size are more reactive than propagating polymer radicals, but this effect is neglectable because the effect of the size vanishes at the dimer or trimer size.[10] Monomer disappears by initiation reaction **(Eq. 1.2)**, in addition to the propagation **(Eq. 1.6)**.

The rate of monomer disappearance, which is synonymous with the rate of polymerisation, is given by **Eq. 1.11**, whereby R_i and R_p are the rates of initiation and propagation, respectively. Nonetheless, the number of monomer molecules reacting in the initiation step is much lower than the number consumed during the propagation step for a process producing high molecular weight polymer. To a very close approximation, the former can be neglected and the polymerisation rate is given simply by the rate of propagation **(Eq. 1.12)**.

$$-\frac{d[\mathrm{M}]}{dt} = R_i + R_p \quad \textbf{(1.11)}$$

$$-\frac{d[\mathrm{M}]}{dt} = R_p \quad \textbf{(1.12)}$$

The rate of propagation, and consequently the rate of polymerisation, can be presented as the sum of many individual propagation steps. Since their rate constants are all identical, the rate of polymerisation can be exemplified as follows:

$$R_p = k_p[\mathrm{M}\cdot][\mathrm{M}] \quad \textbf{(1.13)}$$

where [M] represents the monomer concentration and [M·] the total concentration of all chain radicals. The radical concentration, however, has proven to be difficult to measure, since they are typically very low (10^{-8} M). **Eq. 1.13** is due to the existence of

this term not directly usable and is therefore required to be eliminated from the expression. Radical concentration initially increases with the decomposition of the initiator. Once all the radicals are generated, the concentration of the formed radicals during propagation remains unchanged. With this *steady-state* assumption (*Bodenstein* approximation), it is likewise acceptable to state that the rate of initiation R_i and termination R_t remain equal **(Eq. 1.14)**.

$$R_i = R_t = 2k_t[\mathrm{M}\cdot]^2 \qquad \textbf{(1.14)}$$

The term on the right side of the equation, represents the rate of termination, where the particular mode of termination is unspecified, as both follow the same kinetic expression. The factor two in the rate of termination equation occurs as a result of the disappearance of two radicals at either incident of termination reaction. Rearranging **Eq. 1.14** and substitution into **Eq. 1.15** gives **Eq. 1.16** for the rate of polymerisation.

$$[\mathrm{M}\cdot] = \left(\frac{R_i}{2k_t}\right)^{\frac{1}{2}} \qquad \textbf{(1.15)}$$

$$R_p = k_p[M]\left(\frac{R_i}{2k_t}\right)^{\frac{1}{2}} \qquad \textbf{(1.16)}$$

Thus, **Eq. 1.16** clearly show the dependence of the polymerisation rate on the square root of the initiation rate. The equation shows that doubling the initiation rate, does not double the rate of polymerisation, but increases it by a factor of $\sqrt{2}$ as a consequence of the bimolecular termination reaction between radicals.

1.1.1.1.3 Kinetics of free radical polymerisation

The rate of the production of radicals by thermal homolysis is given by **Eq. 1.18**, where [I] is the initiator concentration and f is the initiator efficiency. The initiation efficiency is defined as the fraction of the radicals produced by thermal hydrolysis and is usually less than one, as side reactions take place which leads to wastage of initiator radicals.

As described above, the initiation step consists of two reactions **(Eq. 1.1** and **1.2)**. In most polymerisations, the second reaction, in which the primary radical adds to the monomer, proceeds much faster. Therefore, the homolysis of the initiator is the rate

determining step which is given in **Eq. 1.18**. Substituting **Eq. 1.18** into **Eq. 1.16** gives **Eq. 1.19**.

$$R_d = 2fk_d[I] \quad \textbf{(1.17)}$$

$$R_i = 2fk_d[I] \quad \textbf{(1.18)}$$

$$R_p = k_p[\mathrm{M}]\left(\frac{fk_d[I]}{k_t}\right)^{\frac{1}{2}} \quad \textbf{(1.19)}$$

The above equation shows that the polymerisation rate is proportional to the square root of the initiator, assuming that f is independent of monomer concentration, which is acceptable for high initiator efficiencies.

Whereas control over polymerisation or dispersity are not relevant factors in for example the industry, more specific applications, such as biological or medicinal applications require more uniform structures where controlled polymerisation techniques can't be neglected. More advanced systems and techniques have been extensively investigated within the last decades to allow more control over the polymerisation, referred to as "controlled" radical polymerisation (CRP). The classes of techniques for such processes are currently being researched intensively worldwide. In the next section those popular techniques will be presented.

1.1.1.2 Controlled radical polymerisation (CRP)

Reversible deactivation radical polymerisation (RDRP)[11], which is also known as controlled/living radical polymerisation, has revolutionised the field of the synthesis of "uniform" polymers with precisely controlled molecular weight, narrow dispersity and the unprecedented maintenance of end-group fidelity. The "living" polymerisation characteristics were pioneered by *Szwarc* in 1956, where early terminations are minimised and molecular weight grows linearly with conversion until full monomer consumption or intentional termination. The most recent IUPAC definition of a living polymerisation is a chain polymerisation, which can take on the character of a living polymerisation with appropriate conditions, *i.e.* chain termination and irreversible chain transfer are absent. As a consequence, the synthesis of homopolymers or block copolymers by sequential addition are possible with narrow molecular weight distributions.[12]

The characteristics have been adapted to radical polymerisation systems in RDRP, where three new representative systems have been developed. Nitroxide-mediated

polymerisation (NMP), metal-catalysed polymerisation (ATRP) and reversible addition-fragmentation chain transfer polymerisation (RAFT) are the most widely employed techniques.

In general, RDRP systems comprise a broad range of monomers, solvent *etc*. to obtain polymers with controlled molecular weight and structures that can be pre-targeted.

1.1.1.2.1 Nitroxide-Mediated Polymerisation (NMP)

A stable radical, which reversibly caps the chain end of a growing polymer establishes a low radical concentration in the solution and minimises deleterious termination reactions. In this way the stable radical of nitroxides[13], (arylazo)oxy[14], triazolinyl[15], verdazyl[16], substituted triphenyl[17] acts as a mediator or deactivator in Stable Free Radical Polymerisation (SFRP). The most investigated and most efficient of the before mentioned stable radicals are nitroxides.

Polymerisation employing nitroxides are therefore called nitroxide-mediated polymerisation (NMP), which was discovered and patented by *Solomon* and *Rizzardo* (CSIRO) in 1985.[18] NMP is in particular useful due to its simplicity as only monomer and an initiator is needed. Additionally, metal catalysts and sulfur can be avoided as used particularly in ATRP and RAFT. NMP is carried out by two methods which are parallel to those in ATRP, which was developed a decade later. One method includes the thermal decomposition of an alkoxyamine such as 2,2,6,6-tetramethyl-1-piperidinoxyl (TEMPO) into a reactive radical and a stable radical.[19]

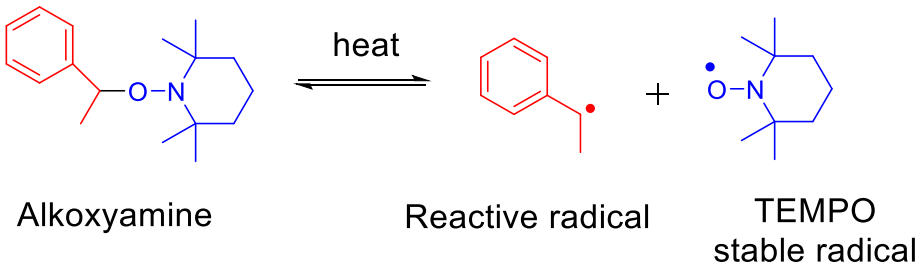

Scheme 1.1: The termal decomposition of alkoxyamine into a reactive radical and a stable radical (TEMPO).

In this way, the alkoxyamine undergoes a homolytical cleavage of the weak C─O bond, initiated by temperature to afford two radicals, a stable nitroxide radical (TEMPO), and a polymeric radical that can undergo chain addition. The nitroxide radical can create a new radical species, but recombines reversibly with active polymeric chains to an unreactive dormant species. The reversible radical generation

and recombination is defined by a temperature dependent equilibrium that allows to conduct the polymerisation under control.

The second method involves a combination of a conventional radical initiator such as azobisisobutyronitrile (AIBN) or benzoyl peroxide (BPO) and the nitroxide radical. The reactive radical depicted in **Scheme 1.1** that is capable to initiate the polymerisation is a styrene monomer. Propagation proceeds in which polymer chains are produced while reversible termination events yield a nitroxide-trapped alkoxyamine as a thermally labile species. The new alkoxyamine mediates the accessibility of the reactive radical species and provides thereby control over the polymerisation.

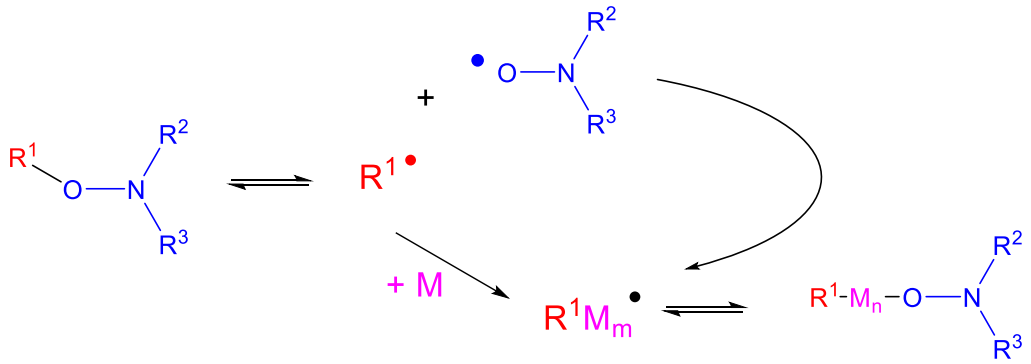

Scheme 1.2: The simplified mechanism of NMP.

However, styrene and 4-vinylpyridine were the only monomers in the early literature of NMP that polymerised well. This system used TEMPO and excessive heat (120-150 °C) and long reaction times (1-3 days).[20] *Hawker et al*. investigated and developed a system for a range of alkoxyamines, evaluated initiators for the polymerisation of styrene, acrylates, acrylamides and acrylonitrile-based monomers. Polymers were obtained with dispersities as low as 1.06.[21] The development of a "universal" initiator (2,2,5-Trimethyl-3-(1-phenylethoxy)-4-phenyl-3-azahexane) allowed control over polymer composition, target molecular weights and definition of the end–group with low dispersities. Furthermore, the initiator confirmed to be compatible with reactive functional monomers, such as carboxylic acids, epoxides, amines and fluorocarbons, resulting in well-defined polymers with low dispersities. Polymerisation of acrylic acid and glycidyl acrylate employing the same initiator however, gave broader dispersities.

1.1.1.2.2 Atom Transfer Radical Polymerisation (ATRP)

Atom transfer radical polymerisation (ATRP) was developed independently by *Sawamoto*[22] and *Matyjazewski*[23] in 1995, in which organic halides undergo a reversible redox process, catalyzed by a transition metal compound (*e.g.* cuprous halide). This method, consists in general of monomers, an initiator with a transferable halogen (P_n-X) and a catalyst (Mt^m, transition metal species in oxidation state m) with a suitable ligand (L_n)) **(Scheme 1.3)**. The generation of radicals in ATRP involves an organic halide undergoing a reversible redox process catalysed by a transition metal compound such as copper halide.

Polymerisation is controlled by an equilibrium between a propagating radical and a dormant species (initiating alkyl halide/macromolecular species: P_nX).[24] The dormant species reacts periodically with a rate constant of activation (k_{act}) with the transition metal complex in their lower oxidation state, Mt^m/L, acting as the activator to form growing radicals P_n and the deactivator-transition metal complex in their higher oxidation state, coordinating with halide ligand X-Mt^m+1. The deactivator reacts then with the propagating radical in a reversible fashion (k_{deact}) to regenerate the dormant species and the activator. Polymer chains are growing by the addition of the intermittently intermediate radicals to the chain. Termination reactions (k_t) occur mainly through radical coupling and disproportionation.[25]

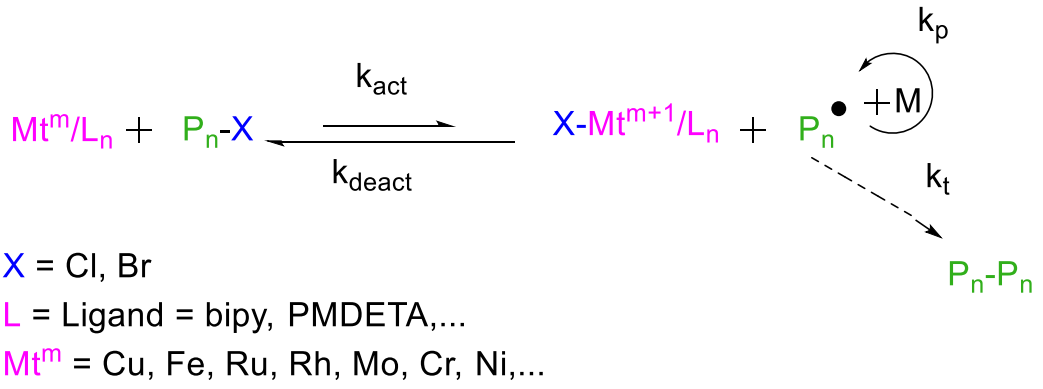

Scheme 1.3: Mechanism of metal-catalyzed ATRP.

In place of copper, many other transition metals can be employed in ATRP, in which the polymerisation proceeds with the same mechanism. Other common transition metals used are ruthenium[26-28], iron[29, 30], nickel[31, 32], palladium[33] and molybdenium[34].

For ATRP various monomers have been successfully polymerised: styrene, (meth)acrylates, dienes, acrylonitriles, *etc*.[35, 36] However, there are only few reports on

ATRP of acrylamides.[37, 38] Acidic monomers, halogenated alkenes, alkyl-substituted olefins and vinyl esters are not suitable monomers for ATRP.

1.1.1.2.3 Single Electron Transfer-Living Radical Polymerisation (SET-LRP)

In 2006 *Percec* and co-workers reported the ultrafast polymerisation of various (meth)acrylates at room temperature using Cu(0). Ever since, the mechanism behind the Cu(0) mediated polymerisation has been under a debate, mainly between *Percec* and *Matyjaszewski*. There are two main models that have been proposed for the mechanism. Both models see Cu(II)Br as the deactivator, however are in disagreement as to which species activates the polymerisation (Cu(0) *vs.* Cu(I)Br) **(Scheme 1.4)**.

The proposed mechanism of SET-LRP by *Percec* is depicted in **Scheme 1.4**. This technique invokes an equilibrium between copper(I) and copper(0) and copper(II) species. With the addition of a ligand, the equilibrium shifts towards copper(0), where the ligand complexes copper(II). With these conditions, it is proposed that Cu(0) acts as the activator, whereas the Cu(II) species deactivate the polymerisation, slowing down the chain growth and allowing better control over the molecular weight distribution and control over polymerisation. Depending on the medium and technique, a broad range of monomers can be used in SET-LRP, including acrylates[39-43], acrylamides[44-46], methacrylates[47-49], methacrylamides[50, 51], zwitterionic monomers[52, 53], semi-fluorinated monomers[54, 55], glycomonomers[56, 57], acrylonitrile[58, 59], vinyl chloride[60], 2-vinyl pyridine[61] and styrene[62, 63].

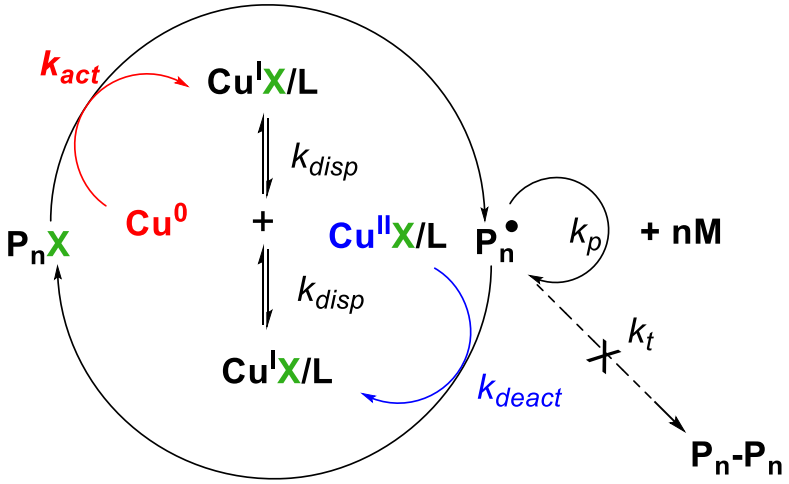

Scheme 1.4: Proposed mechanism for SET-LRP.

Similarly, the first example of CuBr disproportionation in the presence of Me_6-TREN in water, has been reported to generate "*nascent*" Cu(0) for the polymerisation of various acrylamides by *Haddleton et al*. This yielded very well defined polymers of NIPAM, DMA, 2-Hydroxyethyl acrylamide with 100% conversion. The polymerisations are performed at or below room temperature and the ability of chain extension was shown *via* ^{1}H NMR spectroscopy, indicating high chain end fidelity **(Scheme 1.5)**.[64]

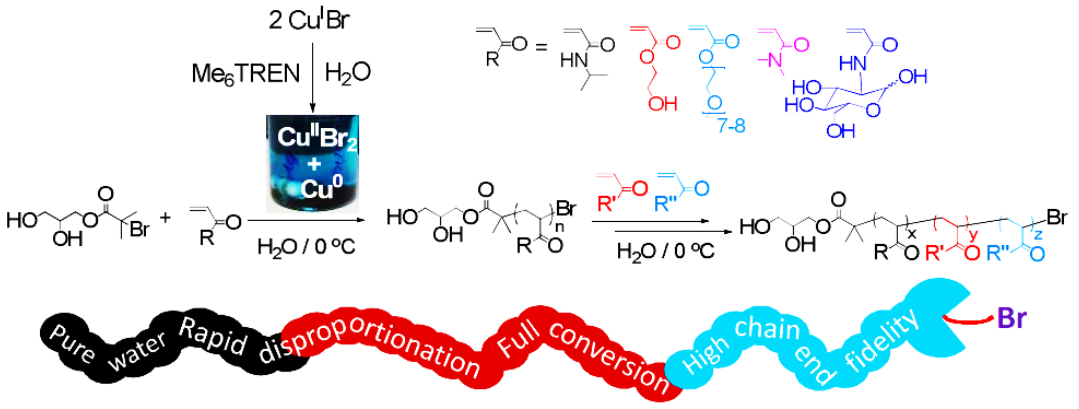

Scheme 1.5: Polymerisation of various water soluble monomers *via* aqueous SET-LRP.[64]

It was later shown that this protocol could also be used to obtain well defined sequence controlled multiblock copolymers. Kinetic studies were carried out in order to find out conditions that allow the polymerisation of acrylamides *via* chain extension. ^{1}H NMR spectroscopy, revealed that employing tertiary acrylamides, contributed more to the

loss of chain end fidelity, in comparison to secondary acrylamides.[65] The same group took this approach further and reported the polymerisation of acrylates *via* photoinduced radical polymerisation. It was shown that acrylates can be polymerised under UV light, in the presence of $CuBr_2$ and Me_6TREN, yielding well defined polymers with dispersities as low as 1.05. Similarly, full monomer conversion was observed, with very high chain end fidelity, allowing further chain extensions of various monomers. The same system was also applied to a telechelic initiator, displaying the versatility of this approach to obtain different structures.[25]

1.1.1.2.4 Reversible Addition-Fragmentation chain transfer (RAFT)

Reversible Addition-Fragmentation Chain Transfer (RAFT) polymerisation was first reported in 1998 by CSIRO, when a dithio-compound had been used as an efficient chain transfer agent (CTA), allowing a rapid exchange between dormant and living chains. The currently approved mechanism of the RAFT process is outlined in **Scheme 1.6** below. Similar to conventional radical polymerisation, the RAFT process follows initiation, chain propagation and chain termination. In a first step, radicals (**I•**) are formed from the initiator and react with monomers (**M**) to give a propagating radical (**P_n•**). The propagating radical (**P_n•**) reacts with the C=S group of the RAFT agent (chain transfer agent, CTA) to form a tertiary radical (**2**). This intermediate radical will control the irreversible termination reaction between the propagating and intermediate radical, which is stabilised by the Z-group and therefore regulates the activity of the C=S bond. On the other hand, the R-group presents a good homolytic leaving group and good initiating species, which can reinitiate the polymerisation rapidly, when the intermediate radical fragments into a new radical (**R•**) and a dormant chain **3** (polymeric thiocarbonylthio compound, RSC(Z)=S). The new propagating radical (**P_m•**) will be formed after reaction of the new radical **R•** with monomer. A rapid equilibrium between active propagating radicals, either **P_n•** or **P_m•** and the dormant polymeric compound **3**, *via* the intermediate **4** provides an equal probability for all chains to grow, leading to low disperse polymers. After termination (either intended or unintended), most of the polymer chains are present as dormant species (**P_nS(Z)C=S (3)**), where the thiocarbonylthio end-group remains and the polymer can be isolated as a stable compound.

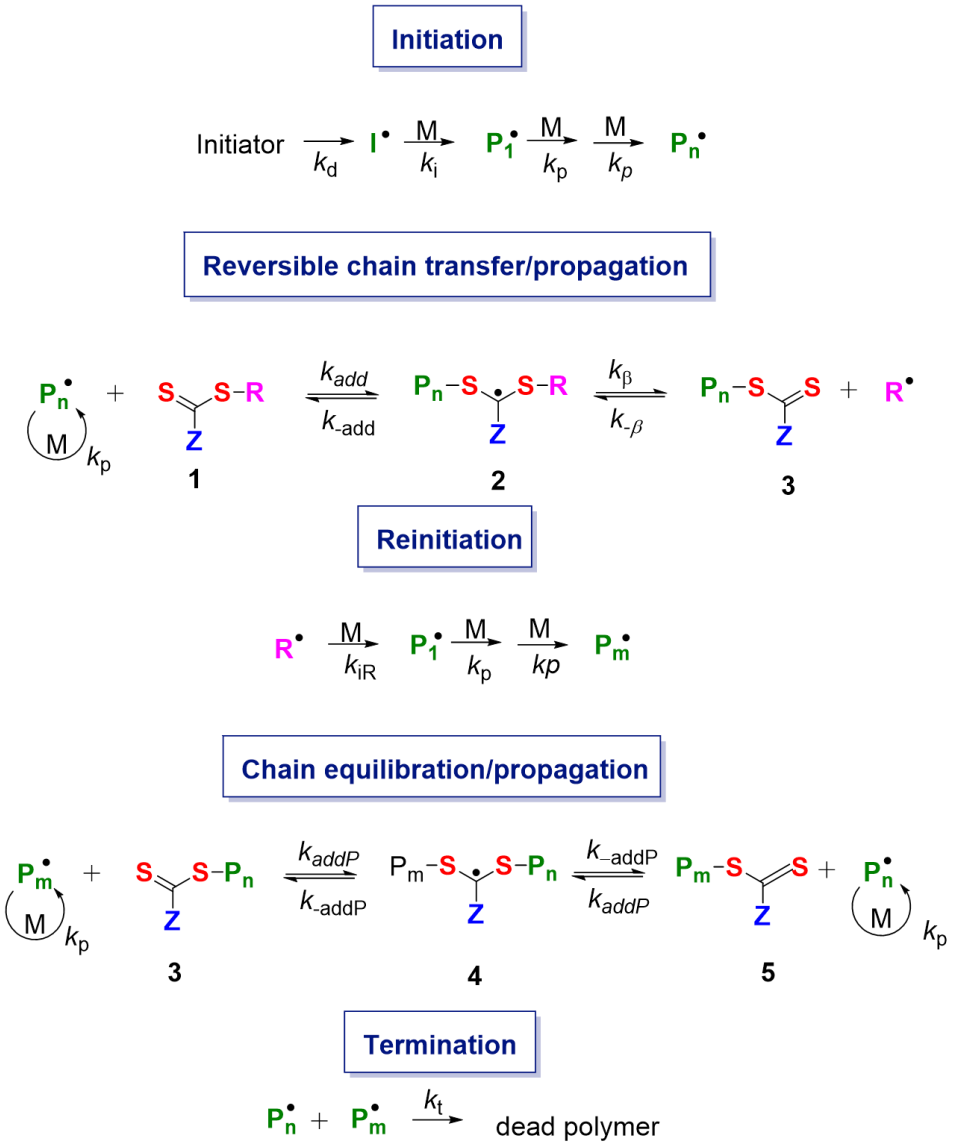

Scheme 1.6: Mechanism of RAFT polymerisation.

An important advantage of RAFT is the broad range of monomers that can be used, which covers in general a broader range than NMP or ATRP. Some of the monomers subjected to RAFT polymerisation are methacrylates, acrylates, methacrylamides, acrylamides, styrene derivatives and diverse monomers. Additionally, no metals are used in the process, however polymers are associated with an odour and colour due to the RAFT agent (purple, red, orange and yellow colours are typical for dithiobenzoates and trithiocarbonates). Because of this, many researchers have examined the possibilities to remove these groups from the polymer chain end to obtain non-coloured materials.

The scope of RAFT is not limited by the choice of monomers, as the variations in the side chain in different monomer classes is possible. The use of different monomers allows more complex architectures to be obtained in a sequence defined fashion. *Perrier et al.* have reported the synthesis of an icosablock polymer with several acrylamides consisting of an average block length of three repeating units, with 94% chain end fidelity (PDI < 1.4).[66] The reaction conditions were further optimised and a decablock homopolymer could be obtained, with an improved control over molecular weight distribution (PDI = 1.15), whilst retaining the high livingness at 97%.[67] Yet an extended polymerisation time of 24 h per block was required to reach complete monomer conversion. The polymerisation conditions were further modified for the homopolymerisation, reducing the reaction times, where only two hours were required per block to reach full conversion. [68] These findings were then extended on the synthesis of a dodecablock copolymer (12 blocks from four different acrylamides) and two high molecular weight pentablock copolymers (five blocks from three different acrylamides) with an average degree of polymerisation of 100 per block.

Interestingly, the RAFT end-group can be used for further modification to functional polymers. For example, *Sumerlin* and co-workers have used the thiocarbonylthio end group of the thermoresponsive PNIPAM for modification with thiols and dienes **(Scheme 1.7)**. Trithiocarbonate end-capped PNIPAM was treated with ethanolamine in the presence of PBu_3 at room temperature to yield a macromolecular thiol (PNIPAM-SH).[69] The thiol terminated polymer was subsequently reacted with 1,8-bismaleimidodiethyleneglycol in the presence of NEt_3 as a base, to give the respective maleimide ω-functional PNIPAM.

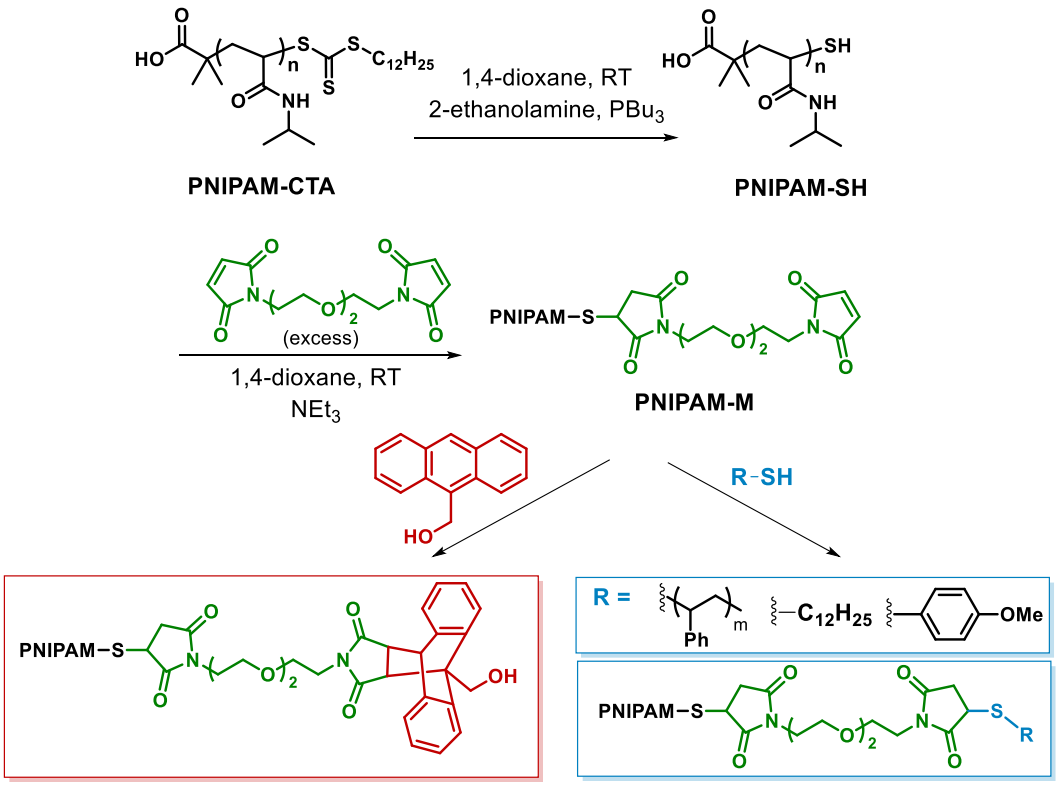

Scheme 1.7: Synthesis of a thermoresponsive macromolecular thiol and its conjugation *via* thiol maleimide chemistry.

The maleimide end groups allowed coupling with small molecule thiols *via* Michael addition and was demonstrated to be an effective route to AB diblock copolymers. The same strategy was applied to dienes and proceeded *via* Diels-Alder reactions. Many other functionalities have been coupled to the thiol terminated RAFT polymer employing the same strategy. For instance, conjugation of a maleimide-terminated PNIPAM (PNIPAM–M) to BSA (bovine serum albumin) and OVA (ovalbumin), gave a thermoresponsive and bioactive conjugate.[70]

Additional to the modification of the end group of a polymer, the side-group of a polymer obtained *via* RAFT can also be altered after the polymerisation process. Well-defined homopolymers and block copolymers of bromoethyl acrylate (BEA), carrying bromide side groups were obtained by RAFT polymerisation **(Scheme 1.8)**. Substitution of terminal bromides using different types of nucleophiles (*e.g.* amines, phosphines, azides, sulfites, and thiols) can produce functional polymers with complex functionalities, from permanently charged polyanions to glycopolymers.[71]

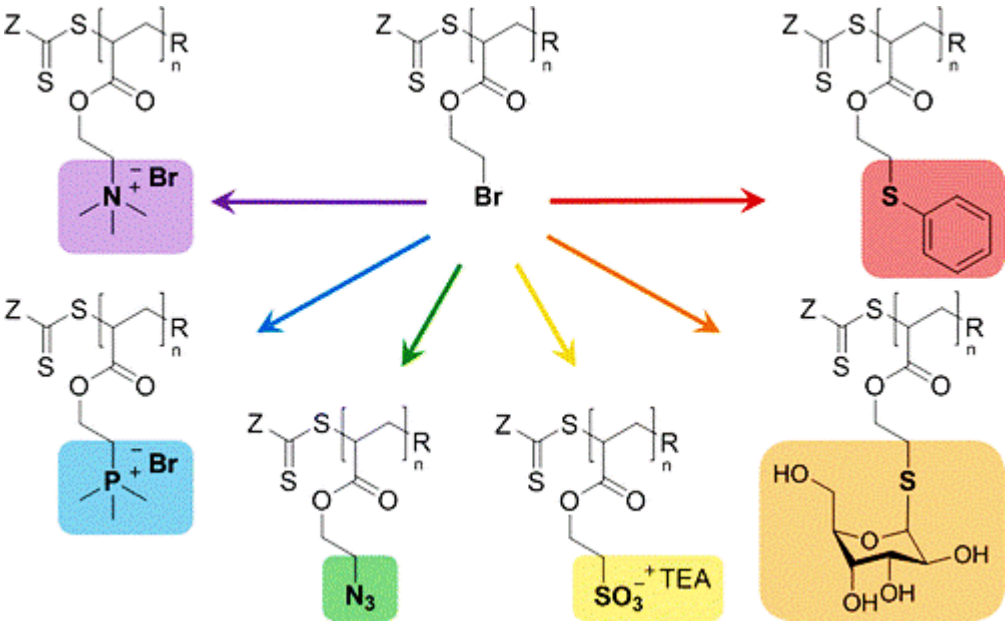

Scheme 1.8: Possible post polymerisation modification routes of a 2-bromoethyl acrylate polymer.[71]

Substitution reaction with sodium azide was followed by ^{1}H NMR and FT-IR and confirming completion of the azide formation by appearance of a strong azide stretch signal at 2200 cm^{-1}. In this way, post modification with an azides provides an alternative route to polyazides and circumvents the use of highly reactive (and explosive) azido monomers. Cationic polyelectrolytes were obtained by quaternisation of PBEA with trimethylamine or trimethylphosphine under mild conditions *(e.g.* room temperature, catalyst-free), maintaining the trithiocarbonate end-group. Substitution with a strong nucleophile, such as tetraethylammonium sulfite was also possible and proceeded fast without any need for optimization. As opposed to the direct polymerisation of protected glycomonomers, the thio-bromo substitution with *β*-thioglucose sodium salt as an alternative route was employed to prepare for well-defined glycopolymers without the use of base. However, the GPC-analysis revealed a higher molecular weight signal indicating some end-group removal of the RAFT agent resulting in disulphide formation. BEA provides an efficient precursor for a catalyst and protecting group free method for the modification of the bromine end-group with a range of functional groups.

1.2 Thioester functional polymers

Sulfur-containing polymers represent an attractive tool for the next generation of functional materials. These materials have already attracted significant interest and led to multifaceted applications, including the construction of thiolated polymers with high mucoadhesive ability[72], optical materials with higher refractive indices[73], robust self-assembled monolayers[74-76] (SAMs) including gold nanoparticles[77] (AuNP) for imaging and bioconjugates of polymers and thiol-containing biomolecules[78]. However, the use of free thiols in polymerisation reactions requires protected thiols due to their low stability and high reactivity compared to esters[79-81], which can be called as their hydroxy counterparts.[82] Nevertheless, there are many straightforward ways to introduce thiols in a protected state into a polymer[83, 84] and numerous studies on various designs, consisting of a source of thiols in acrylic, vinyl or hetereocyclic systems (*e.g.* thiazole[85], thiophene[86, 87] or thiolactones[88-90]) have been reported up to date. The latter one is still of great interest as thiolactones have been demonstrated to be a versatile and unique structural motif in the construction of sequence defined oligomeric and polymeric materials.[88-90]

1.2.1 Structural features of thioesters

The thioester bond is a common functional group in biology as it displays a wealth of attractive properties and exists as a fundamental key component or intermediate in biological systems, such as reactions of Coenzyme A (CoA), which promotes the metabolism of cellular components (*e.g.* peptides, fatty acids, sterols, terpenes, lipids and porphyrins).[91]

Esters are stabilised by a contribution from a resonance structure where the lone pair of the single bonded oxygen atom donates electron density into the antibonding orbital of the carbonyl structure. This is manifested in a partial double bond character and hindered rotation around the C-O single bond. In a similar structure with a thioester as in CoA, the carbonyl is not stabilised by resonance as the ester carbonyl. The poor resonance overlap of the 2p orbital from the carbon and the sulfur 3p orbital makes a thioester less resonance stabilised and thus more reactive.[92] Thioesters are mainly stabilised from a

resonance structure where both electron pairs are localised on the oxygen, resulting in a full negative charge and the carbonyl carbon in a full positive charge and susceptible to nucleophilic attack.[93] Additionally, a thiolate anion and thiol presents a good leaving group because of its high polarisability and low degree of polarisation.[94] The aforementioned factors, makes the more reactive carbonyl in thioesters more favourable against oxoesters for the linkage in CoA.

1.2.2 Synthesis and reactions of thioesters

There are numerous known methodologies for the synthesis of thioesters **(Scheme 1.9)**. Esterification reactions of an acyl compound (*e.g.* carboxylic acid[95-97], acid anhydride[98, 99] or acid chloride[100-103]) with a thiol conducted in the presence of a base is a convenient and a standard protocol for the synthesis of these organosulfur compounds. Aldehydes have also been widely explored for the synthesis of thioesters.[99, 104-109] An alternative methodology is the acylation of thiols using various catalysts (*e.g.* triflates, CsF, NBS, zeolites, rongalite, Lewis acids, zinc, ionic liquids).[110] An inexpensive and efficient method for the synthesis of thioesters by an acid-catalysed *S*-acetylation of a wide range of aromatic and aliphatic thiols with isopropenyl acetate, has also been reported recently.[111]

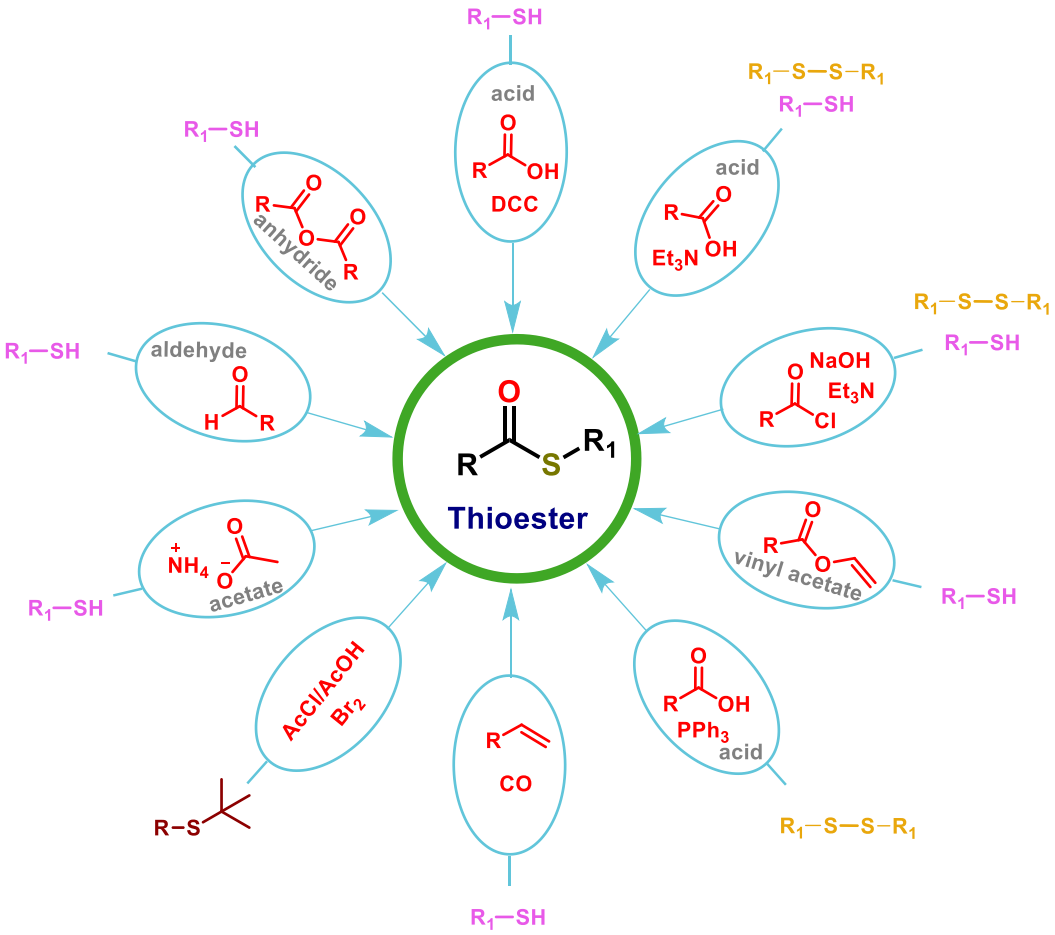

Scheme 1.9: Synthesis of thioesters in the literature.

Additionally, one-step conversion of the thioester group into other functional groups is very attractive in organic synthesis **(Scheme 1.10)**. A particular significant conversion is the transformation of thioesters into amides. Reaction of thioesters with primary amines, azides[112-114] or cysteine-containing structures[115, 116] result in an amide functionality in the molecule, whereas a reaction with a thiol in a thiol-thioester exchange reaction[117, 118] will form a new thioester bond.

Numerous studies have elaborated their reactivity in contrast to oxoester analogues and proven a 100-fold faster reaction rate with amines.[93] The mechanism and progress of this amidation process with mono- and bifunctional amines on a dithioester has been described in 1990[119], catalysed with arylthiols[120], and outlined in more details by *Castro* for thioesters and thiocarbonates.[121]

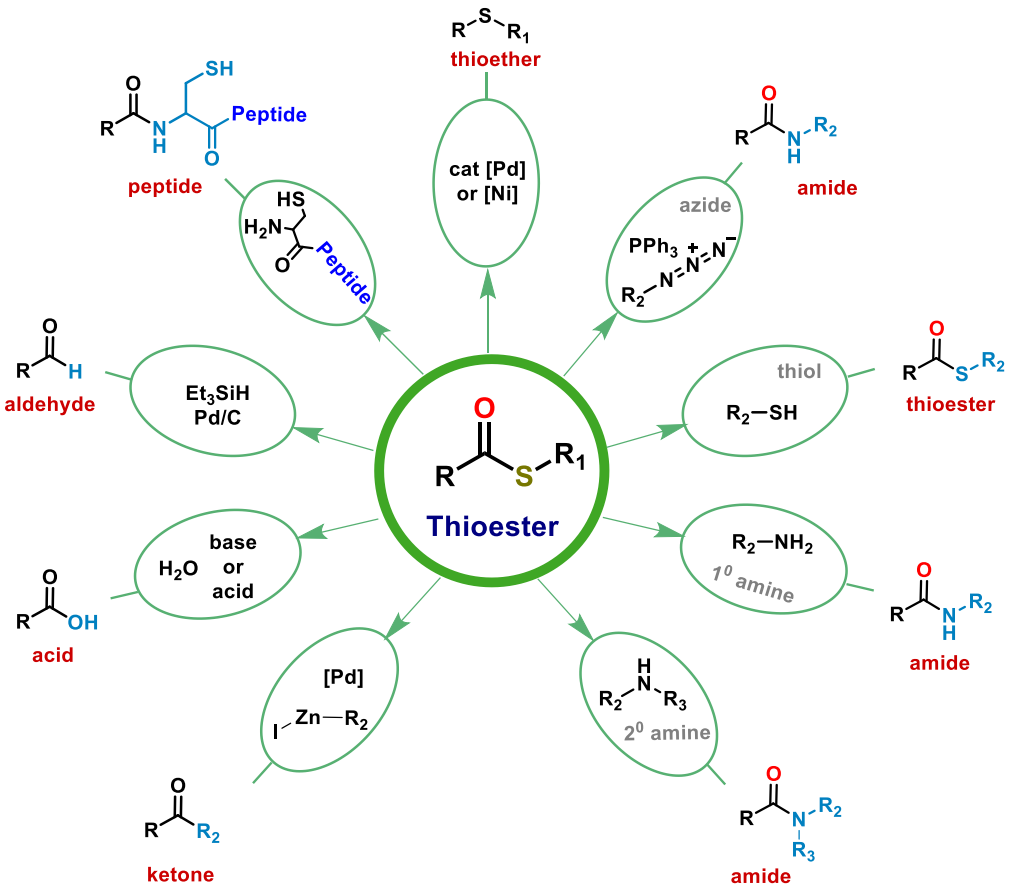

Scheme 1.10: Possible modification routes of thioesters.

Very recently, the transformation of thioesters to their thioethers has been reported on arylthioesters *via* Pd- and Ni-catalysed decarbonylative conversion, under base and thiol free conditions.[122] In an attempt to develop new rigid-rod polymers, the thia-Michael reaction was employed between molecular rods, bearing terminal thiols and bis maleimides.[123] Interestingly, cyclic oligomers were mainly obtained contrary to the expected linear polymers, which was attributed to the folded conformation of the building blocks.

1.2.3 Thioester in Polymers

In the past few years, the manifoldness of thioesters have become widely available and have drawn widespread attention in polymer science **(Scheme 1.11)**. For example, the aminolysis of dithiocarbonates, dithiocarbamates and thioesters has been evaluated as thiol protection groups in atom transfer radical polymerisation (ATRP) and reversible addition fragmentation chain transfer (RAFT) polymerisation. Interestingly, dithiocarbamate group could not be cleaved under mild conditions and led to

side-reactions during the radical polymerisation of styrene and (meth)acrylates. Thiocarbonyl and thioesters did not induce any side-reactions and could be cleaved under mild conditions. Moreover, up to eight times higher reactivity towards amines of the dialkyl xanthate in comparison to an alkyl thioacetate was reported.[82]

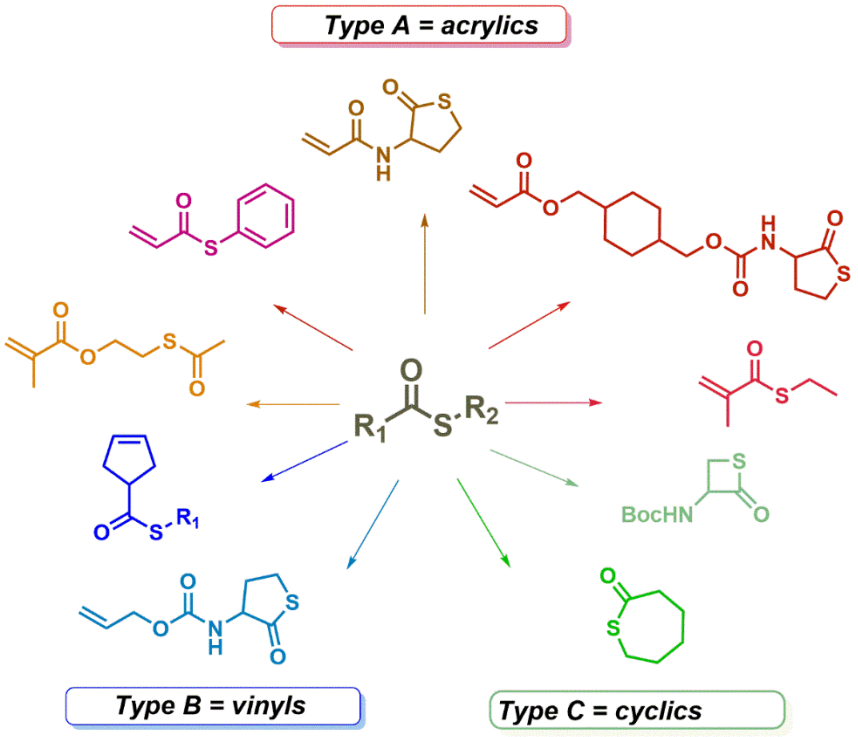

Scheme 1.11: Classification of thioester containing monomers.

Additionally a 100-fold higher reactivity towards thiolate nucleophiles and at least a 2000-fold higher reactivity towards carbanion nucleophiles has been observed in experiments and computational studies, attributed mainly to the lower electron delocalisation in thioesters compared to oxoester.[93]

One approach to incorporate a thioester functionality into a polymer describes the direct utilisation of thioester containing monomers within the polymerisation process and several successful protocols have been reported to date.

Among these in particular are three main classes, each of which correspond to the nature of the monomeric unit, namely acrylics, vinyls, and cyclic monomers. Type A can be classified as acrylics - for instance thio(meth)acrylates, thioester containing (meth)acrylates and (meth)acrylamides. Type B monomers include olefins, such as thioester functionalised cyclopentene and *N*-(allyloxy) carbonyl-homocysteine thiolactone. Cyclic monomers, which are polymerised

by diverse ring-opening polymerisation techniques (*e.g.* thiolactones), fall into Type C.

Polymers that contain thioester functionalities are prepared *via* different routes as listed in (**Table 1.1**). The range of polymerisation techniques, concerning monomers with pendant thioester groups range from free radical polymerisation (FRP) and various reversible deactivation radical polymerisation (RDRP) techniques, such as Copper-mediated RDRP (Cu-RDRP) and RAFT. Furthermore, thioesters can not only be incorporated in form of a thioester containing monomer, but also formed throughout a polymerisation process such as *β*-thioesters *via* reactions of thiols with either an acrylate in a thiol-ene process or in an acid condensation reaction. Thioesters can also be found in the polymer chain end, integrated as thioester functionalised initiators or Chain Transfer Agents (CTAs). Moreover, cyclic thioesters *(e.g.* thiolactones with different number of carbon atoms in the heterocycle) exhibit thioesters distributed along the polymer chain.

Table 1.1 Techniques used for the polymerisation of thioester containing structures (monomers, initiators and CTAs).

Technique	Type	Name	Code	Ref.
FRP	**Monomer**	Thioacrylates (TA)	TE1	124
		Thio methacrylates (TMA)	TE2	125, 126
		Maleimide thiolactone (MITla)	TE3	127
RAFT	**Monomer**	Thioacrylates (TA)	TE1	128
		2-(acetylthio)ethyl methacrylate (AcSEMA)	TE4	129
		N-Thiolactone acrylamide (TLAm)	TE5	130, 131
		Maleimide thiolactone (MITla)	TE3	127
	CTA	Thioester trithiocarbonate	TE6	114
Cu-RDRP	**Monomer**	Thiolactone acrylate (TLA)	TE7	132
	Initiator	Thioester ATRP initiator	TE8	133
ROMP	**Monomer**	Cyclopentene thioesters	TE9	134
ROP	**Monomer**	β-thiolactone	TE10	135
		γ-thiolactone δ-thiolactone	TE11 TE12	136
		ε-thiolactone	TE13	136, 137, 138, 139, 140
eROP	**Monomer**	ε-thiolactone	TE13	141
		Cyclic dithioester	TE14	142

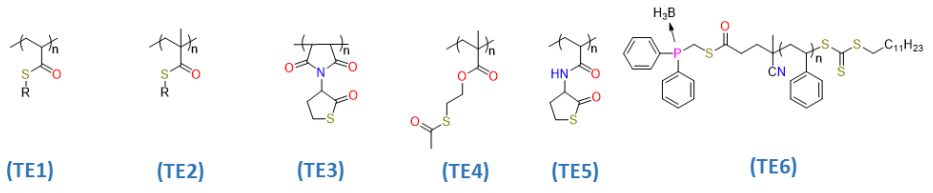

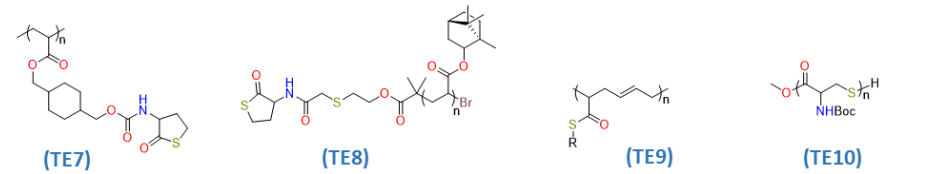

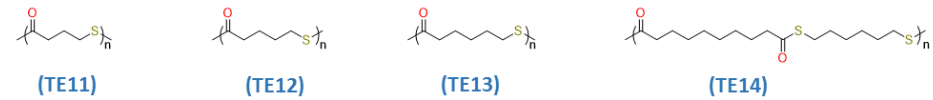

1.2.3.1 Access to thioester containing polymers: thioesters in the monomer side chain

Based on reports in the literature, the introduction of thioester group into a polymerisable unit from Type A can be further divided into three groups, depending on the nature of the thioester. The organosulfur compound can be incorporated as a thioacrylic derivative in form of thio(meth)acrylates, (meth)acrylate or (meth)acrylamide. One very distinct factor is the local occurrence of the thioester, as it can be either somewhere in the sidechain as in a (meth)acrylate or (meth)acrylamide based structure or it can be directly connected to the polymerisable unit as a thio(meth)acrylate. The latter being still of a lower level of esteem than other acrylics, but reports in the past showed promising features. For this class of monomers, sporadic entries to the literature concerning the (meth)acrylic thioester counterpart to (meth)acrylates, have appeared in 1956. In these initial reports *Marvel et al.* showed the synthesis of a range of alkyl thioacrylates by the reaction of *α,β*-dibromopropionyl chloride with alkylthiols.[124]

In 1977 *Hadjichristidis et al.* reported the preparation of thiomethacrylates by treating methacryloyl chloride with respective thiols in aqueous sodium hydroxide solution with successive distillation.[125, 126]

Another elegant and more recent example presents a cyclic monomer with a thioester as a pendant group, such as cyclopent-3-enecarbothioate **(Scheme 1.12)**. In a one-step synthesis, monomers were obtained by simple thioesterfication of 3-cyclopentene-1-carboxylic acid with four alkythiols of different length. Differential scanning calorimetry (DSC) analysis highlighted higher glass transition temperatures (T_g) and melting temperature (T_m) for thioester containing polymers than for the structurally identical counterparts with ester pendants. Thermogravimetric analysis (TGA) elucidated slightly lower thermal stability than their counterparts without sulfur.[134, 143]

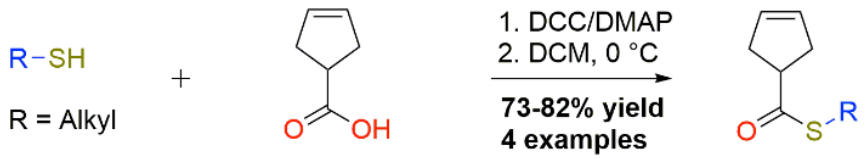

Scheme 1.12: Synthesis of thioester functionalised cyclopentene monomer. Adapted from Ref.[134]

In addition to thiols as starting materials, thiolactones (Tla) have also been proven to be ideal precursors for thioester containing monomers.

Among these in particular, vinylic thiolactones are the most established building blocks. A large set of thiolactone based structures, either derived from itaconic acid or homocysteine thiolactone, have been reported in multi-gram amounts **(Scheme 1.13)** .[144]

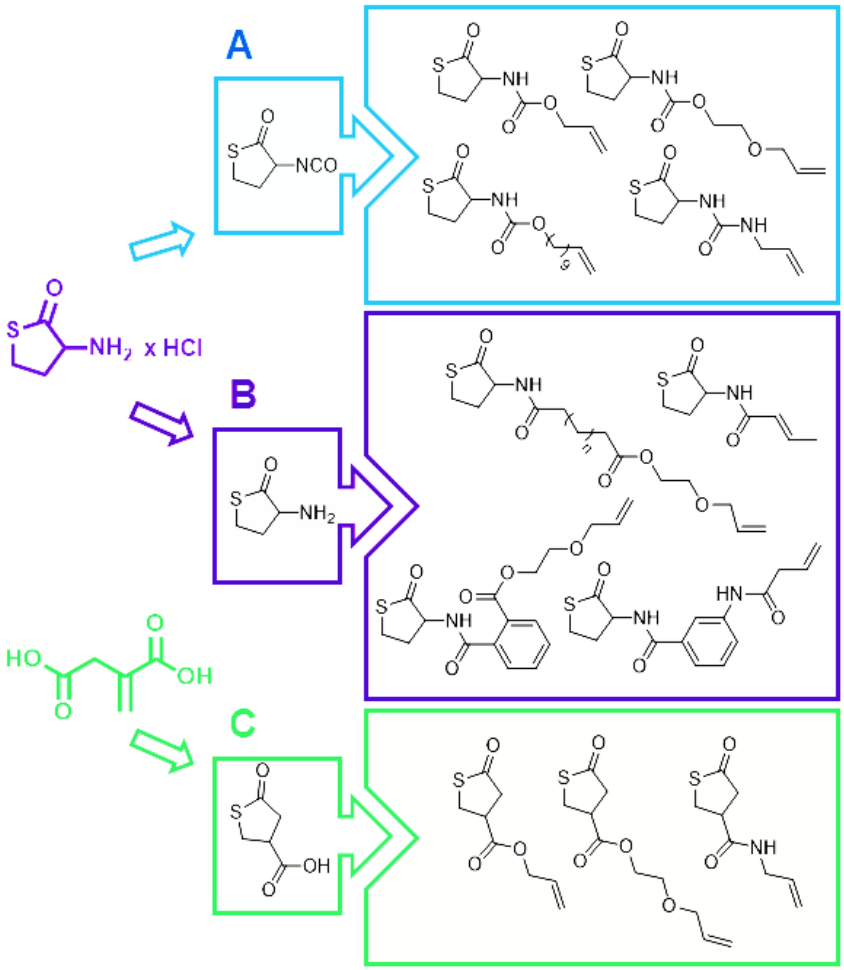

Scheme 1.13: Overview of the chemical synthesis of thiolactone derived vinyl monomers in Ref.[144]

A reaction of thiolactone isocyanate with different alcohols, yielded in thiolactone carbamides. The same thiolactone can functionalised with allylamine and resulted in a thiolactone urea (**Route A** in **Scheme 1.13**).
Homocysteine thiolactone reacted with either an acids or cyclic anhydrides with different alcohols yielded in thiolactone amides. Bisthiolactones derived from difunctional acid chlorides were obtained (**Route B** in **Scheme 1.13**) and the esterification of thioparaconic acid with alcohols lead to a set of thiolactone esters. Additionally, a thiolactone amide could be synthesised from the same starting material, but *via* a thioparaconic acid chloride and allylamine (**Route C** in **Scheme 1.13**).
On the other hand, a prominent example of a thioester bearing methacrylate is 2-(acetylthio)ethyl methacrylate (AcSEMA), resulting from a two-step synthesis.[129, 145] For this, methacryloyl chloride was reacted with 2-bromoethanol under basic conditions **(Scheme 1.14)**.
The resulting 2-bromoethyl methacrylate was further reacted with potassium thioacetate to yield the thioester containing methacrylate.[129]

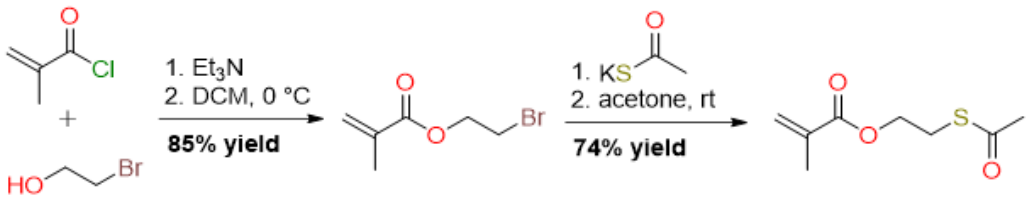

Scheme 1.14: Synthesis of the AcSEMA monomer. Adapted from Ref.[129]

Möller and coworkers reported the synthesis of thiol functionalised poly(meth)acrylates, starting from modified MA or MMA monomers by enzymatic transacylation with Lipase (Novozyme 435, a lipase from C. Antarctica with various alcohols at ambient temperatures. After removal of the enzyme from the reaction mixture, polymerisation were carried out in bulk, utilizing AIBN as initiator in FRP gave polymers with weights up to 40 kDa.[146]

The incorporation of the thioester group into a specific position on a polymer chain proves to be easy and useful when further functionalisation is desired. In general, not only the thioester, but any functional group, if present, is typically found along the backbone, chain end or in the monomeric repeating unit. By

incorporating the thioester function in the monomer, it is possible to tailor the polymer by varying the targeted DP or by introducing comonomers to obtain random or block copolymers. Hence, this methodology allows the further functionalisation of thioesters at specific points along the polymer, which could yield a change in physical, thermal and structural properties.

In the 1980s, *Hadjichristidis et al.* reported the synthesis of a new class of an acrylic monomer, namely thiomethacrylate, in which the methacrylic ester oxygen was replaced with a sulfur atom. A series of phenylic poly methacrylates and poly thiomethacrylates were prepared at different chain lengths *via* free radical polymerisation, using azobisisobutyronitrile (AIBN) at 50 °C with relatively good control (PDI < 1.4). The chain flexibility of the polymers prepared were investigated from their thermal properties. Generally, the substituents in poly(phenyl thiomethacrylate) was found to be more flexible (higher flexibility factor σ) when compared to poly(phenyl methacrylate), which was attributed to the increased length of the less polar bond between the sulfur and carbon, caused by the substitution of the oxygen atom by a sulfur atom.[125, 126]

Similarly, *Song et al*. have reported the polymerisation of a range of thioester functionalised cyclopentenes *via* ring opening metathesis polymerisation (ROMP) with high conversions, while retaining control over dispersity.[134] A comparison of the thermal properties between the oxoester containing polymers and the reported thioester containing polymers displayed a higher T_g.

Another method of incorporating a thioester in to the polymer was shown by *Boyer et al.* in the form of a thioacetate monomer. In this case, 2-(acetylthio)ethyl methacrylate (AcSEMA) was copolymerised with oligo(ethylene glycol) methyl ether methacrylate (OEGMA) *via* RAFT at different molar ratios and thoroughly characterised.[129] The obtained polymers were hydrolysed to yield a free thiol, allowing the formation of gold nanoclusters. Interestingly, random copolymer stabilised gold nanoclusters displayed higher emission intensity in comparison to block copolymer stabilised gold nanoclusters.

Du Prez et al. generated a large library of thiolactone containing monomers, which found application in a wide range of polymerisation techniques. For example, a radical amine-thiol-ene polymerisation has been performed in a one

pot reaction *via* nucleophilic ring opening of a thiolactone with an amine (aminolysis), followed by a radical thiol-ene conjugation. Typically, a free thiol group was generated *in situ* after aminolysis, which reacted with a double bond already present in the same reactor. Using this protocol, a thiolactone bearing a double bond (*i.e.* *N*-(allyloxy)carbonylhomocysteine thiolactone) and various amines were employed to obtain linear polymers and networks in a radical photopolymerisation process.[88] Radical thiol-ene polymerisation has been performed on *N*-(allyloxy)carbonylhomocysteine thiolactone and 10-undecenoyl thiolactonamide after aminolysis.[88] The same group, used a similar strategy to polymerise a thiolactone containing acrylate *via* Cu-RDRP LRP to form the backbone of a graft copolymer. Furthermore, propylamine and poly(ethylene glycol) acrylate were added to react with the thiolactone ring, forming the brush structures.[132]

1.2.3.2 Access to thioester containing polymers: thioester in the chain end

Instead of having a number of thioesters incorporated, initiators for CRP can be functionalised to provide thioester functionality at the chain end of a polymer. Cu(0) mediated polymerisation of isobornyl acrylate using a TL-based initiator has been evaluated as an efficient ATRP initiator, while the presence of the thioester end group of the polymer has been confirmed by ^{1}H NMR **(Scheme 1.15)**.[133]

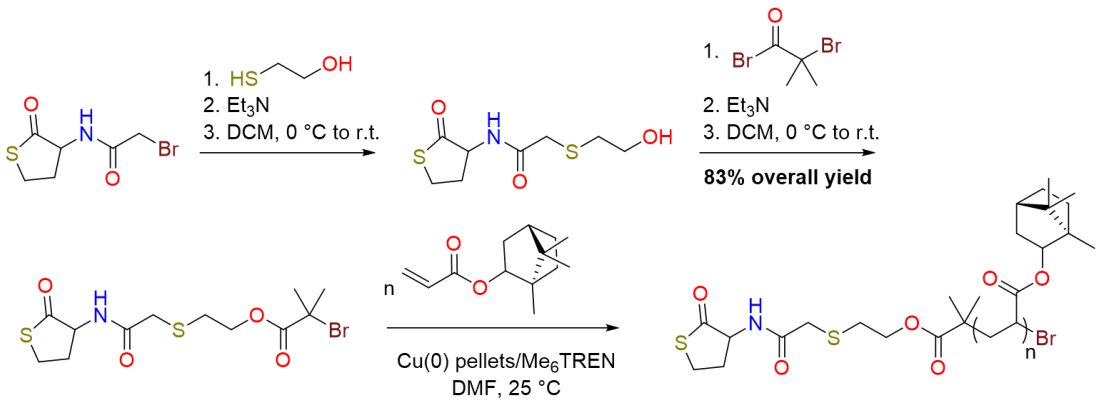

Scheme 1.15: One-pot, two-step synthesis of a thiolactone containing initiator and Cu(0)-mediated polymerisation of isobornyl acrylate *via* a thiolactone-initiator. Adapted from Ref.[133]

In a similar manner, the synthesis of functionalised cyclic polymers *via* RAFT utilizing a thiolactone based CTA was shown. After the aminolysis on the thioester functionality, the free thiol was rearranged with the ω-chain end under high dilution, which afforded the targeted cyclic polymers.[147]

In another approach, a CTA has been tethered to the polymer end group and have been used for the homopolymerisation of styrene with further modification. *Voit et al.* reported a protocol for the esterification of a carboxylic-acid containing CTA with pentaflurophenyl and subsequently reacted with thiolphosphine. The obtained CTA was utilised for the synthesis of polystyrene *via* RAFT **(Scheme 1.16)**.[114]

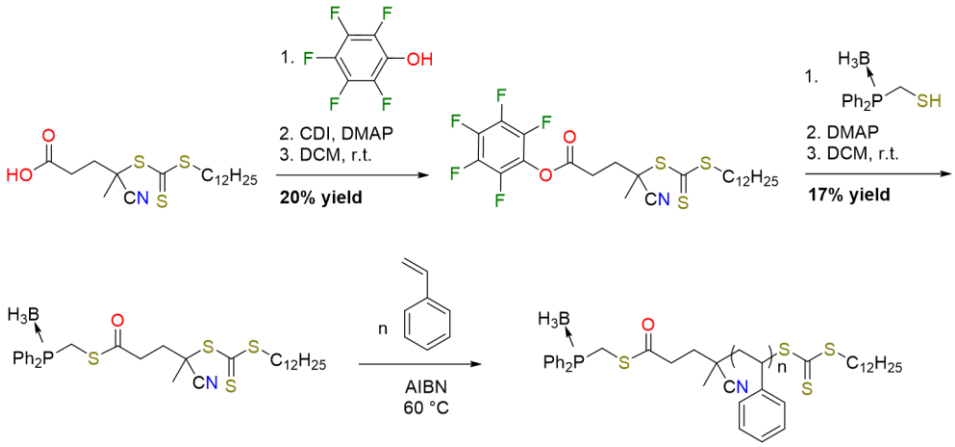

Scheme 1.16: Two step preparation of thioester containing CTA and polymerisation of styrene. Adapted from Ref.[114]

1.2.3.3 Access to thioester containing polymers: Access *via* polymerisation process

As stated above, polythioesters can be described as polymers containing thioester moieties along the backbone. The synthesis of a polythioester was first reported by *Kotch* as early as 1951, where a range of dibasic acid chlorides were reacted with aliphatic dithiols, such as the reaction between adipoyl chloride and hexane-1,6-dithiol.[148] The obtained polythioesters were found to be low in molecular weight and displayed evidence of some crystallinity in their X-ray patterns, with their melting points being higher compared to their oxygen analogues. Similarly, polycondensations of methyl mercaptoacetate at different lengths were also described.[149] Later, the enzyme catalysed polycondensation of hexane-1,6-dithiol with a range of diesters was demonstrated using Lipase

(Novozyme 435), yielding low molecular weight polythioesters with 75-90% yield (M_n 3700-6000 g/mol, PDI 1.7-2.0).[150]

Higher molecular weights could also be obtained, when aromatic groups were included in the backbone. For example, *Kowalewska et al.* showed the synthesis of an aromatic polythioester by interfacial polycondensation of 1,4-di(mercaptomethy1)-tetramethylbenzene phtaloyl, isophtaloyl and terephthaloyl chloride, in which the aqueous to organic solvent ratio, as well as the type of organic phase and molar ratio of reagents was investigated, in order to determine the optimal reaction conditions to allow high conversion.[151]

Another route to polythioesters is the ring-opening-polymerisation (ROP).[140] Further experiments confirmed the same trend for higher melting points compared to corresponding polyesters. Polymers were prepared by anionic ROP of ε-thiocaprolactone for the first time, initiated with potassium tert-butoxide.[152] An extended study by the same group investigated the effect of the number of carbon atoms in the thiolactone ring, and reactivity of the thiolactones towards polymerisation dependent on ring size. Polymerisation occurred for four-, six- and seven-membered thiolactones, whereas the five-membered thiolactone could not be polymerised. While this trend could also be observed for lactones[136], γ-thiolactones have been shown to copolymerise in the presence of trimethylene carbonate. Although NMR and MALDI ToF MS analysis has proven its incorporation, the percentage of thiolactone found was limited to only 9 mol%.[153]

ε-thiocaprolactone has been also used as initiator for the anionic polymerisation of ε-caprolactame, higher polymerisation rate with the initiation by sulfur compound compared to the oxygen analogue was observed.[154]

Moreover, different metal alkoxides (Sn, Cd, Mn, *etc*.) as catalysts and thiols or alcohols initiators have been used for the polymerisation of cyclic thioesters.[138,137] Lipase have also been employed as an alternative "greener" enzymatic-catalysed ROP (eROP) and generated high molecular weight polymers.[141, 142] Polythioesters with higher molecular weight (M_n > 50000 g/mol, PDI 2.3) could be prepared under enzymatic ring opening polymerisation of cyclic polythioesters at 120 °C for 2 days.[155]

Using various dithiols and diacrylates, *Junkers et al.* showed the design and synthesis of biodegradable poly(β-thioesters) *via* step-growth polymerisation.[156]

The obtained polymers were found to be semi crystalline materials with low T_g values due to the incorporation of thiols. Similarly, when more than difunctional thiols and acrylates were used, poly(*β*-thioesters) containing networks with broad molecular weight distributions were synthesised *via* thiol-ene Michael addition.[157]

In the same manner, Michael addition was employed to obtain well-defined amphiphilic triblock copolymers of poly(*β*-thioesters)s, containing an azo linkage in the middle of the chain. TEM images of these polymers have shown their formation into micelles, which could be thermally degraded upon heating to 95 °C.[158] *Long et al.* on the other hand, made use of the thia-Michael addition chemoselectivity towards an acrylate over a methacrylate to synthesise segmented poly(*β*-thioesters) in a one-pot approach.[159] Bis-thiol compounds were initially reacted with diacrylates to obtain thiol terminated soft segment oligomers, which were further reacted with oxamide containing dimethacrylates as the hard segments. *Nishikubo et al.* developed the synthesis of polythioethers by the acyl transfer polymerisation of thiiranes with thioesters.[160] A similar approach was used when cyclic dithioesters were employed, in order to increase the ring size to yield cyclic(thioester-*alt*-thioether).[161]

1.2.3.4 Access to thioester-bearing structures *via* post-modification approach

The second route evolves thiols, which will form thioesters during the polymerisation. These include mainly *β*-thioester from thiol-ene reactions, ring opening with a thiol or exchange reactions. One way to introduce thioesters into a polymer is by using thioacetic acid. For example various dithiols and glycidyl propargyl ether were used in an attempt to obtain polymers *via* thiol-yne chemistry.[162] In further post polymerisation functionalisation, the epoxide in the side chain was ring-opened using thioacetic acid in the presence of triethyl amine, to form thioesters in the side chain. Similarly, a highly efficient synthesis pathway to polysiloxanes containing thiols as end or side groups was demonstrated, when vinyl end-functionalised polydimethylsiloxane or polymethyl-vinylsiloxanes were reacted with thioacetic acid.[163] This allowed the formation of thioesters along the side chain or at the chain ends, which were reduced to the corresponding thiol. Although relatively stable to aminolysis, it

is well known that thioesters can readily undergo transesterification with thiol groups to form new thioesters. An elegant example of a thioester incorporation *via* an exchange reaction was demonstrated by *Liu et al.* **(Scheme 1.17)**.[164]

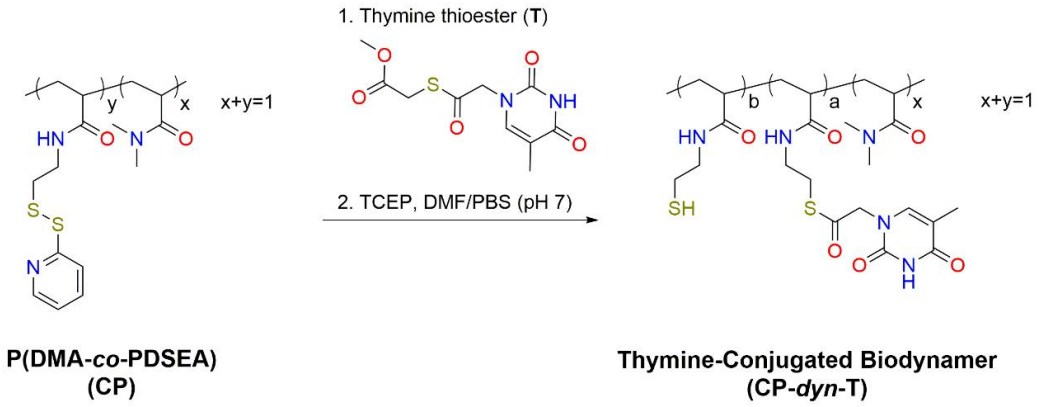

Scheme 1.17: Outline for the synthesis of thymine-conjugated biodynamer CP-dyn-T by RAFT polymerisation *via* a thiol–thioester exchange reaction. Adapted from Ref.[164]

To construct dynamic nucleobase containing copolymers, dimethylacrylamide was copolymerised with pyridyldisulfide ethylacrylamide *via* RAFT. Thymine thioester reacted with the *in situ* generated pendant thiol group *via* a thiol thioester exchange reaction. This newly formed reversible thioester linkage was also shown to be glutathione responsive.

Reactions, where new bonds are formed are the most used tools in synthesis and much progress have been made in the field of thioester containing reaction partners, yielding valuable products such as amides. For example, a thioester can lead to an *S*-acyl intermediate in the presence of cysteine, which can then spontaneously form amide bonds over an *S*- to *N*-acyl migration. This has been reported by *Messersmith et al.*, when initially a four arm poly(ethylene glycol) tetra amine was transformed into a tetra thioester.[165]

The native chemical ligation method was employed to covalently cross-link these macromonomers with a four-arm cysteine macromonomer into a hydrogel. It was also shown that no concurrent reactions to form hydrogels (*i.e.* disulfide bond, thioester exchange) took place during the NCL. *Grinstaff et al.* have similarly obtained hydrogels when a poly(ethylene glycol) based peptide dendron possessing four terminal thiols was crosslinked over thioesters with poly(ethylene glycol disuccinimidyl valerate) (SVA-PEG-SVA) **(Scheme 1.18)**.[166]

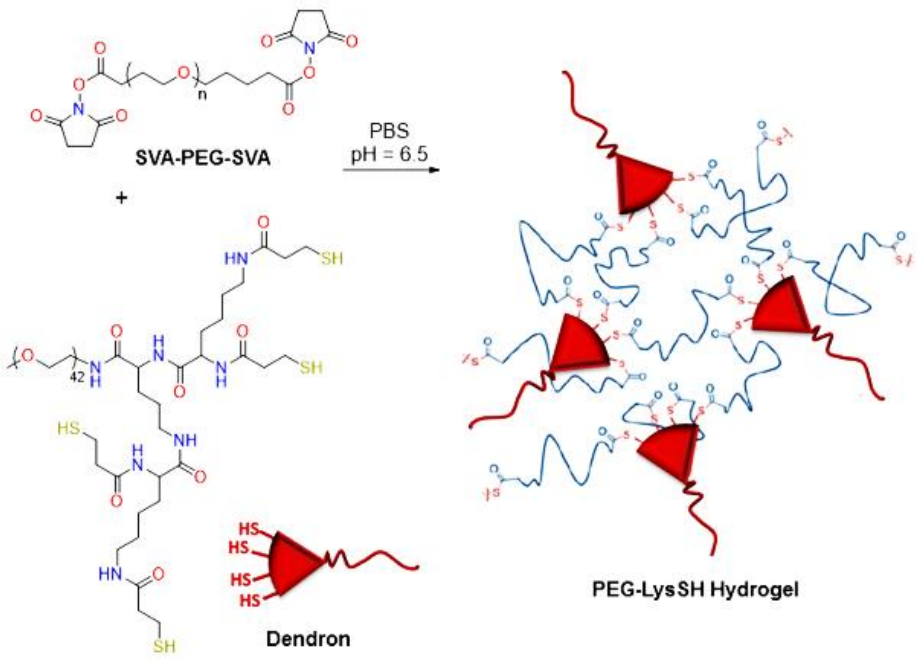

Scheme 1.18: A crosslinked PEG-LysSH hydrogel formed by the reaction of Dendron and SVA-PEG-SVA by thiol–thioester exchange. Adapted from Ref.[166]

Unlike other examples, their dissolution by breaking the thioester bond was shown for the first time. Among others, L-cysteine methyl ester was used to fully promote the dissolution of the hydrogel *via* a thiol-thioester exchange reaction within 12 minutes. As mentioned previously in **Section 1.2.3.2** *Voit et al.* demonstrated the synthesis of poly(styrene) using a phosphine containing thioester based CTA, which was incorporated to allow further functionalisation with an azide *via Staudinger* Ligation. Hence, using 3,6,9-Trioxodecyl azide, the end group modification was carried out on the thioester, yielding an amide bond on the chain end in almost quantitative manner **(Scheme 1.19)**.[114]

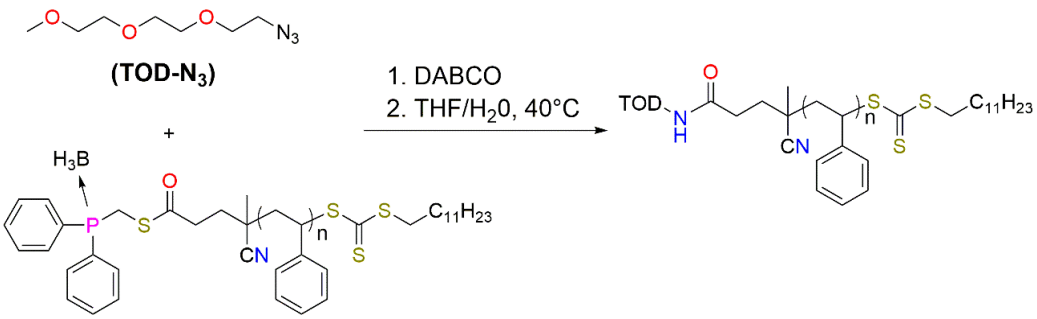

Scheme 1.19: Staudinger Ligation of thioester containing CTA with TOD-N_3. Adapted from Ref.[114]

Furthermore, *París* et al. prepared thioester containing polymers *via* modification on the polymer end of a typical bromine functionalised ATRP initiator.[167] In a one-step protocol, various poly methacrylates have been synthesised and the bromine end group has been transformed into corresponding thioester by substitution reaction with potassium thioacetate. Subsequent hydrolysis a thiol terminated polymer was generated and could be further modified *via* a thiol-ene reaction with a fluorescent alkene (a synthetic alquene tethered to a 4,4-difluoro4-bora-3a,4a-diaza-s-indacene (BODIPY) fragment). By this, quantification of the quantitative thiol-ene process could be calculated from UV-Vis measurements **(Scheme 1.20)**.

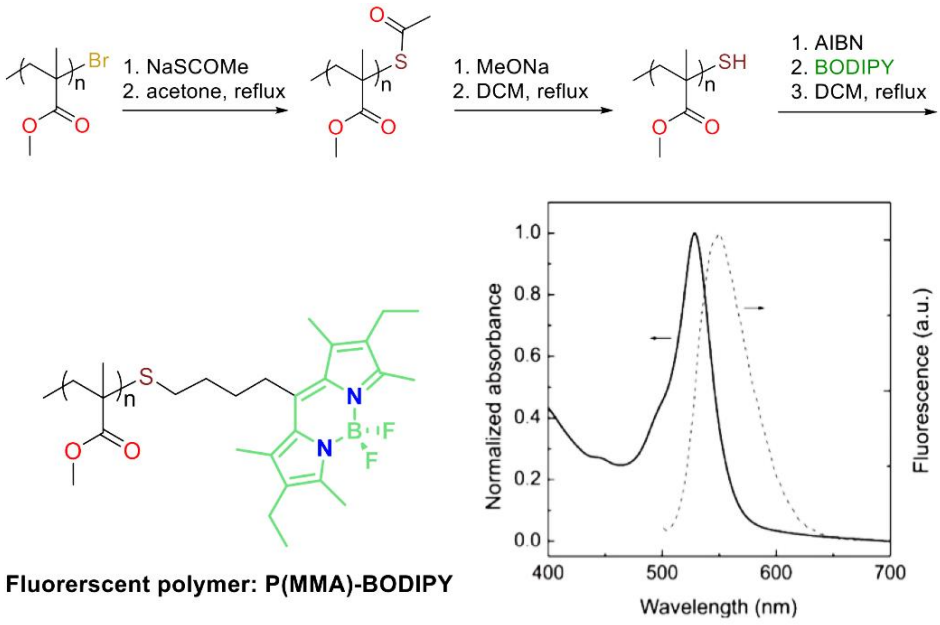

Scheme 1.20: Route for the formation of BODIPY end-functionalised P(MMA) *via* thio-ester end-functionalisation, subsequent hydrolysis to a thiol end-functionalised polymer. "Click" reaction with BODIPY to yield a fluorescent polymer, which absorption spectrum is displayed on the bottom right (solid lines) and fluorescence (dashed lines). Ref.[167]

1.3 Aims and Objectives

The interest of polymer chemists is now moving more and more towards mimicking nature in synthesis. Over millions of years, nature has been optimising the synthesis of complex architectures. To achieve this, a sequence defined linear structure of amino acids is first synthesised (primary structure). By using different sequences, proteins of different functionalities can be obtained. With precise insertion of amino acids in a certain sequence, their interactions lead to secondary structures, for example α-helices or *β*-sheets. At this stage, with further regulation of the amino acid sequence, tertiary or even quaternary structures can be obtained. Current research interest in polymer science include to mimic this regulation of linear chains of single units, to be able to obtain higher order structures to direct or manipulate biological functionalities within living organisms. By using different sequences, proteins of different functionalities can be obtained, however, the monomer library is restricted to the 22 natural amino acids **(Scheme 1.21)**.

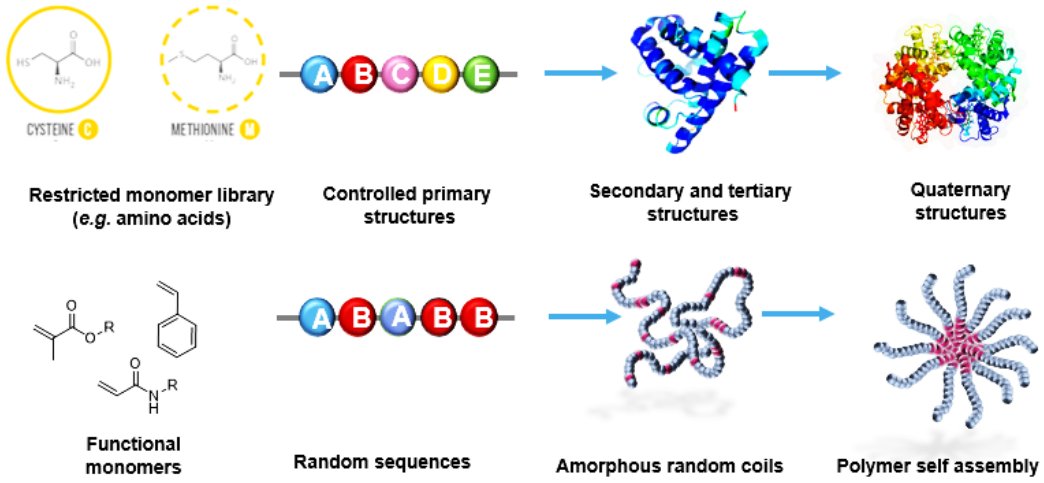

Scheme 1.21: A comparison between a defined sequence of amino acids and its higher order structures (top row) and a polydisperse composition of a polymer and its self-assembly.

The variety of available monomers in polymer synthesis continously grows every year but unfortunately requires to find monomers, which are compatible with many aspects of the polymerisation and a larger range of functionalities. The ability to prepare novel, innovated architecture polymers and the possibility of functionalisation reactions has been an ongoing importance in recent years. As the control over monomer sequence

can lead to novel properties of materials with more complex structures, there is still a need in having a broader monomer library for well-defined polymer based materials. The last century had indeed already witnessed the development and investigation of novel materials, based on new classes of monomers for the synthesis of polymers with unprecedented properties and also monomers which can be employed in regulating the sequence.

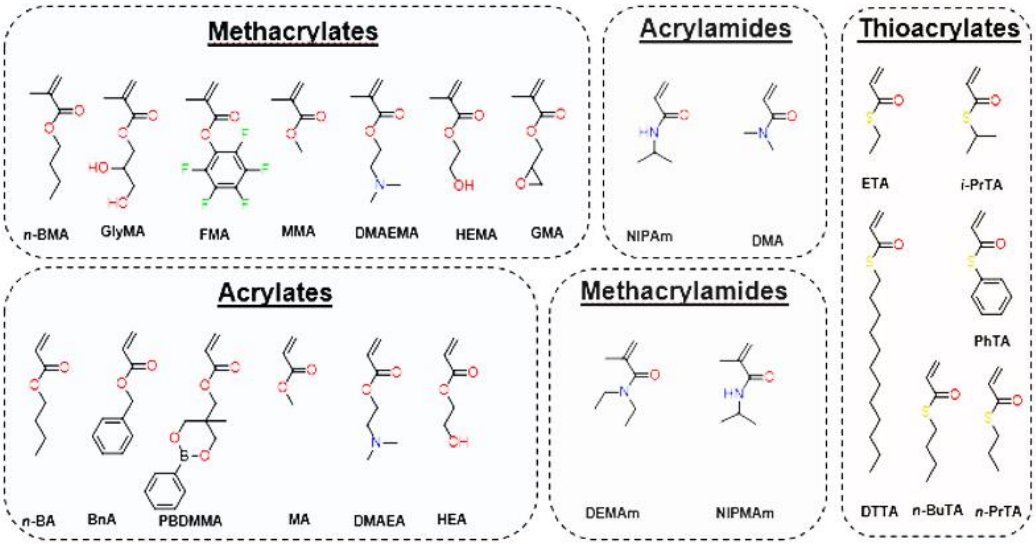

Scheme 1.22: An overview of different monomer classes and their representative examples.

For this purpose, hundreds of (meth)acrylates, (meth)acrylamides and other acrylic monomers have already been developed and have been investigated if they are suitable candidates for sequence controlled polymers. They have been studied thousand-fold with increasing variety since the late 1950s and are still ongoing on gaining the attention of polymer scientists. Although polymerisation techniques are well established, not all monomers are fully compatible with every technique. There are multiple exceptions, but in general, it is accepted that ATRP can be commonly used for methacrylates, acrylates and styrenics, whereas methacrylamides and acrylamides won't polymerise as well. Depending on the SET-LRP system, acrylamides or acrylates can be polymerised in a very well controlled manner in very short times, whereas methacrylates and methacrylamides are not very suitable. Finally, where mostly styrenics work well with NMP, RAFT allows the polymerisation of almost all the various monomer types which are currently available. To date, most of the monomers contain either an activated ester or an amide group next to the double bond. In contrast to monomers, other thioester containing structures are also well known in

polymer synthesis. For example, thioester containing chain transfer agents for RAFT polymerisation allow the positioning in the chain end. Ring-opening-, polycondensation or thia-Michael polymerisation techniques allows the incoporation of (α-,β-) thioesters along the polymer backbone. Although thioesters in polymers are well studied, available structures are still limited. The potential of a thioester bond incoporated into a monomer for example widens the toolbox for polymerisation processes as well as for sequence-controlled polymers as it resembles a more bioligically. Furthermore modification reactions with azides or amines lead to amide-structures, which are typically found in nature.

The aim of the present thesis was to prepare a range of thioester containing acrylics in form of a thioacrylate or thio methacrylate. This class of monomers has never been investigated in controlled radical polymerisations but bear a great potential to study structure-property relationships. The exploration of their potential with the goal to incorporate a functional group for possible modifications *via* different routes will also be discussed.

Although the incorporation of thiols into acrylic monomers, such as thioacrylates (TA) can bring unique functionalities to materials, they have received less attention in research in contrast to their commercially available oxo- and nitro-analogues and have not yet been reported for CRP. With all its facets the incorporation of thioester as a functional group provides a variety of reactions that are fast and which proceed with high yields under benign conditions and make thiols valuable and suitable candidates for polymer science, as even the small difference between (meth)acrylates and (meth)acrylamides can have a big impact on properties, it can be assumed that thioacrylates will provide novel features when used for CRP. The ability to prepare novel, innovated architecture polymers and the possibility of functionalisation reactions have been a topic of interest since many years. The microstructure of polymers, tacticity[168] and monomer sequence[169, 170] are three main properties that can have an influence on the macroscopic nature of those materials. It can be clearly seen, that there are limited functional monomers which can be used in wide fields of CRP methods. When thioacrylates can be used proficiently for polymerisation reactions, subsequent and elaborate modification of polymers with thiols are no longer required. Preparation of thioacrylates to the materials point in the use of novel unexplored applications in material science is essential and need to be analysed in detail. In

Chapter 2, the design of the synthesis to create structurally diverse and thioester-based monomers with aliphatic and aromatic R-groups will be discussed. All obtained compounds were analysed and resulting monomers were used in different polymerisation techniques in subsequent chapters. RAFT polymerisation was used for obtained thio(meth)acrylates to explore the synthesis of homo and block copolymers and compared with an acrylate in Chapter 3. The polymerisation parameters were investigated. Thermal properties and hydrophobicity of obtained polymers are examined and discussed. Copolymerisation of a thioacrylate *via* NMP is discussed in Chapter 4. Furthermore, microwave-assisted side group modification of P(ETA) with primary amines and alcohols were investigated. As the structure of a thioester based polymer gradually changes to its copolymer with respective amide functionality, the thermal properties changes accordingly. The change in the degree of amidation yields polymers with different T_g values and shows the progress and the occurrence of the reaction proposed. In chapter 5, a comparison of an amide-, ester- and thioester based linear ATRP initiator have been studied under SET-LRP conditions. A 4-arm star-shaped thioester initiator was also synthesised and analysed. This was to yield a thioester end-functionalised polymer (initiator) instead of having many thioesters distributed along the side groups (monomer). Furthermore, several reaction kinetics analysis have been carried out on the polymerization of ETA. Instead a copper-based system, a bimetallic system was found to be more suitable for the SET-LRP of ETA in organic media (DMSO). The polymerisation behaviour was investigated by varying DP, amount of deactivator, Cu(0)-wire, ligand and temperature. Finally, Chapter 6 discusses the combination of solid phase thiolactone chemistry and thioacrylates. The addition of acrylamide double bonds to the pendant thiol has been proven to be difficult and incomplete. This problem was overcome in a two-step reaction, by introducing ETA over a thia-michael addition that could be used as a handle for a subsequent amidation reaction to provide amide functionality, as if an acrylamide was introduced to the thiol.

1.4 References

1. J. J. Berzelius, *Jahresbericht über die Fortschritte der physikalischen Wissenschaft*, 1833, **12**, 63.
2. H. Staudinger and J. Fritschi, *Helv. Chim. Acta*, 1922, **5**, 785-806.
3. A. D. Jenkins, P. Kratochvil, R. F. T. Stepto and U. W. Suter, *Pure&Appl. Chem.*, 1996, **12**, 2287-2311.
4. D. N. Schulz and A. O. Patil, in *Functional Polymers*, American Chemical Society, 1998, vol. 704, ch. 1, pp. 1-14.
5. K. Matyjaszewski, *Science*, 2011, **333**, 1104-1105.
6. J. T. Offenloch, H. Mutlu and C. Barner-Kowollik, *Macromolecules*, 2018, **51**, 2682-2689.
7. P. J. Flory, *J. Am. Chem. Soc.*, 1937, **59**, 241-253.
8. G. Moad and D. H. Solomon, *The Chemistry of Radical Polymerization*, Elsevier, Oxford, 2006.
9. D. M. Knauss, *J. Am. Chem. Soc.*, 2004, **126**, 4741-4741.
10. A. A. Gridnev and S. D. Ittel, *Macromolecules*, 1996, **29**, 5864-5874.
11. A. D. Jenkins, R. G. Jones and G. Moad, *Pure&Appl. Chem.*, 2010, **82**, 483-491.
12. A. D. McNaught and A. Wilkinson, *IUPAC. Compendium of Chemical Terminology, 2nd ed. (the "Gold Book")*, WileyBlackwell; 2nd Revised edition edition.
13. R. D. Puts and D. Y. Sogah, *Macromolecules*, 1996, **29**, 3323-3325.
14. J. D. Druliner, *Macromolecules*, 1991, **24**, 6079-6082.
15. M. Steenbock, M. Klapper and K. Müllen, *Macromol. Chem. Phys.*, 1998, **199**, 763-769.
16. S. J. Teertstra, E. Chen, D. Chan-Seng, P. O. Otieno, R. G. Hicks and M. K. Georges, *Macromolecular Symposia*, 2007, **248**, 117-125.
17. E. De León-Sáenz, G. Morales, R. Guerrero-Santos and Y. Gnanou, *Macromol. Chem. Phys.*, 2000, **201**, 74-83.
18. D. H. Solomon, E. Rizzardo and P. Cacioli, *Journal*, 1986.
19. C. J. Hawker, A. W. Bosman and E. Harth, *Chem. Rev.*, 2001, **101**, 3661.
20. M. K. Georges, R. P. N. Veregin, P. M. Kazmaier and G. K. Hamer, *Macromolecules*, 1993, **26**, 2987-2988.
21. D. Benoit, V. Chaplinski, R. Braslau and C. J. Hawker, *J. Am. Chem. Soc.*, 1999, **121**, 3904-3920.
22. M. Kato, M. Kamigaito, M. Sawamoto and T. Higashimura, *Macromolecules*, 1995, **28**, 1721-1723.
23. J. S. Wang and K. Matyjaszewski, *J. Am. Chem. Soc.*, 1995, **117**, 5614-5615.
24. K. Matyjaszewski, *Macromolecules*, 2012, **45**, 4015-4039.
25. A. Anastasaki, V. Nikolaou, Q. Zhang, J. Burns, S. R. Samanta, C. Waldron, D. M. Haddleton, R. McHale, D. Fox, V. Percec, P. Wilson and A. J. Haddleton, *J. Am. Chem. Soc.*, 2013, **136**, 1141-1149.
26. M. Kato, M. Kamigaito, M. Sawamoto and T. Higashimura, *Macromolecules*, 1995, **28**, 1721-1723.
27. V. Percec, B. Barboiu, A. Neumann, J. C. Ronda and M. Zhao, *Macromolecules*, 1996, **29**, 3665-3668.

28. H. Takahashi, T. Ando, M. Kamigaito and M. Sawamoto, *Macromolecules*, 1999, **32**, 6461-6465.
29. T. Ando, M. Kamigaito and M. Sawamoto, *Macromolecules*, 1997, **30**, 4507-4510.
30. K. Matyjaszewski, M. Wei, J. Xia and N. E. McDermott, *Macromolecules*, 1997, **30**, 8161-8164.
31. H. Uegaki, Y. Kotani, M. Kamigaito and M. Sawamoto, *Macromolecules*, 1997, **30**, 2249-2253.
32. H. Uegaki, Y. Kotani, M. Kamigaito and M. Sawamoto, *Macromolecules*, 1998, **31**, 6756-6761.
33. P. Lecomte, I. Drapier, P. Dubois, P. Teyssié and R. Jérôme, *Macromolecules*, 1997, **30**, 7631-7633.
34. E. Le Grognec, J. Claverie and R. Poli, *J. Am. Chem. Soc.*, 2001, **123**, 9513-9524.
35. K. Matyjaszewski, *Chem. Eur. J.*, 1999, **5**, 3095.
36. D. A. Shipp and K. Matyjaszewski, *Macromolecules*, 2000, **33**, 1553.
37. M. Teodorescu and K. Matyjaszewski, *Macromolecules*, 1999, **32**, 4826.
38. J. T. Rademacher, M. Baum, M. E. Pallack, W. J. Brittain and W. J. Simonsick, *Macromolecules*, 2000, **33**, 284.
39. S. R. Samanta, M. E. Levere and V. Percec, *Polym. Chem.*, 2013, **4**, 3212-3224.
40. N. H. Nguyen, B. M. Rosen, G. Lligadas and V. Percec, *Macromolecules*, 2009, **42**, 2379-2386.
41. X. Leng, N. H. Nguyen, B. van Beusekom, D. A. Wilson and V. Percec, *Polym. Chem.*, 2013, **4**, 2995-3004.
42. S. R. Samanta, V. Nikolaou, S. Keller, M. J. Monteiro, D. A. Wilson, D. M. Haddleton and V. Percec, *Polym. Chem.*, 2015, **6**, 2084-2097.
43. A. Simula, V. Nikolaou, A. Anastasaki, F. Alsubaie, G. Nurumbetov, P. Wilson, K. Kempe and D. M. Haddleton, *Polym. Chem.*, 2015, **6**, 2226-2233.
44. C. Waldron, Q. Zhang, Z. Li, V. Nikolaou, G. Nurumbetov, J. Godfrey, R. McHale, G. Yilmaz, R. K. Randev, M. Girault, K. McEwan, D. M. Haddleton, M. Droesbeke, A. J. Haddleton, P. Wilson, A. Simula, J. Collins, D. J. Lloyd, J. A. Burns, C. Summers, C. Houben, A. Anastasaki, M. Li, C. R. Becer, J. K. Kiviaho and N. Risangud, *Polym. Chem.*, 2014, **5**, 57-61.
45. N. H. Nguyen, B. M. Rosen and V. Percec, *J. Polym. Sci. Part A: Polym. Chem.*, 2010, **48**, 1752-1763.
46. Q. Zhang, P. Wilson, A. Anastasaki, R. McHale and D. M. Haddleton, *ACS Macro Lett.*, 2014, **3**, 491-495.
47. S. Fleischmann and V. Percec, *J. Polym. Sci. Part A: Polym. Chem.*, 2010, **48**, 2236-2242.
48. N. H. Nguyen, X. Leng, H.-J. Sun and V. Percec, *J. Polym. Sci. Part A: Polym. Chem.*, 2013, **51**, 3110-3122.
49. V. Percec, T. Guliashvili, J. S. Ladislaw, A. Wistrand, A. Stjerndahl, M. J. Sienkowska, M. J. Monteiro and S. Sahoo, *J. Am. Chem. Soc.*, 2006, **128**, 14156-14165.
50. M. Vorobii, A. de los Santos Pereira, O. Pop-Georgievski, N. Y. Kostina, C. Rodriguez-Emmenegger and V. Percec, *Polym. Chem.*, 2015, **6**, 4210-4220.
51. J. A. Syrett, M. W. Jones and D. M. Haddleton, *Chem. Commun.*, 2010, **46**, 7181-7183.
52. U. Edlund, C. Rodriguez-Emmenegger, E. Brynda and A.-C. Albersson, *Polym. Chem.*, 2012, **3**, 2920-2927.

53. T. Tischer, C. Rodriguez-Emmenegger, V. Trouillet, A. Welle, V. Schueler, J. O. Mueller, A. S. Goldmann, E. Brynda and C. Barner-Kowollik, *Adv. Mater.*, 2014, **26**, 4087-4092.
54. S. R. Samanta, R. Cai and V. Percec, *Polym. Chem.*, 2014, **5**, 5479-5491.
55. S. R. Samanta, R. Cai and V. Percec, *Polym. Chem.*, 2015, **6**, 3259-3270.
56. Q. Zhang, A. Anastasaki, G.-Z. Li, A. J. Haddleton, P. Wilson and D. M. Haddleton, *Polym. Chem.*, 2014, **5**, 3876-3883.
57. Q. Zhang, J. Collins, A. Anastasaki, R. Wallis, D. A. Mitchell, C. R. Becer and D. M. Haddleton, *Angew. Chem. Int. Ed.*, 2013, **52**, 4435-4439.
58. X.-H. Liu, G.-B. Zhang, B.-X. Li, Y.-G. Bai and Y.-S. Li, *J. Polym. Sci. Part A: Polym. Chem.*, 2010, **48**, 5439-5445.
59. J. Ma, H. Chen, M. Zhang and L. Chen, *J. Polym. Sci. Part A: Polym. Chem.*, 2011, **49**, 2588-2593.
60. M. J. Sienkowska, B. M. Rosen and V. Percec, *J. Polym. Sci. Part A: Polym. Chem.*, 2009, **47**, 4130-4140.
61. H. Wu, Y. Wan, W. Wang, Y. Wang, N. Zhou, W. Zhang, X. Li, Z. Zhang and X. Zhu, *Polym. Chem.*, 2015, **6**, 2620-2625.
62. J. Tom, B. Hornby, A. West, S. Harrisson and S. Perrier, *Polym. Chem.*, 2010, **1**, 420-422.
63. J. Gao, Z. Zhang, N. Zhou, Z. Cheng, J. Zhu and X. Zhu, *Macromolecules*, 2011, **44**, 3227-3232.
64. Q. Zhang, P. Wilson, Z. Li, R. McHale, J. Godfrey, A. Anastasaki, C. Waldron and D. M. Haddleton, *J. Am. Chem. Soc.*, 2013, **135**, 7355-7363.
65. F. Alsubaie, A. Anastasaki, P. Wilson and D. M. Haddleton, *Polym. Chem.*, 2015, **6**, 406-417.
66. G. Gody, T. Maschmeyer, P. B. Zetterlund and S. Perrier, 2013, **4**, 2505.
67. G. Gody, T. Maschmeyer, P. B. Zetterlund and S. Perrier, *Macromolecules*, 2014, **47**, 639-649.
68. G. Gody, T. Maschmeyer, P. B. Zetterlund and S. Perrier, *Macromolecules*, 2014, **47**, 3451-3460.
69. M. Li, P. De, S. R. Gondi and B. S. Sumerlin, *J. Polym. Sci. A.*, 2008, **46**, 5093-5100.
70. M. Li, P. De, H. Li and B. S. Sumerlin, *Polym. Chem.*, 2010, **1**, 854-859.
71. T. R. Barlow, J. C. Brendel and S. Perrier, *Macromolecules*, 2016, **49**, 6203-6212.
72. C. E. Kast and A. Bernkop-Schnürch, *Biomaterials*, 2001, **22**, 2345-2352.
73. M. Tatsuhito, F. Yasuaki, Y. Masahiro, Y. Tetsuya and T. Tsuguo, *J. Appl. Polym. Sci.*, 2000, **76**, 45-49.
74. Y. Xue, X. Li, H. Li and W. Zhang, *Nat. Commun.*, 2014, **5**, 4348.
75. H. Häkkinen, *Nature Chemistry*, 2012, **4**, 443.
76. J. C. Love, L. A. Estroff, J. K. Kriebel, R. G. Nuzzo and G. M. Whitesides, *Chem. Rev.*, 2005, **105**, 1103-1170.
77. E. Boisselier and D. Astruc, *Chem. Soc. Rev.*, 2009, **38**, 1759-1782.
78. M. H. Stenzel, *ACS Macro Lett.*, 2013, **2**, 14-18.
79. I.-H. Lee, E. H. Discekici, S. L. Shankel, A. Anastasaki, J. Read de Alaniz, C. J. Hawker and D. J. Lunn, *Polym. Chem.*, 2017, **8**, 7188-7194.
80. G. Delaittre and L. Barner, *Polym. Chem.*, 2018, **9**, 2679-2684.
81. S. Agar, E. Baysak, G. Hizal, U. Tunca and H. Durmaz, *J. Polym. Sci. A.*, 2018, **56**, 1181-1198.
82. M. Le Neindre and R. Nicolay, *Polym. Chem.*, 2014, **5**, 4601-4611.

83. S. H. Yu, F. Ercole, N. A. Veldhuis, M. R. Whittaker, T. P. Davis and J. F. Quinn, *Polym. Chem.*, 2017, **8**, 6362-6367.
84. S. Iimura, K. Manabe and S. Kobayashi, *Org. Lett.*, 2003, **5**, 101-103.
85. K. Nakabayashi, A. Matsumura, Y. Abiko and H. Mori, *Macromolecules*, 2016, DOI: 10.1021/acs.macromol.5b02573.
86. Y. Qiao, X. Yin and C. Tang, *Science China Chemistry*, 2015, **58**, 1641-1650.
87. C. Zhao, Y. Zhang, S. Pan, L. Rothberg and M.-K. Ng, *Macromolecules*, 2007, **40**, 1816-1823.
88. P. Espeel, F. Goethals and F. E. Du Prez, *J. Am. Chem. Soc.*, 2011, **133**, 1678-1681.
89. E. Pieter, C. L. L. G., B. Katarzyna, C. Sven, M. J. C., D. P. F. E. and M. Annemieke, *Angew. Chem. Int. Ed.*, 2013, **52**, 13261-13264.
90. S. Martens, J. Van den Begin, A. Madder, F. E. Du Prez and P. Espeel, *J. Am. Chem. Soc.*, 2016, **138**, 14182-14185.
91. P. Bracher, P. Snyder, B. Bohall and G. Whitesides, *Orig Life Evol Biosph*, 2011, **41**, 399-412.
92. J. F. Marlier, E. J. Fogle, R. L. Redman, A. D. Stillman, M. A. Denison and L. I. Robins, *J. Org. Chem.*, 2015, **80**, 1905-1908.
93. W. Yang and D. G. Drueckhammer, *J. Am. Chem. Soc.*, 2001, **123**, 11004-11009.
94. I. V. Koval, *Russian Journal of Organic Chemistry*, 2005, **41**, 631-648.
95. B. Neises and W. Steglich, *Angew. Chem. Int. Ed.*, 1978, **17**, 522-524.
96. N. Iranpoor, H. Firouzabadi, D. Khalili and S. Motevalli, *J. Org. Chem.*, 2008, **73**, 4882-4887.
97. Y.-L. Chou, Y. Jhong, S. P. Swain and D.-R. Hou, *J. Org. Chem.*, 2017, **82**, 10201-10208.
98. A. Temperini, D. Annesi, L. Testaferri and M. Tiecco, *A simple acylation of thiols with anhydrides*, 2010.
99. K. A. T., C. L. H. and G. Subrata, *Eur. J. Org. Chem.*, 2005, **2005**, 2782-2787.
100. M. Lakouraj, B. Movassagh and Z. Fadaei, *Convenient Synthesis of Thiol Esters from Acyl Chlorides and Disulfides Using Zn/AlCl 3*, 2002.
101. B. C. Ranu, S. S. Dey and A. Hajra, *Green Chem.*, 2003, **5**, 44-46.
102. B. Basu, S. Paul and A. K. Nanda, *Green Chem.*, 2010, **12**, 767-771.
103. P. Singh and R. K. Peddinti, *Harnessing the catalytic behaviour of 1,1,1,3,3,3-hexafluoro-2-propanol (HFIP): An expeditious synthesis of thioesters*, 2017.
104. K. A. Ogawa and A. J. Boydston, *Org. Lett.*, 2014, **16**, 1928-1931.
105. J. M. Yost, G. Zhou and D. M. Coltart, *Org. Lett.*, 2006, **8**, 1503-1506.
106. C. Junyong, S. U. Ryung, C. Supill and C. Y. Keun, *ChemCatChem*, 2016, **8**, 318-321.
107. C. He, X. Qian and P. Sun, *Org. Biomol. Chem.*, 2014, **12**, 6072-6075.
108. Y.-T. Huang, S.-Y. Lu, C.-L. Yi and C.-F. Lee, *J. Org. Chem.*, 2014, **79**, 4561-4568.
109. C.-L. Yi, Y.-T. Huang and C.-F. Lee, *Green Chem.*, 2013, **15**, 2476-2484.
110. M. Kazemi and L. Shiri, *Thioesters synthesis: Recent adventures in the esterification of thiols*, 2015.
111. K. Kuciński and G. Hreczycho, *Org. Process Res. Dev.*, 2018, **22**, 489-493.
112. S. H. and M. Jules, *Helv. Chim. Acta*, 1919, **2**, 635-646.
113. B. L. Nilsson, L. L. Kiessling and R. T. Raines, *Org. Lett.*, 2000, **2**, 1939-1941.
114. R. Pötzsch, S. Fleischmann, C. Tock, H. Komber and B. I. Voit, *Macromolecules*, 2011, **44**, 3260-3269.

115. E. C. B. Johnson and S. B. H. Kent, *J. Am. Chem. Soc.*, 2006, **128**, 6640-6646.
116. W. Chen, G. Qing-Xiang and F. Yao, *Chemistry – An Asian Journal*, 2011, **6**, 1241-1251.
117. M. G. Woll and S. H. Gellman, *J. Am. Chem. Soc.*, 2004, **126**, 11172-11174.
118. X.-H. Sun, H.-Z. Yu, S.-Q. Pei and Z.-M. Dang, *Chin. Chem. Lett.*, 2015, **26**, 1259-1264.
119. M. Deletre and G. Levesque, *Macromolecules*, 1990, **23**, 4733-4741.
120. N. Stuhr-Hansen, N. Bork and K. Stromgaard, *Org. Biomol. Chem.*, 2014, **12**, 5745-5751.
121. E. Castro, *ChemInform Abstract: Kinetics and Mechanism of the Aminolysis of Thioesters and Thiocarbonates in Solution*, 2009.
122. N. Ichiishi, C. A. Malapit, Ł. Woźniak and M. S. Sanford, *Org. Lett.*, 2018, **20**, 44-47.
123. P. Wessig, T. Schulze, A. Pfennig, S. M. Weidner, S. Prentzel and H. Schlaad, *Polym. Chem.*, 2017, **8**, 6879-6885.
124. C. S. Marvel, S. L. Jacobs, W. K. Taft and B. G. Labbe, *Journal of Polymer Science*, 1956, **19**, 59-72.
125. N. Hadjichristidis, *Polymer*, 1981, **22**.
126. N. Hadjichristidis, *Macromolecules*, 1981, **14**, 128-130.
127. T. Rudolph, P. Espeel, F. E. Du Prez and F. H. Schacher, *Polym. Chem.*, 2015, **6**, 4240-4251.
128. S. Aksakal and C. Remzi Becer, *Polym. Chem.*, 2016, **7**, 7011-7018.
129. N. N. M. Adnan, S. Ahmad, R. P. Kuchel and C. Boyer, *Materials Chemistry Frontiers*, 2017, **1**, 80-90.
130. S. Reinicke, P. Espeel, M. M. Stamenovic and F. E. Du Prez, *Polym. Chem.*, 2014, **5**, 5461-5470.
131. S. Montolio, O. Zagorodko, R. Porcar, M. Isabel Burguete, S. V. Luis, H. Tenhu and E. Garcia-Verdugo, *Polym. Chem.*, 2017, **8**, 4789-4797.
132. F. Driessen, R. Herckens, P. Espeel and F. E. Du Prez, *Polym. Chem.*, 2016, **7**, 1632-1641.
133. F. Driessen, F. E. Du Prez and P. Espeel, *ACS Macro Lett.*, 2015, **4**, 616-619.
134. S. Song, Z. Zhang, X. Liu, Z. Fu, J. Xu and Z. Fan, *J. Polym. Sci. A.*, 2017, **55**, 4027-4036.
135. M. Suzuki, K. Makimura and S.-i. Matsuoka, *Biomacromolecules*, 2016, **17**, 1135-1141.
136. C. G. Overberger and J. K. Weise, *J. Am. Chem. Soc.*, 1968, **90**, 3533-3537.
137. P. E. Fritze, *Union Carbide; USA: Thiolactone Polymerization and Catalysts. 3,755,268. US Patent.*, 1972 Jun 16.
138. C. G. Seefried and J. V. Kodeske, *Polym. Eng. Sci.*, 1976, **16**, 526-528.
139. C. G. Overberger and J. K. Weise, *J. Am. Chem. Soc.*, 1968, **90,** 3538–3543.
140. T. J. Bannin and M. K. Kiesewetter, *Macromolecules*, 2015, **48**, 5481-5486.
141. S. W. Duchiron, E. Pollet, S. Givry and L. Avérous, *Eur. Polym. J.*, 2017, **87**, 147-158.
142. M. Kato, K. Toshima and S. Matsumura, *Biomacromolecules*, 2007, **8**, 3590-3596.
143. S. Song, Z. Fu, J. Xu and Z. Fan, *Polym. Chem.*, 2017, **8**, 5924-5933.
144. D. Frank, P. Espeel, S. Claessens, E. Mes and F. E. Du Prez, *Tetrahedron*, 2016, **72**, 6616-6625.

145. M. Liras, I. Quijada-Garrido, M. Palacios-Cuesta, S. Munoz-Durieux and O. Garcia, *Polym. Chem.*, 2014, **5**, 433-442.
146. E. Hrsic, H. Keul and M. Möller, *Eur. Polym. J.*, 2012, **48**, 761-768.
147. M. M. Stamenovic, P. Espeel, E. Baba, T. Yamamoto, Y. Tezuka and F. E. Du Prez, *Polym. Chem.*, 2013, **4**, 184-193.
148. C. S. Marvel and A. Kotch, *J. Am. Chem. Soc.*, 1951, **73**, 1100-1102.
149. H. R. Kricheldorf and K. Bösinger, *Die Makromolekulare Chemie*, 1973, **173**, 67-80.
150. M. Kato, K. Toshima and S. Matsumura, *Macromol. Rapid. Comm.*, 2006, **27**, 605-610.
151. W. Podkoscielny and W. Kowalewska, *Journal of Polymer Science: Polymer Chemistry Edition*, 1984, **22**, 1025-1033.
152. C. G. Overberger and J. Weise, *J. Polym. Sci. B.*, 1964, **2**, 329-331.
153. M. Langlais, O. Coutelier, S. Moins, J. De Winter, O. Coulembier and M. Destarac, *Polym. Chem.*, 2018, **9**, 2769-2774.
154. M. Matzner, J. E. McGrath, S. W. Chow, J. V. Koleske and L. M. Robeson, *J. Appl. Polym. Sci.*, 1973, **17**, 983-986.
155. M. Kato, K. Toshima and S. Matsumura, *Biomacromolecules*, 2005, **6**, 2275-2280.
156. N. Zaquen, B. Wenn, K. Ranieri, J. Vandenbergh and T. Junkers, *J. Polym. Sci. A.*, 2014, **52**, 178-187.
157. J. Vandenbergh, M. Peeters, T. Kretschmer, P. Wagner and T. Junkers, *Cross-linked degradable poly(β-thioester) networks via amine-catalyzed thiol-ene click polymerization*, 2014.
158. H. Sun, D. J. Dobbins, Y. Dai, C. P. Kabb, S. Wu, J. A. Alfurhood, C. Rinaldi and B. S. Sumerlin, *ACS Macro Lett.*, 2016, **5**, 688-693.
159. N. G. Moon, R. J. Mondschein and T. E. Long, *Polym. Chem.*, 2017, **8**, 2598-2608.
160. A. Kameyama, M. Kiyota and T. Nishikubo, *Tetrahedron Lett.*, 1994, **35**, 4571-4574.
161. H. Kudo, S. Makino, A. Kameyama and T. Nishikubo, *Macromolecules*, 2005, **38**, 5964-5969.
162. Y. Zheng, S. Cai, L. Peng, Y. Jin, H. Xu, Z. Weng, Z. Gao, B. Zhao and C. Gao, *Polym. Chem.*, 2016, **7**, 6202-6210.
163. E. Perju, S. J. Dünki and D. M. Opris, *J. Polym. Sci. A.*, 2016, **54**, 2940-2948.
164. L. Liu, L. Wu, J. Tan, L. Wang, Q. Liu, P. Liu and L. Liu, *Polym. Chem.*, 2015, **6**, 3934-3941.
165. B.-H. Hu, J. Su and P. B. Messersmith, *Biomacromolecules*, 2009, **10**, 2194-2200.
166. C. Ghobril, K. Charoen, E. K. Rodriguez, A. Nazarian and M. W. Grinstaff, *Angewandte Chemie International Edition*, 2013, **52**, 14070-14074.
167. M. Liras, O. García, I. Quijada-Garrido and R. París, *Macromolecules*, 2011, **44**, 1335-1339.
168. K. Satoh and M. Kamigaito, *Chem. Rev.*, 2009, **109**, 5120-5156.
169. J.-F. Lutz, M. Ouchi, D. R. Liu and M. Sawamoto, *Science*, 2013, **341**.
170. M. Ouchi, N. Badi, J.-F. Lutz and M. Sawamoto, *Nature Chem.* , 2011, **3**, 917-924.

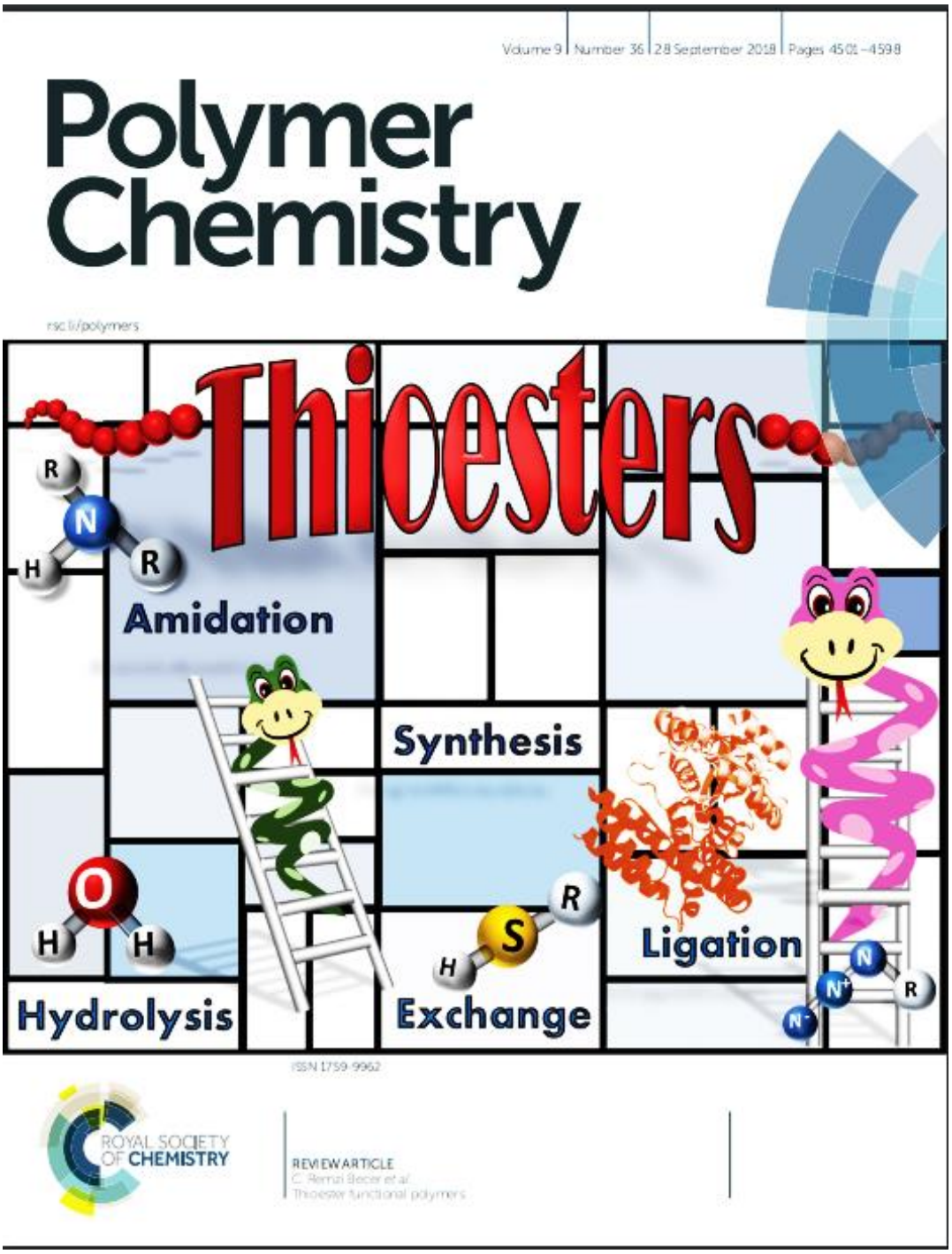

S. Aksakal, R. Aksakal and C.R. Becer, *Polym. Chem.*, **2018**, *9*, 4502-4502

2 Synthesis of thio(meth)acrylate monomers

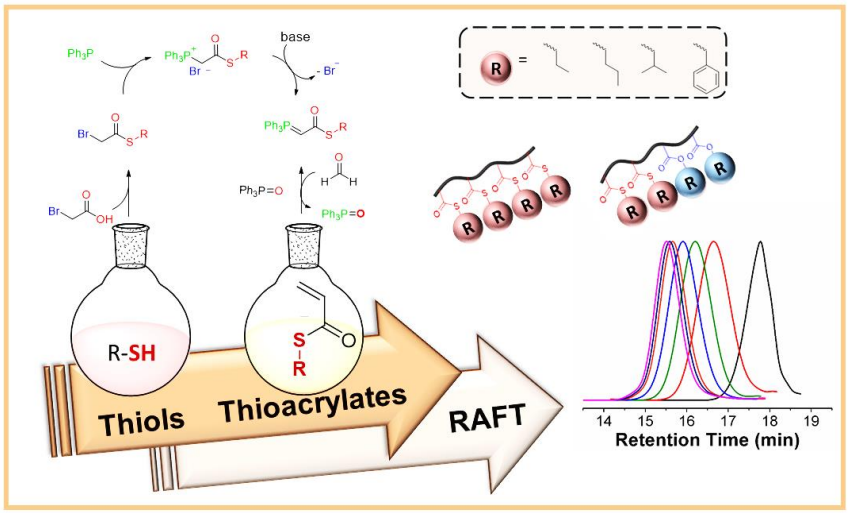

Radically polymerisable monomers such as acrylates, acrylamides, and styrenes have been investigated because of their corresponding polymers for many years. However, thioacrylates are a forgotten class of monomers and have not been studied for decades. Herein, we present a simple synthetic approach to prepare various thioacrylate monomers as well as the modification of a thioacrylate monomer into the corresponding thio(meth acrylate).

Parts of this chapter have been published;

S. Aksakal, C.R. Becer, *Polym. Chem.*, 2016, **7**, 7011-7018

2.1 Introduction

Elemental sulfur is a bright yellow, crystalline non-metal and is the 10th most abundant element in the universe covering almost three percent of the Earths mass.[1] Thiols are the simplest class of organosulfur compounds and are considered to be essential for all divalent sulfur in living creatures in form of certain amino acids, enzymes, coenzymes, vitamins and even hormones.[2] They overtake an important role in many biochemical processes. For instance, the amino acid cysteine is the operating component of proteins in biochemical redox processes and involved in the capture of free radicals.[3] In the presence of cysteine as a residue, formation of disulfide bridges occurs and leads to fixed conformation of proteins and polypeptides. The natural occurrence of free thiols is relatively rare due to their instability towards oxidation to disulfides. These disulfides can be easily reduced back to thiols and are used therefore as a thiol protecting group. The most widely represented form of thiols in nature are the biologically active thioesters.[4] This class of thioesters are the so called high-energy compounds, since they lead to markedly facile cleavage of acyl sulfur bonds by hydrolysis or acyl transfer. They can be found in several forms, for instance Coenzyme A (CoA) which contains an active thiol group, facilitates oxidation pathways, resulting in the synthesis of acetyl-Coenzyme A. This important macromolecule is utilised as a key intermediate in the storage and production of energy rich adenosine 5-triphosphate (ATP), which serves as the primary source of energy used by cells. This ubiquitous and essential molecule serves as a universal fuel source for every process within an organism, which is required for deoxyribonucleic acid (DNA) and protein synthesis, muscle contraction or even generation of electric pulses in nerves for transporting messages across its network.

Several hypothesis have been proposed in an attempt to find out how life had arisen from non-living matter through natural processes billions of years ago with thioesters.[5] There are still debates, whether life started with replication of cells or by metabolism, in which numerous theories ensue from. The discovery of sulfur bacteria in the deep sea linked them as a primitive form to the emergence of the simplest form of life and supported the idea of an iron-sulfur world theory, one of the earliest concepts in which the hypotheses of metabolism without genetics is proposed as the genesis of life.

Christian de Duve associated the prebiotic phase of the primeval earth with the state of development of evolution to generate molecular complexity on early earth. For this chemical procedure he favoured thioesters as the molecular species, based on its unique catalytic and energetic nature, including inauguration of electron transfer, phosphorylation, group transfer and energy coupling. Those functions consequence the possibility of the assembly of amino acids, synthesis of peptides, fatty acids and adenosine monophosphate (AMP) and are therefore considered as precursors of life.[6]

In thiols, we find that the dissociation energies of S-H and C-S bond, are less strong compared to O-H and C-O bond in their alcohol analogues.[7] As the sulfur atom is less electronegative than oxygen, thiols have a reduced affinity to hydrogen bond formation, which results in greater volatility compared to their counterparts. In addition, the solubility in water is also lower of thiols. Inasmuch sulfur withdraw some electronic density from the carbonyl π-bond into nominally empty δ-orbitals through $3d - 2p_z$ bonding, the IR carbonyl stretching vibration of S-H bonds in alkanethiols appear therefore in lower regions than oxygen analogues. Thiols are much more acidic than similar alcohols due to more polar S-H bonds compared to O-H bonds because of greater s-character of the sulfur atom.[8] This property makes them more sensitive to nucleophilic attacks, typically thiols have a pk_a of 7-9, whereas pk_a of alcohols are in the range of 16-18, depending on the nature of the neighbouring groups. As thiols are involved in all the before mentioned roles and even in other significant reactions, they are one of the most interesting classes in almost all fields of chemistry. No other chemical entity has been under constant scrutiny regarding their specific features and therefor the chemistry including their unique reactivity have been studied and reported for more than a century.

Various fields in science and material engineering have made use of all those advantageous properties of natural thiols for synthetic thiol containing materials. Physical and mechanical properties, such as flexibility, network uniformity, high optical clarity, mucoadhesive properties can be envisioned by using thiol-based polymers. Furthermore, the incorporation of disulfide bonds in the polymer backbone provides (bio)degradability.[9] The range of polythiols can be used as cross-linking & chain transfer agents or for optical lenses with high refractive index. There are numerous applications and varity of thiol containing polymers based on sulfur bearing monomers. All those bear free thiols in the sidechain of a polymer or masked in a

heterocycle in common (*e.g.* thiomers[10], thiazoline[11], thiazole[12], thiophene[13, 14] or thiolactones[15]) and are used for various applications.

In the field of polymer science, the ability of preparation of novel, innovative architecture polymers and the possibility of functionalisation reactions have been gaining importance in recent years. As the control over monomer sequence can lead to novel properties of materials with more complex structures, there is still a need in having more monomers for a broader application in well-defined polymer based materials. *Lutz* and coworkers showed, that single monomers can be fairly easily transformed into a well-defined polymer chain when electron-deficient monomers (maleimide derivatives) and electron-rich monomers (styrenic or derivatives thereof) are used.[16, 17]

Not much research was reported in the last seventy years concerning the synthesis and characterisation of a thioester containing acrylic monomer: the thioacrylates. Early investigation in this field can be tracked back to the late 1940s impelled by the discovery of *Reppe*-carbonylation process (**Scheme 2.1**).[18]

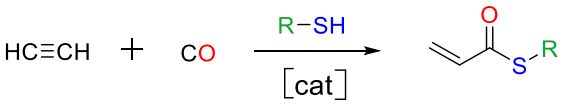

Scheme 2.1: *Reppe*-Carbonylation reaction for thiacrylate (1): synthesis from thiol, acetylene and carbonmonoxide in the presence of nickelcarbonyl catalyst.

The preparation of thioacrylates was carried out by condensation of acetylene and thiols in the presence of metal carbonyls, however no protocol of the synthesis and also no properties of obtained compounds were documented. The acetylene approach with carbon monoxide; and tetracarbonyl nickel has been further refined to the synthesis of thioacrylates by employing acrylic acid.[19] Acylic acid have been used in

another approach, where thiometh acrylates have been synthesised by a DCC/DMAP mediated esterfication of methacrylic acid with thiol.[20]

In 1949 *Mikeska* prepared long chain thioacrylates by reacting chloropropionylchloride and thiols, followed by dehydrohalogenation with diethylaniline (**Scheme 2.2**).[21]

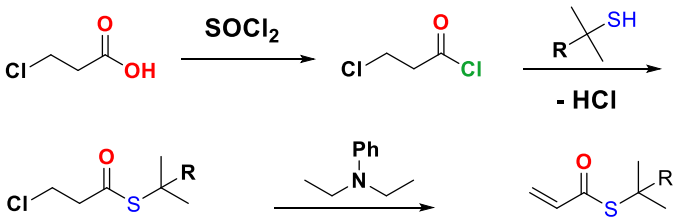

Scheme 2.2: Mikeska, 3 step synthesis, based on chloropropionylchloride.

In 1956 *Marvel* synthesised a range of thioacrylates by the reaction of 2,3-dibromopropionyl chloride with thiols and subsequent treatment with sodium iodine for dehalogenation to yield the respective thioacrylate (**Scheme 2.3**).[22]

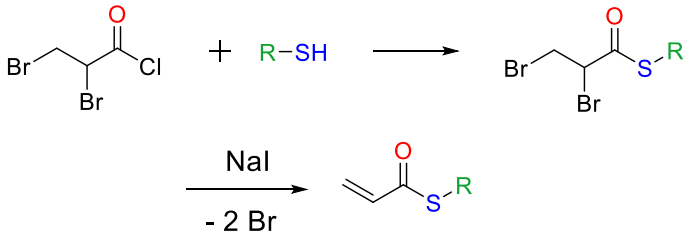

Scheme 2.3: 2 step synthesis starting with dibromopropionylchloride and dehalogenation.

In this way, methyl, ethyl, *n*-propyl, isopropyl, *n*-butyl, isobutyl and *tert*-butyl thioacrylate with an over-all yield of 25-45% were obtained. These monomers were further analysed *via* IR. In a similar reaction, *S*-Ethyl *β*-Bromo(isobutane)thioate was converted to the corresponding acid chloride by refluxing with thionyl chloride, where the resulting acid chloride was treated with a thiol with pyridine and a thiometh acrylate was attained after purification. Another example for an elimination reaction presents the base-catalysed *β*-elimination of 3-acetoxyethiobutyrate by tertiary amines.[23]

Esterification reactions of acryloyl chloride with a thiol conducted in the presence of a base was reported by *Hadjichristidis* in 1977, who analysed the influence of side

groups on the chain flexibility of different acrylates and observed a higher chain flexibility of corresponding polythiomethacrylates (**Scheme 2.4**).[24, 25]

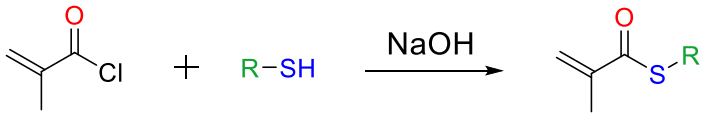

Scheme 2.4: synthesis of methacryloylchloride with thiol.

Thiomethacrylates were prepared with methacryloyl chloride by treatment with thiols in an aqueous sodium hydroxide solution. Repeated distillation needed to be carried out, as *Michael* addition of thiol to the carbon-carbon double bond also took place at the same time with the ester formation. The same method was used with acryloyl chloride to furnish a thioacrylate[26] and in a smiliar approach, where NaOH could be substituted with trimethylamine (NEt_3)[27]. Another methodologies using acryloyl chloride was reported for a nucleophilic conjugate addition either with metal thiolates (PhSLi, *t*-BuSNa, *t*-BuSCu[28]) or NaH and 2,6-dimethyl benzenethiol.[29] Substitution reaction of the silyl group in vinyltrimethylsilane by a Lewis acid activated *S*-ethyl chlorothiocarbonate.[30] Although the reactions were successful with $AlCl_3$, $TiCl_4$, substitution with MgBr failed to catalyse the reaction. A reaction of (meth)acryloyl chloride was also conducted with lead mercaptides to yield respective thio(meth)acrylates.[31]

The Wittig reaction[32-34] is the most commonly used method for the synthesis of alkenes and therefore of acrylates by cross metathesis of a respective Wittig reagent with an aldehyde or ketone to yield acrylates.[35] This method is widely used for the preparation of alkenes because of the wide applicability of an extremely powerful carbon carbon double bond extension. The corresponding carboxylic acid is required for the preparation of acrylates. These carboxylic acids can be used with simple Steglich esterification which usually requires only 10 mol% of Steglich catalyst 4-(N,N-dimethylamino)pyridine (DMAP), carboxylic acids and 1.1 equivalent of N,N-dicyclohexylcarbodiimide (DCC). Depending on the structure of the Wittig

reagent, respective thioacrylates are accessible, the general approach is depicted in **Scheme 2.5** below.[36, 37]

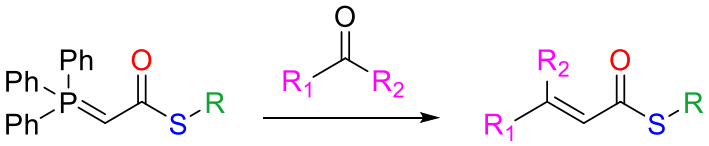

Scheme 2.5: Cross metathesis of respective phosphorene with aldehyde or ketone to yield thioacrylate.

The fundamental understanding on the synthesis and polymerisation of thioacrylate monomers and their physical properties are still very limited, although the introduction of thioesters or thiol groups brings unique functionalities to the macromolecules. Transformation of the thioester group *via* post-polymerisation modification (PPM), allows selective functionalisation into other functional moieties. This tempting idea of having a thioester incorporated into a monomer, point to the use in novel unexplored applications in material science. For this reason there has been a drive towards the development of a synthetic strategy for the synthesis of thioacrylate monomers.

The focus of this chapter is the presentation of an easy and efficient method for the preparation of different thioacrylate monomers that will potentially generate a high level of interest and novel applications in material science. For this, a typical base catalysed reaction from the literature has been used and studied. An alternative route *via* a multi-step reaction for the synthesis of thioacrylate and thiomethacrylate is presented, where the intermediate product in the synthesis has been also used for a modification reaction.

2.2 Results and discussion

2.2.1 Initials attempts to synthesise a thioacrylate monomer (1)

Investigation were started with examining the *S*-acylation of thiophenol as a test thiol starting material with acryloyl chloride with different conditions to produce the corresponding thioacylate **1 (Scheme 2.6)**. At the outset of this study, trimethylamine (NEt_3) was used as base for the reaction. Therefore, the reaction was started with 1.80 equivalents of NEt_3 and 1.50 equivalents of the thiol in THF and stirred for 18 hours. Thereafter, the reaction mixture was washed and the product was analysed by NMR.

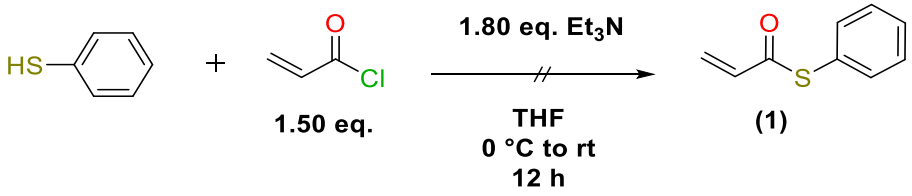

Scheme 2.6: Unsuccessful synthesis of desired thioacrylate (**1**).

However, the desired acrylate functionality could not be observed by ^{1}H NMR, as no characteristic peaks for the olefinic protons appear in the expected range from 5-6 ppm. Under the reaction conditions applied, the acylation between the thiophenol and the acryloyl chloride and simultaneously a Michael-addition of thiophenol and the double bond of the formed thioacrylate occurred in form of *S*-phenyl 3-(phenylthio)propanethioate (**1**). This was confirmed by ^{1}H and ^{13}C NMR, as two triplets at 3.24 and 3.00 ppm appeared. Furthermore, no peak between 160-185 ppm for the carbonyl of the ester, corresponding to acryloyl chloride is absorbed in the ^{13}C NMR. In fact, a new peak in the ^{13}C NMR spectrum appears at 195.21 ppm, corresponding to a thioester (**Figure 2.2**). This observation explains the reaction pathway as follows; as no peak for a carbonyl from an oxoester is present in the NMR, it can be concluded that a thioesterfication occurred as a carbonyl peak from a thioester can be found in the NMR. The absence of vinyl peaks in the proton NMR proofs that a thio-michael addition took place of the newly formed thioacrylate. The chemical shifts and the relative integrations match well with expected values and are assigned and shown in **Figure 2.1** below.

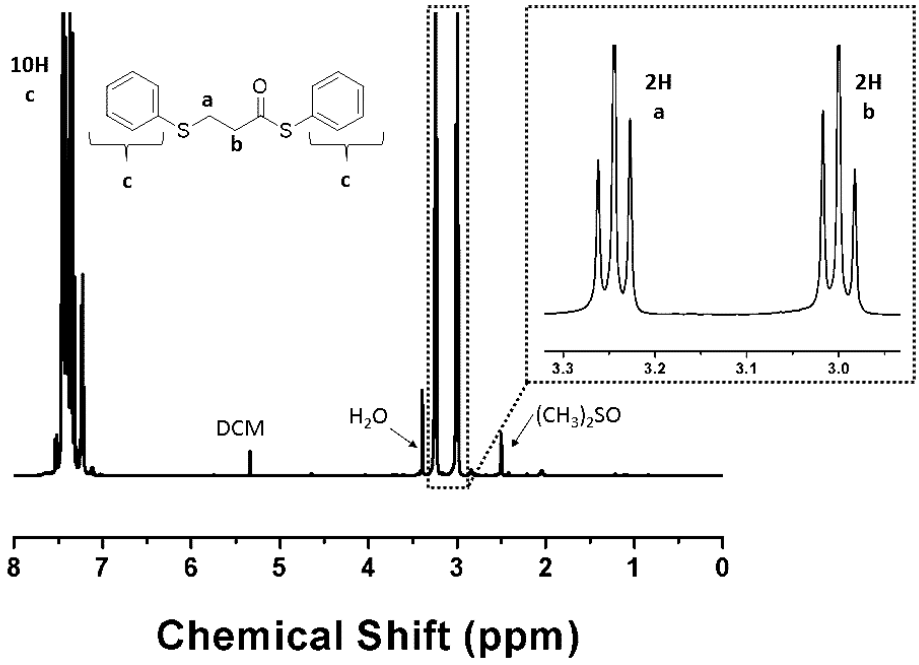

Figure 2.1: ^{1}H NMR spectrum of the diaddition product $(CD_3)_2SO$, 400 MHz, 303 K) of **1**.

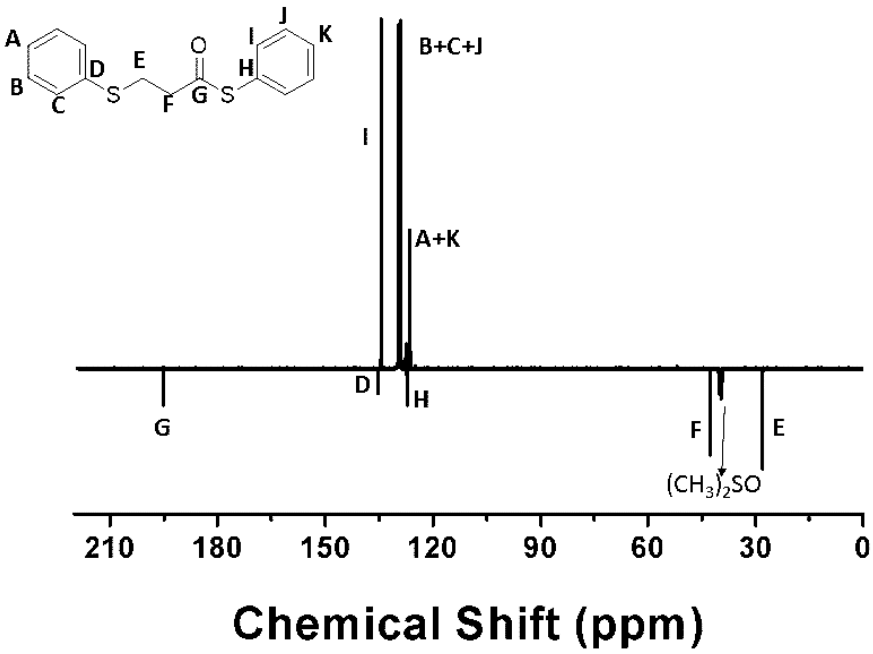

Figure 2.2: ^{13}C NMR spectrum of the diaddition product ($(CD_3)_2SO$, 101 MHz, 303 K) of **1**.

On the other hand, amines are known to catalyse a thiol-Michael addition, which could explain the reaction pathway in this experiment.[38] In a second approach, we applied the conditions from a different report[24, 25], where monomers were obtained by treatment of methacryloyl chloride with thiols in aqueous sodium hydroxide solution.

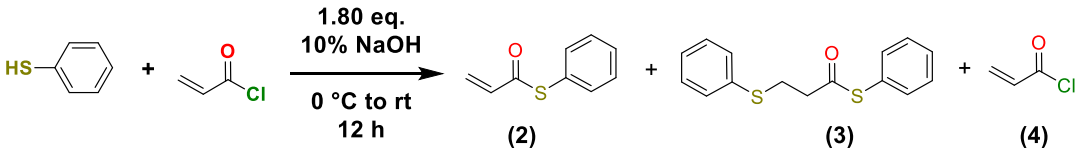

Scheme 2.6: Successful synthesis of thioacrylate **2**.

^{1}H NMR spectrum of the purified compound reveals a small amount of unreacted acryloyl chloride is present in the final product (**Figure 2.4**).

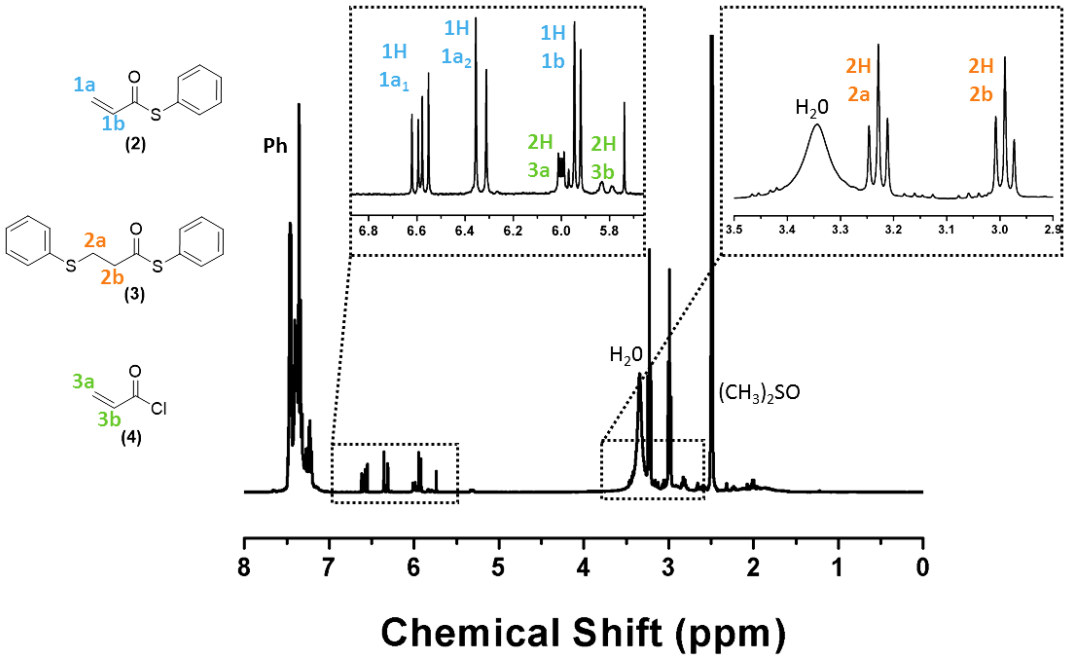

Figure 2.4. ^{1}H NMR spectrum ($(CD_3)_2SO$, 400 MHz, 303 K) of a reaction mixture containing **2**, **3** and **4** from acylation reaction of acryloyl chloride and thiophenol.

The amount of the desired product **2** and the by-product was calculated to be 10% for thioacrylate compound and 87% of **3** from the ^{1}H NMR. Despite the low conversion and the upcoming repeated distillation, this approach was deemed to be not suitable for the synthesis of thioacrylates, due to a necessary extensive purification process.

2.2.2 Synthesis of thioacrylates *via* Wittig reaction

Inspired by a report from *B. L. Feringa* in 2008, in which a protocol *via* a Wittig reaction was used,[39] ethyl thioacrylate (ETA) was prepared by an esterification reaction and subsequent addition of triphenylphosphine to yield a phosphonium salt after treatment with base. After final cross metathesis with paraformaldehyde, the respective thioacrylate was obtained. The resulting monomer was used for another metathesis reaction with various olefins. As the Wittig reagent proofed to be a versatile compound, we first attempted the synthesis of 2-bromoethanethioate for the generation of a Wittig reaction afterwards. As initial attempts to synthesise thioester **5** (*S*-ethyl bromoethanethioate) *via* esterification of an acyl source, the reaction of bromoacetyl bromide with ethanethiol was shown to be successful, however resulting in an unsatisfying yield of 54% (**Scheme 2.7**).

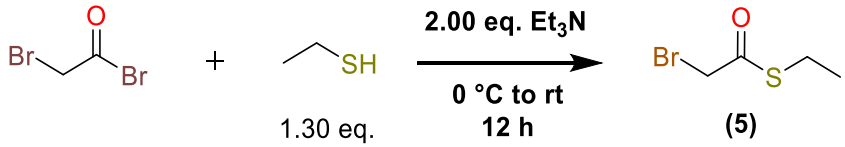

Scheme 2.7. The synthesis of the α-bromo-thioester **5** *via* a base catalysed acylation.

As already discussed in the introduction, there are additional ways to synthesise thioesters. One of them is the use of coupling reagents (**Scheme 2.8**).

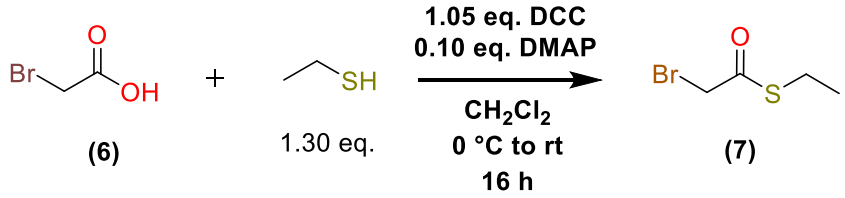

Scheme 2.8. The synthesis of the α-bromo-thioester **7a** via a DMAP-catalysed acylation.

DCC/DMAP coupling has many advantages over common base catalysed esterification. By-products can easily be removed by filtration or extraction. It was hence proposed that the utilization of DCC/DMAP esterification may improve the yield for the first step to generate a thioacrylate monomer. For this purpose ethanethiol and bromoacetic acid was used as the precursor in the presence of a DCC/DMAP catalyst system and gave the corresponding thioester in a higher yield of 70%.

^{1}H NMR was recorded to verify samples purity and the successful esterification reaction between ethanethiol and the acid (**Scheme 2.8**, **Figure 2.3**, bottom).

The NMR displays two additional peaks compared to the CH_2 group in bromoacetic acid.to the starting material, whereby a new resonance signal for the methylene group H_c is shifted high field and appears as a triplet at 1.27 ppm. The coupling constant for this methyl group is 7.4 Hz and is in good accordance with the typical value between 6 – 8 ppm for a methyl group next to a carbon. The appearance as a triplet indicates a methyl group that is coupling to 2 vicinal protons, which supports the presence of an ethyl group. In fact, a new peak arising as a quartet can be found in the NMR at 2.94 ppm and the relative intensities of the triplet and quartet are 2:3.

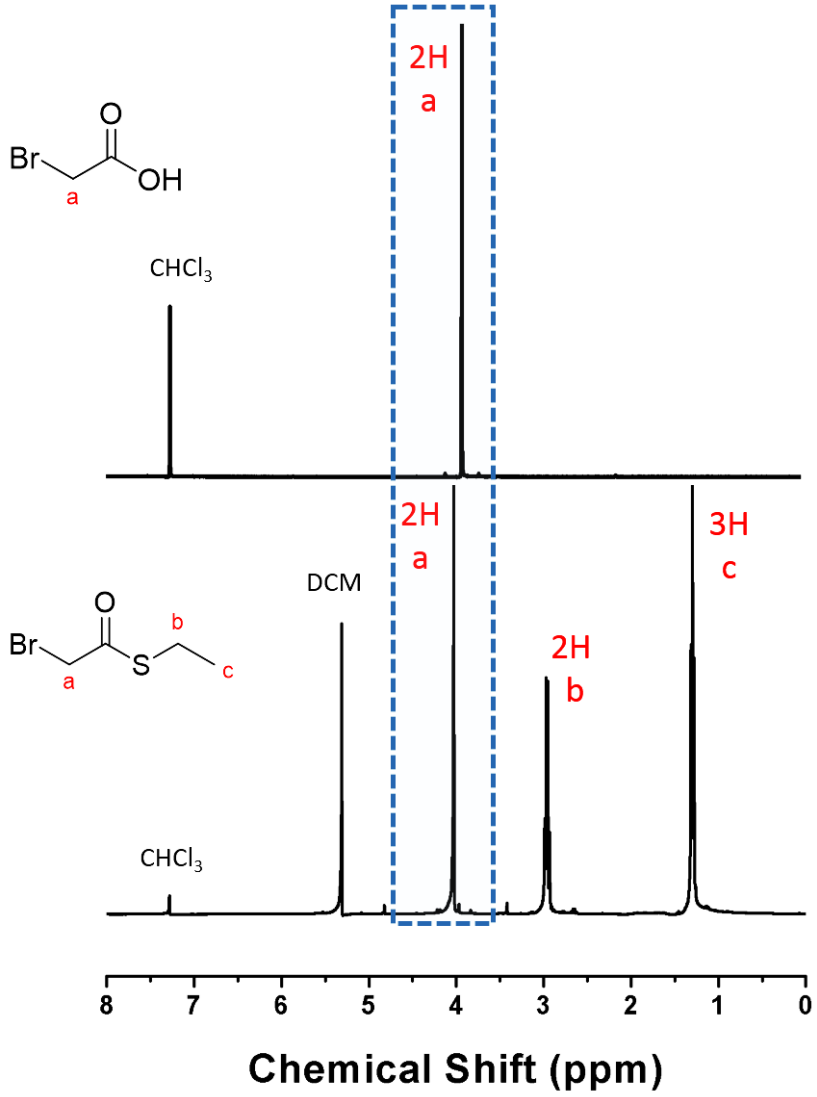

Figure 2.3: ^{1}H NMR spectrum ($CDCl_3$, 400 MHz, 303 K) overlay of starting material (**6**) and thioester product (**7a**) in a DCC/DMAP-catalysed esterification reaction.

In the mid field region of the NMR the singlet of the starting material has slightly shifted from 3.91 to 4.01 ppm and proofs a change of the carbonyl group from an oxoester to a thioester in H_a. This shift is highlighted in blue in **Figure 2.3**.

As the reaction proceed with good yield, it was used for further esterification reactions with other thiols (thiophenol, propanethiol, isopropylthiol and dodecane thiol). The thioester formation was verified for all compounds by ^{1}H NMR, the general approach is depicted below in **Scheme 2.9**.

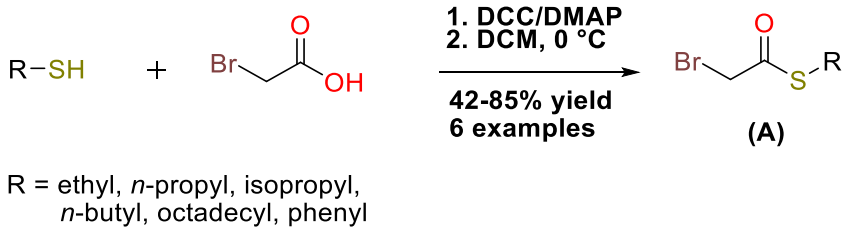

Scheme 2.9. Step 1: Synthesis of thioester **A** via Steglich esterification.

In a next step, the thioester was reacted with a tertiary phosphine to yield a phosphonium salt, subsequent *in situ* deprotonation promotes the formation of the parent phosphor-ylide.

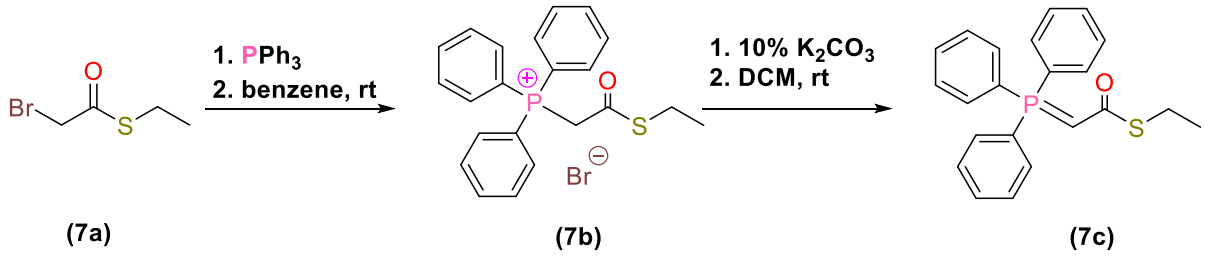

Scheme 2.10: Step 3: Reaction of thioester **7a** with triphenylphosphine and subsequent deprotonation to yield the phosphor ylide **7c**.

The reaction was followed by ^{1}H NMR and is depicted below in **Figure 2.4**. Although the NMR was recorded in DMSO for the triphenylphosphonium salt (**7b)** instead of chloroform, an immense shift of the resonance of H_a in **7c** from the midfield region (4.01 ppm) to low field (5.71 ppm) for H_p in **7b**, indicates the change of the chemical

environment. The singlet from the previous step, splits into a doublet, this can be explained by the fact that the P^+ next to the CH_2 entirely exists as ^{31}P with a magnetic moment of ½. One single ^{31}P will split the protons to a doublet, a phenomena which is well known in the literature. Additionally, the aromatic protons of the phenyl groups are in expected deshielded side in high ppm region (7.93-7.70 ppm).

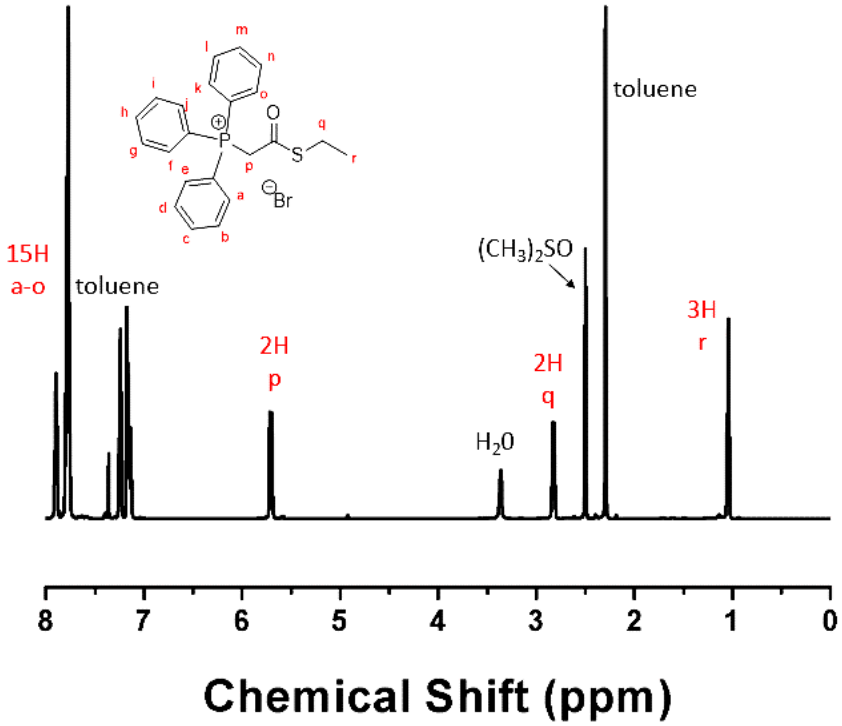

Figure 2.4: ^1H NMR spectrum ($(CD_3)_2SO$, 400 MHz, 303 K) of **7b.**

The formation of the phosphonium bromide **7b** was accelerated, when the thioester and triphenylphosphine were heated to reflux under nitrogen in DCM for an hour and have been used as an alternatively way for phosphonium salts **7b**, which represents the precursors of the ylides for the Wittig olefination reaction in the last step.

For the formation of phosphorane **7c**, Na_2CO_3 was initially used as a base according to a literature procedure.[35] It was proposed that the yield of the obtained phosphorane **7c** could be increased by varying the size of the alkali metal cation, and in fact, the yield was increased when Na_2CO_3 was replaced with K_2CO_3. Therefore, the choice of K_2CO_3, which has been reported as a remarkable base[40] led to the necessity of using this base for all Wittig reactions.

The ^{1}H NMR of phosphorane 7c is depicted below in **Figure 2.5** and indicates a chemical shift of the signal H_p (5.71 ppm) to lower frequency at 3.66 ppm.

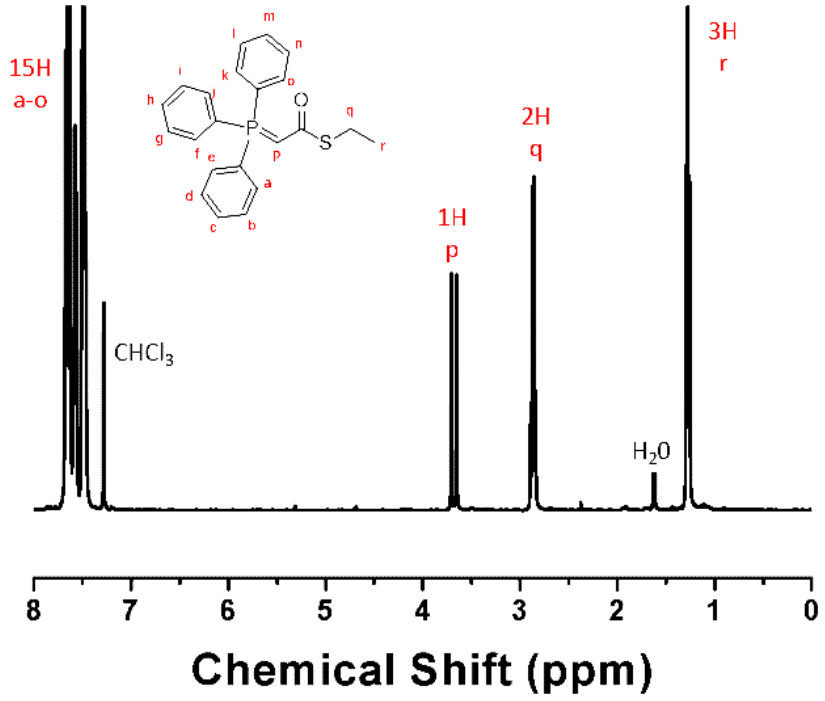

Figure 2.5. ^{1}H NMR spectrum ($CDCl_3$, 400 MHz, 303 K) of **7c**.

The relative intensities of the triplett for H_r in **7c** and singlet from H_p in **7c** are 3:1. The approach for thioesters with different alkyl and aryl groups is depicted below in **Scheme 2.11**.

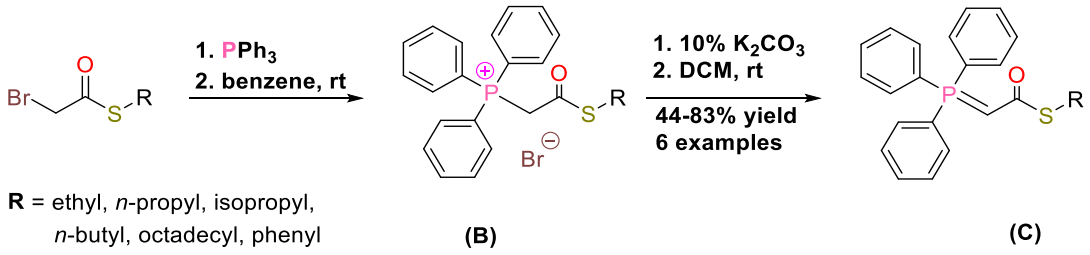

Scheme 2.11: Step 2: Synthesis of Wittig reagent **C**.

In a final step, the olefination has been carried out for the synthesis of thioacrylate **7**, by refluxing ylide **7c** with paraformaldehyde for. The metathesis reaction gives the

corresponding alkenes (thioacrylates) with phosphine oxide as the by-product, which could be removed by column chromatography or purified by distillation.

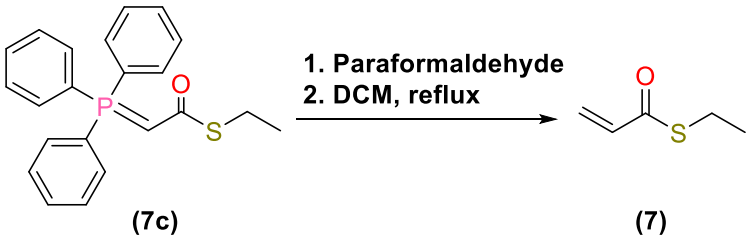

Scheme 2.12: Wittig reaction of phosphorane **7c** with paraformaldehyde to yield ethyl thioacrylate **7**.

Cross metathesis of the Wittig reagent **7c** and paraformaldehyde, followed by flash chromatography and distillation, was carried out for thioacrylates (**7**) according to the literature.[35] The ^{1}H NMR for ethyl thioacrylate (ETA) **7** is depicted below. The triplet for the methyl group in H_d and the ethyl group for H_c remains at lower frequencies as expected. As a C=C bond was formed from the carbon-phosphorus double bond in **7c**, the disappearance of H_p and from the aromatic groups in **7c** are expected. The new signals between δ 6.32 –. 5.59 ppm correspond to the three vinyl protons of ETA (**Figure 2.6**).

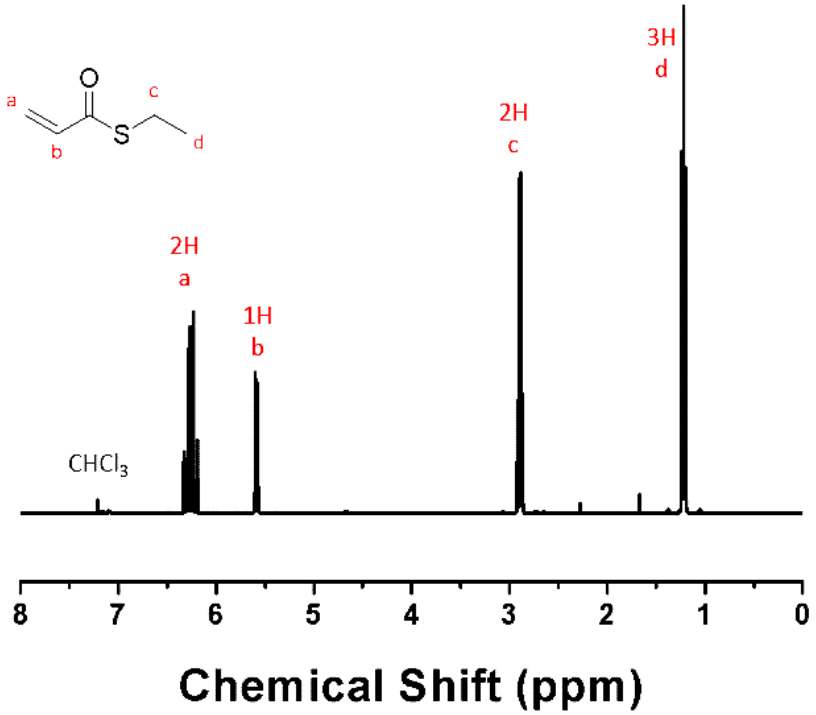

Figure 2.6: ^{1}H NMR spectrum ($CDCl_3$, 400 MHz, 303 K) of **7**.

ETA has five distinct carbons; one signal phase up at 14.6 ppm for the methyl group and another positive peak for the CH of the C=C bond d at the low-field end at 135.1 ppm. In DEPTQ non protonated carbon can be detected as well, the carbonyl carbon appears in the low-field end of the spectrum at 190.1 ppm phase down. It should be noted that the thioester carbonyl is shifted more down field than the carbonyl ester in ethyl acrylate (~180 ppm). Both CH_2 peaks appear phase down; the CH_2 ofdthe C=C double bond appears at 125.9 ppm and the CH2 of the alkyl group in the up field (**Figure 2.7**).

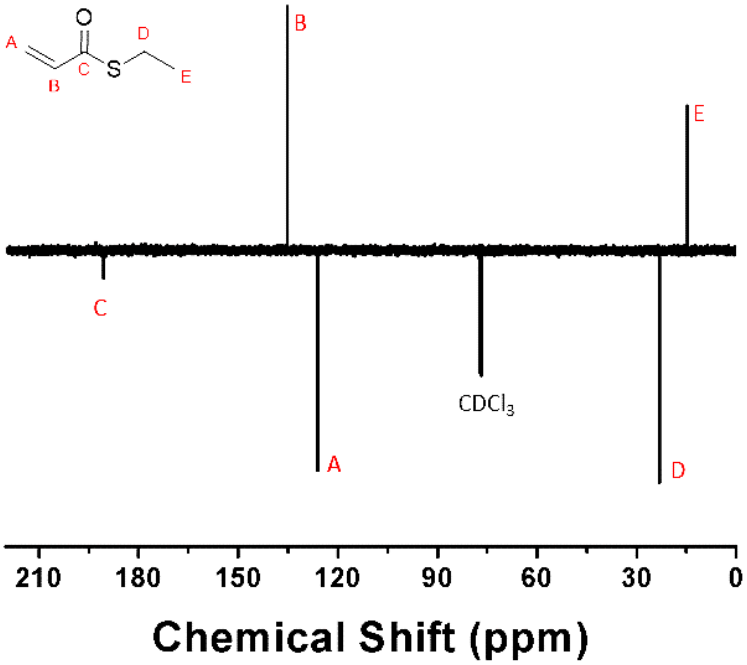

Figure 2.7: ^{13}C NMR spectrum ($CDCl_3$, 101 MHz, 303 K) of **7**.

Wittig reaction has been used for all other thioacrylate monomers with quantitative yields as the last step of the approach, which is depicted in **Scheme 2.13** below.

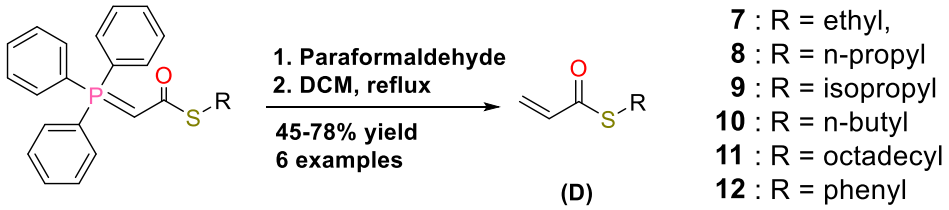

Scheme 2.13. Step 3: Synthesis of thioacrylate monomer **D** *via* a Wittig reaction.

2.2.3 Modification of Wittig reagent C

Further, the phosphorus-carbon double bond in the Wittig reagent C is a versatile bond, easily tuneable from a synthetic standpoint and alkylation[41], acylation and halogenation[42] can yield in modified phosphoranes. For example, methylation of an ylide with iodomethane is possible, and could lead from an ylide from a thioacrylate to a precursor for thio methacrylates. The polymerisation of thioacrylates would be analogous to the polymerisation of thio methacrylates, yielding another thioester containing monomer.

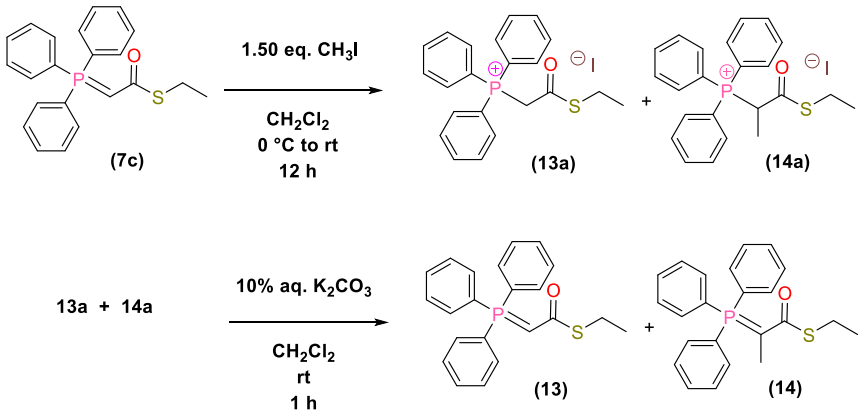

Scheme 2.10. Methylation of phosphorane **7c**.

As compound **C** can possibly serve as a precursor for either thioacrylates and/or thiometh acrylates, the methylation in DCM was performed on this compound. The existence of a methylated phosphorane (13) can be evidenced by a very abundant H^+ ionised the species at 379.11 m/z (m/z^{theo} 378.12). A second characteristic ion was detected: a low abundant peak with 365.23 m/z, which represents the starting material 7c ((m/z_{theo} 365.11). The methylation suggest that the desired product **13** could not be generated completely, but could serve as a precursor for the generation of alkylated ylides and therefore functionalised thioacrylates.

2.2.4 Synthesis of thio methacrylates *via* Wittig reaction

The synthesis of thioacrylates can be also be adopted for the synthesis of thio methacrylates by directly employing bromopropionic acid instead of bromo acetic acid as starting material (**Scheme 17**).

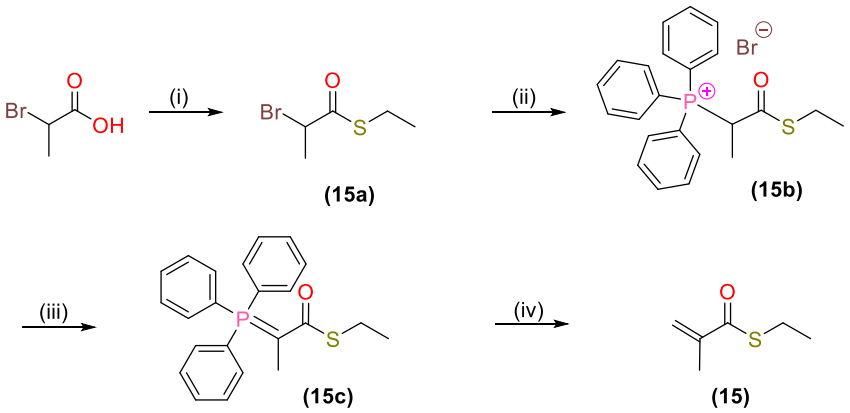

Scheme 2.11. General synthetic scheme, exemplifying chemical synthesis of ethyl thiomethacrylate monomer 15.

The synthesis of ethyl thiomethacrylate (**15**) *via* Wittig reaction was carried out with an overall yield of 41% and proofed the versatility of the described multi step synthesis. In the following pages, the synthesis of all thio(meth)acrylates are presented.

The NMR in **Figure 2.8** displays two additional peaks compared to the CH_2 and methyl group in bromopropionic acid as the starting material. A new resonance signal for the methylene group H_d is shifted high field and appears as a triplet at 1.22 ppm and splits as triplet. The coupling constant for this methyl group is 7.4 Hz and is in good accordance with the typical value between 6 – 8 ppm for a methyl group next to a carbon. The appearance as a triplet indicates a methyl group that is coupling to 2 vicinal protons, which supports the presence of an ethyl group. Indeed, a new peak arising as a quartet can be found in the NMR at 1.77 ppm and the relative intensities of the triplet and quartet are 2:3.The fact that the alkyl group from the thiol is visible in the NMR along with the resonance signals for the bromopropionic acid and a shift is visible for the CH_2 of the acid used, proofs a successful coupling reaction between the bromopropionic acid and ethanethiol. The secondary carbon H_a appears in the midfield region of the NMR (4.45 ppm) as a quartet due to the coupling to the methyl

group H_b. The vicinal protons of the methy group H_b couple to the proton in H_a as a doublet.

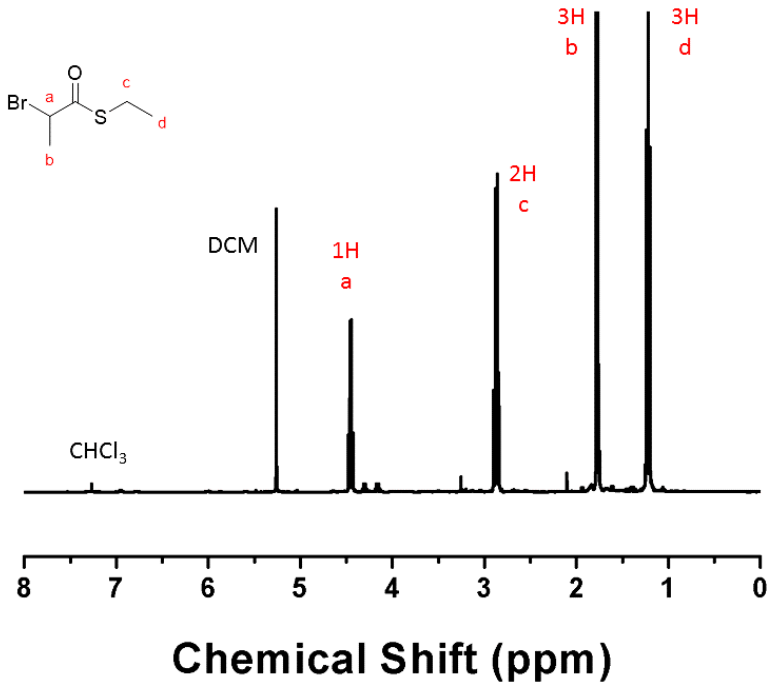

Figure 2.8: ^{1}H NMR spectrum ($CDCl_3$), 400 MHz, 303 K) of **15a**.

The thioester was further reacted with triphenylphosphine under reflux to yield a respective phosphonium salt. The reaction was left for 24h and after filtration the salt was stirred with 10% aqueous solution of K_2CO_3. The obtained wittig reagent **15c** was analysed *via* NMR and the assigned spectrum is shown below in **Figure 2.9**. At high frequency (δ = 7.70-7.45) aromatic peaks of the triphenyl group appears as multiplet. Due to the formation of a P=C bond the proton H_a in thioester **15** has disappeared as expected. The methyl group on the C=P bond Hq stays at low frequency in the NMR spectrum as well as the methyl group H_s and the CH_2 group H_r. The ratios of the hydrogen atoms in the three different environments of H_q, H_r and H_s is 3:2:3 Besides the NMR solvent and the peaks for cyclohexane, the NMR shows a pure product without any left over thioester or phosphonium salt.

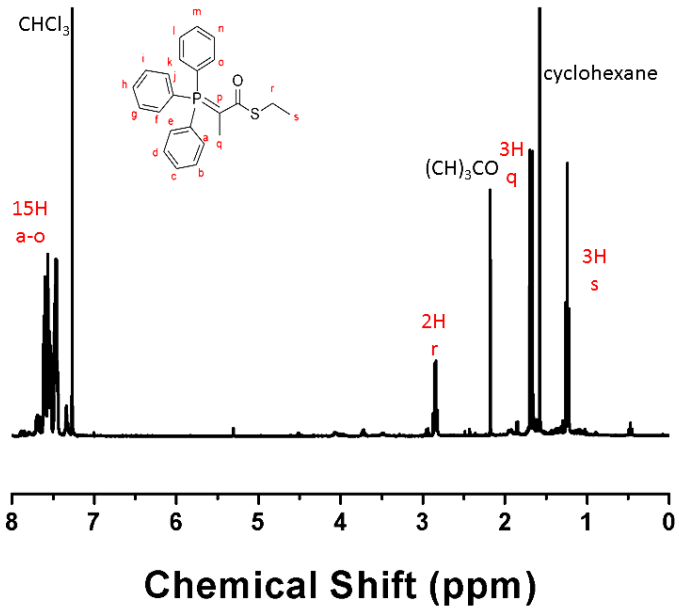

Figure 2.9: ^{1}H NMR spectrum ($CDCl_3$), 400 MHz, 303 K) of **15c**.

The crucial point of the thio(meth)acrylate synthesis was the wittig reaction in the final step, which was also used for the reaction of Wittig reagent **15c** with paraformaldehyde. The obtained and purified monomer is depicted below in **Figure 2.10**.

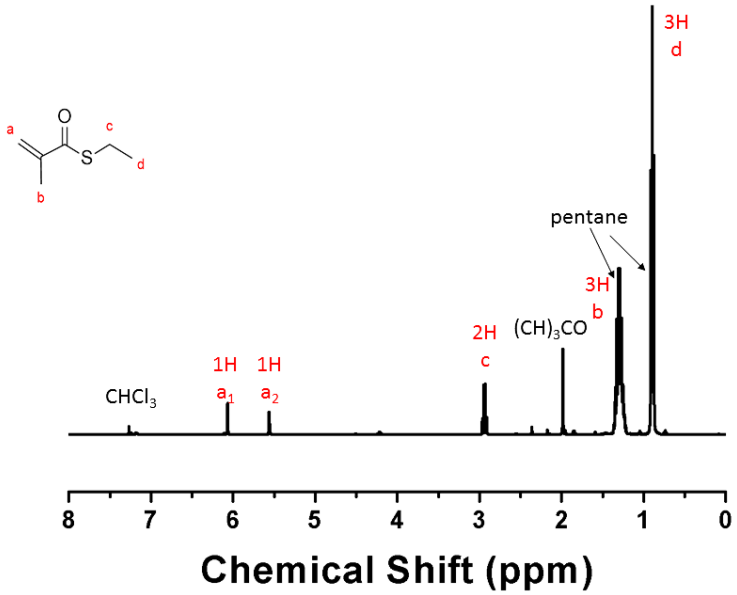

Figure 2.10: ^{1}H NMR spectrum ($CDCl_3$), 400 MHz, 303 K) of **15**.

The characteristic vinyl peaks are detected in the deshielded region as two singlets with a ratio of 1:1. In the shielded region, the two methyl groups and the CH_2 appear, where the latter signal splits as a triplet at 2.93 ppm with a coupling constant of 7.4 Hz. However, coupling constant for the methyl group H_d could not be measured due to the solvent peaks of pentane. Nevertheless, besides some small impurities from reaction solvents, no other impurity such as a side product or starting material were evident in the NMR spectra. The residual solvent can be easily removed and do not require any other additional step. It is important to note that if monomers are used for a polymerization reaction, the added inhibitor used for storage should be easy to remove but also a high purity is necessary. The pureness of the monomer is of particular importance as small amounts of initiator are used most of the time for the polymerization and a small error of weight of the monomer caused by a small trace of solvent can affect the aimed degree of polymerisation drastically.

2.3 Conclusion and Outlook

In summary, we have developed an efficient synthetic approach for the synthesis of thioacrylates, a class of compounds with an interesting functional group. The monomer alphabet could extend the variety of acrylics, allowing access to post modifications with various other groups. The described method allows the introduction of all available thiols in the synthetic scheme, therefore greatly facilitating the preparation of thioacrylates with diversity of the sidegroup. The synthetic steps described in this chapter were carried out in easy experimental setups and with suffiecient yields. With this monomer in hand and with current methods in controlled radical polymerisations further experiments could lead to well-defined poly(thioacrylates) with higher conversions, as experiments in the past on free radical polymerisation of thio(meth)acrylates reported the low conversion and less definition compared to current polyacrylates.

2.4 Experimental

2.4.1 Instrumentation

^{1}H NMR and ^{13}C spectra were recorded on a Bruker AV-400 at 303 K. CDCl3 and the resonance signal at 7.26 ppm (^{1}H) was used as residual $CDCl_3$ or for $(CD_3)_2CO$ at 2.05 ppm peak for the chemical shift (δ).

LC–MS studies were carried out on a system in which the LC part consisted of a 1100 series HPLC (Agilent Technologies, USA) comprising of a vacuum degasser (G1322A), a quaternary pump (G1311A), an auto sampler (G1313A), a UV/visible detector (G1314A) and an Agilent 1100 Series G2244D MSD Ion Trap.

2.4.2 Materials

1-octadecane thiol (Aldrich, ODT, 98%), 2-bromopropionic acid (Aldrich, ≥99%), 2-propanethiol (Aldrich, ≥97%), 4-(dimethylamino)pyridine (DMAP, Aldrich, 99%), acryloyl chloride (Sigma, 97%), bromoacetic acid (Aldrich, reagent grade, 97%), bromoacetyl bromide (Aldrich, ≥98%), dicyclohexylcarbodiimide (DCC, Aldrich, puriss., ≥99% (GC)), ethanethiol (Sigma, 97%), iodomethane (Sigma, purum, ≥99% (GC)), paraformaldehyde (Sigma, powder, 95%), potassium carbonate (Sigma, BioXtra, ≥99%), propanethiol (Sigma, 99%), sodium hydroxide(Fisher, 98.5% for analysis, pellets), thiophenol (Sigma, 97%) and triethylamine (TEA, Sigma, ≥99%). All solvents were purchased from Sigma-Aldrich (UK) and used as received at the highest purity available.

2.4.3 Procedures

2.4.3.1 Experimental Procedure for thiophenol acrylate (PhTA) monomer (1)

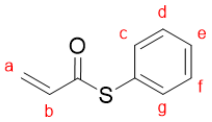

In a typical reaction, thiophenol (5.27 g, 5.00 mL, 48.5 mmol) was dissolved in THF (50 mL), to which triethylamine (12.0 mL, 8.84 g, 87.3 mmol) was added under an atmosphere of argon, and the reaction was cooled to 0 °C. Acryloyl chloride (6.61 g, 7.00 mL, 73.0 mmol) in THF (50 mL) was subsequently added dropwise over 30 minutes with stirring. The reaction was allowed to warm to room temperature overnight with continued stirring. The reaction mixture was then filtered, and the solvent was evaporated in *vacuo*. DCM was added and the organic layer washed with 1M HCl (3x200 mL), 1M NaOH (3x200 mL) and then washed with water (3x200 mL). The organic layer was dried over anhydrous $MgSO_4$ and the solvent was removed *in vacuo* to yield a yellow oil (1.20 g).**^{1}H NMR** ($(CD_3)_2SO$, 400 MHz) δ = 7.26 (m, 5H, H_c – H_g), 6.37 (dd, J = 10.4, 6.7 Hz, 1H, H_b) 6.13 (d, J = 17.2 Hz, 1H, H_{a1} and 5.72 (d, J = 10.4 Hz, 1H, H_{a2}). **^{13}C NMR** (101 MHz, $(CH_3)_2SO$, *δ*): 188.0, 135.1, 134.8, 130.1, 129, 129.1.

2.4.3.2 Experimental Procedure for thiophenol acrylate (PhTA) monomer (2)

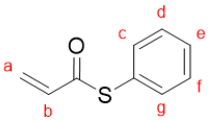

For this, acryloyl chloride (2.23 g, 2.00 mL, 24.0 mmol) was added to a suspension of thiophenol (1.76 g, 1.65 mL, 16.0 mmol) in 10% aqueous sodium hydroxide solution (25 mL) under an atmosphere of argon and was stirred at 0°C. After 12 h the organic layer was extracted with DCM and washed with 1M HCl (3 × 50 mL), 1M NaOH (3 × 50 mL) and then washed with water (3 x 50.0 mL). The organic layer was dried over anhydrous $MgSO_4$ and the solvent was removed in *vacuo*. **^{1}H NMR** ($(CD_3)_2SO$, 400 MHz) δ = 7.26 (m, 5H, H_c – H_g), 6.37 (dd, J = 10.4, 6.7 Hz, 1H, H_b) 6.13 (d, J = 17.2 Hz, 1H, H_{a1} and 5.72 (d, J = 10.4 Hz, 1H, H_{a2}). **^{13}C NMR** (101 MHz, $(CH_3)_2SO$, *δ*): 188.0, 135.1, 134.8, 130.1, 129, 129.1.

2.4.3.3 Experimental Procedure for ethylthioacrylate (ETA) monomer (7)

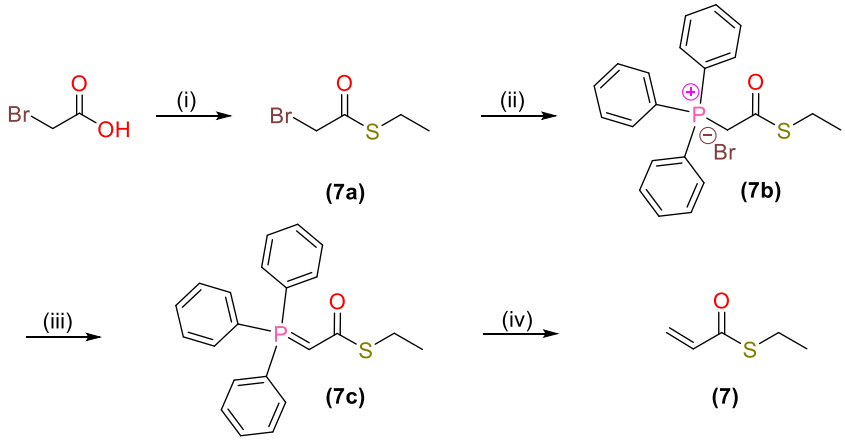

Scheme 12: Synthesis of *S*-Ethyl 2-bromoethanethioate (7), Reagents and conditions: (i) ethanethiol, DCC/DMAP, CH_2Cl_2, 0 °C to rt, 16 h. (ii) Triphenylphosphine, benzene, reflux, 30 min. (iii) 10 wt% K_2CO_3, CH_2Cl_2, rt, 30 min. (iv) paraformaldehyde, CH_2Cl_2, reflux, 1 h.

2.4.3.3.1 Synthesis of S-ethyl bromoethanethioate (7a)

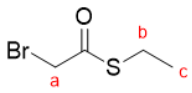

A two-necked 5-L round bottom flask was charged with bromoacetic acid (200 g, 1.44 mol), ethanethiol (140 mL, 189 mmol) and a catalytic amount of DMAP (17.6 g, 0.144 mol). 1 L of DCM was added and the solution was cooled to 0 °C with stirring under an atmosphere of nitrogen. DCC (17.6 g, 144 mmol) was diluted in 200 mL of DCM and added dropwise and the solution slowly warmed to room temperature overnight until esterification was complete. The solution was then filtered through Silica and the filtercake was washed several times with DCM. The filtrate was washed with saturated $NaHCO_3$ solution, water and brine and was dried over Na_2SO_4. Evaporation of the solvent in *vacuo* gave a yellowish oil. (**Yield** = 181,68 g, 70%) **^{1}H NMR** ($CDCl_3$, 400 MHz) δ = 4.01 (s, 2H, H_a), 2.94 (q, J = 7.5 Hz, 2H, H_b) and 1.27 (t, J = 7.4 Hz, 3H, H_c).

2.4.3.3.2 Synthesis of (2-(ethylthio)-2-oxoethyl)triphenylphosphonium bromide (7b)

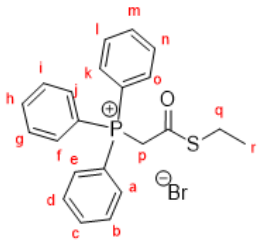

Product 7a (181 g, 0.99 mol) and triphenylphosphine (337 g, 1.28 mol) in 750 mL of benzene was heated to reflux under nitrogen for one hour. The solvent was evaporated under reduced pressure to yield white crystals after filtering and washing with toluene. **^{1}H NMR** $(CH_3)_2SO$, 600 MHz) δ = 7.93-7.70 (m, 15H, H_a – H_o), 5.71 (d, J = 14.5 Hz, 2H, H_p), 2.82 (q, J = 7.3 Hz, 2H, H_q) and 1.04 (t, J = 7.3 Hz, 3H, H_r).

2.4.3.3.3 Synthesis of *S*-ethyl 2-(triphenyl-λ^5-phophanylidene)ethanethioate (7c)

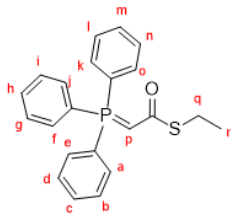

7b was then dissolved in 500 mL of DCM and vigorously stirred with 200 mL of 10% aqueous K_2CO_3 solution for 30 min. The organic layer was separated and the aqueous layer was extracted twice with DCM. The combined organic phases were dried over magnesium sulfate and partially concentrated in *vacuo* and diluted in pentane which afforded 7b (259 g, 72% yield) of light-brown crystals after 24h. **^{1}H NMR** ($CDCl_3$, 400 MHz) δ = 7.70-7.40 (m, 15H, H_a – H_o), 3.66 (d, J = 22.7 Hz, 1H, H_p), 2.84 (q, J = 7.4 Hz, 2H, H_q) and 1.25 (t, J = 7.4 Hz, 3H, H_r).

2.4.3.3.4 Synthesis of *S*-ethyl prop-2-enethioate (7)

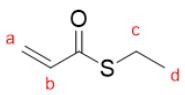

In a 1-L two-necked flask equipped with a cooling system and magnetic stirrer, (100 g, 270 mmol) of Wittig reagent 7c were introduced into 700 mL of DCM. Then, (41.7 g, 1.37 mol) of paraformaldehyde was poured into the solution. The mixture was heated for 1 hour under then concentrated in *vacuo* and the residue was suspended in cold pentane (250 mL) and filtered over silica. The filtercake was washed with cold (10:90 Et_2o/pentane). Hydroquinone was added to the solution to prevent polymerisation. The solution was distilled over CaH_2 (2 g/L) at reduced pressure (11 mbar/80°C) to yield (17,96 g, 57% yield) of a colorless oil.**^{1}H NMR** ($CDCl_3$, 400 MHz), δ = 6.32 (dd, J = 17.2, 9.7 Hz, 1H, H_{a1}), 6.28 (dd, J = 17.2, 1.6 Hz, 1H, H_{a2}), 5.59 (dd, J = 9.8, 1.6 Hz, 1H, H_b), 2.89 (q, J = 7.4 Hz, 2H, H_c), 1.21 (t, J = 7.4 Hz,3H, H_d). **^{13}C NMR** (101 MHz, $CDCl_3$, *δ*): 190.1, 135.1, 125.9, 23.1, 14.6.

2.4.3.4 Preparation of *S*-Propyl prop-2-enethioate (PTA) monomer (8)

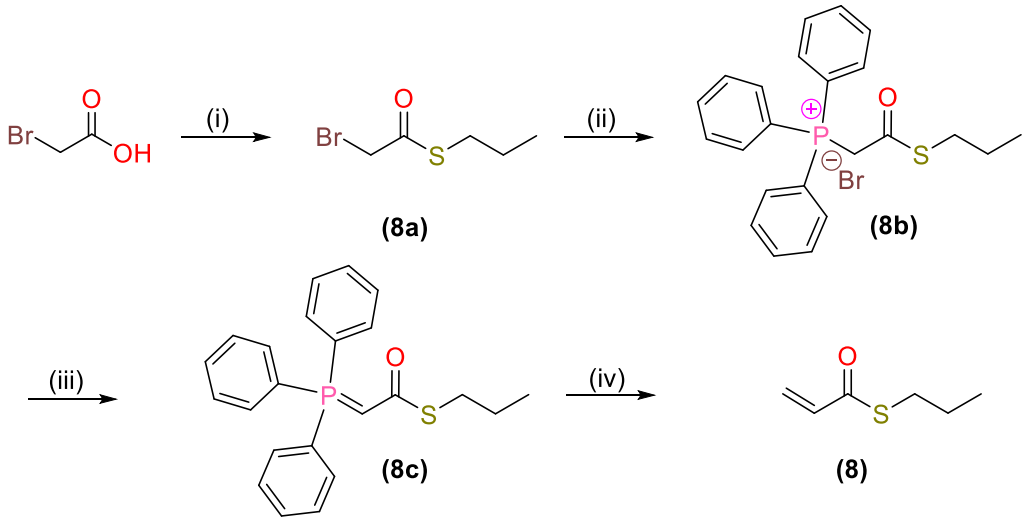

Scheme 2.13: Synthesis of S-Propyl prop-2-enethioate (8), Reagents and conditions: (i) 1-propanethiol, DCC/DMAP, CH_2Cl_2, 0 °C to rt, 16 h. (ii) Triphenylphosphine, benzene, reflux, 30 min. (iii) 10 wt% K_2CO_3, CH_2Cl_2, rt, 30 min. (iv) paraformaldehyde, CH_2Cl_2, reflux, 1 h.

2.4.3.4.1 Synthesis of S-Propyl 2-bromoethanethioate (8a)

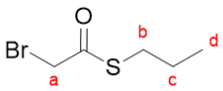

A two-necked 5-L round bottom flask was charged with bromoacetic acid (54.0 g, 0.39 mol), 1-propanethiol (50.0 mL, 0.50 mol) and a catalytic amount of DMAP (5.05 g, 0.04 mmol). 200 mL of DCM was added and the solution was cooled to 0°C with stirring under an atmosphere of nitrogen. DCC (89.5 g, 0.43 mol) was diluted in 100 mL of DCM and added dropwise and the solution slowly warmed to room temperature overnight until esterification was complete. The solution was then filtered through Silica and the filtercake was washed several times with DCM. The filtrate was washed with saturated $NaHCO_3$ solution, water and brine and was dried over $Na2SO_4$. Evaporation of the solvent in *vacuo* gave (60 g, 74%) of a yellowish oil. **^{1}H NMR** ($CDCl_3$, 400 MHz) δ = 4.01 (s, 2H, H_1), 2.94 (t, J = 7.5 Hz, 2H, H_2), 1.63 (sxt, J = 7.3 Hz, 2H, H_3) and 1.27 (t, J = 7.4 Hz, 3H, H_4).

2.4.3.4.2 Synthesis of (2-oxo-2-(propylthio)ethyl)triphenylphosphonium bromide (8b)

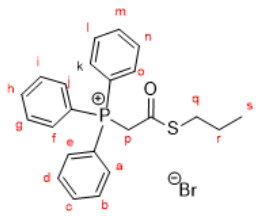

8a (60.0 g, 0.30 mol) and triphenylphosphine (104 g, 0.40 mol) in 200 mL of benzene was heated to reflux under nitrogen for one hour. The solvent was evaporated under reduced pressure to yield white crystals after filtering and washing with toluene. **^{1}H NMR** ($CDCl_3$, 400 MHz) δ = 7.85 – 7.57 (m, 15H, H_{a-o}), 5.86 (d, J = 13.3 Hz, 1H, H_p), 2.69 (t, J = 7.2 Hz, 2H, H_q), 1.36 (sxt, J = 7.3 Hz, 2H, H_r), 0.76 (t, J = 7.5, H_s).

2.4.3.4.3 Synthesis of *S*-Propyl 2-(triphenyl-λ^5-phosphanylidene)ethanethioate (8c)

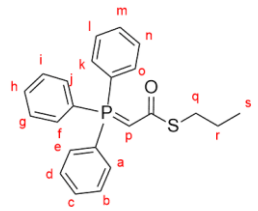

8b was then dissolved in 200 mL of DCM and vigorously stirred with 200 mL of 10% aqueous K_2CO_3 solution for 30 min. The organic layer was separated and the aqueous layer was extracted twice with DCM. The combined organic phases were dried over magnesium sulfate and partially concentrated in *vacuo* and diluted in pentane which afforded 4 (58.9 g, 50%) of light-brown crystals after 24h. **^{1}H NMR** ($CDCl_3$, 400 MHz) δ = 7.70-7.43 (m, 15H, H_1 – H_{16}), 3.66 (d, J = 20.6 Hz, 1H, H_{16}), 2.82 (t, J = 7.2 Hz, 2H, H_{17}), 1.61 (sxt, J = 7.3 Hz, 2H, H_{18}) and 0.96 (t, J = 7.4 Hz, 3H, H_{19}).

2.4.3.4.4 Synthesis of S-Propyl prop-2-enethioate (8)

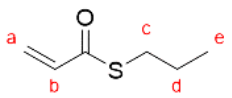

8c (35.0 g, 0.09 mol) and paraformaldehyde (12.8 g, 0.36 mol) were poured into a nitrogen flushed round bottom flask. The mixture was heated for 1 hour under an atmosphere of argon at reflux temperature, then concentrated in *vacuo* and the residue was suspended in cold pentane (100 mL) and filtered over silica. The filtercake was washed with cold (10:90 Et_2O/pentane). Hydroquinone was added to the solution to prevent polymerisation. The solution was

distilled over CaH_2 (2 g/L) at reduced pressure to yield a yellowish oil (8.8 g, 74%). **^{1}H NMR** ($CDCl_3$, 400 MHz) δ = 6.39-6.15 (m, 2H, H_a), 5.59 (dd, J = 9.9, 1.25 Hz, 1H, H_b), 2.89 (t, J = 8.3 Hz, 2H, H_c), 1.58 (sxt, J = 8.4 Hz, 2H, H_d) and 0.93 (t, J = 7.4 Hz, 3H, H_e). **^{13}C NMR** (101 MHz, $CDCl_3$, *δ*): 144.2, 134.8, 39.6, 31.9, 22.3.

2.4.3.5 Preparation of *S*-Isopropyl prop-2-enethioate (IPTA) monomer

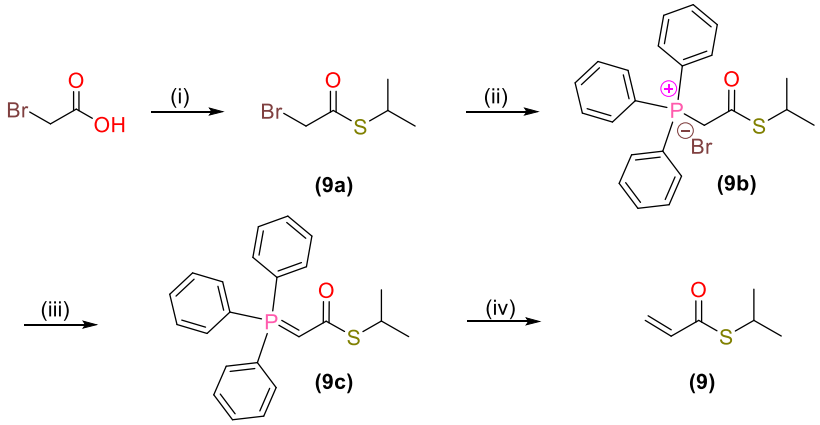

Scheme 2.14: Synthesis of S-Isoropyl prop-2-enethioate (9), Reagents and conditions: (i) 1-propanethiol, DCC/DMAP, CH_2Cl_2, 0 °C to rt, 16 h. (ii) Triphenylphosphine, benzene, reflux, 30 min. (iii) 10 wt% K_2CO_3, CH_2Cl_2, rt, 30 min. (iv) paraformaldehyde, CH_2Cl_2, reflux, 1 h.

2.4.3.5.1 Synthesis of S-Isopropyl 2-bromoethanethioate (9a)

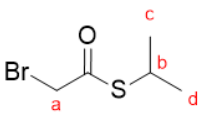

A two-necked 5-L round bottom flask was charged with bromoacetic acid (70.0 g, 0.51 mol), 2-propanethiol (60.0 mL, 0.66 mol) and a catalytic amount of DMAP (6.06 g, 0.05 mmol). 200 mL of DCM was added and the solution was cooled to 0°C with stirring under an atmosphere of nitrogen. DCC (107 g, 0.52 mol) was diluted in 100 mL of DCM and added dropwise and the solution slowly warmed to room temperature overnight until esterification was complete. The solution was then filtered through Silica and the filtercake was washed several times with DCM. The filtrate was washed with saturated $NaHCO_3$ solution, water and brine and was dried over Na_2SO_4. Evaporation of the solvent in *vacuo* gave (76 g, 77%) of a yellowish oil. **^{1}H NMR** ($CDCl_3$, 400 MHz) δ = 3.99 (s, 2H, H_1), 2.94 (q, J = 6.9 Hz, 1H, H_2 and 1.33 (d, J = 6.9 Hz, 6H, $H_{3/4}$).

2.4.3.5.2 Synthesis of (2-(isopropylthio)-2-oxoethyl)triphenylphosphonium bromide (9b)

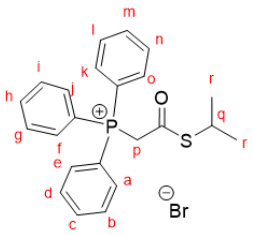

9a (30.0 g, 0.152 mol) and triphenylphosphine (51.5 g, 0.20 mol) in 120 mL of benzene was heated to reflux under nitrogen for one hour. The solvent was evaporated under reduced pressure to yield white crystals after filtering and washing with toluene.

2.4.3.5.3 Synthesis of *S*-Isopropyl 2-(triphenyl-λ^5-phosphanylidene)-ethanethioate (9c)

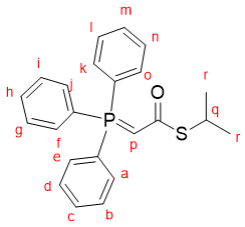

9b was then dissolved in 150 mL of DCM and vigorously stirred with 150 mL of 10% aqueous K_2CO_3 solution for 30 min. The organic layer was separated and the aqueous layer was extracted twice with DCM. The combined organic phases were dried over magnesium sulfate and partially concentrated in *vacuo* and diluted in pentane which afforded 4c (30 g, 49%) of lightbrown crystals after 24h. **^{1}H NMR** ($CDCl_3$, 400 MHz) δ = 7.89-7.39 (m, 15H, H_1 – H_{15}), 5.64 (dd, J = 9.41, 1.88 Hz, 1H, H_{16}), 3.74 (quint, J = 6.9 Hz, 1H, H_{17} and 1.34 (d, J = 6.9 Hz, 6H, $H_{18/19}$).

2.4.3.5.4 Synthesis of *S*-Isopropyl prop-2-enethioate (9)

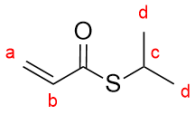

9c (30.0 g, 0.07 mol) and paraformaldehyde (11.0 g, 0.36 mol) were poured into a nitrogen flushed round bottom flask. The mixture was heated for 1 hour under an atmosphere of argon at reflux temperature, then concentrated in *vacuo* and the residue was suspended in cold pentane (100 mL) and filtered over silica. The filtercake was washed with cold (10:90 Et_2O/pentane). Hydroquinone was added to the solution to prevent polymerisation. The solution was distilled over CaH_2 (2 g/L) at reduced pressure to yield 10 (7.7 g, 75%). **^{1}H NMR** ($CDCl_3$, 400 MHz) δ = 6.38-6.20 (m, 2H, H_1), 5.62 (dd, J = 9.54, 1.88 Hz, 1H, H_2) 3.72 (quint, J = 6.9 Hz, 1H, H_3) and 1.33 (d, J = 7.0 Hz, 6H, $H_{4/5}$).

2.4.3.6 Synthesis of Butyl thioacrylate (BuTA) monomer (10)

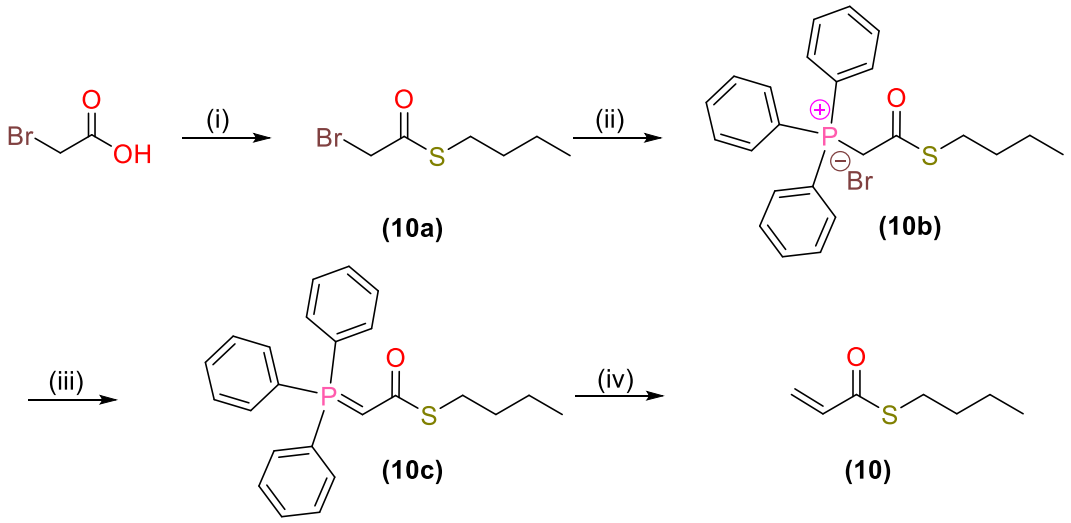

Scheme 2.15: Synthesis of S-butyll prop-2-enethioate (10), Reagents and conditions: (i) butanethiol, DCC/DMAP, CH_2Cl_2, 0 °C to rt, 16 h. (ii) Triphenylphosphine, benzene, reflux, 30 min. (iii) 10 wt% K_2CO_3, CH_2Cl_2, rt, 30 min. (iv) paraformaldehyde, CH_2Cl_2, reflux, 1 h.

2.4.3.6.1 Synthesis of *S*-butyl 2-bromoethanethioate (10a)

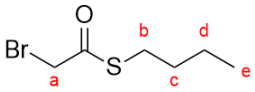

A two-necked 2 L round bottom flask was charged with bromoacetic acid (55.3 g, 0.40 mol), butanethiol (50.0 mL, 0.46 mol) and a catalytic amount of DMAP (5.01 g, 0.04 mmol). 200 mL of DCM was added and the solution was cooled to 0°C with stirring under an atmosphere of nitrogen. DCC (90.0 g, 0.43 mol) was diluted in 100 mL of DCM and added dropwise and the solution slowly warmed to room temperature overnight until esterification was complete. The solution was then filtered through Silica and the filtercake was washed several times with DCM. The filtrate was washed with saturated $NaHCO_3$ solution, water and brine and was dried over $Na2SO_4$. Evaporation of the solvent in *vacuo* gave (70 g, 85%) of a yellowish oil. (**^{1}H NMR** ($CDCl_3$, 400 MHz) δ = 4.01 (s, 2H, H_a), 2.93 (t, J = 7.3 Hz, 2H, H_b), 1.58 (d, J = 10.2 Hz, 2H, H_c), 1.38 (sxt, J = 10.2 Hz, 2H, H_d) and 0.91 (t, J = 7.3 Hz, 3H, H_e).

2.4.3.6.2 Synthesis of (2-(butylthio)-2-oxoethyl)triphenylphosphonium bromide (10b)

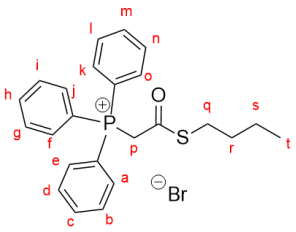

Product 10a (41.0 g, 0.19 mol) and triphenylphosphine (65.2 g, 0.25 mol) in 750 mL of benzene was heated to reflux under nitrogen for one hour. The solvent was evaporated under reduced pressure to yield white crystals after filtering and washing with toluene to yield white crystals. (**^{1}H NMR** ($CDCl_3$, 400 MHz) δ = 7.89-7.67 (m, 15H, H_a -H_o), 5.9 (d, 1H, J = 13.3 Hz, H_p), 2.78 (t, J = 7.3 Hz, 2H, H_q), 1.37 (sxt, 2H, J = 8.4 Hz, H_r), 1.22 (sxt, 2H, J = 8.4 Hz, H_s) and 0.81 (t, 7.3 Hz, 3H, H_t).

2.4.3.6.3 Synthesis of S-butyl 2-(triphenyl-λ^5-phosphanylidene)ethanethioate (10c)

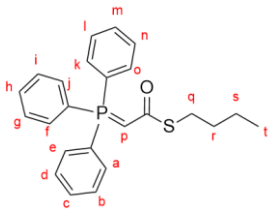

10b was then dissolved in 250 mL of DCM and vigorously stirred with 350 mL of 10% aqueous K_2CO_3 solution for 30 min. The organic layer was separated and the aqueous layer was extracted twice with DCM. The combined organic phases were dried over magnesium sulfate and partially concentrated in *vacuo* and diluted in pentane which afforded 12c (129 g, 83%) of lightbrown crystals after 24h. (**^{1}H NMR** ($CDCl_3$, 400 MHz) δ = 7.65-7.36 (m, 15H, H_a -H_o), 3.66 (d, J = 20 Hz, 1H, H_p), 2.85 (t, J = 7.3 Hz, 2H, H_q), 1.57 (q, 2H, J = 7.4 Hz, H_r), 1.4 (sxt, 2H, J = 7.4 Hz, H_s) and 0.89 (t, 7.2 Hz, 3H, H_t).

2.4.3.6.4 Synthesis of S-butyl prop-e-enethioate (10)

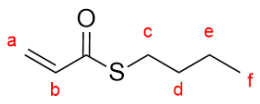

10c (15.6 g, 0.07 mol) and paraformaldehyde (11.0 g, 0.36 mol) were poured into a nitrogen flushed round bottom flask. The mixture was heated for 1 hour under an atmosphere of argon at reflux temperature, then concentrated in *vacuo* and the residue was suspended in cold pentane (100 mL) and filtered over silica. The filtercake was washed with cold (10:90 Et_2O/pentane). Hydrochinone was added to the solution to prevent polymerisation. (3.10 g, 64%). (**^{1}H NMR** ($CDCl_3$, 400 MHz) δ = 6.40 (dd, 1H, J = 9.8 Hz, H_{a1}), 6.29 (dd, 1H, J = 12.2 Hz, H_b), 5.66 (dd, 1H, J = 9.9 Hz),

2.97 (t, J = 7.3 Hz, 2H, J = 7.3 Hz, H_c), 1.6 (quin, 2H, J = 7.4 Hz, H_d), 1.42 (sex, 2H, J = 7.4 Hz, H_e) and 0.94 (t, 3H, J = 7.3 Hz, H_f).

2.4.3.7 Synthesis of *S*-Octadecyl prop-2-enethioate (ODTA) monomer (11)

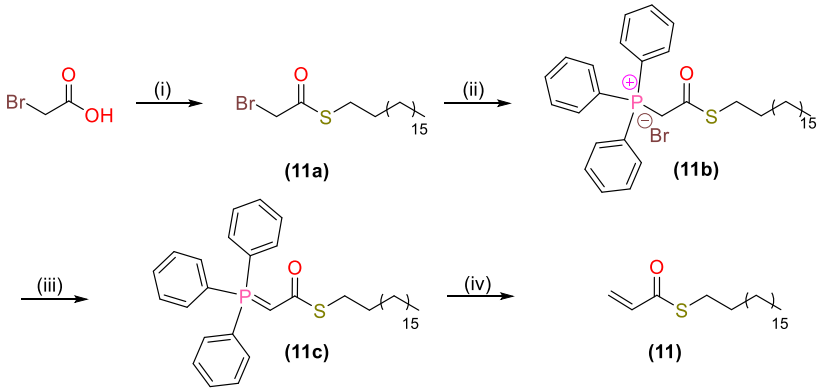

Scheme 2.16: Synthesis of S-Octadecyl prop-2-enethioate (11), Reagents and conditions: (i) thiophenol, DCC/DMAP, CH_2Cl_2, 0 °C to rt, 16 h. (ii) Triphenylphosphine, benzene, reflux, 30 min. (iii) 10 wt% K_2CO_3, CH_2Cl_2, rt, 30 min. (iv) paraformaldehyde, CH_2Cl_2, reflux, 1 h.

2.4.3.7.1 Synthesis of S-octadecyl 2-bromoethanethioate (11a)

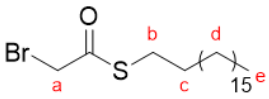

A two-necked 5 L round bottom flask was charged with bromoacetic acid (31.0 g, 225 mmol), 1-octadecanethiol (84.0 g, 290 mmol) and a catalytic amount of DMAP (2.75 g, 22.5 mmol). 400 mL of THF was added and the solution was cooled to 0°C with stirring under an atmosphere of nitrogen. DCC (49.0 g, 230 mmol) was diluted in 200 mL of THF and added dropwise and the solution slowly warmed to room temperature overnight until esterification was complete. The solution was then filtered through Silica and THF was evaporated in *vacuo*. The solid was dissolved in DCM. The filtrate was washed with saturated $NaHCO_3$ solution, water and brine and was dried over Na_2SO_4. Evaporation of the solvent in *vacuo* gave (23.2 g, 52%) of a brown solid. **^{1}H NMR** ($CDCl_3$, 400 MHz) δ = 4.01 (s, 2H, H_1), 2.94 (t, J = 7.3 Hz, 2H, H_2), 1.60 (q, J = 7.3 Hz, 2H, H_4), 1.25 (s, 30H, H_{15}), 0.88 (t, J = 6.8 Hz, 3H, H_5).

2.4.3.7.2 Synthesis of *S*-octadecyl 2-(triphenyl-λ^5-phosphanylidene)-ethanethioate (11c)

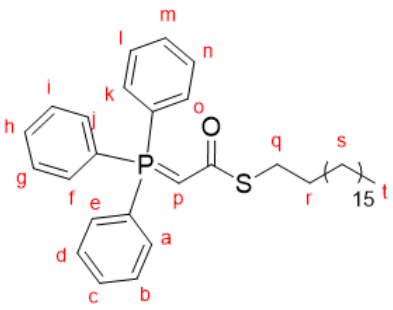

The obtained oil (8.80 g, 21.0 mmol) and triphenylphosphine (7.30 g, 28.0 mmol) in 120 mL of benzene was heated to reflux under nitrogen for one hour. The solvent was evaporated under reduced pressure to yield yellow-brown crystals after filtering and washing with toluene. The product was then dissolved in 150 mL of DCM and vigorously stirred with 150 mL of 10% aqueous K_2CO_3 solution for 40 min. The organic layer was separated and the aqueous layer was extracted twice with DCM. The combined organic phases were dried over magnesium sulfate and partially concentrated in *vacuo* and diluted in pentane which afforded 5c (7.50 g, 57%) of lightbrown crystals after 24h. **^{1}H NMR** ($CDCl_3$, 400 MHz) δ = 7.69-7.45 (m, 15, H_a - H_o), 3.66 (d, 1H, H_p), 2.85 (t, J = 7.2 Hz, 2H, H_q), 1.58 (q, 2H, H_r), 1.25 (m, 30H, H_s) and 0.89 (t, 3H, H_s).

2.4.3.7.3 Synthesis of *S*-Octadecyl prop-2-enethioat (11)

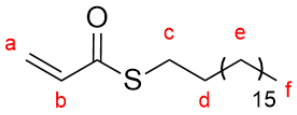

11c (5.00 g, 8.50 mmol) and paraformaldehyde (1.27 g, 42.5 mmol) were poured into a nitrogen flushed round botton flask. The mixture was heated for 1 hour under an atmosphere of argon at reflux temperature, then concentrated in *vacuo*. The crude product was dissolved in hexane and purified using silica column chromatography (90:10 hexane/ethylacetate) as a pale brown solid (1.30 g, 45% yield).

2.4.3.8 Experimental Procedure for *S*-Phenyl prop-2-enethioate (PhTA) monomer (12)

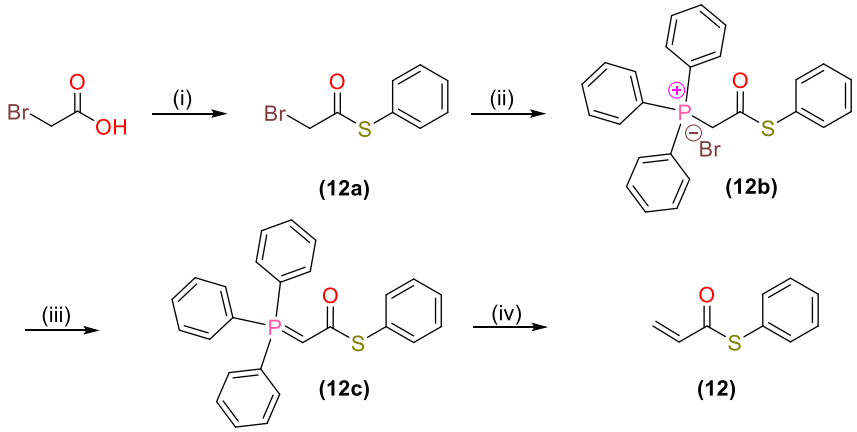

Scheme 2.16: Synthesis of S-Phenyl prop-2-enethioate (12), Reagents and conditions: (i) thiophenol, DCC/DMAP, CH_2Cl_2, 0 °C to rt, 16 h. (ii) Triphenylphosphine, benzene, reflux, 30 min. (iii) 10 wt% K_2CO_3, CH_2Cl_2, rt, 30 min. (iv) paraformaldehyde, CH_2Cl_2, reflux, 1 h.

2.4.3.8.1 Synthesis of *S*-phenyl 2-bromoethanethioate (12a)

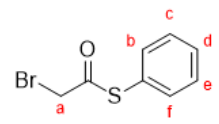

A two-necked 2-L round bottom flask was charged with bromoacetic acid (14.1 g, 0.10 mol), thiophenol (13.4 mL, 0.13 mol) and a catalytic amount of DMAP (1.26 g, 10.0 mmol). 300 mL of DCM was added and the solution was cooled to 0 C with stirring under an atmosphere of nitrogen. DCC (22.0 g, 0.11 mol) was diluted in 200 mL of DCM and added dropwise and the solution slowly warmed to room temperature overnight until esterification was complete. The solution was then filtered through Silica and the filtercake was washed several times with DCM. The filtrate was washed with saturated $NaHCO_3$ solution, water and brine and was dried over $Na2SO_4$. Evaporation of the solvent in *vacuo* gave (14.1 g, 42%) of a yellowish oil.**^{1}H NMR** ($CDCl_3$, 400 MHz) δ = 7.30-7.01 (br-m, 5H, H_b – H_f) and 3.94 (s, 2H, H_a).

2.4.3.8.2 Synthesis of (2-oxo-2-(phenylthiol)ethyl)triphenylphosphonium bromide (12b)

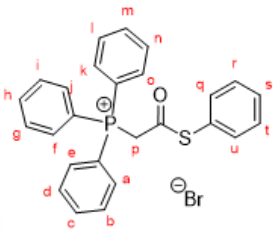

12a (13.9 g, 0.10 mol) and triphenylphosphine (5.13 g, 0.17 mol) in 75.0 mL of benzene was heated to reflux under nitrogen for one hour. The solvent was evaporated under reduced pressure to yield white crystals after filtering and washing with toluene. **^{1}H NMR** ($(CD_3)_2SO$, 400 MHz) δ = 7.91-7.78 (m, 15H, H_{a-o}), 7.47-7.36 (br-m, 5H, H_q – H_u) and 5.87 (d, J = 14.3 Hz, 2H, H_p).

2.4.3.8.3 Synthesis of S-phenyl 2-(triphenyl-λ^5-phosphanylidene)-ethanethioate (12c)

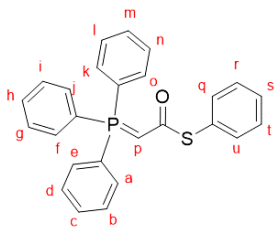

12b was then dissolved in 7.05 mL of DCM and vigorously stirred with 50.0 mL of 10% aqueous K_2CO_3 solution for 30 min. The organic layer was separated and the aqueous layer was extracted twice with DCM. The combined organic phases

were dried over magnesium sulfate and partially concentrated in *vacuo* and diluted in pentane which afforded (16.14 g, 44% yield) of light-brown crystals after 24h. **^{1}H NMR** ($(CD_3)_2SO$, 400 MHz) δ = 7.80-7.45 (m, 15H, $H_{a\text{-}o}$), 7.45-7.24 (br-m, 5H, H_q – H_u) and 3.52 (d, J = 22.1 Hz, 1H, H_p).

2.4.3.8.4 Synthesis of S-phenyl prop-2-enethioate (12)

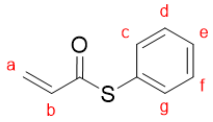

In a 1 L two-necked flask equipped with a cooling system and magnetic stirrer, of Wittig reagent 12c were introduced into 700 mL of DCM. Then, (4.59 g, 152 mmol) paraformaldehyde were poured into the solution. The mixture was heated for 1 hour under an atmosphere of argon then concentrated in *vauo* and the residue was suspended in cold pentane (50.0 mL) and filtered over silica. The filtercake was washed with cold (10:90 Et_2O/pentane). Hydrochinone was added to the solution to prevent polymerisation. The solution was distilled over CaH_2 (2 g/L) at reduced pressure to yield (3.20 g, 62% yield) of a colorless oil. **^{1}H NMR** ($(CD_3)_2SO$, 400 MHz) δ = 7.26 (m, 5H, H_c – H_g), 6.37 (dd, J = 10.4, 6.7 Hz, 1H, H_b) 6.13 (d, J = 17.2 Hz, 1H, H_{a1} and 5.72 (d, J = 10.4 Hz, 1H, H_{a2}). **^{13}C NMR** (101 MHz, $(CH_3)_2SO$, *δ*): 188.0, 135.1, 134.8, 130.1, 129, 129.1.

2.4.3.9 Synthesis of *S*-ethyl 2-(triphenyl-λ^5-phosphanylidene)propanethioate (14)

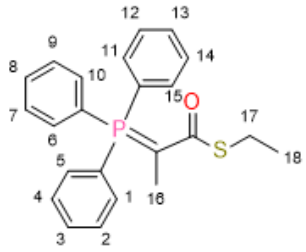

To the stabilised ylide 7b (14.9 g, 40.0 mmol), 120 mL dry DCM was added under an atmosphere of argon and was stirred at 0°C. CH_3I (3.83 mL, 61.0 mmol) in 25 mL dry DCM was added through an addition funnel and the solution was allowed to warm to room temperature overnight with continued stirring. 250 mL of a 10% aqueous K_2CO_3 was added to the solution and stirred for 30 minutes. The organic layer was separated and washed with water (3 x 100 mL) and dried over $MgSO_4$, and the solvent removed *in vacuo*. The resulting pale yellow solid was analysed by ESI MS. m/z^{theo} 365.11.

2.4.3.10 Synthesis of ethyl thiomethacrylate (ETMA) (15)

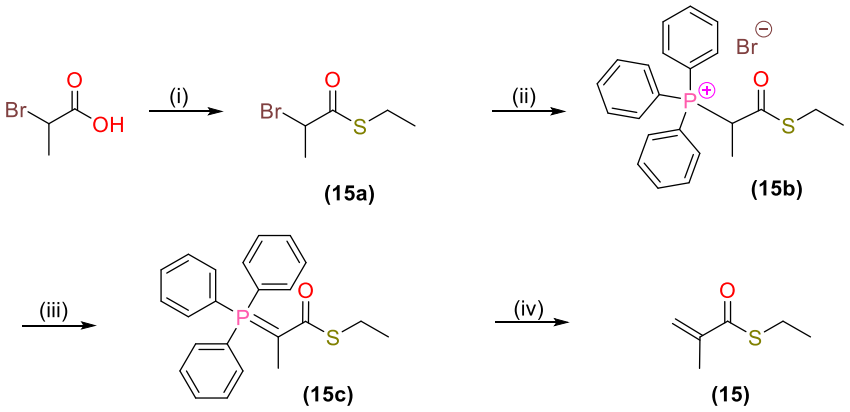

Scheme 2.14: General synthetic scheme, exemplifying chemical synthesis of ethyl thiomethacrylate monomer 15.

2.4.3.10.1 Synthesis of S-ethyl 2-bromopropanethioate (15a)

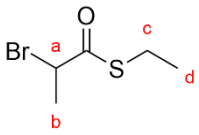

Bromopropionic acid (45.0 mL, 500 mmol), DMAP (6.10 g, 50.0 mmol) and ethanethiol (57.0 mL, 772 mmol) were mixed in 200 mL DCM in a 500 mL 2 neck round bottom flask and the solution was cooled to 0°C with stirring under an atmosphere of nitrogen. DCC (108 g, 524 mmol) was diluted in 200 mL of DCM and added dropwise and the solution slowly warmed to room temperature overnight until esterification was complete. The solution was then filtered and the filtrate was washed with saturated $NaHCO_3$ solution, water and brine and was dried over Na_2SO_4. Evaporation of the solvent in *vacuo* gave (75.19 g, 74%) of a brown oil. (**^{1}H NMR** ($CDCl_3$, 400 MHz) δ = 4.45 (q, J = 6.9 Hz, 1H, H_a), 2.87 (q, J = 7.4 Hz, 2H, H_c), 1.77 (d, J = 6.9 Hz, 3H, H_b) and 1.22 (t, J = 7.47 Hz, 3H, H_d).

2.4.3.10.2 Synthesis of (1-(ethylthio)-1-oxopropan-2-yl)triphenylphosphonium bromide (15b)

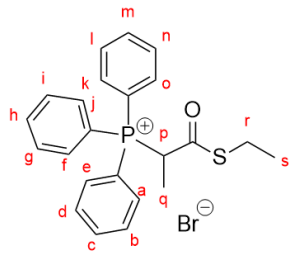

15a (71.3 g, 360 mmol) and triphenylphosphine (104 g, 400 mmol) in 500 mL of benzene was heated to reflux under nitrogen for 24 h. The solvent was evaporated under reduced pressure to yield white crystals after filtering and washing with toluene.

2.4.3.10.3 Synthesis of S-ethyl 2-(triphenyl-λ^5-phosphanylidene)propanethioate (15c)

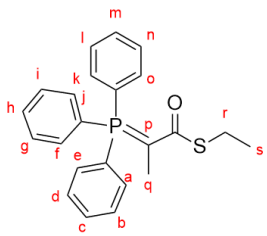

15b was then dissolved in 150 mL of DCM and vigorously stirred with 150 mL of 10% aqueous K_2CO_3 solution for 40 min. The organic layer was separated and the aqueous layer was extracted twice with DCM. The combined organic phases were dried over magnesium sulfate and partially concentrated in *vacuo* and diluted in cyclohexane which afforded 14c (98.95 g, 72%)

of lightbrown crystals after 24h. **^{1}H NMR** ($CDCl_3$, 400 MHz) δ = 7.70-7.45 (m, 15H, H_{a-o}), 2.65 (q, J = 7.4, 2H, H_r), 1.68 (d, J = 15.1, 3H, H_q) and 1.24 (t, J = 7.3, 3H, H_S).

Synthesis of *S*-ethyl 2-methylprop-2-enethioate (15)

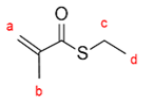

15c (9.15 g, 24.0 mmol) and paraformaldehyde (3.63 g, 121 mmol) were poured into a nitrogen flushed round botton flask. The mixture was heated for 1 hour under an atmosphere of argon at reflux temperature, then concentrated in *vacuo*. The crude product was dissolved in hexane and purified using silica column chromatography (90:10 hexane/ethylacetate) as a pale brown solid (2.4 g, 77% yield). **^{1}H NMR** ($CDCl_3$, 400 MHz) δ = 6.07 (s, 1H, H_{a1}), 5.56 (s, 1H, H_{a2}), 2.93 (t, J = 7.4, 2H, H_c), 1.29 (3H, H_b) and 0.90 (3H, H_d).

Characterisation of compounds

8a

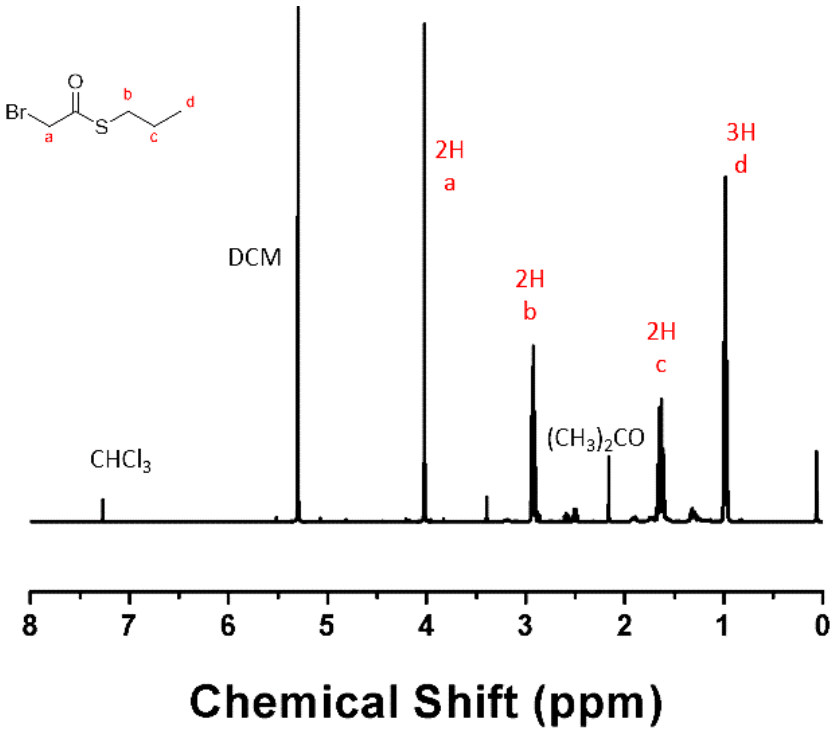

Figure 2.11: ^{1}H NMR spectrum ($CDCl_3$, 400 MHz, 303 K) of **8a**

8b

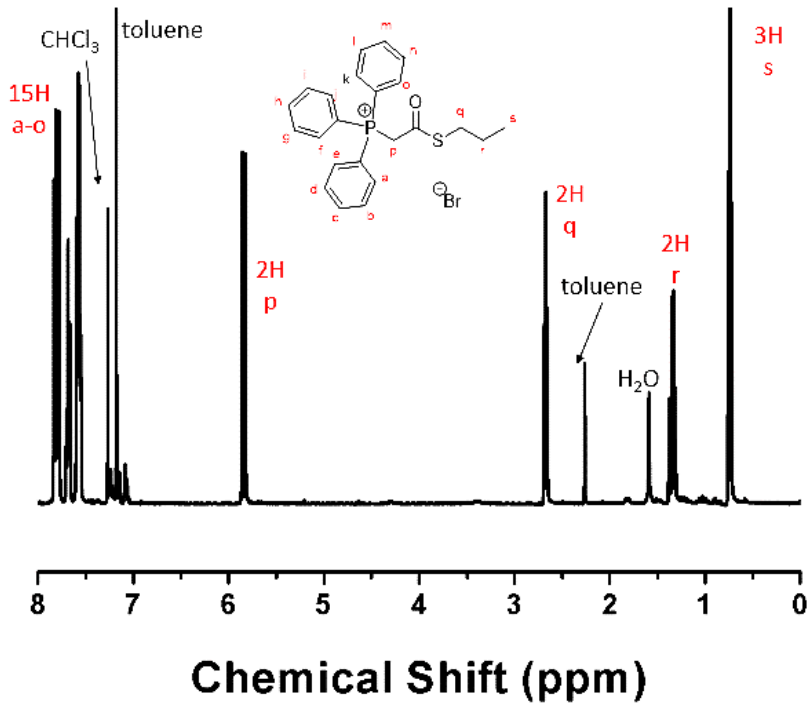

Figure 2.12: ^{1}H NMR spectrum ($CDCl_3$, 400 MHz, 303 K) of **8b.**

8c

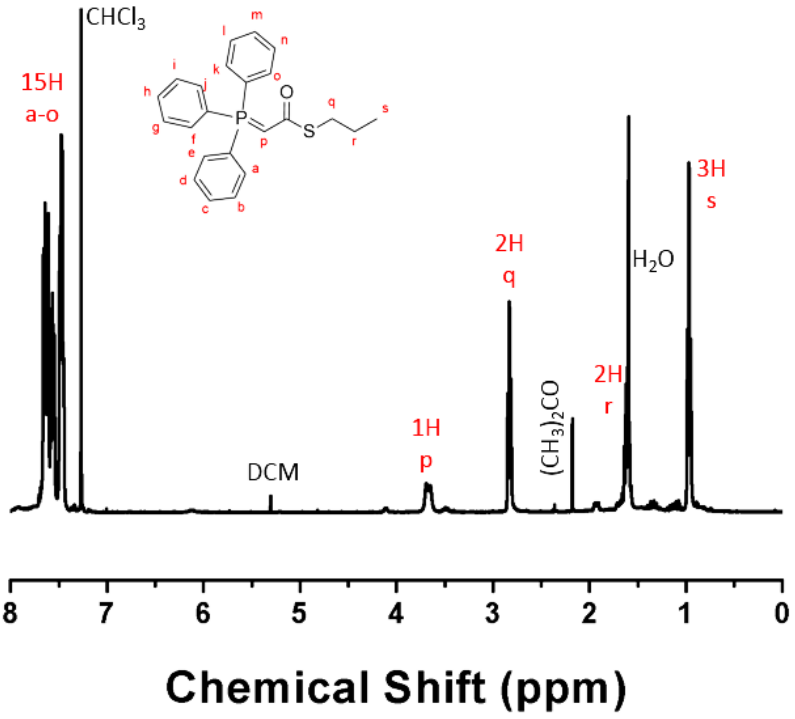

Figure 2.13: ^{1}H NMR spectrum ($CDCl_3$, 400 MHz, 303 K) of **8c.**

8

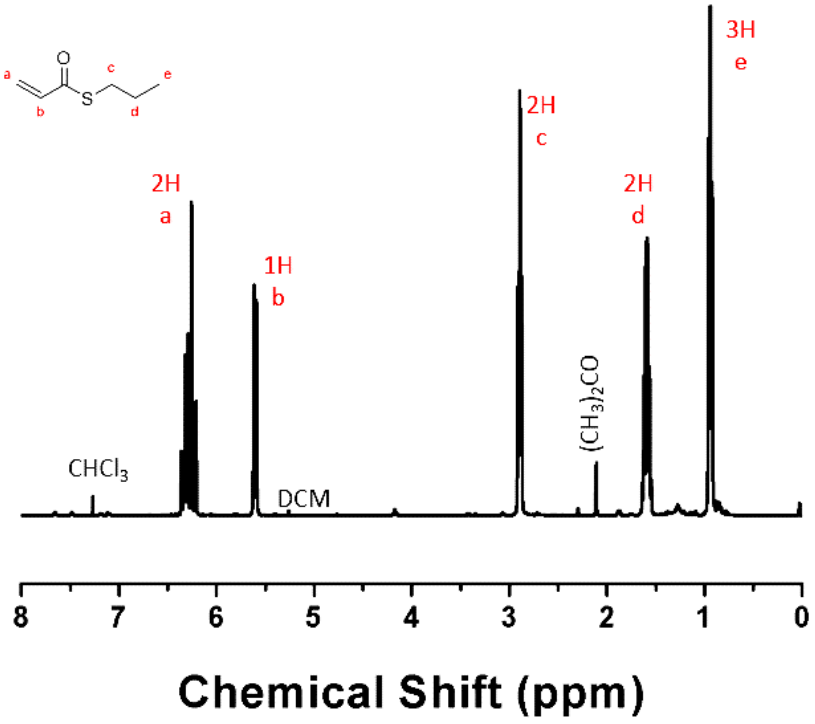

Figure 2.14: ^{1}H NMR spectrum ($CDCl_3$, 400 MHz, 303 K) of **8.**

9a

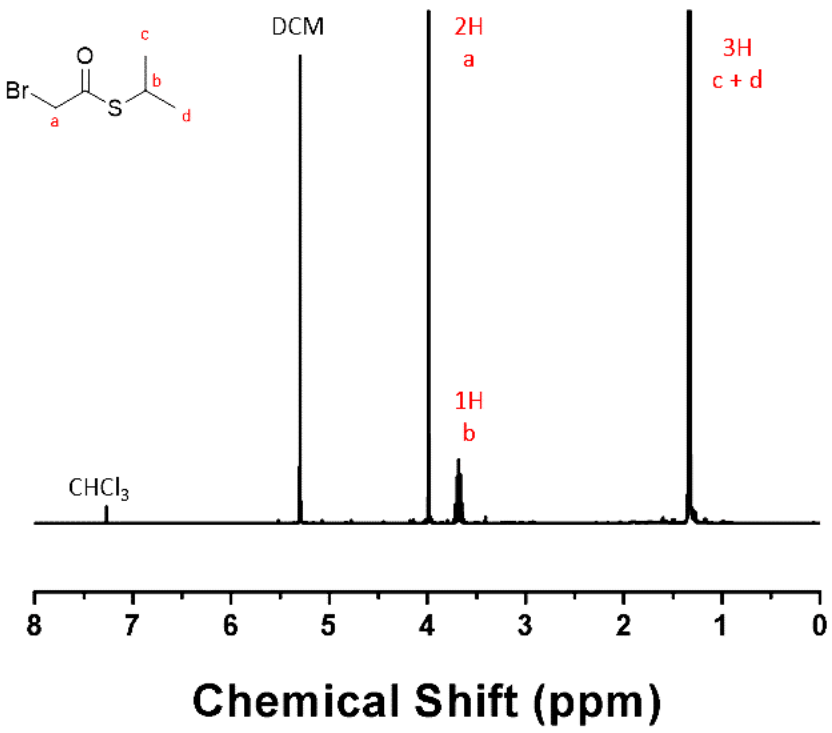

Figure 2.15: ^{1}H NMR spectrum ($CDCl_3$, 400 MHz, 303 K) of **9a.**

9b

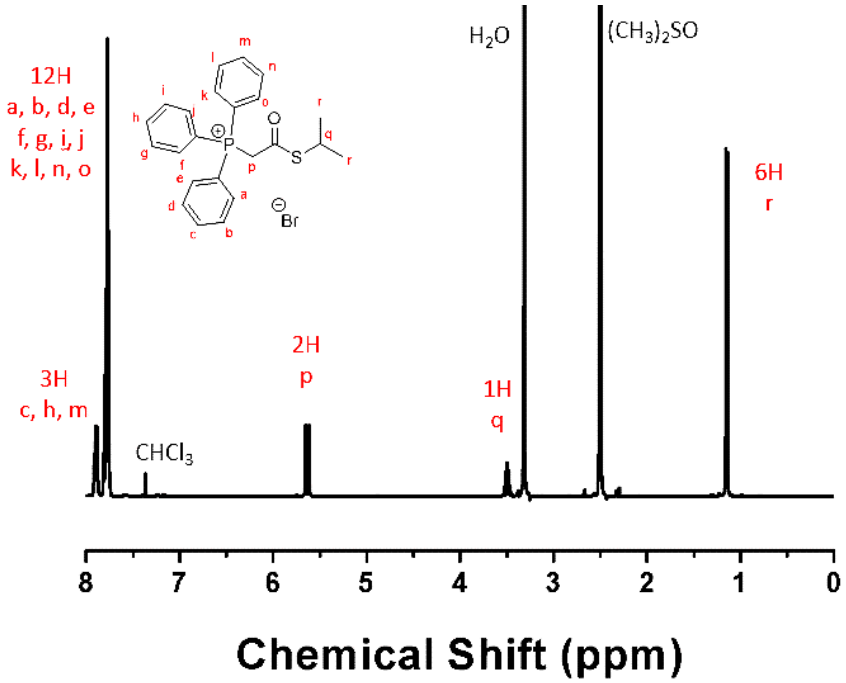

Figure 2.16: ^{1}H NMR spectrum ($CDCl_3$, 400 MHz, 303 K) of **9b.**

9c

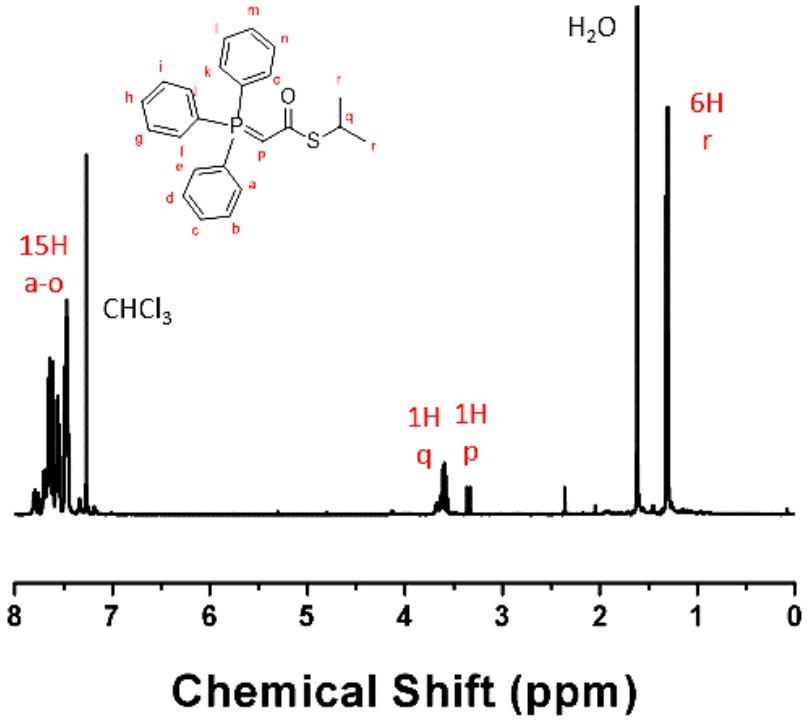

Figure 2.17: ^{1}H NMR spectrum ($CDCl_3$, 400 MHz, 303 K) of **9c.**

9

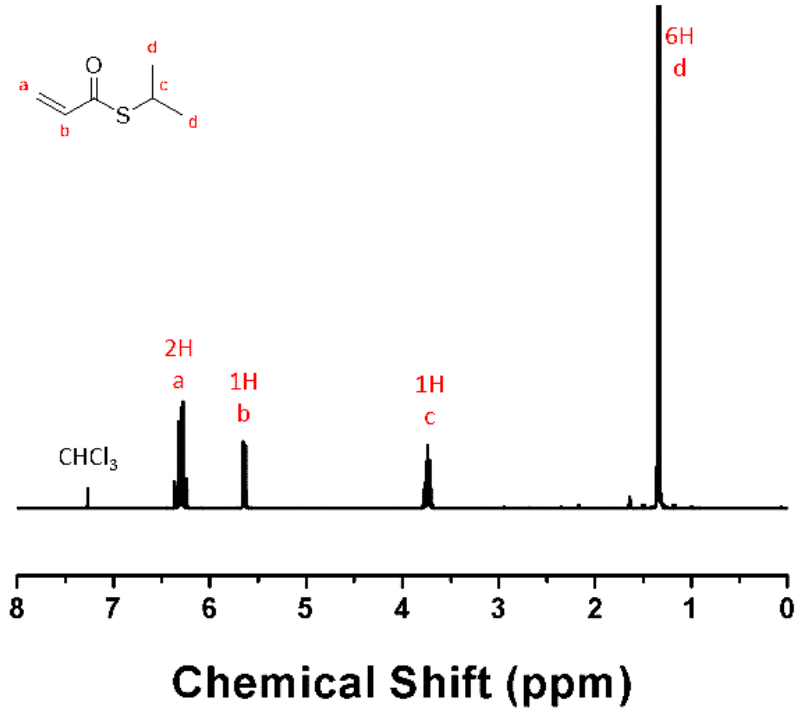

Figure 2.18: ^{1}H NMR spectrum ($CDCl_3$, 400 MHz, 303 K) of **9.**

9

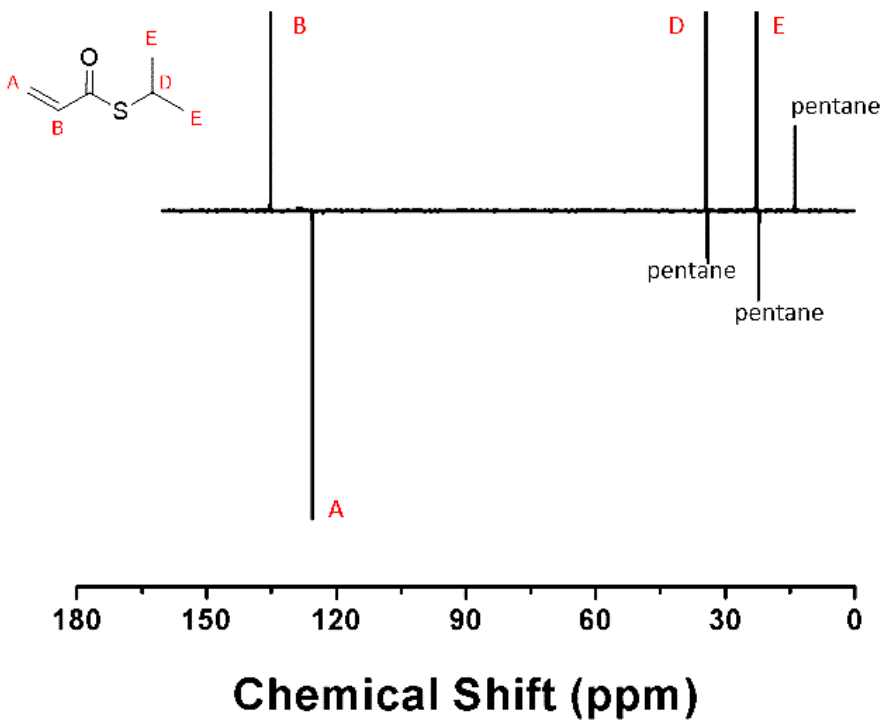

Figure 2.19: ^{13}C NMR spectrum ($CDCl_3$, 400 MHz, 303 K) of **9.**

10

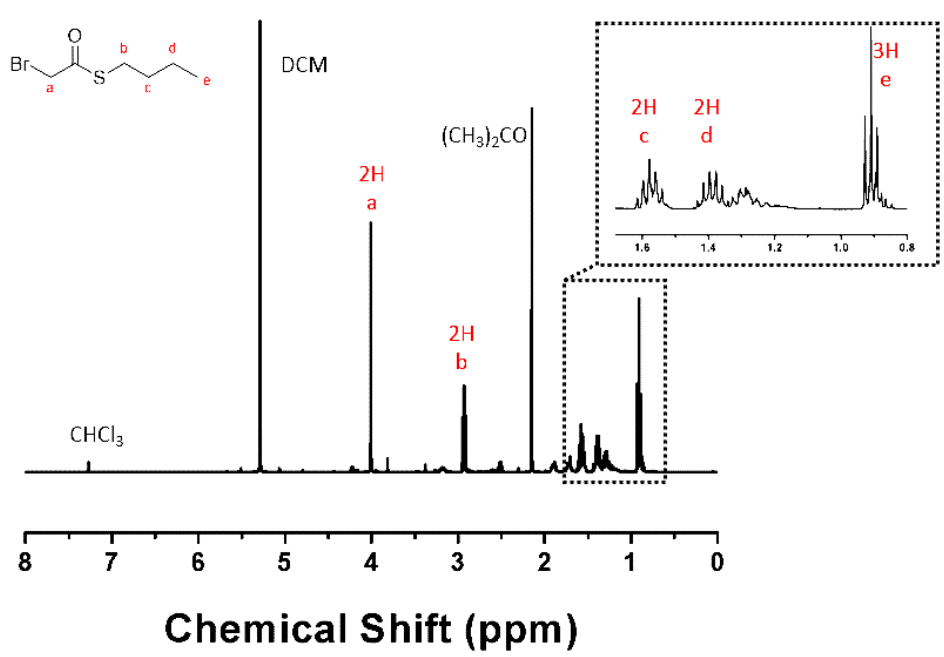

Figure 2.20: ^{1}H-NMR spectrum ($CDCl_3$, 400 MHz, 303 K) of **10**.

10a

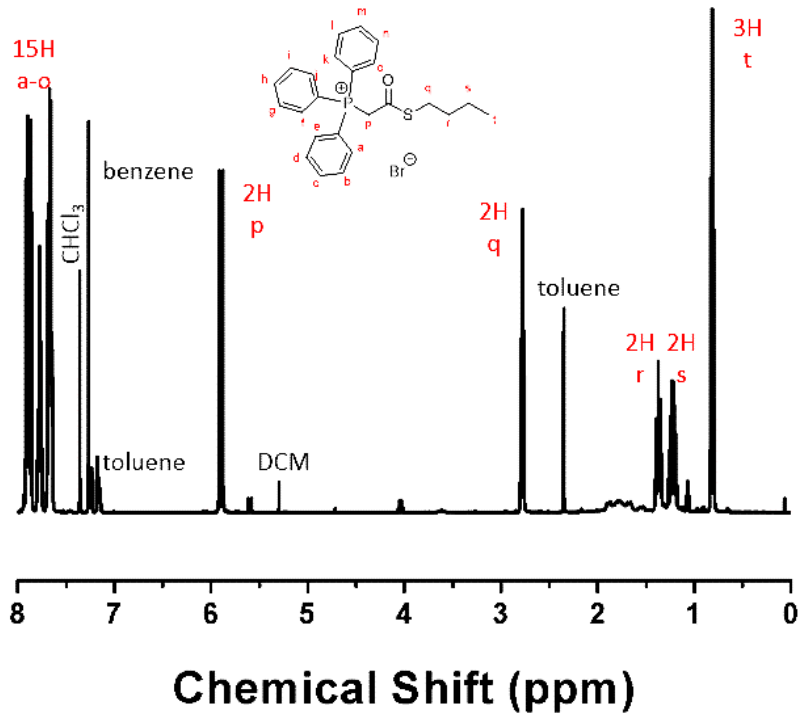

Figure 2.21: ^{1}H-NMR spectrum ($CDCl_3$, 400 MHz, 303 K) of **10a**.

10b

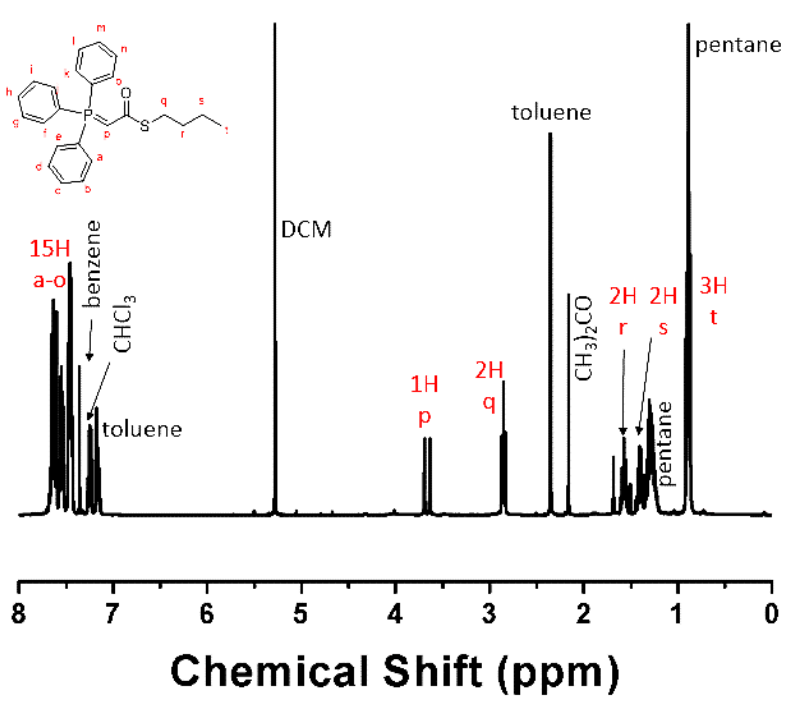

Figure 2.22: ^{1}H-NMR spectrum ($CDCl_3$, 400 MHz, 303 K) of **10b**.

10

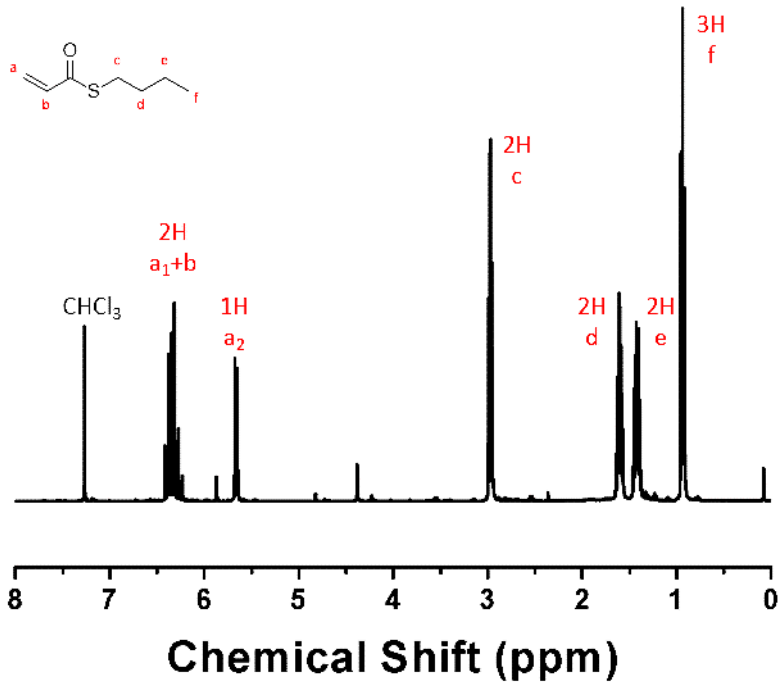

Figure 2.23: ^{1}H-NMR spectrum ($CDCl_3$, 400 MHz, 303 K) of **10**.

10

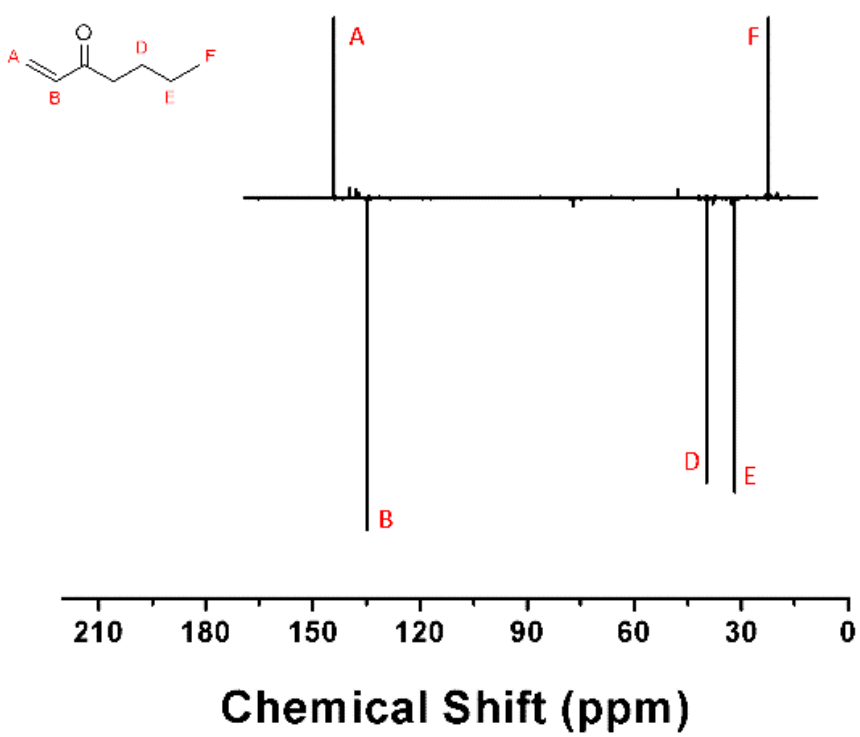

Figure 2.24: ^{13}C NMR spectrum ($CDCl_3$, 101 MHz, 303 K) of **10.**

11a

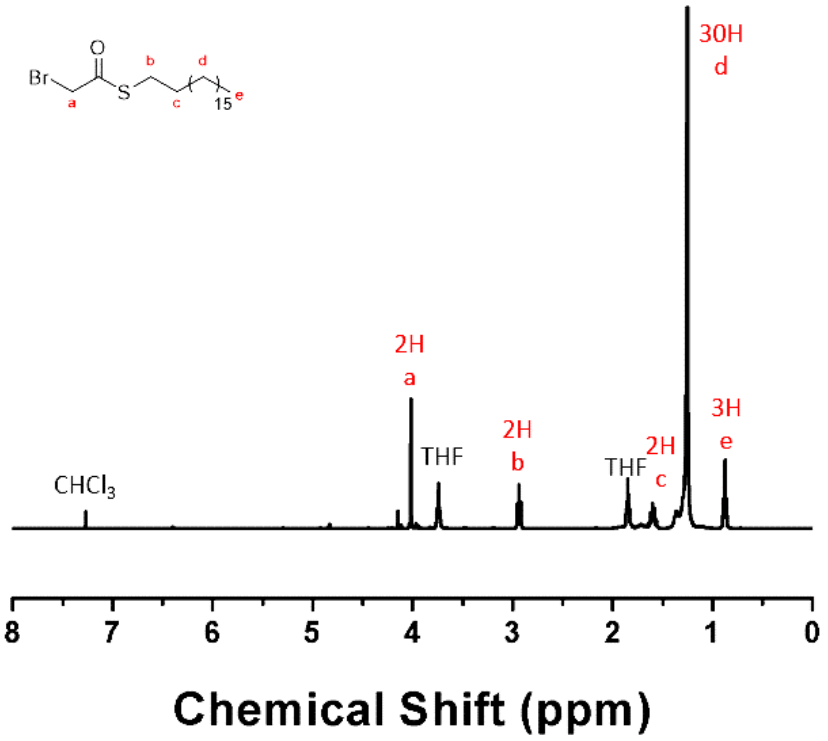

Figure 2.25: ^{1}H NMR spectrum ($CDCl_3$, 400 MHz, 303 K) of **11a.**

11b

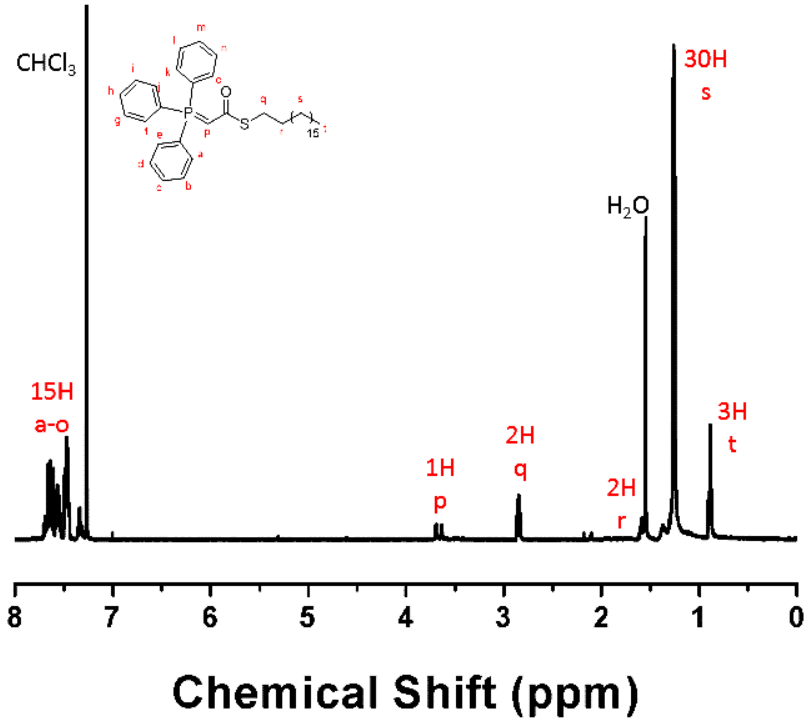

Figure 2.26: ^{1}H NMR spectrum ($CDCl_3$, 400 MHz, 303 K) of **11b.**

11

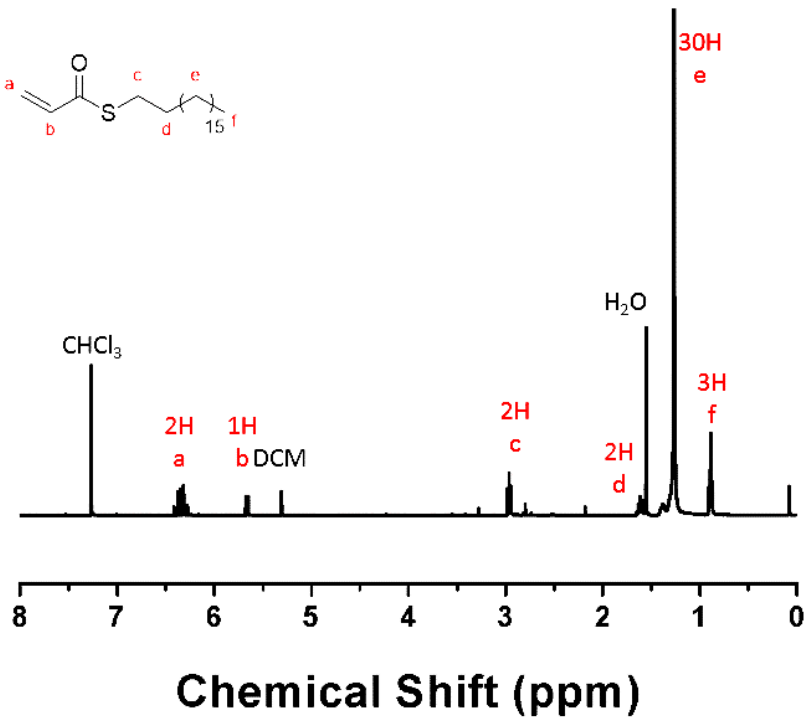

Figure 2.27: ^{1}H-NMR spectrum ($CDCl_3$, 400 MHz, 303 K) of **11**.

12a

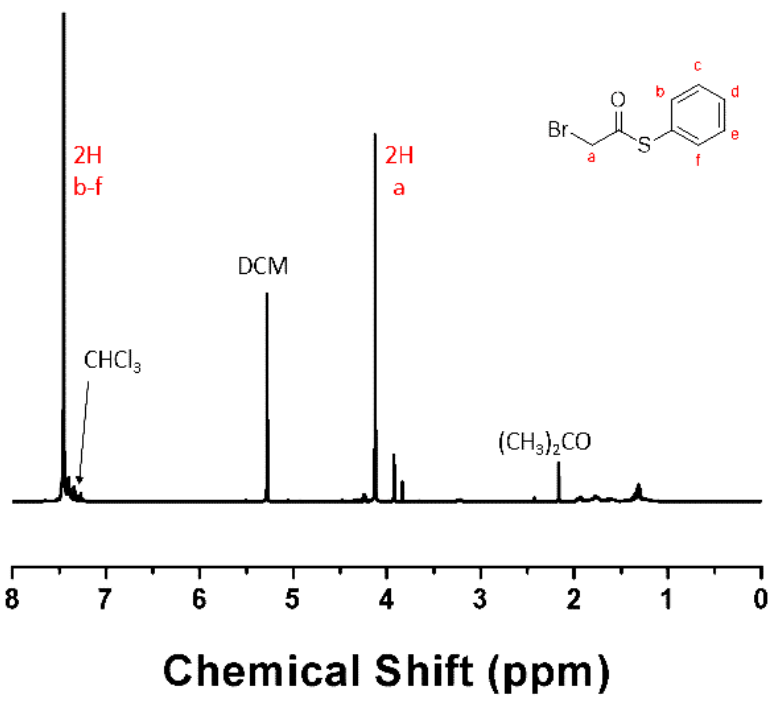

Figure 2.28: ^{1}H NMR spectrum ($CDCl_3$, 400 MHz, 303 K) of **12a**.

12b

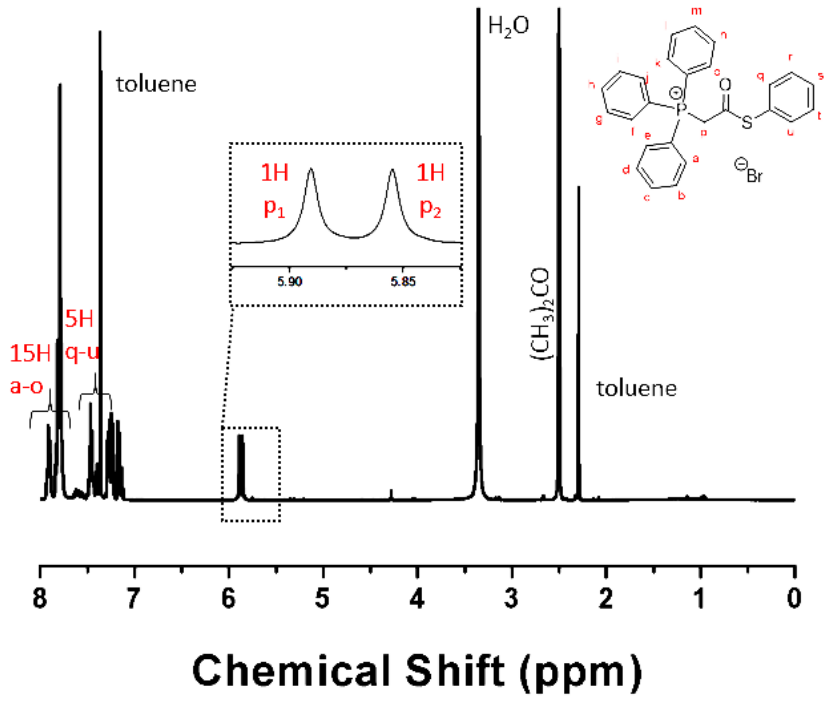

Figure 2.29: ^{1}H NMR spectrum $(CD_3)_2SO$, 400 MHz, 303 K) of **12b**.

12c

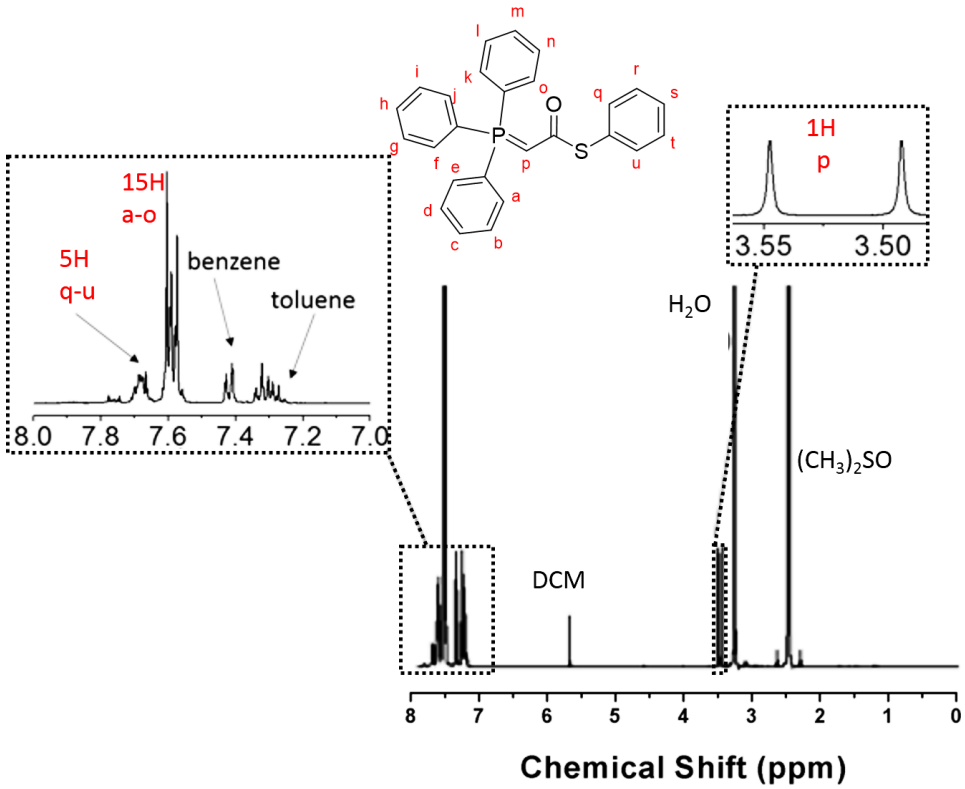

Figure 2.30: ^{1}H NMR spectrum $(CD_3)_2SO$, 400 MHz, 303 K) of **12c**.

12

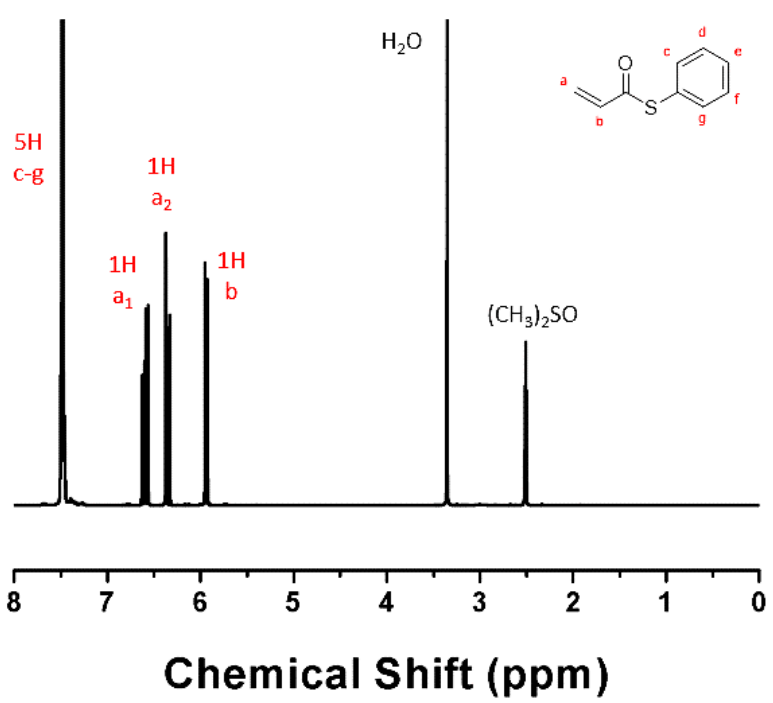

Figure 2.31: ^{1}H NMR spectrum $(CD_3)_2SO$, 400 MHz, 303 K) of **12**.

12

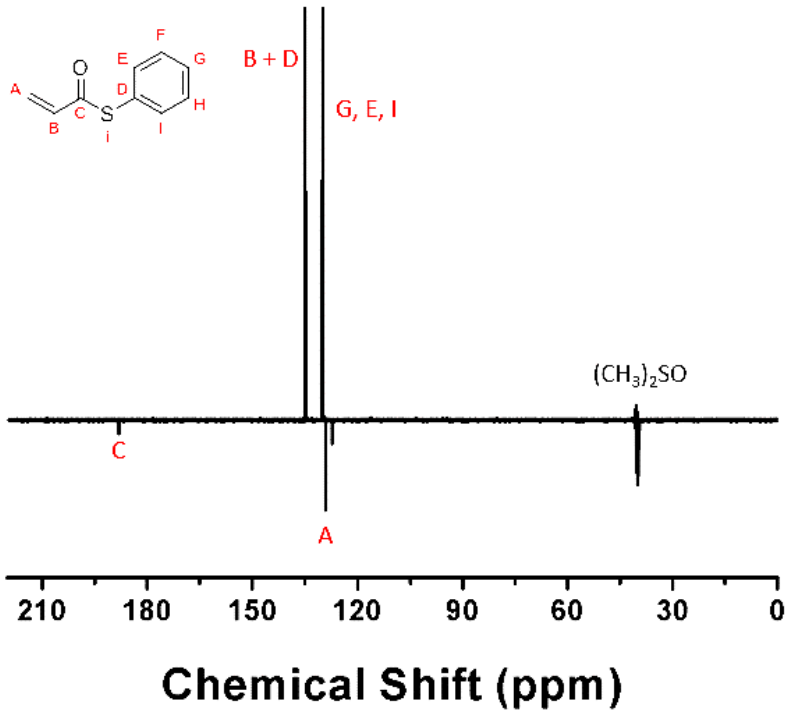

Figure 2.32: ^{13}C NMR spectrum $(CD_3)_2SO$, 101 MHz, 303 K) of **12.**

2.5 References

1. H. E. Suess and H. C. Urey, *Reviews of Modern Physics*, 1956, **28**, 53-74.
2. I. V. Koval, *Russ. J. Organ. Chem.*, 2005, **41**, 631-648.
3. G. Lowe, *Tetrahedron*, 1976, **32**, 291.
4. C. de Duve, *American Scientist*, 1995, **83**, 428.
5. G. Wächtershäuser, *Prog. Biophys. molec. Biol.*, 1992, **58**, 85-201.
6. P. Bracher, P. Snyder, B. Bohall and G. Whitesides, *Orig Life Evol Biosph*, 2011, **41**, 399-412.
7. I. V. Koval, *Usb. Khim.*, 1993, **62**, 813.
8. I. V. Koval, *Zh. Organ. Khim*, 1995, **31**, 961.
9. S. Onbulak, S. Tempelaar, R. J. Pounder, O. Gok, R. Sanyal, A. P. Dove and A. Sanyal, *Macromolecules*, 2012, **45**, 1715-1722.
10. S. Bonengel and A. Bernkop-Schnuerch, *J. Control Release* 2014, **195**, 120-129.
11. Y. Iwakura, K. Kurita and F. Hayano, *Journal of Polymer Science Part A-1: Polymer Chemistry*, 1969, **7**, 3075-3087.
12. K. Nakabayashi, A. Matsumura, Y. Abiko and H. Mori, *Macromolecules*, 2016, **49**, 1616-1629
13. Y. Qiao, X. Yin and C. Tang, *Science China Chemistry*, 2015, **58**, 1641-1650.
14. C. Zhao, Y. Zhang, S. Pan, L. Rothberg and M.-K. Ng, *Macromolecules*, 2007, **40**, 1816-1823.
15. S. Reinicke, P. Espeel, M. M. Stamenovic and F. E. Du Prez, *Polym. Chem.*, 2014, **5**, 5461-5470.
16. S. Pfeiffer and J.-F. Lutz, *J. Am. Chem. Soc.*, 2007, **129**, 9542-9543.
17. M. Ouchi, N. Badi, J.-F. Lutz and M. Sawamoto, *Nature Chem.* , 2011, **3**, 917-924.
18. W. Reppe, *Experientia*, 1949, **5**, 93-110.
19. E. J. Kelley, U.S. Patent 2888480A, 1959
20. J. Du and T. P. Yoon, *J. Am. Chem. Soc.*, 2009, **131**, 14604-14605.
21. L. A. Mikeska, U.S. Patent 2, 475, 246, 1949,

22. C. S. Marvel, S. L. Jacobs, W. K. Taft and B. G. Labbe, *Journal of Polymer Science*, 1956, **19**, 59-72.

23. L. R. Fedor, *J. Am. Chem. Soc.*, 1969, **91**, 913-917.

24. N. Hadjichristidis, *Macromolecules*, 1981, **14**, 128-130.

25. N. Hadjichristidis, *Polymer*, 1981, **22**.

26. C. L. Rigby and D. J. Dixon, *Chemical Communications*, 2008, 3798-3800

27. R. Fausto, P. J. Tonge and P. R. Carey, *Journal of the Chemical Society, Faraday Transactions*, 1994, **90**, 3491-3503.

28. R. Haynes, S. Vonwiller, J. Stokes and L. Merlino, *Australian Journal of Chemistry*, 1988, **41**, 881-895.

29. G. Zhou, J. M. Yost, S. J. Sauer and D. M. Coltart, *Org. Lett.*, 2007, **9**, 4663-4665.

30. E. Schaumann and B. Mergardt, *Journal of the Chemical Society, Perkin Transactions 1*, 1989, 1361-1363.

31. G. Braude, *J. Org. Chem.*, 1957, **22**, 1675-1678.

32. B. E. Maryanoff and A. B. Reitz, *Chem. Rev.*, 1989, **89**, 863.

33. G. Wittig and G. Geissler, *Justus Liebig ann. Chem.*, 1953, **580**.

34. M. G. Russel and S. Warren, *J. Chem. Soc., Perkin Trans.*, 2000, 505.

35. G. E. Keck, E. P. Boden and S. A. Mabury, *J. Org. Chem.*, 1985, **50**, 709-710.

36. B. Neises and W. Steglich, *Angew. Chem. Int. Ed.*, 1978, **17**, 522-524.

37. P. A. Byrne and D. G. Gilheany, *Chem. Soc. Rev.*, 2013, **42**, 6670-6696.

38. G.-Z. Li, R. K. Randev, A. H. Soeriyadi, G. Rees, C. Boyer, Z. Tong, T. P. Davis, C. R. Becer and D. M. Haddleton, *Polym. Chem.*, 2010, **1**, 1196-1204.

39. A. W. van Zijl, A. J. Minnaard and B. L. Feringa, *J. Org. Chem.*, 2008, **73**, 5651-5653.

40. R. Salem, *Anionic activation of the Wittig reaction using a solid-liquid phase transfer: Examination of the medium-, temperature-, base- and phase-transfer catalyst effects*, 2006.

41. G. Wittig and M. Rieber, *Justus Liebigs Annalen der Chemie*, 1949, **562**, 177-186.

42. G. Märkl, *Chemische Berichte*, 1961, **94**, 3005-3010.

Chapter 3

3 Polymerisation of thio(meth)acrylate monomers

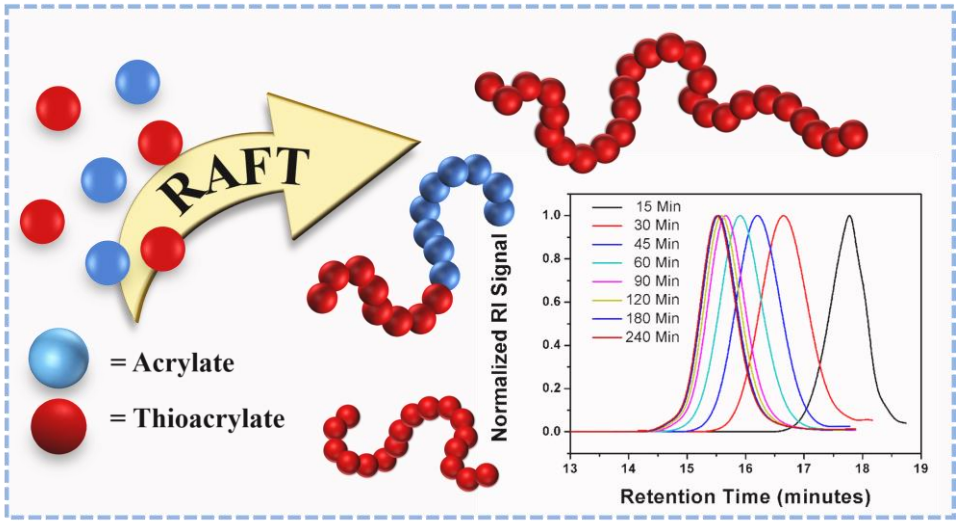

Herein, we present the controlled radical polymerisation of thioacrylates for the first time. Four different thioacrylate (TA) monomers namely, ethyl thioacrylate, phenyl thioacrylate, n-propyl thioacrylate and isopropyl thioacrylate have been polymerised via RAFT polymerisation. A trithiocarbonate chain transfer agent was utilised to control the molar mass and dispersity of thioacrylate polymers. Homopolymers of thioacrylates with different degrees of polymerisations were prepared and their block copolymerisations were studied with ethylacrylate and thioacrylates. Initial screening of suitable RAFT agents for the homopolymerisation of ethylthio methacrylate was additionally performed. Obtained polythioacrylates were analysed in detail using GPC, NMR, TGA, DSC and water contact angle.

Parts of this chapter have been published;

S. Aksakal, C.R. Becer, *Polym. Chem.*, 2016, **7**, 7011-7018

3.1 Introduction

Sulfur-containing polymers are attractive materials within the polymer chemistry field, due to their remarkable features that determine their outstanding properties. The presence of sulfur in polymer structures enhances a wide variety of material properties such as mechanical, electrical, optical, adhesion, heat resistance, and biocompatibility.[1-4] Thiols are known as softer nucleophiles in comparison to alcohols and amines and are able to form disulphide bonds, which can be further used as a reactive group. Due to their numerous advantages over their non-functionalised counterparts, thiol-containing polymers open new avenues for advanced functional materials. Detailed studies on various molecular designs including pendant groups, chain end functionalisation, graft and hyperbranched polymers have been reported to fine-tune their physical properties. For instance, much effort has been devoted for the preparation of thiol-containing monomers that consist of either free thiols in the side chain or in heterocyclic systems (e.g. thiomers[5], thiazoline[6], thiazole[7], thiophene[8, 9] or thiolactones[3]).

Sulfur containing polymers are of significant interest for researchers and form the basis of an emerging platform in material science.[10] Unfortunately, due to their relatively high reactivity, thiol containing monomers are known to be incompatible with most polymerisation techniques as they are prone to undergo chain transfer reactions with monomers, active species or even catalysts. Protection and deprotection of the thiol group becomes therefore necessary in order not to induce transfer reactions during polymerisation and also to improve their storage, as they are not stable under oxidative conditions. Mostly because of these reasons very few examples have been reported to date. Three main synthetic routes can be listed for the preparation of thiol containing polymers. The first one is by polymerisation of monomers with protected thiols as pendant groups.[11, 12] Polymerisation of thiol monomers, which does not have to be protected under specific conditions, can also be carried out, especially with polycondensation.[13] The synthesis of linear polymers with secondary thiols as pendant group have been shown by *Matsumara et al.* by taking the advantage of highly selective biological processes between hydroxyl and mercapto groups

using a lipase enzyme.[14] Furthermore, linear polythiols have been prepared by metal catalysis of polyesters with pendant mercapto groups from the reaction of diols and thiomalic acid in the presence of scandium(III) triflate. Subsequent functionalisation by thiol-ene glycosidation or crosslinking with 1,1'-thiocarbonyldiimidazole leads to linear polythiols.[15] The final route is based on the Sol-gel process that was also successfully used for the reaction of dimethoxysiloxane with free thiols as pendant group in acidic medium, to synthesise co(polymers) carrying thiol moieties.[16] The most widely applied utilisation of polythiols is based on the post-polymerisation modification, which has been demonstrated for thiolated polymers (thiomers) for mucoadhesive drug delivery, generally carried out *via* thiol Michael addition.[17]

The synthesis and free radical polymerisation of a couple of thioacrylate monomers was first described in 1956, when *Marvel* prepared a range of thioacrylates by the reaction of 2,3-dibromopropionyl chloride with thiols and subsequent treatment with sodium iodide for dehalogenation.[18] In this way, methyl, ethyl, *n*-propyl, isopropyl, *n*-butyl, isobutyl and *tert*-butyl thioacrylates with an over-all yield of 25-45% were obtained. These monomers were further analysed *via* IR. Free radical polymerisation was carried out in bulk using benzoyl peroxide as initiator. Conversions were calculated to be between 33-73%. Another example for the preparation of thio methacrylates was published in 1977 by *Hadjichristidis.*[19, 20] This article elucidated higher chain flexibility of polythio methacrylates compared to their polymethacrylate counterparts. Monomers were obtained by the reaction of methacryloylchloride with thiols in an aqueous sodium hydroxide solution and repeated distillation. Their free radical polymerisation was followed with AIBN. Furthermore, copolymerisation with styrene *via* free radical polymerisation has been investigated by *Otsu et al.*.[21] Relative reactivity values for different ester alkyl groups in thioacrylates for their copolymerisation with styrene was found higher compared to copolymerisation with similar alkylacrylates. Even polymerisation with some anionic catalysts (*e.g. n*-BuLi, PhMgBr, $LiAlEt_3Bu$) has been studied for ethyl, *n*-propyl, isopropyl, *n*-butyl, isobutyl, *sec*- and *tert*-butyl thioacrylates[22] and for methylthio methacrylate respectively[23]. However, neither their controlled polymerisation nor their complete physical properties were investigated so far. The fundamental interest on the synthesis and

polymerisation of thioacrylate monomers and their physical properties are still very limited, although the introduction of thioesters or thiol groups could bring unique functionalities to the macromolecules. Transformation of thioester groups *via* post-polymerisation modification (PPM), would for example allow selective functionalisation into other functional moieties.

For instance, one of the main versatility of thioesters, are reversible trans-thioesterification reactions for generation of higher order structures in peptides or proteins. In consideration to post polymerisation functionalisation, thioester containing peptides can participate in a native chemical ligation (NCL) reaction to generate a peptide bond from an *n*-terminal cysteine containing peptide under mild conditions in the presence of a thiol.[24] These and other promising properties of thioesters point to the use in novel unexplored applications in material science and for this reason there has been a drive towards the development of a synthetic strategy for the syntheses of thioacrylate monomers.

Recent progress in living radical polymerisation has started a new era of well-defined polymers *via* well-known controlled radical polymerisation techniques such as single electron transfer-living radical polymerisation (SET-LRP)[25-27], nitroxide mediated polymerisation (NMP)[28-32], atom transfer radical polymerisation (ATRP)[33-35] and reversible addition-fragmentation chain transfer (RAFT) polymerisation[36-38]. The latter was introduced in 1998 and has revolutionised the field of polymer synthesis since then.[39] The main advantage of RAFT polymerisation is the possibility of polymerising a wide range of monomer classes under appropriate choice of reagents and polymerisation conditions. As this process enables access to polymerise a wide range of monomers and in addition tolerates many functional groups, RAFT polymerisation is preferred to prepare well-defined poly(thioacrylate)s in this study.

Within this chapter, an easy and efficient method for the preparation of aliphatic and aromatic thio(meth)acrylate monomers that will potentially generate a high level of interest and novel applications in material science is described. Additionally, the polymerisation of these monomers *via* a controlled radical polymerisation technique is investigated for the first time. Detailed kinetic studies under different reaction conditions have been performed and the

obtained poly(thioacrylate)s are characterised in detail by ^{1}H NMR, GPC, water contact angle. In addition, their thermal stability and transitions were determined using TGA and DSC.

3.2 Results and Discussion

3.2.1 RAFT polymerisation of thioacrylate monomers

The polymerisation of thioacrylates have been investigated using a trithiocarbonate ester chain transfer agent (CTA), namely butyl 2-(((dodecylthio)carbonothioyl)thio)2-methyl propanoate (BDTMP), which enables polymerisation of a wide variety of functional monomers, including acrylates and acrylamides. To identify optimised conditions for the preparation of well-defined polymers, the polymerisation kinetics of chosen thioacrylates *via* RAFT was studied. The thioacrylates used in this polymerisation are listed in **Figure 3.1**.

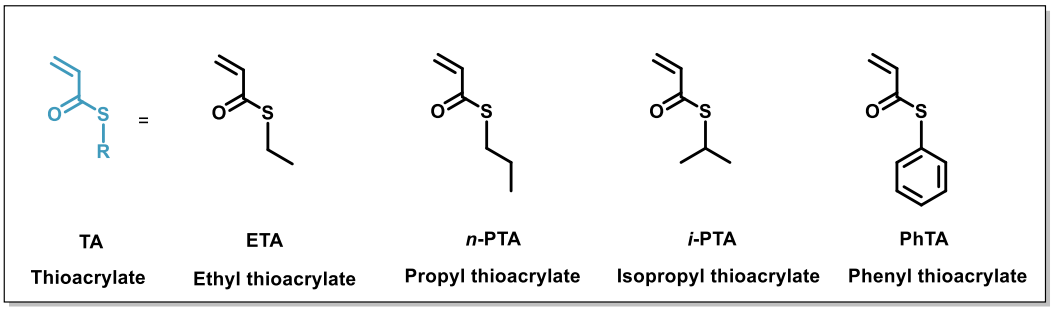

Figure 3.1: Thioacrylate monomers used for the polymerisation *via* RAFT.

The homopolymerisation of ETA, PhTA, *n*-PTA and *i*-PTA using BDTMP as the CTA were studied, examining the influence of several experimental parameters on the rate of polymerisation, the influence of initiator concentration and the influence of degree of polymerisation

The overall conditions for the RAFT homopolymerisation of thioacrylates are shown below in **Scheme 3.1.**

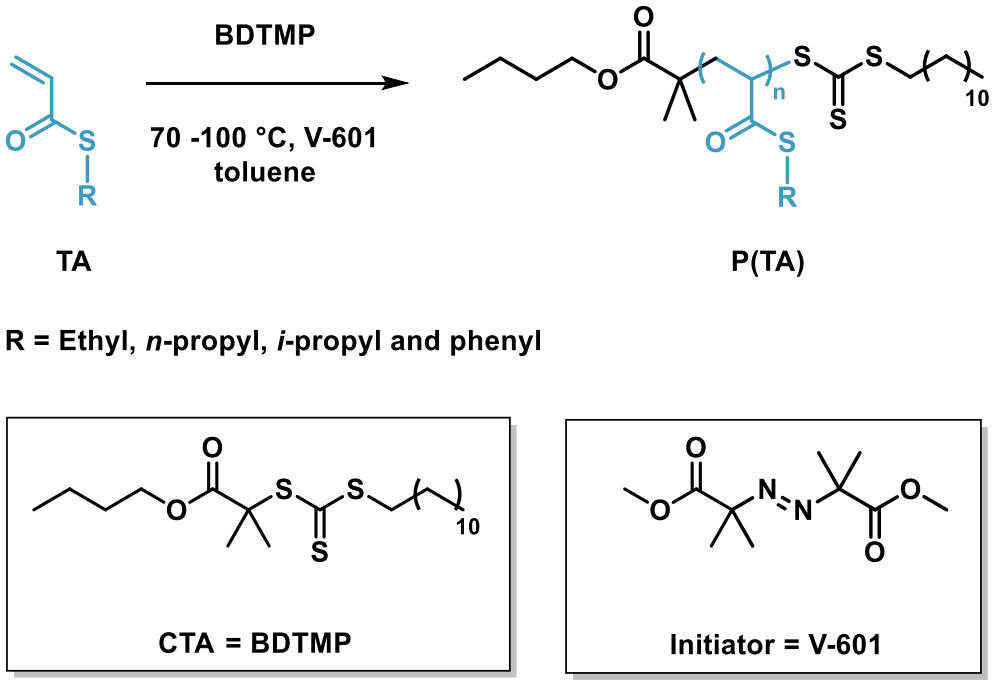

Scheme 3.1: Schematic for the synthetic pathway of RAFT polymerisation of thioacrylate monomers: $[CTA]_0$: $[V\text{-}601]_0$ = 10 in toluene at 70 and 100 °C.

3.2.2 Homopolymerisation

Homopolymerisation was first attempted using 3-butyl-2-(dodecylthiocarbonothioylthio)-2-methylpropionate (BDTMP, 1 eq.) as RAFT agent and Dimethyl 2,2′-azobis(isobutyrate) (V-601, 0.10 eq.) as initiator in toluene at 70 °C (**Scheme 3.2**).

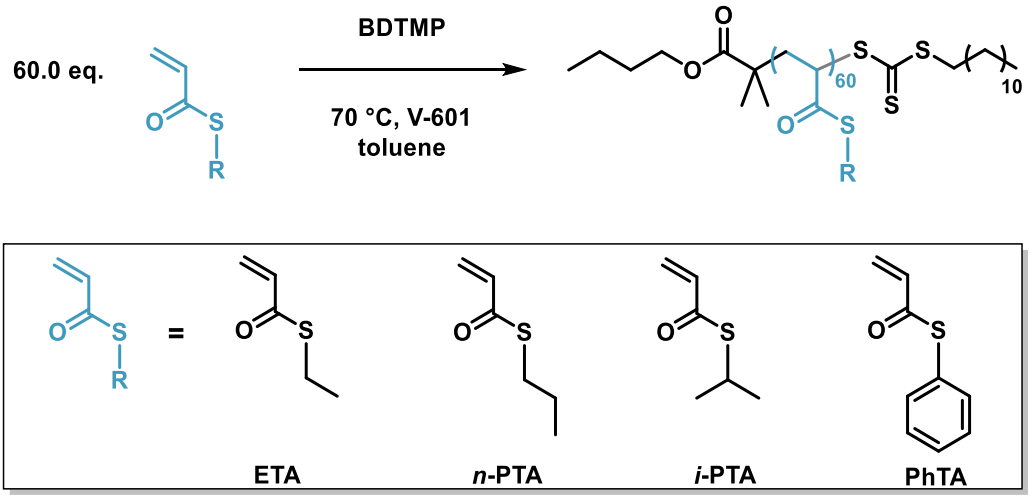

Scheme 3.2: General conditions for the polymerisation of different thioacrylates: ETA, *n*-PTA, *i*-PTA and PhTA *via* RAFT polymerisation with $[M]_0$: $[CTA]_0$ = 60, BDTMP as CTA and V-601 as initiator.

Samples were periodically taken from the polymerisation to determine the conversion and average molecular weight of the polymers. The conditions were subsequently applied for a homopolymerisation with chain length of DP_n = 60 ($[M]_0$:$[CTA]_0$:$[V\text{-}601]_0$=[60]:[1]:[0.01] in **P2**. In the following, the polymerisation of ETA will be described in detail as an example for the thioacrylate (**Table 3.1**).

Table 3.1: Experimental details on synthesis of homopolymerisation of ETA, **P2**.

Time (min)	$M_{n,theo}$ **(g/mol)**	$M_{n,GPC}$[b] **(g/mol)**	**PDI**[b]	**Conv.**[a] **(%)**
15	2020	2790	1.11	23
30	3849	5130	1.10	49
45	5010	6370	1.09	66
60	5790	7060	1.10	77
90	6200	7820	1.10	86
120	6690	8130	1.10	90

Polymerisation condition: ($[M]_0$: $[CTA]_0$: $[V\text{-}601]_0$ = 60 : 1 : 0.1) in toluene at 70 °C for ETA. [a] Conversion measured by ^{1}H NMR spectroscopy. [b] THF eluent, linear PMMA standard.

Initial screening of homopolymerisation of ETA presented a low dispersity and high conversion (90%, PDI = 1.10). The polymerisation data for the homopolymer is presented and summarised in **Figure 3.2** and **Figure 3.3** below.

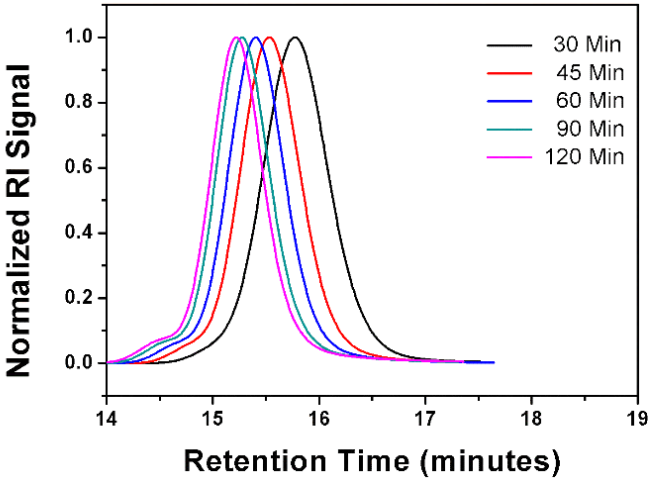

Figure 3.2: GPC traces of the obtained poly(ethyl thioacrylate)s with DP = 60 in toluene at 70°C, **P2**.

Kinetic investigations revealed quantitative conversion (~ 90%) within 2 h, following with no evident induction period in the first 15 minutes.

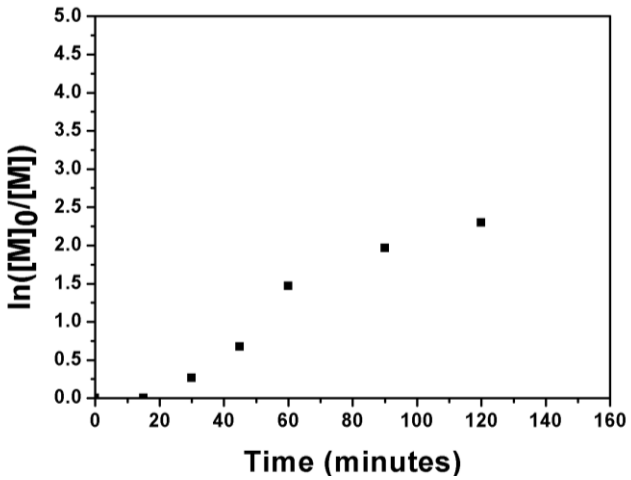

Figure 3.3: Ln([M]$_0$: [M]) vs. time plot for P(ETA).

A linear dependence of ln[M]$_0$/[M] *vs*. time indicated first order kinetics with respect to monomer concentration between 15 and 60 minutes (**Figure 3.3**), while M_n increased linearly with time and PDI values remained narrow ($\leq$ 1.11) throughout the reaction (**Figure 3.4**).

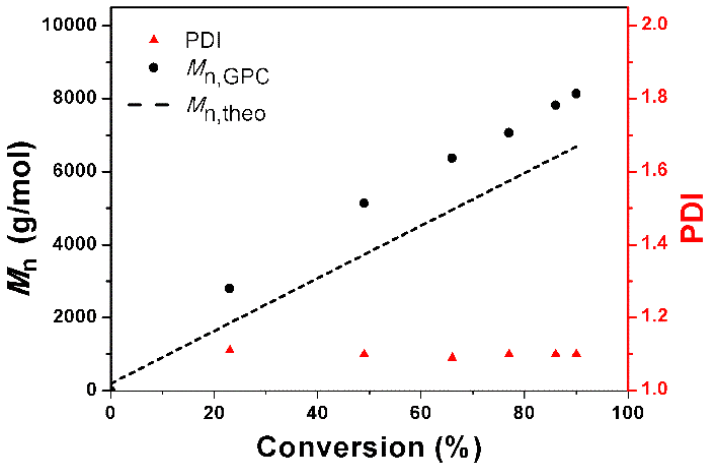

Figure 3.4: M_n vs. conversion plot for P(ETA).Black symbols represent $M_{n,GPC}$, dashed lines represents respective $M_{n,theo}$ and red symbols represents their PDI for **P2**.

Additionally, close correlation between $M_{n,theo}$ and $M_{n,GPC}$ values further confirms a controlled/living character of this polymerisation. GPC analysis discovered a peak forming at higher molecular weight already after 45 minutes, indicating a coupling reactions of two chains and possible termination. However, different results were obtained when ETA was changed with the aromatic thioacrylate PhTA (**P6**), the results are summarised in **Table 3.2**.

Table 3.2: Experimental details on synthesis of homopolymerisation of PhTA, **P6**.

Time (min)	$M_{n,theo}$ (g/mol)	$M_{n,GPC}$[b] (g/mol)	PDI[b]	Conv.[a] (%)
15	1410	2130	1.16	10
30	2590	4000	1.12	22
45	4070	5100	1.14	37
60	5100	5400	1.14	47
90	6280	6290	1.14	59
120	6530	6430	1.14	62

Polymerisation condition: ($[M]_0$:$[CTA]_0$:$[V\text{-}601]_0$ = 60:1:0.1) in toluene at 70 °C for PhTA.
[a] Conversion measured by ^{1}H NMR spectroscopy. [b] THF eluent, linear PMMA standard.

Similar to **P2**, GPC analysis revealed narrow, mono-modal distribution for **P6** (**Figure 3.5**) whereas dispersity indices slightly increased (≤ 1.16).

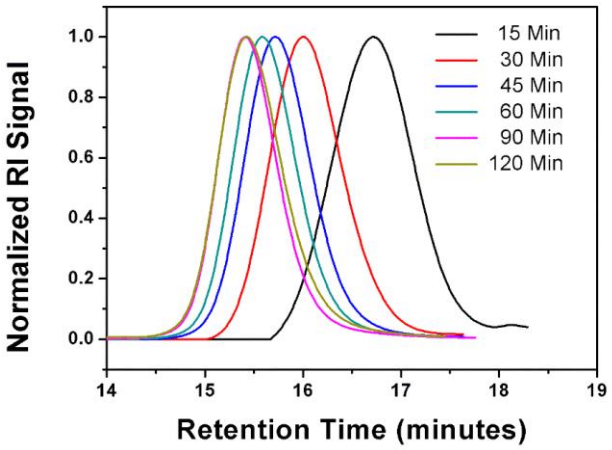

Figure 3.5: GPC traces of the obtained poly(thiophenol acrylate)s with DP = 60 in toluene at 70 °C, **P6**.

There was no indication of a termination reactions, neither at low molecular weight, nor at higher molecular weight (bimolecular termination, evident as a shoulder in the GPC). However, the polymerisation of PhTA compared to ETA was found to be significantly slower and showed no recognisable increase in molecular weight observed after 2 hours according to the GPC and ^{1}H NMR analysis. The polymerisation at 70 °C, attaining relatively low conversion (62%) in 2 hours. The GPC analysis revealed a linear increase in number-average molecular weight (M_n) with increasing conversion (**Figure 3.6b**). Ideally the calculated $M_{n,theo}$ and the experimental M_n obtained by GPC should show no or little deviation from each other, which is also not the case for **P6**. Nevertheless, no observable evidence of high or low molecular weight termination events was present in the GPC analysis.

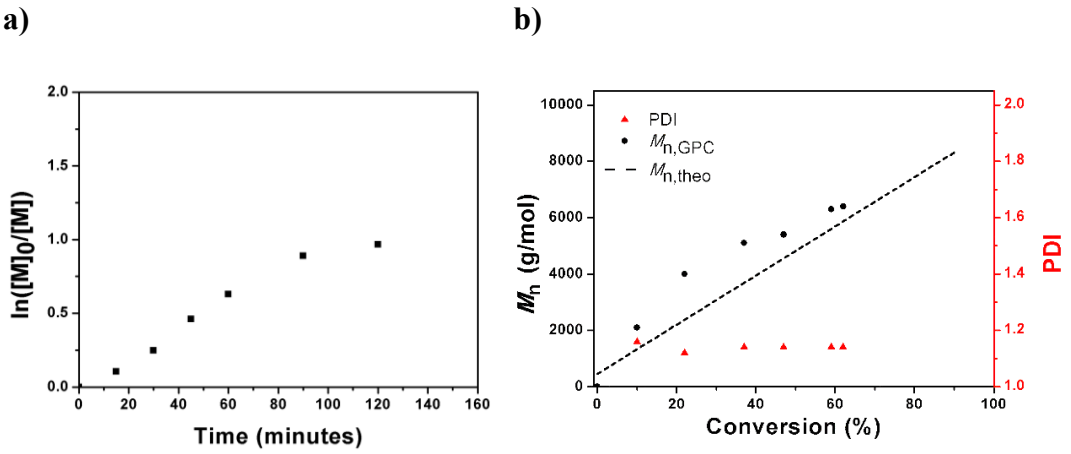

Figure 3.6: a) Ln([M]$_0$: [M]) vs. time plot for P(PhTA). **b)** M_n vs. conversion plot for P(PhTA).Black symbols represent $M_{n,GPC}$, dashed lines represents respective $M_{n,theo}$ and red symbols represents their PDI.

The results for the homopolymerisations for all four monomers; the number average molecular weight (M_n) *vs* conversion and the semi-logarithmic kinetic plots are shown in **Figure 3.7a**. PDIs determined by GPC were found to be below 1.2 for all poly(thioacrylate)s indicative of a well-controlled polymerisation and a high chain transfer efficiency of the used CTA under the conditions investigated. For ETA, *n*-PTA, *i*-PTA and PhTA, linear relationship between molecular weight and conversion indicates the controlled nature of the polymerisation (**Figure 3.7b**).

The M_n *vs* conversion plots are showing similar de*via*tions at low and high monomer conversions compared to the theoretical values ($M_{n,theo}$ = MW_{CTA} + ($MW_{monomer}$ × DP × Conversion)). However, measured average molecular weight of P(ETA) against linear poly(methyl methacrylate) as standard, showed higher M_n than the theoretical values for **P2** (**Table 3.3**), as mentioned earlier. There may be two reasons that led to this observation. The first possible reason is that the transfer between RAFT agent and a propagating radical is less efficient than the subsequent transfer between a dormant chain and a propagating radical. The second possible reason is that in this study the obtained M_n values are calculated using PMMA calibration standards and the discrepancy may be attributed to the inadequacy of PMMA standards to approximate the hydrodynamic volume of obtained poly(thioacrylate)s in THF. It is believed that the latter is more likely as the polymers display narrow PDI. The linear increase

of M_n values with increase in conversion and the low dispersities strongly indicated the controlled nature of the reactions and confirm that the polymerisation of thioacrylates by the RAFT process follows virtually "living" polymerisation mechanism. Semi-logarithmic kinetic plot of homopolymerisations of ETA, *n*-PTA, *i*-PTA and PhTA, is shown in **(Figure 3.7a).**

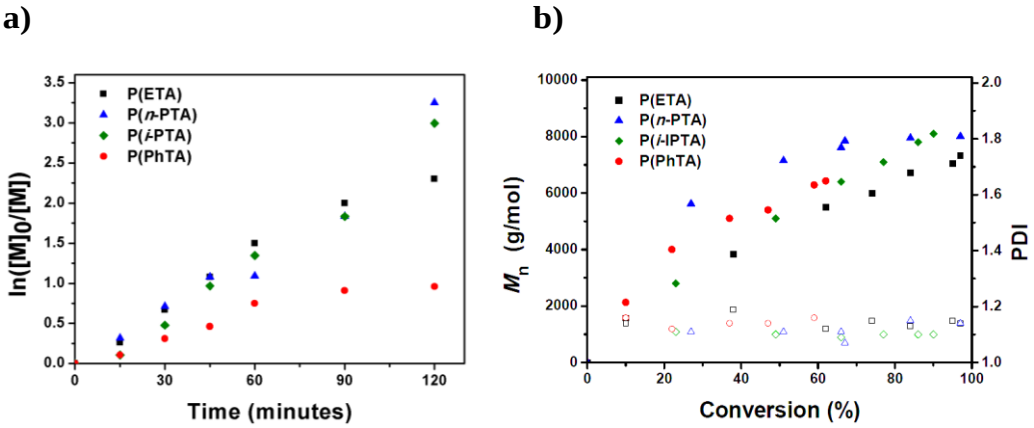

Figure 3.7: Investigation of homopolymerisation of different thioacrylates *via* RAFT, DP = 60 in toluene at 70 °C. **a)** Ln($[M]_0/[M]$) *vs*. time plot for P(ETA), P(*n*-PTA) and P(*i*-PTA) and P(PhTA); **b)** M_n vs. conversion plot for P(ETA), P(*n*-PTA) and P(*i*-PTA) and P(PhTA). Filled symbols represent $M_{n,GPC}$ and blank symbols represent their corresponding PDI.

The linear relationships indicates a constant radical concentration throughout the RAFT polymerisation and an absence of termination reactions, as well as a small effect of decreasing initiator concentration of thioacrylates. The resulting polymers maintained low dispersities (PDI = 1.07 to 1.19) and verified the living characteristics of the polymerisation process with linear agreement between polymer molecular weight and monomer conversion. The apparent propagation rates (k_p^{app}) can be estimated from the slopes of the semi-logarithmic kinetic plots and are listed in **Table 3.3** below.

Table 3.3: Experimental details on synthesis of homopolymerisation of ETA, PhTA, *n*-PTA and *i*-PTA.

Polymer	Monomer	$[M]_0$: $[CTA]_0$	Conv.[a] (%)	$M_{n,theo}$ (g/mol)	$M_{n,GPC}$[b] (g/mol)	PDI[b]	k_p^{app} (s^{-1})
P1	EA	60	78	5110	5300	1.11	$3.57x10^{-4}$
P2	ETA	60	77	5790	7060	1.10	$3.37x10^{-4}$
P3	ETA	120	78	11300	12700	1.12	$3.57x10^{-4}$
P4	ETA	180	56	12110	12100	1.11	$2.29x10^{-4}$
P5	PhTA	30	60	3370	2870	1.19	$1.90x10^{-4}$
P6	PhTA	60	53	5640	5700	1.14	$2.06x10^{-4}$
P7	*n*-PTA	60	67	5646	7850	1.07	$4.11x10^{-4}$
P8	*i*-PTA	30	87	3800	3770	1.13	$3.92x10^{-4}$
P9	*i*-PTA	60	76	6350	6930	1.07	$3.95x10^{-4}$

Polymerisation condition: ($[M]_0$:$[CTA]_0$:$[V\text{-}601]_0$ = 30; 60; 120; 180:1:0.1) in toluene at 70° C.
[a] Conversion measured by ^{1}H NMR spectroscopy. [b] THF eluent, linear PMMA standards

In the case of PhTA (**P6**), first-order kinetics were maintained for the first hour (**Figure 3.7**) and a maximum conversion of 62% was obtained after 120 minutes. Even though polymerisation rate was relatively low a polymer with a PDI of 1.16 was obtained. The low propagation rate indicates a slow initiation although appearance of an uncontrolled period in the early stage was evident, due to equilibrium between active radical-containing chains and dormant species, which potentially lead to early termination events. Whereas, k_p^{app} for the homopolymerisation of ETA (**P2**) shows a two-fold increase ($3.37x10^{-4}$ s^{-1}), isomeric monomers, *n*-PTA (**P7**, $4.11x10^{-4}$ s^{-1}) and *i*-PTA (**P9**, $3.95x10^{-4}$ s^{-1}) display very similar propagation rates, but are relatively higher than ETA and PhTA.

A detailed ^{1}H NMR analysis of a purified polymer of *n*-PTA (**P7**) is provided in **Figure 3.8** and for all purified polymers in **Figure 3.9.**

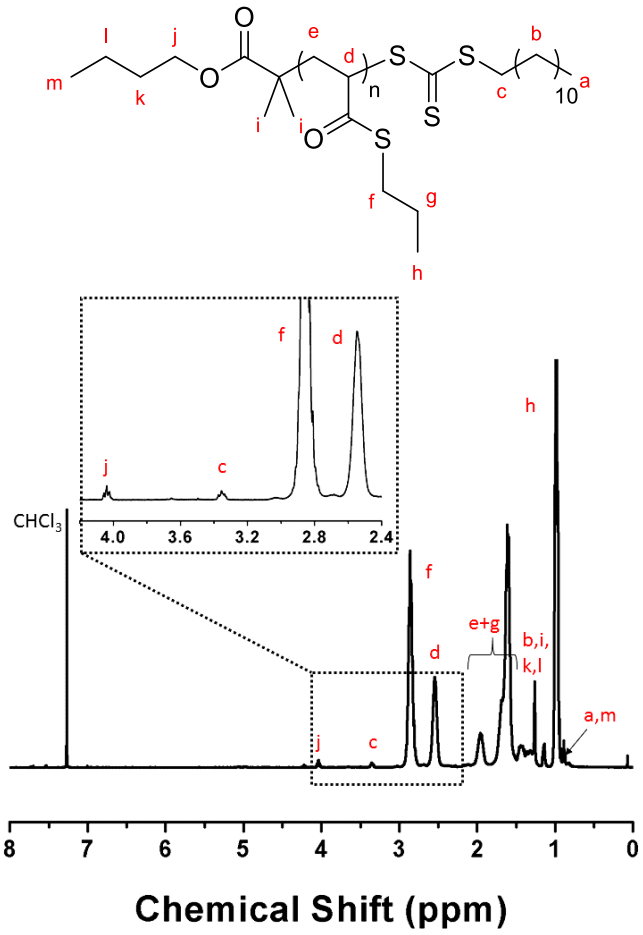

Figure 3.8: ^{1}H NMR spectrum of *n*-PTA, **P7** ($CDCl_3$, 400 MHz, 303 K).

Additionally, end group fidelity is a very important factor as the RAFT end group must be kept on the polymer for the generation of block copolymers and further polymerisation. ^{1}H NMR spectroscopy is a useful tool to determine the end group fidelity of polymers synthesised *via* RAFT or other CRP methods. The ^{1}H NMR spectrum of the purified P(*n*-PTA) (**P7**) is presented in **Figure 3.8**. Integration of the -C*H*- broad polymer backbone peak at 2.5 ppm (H_d) against the –CH_2- (H_c) at 3.3 ppm immediately adjacent to the trithioacarbonate end group, indicates a DP of 59 and agrees well with an expected value of 57, which was calculated from the ratios of the initial *n*-PTA to initiator ratio multiplied by the conversion of the monomer.

Additionally, the end group fidelity was calculated by comparing the –CH_2COO- protons of the CTA (H_j) at 3.9 ppm and the –SCH_2- (H_c) at 3.3 ppm **(Figure 3.8).** Integration of H_j and H_c should be 2:2. However, the analysis revealed an 93% end-

group fidelity, the remaining 7% of the P(*n*-PTA) chains were initiated by the radicals from the initiator decomposition.

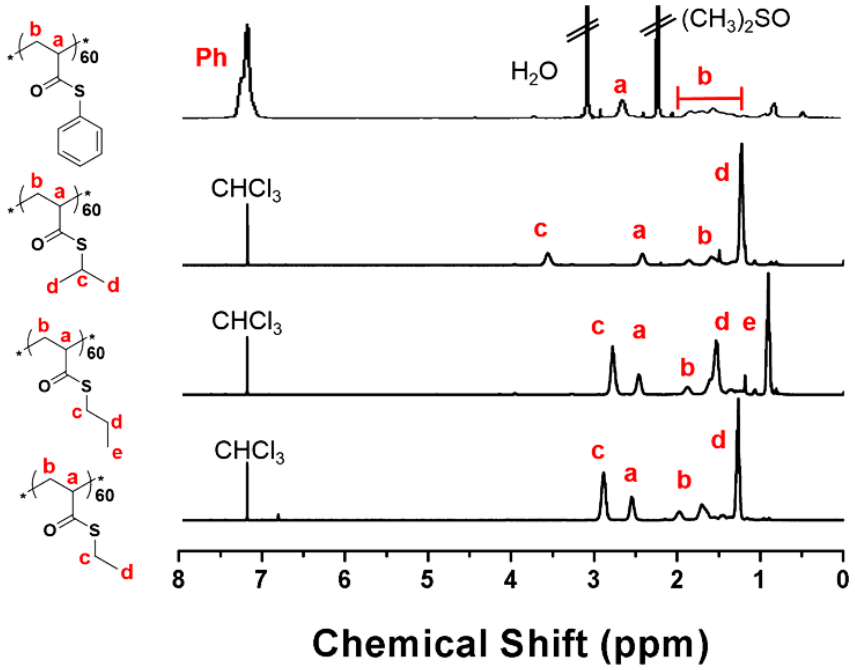

Figure 3.9: ^{1}H NMR spectra ($CDCl_3$, $(CD_3)_2SO$) of purified **P2**, **P6**, **P7** and **P9**.

3.2.3 The effect of the initiator concentration

In all of the above experiments 0.1 molar ratio of initiator were used, resulting in a $[CTA]_0$:$[V\text{-}601]_0$ ratio of 10. It is known that, in RAFT process the fractions of living chains at the end of the polymerisation, and thus the obtained degree of control, are strongly dependent on this ratio. Therefore, the concentration of RAFT agent to initiator was optimised by changing the ratio of RAFT agent to initiator (V-601) while maintaining constant monomer-to-RAFT molar ratio of 60 in toluene at 70°C (**Scheme 3.3**). The concentration of initiator with respect to chain transfer agent (BDTMP) was reduced from 0.1 (**P9**) to 0.01 (**P10**) molar ratios.

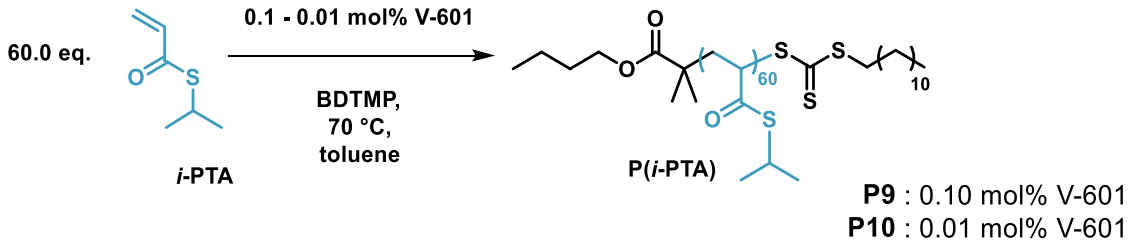

Scheme 3.3: General conditions for the polymerisation of *i*-PTA *via* RAFT polymerisation with 0.10 (**P9**) and 0.01 mol% (**P10**) V-601.

i-PTA could be homopolymerised with an initiator concentration of 0.10 mol% in a controlled manner using same conditions as applied for **P7**, **P8** and **P9.** The data obtained for *i*-PTA with 0.10 mol% initiator (V-601) are summarised in **Table 3.4** below.

Table 3.4: Experimental details on synthesis of homopolymerisation of *i*-PTA.

Time (min)	$M_{n,theo}$ (g/mol)	$M_{n,GPC}$[b] (g/mol)	PDI[b]	Conv.[a] (%)
15	1200	1570	1.14	10
30	3390	3840	1.19	38
45	5300	5490	1.12	62
60	6200	5990	1.15	74
90	6900	6710	1.13	84
120	7840	7050	1.15	95
180	8000	7330	1.14	97

Polymerisation condition: **P9**: ($[M]_0$:$[CTA]_0$:$[V\text{-}601]_0$ = 60:1:0.1) in toluene at 70 °C for *i*-PTA. [a] Conversion measured by ^{1}H NMR spectroscopy. [b] THF eluent, linear PMMA standard.

GPC traces of P(*i*-PTA) (**P9**) synthesised by RAFT polymerisation show well-defined symmetrical peaks with minimal formation of a high molecular weight shoulder at 180 minutes (**Figure 3.10**), potentially caused by recombination of propagating radicals. M_n measured by GPC matches closely the theoretical M_n (**Table 3.4**).

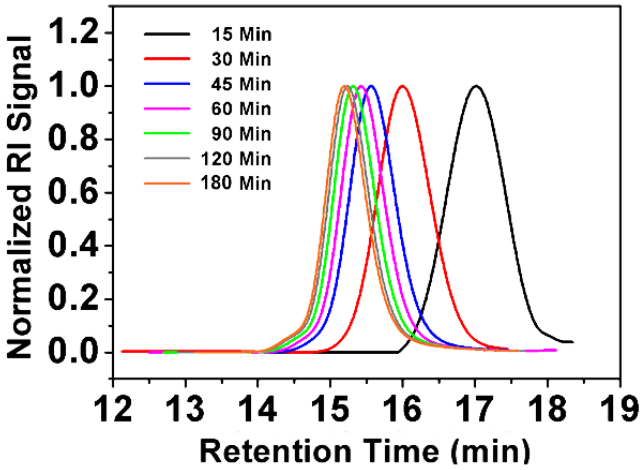

Figure 3.10: GPC traces of the homopolymerisation of *i*-PTA with DP = 60 in toluene at 70 °C, **P9**.

Furthermore, the initiator concentration was reduced to 0.01 mol%, this has been shown to be an optimal ratio for the generation of a well-defined poly(thioacrylate) with an isopropyl side-group. Dispersities stay relatively low (PDI = 1.13 to 1.19) (**Table 3.5**) with a symmetrical peak (**Figure 3.11**).

Table 3.5: Experimental details on synthesis of homopolymerisation of *i*-PTA.

Time (min)	$M_{n,theo}$ (g/mol)	$M_{n,GPC}$[b] (g/mol)	PDI[b]	Conv.[a] (%)
15	730	800	1.10	4
30	2220	2090	1.17	23
45	3390	3170	1.13	38
60	4330	4130	1.13	50
90	5730	5010	1.17	68
120	6440	5340	1.14	77
180	6590	5520	1.19	79

Polymerisation condition: **P10**: ($[M]_0$:$[CTA]_0$:$[V\text{-}601]_0$ = 60:1:0.01) in toluene at 70 °C for *i*-PTA. [a] Conversion measured by ^{1}H NMR spectroscopy. [b] THF eluent, linear PMMA standard.

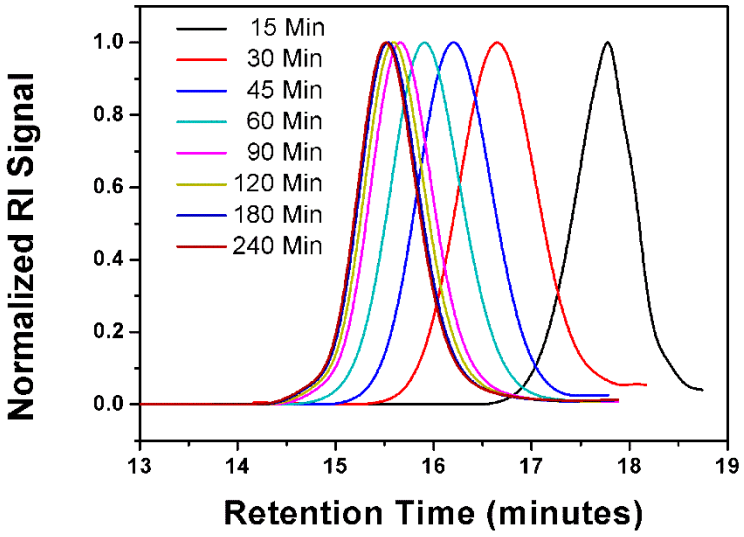

Figure 3.11: GPC traces of the homopolymerisation of *i*-PTA with 0.01 mol% Initiator in toluene at 70 °C, **P10**.

A decrease in the amount of V-601 resulted in a decrease in the rate of polymerisation, as propagation rate of polymerisation is proportional to the square root of the initiator concentration, $[I]^{1/2}$. Both polymerisation reactions exhibited linear kinetics (**Figure 3.12**) and provided M_n *vs* conversion plots that were linear. Polymerisation with 0.01 mol% V-601 to BDTMP showed a decrease in the rate of polymerisation from 3.95×10^{-4} s^{-1} to 2.28×10^{-4} s^{-1}. Furthermore, dispersity decreased slightly as the initiator concentration was decreased.

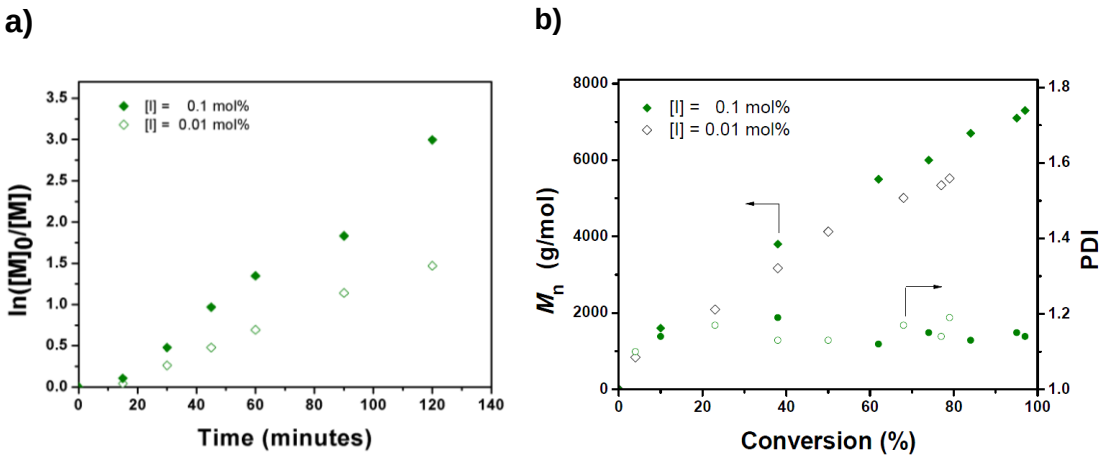

Figure 3.12: Influence of monomer-to-initiator ratio on the homopolymerisation of *i*-PTA *via* RAFT with BDTMP as CTA agent. **a)** Ln($[M]_0/[M]$) *vs*. time plot for P(*i*-PTA). **b)** M_n vs. conversion plot for P(*i*-PTA). Diamond shaped symbols represent $M_{n,GPC}$ and circles represents their corresponding dispersity.

3.2.4 Investigation of the relative ratio of monomer to chain transfer agent

The influence of the relative concentrations of monomer to chain transfer agent was evaluated by a series of experiments that involved variations of the $[monomer]_0$: $[BDTMP]_0$ values from 60, 120 and 180 in toluene (**Scheme 3.4**).

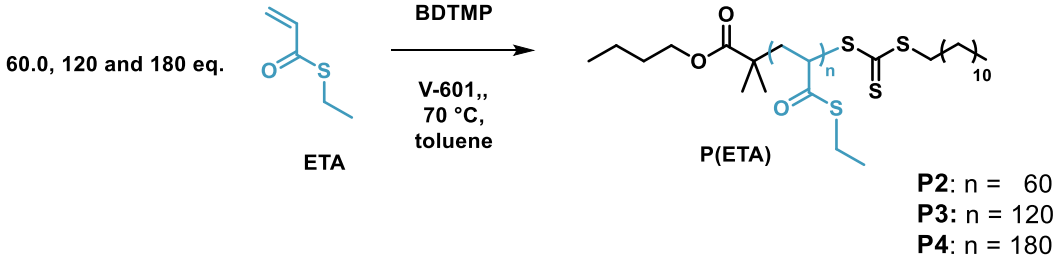

Scheme 3.4: General conditions for the polymerisation of ETA with DP = 60; 120 and 180 *via* RAFT polymerisation with BDTMP as CTA and V-601 as initiator

The ratio of initiator and CTA were hold constant at 0.10 mol% and the temperature was kept at 70 °C. Results are listed for **P2** in **Table 3.1**, **P3** in **Table 3.6** and **P4** in **Table 3.7.**

Table 3.6: Experimental details on synthesis of homopolymerisation of ETA, **P3**.

Time (min)	$M_{n,theo}$ (g/mol)	$M_{n,GPC}$[b] (g/mol)	PDI[b]	Conv.[a] (%)
15	2230	7100	1.11	13
30	7390	10600	1.11	50
45	9480	12310	1.12	65
60	12290	12700	1.12	78
90	12550	13600	1.14	87
120	13100	13800	1.16	91

Polymerisation condition: $([M]_0:[CTA]_0:[V\text{-}601]_0 = 120:1:0.1)$ in toluene at 70 °C for ETA. [a] Conversion measured by ^1H NMR spectroscopy. [b] THF eluent, linear PMMA standard.

Variable molecular weight was possible by targeting different DP of ETA, where conversion and low dispersity remained the same (**Table 3.7**).

Table 3.7: Experimental details on synthesis of homopolymerisation of ETA, **P4**.

Time (min)	$M_{n,theo}$ **(g/mol)**	$M_{n,GPC}$[b] **(g/mol)**	**PDI**[b]	**Conv.**[a] **(%)**
15	2510	2830	1.22	10
30	6680	7610	1.11	30
45	10440	10600	1.11	48
60	12110	12100	1.11	56
90	15400	15560	1.09	72
120	17120	17280	1.09	80
150	18000	17920	1.12	84
180	18170	19000	1.13	85
240	19210	19630	1.15	90

Polymerisation condition: ($[M]_0$:$[CTA]_0$:$[V\text{-}601]_0$ = 180:1:0.1) in toluene at 70 °C for ETA. [a] Conversion measured by ^{1}H NMR spectroscopy. [b] THF eluent, linear PMMA standard.

A shift towards higher molecular weight, shown by an increase of M_n is observed. A molecular weight of 19630 g/mol at the final sampling point at 4 hours is obtained with low dispersity (1.15), measured by GPC in THF +2% TEA and calibrated with PMMA standards. A slightly higher dispersity was observed for the time point at 15 minutes, whereas dispersity became lower after this time (**Table 3.7**).

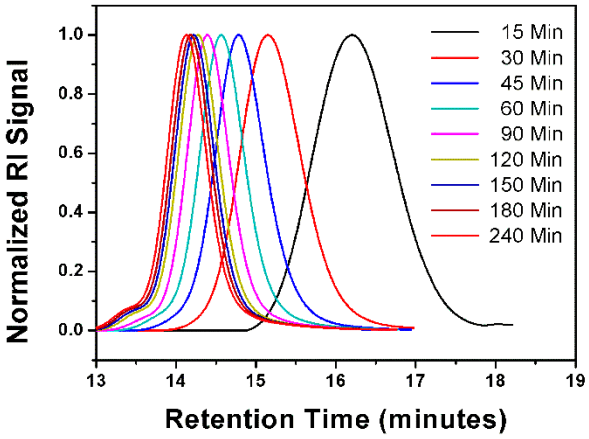

Figure 3.13:GPC traces of the homopolymerisation of ETA with DP = 180 in toluene at 70 °C.

a) **b)**

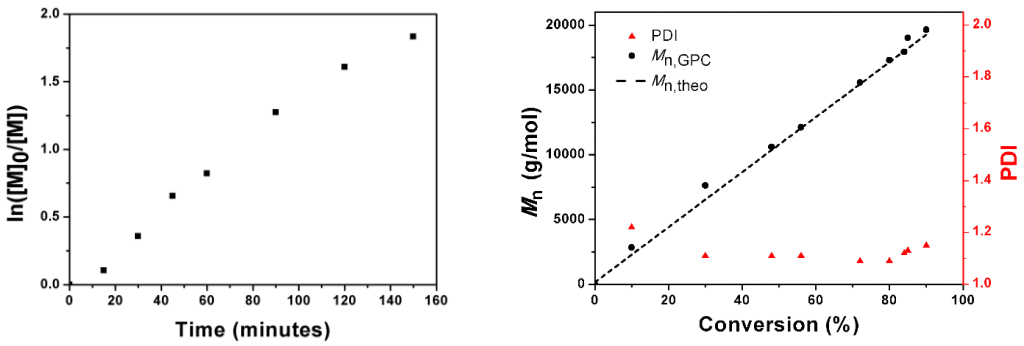

Figure 3.14. a) Ln($[M]_0$: [M]) vs. time plot for P(ETA). **b)** M_n vs. conversion plot for P(ETA).Black symbols represent $M_{n,GPC}$, dashed lines represents respective $M_{n,theo}$ and red symbols represents their PDI.

Increase of the targeted DP corresponded to a dilution of radicals and therefore in a decrease in the rate of polymerisation (**Figure 3.15**). Interestingly, conversion values were similar for targeted DP of 60 and 120, in comparison to low conversion values obtained with DP 180. All polymers showed narrow PDI in the range of 1.09 to 1.12.

a) b)

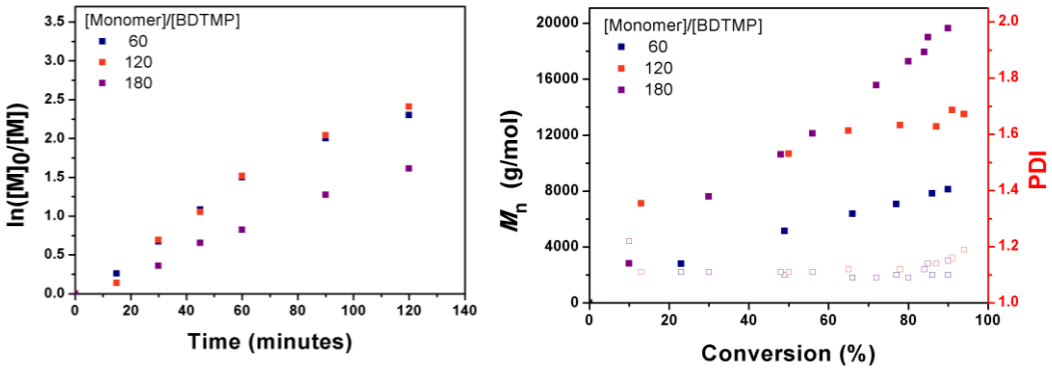

Figure 3.15: Influence of ETA-to-[CTA] on the polymerisation of ETA *via* RAFT. **a)** Ln(([M]$_0$/[M]) *vs.* time plot for P(ETA) with different DPs. **b)** M_n vs. conversion plot for P(ETA). Filled and empty symbols represent $M_{n,GPC}$ and PDI, respectively.

3.2.5 Block copolymerisations of thioacrylate and ethyl acrylate

The living nature of polymers was further verified by block copolymerisation. In order to assess the end-group fidelity, chain extension of P(ETA) or P(EA) was attempted with the addition of EA or ETA (DP = 60), respectively. The first block copolymerisation was initiated with EA, as it showed higher transfer ability for the CTA selected (**Scheme 3.5**).

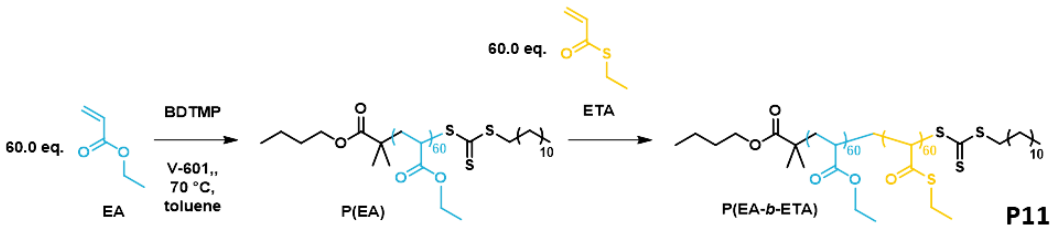

Scheme 3.5: RAFT polymerisation of EA and subsequent chain extension with ETA to synthesise diblock copolymer (**P11**).

Table 3.8: Experimental details on synthesis of block copolymer P(EA-*b*-ETA).

	Time (min)	$M_{n,theo}$ (g/mol)	$M_{n,GPC}$[b] (g/mol)	PDI[b]	Conv.[a] (%)
1st block	270	5940	6910	1.17	92
2nd block	15	6850	8400	1.19	13
	30	8240	9500	1.20	33
	45	9070	10660	1.20	45
	60	9700	10950	1.22	54
	90	10600	11700	1.23	66
	120	10900	12400	1.21	71
	150	11400	12600	1.23	79
	240	11800	12900	1.23	80

Polymerisation condition for chain extension of $P(EA)_{60}$ with ETA (DP = 60). [a] Conversion measured by ^1H NMR spectroscopy. [b] THF eluent, linear PMMA standard.

Therefore, the block copolymerisation was initiated with EA and followed by sequential addition of ETA as the second monomer without performing any purification step in between. The conversion of the first block was higher than 94% with the GPC traces revealing a monomodal peak, which suggests the absence of bimolecular coupling or early termination reactions (**Figure 3.16a**).

a) **b)**

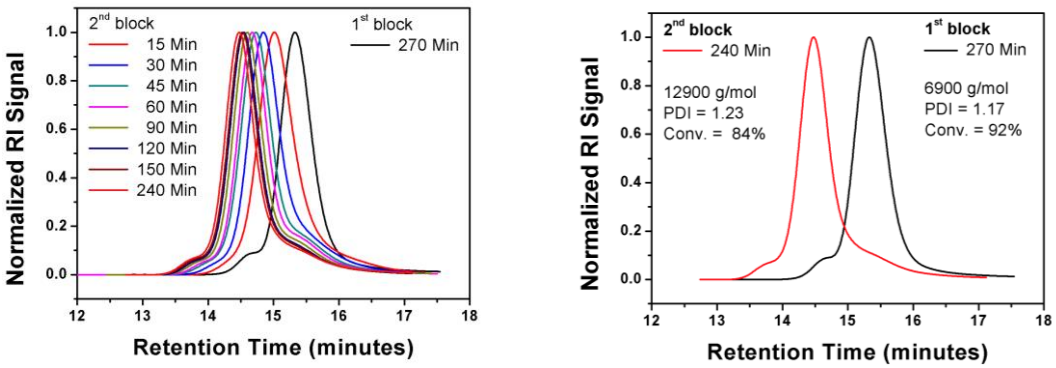

Figure 3.16: Chain extension experiment of $P(EA)_{60}$ with ETA (DP = 60). **a)** GPC traces of the kinetic experiments. **b)** GPC traces of the first block in black and the final time point of the second block for **P11**.

The second block of poly(ETA) was grown in a controlled fashion (**Figure 3.16b**), as a good correlation between the theoretical and the

experimental values and narrow PDI (1.12-1.15) were achieved throughout the chain extensions, further confirming the controlled/living character of the polymerisation. M_n increased linearly with conversion (**Figure 3.17a**) and relatively low dispersity values (~1.17) with good correlation between theoretical and experimental M_n were observed (**Table 3.8**, **Figure 3.17**).

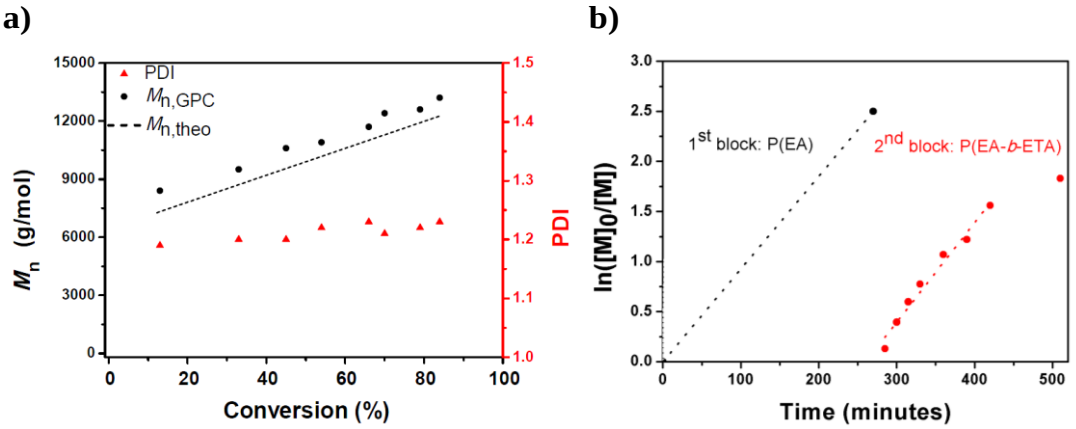

Figure 3.17: a) M_n vs. conversion plot for the second block of P(EA-*b*-ETA). Black and red symbols represent $M_{n,GPC}$ and PDI, respectively. **b)** Ln(([M]$_0$/[M]) vs. time plot for P(EA-*b*-ETA).

A reverse block order strategy of starting first with poly(ETA) and growing a second block of poly(EA), was also investigated (**Scheme 3.6**).

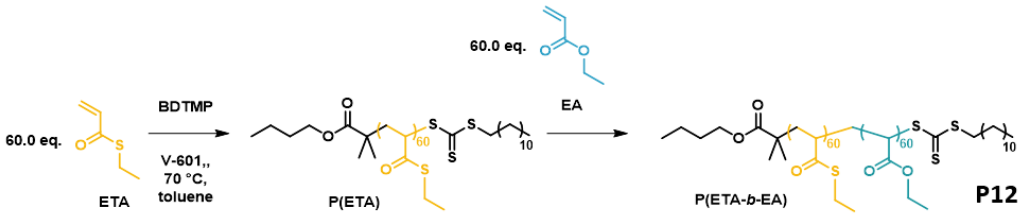

Scheme 3.6: RAFT polymerisation of ETA and subsequent chain extension with EA to synthesise diblock copolymer (**P12**).

As expected the block copolymers were grown to satisfactory molecular weights as in **P11**, however the PDI slightly increases (PDI ~ 1.20 - 1.23), whereby theoretical and experimental M_n values were still in good correlation (**Table 3.9**, **Figure 3.19b**).

Table 3.9: Experimental details on synthesis of block copolymer P(ETA-*b*-EA).

	Time (min)	$M_{n,theo}$ (g/mol)	$M_{n,GPC}$[b] (g/mol)	PDI[b]	Conv.[a] (%)
1st block	270	6960	7070	1.12	94
2nd block	15	7640	8280	1.13	11
	30	8220	8900	1.13	21
	45	9120	10150	1.17	36
	60	9780	10800	1.13	47
	90	10500	11800	1.14	59
	120	10980	12400	1.14	67
	150	11580	13300	1.14	77
	240	12060	13800	1.14	85

Polymerisation condition for chain extension of $P(ETA)_{60}$ with EA (DP = 60). [a] Conversion measured by ^1H NMR spectroscopy. [b] THF eluent, linear PMMA standard.

GPC traces, as shown in **Figure 3.18a** have a similar shape with shoulders indicating some bimolecular coupling.

a) **b)**

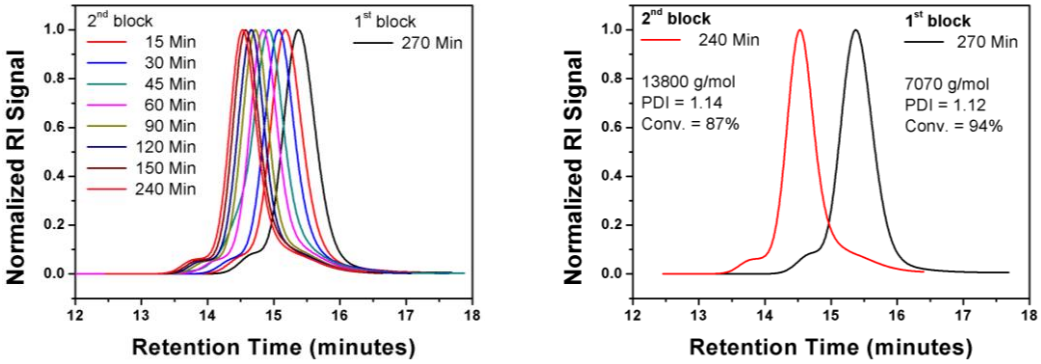

Figure 3.18: Chain extension experiment of $P(ETA)_{60}$ with EA (DP = 60). **a)** GPC traces of the kinetic. **b)** GPC traces of the first block in black and the final time point of the second block.

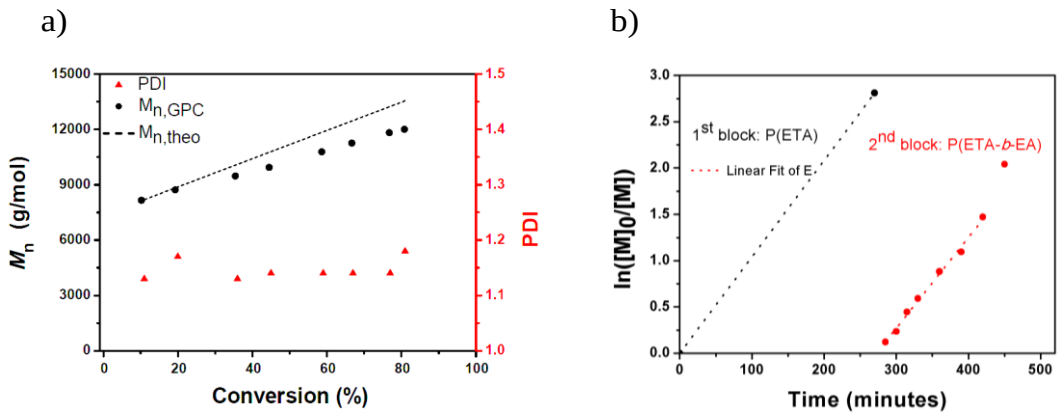

Figure 3.19: a) M_n vs. conversion plot for second block of P(ETA-*b*-EA). Black and red symbols represent $M_{n,GPC}$ and PDI, respectively for **P12**. **b)** Ln(($[M]_0$/[M]) vs. time plot for P(ETA-*b*-EA).

In summary, for a block copolymer formation for which an acrylate and a thioacrylate with similar polymerisation rate is employed, the order of the blocks does not have a significant difference in the preparation of block copolymers as the initial linear region up to 150 minutes for **P11** 1.60×10^{-4} s^{-1} and for **P12** 1.50×10^{-4} s^{-1} are very similar.

3.2.6 Physical properties of poly(thio acrylates)

Thermal properties of the obtained polymers were investigated using thermal gravimetric analysis (TGA) and differential scanning calorimetry (DSC) (**Figure 3.20**). P(ETA) exhibited thermal properties with 5% mass loss at T > 316 °C and a glass transition temperature (T_g) of 12 °C. Weight loss of the polymers occurring above 300 °C was ascribed to the decomposition of the polymers. Poly(thioacrylate)s have relatively higher T_g than the corresponding acrylate polymers P(EA) (T_g = -21 °C) possibly due to the replacement of thioester into an ester in the polymer side chain. The 5% mass loss for P(EA) occurs at a lower temperature (293 °C).

After an initial weight loss, associated with some humidity absorbed by the environment, main loss occurs in the range between 199°C and 269°C for poly(thioacrylate)s. Derivative curves of heat flow, indicates the temperature for maximum weight loss (T_{max}). Poly(ethyl thioacrylate) provides more stable homopolymers, as the degradation of P(EA) starts at 247.2 °C and shows 50% weight loss at 385.6 °C, whereas thioester-analogues is stable up to 269.7 °C,

with a weight loss of 50% at higher temperature (T_{50} = 393.6 °C). Poly(ethyl thioacrylate) shows the highest thermal stability of all poly(thioacrylate)s as well as in comparison to poly(ethyl acrylate). A large solid residue at 600 °C of homopolymer of thiophenylacrylate is worth noticing (5.9% residue) as for all other samples it has been found to be between 1.2% and 1.9%, including P(EA).

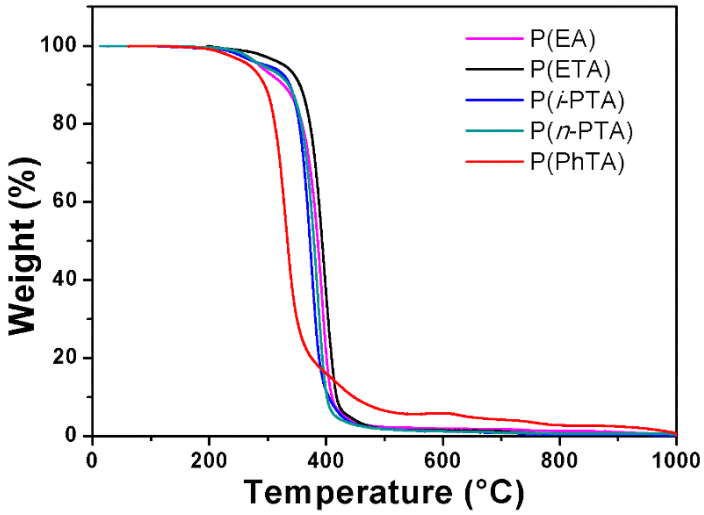

Figure 3.20: TGA thermogram of poly(ethyl acrylate) P(EA), poly(thioacrylate)s: P(ETA), P(PhTA), P(*n*-PTA) and P(*i*-PTA).

Calorimetric behaviour of polymers was studied by differential scanning calorimetry (DSC). The only thermal event that has been detected in the DSC curve is an exothermal baseline shift, associated with the glass transition temperature (T_g), which are listed in **Table 3.10**. In addition, the absence of crystallisation and also melting transitions indicates that obtained polymers were amorphous. As T_g depends primarily on the flexibility of polymer backbone, the exchange of an oxygen with a bigger sulfur atom in the side-group possibly restricts the flexibility and therefore leads to an increase of the T_g. Varying the length of the side-group, results in a change of the movement of the individual repeating units, which can lead to an inefficient packing and therefore higher fragility. This effect can be seen by varying the side-groups of thioacrylates for P(*n*-PTA) (T_g = -37 °C) and P(ETA) (T_g = 12 °C) due to increase of side group flexibility (**Figure 3.21**, **Table 3.10**).

As the thiophenol side group in P(PhTA) presents a bulky and stiff group, the barrier for segmental motion is higher than for alkyl chain. The T_g of this polymer increases to -26 °C. Homopolymer of isomeric analogue of *n*-PTA, *i*-PTA is assumed to be related to the value of poly(*n*-PTA).

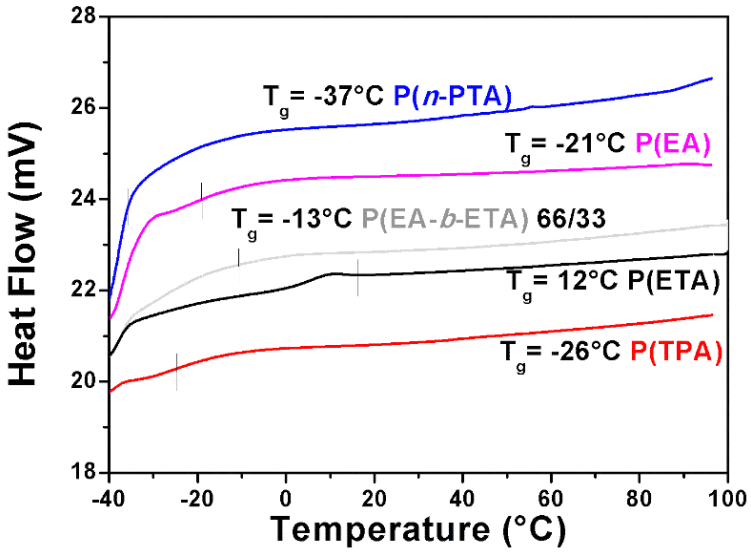

Figure 3.21: DSC thermograms of poly (ethyl acrylate): P(EA), poly(thioacrylate)s: P(ETA), P(PhTA), P(*n*-PTA) and block copolymer P(EA-*b*-ETA).

Table 3.10: Thermal properties and water contact angles (WCA) of P(EA) and Poly(thioacrylate)s with $[M]_0:[CTA]_0 = 60$.

	Polymer	T_d[a] (°C)	T_{max}[a] (°C)	Residue at 600°C[a] (%)	T_g[b]	WCA[c] (°)
P1	$P(EA)_{60}$	247.2	385.6	1.925	-21	71.20 ± 0.26
P2	$P(ETA)_{60}$	269.7	393.6	1.507	12	109.10 ± 0.44
P9	$P(i\text{-PTA})_{60}$	242.9	370.2	1.211	N/A	100.10 ± 0.03
P7	$P(n\text{-PTA})_{60}$	211.3	381.7	1.210	-37	94.45 ± 0.03
P6	$P(PhTA)_{60}$	199.6	332.7	5.904	-26	N/A

[a] measured by thermogravimetric analysis. [b] Temperature determined by differential scanning calorimetry and [c] determined by water contact angle of water on polymer films.

Furthermore, water contact angles of poly(thioacrylate)s were measured. Water contact angle (WCA, θ) measurements were performed on the homopolymers and on selected block copolymers. Compared to P(EA) (θ = 71.2°), P(ETA) is much more hydrophobic (θ = 109.1°). Hydrophobicity is also highlighted by

other poly(thioacrylate)s, which corresponds to the insolubility of poly(thioacrylate)s in water. In **Table 3.10**, the experimental water contact angle values for P(ETA), P(EA-*b*-ETA), P(*n*-PTA) and P(*i*-PTA) are given. The hydrophilicity of P(EA) can be modified by copolymerisation with more hydrophilic monomers such as ETA. For example, the addition of 66% ETA increased the contact angle value by around 30%.

3.2.7 Initial attempts for homopolymerisation of thio methacrylates

Of the CRP techniques available, RAFT polymerisation was used for the polymerisation of thio(meth)acrylates, as it has been proved for thioacrylates to be effective. In the following experiments, different RAFT agents (dithiocarbonates and trithiocarbonate) have been screened to mediate the homopolymerisation of $ETMA_{60}$ (**Scheme 3.7**).

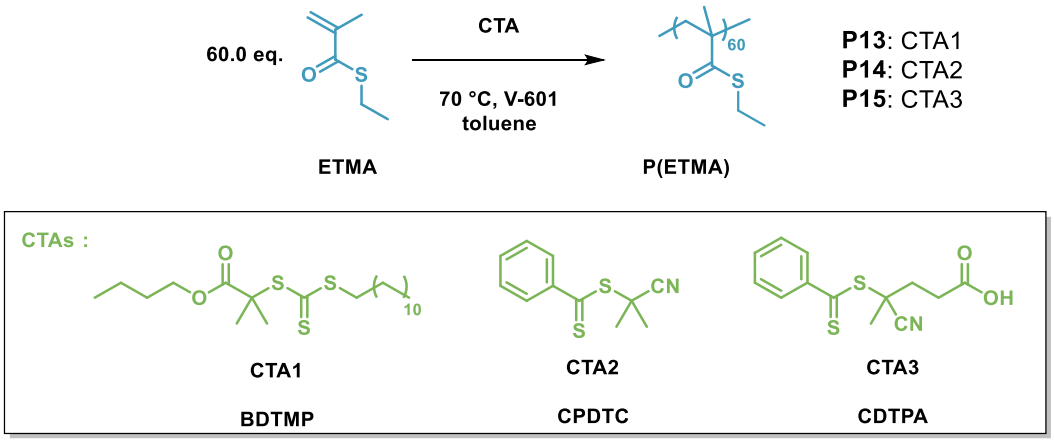

Scheme 3.7: RAFT homopolymerisation of ETMA, initiated by V-601 and mediated either by BDTMP, CPDTC or CDTPA in toluene at 70 °C.

The homopolymerisation with 3-butyl-2-(dodecylthiocarbonothioylthio)-2-methylpropionate (BDTMP) as RAFT agent and Dimethyl 2,2′-azobis(isobutyrate) (0.10 eq., V-601, **P13**) as initiator in toluene at 70 °C has been carried out. However, ^{1}H NMR analysis showed that the conversion of ETMA remained at 28% for 2 and 18 hours. Utilising 2-Cyano-2-propyl dodecyl trithiocarbonate (CPDTC), resulted in significantly higher conversion with 48%

and high molecular weight, but multi-modal peaks, which is evidenced by GPC (**Figure 3.22b**).

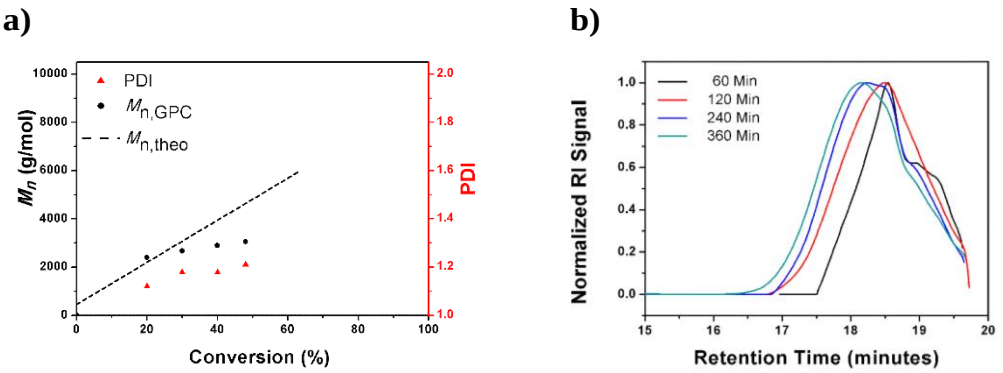

Figure 3.22: a) M_n vs. conversion plot for P(ETMA), prepared by RAFT polymerisation in toluene at 70 °C, mediated by CPDTC and initiated by V-601 (0.10 eq.).Black and red symbols represent $M_{n,GPC}$ and PDI, respectively. **b)** GPC traces (RID) of P(ETMA) (**P13**).

Furthermore, ETMA conversion could be slightly increased to 55% by increasing the equivalents of V-601 to 0.25. GPC revealed a multi-modal peak during the polymerisation (**Figure 3.23a**).

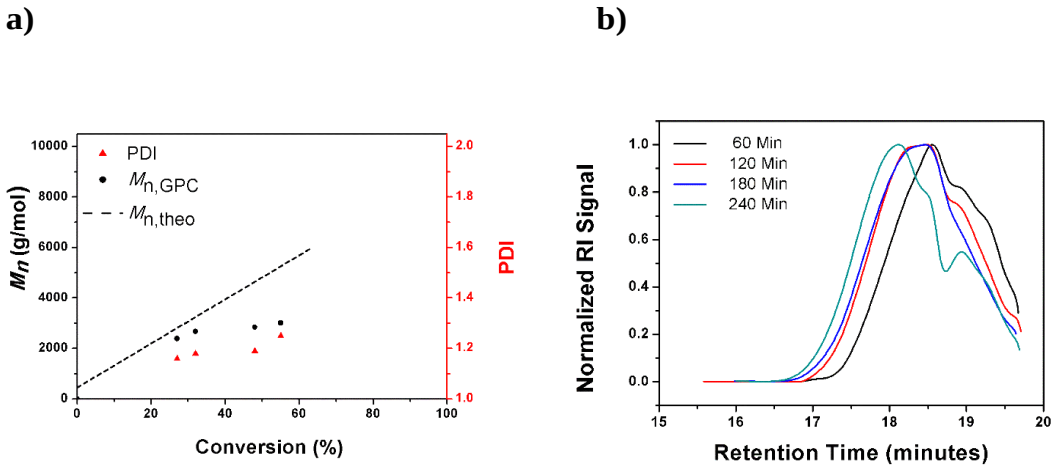

Figure 3.23: a) M_n vs. conversion plot for P(ETMA), prepared by RAFT polymerisation in toluene at 70 °C, mediated by CPDTC and initiated by V-601 (0.25 eq.).Black and red symbols represent $M_{n,GPC}$ and PDI, respectively. **b)** GPC traces (RID) of P(ETMA) (**P14**).

However, P(ETMA) initiated by either 0.10 (**P13**) or 0.25 equivalents (**P14**) of V-601 are very poorly defined, as evidenced by GPC traces with unsymmetrical distribution. This suggests that the R group (–C(CH$_2$)$_3$CN) was not relatively

sufficient as a radical leaving group and radicals would not add to and fragment the RAFT agent.

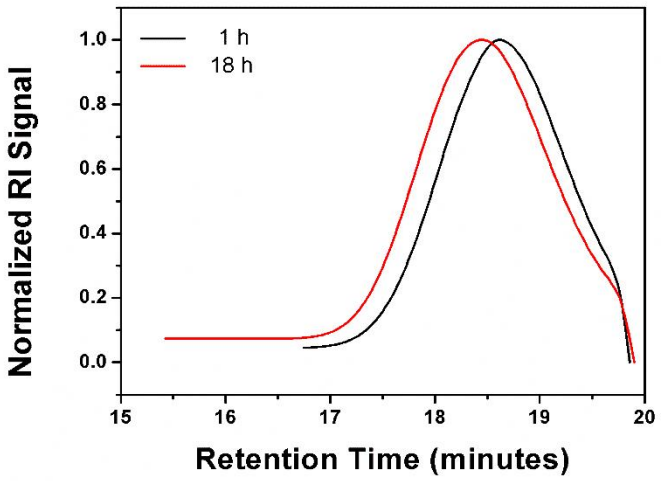

Figure 3.24: GPCs for P(ETMA), prepared by RAFT polymerisation in toluene at 70 °C, mediated by CDTPA and initiated by V-601 (0.10 eq.).

For this reason, homopolymerisation of ETMA was repeated with (CDTPA), bearing the following R group: –C(CN)(CH_3)CH_2CH_2COOH as this is a better radical leaving group and as such more appropriate for controlling polymerisations of α-methyl containing monomers (**Figure 3.24**). However, RAFT polymerisation of ETMA mediated by CDTPA reached 70%, the highest conversion obtained for this monomer. As such, the polymerisation seemed to be less "disturbed", indicated by a more symmetrical distribution when compared with other CTA's. Changes in the choice of RAFT agent to mediate the RAFT homo polymerisation of thio(meth)acrylates, deliver incremental improvement in terms of conversion and molecular weight distribution. However, conversions remained low and reached to a maximum of 70% when CDTPA was employed.

3.3 Conclusions

RAFT has been utilised to synthesise thioacrylate homopolymers with different side groups (aromatic and aliphatic), as a first report utilising thioacrylates in conjunction with RAFT. Homopolymers could be synthesised to different molecular weights, differing in the block length, where the M_n measured by GPC was close to the theoretical M_n values. The high end-group fidelity was subsequently exemplified by *in situ* chain extension upon addition of second blocks in **P12** (1^{st} block, DP = 60, 94% in 4.5 h, $M_{n,GPC}$ = 7070, PDI = 1.12) with the molecular weight distribution shifting to lower retention times with an increase of molecular weight ($M_{n,GPC}$ = 13800) and dispersity (DP = 1.14). Thereby, the kinetics of homo- and block polymerisations were followed by NMR and GPC analysis.

The obtained polymers were further analysed by TGA and DSC, which showed degradation temperatures around 332°C and glass transition temperatures in the range of -37°C – 12°C. Finally, poly(thio acrylate)s resulted in a significant increase of water contact angles compared to P(EA). Poly(thioacrylates) are shown to be easily accessible and can be adapted in most of the controlled radical polymerisation techniques. Last but not least, the thioester group has the potential to be used in thio-exchange reactions, which can open new avenues for the preparation of polymer-peptide bioconjugates. In contrast to the polymerisation of thioacrylates, the homopolymerisation of thio(meth)acrylates are still at the very beginning and more investigations, such as a screening of solvents are required. The investigation of even reactions in bulk to evade possible transfer to solvent, which can lead to dead chains would certainly be of interest. This effect is different for certain solvents but high for the employed toluene and needs to be explored further.

3.4 Experimental

3.4.1 Instrumentation

3.4.1.1 Differential Scanning Calorimetry (DSC)

A PerkinElmer DSC4000 was used to study glass transition (T_g). An indium standard (T_m = 156.6 °C and ΔH = 28.72 J/g) was used to calibrate the instrument and ensure accuracy and reliability of the obtained thermograms. Weights of specimen ranged from 5 to 10 mg and were loaded into the calorimeter, using a sealed 50 µL aluminium pan. Instrument was equilibrated at 25°C, cooled to -40°C at a rate of 10°C /min and heated to 100°C at a rate of 10°C/min. The cooling and heating scans were repeated twice to erase the effect of previous thermal history of the samples. From DSC curves T_g were determined from the inflection point temperature.

3.4.1.2 Thermogravimetric Analysis (TGA)

A TGA Q500 thermo thermogravimetric analyzer (TA Instruments, USA) was used to study thermal stability. The samples were heated from 30°C ton 1000°C at a ramp rate of 10°C/min in a nitrogen environment (the balance nitrogen purge flow was 40 mL/min and the sample purge flow was 60 mL/min). Extrapolated onset temperature was calculated, which denotes the temperature at which weight loss begins (T_0). For the next calculation, the first derivative of the weight loss was determined and indicates the point of greatest rate of change on the weight loss curve (T_p).

3.4.1.3 Static Contact Angel Measurement to Determine Surface Wettability

Contact angle (θ) measurements were obtained using a goniometer (DSA100, Kruss, Germany) equipped with a digital camera and image analysis software (DSA1 version 1.80, Kruss, Germany). Static contact angle of a 5-µl drop of deionised water deposited on spincoated solid surface. Sessile drop method was used to analyse contact angles of the water-substrate interface, which results are the average of six measurements.

3.4.1.4 Gel permeation chromatography (GPC)

GPC was utilised to determine molecular weight averages and polymer dispersity. GPC measurements were performed on an Agilent 390-LC system equipped with a PL-AS RT autosampler, 2PLgel 5 μm mixed-C columns (300×7.5 mm), a PLgel 5 mm guard column (50×7.5 mm), and a differential refractive index (DRI). The system was eluted with THF containing 2% triethylamine (TEA) at a flow rate of 1 mL min^{-1} and the DRI was calibrated with linear narrow poly(methyl methacrylate) standards, ranging from 1010 to 2136000 g/mol.

3.4.1.5 Nuclear magnetic resonance (NMR)

^{1}H NMR spectra were recorded on a Bruker AV-400 at 303 K. $CDCl_3$ and the resonance signal at 7.26 ppm (^{1}H) was used as residual $CDCl_3$ or for $(CD_3)_2CO$ at 2.05 ppm peak for the chemical shift (δ).

3.4.1.6 Gas Chromatography

Gas chromatography – flame ionisation detection (GC-FID) analysis was performed using Agilent Technologies 7820A. An Agilent J&W HP-5 capillary column of 30 m x 0.320 mm, film thickness 0.25 μm was used. The oven temperature was programmed as follows: 40°C (hold for 1 minute) increase at 30°C min^{-1} to 300°C (hold for 2.5 minutes). The injector was operated at 250°C and the FID was operated at 320°C. Nitrogen was used as carrier gas at a flow rate of 6.5 mL min^{-1} and a split ratio of 1:1 was applied. Chromatographic data was processed using OpenLab CDS ChemStation Edition, version C.01.05. Conversions were obtained by the comparing the integral of the monomer with the solvent for block copolymers.

3.4.2 Materials

All chemicals were purchased from Sigma-Aldrich (UK) and used as received at the highest purity available. Dichloromethane (DCM, HPLC grade), benzene (HPLC grade), pentane (HPLC grade), methanol (HPLC grade), tetrahydrofuran (THF, HPLC grade) and toluene (HPLC grade), were used as received. Dimethyl 2,2′-azobis(isobutyrate) and 3-butyl-2-(dodecylthiocarbonothioylthio)-2-methyl-propionate were provided by University of Warwick and used as received. Ethyl acrylate (EA, Aldrich, 99%) was destabilised by passing through a short column of basic aluminium oxide prior to polymerisation. All other chemicals and solvents were purchased from Sigma-Aldrich (UK) at the highest purity available and used as received unless mentioned otherwise.

3.4.3 Procedures

3.4.3.1 Synthesis of poly(thiophenol acrylate), DP = 60 (P6)

In a typical polymerisation, (0.4092 g, 2.492 mmol) thiophenol acrylate, BDTMP (14.7 mg, 0.041 mmol), V-601 (1.00 mg, 4.34 mmol), 0.04 mL of mesitylene and 50% 0.4 mL toluene were charged into a schlenk tube and degassed by gentle bubbling of N_2 gas for 30 minutes. Schlenk tube was submerged into an oil bath at 70°C or 100°C. Samples were taken *via* degassed syringe at desired time points and analysed. The samples were then analysed by GPC, GC and ^{1}H NMR.

3.4.3.2 Synthesis of poly(ethylthio acrylate), DP = 60 (P2)

In a typical polymerisation, (0.629 g, 5.414 mmol) ethylthioacrylate, BDTMP (33.9 mg, 0.081 mmol), V-601 (1.92 mg, 0.008 mmol), 5% v/v mesitylene and 50% v/v toluene were charged into a schlenk tube and degassed by gentle bubbling of N_2 gas for 30 minutes. Schlenk tube was submerged into an oil bath at 70°C or 100°C. Samples were taken *via* degassed syringe at desired time points and analysed. The samples were then analysed by GPC, GC and ^{1}H NMR.

3.4.3.3 Synthesis of poly(isopropylthio acrylate), DP = 60 (P9)

In a typical polymerisation, (0.40 g, 3.077 mmol) isopropylthioacrylate, BDTMP (21.5 mg, 0.051 mmol), V-601 (1.18 mg, 0.005 mmol), 0.04 mL mesitylene and 0.4 mL of toluene were charged into a schlenk tube and degassed by gentle bubbling of N_2 gas for 30 minutes. Schlenk tube was submerged into an oil bath at 70°C or 100°C. Samples were taken *via* degassed syringe at desired time points and analysed. The samples were then analysed by GPC, GC and ^{1}H NMR (**Figure 3.25)**.

a) **b)**

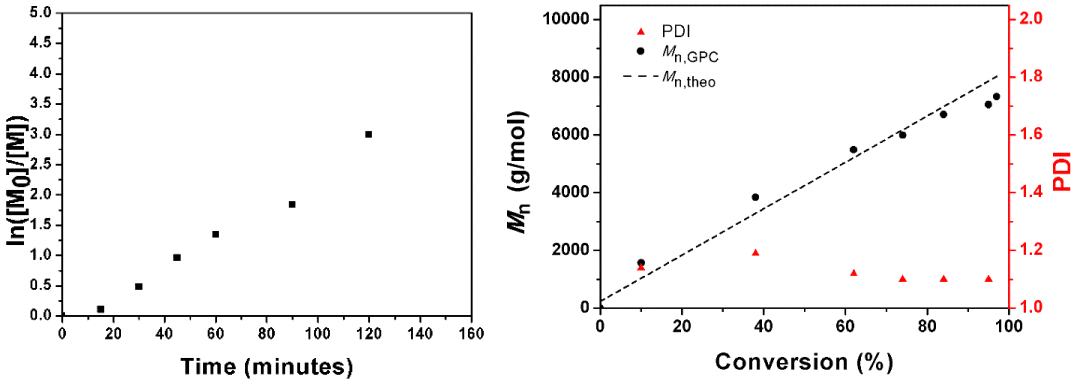

Figure 3.25: a) ln([M]$_0$: [M]) vs. time plot for P(*i*-PTA). **b)** M_n vs. conversion plot for P(*i*-PTA).Black symbols represent $M_{n,GPC}$, dashed lines represents respective $M_{n,theo}$ and red symbols represents their PDI.

3.4.3.4 Synthesis of poly(propyl thioacrylate), DP = 60 (P7)

In a typical polymerisation, (0.65 g, 4.99 mmol) propylthioacrylate, BDTMP (34.05 mg, 0.081 mmol), V-601 (1.88 mg, 0.008 mmol), 0.04 mL mesitylene and 0.4 mL of toluene were charged into a schlenk tube and degassed by gentle bubbling of N_2 gas for 30 minutes. Schlenk tube was submerged into an oil bath at 70°C or 100°C. Samples were taken *via* degassed syringe at desired time points and analysed. The samples were then analysed by GPC, GC and ^{1}H NMR (**Table 3.11**, **Figure 3.26**, **Figure 3.27**)

Table 3.11: Experimental details on synthesis of homopolymerisation of *n*-PTA.

Time (min)	$M_{n,theo}$ (g/mol)	$M_{n,GPC}$[b] (g/mol)	PDI[b]	Conv.[a] (%)
15	5100	5500	1.11	60
30	6270	7000	1.11	75
45	6970	7600	1.11	84
60	7270	7820	1.07	87
90	7440	7900	1.15	90
120	7910	8000	1.14	96

Polymerisation condition: ($[M]_0$: $[CTA]_0$: $[V\text{-}601]_0$ = 60 : 1 : 0.1) in toluene at 70°C for *n*-PTA. [a] Conversion measured by ^{1}H NMR spectroscopy. [b] THF eluent, linear PMMA standard.

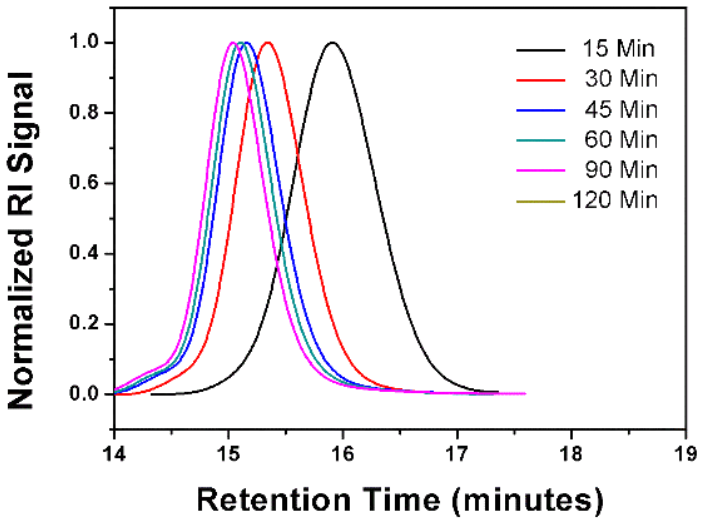

Figure 3.26: GPC traces of the homopolymerisation of *n*-PTA with DP = 60 in toluene at 70°C.

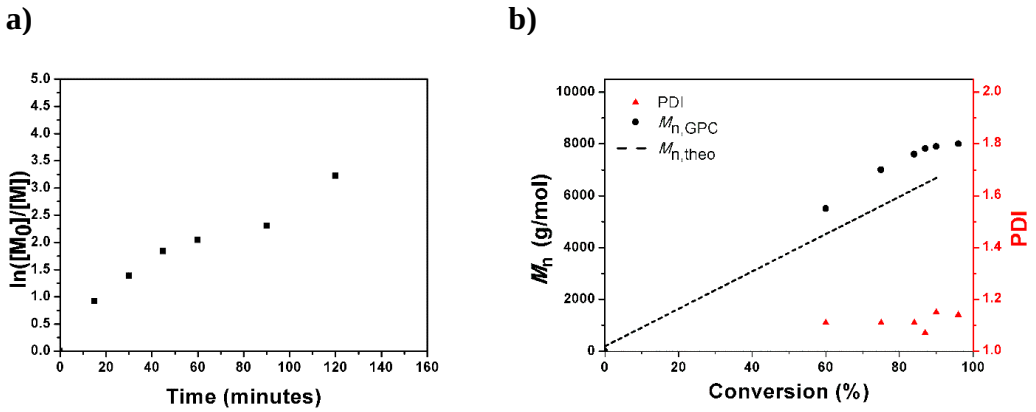

Figure 3.27: a) ln([M]$_0$: [M]) vs. time plot for P(*n*-PTA). **b)** M_n vs. conversion plot for P(*n*-PTA). Black symbols represent $M_{n,GPC}$, dashed lines represents respective $M_{n,theo}$ and red symbols represents their PDI.

3.4.3.5 Synthesis of poly(ethylthio acrylate), DP = 120 (P3)

In a typical polymerisation, (0.58 g, 5.00 mmol) ethylthioacrylate, BDTMP (17 mg, 0.04 mmol), V-601 (0.9 mg, 0.004 mmol), 0.06 mesitylene and 0.6 mL toluene were charged into a schlenk tube and degassed by gentle bubbling of N_2 gas for 30 minutes. Schlenk tube was submerged into an oil bath at 70°C or 100°C. Samples were taken *via* degassed syringe at desired time points and analysed. The samples were then analysed by GPC, GC and ^{1}H NMR.

3.4.3.6 Homopolymerisation of ethyl thioacrylate with DP = 180 (P4)

In a typical polymerisation, (1.14 g, 9.83 mmol) ethylthioacrylate, BDTMP (23.00 mg, 0.05 mmol), V-601 (1.26 mg, 0.005 mmol), 0.11 mL mesitylene and 1.14 mL of toluene were charged into a Schlenk tube and degassed by gentle bubbling of N_2 gas for 30 minutes. Schlenk tube was submerged into an oil bath at 70°C or 100°C. Samples were taken *via* degassed syringe at desired time points and analysed. The samples were then analysed by GPC, GC and ^{1}H NMR.

3.4.3.7 Homopolymerisation of isopropyl thioacrylate with DP = 60 and [I] = 0.01 mol% (P10)

In a typical polymerisation, (0.408 g, 3.138 mmol) isopropyl thioacrylate, BDTMP (23.6 mg, 0.056 mmol), V-601 (0.117 mg, 0.0005 mmol), 0.11 mL mesitylene and 1.14 mL of toluene were charged into a Schlenk tube and degassed by gentle bubbling of N_2 gas for 30 minutes. Schlenk tube was submerged into an oil bath at 70°C. Samples were taken *via* degassed syringe at desired time points and analysed. The samples were then analysed by GPC, GC and ^{1}H NMR (**Figure 3.28**)

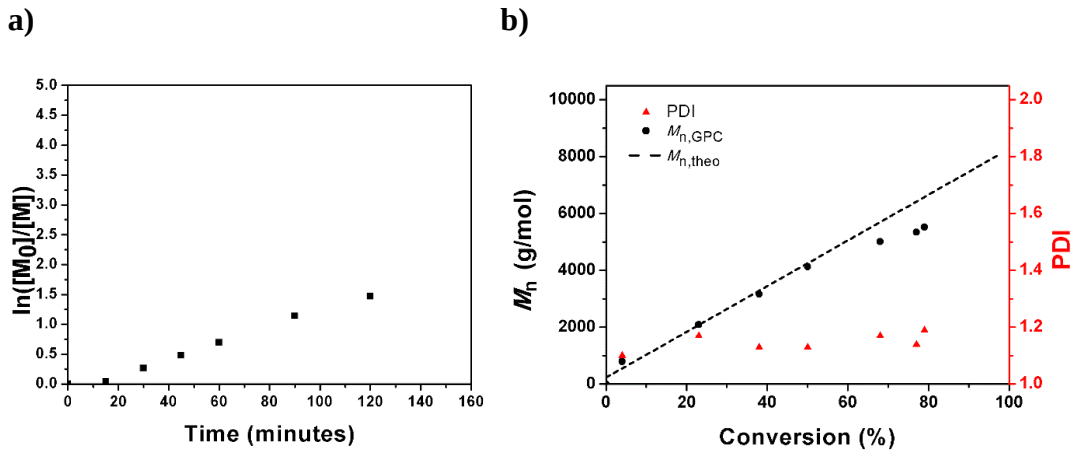

Figure 3.28: a) Ln([M]$_0$: [M]) vs. time plot for P(*i*-PTA). **b)** M_n vs. conversion plot for P(*i*-PTA).Black symbols represent $M_{n,GPC}$, dashed lines represents respective $M_{n,theo}$ and red symbols represents their PDI.

3.4.3.8 Block copolymerisation of EA with ETA, DP = 60 (P11)

In a typical chain extension experiment, (0.4946 g, 4.94 mmol) ethylacrylate, BDTMP (36.0 mg, 0.086 mmol), V-601 (2 mg, 0.0087 mmol), 0.05 mL mesitylene and 0.5 mL of toluene were charged into a schlenk tube and degassed by gentle bubbling of N_2 gas for 30 minutes. Schlenk tube was submerged into an oil bath at 70°C. Sample was taken *via* degassed syringe after 4.5 h and block was chain extended with 0.58 g (5.00 mmol) ethylthioacrylate in 0.49 mL of toluene and samples were measured at desired time intervals.

3.4.3.9 Block copolymerisation of ETA with EA, DP = 60 (P12)

In a typical chain extension experiment, (0.59 g, 5.08 mmol) ethylthioacrylate, BDTMP (34.4 mg, 0.082 mmol), V-601 (2 mg, 0.0087 mmol), 0.06 mL mesitylene and 0.6 mL of toluene were charged into a schlenk tube and degassed by gentle bubbling of N_2 gas for 30 minutes. Schlenk tube was submerged into an oil bath at 70°C. Sample was taken *via* degassed syringe after 4.5 h and block was chain extended with 0.4924 g (4.924 mmol) ethylacrylate in 0.49 mL of toluene and samples were measured at desired time intervals.

3.5 References

1. M. Le Neindre and R. Nicolay, *Polym. Chem.*, 2014, **5**, 4601-4611.
2. R. K. Iha, K. L. Wooley, A. M. Nyström, D. J. Burke, M. J. Kade and C. J. Hawker, *Chem. Rev.*, 2009, **109**, 5620-5686.
3. S. Reinicke, P. Espeel, M. M. Stamenovic and F. E. Du Prez, *Polym. Chem.*, 2014, **5**, 5461-5470.
4. G.-Z. Li, R. K. Randev, A. H. Soeriyadi, G. Rees, C. Boyer, Z. Tong, T. P. Davis, C. R. Becer and D. M. Haddleton, *Polym. Chem.*, 2010, **1**, 1196-1204.
5. S. Bonengel and A. Bernkop-Schnuerch, *J. Control Release* 2014, **195**, 120-129.
6. Y. Iwakura, K. Kurita and F. Hayano, *Journal of Polymer Science Part A-1: Polymer Chemistry*, 1969, **7**, 3075-3087.
7. K. Nakabayashi, A. Matsumura, Y. Abiko and H. Mori, *Macromolecules*, 2016, **49**, 1616-1629.
8. Y. Qiao, X. Yin and C. Tang, *Science China Chemistry*, 2015, **58**, 1641-1650.
9. C. Zhao, Y. Zhang, S. Pan, L. Rothberg and M.-K. Ng, *Macromolecules*, 2007, **40**, 1816-1823.
10. A. Kausar, S. Zulfiqar and M. I. Sarwar, *Polymer Reviews*, 2014, **54**, 185-267.
11. C. G. Overberger and H. Aschkenasy, *J. Am. Chem. Soc.*, 1960, **82**, 4357-4360.
12. C. G. Overberger and H. Aschkenasy, *J. Org. Chem.*, 1960, **25**, 1648-1651.
13. S. Matsumura, N. Kihara and T. Takata, *Synthesis of All Aromatic Poly(Thioether-Ketone)s, Sulfur-Containing High Performance Polymers with High Solubility*, 2001.
14. M. Kato, K. Toshima and S. Matsumura, *Biomacromolecules*, 2009, **10**, 366-373.
15. K. Yamamoto and A. Takasu, *Macromolecules*, 2010, **43**, 8519-8523.
16. P. J. Evans, R. C. T. Slade, J. R. Varcoe and K. E. Young, *Journal of Materials Chemistry*, 1999, **9**, 3015-3021.
17. A. Bernkop-Schnürch, A. H. Krauland, V. M. Leitner and T. Palmberger, *European Journal of Pharmaceutics and Biopharmaceutics*, 2004, **58**, 253-263.
18. C. S. Marvel, S. L. Jacobs, W. K. Taft and B. G. Labbe, *Journal of Polymer Science*, 1956, **19**, 59-72.
19. N. Hadjichristidis, *Macromolecules*, 1981, **14**, 128-130.
20. N. Hadjichristidis, *Polymer*, 1981, **22**.
21. T. Otsu, K. Tsuda and T. Fukumizu, *Die Makromolekulare Chemie*, 1968, **119**, 140-146.
22. Y. Nakayama, T. Tsuruta, J. Furukawa, A. Kawasaki and G. Wasai, *Die Makromolekulare Chemie*, 1961, **43**, 76-83.
23. Y. Okamoto, M. Toki and H. Yuki, *Journal of Polymer Science: Polymer Chemistry Edition*, 1979, **17**, 3705-3712.
24. P. Thapa, R.-Y. Zhang, V. Menon and J.-P. Bingham, *Molecules*, 2014, 14461-14483.
25. A. Anastasaki, V. Nikolaou and D. M. Haddleton, *Polym. Chem.*, 2016, **7**, 1002-1026.
26. Q. Zhang, J. Collins, A. Anastasaki, R. Wallis, D. A. Mitchell, C. R. Becer and D. M. Haddleton, *Angew. Chem. Int. Ed.*, 2013, **52**, 4435-4439.

27. Q. Zhang, L. Su, J. Collins, G. Chen, R. Wallis, D. A. Mitchell, D. M. Haddleton and C. R. Becer, *J. Am. Chem. Soc.*, 2014, **136**, 4325-4332.
28. E. L. Malins, S. Amabilino, G. Yilmaz, F. H. Isikgor, B. M. Gridley and C. R. Becer, *Eur. Polym. J.*, 2015, **62**, 347-351.
29. J. Nicolas, Y. Guillaneuf, C. Lefay, D. Bertin, D. Gigmes and B. Charleux, *Progress in Polymer Science*, 2013, **38**, 63-235.
30. R. B. Grubbs, *Polym. Rev.*, 2011, **51**, 104-137.
31. J. Nicolas, Y. Guillaneuf, C. Lefay, D. Bertin, D. Gigmes and B. Charleux, *Prog. Polym. Sci*, 2013, **38**.
32. E. L. Malins, S. Amabilino, G. Yilmaz, F. H. Iskigor, B. M. Gridley and C. R. Becer, *Eur. Polym. J.*, 2015, **62**.
33. C. Boyer, N. A. Corrigan, K. Jung, D. Nguyen, T.-K. Nguyen, N. N. M. Adnan, S. Oliver, S. Shanmugam and J. Yeow, *Chem. Rev.*, 2016, **116**, 1803-1949.
34. V. Coessens, T. Pintauer and K. Matyjaszewski, *Prog. Polym. Sci*, 2001, **26**, 337-377.
35. C. R. Becer, R. M. Paulus, S. Höppener, R. Hoogenboom, C.-A. Fustin, J.-F. Gohy and U. Schubert, *macromolecules*, 2008, **41**.
36. G. Moad, E. Rizzardo and S. H. Thang, *Polymer*, 2008, **49**, 1079-1131.
37. G. Moad, E. Rizzardo and S. H. Thang, *Aust. J. Chem.*, 2009, 1402-1472.
38. K. Kempe, A. Krieg, C. R. Becer and U. S. Schubert, *Chem. Soc. Rev.*, 2012, **41**, 176-191.
39. G. Moad and D. H. Solomon, *The Chemistry of Radical Polymerization*, Elsevier, Oxford, 2006.

4 Nitroxide mediated polymerisation of thioacrylates and their modification

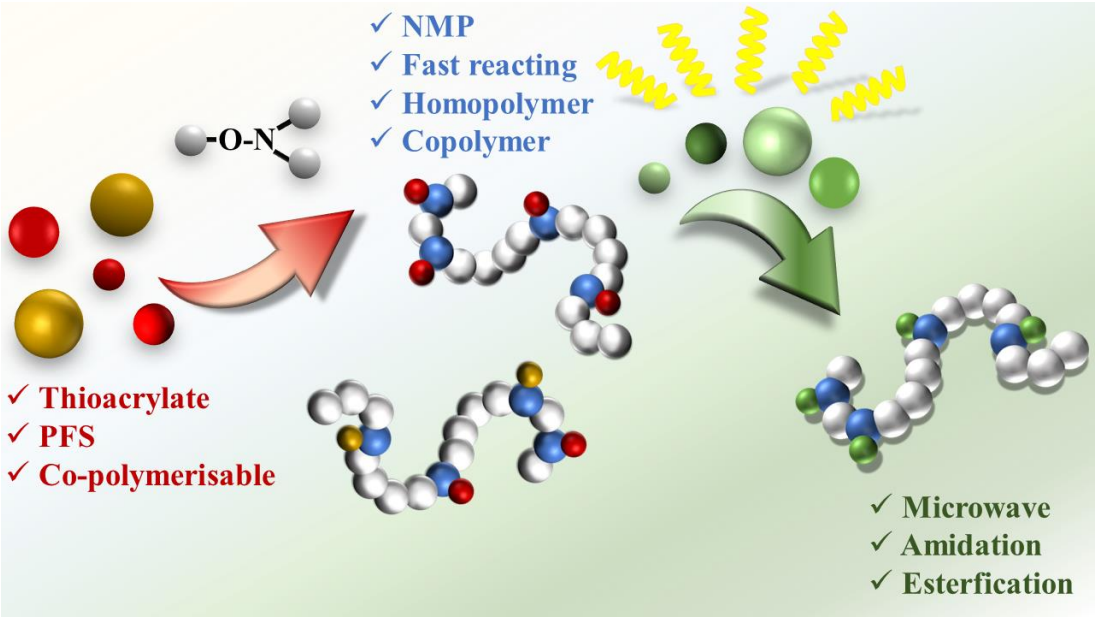

One long-standing challenge in polymer science is the development of transformation reactions, in which the conversion of a functional group to another is targeted. In the past years advances have been made with regards to amidation of unactivated and activated esters and amides, whereas the amidation of thioester containing polymers has remained elusive. In this chapter, a simple approach that allows nucleophilic substitution with primary amines and alcohols on a poly(thioacrylate) has been discussed. A thioacrylate monomer has been polymerised via nitroxide mediated polymerisation (NMP) and post modification in a metal-free and thiophenol catalysed reaction is investigated. Copolymerisation reactions with other classes of functional monomers are also studied and evaluated.

4.1 Introduction

Within the field of chemical synthesis, transformation reactions play a pivotal role. In particular the amide-bond formation has a widespread occurrence in the synthesis of pharmaceuticals, natural products and fine chemicals.[1] In particular, a huge area of transformation reactions have emerged that address the modification of polymers, in which one particularly interesting reaction is the transamination reaction with amines under specific conditions. The ability to convert a functional group into an amide remains an important endeavour with a remarkable impact as it allows access to more natural amide-based polymers and mimic biostructures to help to understand their functions.[2] Over the past years, many examples of substitution reactions on polymers have been reported and open a new avenue into value-added materials.[3] Two aspects play a role when a modification reaction is considered. On one hand, the modification of a polymer is the only route to the functional material as no direct polymerisation of monomer can be performed. For example, reactive monomers cannot be employed within the polymerisation process due to side reactions, where a protecting strategy becomes necessary. Modification reactions also offer a way, when a starting material is not commercially available at all and a precursor becomes necessary. For this, post polymerisation modification (PPM) is conducted after polymerisation under various conditions with different functional groups. Couplings reactions such as thiol-ene, thiol-yne, *Michael* addition, exchange reactions[4], cycloadditions have been summarised as a possible pathway to modify a polymer. Numerous functional groups have been employed and one in particular is the example of chemical transformation reactions of activated esters in a macromolecular context, where a large range of amines from natural or commercial sources can be used.[5] The monomers can be easily polymerised to yield the reactive precursor. Prominent examples are pentafluorophenyl (PFP) ester, NHS-ester monomers[6], pentafluorophenyl ester-based acrylates (PFPA) or methacrylates (PFPMA)[7], and vinylbenzoates (PFP4VP). To overcome extended reaction times and high temperatures, more latterly catalytic approaches of ester derivatives have been reported. For example, unactivated esters have been used for catalytic activation with nucleophilic organocatalyst (1,5,7-triazabicyclo[4.4.0]undec-5-ene (TBD)) with primary amines and alcohols[8] or by involving a base-catalysed amidation with an exogenous alcohol-derived additive to

form an active ester in situ.[9] More recently, *Hillmyer* and co-workers have employed a metal-free nucleophilic substitution with amines and alcohols of an activated amide containing polymer of the less reactive di(Boc)-acrylamide (DBAm).[10]

Inspired by a report on a metal-free, thiol-catalysed amidation on a thioester[11] and a similar approach on solid phase through thiol-catalysed substitution[12], amidation on a polythioacrylate was investigated on a macromolecular level. For this, two different thioacrylates were polymerised *via* NMP for the first time. Reaction kinetics of their homopolymerisation and copolymerisation behaviour with a styrene derivative (2,3,4,5,6-pentaflurostyrene, PFS) as a second type of functional monomer were followed by periodic sampling. Kinetic studies of the reaction between primary amines where poly(ethyl thioacrylate) was used as a representative polythioacrylate and benzylamine as a model for a free amine were investigated. The strategy was additionally tested using isopropylamine and benzylalcohol. Functionalisation was carried out in the presence of thiophenol and base on the thioester moiety.

4.2 Results and Discussion

4.2.1 Homopolymerisation of butyl thioacrylate and butylacrylate *via* NMP

SG1-MAMA is an efficient initiator for the polymerisation of a broad variety of different acrylic esters.[13] Butylacrylate (BuA) is a representative acrylic ester often polymerised *via* NMP and many studies under various conditions have been reported to date.[14-17] BuA has been therefore used as a model acrylate to compare it to its sulfur-containing counterpart, butyl thioacrylate (BuTA). In the following section, the polymerisation of butyl thioacrylate (BuTA) and butylacrylate (BuA) have been investigated using an SG1-based alkoxyamine *N*-(tert-butyl)-N-(1-diethylphosphono-2,2-dimethylpropyl)-*O*-(2-carboxylprop-2-yl)-hydroxylamine (SG1-MAMA, BlocBuilder^{TM}) as NMP initiator, which enables polymerisation of a broad range of monomers, including acrylates and acrylamides. The polymerisation kinetics were followed for high and lower temperatures. The general reaction conditions for both monomers are shown below (**Scheme 4.1**).

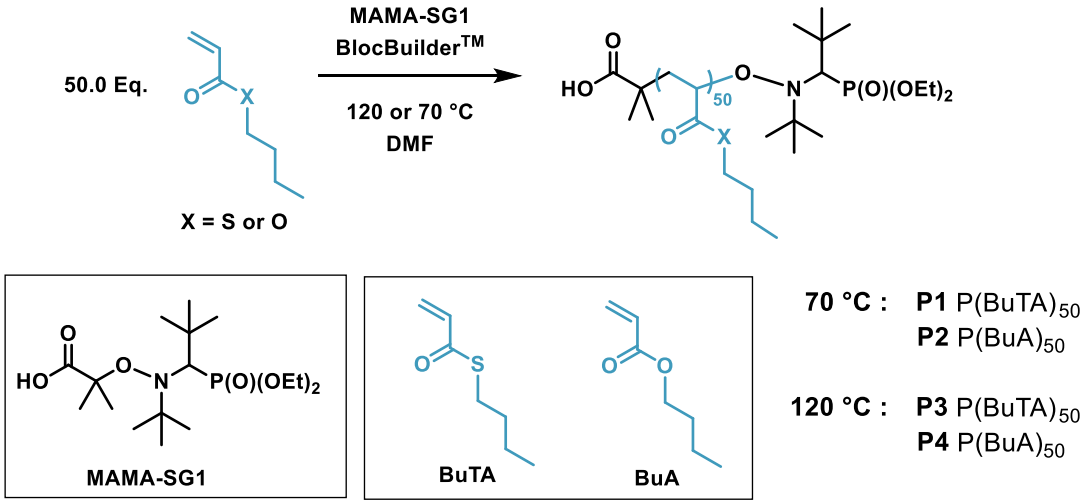

Scheme 4.1: Homopolymerisation of BuTA and BuA *via* NMP.

The homopolymerisation of BuTA and BuA using SG1-MAMA were studied, examining the influence of temperature at 70 and 120 °C and the type of related monomers. Samples were taken periodically from the polymerisation reactor to determine the conversion and average molecular weight of the polymers. The conditions were subsequently applied for a homopolymerisation with chain length of DP_n = 50 ($[M]_0$:$[SG1\text{-}MAMA]_0$ = [50]:[1] in **P1, P2, P3** and **P4**. In the following, the details of the polymerisations will be described.

Initial screening of the homopolymerisation of BuTA in **P1** presented a relatively good control over molecular weight distribution (PDI ~ 1.36 – 1.78). Yet the polymerisation did not proceed to high conversion and stopped after 240 minutes with 59% of monomer conversion. This observation is explained as follows: the NMP process requires higher polymerisation temperature, sufficiently high for the dissociation of SG1-MAMA and high enough to allow a reversible dissociation of the alkoxyamine product.

The employed temperature was increased in a next attempt to obtain higher conversion. Kinetic investigation revealed full conversion within 2 h, with more narrow PDIs (1.46 – 1.67) at a higher polymerisation temperature of 120 °C for **P3**.

Table 4.1: Data obtained from the homopolymer of BuTA, at 70 °C in DMF (**P1**).

Time (min)	$M_{n,theo}$ (g/mol)	$M_{n,GPC}$[b] (g/mol)	PDI[b]	Conv.[a] (%)
30	1680	1800	1.71	18
60	1820	2070	1.59	20
90	2110	2060	1.62	24
120	2250	2490	1.46	26
240	4630	3470	1.78	59

Polymerisation condition: ($[M]_0$:$[SG1\text{-}MAMA]_0$ = 50:1) in DMF at 70 °C for BuTA for **P1**. [a] Conversion measured by ^{1}H NMR spectroscopy. [b] THF eluent, linear PMMA standard.

Again, the evolution of the monomer concentration was monitored throughout the reaction both by GPC and by ^{1}H NMR to follow conversions with increasing time for **P3**. At the bottom of **Figure 4.1**, the NMR spectrum of the initial reaction mixture, containing BuTA, 5% internal standard (mesitylene) in DMF is depicted. The signals between 5.58 – 6.25 ppm originate from the three protons of the CH_2- and CH- group of the thioacrylate repeating unit. The triplet at 0.83 ppm arises from the methyl group of the sidegroup (H_f), whereas the two CH_2-groups appear as a quintet at 1.31 ppm for H_d and as a sextet at 1.49 ppm for H_e. However, the CH_2-group located next to the thioester is located 2.86 ppm and is overlapping with the methyl group of the DMF and will not be used for further calculations. Conversion was calculated as the ratio of the integral of the CH-resonance of the double bond (H_{a2}) of BuTA at 5.58 ppm and the methyl group of BuTA and P(BuTA) resonance at 0.85 ppm.

The spectra above the spectrum of the initial reaction mixture (t_0) were acquired at 15, 30, 45, 60, and 120 minute time-points over the course of polymerisation. The insert shows a decrease in intensity of the vinyl protons of BuTA at δ 5.58 – 6.25 ppm as the reaction progresses and are not visible at 120 minutes due to full consumption of the monomer. Additionally, a broadening of the signals throughout the reaction can be observed for the polymer backbone and side group-peaks, which is typical for a polymer.

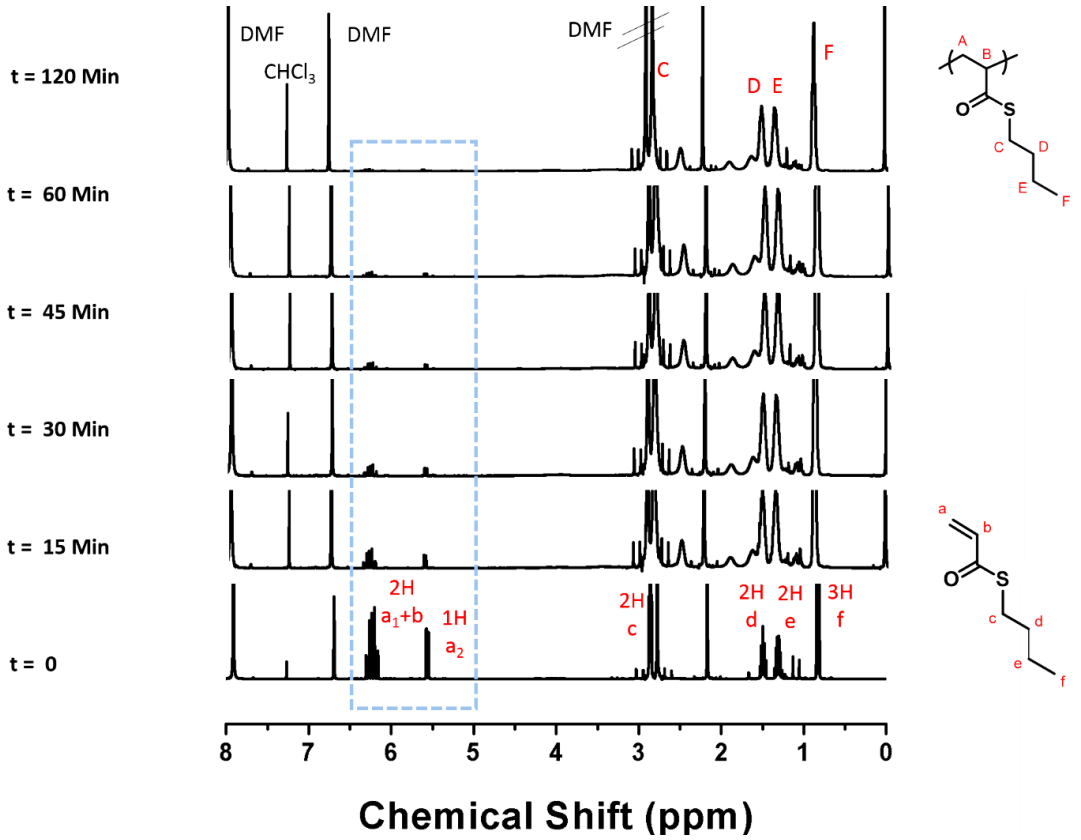

Figure 4.1: Stacked spectra of measured ^{1}H NMR samples, showing the monomer conversion during the homopolymerisation of BuTA (DP=20) obtained *via* NMP in DMF ($CDCl_3$, 400 MHz, 303 K).

GPC analysis revealed a linear increase in number-average molecular weight (M_n) with increasing conversion. Whereby excellent agreement with theoretical M_n and low dispersity are obtained for **P1**, higher theoretical values for number-average molecular weight ($M_{n,theo}$) compared to obtained M_n are obtained for **P3**. The difference in the calculated and experimental molecular weight arises due to the fit in the GPC calibration that gives higher difference in higher molecular weight compared to the low molecular weight region.

The kinetics of the polymerisation and control of the resulting polymer molecular weight (MW) and molecular weight distribution depend on the dissociation and recombination rate coefficients of the SG1-MAMA. The chosen temperature plays an important role in the thermal dissociation and therefore the initiation of the polymerisation and hence, can lead to a faster polymerisation rate. In a comparison experiment, homopolymerisation of butylacrylate at 70 °C were found to be significantly slower in the first 2 hours. The polymerisation stopped with no recognisable increase in conversion observed according to ^{1}H NMR at 3 hours with a

conversion of 13%. The semi-logarithmic kinetic plots for BuTA and BuA at 70 and 120 °C are shown in **Figure 4.2** and summarised in **Table 4.2**.

Table 4.2: Data obtained from the homopolymer of BuTA, at 120 °C in DMF (**P3**).

Time (min)	$M_{n,theo}$ (g/mol)	$M_{n,GPC}$[b] (g/mol)	PDI[b]	Conv.[a] (%)
15	6790	4240	1.46	89
30	7080	4220	1.52	93
45	7220	4250	1.54	95
60	7370	4200	1.60	97
90	7440	4240	1.63	98
120	7580	4310	1.67	100

Polymerisation condition: ($[M]_0$:$[SG1\text{-}MAMA]_0$ = 50:1) in DMF at 120 °C for BuTA for **P3**. [a] Conversion measured by ^{1}H NMR spectroscopy. [b] THF eluent, linear PMMA standard.

The linear relationships indicate a constant radical concentration throughout the NMP process and the apparent propagation rates (k_p^{app}) can be estimated from the slopes of the second linear region of the semi-logarithmic kinetic plots (**Figure 4.2**).

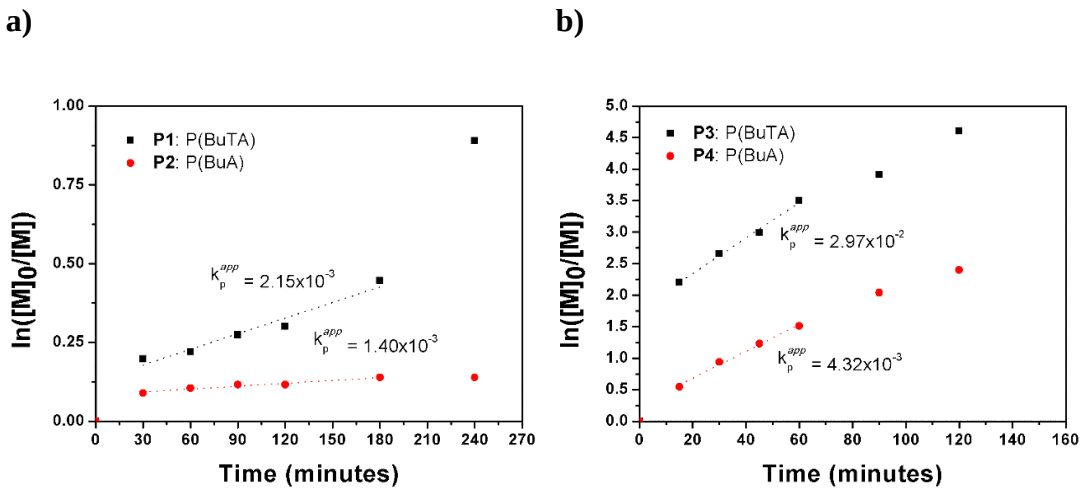

Figure 4.2: Investigation of homopolymerisation of BuTA and BuA *via* NMP, DP = 50 in DMF using a unimolecular initiator SG1-MAMA. **a)** Ln($[M]_0$/[M]) vs. time plot for P(BuTA), and P(BuA) at 70 °C. **b)** Ln($[M]_0$/[M]) vs. time plot for P(BuTA) and P(BuA) at 120 °C.

Figure 4.2 illustrates the effect of temperature on polymerisation rate in the presence of a low-molecular-weight alkoxyamine (M_n = 381 g/mol). As expected, at a higher temperature, the polymerisation rate is significantly higher. k_p^{app} for the homopolymerisation of BuTA (**P1**) shows a 1.5-fold increase ($2.15x10^{-3}$ s^{-1}), to the counterpart monomer, BuA (**P2**, $4.32x10^{-3}$ s^{-1}) at 70 °C. For both monomers an expected increase of k_p^{app} was observed when temperature was increased to 120 °C. The increase led to a 13-fold increase of the propagation rates for BuTA in **P1** to **P3**, whereas the increase for BuA is only 3-fold (**P4**).

The Arrhenius equation $k_p = A\exp(-E/RT)$, where E represents the activation energy and A the frequency factor with R as the universal gas constant and T as temperature in K, shows that, increasing T will increase k_p. As the dissociation of the C-ON bond is an endothermic process, the increase in temperature will therefore enhance the rate of dissociation of C-ON and subsequently K will increase. All four polymerisations for BuTA and BuA showed that higher temperatures increase the polymerisation rate. The progress of polymerisation was followed by GPC for **P3** and **P4** and showed a clear shift to higher molecular weight after every 15 minutes for the first hour for BuA at 120 °C (**P4**) (**Figure 4.3**).

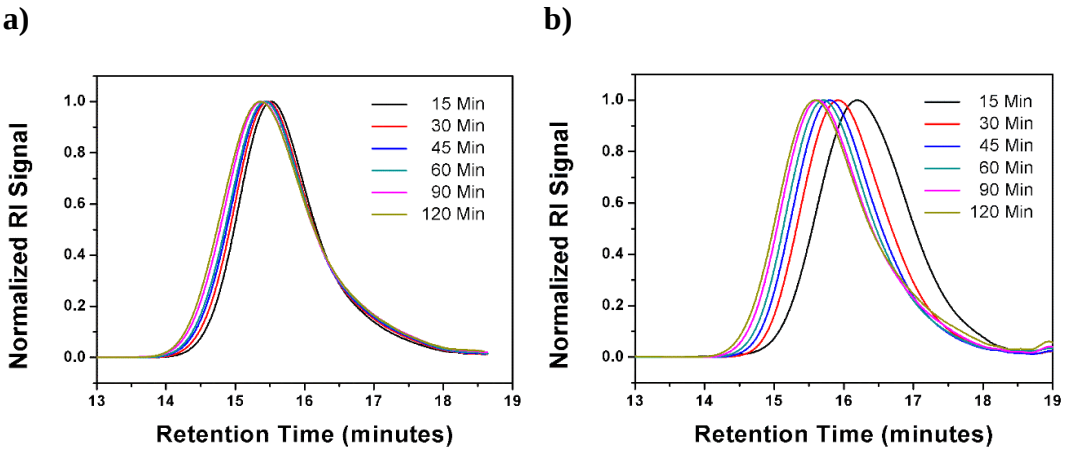

Figure 4.3: GPC traces of the homopolymerisation at 120 °C in DMF. **a)** For BuTA with DP = 50 (**P3**), **b)** For BuA with DP = 50 (**P4**).

Approximately 7-fold higher propagation rate for the homopolymerisation of BuTA is also manifested in the first peak at 15 minutes appearing already at a high molecular weight. The progress of the reaction can be followed by a shift of the molecular weight distributions to higher molecular weights with an observable increase in dispersity (PDI ~1.67).

4.2.2 Copolymerisation of butyl thioacrylate and butylacrylate with PFS *via* NMP

The alkoxamide employed in the previous experiments enables the controlled polymerisation of a selection of monomers and functional groups. The monomer families compatible with SG1-MAMA ranges from styrenes to acrylates, acrylamides 1,3,-dienes, and acrylonitrile-based monomers and also allow the facile synthesis of copolymers of different classes. In a series of kinetic experiments, a second functional monomer, PFS was copolymerised with BuTA to yield a bifunctional linear polymer.

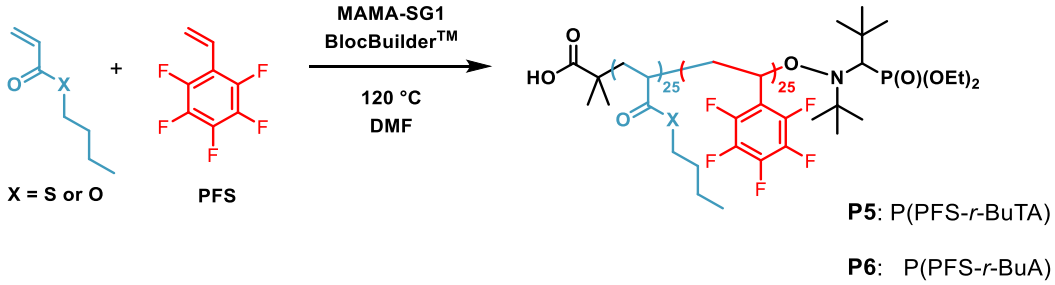

Scheme 4.2: Schematic representation of the overall reaction scheme for the preparation of copolymers **P5** and **P6**.

The use of PFS carries certain advantages, for example it is commercially available and is one of the most often employed monomer for post-modifications.[18, 19] The para-fluorine atom of the pentaflurophenyl (PFP) moiety is susceptible to nucleophilic attack by alcohols, amines, phosphines, and a range of sulfur-based compounds, particularly thiols. In combination with a thioacrylate, the resulting copolymer will furnish the polymer with a second pendant functional group for a nucleophilic attack. In the following, the copolymerisation of BuTA with PFS at 120 °C in DMF was explored. Additionally, the radical copolymerisation of BuTA with PFS in a feed ratio of [BuTA; BuA]:[PFS] = 1:1 was investigated for comparison and the representative results are summarised in **Table 4.3**.

Within an hour, a well-defined poly(PFS)-*r*-(BuA) and poly(PFS)-*r*-(BuTA) copolymer was obtained **(Figure 4.4)**. Whereas **P5** indicates a significantly increased polymerisation rate, a drift in the dispersity was observed (PDI~1.46). Interestingly, by employing BuA instead of BuTA, an opposing trend can be observed, where the polymerisation rate is reduced but the dispersity remains low with 1.27.

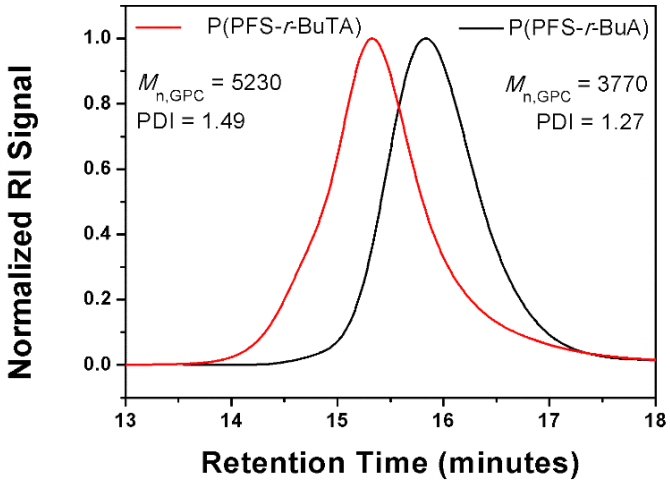

Figure 4.4: GPC traces of the homopolymerisation of PFS with BuA (**P5**, black trace) and PFS with BuTA (**P6**, red trace) with DP = 50 in DMF at 120 °C.

Butylacrylate was copolymerised successfully with PFS. Thioacrylates were found to be compatible with this polymerisation technique as well, showing a higher rate of polymerisation in the homopolymerisation and copolymerisation with PFS in **P6** relative to butylacrylate. For example, when butylacrylate was employed as a comonomer, a lower conversion of PFS (10%) was obtained in 60 minutes compared to 94% of PFS in **P5** with BuTA.

A linear dependence of $\ln[M]_0/[M]$ *vs*. time indicated first order kinetics with respect to monomer concentration between 15 and 90 minutes (**Figure 4.6**) for both monomers in polymers **P5** and **P6**. As well as in the hompolymerisation of BuTA and BuA, a higher propagation rate for a polymer, where a thioacrylate is used was observed. Obtained data from the copolymer of PFS with BuTA and BuA at 120 °C in DMF are summarised in **Table 4.3.**

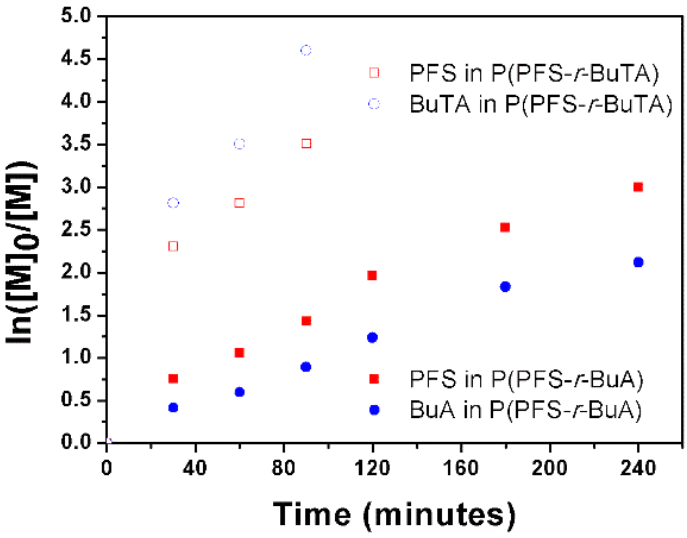

Figure 4.5: Influence of monomer composition in copolymer of **P5** and **P6**: ln([M]$_0$/[M]) *vs*. time plot for P(PFS)-*r*-(BuTA) and P(PFS)-*r*-(BuA).

For instance, when BuTA is used in a copolymerisation with PFS instead of BuA, a 1.8-fold higher k_p^{app} could be achieved for PFS. BuTA in **P5** evidenced a significantly higher propagation rate coefficient of 4.96x10^{-4} s^{-1} compared to BuA (1.32x10^{-4} s^{-1}) (**Figure 4.6**).

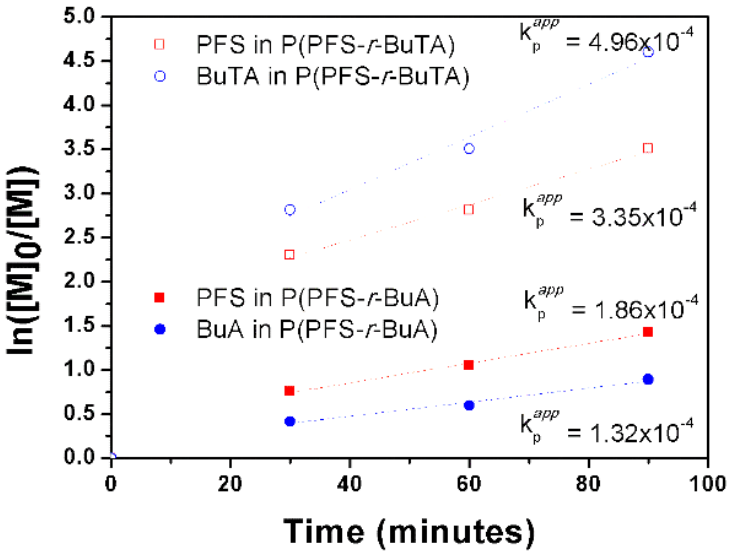

Figure 4.6: Influence of monomer composition in copolymer of **P5** and **P6**. Zoom of the second linear region of the ln([M]$_0$/[M]) *vs*. time plot.

Table 4.3: Data obtained from the copolymers of PFS with BuTA and BuA at 120 °C in DMF.

Code	Polymer	Monomer	k_p^{app} (s^{-1})
P5	P(PFS-*r*-BuTA)	PFS	$3.35x10^{-4}$
P5	P(PFS-*r*-BuTA)	BuTA	$4.96x10^{-4}$
P6	P(PFS-*r*-BuA)	PFS	$1.86x10^{-4}$
P6	P(PFS-*r*-BuA)	BuA	$1.32x10^{-4}$

4.2.3 Synthesis of P(ETA) for modification reactions

In the following, modification reactions of a poly thioacrylate will be presented. For this purpose, ethyl thioacrylate (ETA) was chosen as a homopolymer of a thioacrylate for further modification as it gives fewer signals in the ^{1}H NMR and therefore less peaks overlapping with the newly formed peak in the analysis of the modified polymer **(Scheme 4.3)**. ETA was polymerised under the same conditions and full conversion was attained within 1.5h as calculated by ^{1}H NMR spectroscopy.

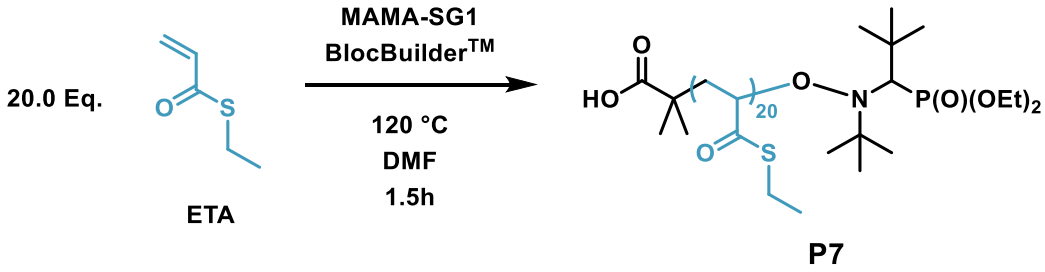

Scheme 4.3: Schematic representation of the overall reaction scheme for the preparation of homopolymer **P7**.

Figure 4.7 below, displays the ^{1}H NMR spectrum of the initial reaction mixture at the bottom and the spectrum collected at 1.5 hours. The insert at the top clearly demonstrates that the resonances signals from the vinyl protons of ETA (δ 5.59 - 6.32 ppm) are not visible at 120 minutes due to full consumption of the monomer.

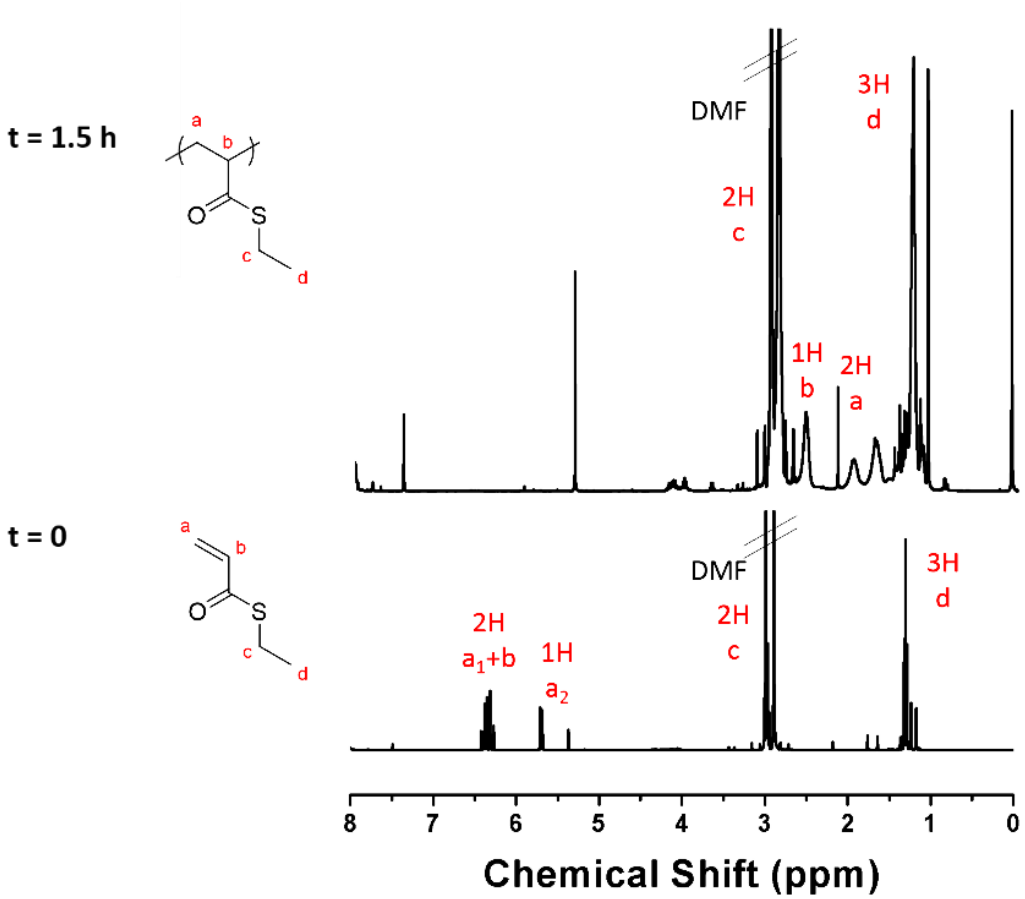

Figure 4.7: ^{1}H NMR spectra displaying full monomer consumption for homopolymerisation of ethyl thioacrylate ($CDCl_3$, 400 MHz, 303 K).

The reaction solvent was distilled off from the polymer under reduced pressure to yield a pale yellow, sticky polymer. The purified polymer **P7** has the ^{1}H NMR spectrum shown in **Figure 4.8**. While the spectrum of the crude reaction mixture only contained DMF and mesitylene, the spectrum of the purified polymer shows no residual peaks of the impurities.

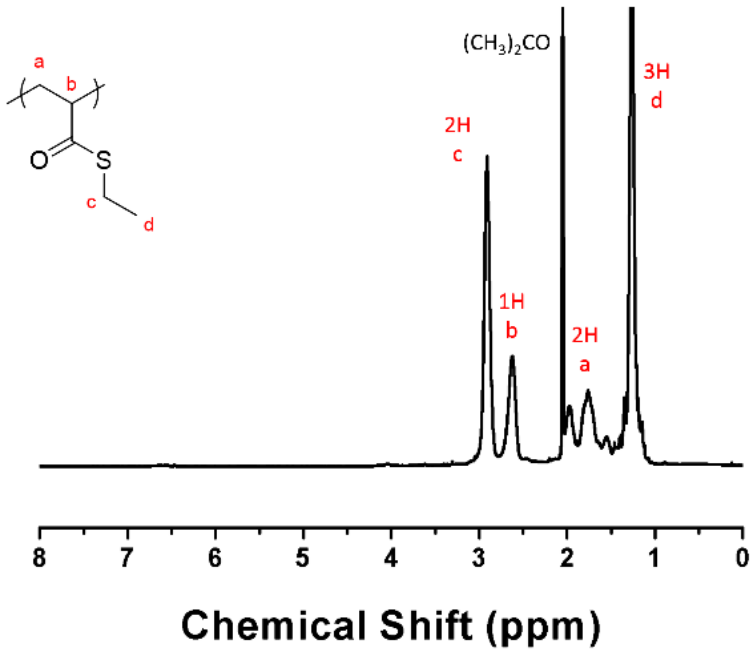

Figure 4.8: ^{1}H NMR spectra of purified poly(ethyl thioacrylate) $(CD_3)_2CO$, 400 MHz, 303 K).

Specifically, a broad peak due to the CH_3- group (H_d) of the alkyl side group appears at δ 1.36, a peak of the SCH_2- that is next to the thioester side group (H_c) appears at δ 2.91, the backbone peaks for the CH- group (H_b) at 2.61 ppm and the neighboring CH_2- (H_a) between 1.76 – 1.99 ppm. Integration of the methyl peak at δ 1.36 and the CH- polymer backbone peak at 2.61 ppm shows that these protons are present in a 3:1 ratio. ^{13}C NMR spectrum was measured and is depicted and assigned in **Figure 4.9** below.

In the ^{13}C NMR spectrum, taken in $CDCl_3$, the CH_2CH_3 side group in poly(ethyl thioacrylate) give rise to two resonances with high intensity peaks at 14.6 and 23.2 ppm . The low field chemical shift of the carbonyl resonance of the thioester (201.2 ppm) is in the range in which the carbonyl carbon resonance of aliphatic thioesters are found (193–203 ppm).[20]

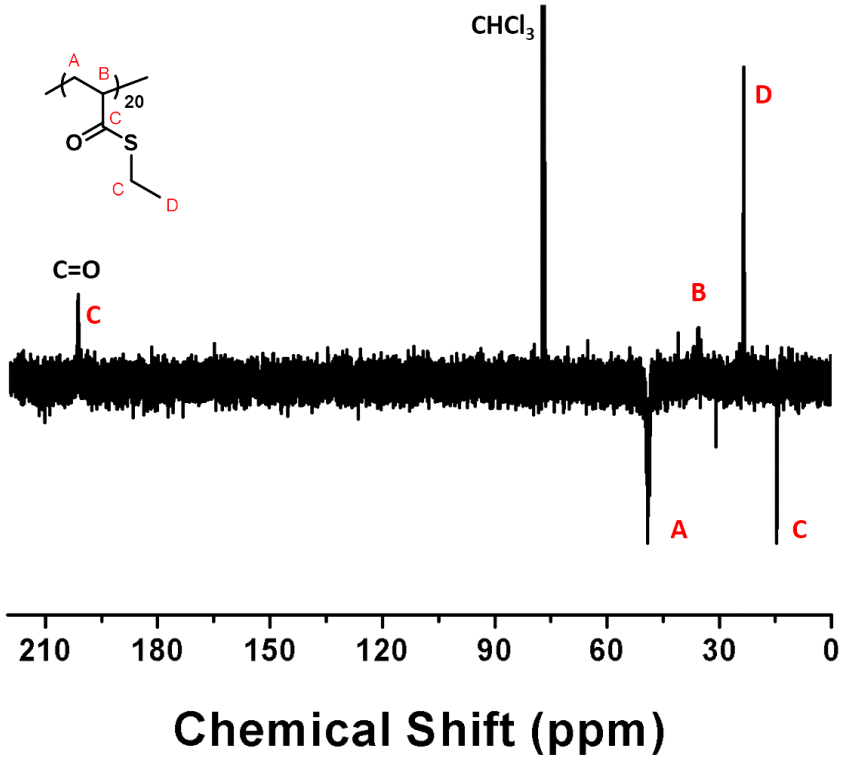

Figure 4.9: ^{13}C NMR spectrum of P(ETA) (DP=20) in $CDCl_3$ by NMP at 120 °C. The numbering of the carbon atoms used for the NMR peak assignment is shown in the spectrum.

Peaks corresponding to the polymeric backbone were observed at 49.1 and 35.6 ppm. The latter one appears as a low intensity peak and was assigned to the tertiary carbon of the CH_2CH-backbone due to the nuclear *Overhauser* effect (NOE).

GPC analysis of the purified polymer reveals a slight improvement in polymerisation control, represented by a narrower molecular weight distribution by GPC (PDI = 1.35) compared to P(BuTA) in **P3** (**Figure 4.10**).

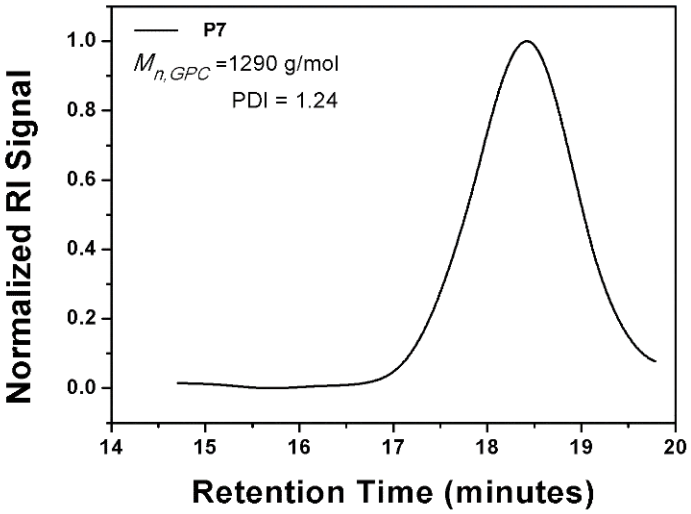

Figure 4.10: GPC trace of the obtained poly(ethyl thioacrylate)s with DP = 20 in DMF at 120°C *via* NMP.

However, experimental M_n (1520 g/mol) obtained by GPC was almost half the theoretical M_n (2700 g/mol). It is believed that this deviation from the theoretical molecular weight arises due to 1) the fact that M_n is calculated from a linear PMMA calibration, which is a different polymer in nature and 2) the fact that the slope of the calibration fit is steeper in the lower molecular weight region and hence a small difference in the hydrodynamic volume, gives a bigger difference between $M_{n,theo}$ and $M_{n,GPC}$ compared to a less steeper region.

4.2.4 Post-modification of Poly(ethyl thioacrylate) with nucleophiles

In order to investigate the modification with primary amines, the purified polymer **P7** was further used for a series of reactions. The experiments were carried out with varying quantities of the amine employed relative to the thioester moiety in the polymer **(Scheme 4.4)**.

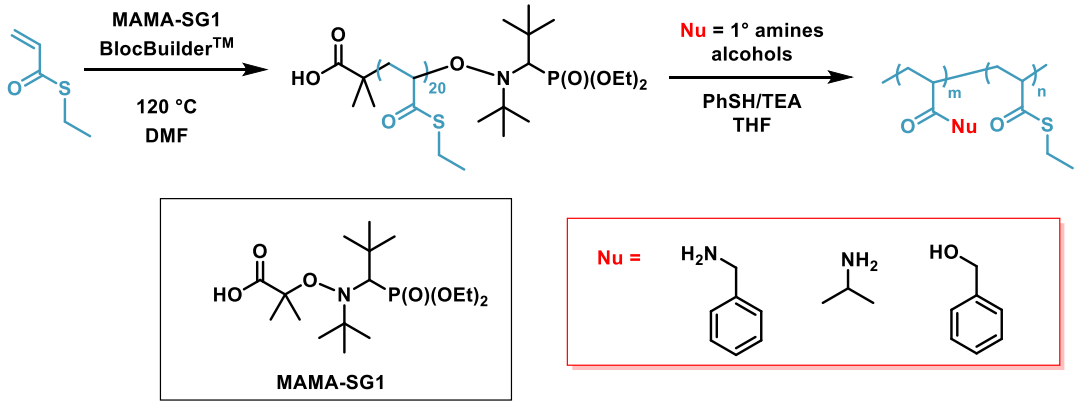

Scheme 4.4 Nitroxide mediated polymerisation of ETA, yielding Poly(ETA) and subsequent substitution of Poly(ETA) with generic nucleophile Nu.

4.2.4.1 Post-modification of Poly(ethyl thioacrylate) with benzylamine

Benzylamine was employed as a model amine as it will show a distinct proton resonance in the low field region. Additionally, the parallel experiments were performed in which every other reactant (*e.g.* base, thiol) was varied. The general concept is depicted in **Scheme 4.5** below.

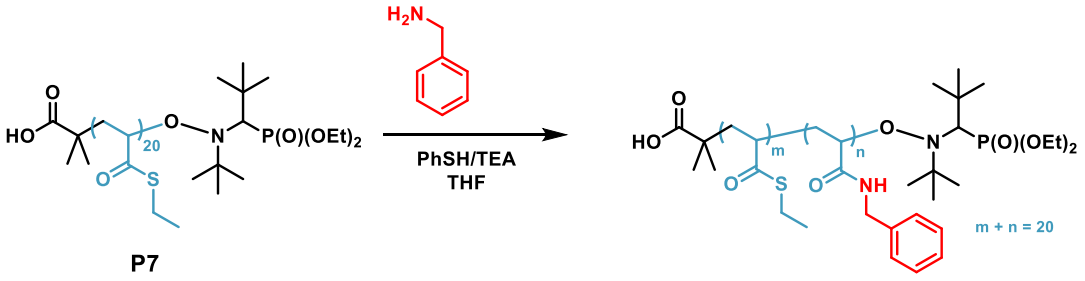

Scheme 4.5: Expected amidation product of **P7** using benzylamine as a nucleophile.

In a first reaction, thiophenol was used as a catalyst to undergo a base-catalysed amide bond formation *via* a trans-thioesterification from an attack of arylthiolate, followed by amidation of the thioester.[21-24] For this, in a 15 mL vial, the purified polymer was

dissolved in dry THF. 2.50 equivalents of benzylamine was added to the mixture followed by 2.00 equivalents of TEA and thiophenol (2.00 equivalents with respect to a single repeating unit) and stirred for 48 hours at room temperature. The mixture was then dialysed against THF/H_2O (9:1), concentrated and freeze dried to give the corresponding polymer **P8**. ^{1}H NMR comparison of the starting polymer (**P7**) and the obtained polymer from the amidation reaction, indicates that the amide bond is present in 22% of **P8**. In the final polymer **(Figure 4.11)** a broad polymeric peak in the downfield area can be detected at 7.28 ppm. When the catalyst was changed to DBU, TBD or DMAP conversions varied from 21% to 22% at 25 °C.

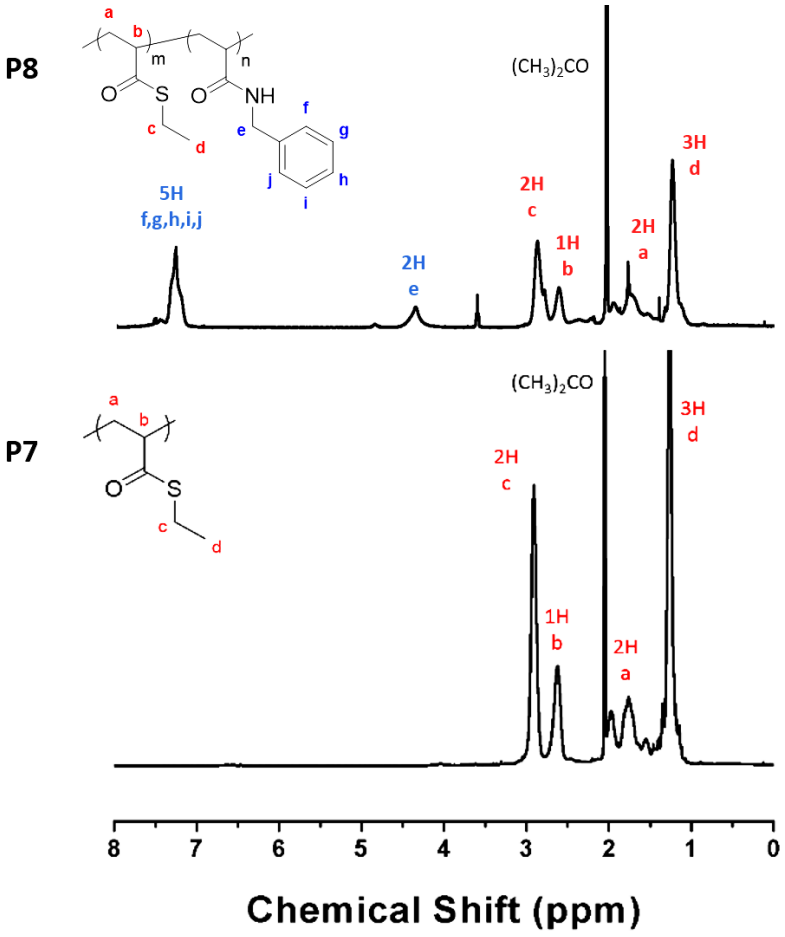

Figure 4.11: ^{1}H NMR analysis of the reaction between the thioester containing polymer **P7** and benzylamine in the presence of thiophenol forming thioester-amide containing polymer **P8**.

The resonance position of protons in **P8** bonded to a carbon of an aromatic ring are in a typical range in the down field area and can be attributed to the resonance of H_f, H_g, H_h, H_i and H_j. A second peak appears in the final polymer at 4.35 ppm and can be assigned as the CH_2-group of the incorporated benzylamine H_e. The Integration of the

aromatic peaks at δ 7.28 and the CH_2-group peak at 4.35 ppm shows that these protons are present in a 5:2 ratio. Furthermore, as the thioester pendant group will be substituted with the benzylamine, a decrease of H_c and H_d is observed as expected.

It is important to note, that the CH_2-group of the incorporated benzylamine in the middle region of the ^1H NMR will be used for calculation of the rate of the incorporation of the amine into the polymer in relation to the CH_2-peak of the alkyl side group of P(ETA) at 2.87 ppm. The reason for not taking the methyl group of the side group in P(ETA) in consideration is, that the methyl groups of the SG1-MAMA also appear in this region and will therefore let to incorrect percentages.

In order to confirm the partial substitution of an ethanethiol group with a benzylamine with a higher mass, GPC was measured for both polymers **P7** and **P8** (**Figure 4.12**).

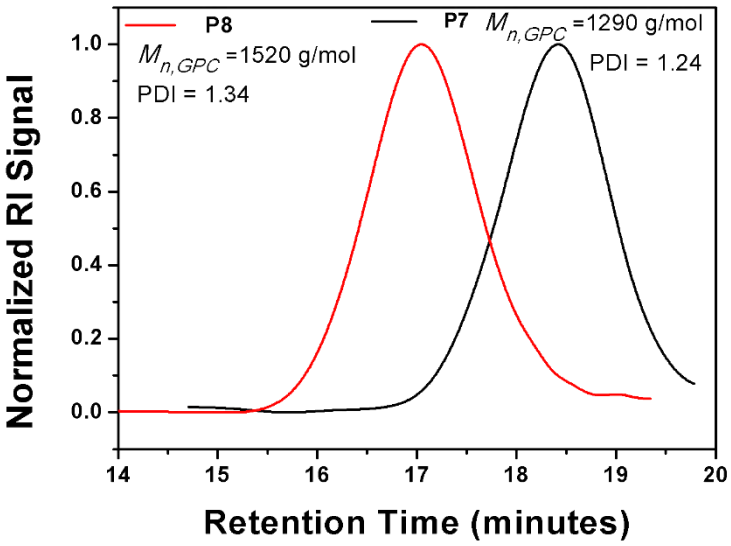

Figure 4.12: GPC traces (RID) of P(ETA) before (**P7**) and after nucleophilic substitution with benzylamine (**P8**).

The GPC measurements following the substitution of P(ETA) with benzylamine, displays a shift to higher molecular weights in (**Figure 4.12**) *M*n increased from 1290 g/mol to 1520 g/mol after substitution with the amine. Furthermore, dispersity increased to a higher value of 1.34. Interestingly, even the appearance of the polymer has changed. Whereas P(ETA) appears as a very viscous, sticky polymer with a yellow colour (**Figure 4.13a**), it becomes a powdery pale-yellow compound (**P8**) (**Figure 4.13b**).

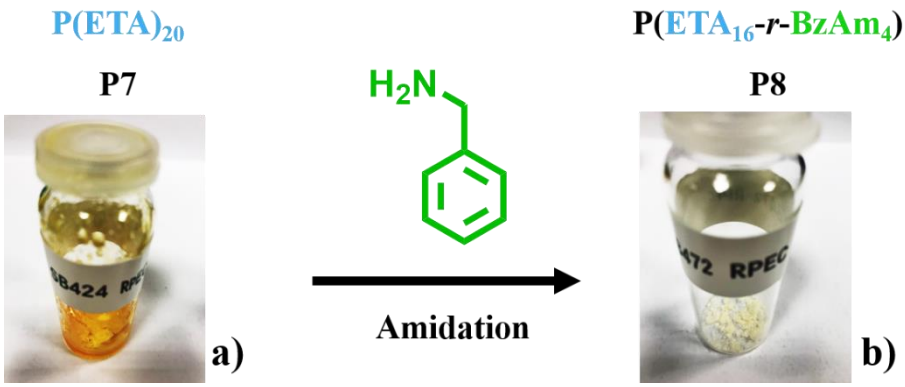

Figure 4.13. a) Visual appearance of Poly(ethyl thioacrylate) **P7**. **b)** Appearance of the post-polymerisation modified polymers with 22% of BzAm in the final copolymer **P8**.

Planned modifications of P(ETA) in later sections will discuss the influence of the amount of all reactants as well as reaction temperature. In a second attempt, the amount of amine has been quadrupled to 10.0 equivalents and the reaction was followed by ^{1}H NMR spectroscopy (**Figure 4.14**).

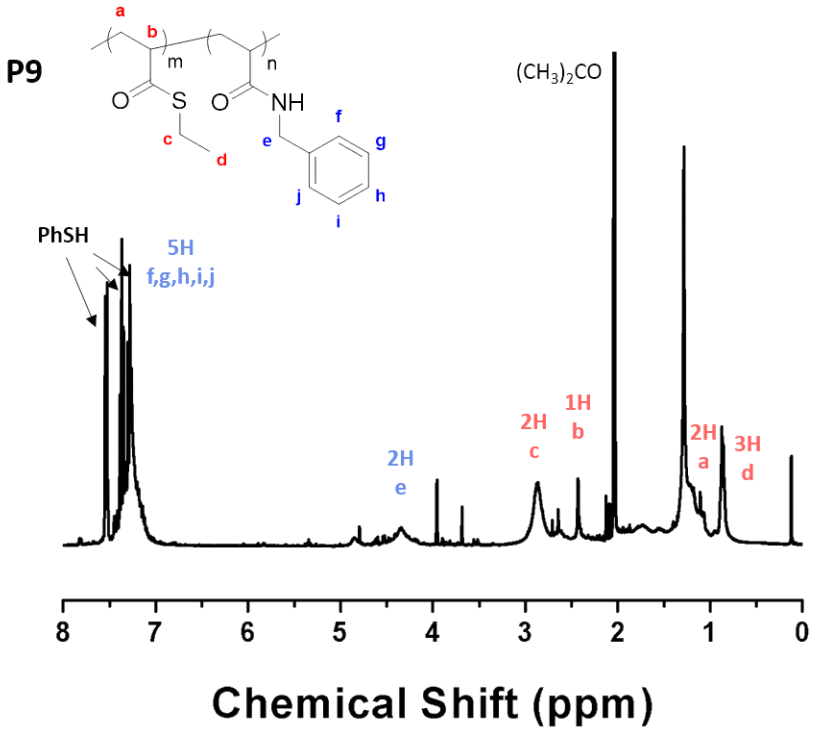

Figure 4.14: ^{1}H NMR analysis of the reaction between the thioester containing polymer **P7** and benzylamine in the presence of thiophenol forming thioester-amide containing polymer **P9**.

The reaction mixture was dialysed against THF/H_2O (9:1), concentrated and freeze dried to give the corresponding polymer. Although some residual thiophenol is left in the spectrum of the purified **P9**, the degree of amidation (DA, indicates the percent of carboxyl group in the amide structure) can be calculated by comparing the ratios of H_e and H_c (2:5) with 28%. Given a suitable higher reaction temperature of 50 °C, the amidation process could be accelerated to higher yields of 44% for **P10 (Table 4.4).**

Table 4.4: Data obtained from the amidation of P(ETA) with model nucleophile $BzNH_2$. 100 mg polymer in 1 : 6.5 *w/v* THF.

Code	**$BzNH_2$ (eq.)**	**Catalyst (eq)**	**Temp (°C)**	**Conv.** [a] **(%)**
P8	2.50	2.00 PhSH	25	22
P9	10.0	2.00 PhSH	25	28
P10	10.0	2.00 PhSH	50	44
P11	10.0	2.00 PhSH	75 (microwave)	100

[a] Measured by ^{1}H NMR.

The resulting reaction mixture was dialysed for 2 days in THF and an NMR was taken to calculate the degree of amidation (**Figure 4.15**). Altough some traces of the solvent from the dialysis are still visible in the ^{1}H NMR spectrum, the decreasing peaks of the alkyl thioester side-group can be seen with a simultaneous appearance of a high intensity peak in the low field at 7.25 ppm.

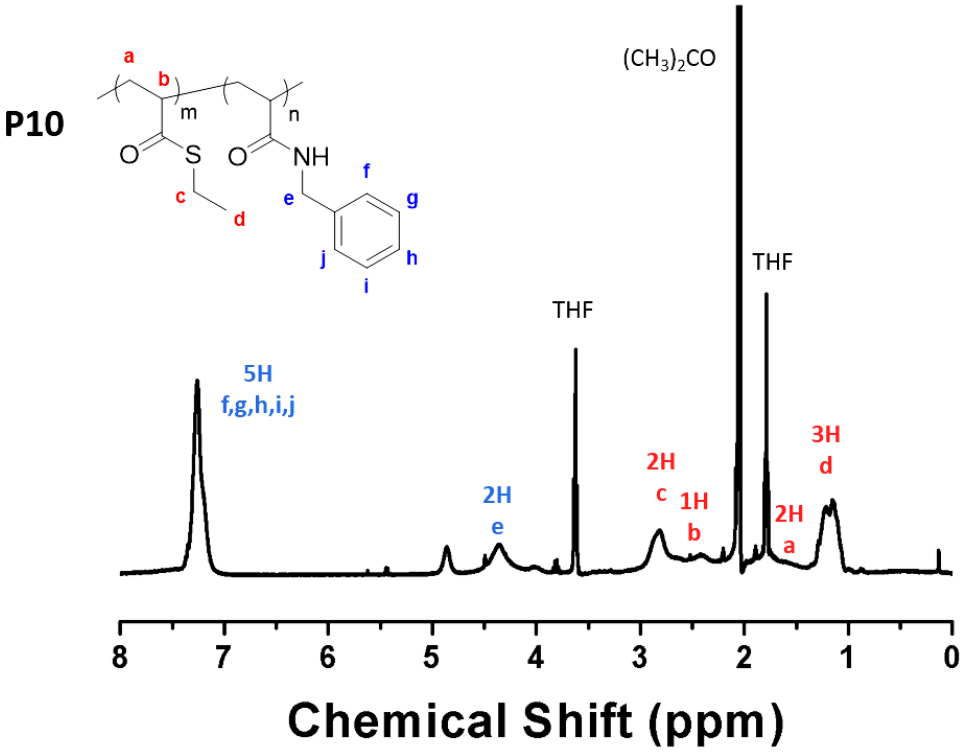

Figure 4.15: ^{1}H NMR analysis of the reaction between the thioester containing polymer **P7** and benzylamine in the presence of thiophenol forming thioester-amide containing polymer **P10**.

A second peak at 4.35 ppm can be seen and assigned to the CH_2-group of the benzylamine. The ratio of this peak and the peak at 2.81 ppm, resulting from the CH_2-group of the ethanethiol side-group in **P7** is 2:2.45, demonstrating a yield of 44% for the amidation process. The degree of amidation could be therefore increased by employing a higher reaction temperature. The temperature was further increased to 75 °C and the reaction was carried out under microwave irradiation, as the heating can be easily controlled but also a closed system for higher temperatures can be used.

For this reaction, a full substitution with benzylamine was achieved and verified by NMR and GPC analysis. In the ^{1}H NMR spectrum of **P11**, no resonance for the SCH_2-group (H_c) of the sidechain is detectable in the mid-field at 2.87 ppm (**Figure 4.16**). Additionally, the methyl group at 1.36 ppm for H_d from the pendant group disappears as well, and the resonances for the methyl group of SG1-MAMA are visible. Furthermore, the transformation entails the formation of a new CH_2-peak of the NCH_2-group for H_c as well as an aromatic peak for H_d-H_h. The full spectrum is depicted below and respective peaks are assigned (**Figure 4.16**).

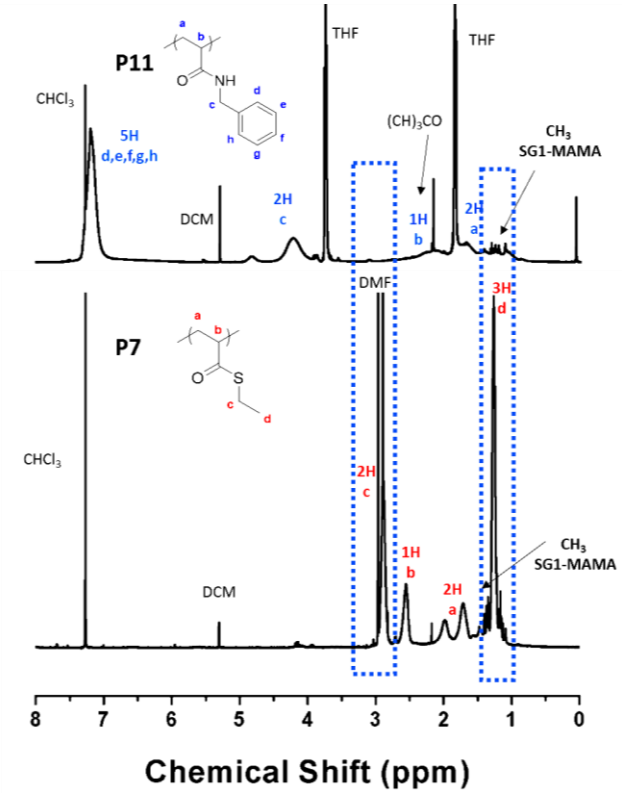

Figure 4.16: ^{1}H NMR analysis of the reaction between the thioester containing polymer **P7** (bottom) and benzylamine in the presence of thiophenol forming thioester-amide containing polymer **P11** (top).

Full amidation for **P7** was additionally verified by GPC analysis and revealed a molecular weight distribution shifting to higher molecular weight. An observable decrease in dispersity (PDI ~ 1.56) upon reaction with benzylamine (**Figure 4.17,** ~44% conversion attained within 48 hours at 75 °C) was observed.

The GPC measurements following the full substitution of P(ETA) with benzylamine, displays a shift to high molecular weights **(Figure 4.17)**. *M*n increased from 1290 g/mol to 2430 g/mol where dispersity increased to a higher value of 1.56.

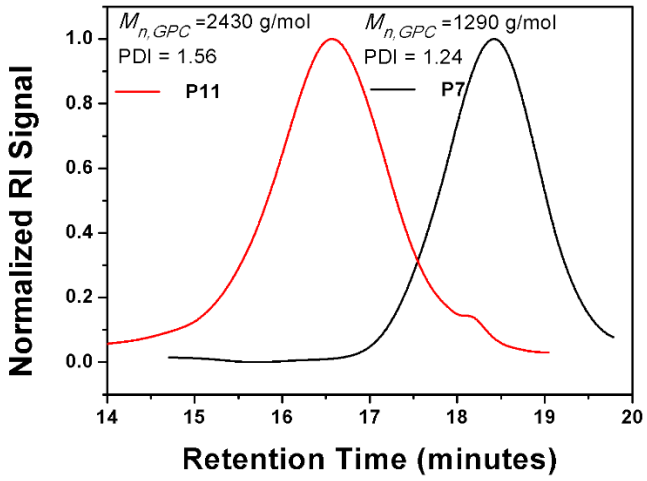

Figure 4.17: GPC traces (RID) of P(ETA) before (**P7**) and after nucleophilic substitution with benzylamine (**P11**).

4.2.4.2 Reaction kinetics of microwave assisted amidation of Poly(ethyl thioacrylate)

A microwave vial was charged with poly(ethyl thioacrylate), benzylamine, triethylamine and thiophenol with a stirrer bar. The vial was sealed with a rubber septum and the reaction mixture was stirred under the respective conditions for a designated period of time (0.5, 10, 20, 34, 48h) at 75°C (**Scheme 4.6).**

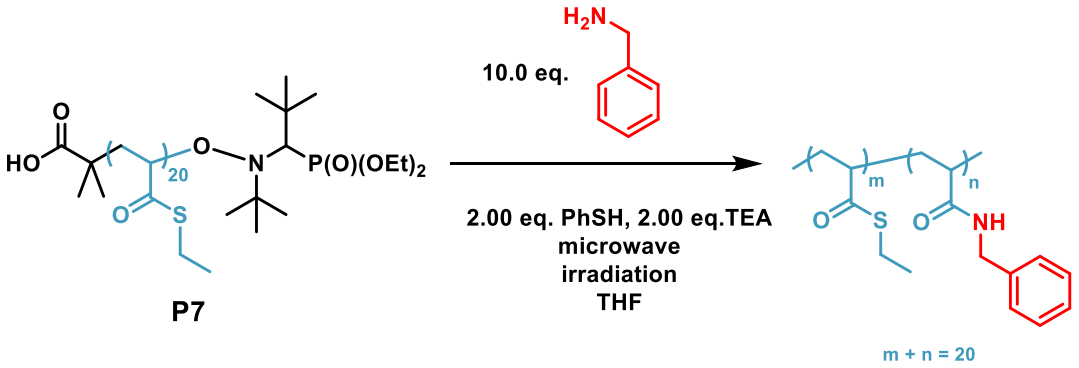

Scheme 4.6: Microwave-assisted amidation of **P7** using benzylamine as a nucleophile.

After the reaction the crude mixture was dialysed against THF/H_2O (9:1), concentrated and freeze dried to give the corresponding polymer. The polymer was further characterised by ^{1}H NMR, GPC and DSC and the results for the final polymer composition is depicted in **Table 4.5** below.

Table 4.5: Data obtained from the amidation of **P7** with model nucleophile $BzNH_2$. 100 mg [polymer], $[BzNH_2]$:[PhSH]:[TEA] = 10:2.0:2.0 in 1 : 6.5 *w/v* THF at 75 °C.

	Time (h)	Conv. [a] (%)	m	n
P7	0	0	20	0
P12	0.5	24	5	15
P13	10	45	9	11
P14	20	92	2	18
P15	34	98	1	19
P16	48	100	0	20

[a] measured by ^{1}H NMR.

4.2.4.3 Post-modification of Poly(ethyl thioacrylate) with isopropylamine

It was then sought to generate a thermoresponsive polymer through the addition of isopropylamine in the amidation process **(Scheme 4.7**). For this, a vial was charged with the purified polymer (**P7**) and dissolved in dry THF. Ten equivalents of isopropylamine was added to the mixture followed by two equivalents of TEA and two equivalents of thiophenol (in respect of a polymer single unit) and reacted in the microwave for 48h at 75 °C. The mixture was then dialysed against THF/H_2O (9:1), concentrated and freeze dried to give the corresponding polymer.

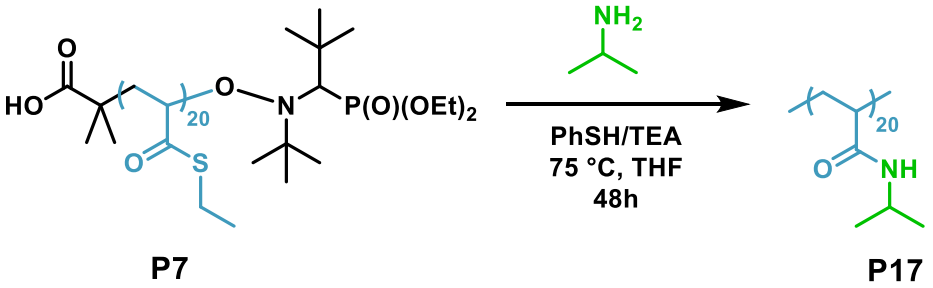

Scheme 4.7: Amidation of **P7** using isopropylamine as a nucleophile.

Amidation with ispropylamine resulted in successful substitution with full conversion by ^{1}H NMR (**Figure 4.19**) and a clear shift of the molecular weight distribution by GPC analysis. M_n increased from 1290 g/mol to 1410 g/mol, where dispersity increased to a higher value of 1.548 (**Figure 4.18**).

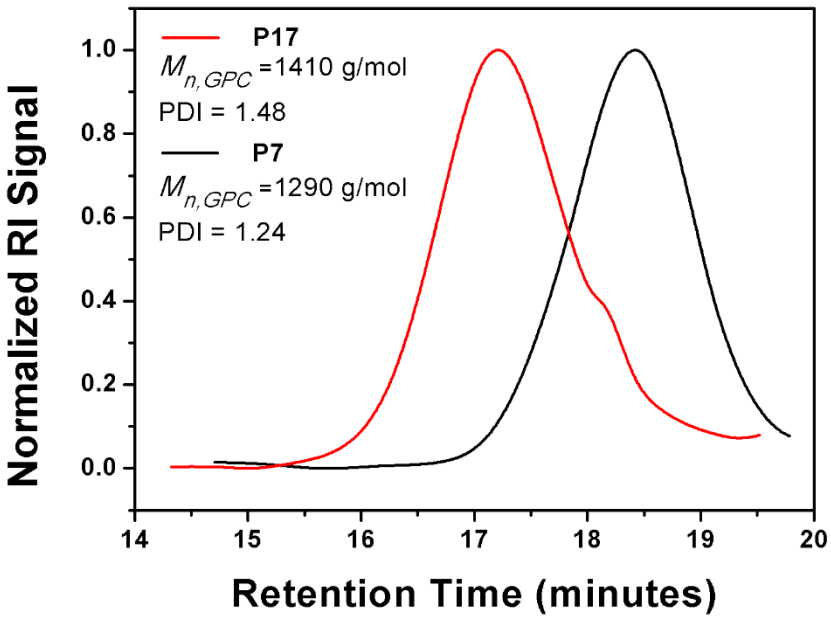

Figure 4.18: Obtained GPC traces of **P17** and **P7**.

For the nucleophilic substitution reaction with isopropylamine, a full substitution with was achieved and verified by NMR spectroscopy. In the ^{1}H NMR spectrum of **P17**, no resonance for the SCH_2-group (H_c) of the sidechain is measureable in the mid-field at 2.87 ppm (**Figure 4.19**).

Additionally, the methyl group at 1.36 ppm for H_d from the pendant group of the thioacrylate disappears and a new peak appears for the two methyl groups for the isopropyl group shifted to 1.16 ppm. The proton from the tertiary carbon in H_e appears as a new peak at 4.03 ppm, while the SCH_2-proton disappears next to it. The full spectrum is depicted below and respective peaks are assigned to illustrate the progress of amidation (**Figure 4.19**).

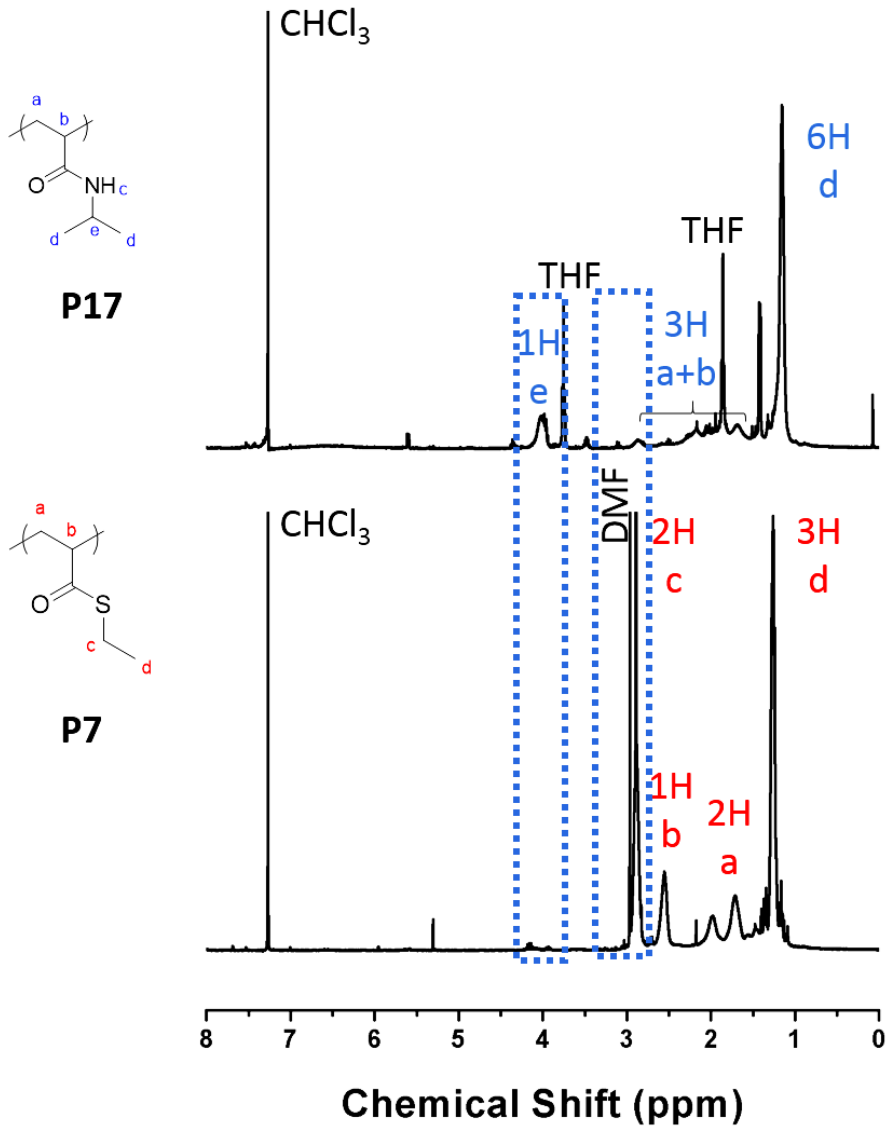

Figure 4.19: ^{1}H NMR spectra of P(ETA) obtained by NMP polymerisation in the presence of BlocBuilder^{TM} (**bottom**) before and (**top**) after amidation in the presence of isopropylamine and thiophenol as catalyst.

Conversion was calculated by comparing the ratio of the integral of the proton resonance in the SCH_2-group (H_c) of **P7** at 2.86 ppm and the methyl group H_d in **P17.** In the recorded NMR spectrum of **P17,** traces of THF are still visible as multiplets at 3.45 and 1.43 ppm. However, the doublet at 1.42 ppm could not be identified. As well as for all polymers obtained by amidation with benzylamine, the appearance of the sticky polymer **P7** (**Figure 4.20a**) results in a white powder (**Figure 4.20b**) for the amidation with isopropylamine.

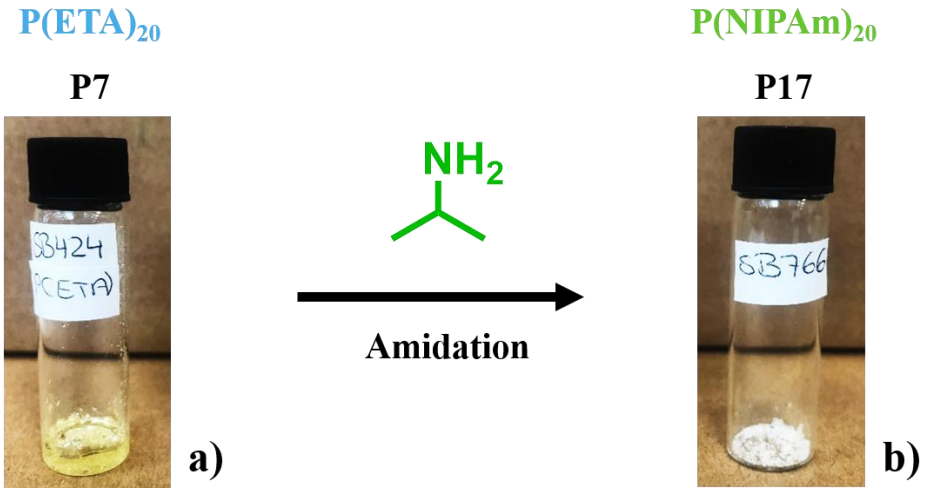

Figure 4.20: Visual appearance of Poly(ethyl thioacrylate) **P7**. **b)** Appearance of the post-modified polymer **P17**.

4.2.4.4 Post-modification of Poly(ethyl thioacrylate) with benzyl alcohol

In a next attempt, it was sought to introduce functional alcohols capable of broadening the spectrum of the functionalisation. The resultant polymers **P18**, containing ester functionality was prepared *via* post modification reaction with benzylalcohol (**Scheme 4.8**).

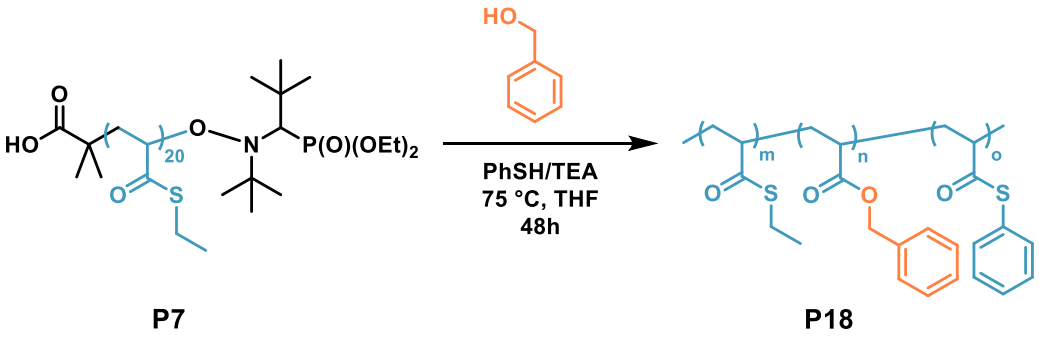

Scheme 4.8: Esterification of **P7** using benzyl alcohol as a nucleophile.

When **P7** was subjected to 10.0 equivalents benzylalcohol (BnOH) in the presence of thiophenol (PhSH, 2.00 eq.) and TEA (2.00 eq.) at 75 °C in a microwave vial under microwave irradiation for 48 h, incomplete conversion was observed. In the ^{1}H NMR spectrum of the purified polymer **P18**, the resonance of the OCH_2-group is visible at 5.12 ppm and proves that an esterification reaction took place (**Figure 4.21**). Furthermore, a resonance at high frequencies can be identified as the protons on the aromatic ring at 7.38 ppm. A second peak is however visible in close distance at

7.48 ppm and can be attributed to thiophenol. This observation can be explained by a competitive thiol-thioester exchange reaction and the aromatic group shows that these protons are present in a 5.5:1 ratio, supporting the replacement with a thiophenol as well as with a benzylalcohol.

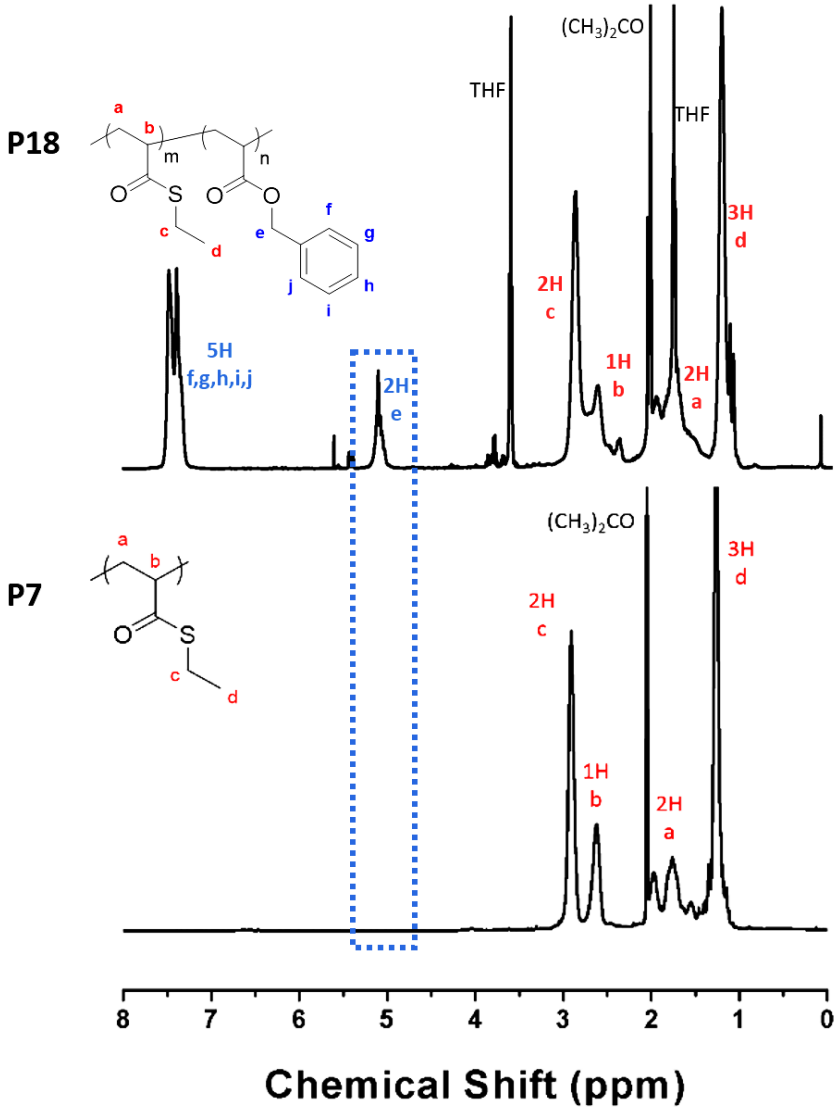

Figure 4.21: ^{1}H NMR spectra of P(ETA) obtained by NMP polymerisation in the presence of BlocBuilder^{TM} (**bottom**) before and (**top**) after esterification reaction with benzylalcohol.

4.2.5 Thermal properties

The change in polymer properties, such as glass transition temperature (T_g) is characterised by performing differential scanning calorimeter (DSC) analysis on the polymers obtained by postpolymerisation modification with different types of nucleophiles. To evaluate and verify the change in T_g, obtained DSC chromatograms were analysed and compared to the representative DSC curves from the starting polymer (**P7**). NMP of ETA initiated by SG1-MAMA yielded a polythioacrylate with a glass transition temperature T_g = 32.2 °C. Benzyl acrylamide (BzAm) has been homopolymerised *via* RAFT (**P18**) and the T_g value of 61.8 ℃ will be used as a comparison value for the progress of the amidation on P(ETA). The polymers (**P12-P16**) from the amidation reactions on **P7** exhibit various Am (Acrylamide) content with 24%, 45%, 92%, 98% and 100% according to the repeating units respectively. The T_g value of **P7** was increased by the incorporation of 24% of Am units (P(ETA_{15}-*r*-$BzAm_5$)) in the homopolymer to 4.4 °C (**Figure 4.22**).

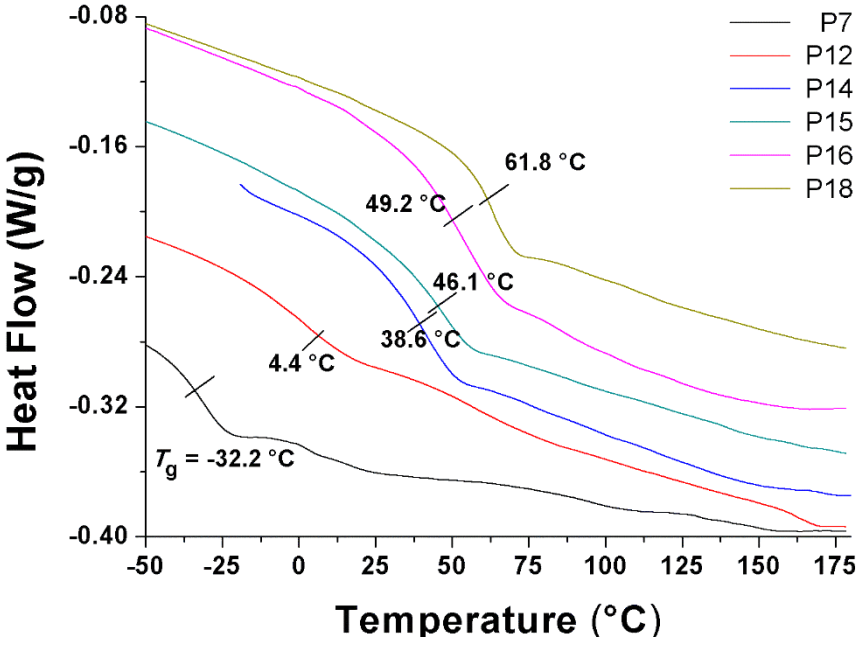

Figure 4.22: DSC thermographs (Exo. up) for the second heating of homopolymer of ETA (**P7**) and polymers obtained by modification with benzylamine (**P12**, **P14**, **P15** and **P16**) and a homopolymer of BzAm (**P18**) as reference.

In **P14**, 92% of the Am were incorporated, yielding the copolymer P(ETA$_2$-*r*-BzAm$_{18}$) and the T_g for this polymer was 28.6 °C. The T_g values of all modified P(ETA) have risen steadily with increased incorporation of Am units in the polymer. The highest T_g value was recorded for **P16** with 49.2 °C for the polymer where all thioester pendant groups were successfully transformed into amide groups. This result is also closer to the value of P(BzAm) obtained *via* RAFT (T_g = 61.8 °C), but still lower as **P18** contains the trithiocarbonate groups from the RAFT agent.

Table 4.6: Specifications for homopolymers of ETA, BzAm and amidated **P7**.

Code	**Composition**	**Amidation** [a] **(%)**	T_g [b] **(°C)**
P7	P(ETA)$_{20}$	-	-32.2
P12	P(ETA$_{15}$-*r*-BzAm$_5$)	24	4.4
P14	P(ETA$_2$-*r*-BzAm$_{18}$)	92	38.6
P15	P(ETA$_1$-*r*-BzAm$_{19}$)	98	46.1
P16	P(BzAm)$_{20}$	100	49.2
P18	P(BzAm)$_{20}$	-	61.8

[a] measured by ^{1}H NMR. [b] Measured by DSC.

Overall, the amide moieties in the pendant group affect the physical and chemical properties when the structure changes to an acrylamide. From a polythioacrylate to its corresponding polyacrylamide, the T_g changed in total 93 °C which illustrates the change of the polymer structure.

4.3 Conclusions and Outlook

In summary, NMP has been used for the polymerisation thioacrylates with short hydrocarbon chains (C_2 and C_4) for the first time. Polymerisation of both alkyl-thioacrylates (ETA and BuTA) were synthesised in DMF with controlled polymerisation, maintained to high conversions. Obtained polymers displayed moderate dispersity values (~1.46) and good agreement with theoretical $M_{n,GPC}$ and experimental number-average molecular weight ($M_{n,theo}$) for **P1**. However, higher theoretical values are obtained, when higher temperatures were used in **P3**. When comparing BuTA with its oxo-ester counterpart BuA at 70 °C and 120 °C, in both cases polymerisation rates are obtained for the thioacrylate (**P1** and **P3**) were compared to the acrylate (**P2** and **P4**). Interestingly, BuTA could be even polymerised at low temperatures of 70 °C with relatively high conversion of 59% in **P1**, whereas only 13% could be achieved after 240 minutes with BuA (**P2**). However, the polymerisation *via* NMP presents an additional technique of controlled radical polymerisation (CRP) next to the RAFT polymerisation reported in **Chapter 2** of this thesis. While acrylates have been successfully employed to copolymerise thioacrylates *via* RAFT, another class of monomer could be used by employing NMP. PFS represents a styrenic monomer and could be copolymerised as a second functional monomer. As well as for the homopolymers of BuTA compared to BuA, higher k_p^{app} were also obtained when employing BuTA in the copolymerisation with PFS compared to BuA. For instance, when BuTA is used in a copolymerisation with PFS in **P5** instead of BuA (**P6**), a 1.8-fold higher k_p^{app} could be achieved for PFS. A 2.5-fold higher value was obtained for the thioacrylate monomer in comparison to the acrylate in the copolymerisation in PFS.

Additionally, a simple modification approach that allows an overall transformation to take place using thiophenol as a catalyst under microwave conditions was investigated for **P7**. The methodology proceeds under exceptionally mild reaction conditions and is tolerant to amine and alcohols as nucleophiles. The polymers could be purified by dialysis to allow a facile purification of the desired polymer from the by-product of a thiol. The modification progressed *via* an activation of the thioester, accomplished by the introduction of a thiophenol and subsequent displacement with primary amines and alcohol led to amide or ester containing

polymer. While full amidation was achieved with benzylamine and isopropylamine in **P11** and **P16**, incomplete substitution was observed with benzylalcohol in an esterification reaction for **P18**. However, this approach offers a new way to synthesise copolymers starting from a homopolymer and adding amines or alcohols as required. The post-polymerisation modification of the thioacrylate containing is also useful to deliver polymers with tuneable properties, such as physical, thermal and mechanical properties. For example, **P7** could be changed to PNIPAm by replacement which isopropylamine, which is the most known example for thermoresponsive polymer (**P17**). Furthermore, the T_g of P(ETA) could also be tuned by stopping the amidation reaction with benzylamine at a certain time, to obtain a specific DA. By this, the range of T_g was varied from -32.2 °C for a poly(thioacrylate) to 49.2 °C for the respective modified polymer.

4.4 Experimental

4.4.1 Instrumentation

4.4.1.1 Differential Scanning Calorimetry (DSC)

Differential scanning calorimetry was performed by use of a Model DSC 25 Differential Scanning Calorimeter (TA Instruments) under N_2 atmosphere (50 mL/min). An indium standard (T_m = 156.6 °C and ΔH = 28.72 J/g) was used to calibrate the instrument according to the manufacturer instructions.and ensure accuracy and reliability of the obtained thermograms. Preweighted (3−8 mg) finely powdered samples were taken in a standard sealed 50 μL hermetic aluminium pan for the measurement. Instrument was equilibrated at 25 °C and then heated to 180 °C at a rate of 10 °C/min, holding for 1 minute, and then cooling back to −80 °C. DSC was then conducted while heating to 180 °C at 10 °C/min. The cooling and heating scans were repeated twice to erase the effect of previous thermal history of the samples. Data were collected with TA software (version V4.3.1.39215) where from the DSC curves T_g were determined from the inflection point temperature and from the heat flow derivative (DDSC) curve.

4.4.1.2 Gel permeation chromatography (GPC)

GPC was utilised to determine molecular weight averages and polymer dispersity. GPC measurements were performed on an Agilent 390-LC system equipped with a PL-AS RT autosampler, 2PLgel 5 μm mixed-C columns (300×7.5 mm), a PLgel 5 mm guard column (50×7.5 mm), and a differential refractive index (DRI). The system was eluted with THF containing 2% trimethylamine (TEA) at a flow rate of 1 mL min^{-1} and the DRI was calibrated with linear narrow poly(methyl methacrylate) standards ranging from 1010 to 2136000 g/mol, purchased from Agilent Technologies (UK).

4.4.1.3 Nuclear magnetic resonance (NMR)

^1H NMR and ^{13}C NMR spectra were recorded on a Bruker AV-400 at 303 K. $CDCl_3$ and the resonance signal at 7.26 ppm (^1H) was used as residual $CDCl_3$ or for $(CD_3)_2CO$ at 2.05 ppm peak for the chemical shift (δ).

4.4.1.4 Materials

All chemicals and solvents were commercially available and used as received unless otherwise stated. 1-butanethiol (Aldrich, 99%), 14-(dimethylamino)pyridine (DMAP, Aldrich, 99%), bromoacetic acid (Aldrich, reagent grade, 97%), butanethiol Aldrich, 99%), dicyclohexylcarbodiimide (DCC, Aldrich, puriss., ≥99% (GC)), ethanethiol (Sigma, 97%), paraformaldehyde (Sigma, powder, 95%), potassium carbonate (Sigma, BioXtra, ≥99%), thiophenol (Sigma, 97%) and triethylamine (TEA, Sigma, ≥99%). All solvents were purchased from Sigma-Aldrich (UK) and used as received at the highest purity available. SG1-MAMA was kindly provided from Arkema and used as received.

4.4.1.5 Procedures

4.4.1.5.1 Synthesis of Poly(butyl thioacrylate) (P1)

To a flame-dried Schlenk flask, equipped with a magnetic stir bar and under N_2-atmosphere, SG1-MAMA (15.6 mg, 0.04 mmol), butylacrylate (300 mg, 2.08 mmol) and 1.06 mL dry DMF was added. The reaction mixture was degassed by gentle bubbling of N_2 gas for 30 minutes at room temperature. The Schlenk tube was submerged into the pre-heated oil bath at 70 °C to start the polymerisation. Samples were taken *via* degassed syringe at desired time points and analysed. The samples were then analysed by GPC and ^{1}H NMR.

4.4.1.5.2 Synthesis of Poly(butyl acrylate) (P2)

To a flame-dried Schlenk flask, equipped with a magnetic stir bar and under N_2-atmosphere, SG1-MAMA (31.4 mg, 0.08 mmol), butylacrylate (532 mg, 4.15 mmol) and 1.06 mL dry DMF was added. The reaction mixture was degassed by gentle bubbling of N_2 gas for 30 minutes at room temperature. The Schlenk tube was submerged into the pre-heated oil bath at 70 °C to start the polymerisation. Samples were taken *via* degassed syringe at desired time points and analysed. The samples were then analysed by GPC and ^{1}H NMR.

4.4.1.5.3 Synthesis of Poly(butyl thioacrylate) (P3)

To a flame-dried Schlenk flask, equipped with a magnetic stir bar and under N_2-atmosphere, SG1-MAMA (15.9 mg, 0.04 mmol), butylacrylate (300 mg, 2.08 mmol) and 0.60 mL dry DMF was added. The reaction mixture was degassed by gentle bubbling of N_2 gas for 30 minutes at room temperature. The Schlenk tube was submerged into the pre-heated oil bath at 120 °C to start the polymerisation. Samples were taken *via* degassed syringe at desired time points and analysed. The samples were then analysed by GPC and ^{1}H NMR.

4.4.1.5.4 Synthesis of Poly(butyl acrylate) (P4)

To a flame-dried Schlenk flask, equipped with a magnetic stir bar and under N_2-atmosphere, SG1-MAMA (31.6 mg, 0.08 mmol), butylacrylate (533 mg, 4.16 mmol) and 1.06 mL dry DMF was added. The reaction mixture was degassed by gentle bubbling of N_2 gas for 30 minutes at room temperature. The Schlenk tube was submerged into the pre-heated oil bath at 120 °C to start the polymerisation. Samples were taken *via* degassed syringe at desired time points and analysed. The samples were then analysed by GPC and ^{1}H NMR.

4.4.1.5.5 Synthesis of copolymer of BuTA with PFS (P5)

To a flame-dried Schlenk flask, equipped with a magnetic stir bar and under N_2-atmosphere, SG1-MAMA (69.8 mg, 0.18 mmol), butyl thioacrylate (659 mg, 4.58 mmol), PFS (887 mg, 4.57 mmol) and 3.10 mL dry DMF was added. The reaction mixture was degassed by gentle bubbling of N_2 gas for 30 minutes at room temperature. The Schlenk tube was submerged into the pre-heated oil bath at 120 °C to start the polymerisation. Samples were taken *via* degassed syringe at desired time points and analysed. The samples were then analysed by GPC and ^{1}H NMR.

4.4.1.5.6 Synthesis of copolymer of BuA with PFS (P6)

To a flame-dried Schlenk flask, equipped with a magnetic stir bar and under N_2-atmosphere, SG1-MAMA (69.4 mg, 0.18 mmol), butylacrylate (585 mg, 4.58 mmol), PFS (887 mg, 4.57 mmol) and 3.00 mL dry DMF was added. The reaction mixture was degassed by gentle bubbling of N_2 gas for 30 minutes at room temperature. The Schlenk tube was submerged into the pre-heated oil bath at 120 °C to start the polymerisation. Samples were taken *via* degassed syringe at desired time points and analysed. The samples were then analysed by GPC and ^{1}H NMR.

4.4.1.5.7 Synthesis of Poly(ethyl thioacrylate) (P7)

To a flame-dried Schlenk flask, equipped with a magnetic stir bar and under N_2-atmosphere, SG1-MAMA (1.00 g, 2.62 mmol), ethyl thioacrylate (6.10 g, 52.5 mmol) and 12 mL dry DMF was added. The reaction mixture was degassed by gentle bubbling of N_2 gas for 30 minutes at room temperature. The Schlenk tube was submerged into the pre-heated oil bath at 120 °C to start the polymerisation. Samples were taken *via* degassed syringe at desired time points and analysed. The samples were then analysed by GPC, GC and ^{1}H NMR. The reaction was stopped immersion of the reaction flask into liquid N_2. After 1.5h ^{1}H NMR showed full conversion, DMF was distilled of and the polymer was dried until constant weight to yield P(ETA) as a yellow sticky compound (4.00 g, 56% yield). $M_{n,theo}$ = 2700 g/mol, $M_{n,GPC}$ = 1290 g/mol, PDI = 1.24.

4.4.1.5.8 General procedure for microwave assisted functionalisation (P12-P16)

Microwave syntheses were performed using a Biotage microwave synthesiser (Biotage® Initiator+) using a 4 mL borosilicate sealable microwave tube. P7 was weighed into the microwave tube. THF was added, a magnetic stirrer bar added and TEA and PhSH was subsequently added. The vessel was sealed and the reaction mixture was sonicated briefly and then heated under microwave irradiation for a predetermined time. After the reaction was finished, the reaction vessel was allowed to cool down and diluting in THF. The work-up procedure consisted of dialysing against 2 x 3 L THF/H_2O (9:1). THF was evaporated and the resulting mixture was freeze dried to give the pure polymers.

4.4.1.5.9 General procedure for microwave assisted functionalisation with isopropylamine (P17)

In a vial, 156 mg of the purified polymer was dissolved in 1.20 mL of dry THF. Ten equivalents of isopropylamine was added to the mixture followed by two equivalents of TEA and two equivalents of thiophenol (in respect of a polymer single unit) and stirred overnight at 75 °C in the microwave for 48h. The mixture was then dialysed against THF/H_2O (9:1), evaporated and freeze dried to give the corresponding polymer.

4.4.1.5.10 General procedure for microwave assisted functionalisation with benzylalcohol (P18)

In a vial, 80.0 mg of the purified polymer was dissolved in 0.60 mL of dry THF. Ten equivalents of benzylalcohol (0.24 mL, 2.20 mg) was added to the mixture followed by two equivalents of TEA and two equivalents of thiophenol (in respect of a polymer single unit) and stirred overnight at 75 °C in the microwave for 48h. The mixture was then dialysed against THF/H_2O (9:1), evaporated and freeze dried to give the corresponding polymer.

4.4.1.5.11 Synthesis of Poly(benzyl acrylamide) (P19)

In a typical polymerisation, to benzyl acrylamide (0.32 g, 1.99 mmol) was added V-601 (2.28 mg, 9.90 μmol), dioxane (0.3 mL) and BDTMP (41.6 mg, 98.9 μmol). The constituents were mixed together with a vortex mixer and charged into a Schlenk tube, sealed with a rubber septum and degassed by gentle bubbling of N_2 gas for 30 minutes. The Schlenk tube was then immersed into into an oil bath at 100 °C. Samples were taken *via* degassed syringe at desired time points and analysed. Dioxane was distilled of and the polymer was dried until constant weight to yield a white compound. $M_{n,theo}$ = 3640 g/mol, $M_{n,GPC}$ = 3300 g/mol, PDI = 1.27. The samples were then analysed by GPC, DSC and ^{1}H NMR.

4.4.1.6 Characterisation of compounds

P19

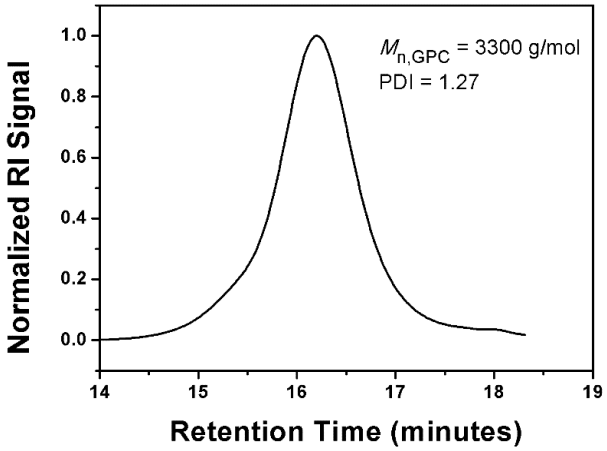

Figure 4.23: GPC trace of the obtained poly(benzylacrylamide) with DP = 20 in dioxane at 100 °C *via* RAFT.

P7

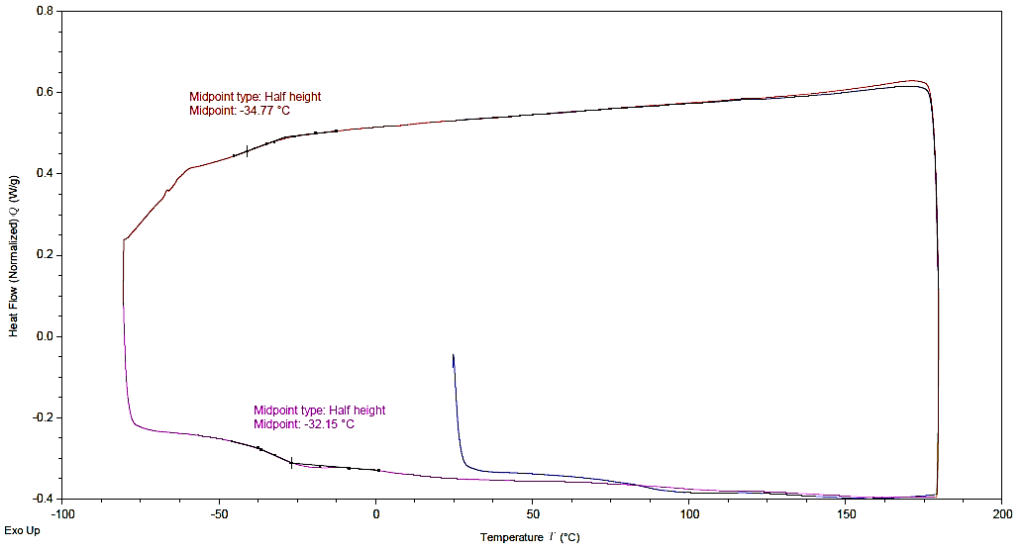

Figure 4.24: P7 DSC Thermogram

P12

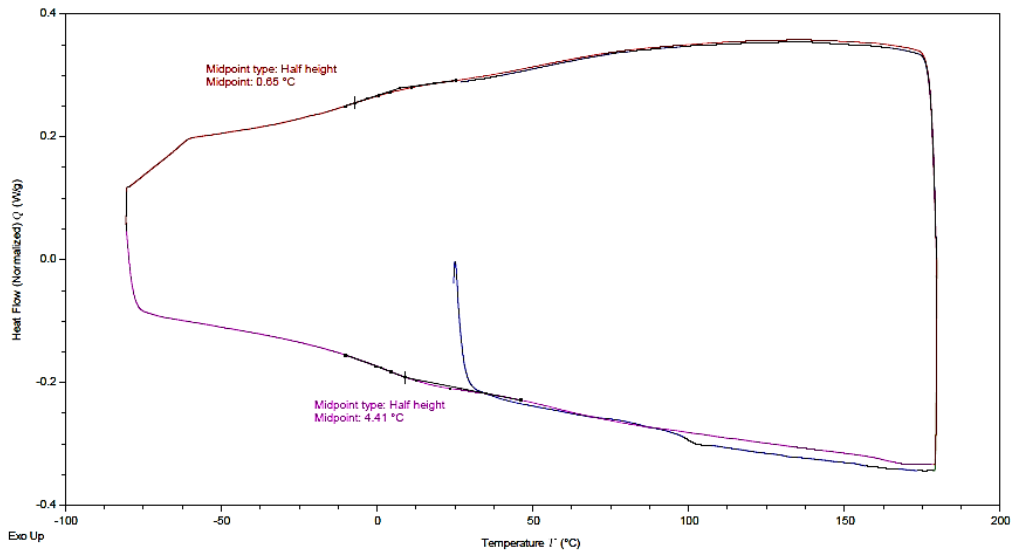

Figure 4.25: P12 DSC Thermogram

P13

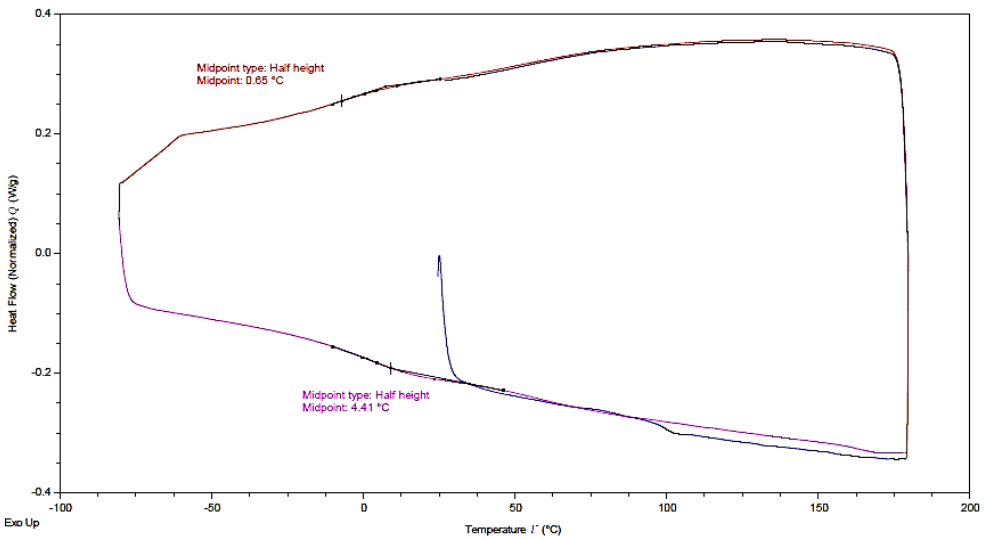

Figure 4.26: P13 DSC Thermogram

P14

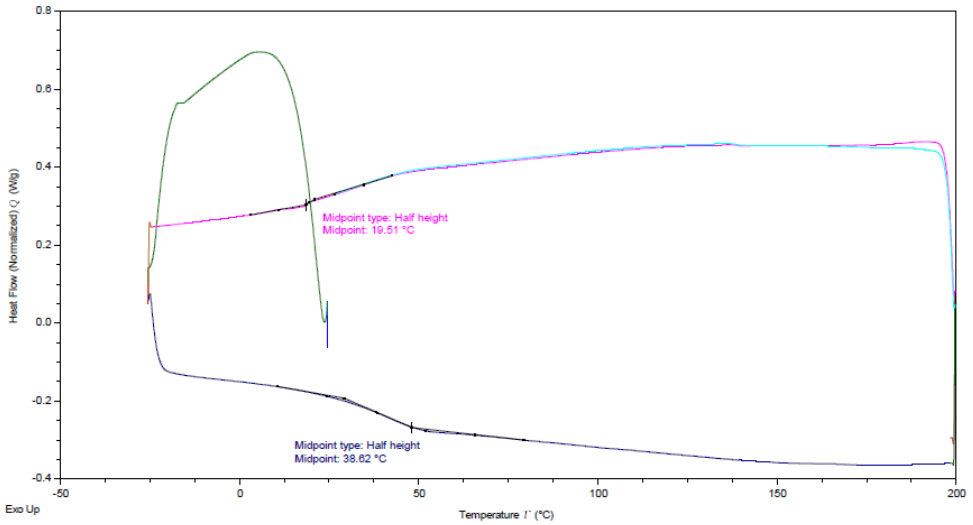

Figure 4.27: P14 DSC Thermogram

P15

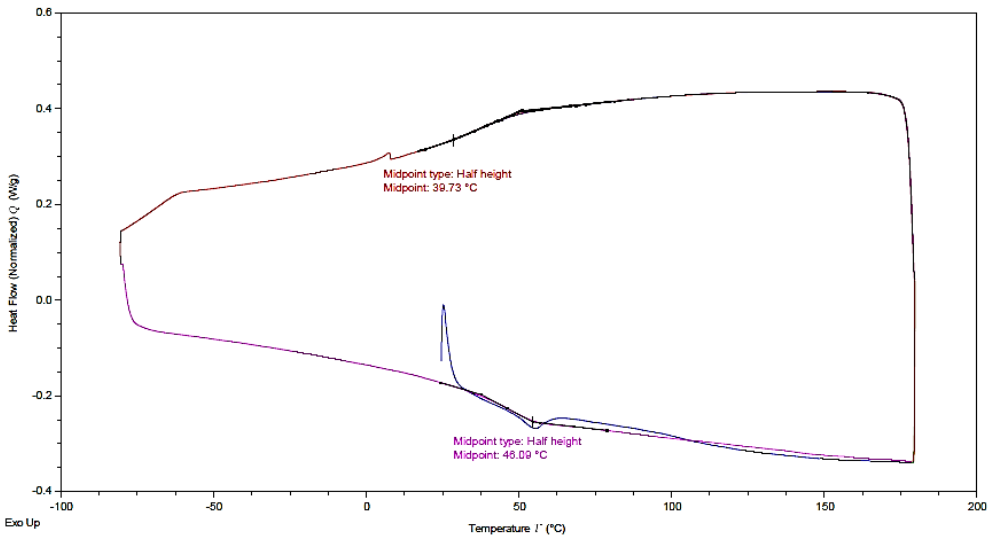

Figure 4.28: P15 DSC Thermogram

P16

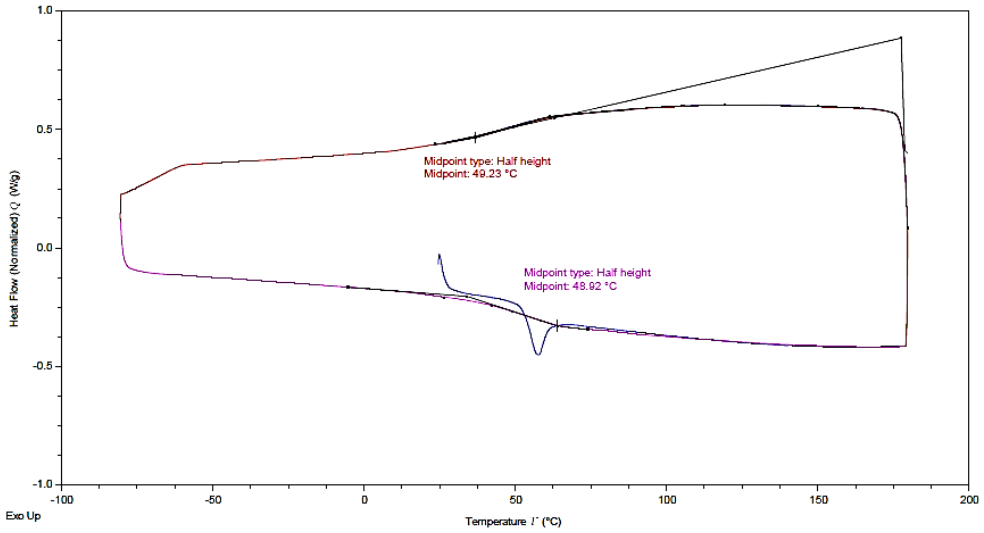

Figure 4.29: P16 DSC Thermogram

P18

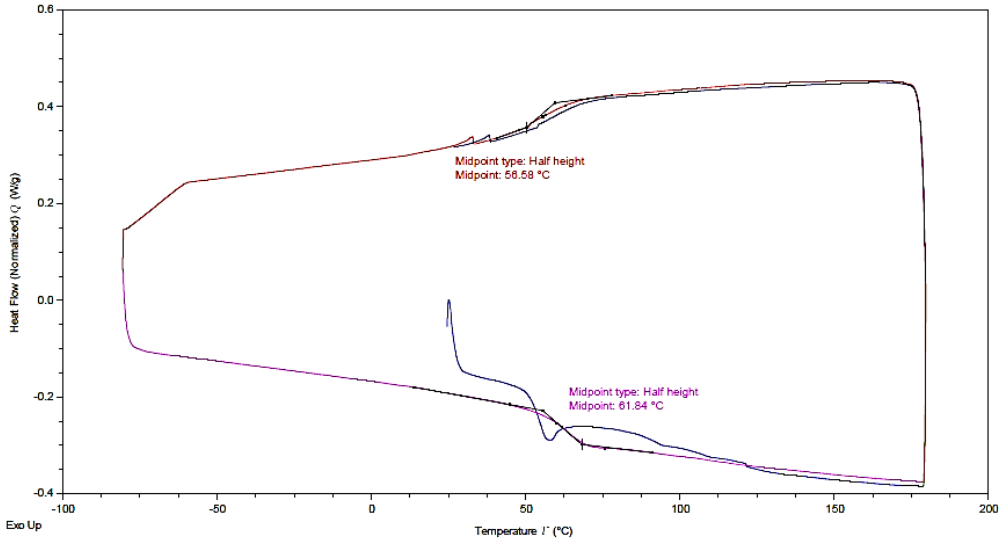

Figure 4.30: P18 DSC Thermogram

4.5 References

1. V. R. Pattabiraman and J. W. Bode, *Nature*, 2011, **480**, 471-479.
2. E. L. Baker, M. M. Yamano, Y. Zhou, S. M. Anthony and N. K. Garg, *Nat. Commun.*, 2016, **7**, 11554.
3. G. Li and M. Szostak, *Nat. Commun.*, 2018, **9**, 4165.
4. B. T. Worrell, S. Mavila, C. Wang, T. M. Kontour, C.-H. Lim, M. K. McBride, C. B. Musgrave, R. Shoemaker and C. N. Bowman, *Polym. Chem.*, 2018, **9**, 4523-4534.
5. A. Das and P. Theato, *Chem. Rev.*, 2016, **116**, 1434-1495.
6. P. Ferruti, A. Bettelli and A. Feré, *Polymer*, 1972, **13**, 462-464.
7. M. Eberhardt, R. Mruk, R. Zentel and P. Théato, *Eur. Polym. J.*, 2005, **41**, 1569-1575.
8. C. P. Easterling, T. Kubo, Zachary M. Orr, G. E. Fanucci and B. S. Sumerlin, *Chemical Science*, 2017, **8**, 7705-7709.
9. N. Caldwell, C. Jamieson, I. Simpson and A. J. B. Watson, *Chemical Communications*, 2015, **51**, 9495-9498.
10. M. B. Larsen, S. E. Herzog, H. C. Quilter and M. A. Hillmyer, *ACS Macro Lett.*, 2018, **7**, 122-126.
11. N. Stuhr-Hansen, N. Bork and K. Stromgaard, *Org. Biomol. Chem.*, 2014, **12**, 5745-5751.
12. J. O. Holloway, S. Aksakal, F. E. Du Prez and C. R. Becer, *Macromol. Rapid. Comm.*, 2017, **38**, n/a-n/a.
13. F. Chauvin, P.-E. Dufils, D. Gigmes, Y. Guillaneuf, S. R. A. Marque, P. Tordo and D. Bertin, *Macromolecules*, 2006, **39**, 5238-5250.
14. C. Farcet, J. Nicolas and B. Charleux, *J. Polym. Sci. A.*, 2002, **40**, 4410-4420.
15. P. Lacroix-Desmazes, J.-F. Lutz, F. Chauvin, R. Severac and B. Boutevin, *Macromolecules*, 2001, **34**, 8866-8871.
16. J. Nicolas, B. Charleux, O. Guerret and S. Magnet, *Angew. Chem. Int. Ed.*, 2004, **43**, 6186-6189.
17. J. Nicolas, B. Charleux and S. Magnet, *J. Polym. Sci. A.*, 2006, **44**, 4142-4153.
18. C. R. Becer, R. M. Paulus, S. Höppener, R. Hoogenboom, C.-A. Fustin, J.-F. Gohy and U. Schubert, *macromolecules*, 2008, **41**.
19. G. Delaittre and L. Barner, *Polym. Chem.*, 2018, **9**, 2679-2684.
20. C. M. Hall and J. Wemple, *J. Org. Chem.*, 1977, **42**, 2118-2123.
21. P. E. Dawson, M. J. Churchill, M. R. Ghadiri and S. B. H. Kent, *J. Am. Chem. Soc.*, 1997, **119**, 4325-4329.
22. E. C. B. Johnson and S. B. H. Kent, *J. Am. Chem. Soc.*, 2006, **128**, 6640-6646.
23. W. Chen, G. Qing-Xiang and F. Yao, *Chemistry – An Asian Journal*, 2011, **6**, 1241-1251.
24. G. L. Thomas, Y. S. Y. Hsieh, C. K. Y. Chun, Z.-L. Cai, J. R. Reimers and R. J. Payne, *Org. Lett.*, 2011, **13**, 4770-4773.

Chapter 5

5 SET-LRP of Thioacrylates and the Dissociation of a Thioester Containing Star-shaped Polymer *via* NCL

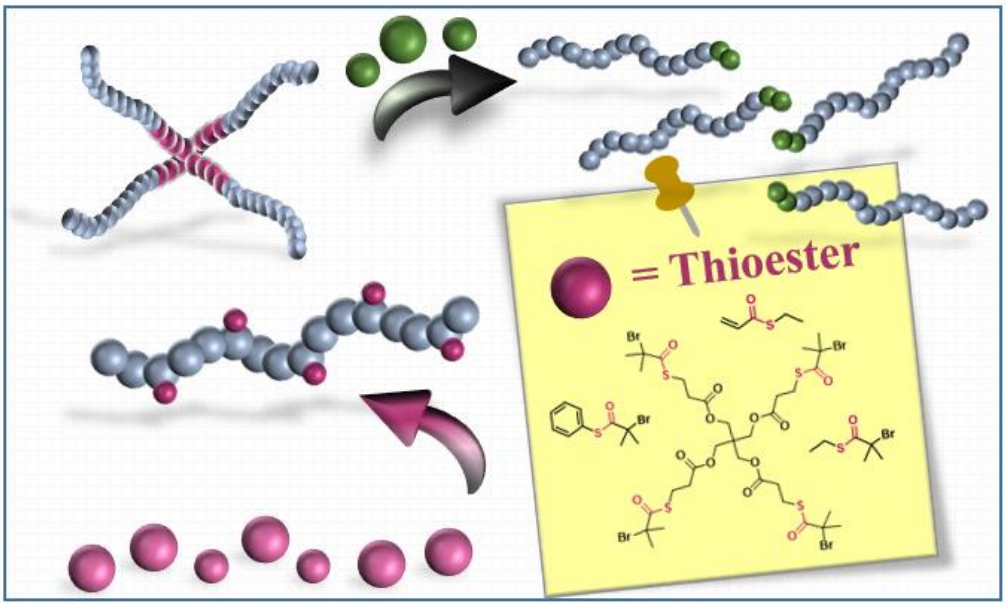

The controlled polymerisation and optimisation of thioacrylates via SET-LRP is reported for the first time. The polymerisation kinetics were investigated with periodic sampling resulting in the substitution of the deactivator $CuBr_2$ with $FeBr_2$ to reach full monomer consumption. Furthermore, a new class of thioester based initiators were reported, proceeding identically to ester initiators. Hence a four-arm star shaped polymer containing four thioesters in the core was polymerised via the core first method and its full dissociation into its linear arms was shown with NCL using a cysteine derivative. The full dissociation was followed via GPC and MALDI-ToF-MS.

5.1 Introduction

Thioester intermediates hold an important place in nature's synthetic toolbox, which can be found throughout various reactions, such as in native chemical ligation, formation and degradation of fatty acids, steroids, as well as in the synthesis of various coenzyme A (CoA) derivatives over acetyl-CoA and many more. From the above, especially native chemical ligation (NCL) offers exciting possibilities in the synthesis and functionalisation of thioester containing small peptides into higher order structures, such as enzymes or proteins. In fact, thioesters are considered to possibly be precursors to life, being obligatory intermediates in several key processes, where ATP is generated or used. Hence, it is not only highly desirable to incorporate thioester functionalities in biomacromolecules, but also into polymers, in order to be able to efficiently replicate biomimetic modification of polymers.

For reaction conditions which are typical in ATRP or SET-LRP, three main structural features of an initiator should be considered for its efficiency, namely (*i*) the initiator halogen, (*ii*) the R-groups that substitute the α-carbon and (*iii*) the nature of the neighbouring group. With the right combination of these features, almost any class of monomer can be polymerised (**Scheme 5.1**).[1-3]

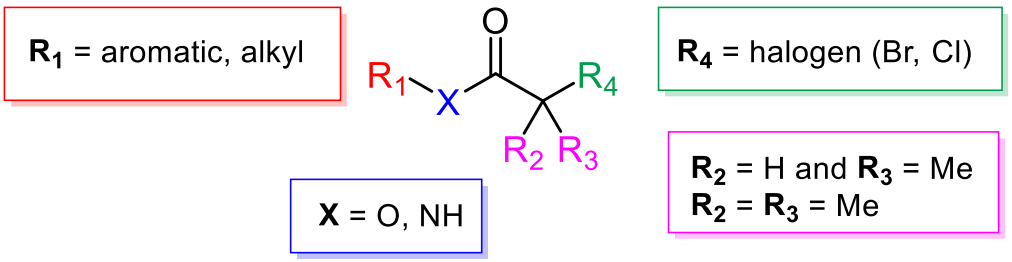

Scheme 5.1: General structure of an initiator and common functional groups that are widely used throughout the literature for ATRP or SET-LRP.

Two of the most popular ester initiators bearing a bromine chain end are methyl bromoproprionate (MBP) and ethyl α-bromoisobutyrate (EBiB) mainly used to polymerise acrylates, as well as methacrylates and acrylonitrile. Chlorine bearing initiators on the other hand such as methyl-2-chloropropionate (MCP) or ethyl 2-chloropropanoate (ECP) are also widely used, typically for the polymerisation of acrylamides, methacrylates and acrylates to yield well defined polymers. Similarly, phenolic-ester based initiators such as 2-bromo-2-methylpropionic acid phenyl ester

(BMPAPE) or 2-chloro-2-methylpropionic acid phenyl ester (CMPAPE) find wide use in polymerisations. Complimentarily, amide based initiators such as 2-chloropropionamide (CPA) or 2-bromo-2-N-phenyl-propionamide (BPPA) can also be applied. Additionally, multifunctional initiators based on the above mentioned structural varieties can also be found throughout the literature (**Figure 5.1**).[4]

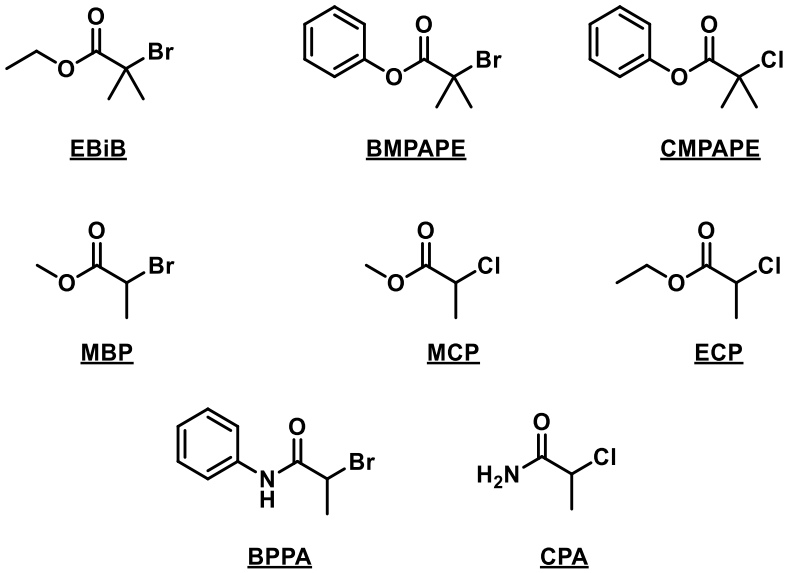

Figure 5.1: Commonly used monofunctional initiators employed in ATRP or Cu(0)-mediated LRP.

Although there are investigations looking into activation rate constants (k_{act}) and the polymerisation kinetics of initiators with different halogens and the substituent, no evaluation of the "neighbouring group effect" is reported. In the following, a comparison of initiators based on an ester, thioester and an amide is made to investigate their polymerisation behaviour under identical conditions, where ethyl acrylate (EA) is used as a model monomer. Parallel to this study, the copolymerisation behaviour of an acrylate and a thioacrylate was studied *via* kinetic investigation. The thioacrylate block was partly transformed into a acrylamide *via* amidation to obtain an "*all-acrylic*" copolymer consisting of a poly(acrylate), poly(acrylamide) and a poly(thioacrylate) along the same chain. Finally, a thioester based tetrafunctional initiator was used to obtain a star shaped polymer, which was subsequently dissociated into a linear polymer *via* native chemical ligation (NCL) of the thioester moieties using L-cysteine methyl ester hydrochloride.

5.2 Results and Discussion

5.2.1 Homopolymerisation of a thioacrylate monomer *via* SET-LRP

5.2.1.1 Optimisation of the homopolymerisation of ETA

Chapter 2 and 3 of this thesis discuss the synthesis of thioacrylates as a new class of monomers and their controlled polymerisation *via* RAFT polymerisation.[5] Thioacrylates are the thioester equivalents of acrylates and acrylamides. Analogous thioacrylate and acrylate monomers have been shown to polymerise with similar kinetic rates, which displays the ease of thioester incorporation in a polymer. By varying the DP, the number of thioester units along a polymer chain can be targeted, allowing control over the physical and thermal properties of the polymer. While RAFT was found to be a suitable method to obtain well defined (co)polymers of thioacrylates, their polymerisation *via* any other controlled polymerisation technique had not yet been reported to date. In order to investigate their polymerisation under SET-LRP conditions, EBiB was employed and a series of optimisation conditions for the polymerisation of ETA was investigated **(Scheme 5.2**, **Table 5.1**). Samples were taken periodically during the screening reactions and analysed to determine conversion and molecular weight distribution by ^{1}H NMR spectroscopy and GPC.

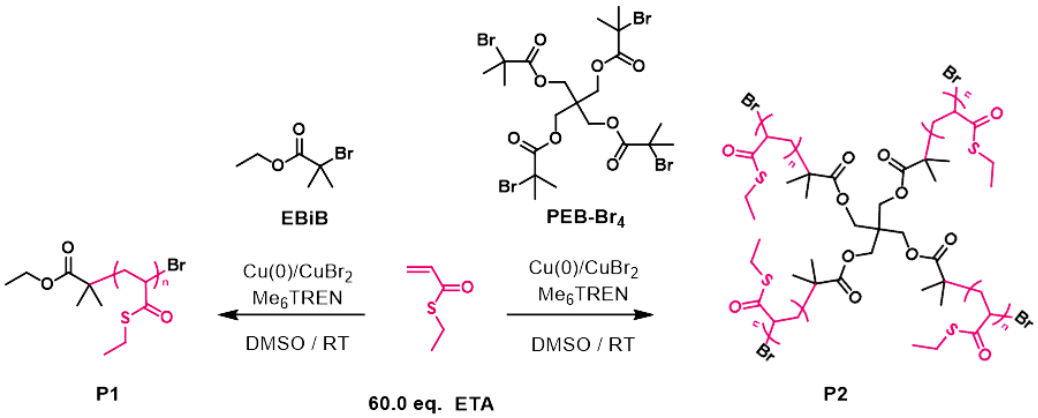

Scheme 5.2: General conditions for the polymerisation of ETA *via* SET-LRP. **P1** was obtained using EBiB with [ETA]:[I]:[$CuBr_2$]:[Me_6TREN] = 60:1:0.1:0.19 and **P2** using PEB-Br_4 with [ETA]:[I]:[$CuBr_2$]:[Me_6TREN] = 60:1:0.4:0.76 in DMSO at RT.

Table 5.1: Summary of the optimisation reactions obtained from the polymerisation of ETA under various reaction conditions.

Entry	DP_{ETA}	[$CuBr_2$]:[I]	[Me_6TREN]:[I]	Cu(0) (cm)	T (°C)	Solvent 1:2 (*m*/*v*)	ρ (%)
P1	60	0.1	0.19	4.0	25	DMSO	60
P3	20	0.1	0.19	4.0	25	DMSO	80
P4	10	0.1	0.19	4.0	25	DMSO	92
P5	20	0.2	0.19	4.0	25	DMSO	50
P6	20	0.1	0.38	4.0	25	DMSO	81
P7	20	0.1	0.19	4.0	25	DMSO (1:8)	80
P8	20	0.1	0.19	4.0	25	TFE	80
P9	20	0.1	0.19	4.0	40	DMSO	91
P10	20	0.1	0.19	10.0	25	DMSO	90
P11	10	0.1 $CuCl_2$	0.19	4.0	25	DMSO	86
P12	10	0.05	0.19	4.0	25	DMSO	86
P13	10	0.1 $FeBr_2$	0.19	4.0	25	DMSO	99
P14	10	0.1 $FeBr_3$	0.19	4.0	25	DMSO	99
P15	10	0.1 $FeBr_3$	0.19	4.0 Fe(0)	25	DMSO	30
P16	10	0.1 $FeBr_3$	0.19	-	25	DMSO	87

Note that **P1** is obtained after kinetic sampling, while entries **P3**-**P16** were allowed to polymerise uninterrupted for 16 hours.[a] Conversion measured by ^{1}H NMR spectroscopy.

Initially, the reaction conditions for the polymerisations were kept the same at [Monomer]:[EBiB]:[Me_6TREN] = 10:1:0.19 (**Table 5.1**). Interestingly, the first order kinetic plot for the polymerisation of ETA (Entry **P1**) displays a linear correlation for the initial four hours (k_p^{app} = 5.283x10^{-5} sec^{-1}), after which the linear fit levels off to a horizontal at 60% conversion yielding a polymer with $M_{n,GPC}$ = 4000 g/mol and PDI = 1.11. GPC analysis revealed a symmetrical chromatogram throughout the polymerisation without any detectable trace of low or high molecular weight signal, which would indicate potential termination or coupling events (**Figure 5.2**).

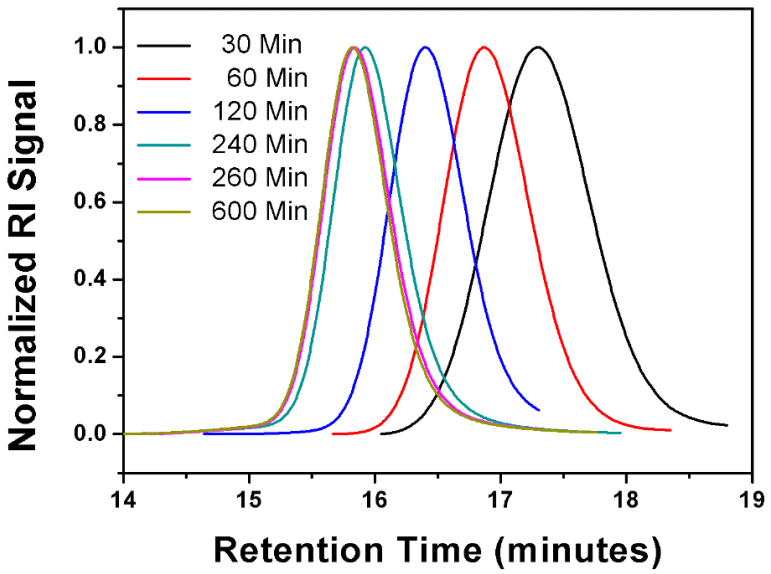

Figure 5.2: GPC traces of the homopolymerisation of ETA with linear initiator (EBiB) at DP = 60 in DMSO, **P1**.

A linear dependence of $\ln[M]_0/[M]$ *vs*. time indicated first order kinetics with respect to monomer concentration between 30 and 240 minutes (**Figure 5.3a**), while M_n increased linearly with conversion and PDI values remained narrow (1.07-1.15) throughout the reaction (**Figure 5.3b**). However, no more increase in conversion or in molecular weight could be observed after 360 minutes.

a) **b)**

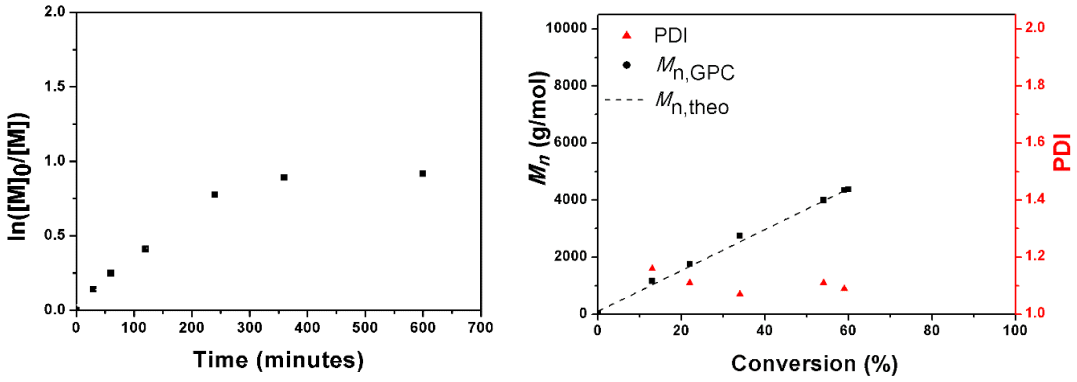

Figure 5.3: a) Ln([M]$_0$:[M]) *vs*. time plot for **P1**. **b)** M_n *vs*. conversion plot for **P1**. Black symbols represent $M_{n,GPC}$, dashed line represents respective $M_{n,theo}$ and red symbols represents their PDI.

The data obtained for the homopolymerisation of ETA for **P1** are summarised in **Table 5.2** below.

Table 5.2: Experimental details of the homopolymerisation of ETA with linear initiator (EBiB) at DP = 60 in DMSO, **P1**.

Time (min)	$M_{n,theo}$ (g/mol)	$M_{n,GPC}$[b] (g/mol)	PDI[b]	Conv.[a] (%)
30	1170	1100	1.15	13
60	1760	1730	1.11	22
120	2750	2570	1.07	34
240	4000	3960	1.11	54
360	4350	4310	1.09	59
600	4380	4380	1.10	60

[ETA]:[EBiB]:[$CuBr_2$]:[Me_6TREN] = 60:1:0.1:0.19. [a]Conversion measured by ^{1}H NMR spectroscopy. [b] THF eluent, linear PMMA standard.

Identical conditions were subsequently applied for a star-shaped polymer with PEB-Br_4 as initiator. ([ETA]:[I]:[$CuBr_2$]:[Me_6TREN] = 60:1:0.4:0.76. Initially homopolymerisation of ETA presented a low dispersity throughout the polymerisation (1.04-1.08). However, after 24 hours, the conversion was limited to 65% with no detectable increase in molecular weight (**Figure 5.4**). Nevertheless, a star polymer was attained with relatively narrow dispersity and molecular weight of 5300 g/mol, with minor star-star coupling, visible as a high molecular weight peak around 15.5 minutes. The obtained results for **P2** are summarised below in **Table 5.3**

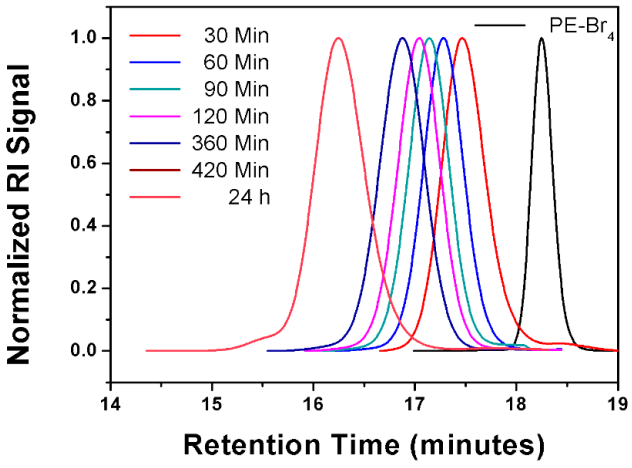

Figure 5.4: GPC traces of the homopolymerisation of ETA with 4-arm initiator (PEB-Br_4) at DP = 60 in DMSO, **P2**.

Table 5.3: Experimental details of the homopolymerisation of ETA with 4-arm initiator (PEB-Br_4) at DP = 60 in DMSO, **P2**.

Time (min)	$M_{n,theo}$ (g/mol)	$M_{n,GPC}$[b] (g/mol)	PDI[b]	Conv.[a] (%)
30	1280	1100	1.08	8
60	1980	1400	1.04	18
90	2190	1600	1.04	21
120	2680	1760	1.04	28
360	3230	2030	1.05	36
420	3580	2180	1.08	41
24 h	5250	3310	1.08	65

[ETA]:[PEB-Br_4]:[$CuBr_2$]:[Me_6TREN] = 60:1:0.4:0.76. [a]Conversion measured by ^{1}H NMR spectroscopy. [b] THF eluent, linear PMMA standard.

Attributing this to high monomer concentration, the targeted degree of polymerisation (DP) was gradually decreased to 20 and 10, which afforded an increase in conversion to 80% and 92% respectively (Entries **P2** and **P3**)

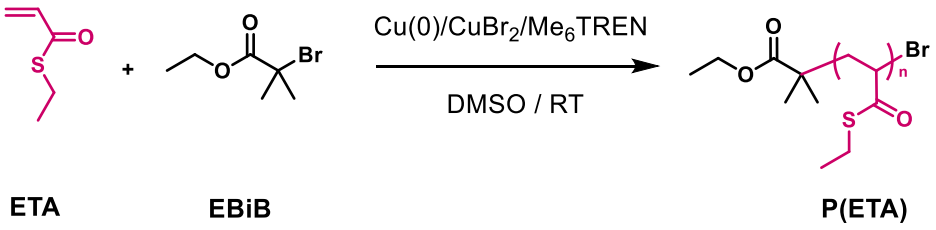

ETA **EBiB** **P(ETA)**

P1 : 60.0 eq.
P3 : 20.0 eq.
P4 : 10.0 eq.

Scheme 5.3: General conditions for the polymerisation of ETA with EBiB *via* SET-LRP with [ETA]:[I]:[$CuBr_2$]:[Me_6TREN] = 60, 20 or 10:1:0.1:0.19 for **P1**, **P3** and **P4**.

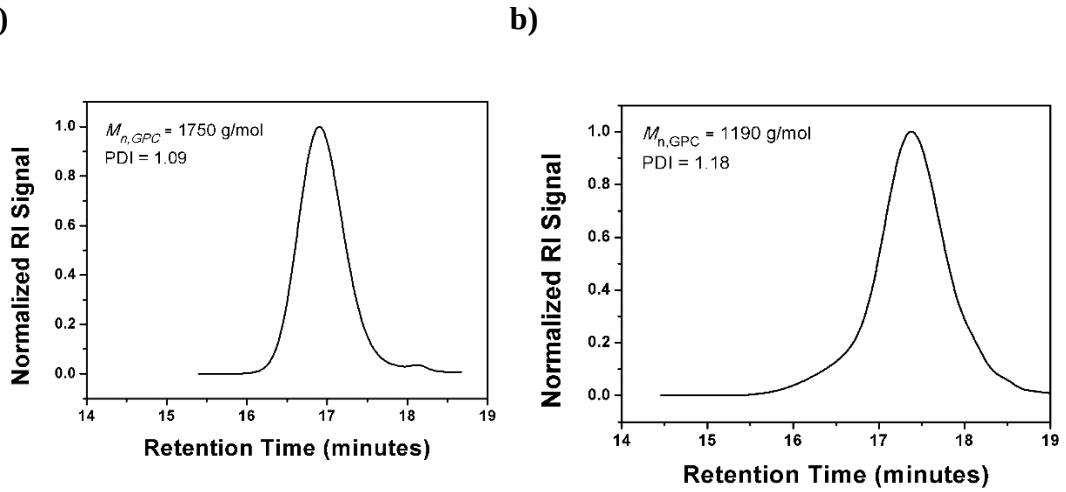

Figure 5.5: GPC traces obtained from the homopolymerisation of ETA with [I]:[$CuBr_2$]:[Me_6TREN] = 1:0.1:0.19 **a)** DP = 20, showing an $M_{n,GPC}$ = 1750, PDI = 1.09 and 80% conversion, **P3**. **b)** DP = 10, showing an $M_{n,GPC}$ = 1190, PDI = 1.18 and 92% conversion, **P4**.

The standard conditions for DP = 20 were further modified to [I]:[$CuBr_2$]:[Me_6TREN] = 1:0.2:0.19 for **P5**. An increase of $CuBr_2$ entails a reduction in the rate of polymerisation. While employing 0.10 eq. of $CuBr_2$ led to a conversion of 80% in **P3**, an increase to 0.20 eq. of $CuBr_2$ resulted in a lower conversion of 50% for **P5**. There are two explanations for obtaining lower conversions with higher concentration of the deactivator; Increasing [$CuBr_2$] entails in an increase of [$Cu^{II}(Me_6TREN)Br_2$] deactivator, causing a shift of the polymerisation equilibrium to the dormant chains and a reduction in free [Me_6TREN] coincides. The conversion was calculated by comparing the multiplet for H_{a1} and H_b at 6.21 – 6.34 ppm of the monomer to the peaks at 2.75 – 2.94 ppm (**Figure 5.6**). The latter includes the *S*CH_2-protons from the monomer, as well as for the polymer, the ratio of both resonances is 1:2, showing 50% of monomer consumed during the polymerisation with a yield of 50%.

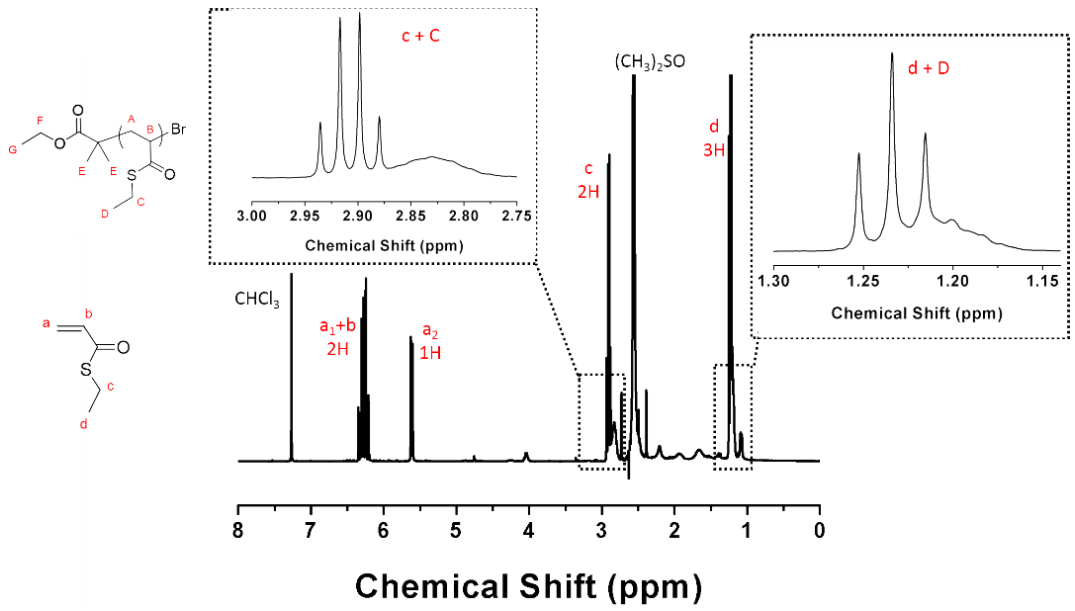

Figure 5.6: ^{1}H NMR spectrum of P(ETA), **P5** ($CDCl_3$, 400 MHz, 303 K) at 16 h.

The increase of [$CuBr_2$] results in a lower molecular weight of 1340 for **P5**, compared to **P3** ($M_{n,GPC}$ = 1750). Furthermore, the increase of deactivator resulted in a broader molecular weight distribution (~ 1.13) for **P5** compared to 1.09 for **P3** (**Figure 5.7**).

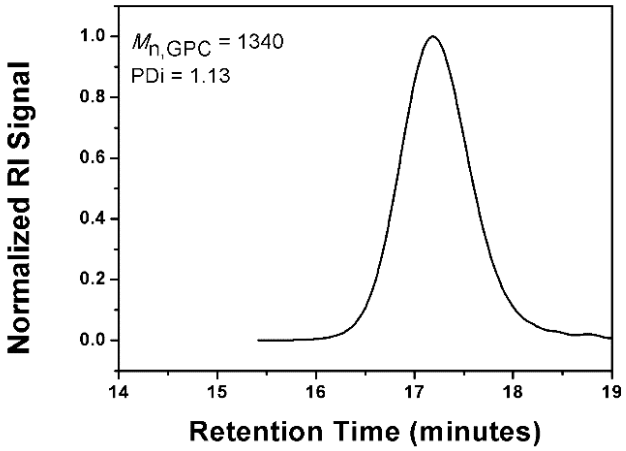

Figure 5.7: GPC trace obtained from the homopolymerisation of ETA with [ETA]:[I]:[$CuBr_2$]:[Me_6TREN] = 20:1:0.2:0.19, showing an $M_{n,GPC}$ = 1340, PDI = 1.13 and 50% conversion, **P5**.

The reaction conditions for further optimisation reactions for P(ETA) chosen were: [M]:[I]:[$CuBr_2$]:[Me_6TREN] = 20:1:0.1:0.19 with a 4 cm piece of Cu(0)-wire. In particular, attention was paid to the concentration of the ligand, where in a next reaction, [Me_6TREN] was increased from 0.19 to 0.38 eq for **P6**. Surprisingly,

conversion remained at 81%, when the ligand concentration of **P3** was doubled (**P6**, $M_{n,GPC}$ = 1630 g/mol, PDI = 1.17), which is also confirmed by similar $M_{n,GPC}$ values.

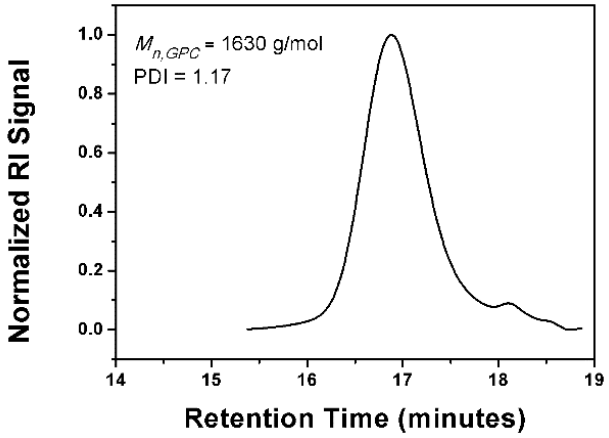

Figure 5.8: GPC trace obtained from the homopolymerisation of ETA with [ETA]:[I]:[$CuBr_2$]:[Me_6TREN] = 20:1:0.1:0.38, showing an $M_{n,GPC}$ = 1630, PDI = 1.17 and 81% conversion, **P6**.

However, by using a higher concentration of ligand, molecular weight distribution measured by GPC increases from 1.09 to 1.17. It is important to mention, that lowering the concentration of ligand can lead to a prohibitive reduction in polymerisation rate.[6] In a further experiment, the amount of DMSO was increased 4-folds to 8:1 (*v*/*v*). DMSO enhances the polarity of the medium and thus aiding electron transfer.[7, 8] Furthermore, DMSO stabilises the CuX_2 species as a coordinating solvent and shifts the k_{dis} and the equilibrium of the polymerisation further to the right.[7] However, the conversion remained at 80% by increasing [DMSO] in **P7** (**Figure 5.9a**).

Percec and coworkers reported 2,2,2-trifluoroethanol (TFE) to be another suitable solvent that yields "*nascent"* Cu(0) and therefore an alternative to DMSO, especially for the polymerisation of hydrophobic monomers.[9-11] Neither a change in the solvent amount, nor the use of TFE as a solvent (Entries **P7** and **P8,** $M_{n,GPC}$ = 1220 g/mol, PDI = 1.10 and $M_{n,GPC}$ = 1280 g/mol, PDI = 1.43 respectively), changed the conversion obtained. However, a bigger deviation in polymerisation control was indicative by a broader molecular weight distribution in the GPC chromatogram (**Figure 5.9b**).

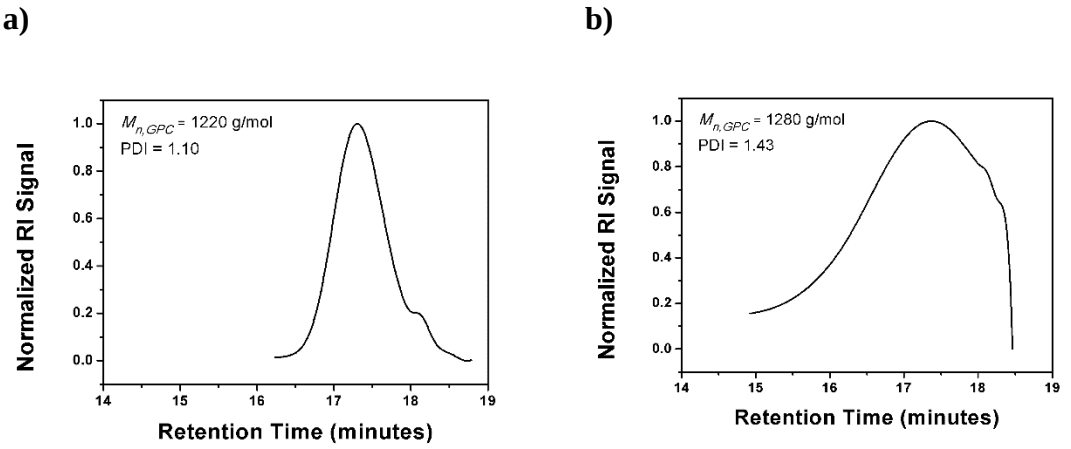

Figure 5.9: GPC traces obtained from the homopolymerisation of ETA with [ETA]:[I]:[$CuBr_2$]:[Me_6TREN] = 20:1:0.1:0.19 **a)** with DMSO (8:1 *v*/*v*) showing an $M_{n,GPC}$ = 1220, PDI = 1.10 and 80% conversion, **P7**. **b)** with TFE, showing an $M_{n,GPC}$ = 1280, PDI = 1.43 and 80% conversion, **P8**.

A slight increase in conversion was only observed, when the reaction temperature was increased to 40 °C for **P9** (**Figure 5.10a**) or a longer piece of Cu(0)-wire (10 cm) was used in **P10** (**Figure 5.10b**), reaching 90% monomer conversion in both polymerisations.[12]

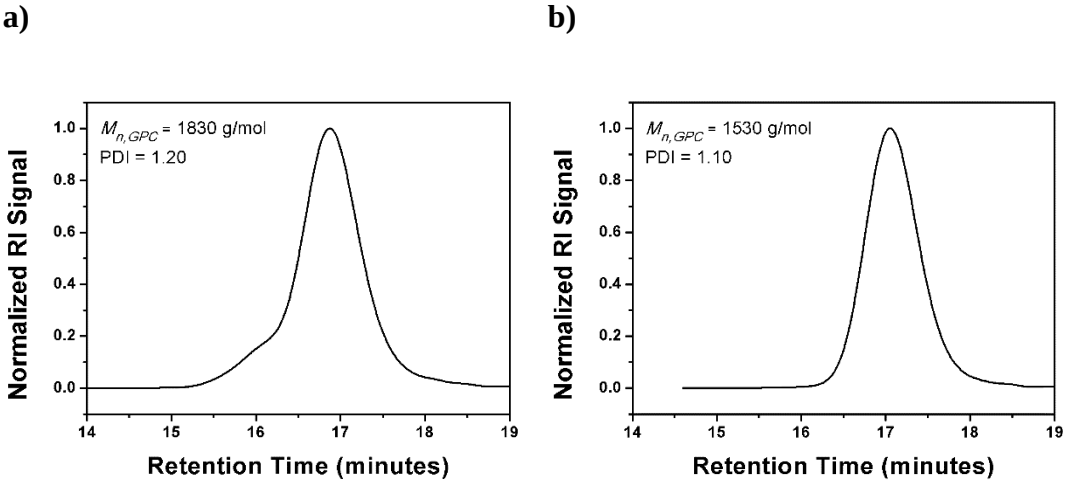

Figure 5.10: GPC traces obtained from the homopolymerisation of ETA with [ETA] : [I] : [$CuBr_2$]:[Me_6TREN] = 20:1:0.1:0.19 **a)** at 40 °C, showing $M_{n,GPC}$ = 1830, PDI = 1.20 and 91% conversion, **P9**. **b)** with 10 cm Cu(0)wire, showing an $M_{n,GPC}$ = 1530, PDI = 1.10 and 90% conversion, **P10**.

With the advances in novel polymerisation techniques in the recent years, it was shown that interesting properties can be gained by simply iteratively polymerising two different monomers to block copolymers. However, to be able to truly obtain block

copolymers, conversions near or equal to 100% need to be obtained for every block prior to chain extension, avoiding exhaustive in between purification steps. Therefore, the polymerisation conditions for ETA were further optimised by changing the metal halide (MH_x) to achieve quantitative conversion (**Scheme 5.4**).

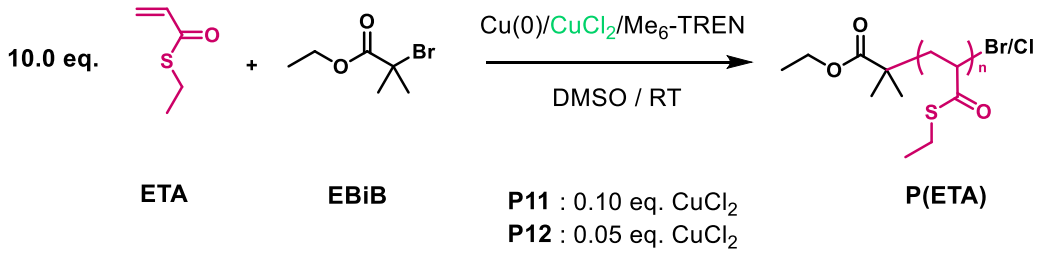

Scheme 5.4: General conditions for the polymerisation of ETA with EBiB *via* SET-LRP with [ETA]:[I]:[Me_6TREN] = 10:1:0.19 using $CuCl_2$.

For instance, when different concentrations of $CuCl_2$ was employed as the deactivator, it was found that the conversion slightly dropped to 86% in both cases (Entries **P11** and **P12, Figure 5.11**).

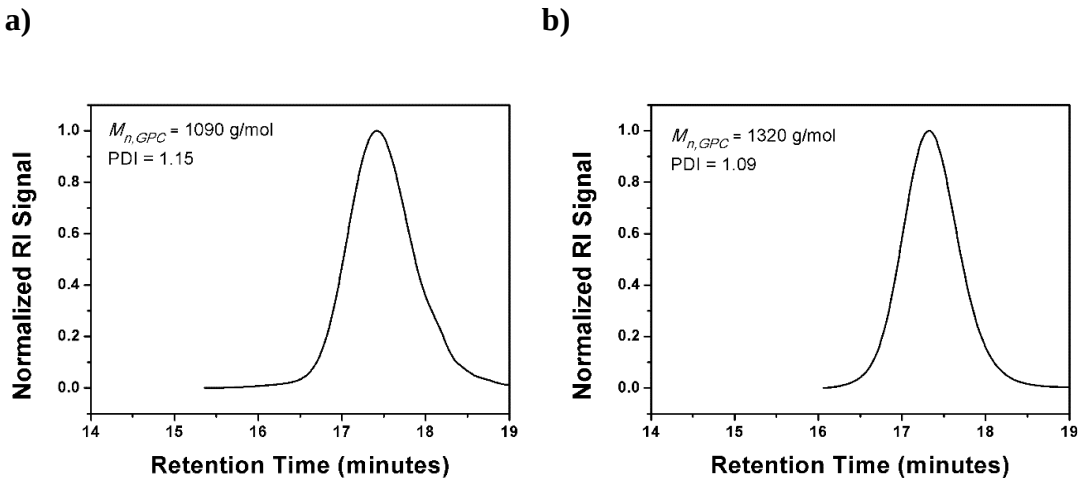

Figure 5.11: GPC traces obtained from the homopolymerisation of ETA with [ETA] : [I] : [Me_6TREN] = 10:1:0.19 **a)** with 0.10 eq. $CuCl_2$, showing $M_{n,GPC}$ = 1090, PDI = 1.15 and 86% conversion, **P11**. **b)** with 0.05 eq. $CuCl_2$, showing an $M_{n,GPC}$ = 1320, PDI = 1.09 and 86% conversion, **P12**.

This was found to be in agreement with previous reports, considering the higher deactivation rate constant of -Cl based deactivators.[13] However, when iron based deactivators namely $FeBr_2$ or $FeBr_3$ were used, conversions of >99% were reached, (**Scheme 5.5, Figure 5.12**).

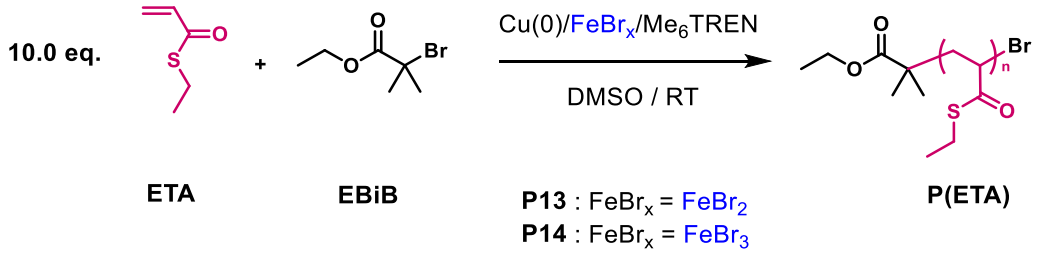

Scheme 5.5: General conditions for the polymerisation of ETA with EBiB *via* SET-LRP with [ETA]:[I]:[$FeBr_x$]:[Me_6TREN] = 10:1:0.1:0.19.

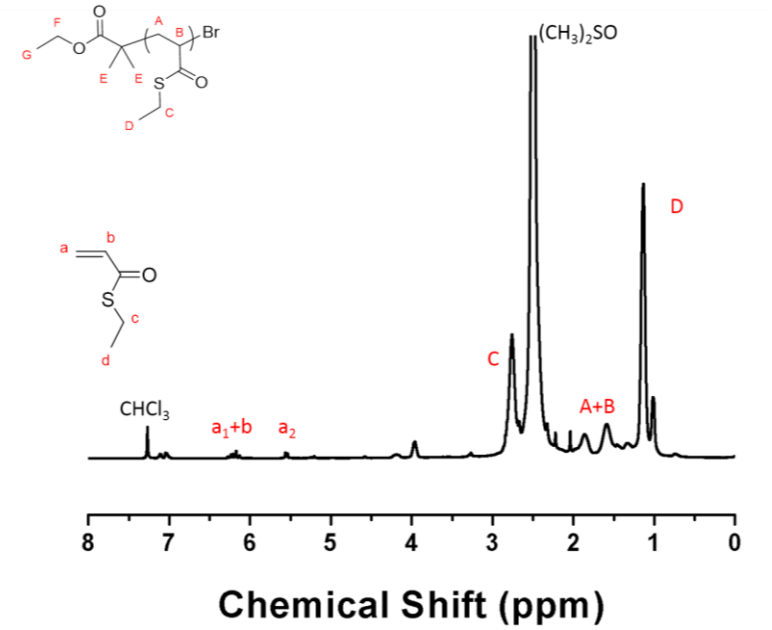

Figure 5.12: ^{1}H NMR spectrum of P(ETA), **P13** ($(CH_3)_2SO$, 400 MHz, 303 K) at 16 h.

Furthermore, the obtained polymers were analysed *via* GPC and were found to be well-defined polymers with low dispersities (**Figure 5.13**, **P13:** $M_{n,GPC}$ = 1290 g/mol, PDI = 1.17 and **P14:** $M_{n,GPC}$ = 1360 g/mol, PDI = 1.21).

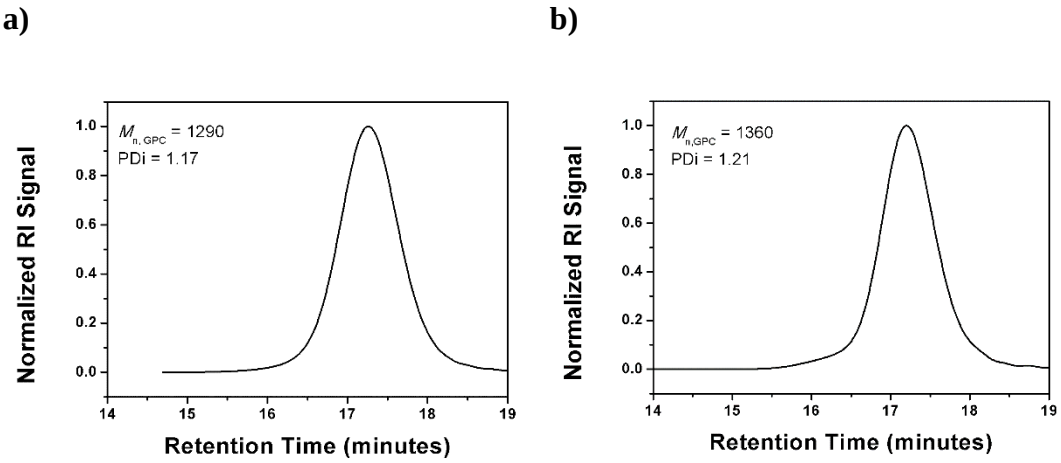

Figure 5.13: GPC traces obtained from the homopolymerisation of ETA with [ETA]:[I]:[Me_6TREN] = 10:1:0.19. **a)** with 0.10 eq. $FeBr_2$ showing $M_{n,GPC}$ = 1290, PDI = 1.17 and 99% conversion, **P13**. **b)** with 0.10 eq. $FeBr_3$ showing an $M_{n,GPC}$ = 1360, PDI = 1.21 and 99% conversion, **P14**.

This caused speculation for a potential thioester-copper complexation or interaction that could be decreasing the reactivity of the polymerisation system, hence resulting in low conversions (compare entries **P4** and **P13**).[14, 15] To our surprise, the conversion dropped much lower, when the Cu(0)-wire was replaced with 4 cm of Fe(0)-wire in the presence of $FeBr_2$ (**Scheme 5.6, Entry P15**), displaying no control over dispersity (**Figure 5.14a**, $M_{n,GPC}$ = 21400 g/mol, PDI = 3.21). The same experiment was repeated without Fe(0)-wire (**Scheme 5.6, Entry P16**).

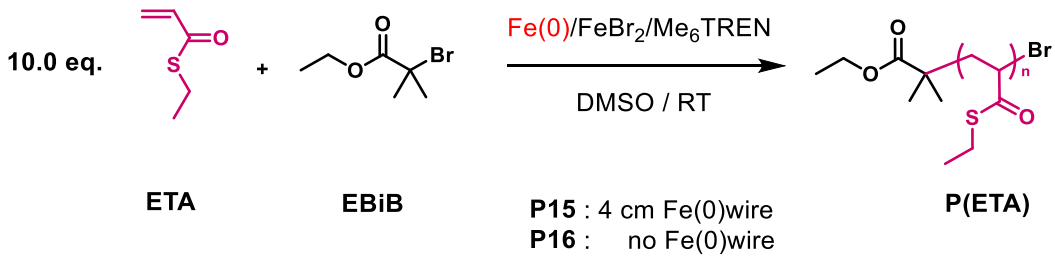

Scheme 5.6: General conditions for the polymerisation of ETA with EBiB *via* SET-LRP with [ETA]:[I]:[$FeBr_2$]:[Me_6TREN] = 10:1:0.1:0.19 with Fe(0)-wire for **P15** and without for **P16**.

When the reaction was carried out without Fe(0)-wire, higher conversion of 87% was obtained. The GPC analysis additionally revealed a narrower molecular weight distribution of 1.25 (**Figure 5.14b**).

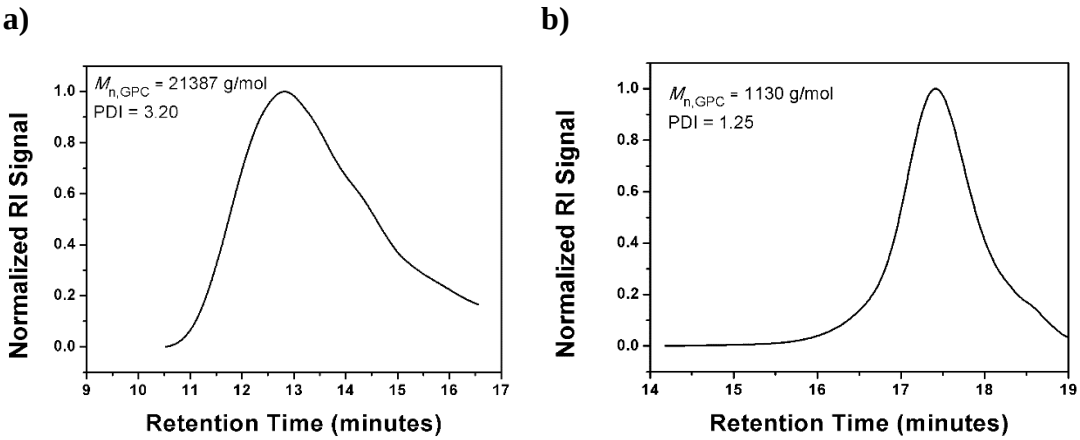

Figure 5.14: GPC traces obtained from the homopolymerisation of ETA with [ETA]:[I]:[$FeBr_2$]:[Me_6TREN] = 10:1:0.1:0.19. **a)** with Fe(0)-wire for **P15,** showing an $M_{n,GPC}$ = 21390, PDI = 3.22 and 30% conversion. **b)** with no Fe(0)-wire, showing an $M_{n,GPC}$ = 1130, PDI = 1.25 and 87% conversion, **P16**.

From the above, it was concluded that only the use of iron halide in the presence of a Cu(0)-wire resulted in quantitative monomer conversion for the polymerisation of thioacrylates with low dispersities. Therefore, different metal halides were compared in a set of identical reactions conditions, for the polymerisation of ETA and EA and discussed further in the following.

5.2.2 Kinetic comparison of different metal halides for the homopolymerisation of ethyl acrylate and ethyl thioacrylate

While Fe-based deactivators helped to increase monomer conversion for a thioacrylate based monomer, its impact as metal halide on acrylates compared to $CuBr_2$ was demonstrated below in a set of polymerisations for EA (**Scheme 5.7**)

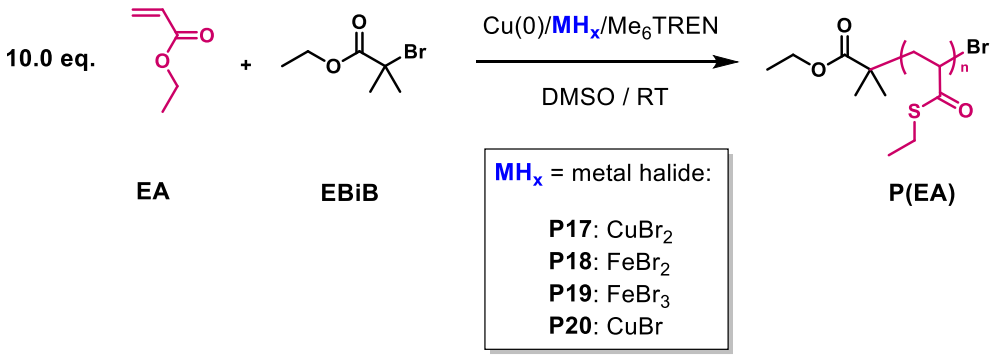

Scheme 5.7: General conditions for the polymerisation of EA with EBiB *via* SET-LRP with [EA]:[I]:[MH_x]:[Me_6TREN] = 10:1:0.1:0.19 with Cu(0)-wire and different metal halides (MH_x).

A summary of the polymerisations are given below in **Table 5.4** below. Additionally, further polymerisation kinetics were carried out for ethyl thioacrylate (ETA) as a model comparison for ETA with [ETA]:[EBiB]:[Me_6TREN] = 10:1:0.19 and 0.1 equivalents of $CuBr_2$ (**P21**), $FeBr_2$ (**P22**), $FeBr_3$ (**P23**) or CuBr (**P24**), the polymerisation conditions are depicted in **Scheme 5.8** below.

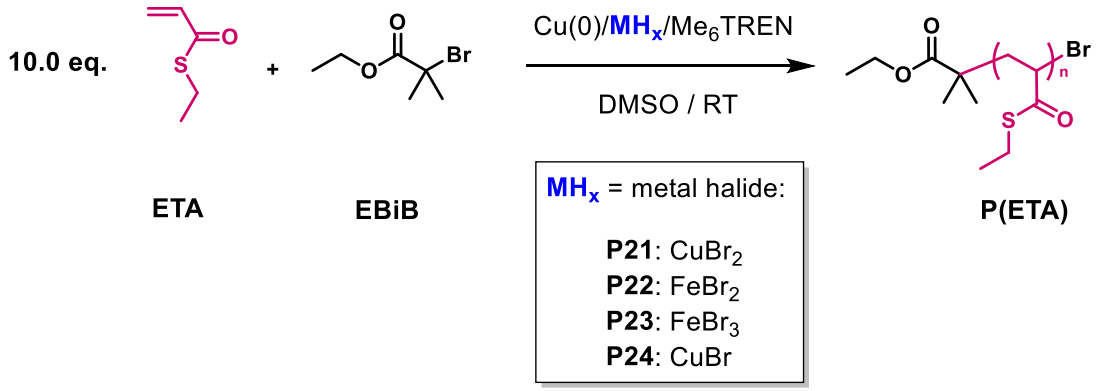

Scheme 5.8: General conditions for the polymerisation of ETA with EBiB *via* SET-LRP with [ETA]:[I]:[MH_x]:[Me_6TREN] = 10:1:0.1:0.19 with Cu(0)-wire and different metal halides.

When ETA was polymerised with 0.10 eq. $CuBr_2$, the reaction was very poorly defined, as evidenced by GPC traces with unsymmetrical distribution at higher conversions for **P21**. The polymerisation resulted in significant loss over the control for the homopolymer, characterised by incomplete conversion (90%) and by significant high molecular weight signal (**Figure 5.15**).

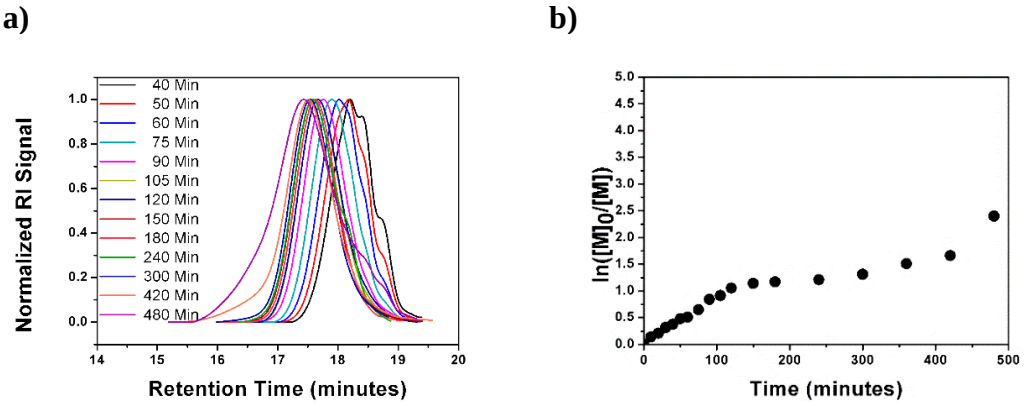

Figure 5.15: Homopolymerisation of ETA *via* SET-LRP with [ETA]:[I]:[$CuBr_2$]:[Me_6TREN] = 10:1:0.1:0.19 **a)** GPC traces of the homopolymerisation of ETA, **P21**. **b)** Ln($[M]_0$/[M]) vs. time plot for **P21**.

The GPC analysis furthermore revealed a constant increase of measured molecular weight by GPC with increasing conversion with relatively low dispersities under 80% conversion. However, after 80% conversion has reached, molecular weight stagnates and broader molecular weight distributions are detected (**Figure 5.16**).

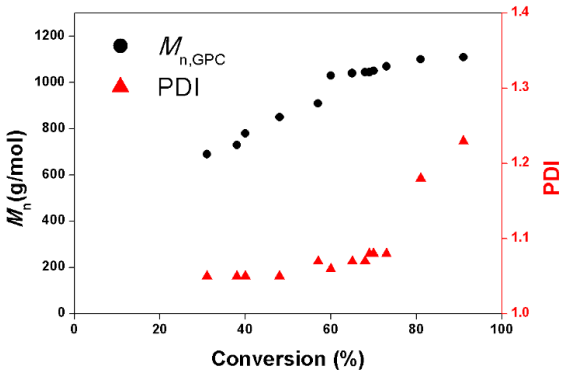

Figure 5.16: M_n *vs*. conversion plot for **P21**. Black circles represent $M_{n,GPC}$ and red triangles represent their corresponding dispersity.

When $CuBr_2$ was replaced with $FeBr_2$ for **P22**, GPC analysis revealed narrow, symmetrical molecular weight distributions (**Figure 5.17a**) with dispersity indices around 1.10 (**Figure 5.17b**). Furthermore, measured molecular weight steadily increased with increasing conversion, resulting in full conversion.

a) **b)**

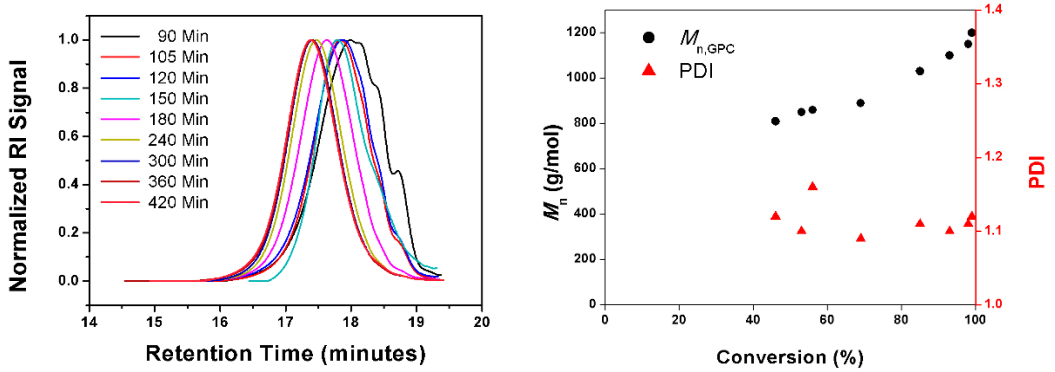

Figure 5.17: Homoppolymerisation of ETA *via* SET-LRP with [ETA]:[I]:[$FeBr_2$]:[Me_6TREN] = 10:1:0.1:0.19 **a)** GPC traces of the homopolymerisation of ETA, **P22**. **b)** M_n *vs*. conversion plot for **P22**. Black circles represent $M_{n,GPC}$ and red triangles represent their corresponding dispersity.

In a next experiment, $CuBr_2$ was replaced with $FeBr_3$ for **P23** and resulted again in full conversion of ETA (**Figure 5.18**), following a non-linear increase of $(\ln[M]_0/[M])$ with time.

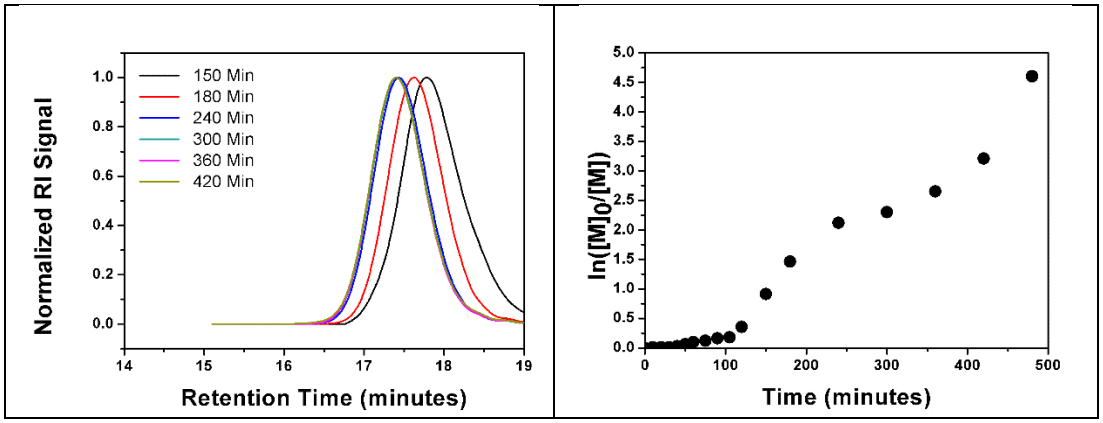

Figure 5.18: Results obtained from the homopolymerisation of ETA *via* SET-LRP with [ETA]:[I]:[$FeBr_3$]:[Me_6TREN] = 10:1:0.1:0.19. **a)** GPC traces of the homopolymerisation of ETA, **P23**. **b)** Ln($[M]_0$/[M]) vs. time plot for the in **P23**.

CuBr was employed in a further experiment for **P24**. GPC analysis revealed no shift of the GPC traces to higher molecular weights as the polymerisation did not proceed to full conversion (**Figure 5.19**).

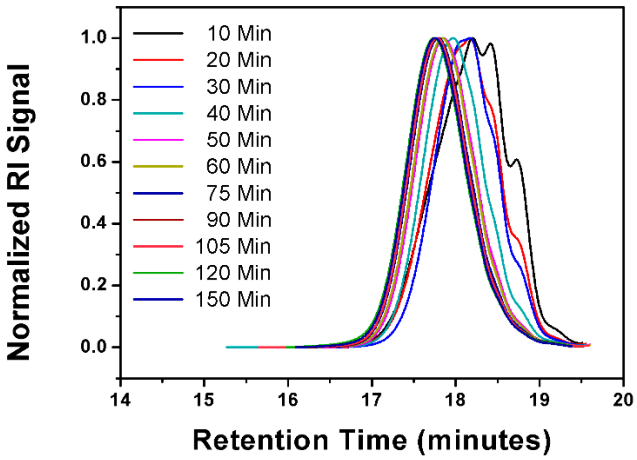

Figure 5.19: GPC traces of the homoppolymerisation of ETA *via* SET-LRP with [ETA]:[I]:[CuBr]:[Me_6TREN] = 10:1:0.1:0.19 in **P24**.

A summary of the polymerisation of ethyl acrylate and ethyl thioacrylate are given below in **Table 5.4** below.

Table 5.4: Overview of the carried out polymerisations with different metal halides for ethyl thioacrylate and ethyl acrylate (**P17**-**P24**).

Entry	Monomer	Metal halide	k_p^{app} (s^{-1})	Induction period (min)	Time for quantitative conversion (min)
P17		$CuBr_2$	$8.36x10^{-4}$	20	105
P18	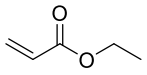	$FeBr_2$	$7.36\ x10^{-4}$	50	150
P19		$FeBr_3$	$9.90\ x10^{-4}$	75	180
P20	EA	CuBr	$4.74\ x10^{-4}$	20	> 120
P21		$CuBr_2$	$1.43\ x10^{-4}$	not observed	> 480
P22	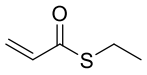	$FeBr_2$	$1.29\ x10^{-4}$	not observed	360
P23		$FeBr_3$	$8.08\ x10^{-5}$*	40	480
P24	ETA	CuBr	$4.70\ x10^{-5}$	not observed	n.a.

* For easier comparison, the rate reported is determined from the initial linear regime between 40-105 minutes (See **Figure 5.21b**).

It was found that for acrylates, all metal halides could be employed interchangeably (**P17**, **P18, P19** and **P20** all resulted in $M_{n,GPC}$ = 1400 g/mol, PDI = 1.10). However, it should be noted that a difference in the time required to reach full conversion was observed, where **P17** required 105 minutes, **P18** 150 minutes and **P19** 180 minutes. Additionally, for ethyl acrylate, the kinetic rate constants appear to be similar, yet there is a notable difference in the induction period, ranging from 20 minutes with CuBr and $CuBr_2$, to 75 minutes for $FeBr_3$. Once monomer conversion started, the polymerisation rates were found to be independent of the deactivator used. A comparable trend was observed for the initial 120 minutes of the polymerisation for ethyl thioacrylate (**Figure 5.20**). For example both **P21** and **P22** proceed nearly identical, with comparable polymerisation rates and no evidence for an induction period. After 150 minutes however, a steeper second linear regime appears for **P22** leading to quantitative conversion, while **P21** plateaus for the next *ca*. 3h, whereafter no polymerisation took place. **P23** on the other hand is initially observed to have an induction period of 40 minutes, after which it proceeds to full monomer consumption within 8 hours. From these results, it can be concluded that, the only difference observed for ethyl acrylate was in the duration of the induction period, resulting in nearly identical polymers.

For ethyl thioacrylate, $CuBr_2$ was found to terminate the polymerisation at about 92%. Contrary, iron based deactivators where found to be more suitable, as they allowed monomer conversion to reach 100%, resulting in well-defined polymers. From the two, $FeBr_2$ showed more controlled characteristics, as the kinetic plots displayed distinct linear regimes compared to a sigmoidal trend of $FeBr_3$. In short, while the presence of $FeBr_2$ allowed the polymerisation of thioacrylates, $CuBr_2$ was found to be unsuitable.

a) Ethyl acrylate **b)** Ethyl thioacrylate

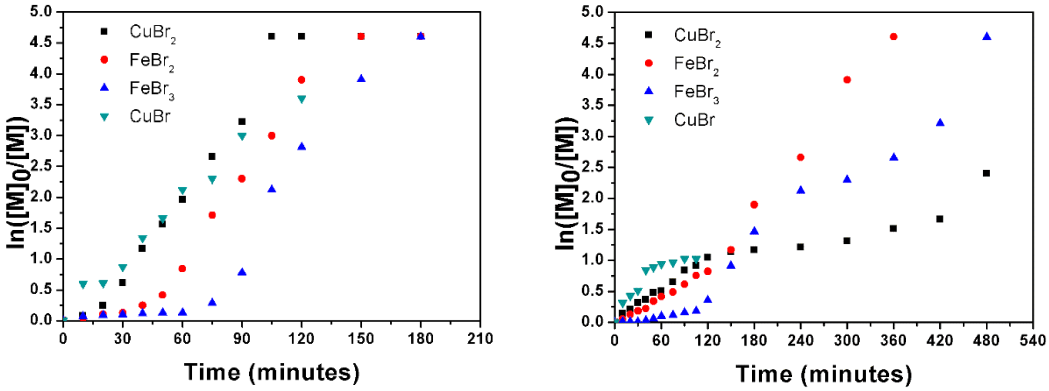

Figure 5.20: First order kinetic plot of different deactivators (0.1 equivalents) for [Monomer]:[EBiB]:[Me_6TREN]=10:1:0.19, **a)** using ethyl acrylate and **b)** ethyl thioacrylate.

a) Ethyl acrylate **b)** Ethyl thioacrylate

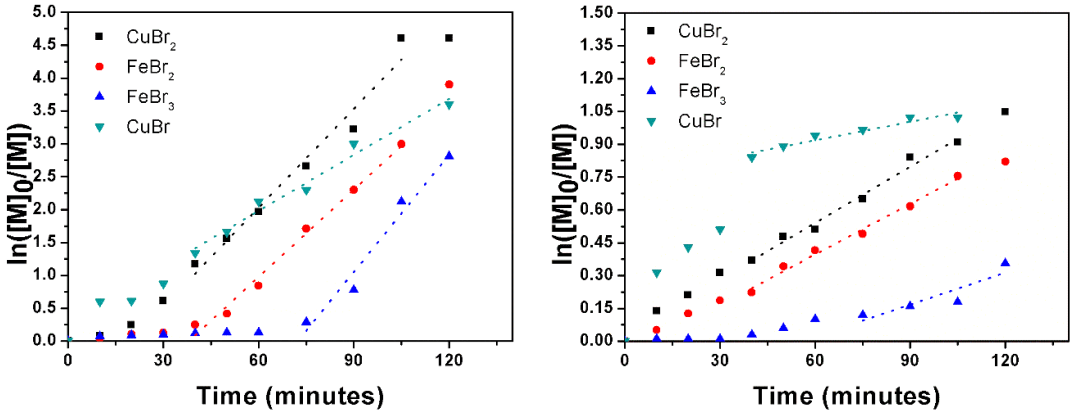

Figure 5.21: First order kinetic plot of different deactivators (0.1 equivalents) for [Monomer]:[EBiB]:[Me_6TREN]=10:1:0.19, **a)** using ethyl acrylate and **b)** ethyl thioacrylate.

Encouraged by these results, the extension of the monomer library was tried with dimethyl acrylamide (DMA). DMA is a well-known acrylamide, preferably polymerised *via* RAFT or other CRP techniques,[16] due to unfavourable side reactions and termination occurring in transition metal mediated (TMM) polymerisations.[17, 18] In an effort to obtain PDMA, the optimised conditions for ETA were used. Unfortunately, the conversion of DMA only reached 21% with $CuBr_2$ (**P25**), 49% with $FeBr_2$ **(P26)** and 45% with $FeBr_3$ **(P27).** The low conversion obtained for DMA was predictable from previous reports found throughout the literature of the inefficient polymerisation of acrylamides. On the other hand, a complexation with $CuBr_2$ seems to be having a more negative impact on the polymerisation, whereas higher conversions are reached, when iron based halides are used. It should be noted that a similar trend was observed for thioacrylates as mentioned above.

Incorporation of monomers, which are difficult to polymerise is typically achieved *via* protecting groups or post polymerisation functionalisation. Thiol bearing monomers for example can be converted into thioesters to avoid their interference with the polymerisation system, which can be hydrolysed back after the completion of the polymerisation to their free thiols.[19] Similarly, anchoring points or functional groups can be inserted along a polymer backbone that can be transformed into other chemical moieties.[20] With the obtained results described above, we theorised that not only would it be possible to convert poly(ethyl thioacrylate) into a poly(acrylamide) *via* amidation, but that its copolymer with an acrylate could be transformed into an "*all-acrylic polymer*", a chain consisting of three different building blocks, namely of acrylates, acrylamides and thioacrylates along a single polymer chain. Since such a polymer has not yet been reported, investigation of its characteristics could unveil interesting new properties. For this hypothesis, the block copolymerisation of an acrylate with a thioacrylate required to be optimised, which is further discussed in the following section.

5.2.2.1 Chain extension of P(MA) with ETA

Under SET-LRP conditions, polymerisations can reach very high conversion for ethyl thioacrylate and ethyl acrylate. The level of livingness/control can be further investigated by *in situ* chain extension of acrylic polymers for the preparation. For this purpose, full kinetic investigation on the homopolymerisation of methyl acrylate (MA) with either $CuBr_2$ (**P51**) or $FeBr_2$ (**P52**) was performed, see in **Section 5.4.2.19** and **Section 5.4.2.20**. Reaction was repeated with $FeBr_2$ for the next experiment to yield P(MA) (P28) and was subsequently chain-extended with the addition of a degassed solution of ETA in DMSO (**Scheme 5.9**).

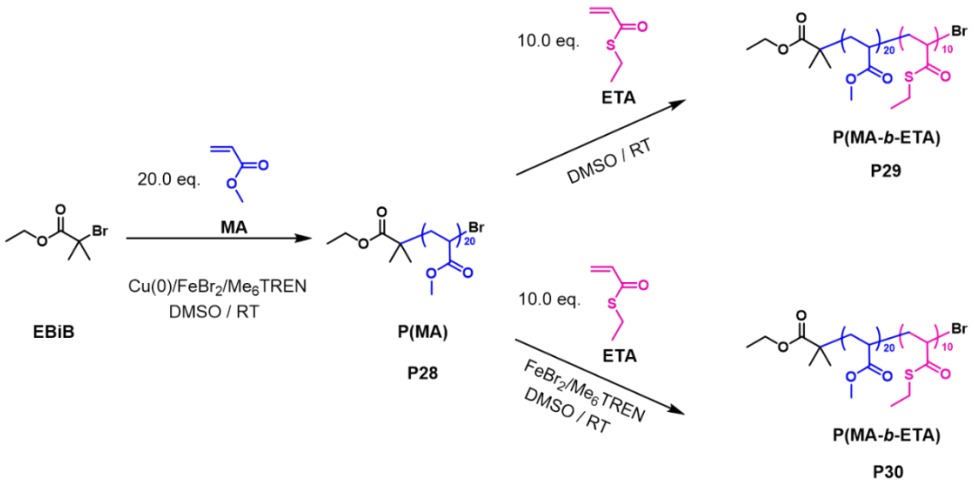

Scheme 5.9: Block copolymers of MA and ETA obtained *via* conventional chain extension (**P29**) and additional $FeBr_2$/Me_6TREN (**P30**).

^{1}H NMR analysis revealed full conversion within 120 minutes for **P51** and 140 minutes for **P52** (**Figure 5.49** and **Figure 5.50**). Furthermore, an initial induction of 20 to 30 minutes and an almost linear dependence of $\ln[M]_0/[M]$ *vs*. time, indicating a first order kinetic with respect to monomer concentration was observed. Polymerisation conditions applied were: [MA]:[EBiB]:[$FeBr_2$]:[Me_6TREN] = [20]:[1]:[0.1]:[0.19] with 4 cm of Cu(0)-wire, generating the first block in 140 minutes. $FeBr_2$ was selected for the initial block as earlier results obtained displayed better polymerisation conditions for thioacrylates. Chain extension by the addition of ETA in DMSO furnished higher molecular weight polymers with an increase in dispersity (DP = 1.40) for **P29** after 16 hours (**Figure 5.22a**) with 80% conversion of the second block. A similar chain extension was performed, adding extra ligand and $FeBr_2$ to the second block of ETA in **P30**. The addition of extra $FeBr_2$/Me_6TREN

allowed the second block of ETA to reach higher conversions (91%), while remaining a narrow dispersity (**Figure 5.22b**).

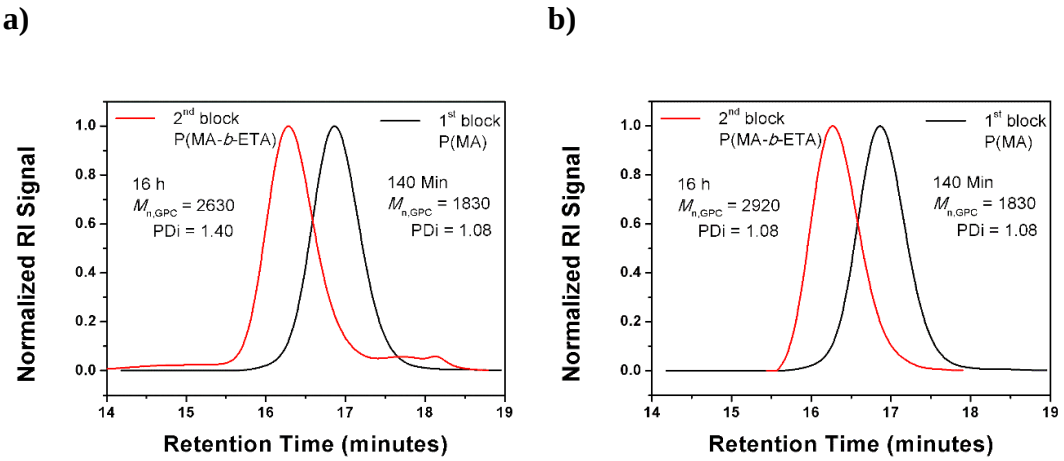

Figure 5.22: Overlay of the GPC traces for **a) P28** and **P29,** and **b) P28** and **P30.**

As the addition of extra ligand and $FeBr_2$ resulted in higher yields for the second block, the conditions from **P30** were applied for a chain extension with 5.00 equivalents of ETA (**P32** in **Scheme 5.10**). This time the conversion could be increased to 97% for the second block.

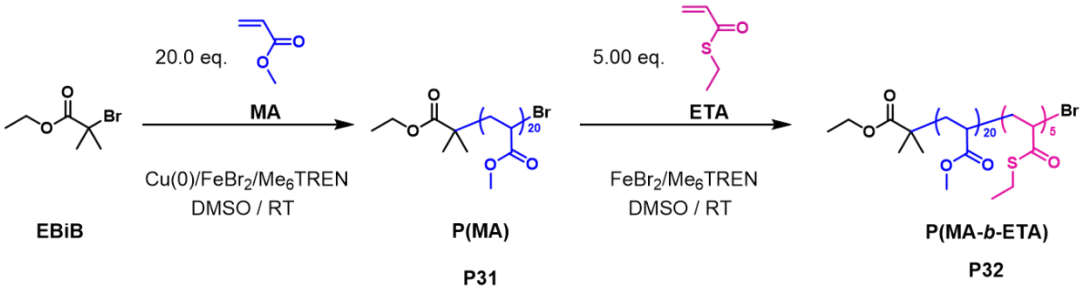

Scheme 5.10: Synthetic route for the polymerisation of MA (**P31**) and successive chain extension with ETA with additional $FeBr_2$/Me_6TREN to obtain **P32**.

GPC analysis revealed a shift towards higher molecular weights and a slight increase in dispersity of 1.10 for **P32** (**Figure 5.23**).

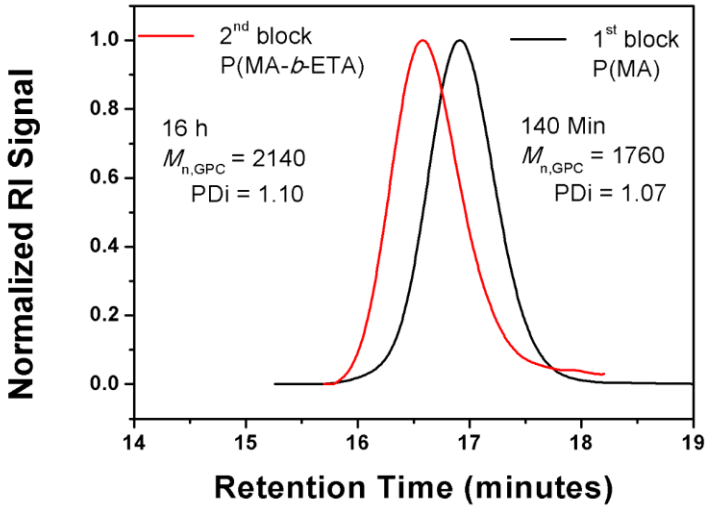

Figure 5.23: Overlay of the GPC traces for **P31** (black) and **P32** (red)**.**

In a further experiment the amount of MA for the first block was decreased to DP = 10 and the amount of the second block was increased to 60.0 equivalents of ETA **(Scheme** 5.11).

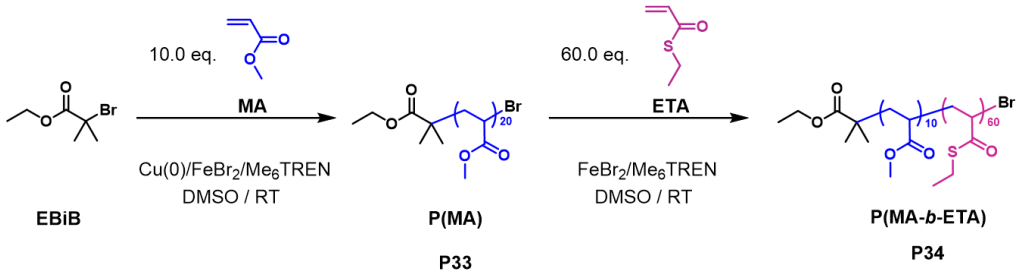

Scheme 5.11: Synthetic route for the polymerisation of MA (**P33**) and successive chain extension with ETA with additional $FeBr_2/Me_6TREN$ to obtain **P34**.

Chain extension by addition at 100 minutes with 60.0 equivalents of ETA in DMSO with ligand and $FeBr_2$, furnished higher molecular weight polymers with almost a 6-fold increase. From the GPC traces it is visible that, all chains have initiated during the chain extension, which can be concluded from the disappearance of the signal for the first block in the region of 17 to 19 minutes. The second block only reached a monomer conversion of 78%, while a broadening of the dispersity was observed (**P34**, $M_{n,GPC}$ = 6280, PDI = 1.76). The overlay of the first block and second block obtained by GPC is depicted below in **Figure 5.24**.

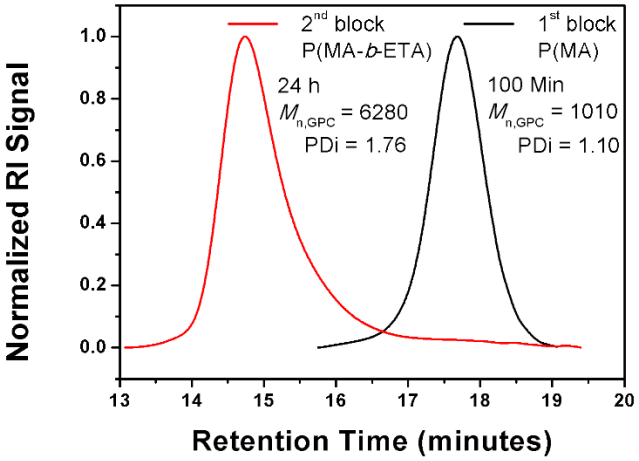

Figure 5.24: Overlay of the GPC traces for **P33** (black) and **P34** (red).

5.2.2.2 Chain extension of P(ETA) with MA

To investigate the livingness of P(ETA) under SET-LRP conditions, the reverse strategy was followed by chain extension of P(ETA) with MA (**Scheme 5.12**).

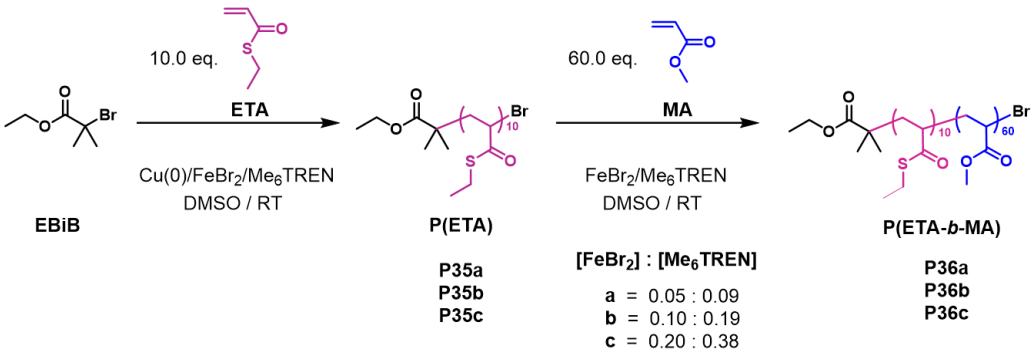

Scheme 5.12: Synthetic route for the polymerisation of ETA (**P35a-c**) and successive chain extension with MA with additional $FeBr_2$/Me_6TREN to obtain **P36a-c**.

Additionally, the amount of [$FeBr_2$]:[Me_6TREN] was varied to explore the consequences for the second block under the conditions applied. For this, *in situ* chain extension of P(ETA) with 60 equivalents of MA was followed by the addition with different ratios of 0.05:0.09 (**P36a**), 0.10:0.19 (**P36b**) and 0.20:0.38 for **P36c**. In all cases, P(ETA) (**P35**) could be chain extended with MA, but GPC analysis additionally revealed that not all chain ends from P(ETA) initiated during the chain extension.

When a low concentration of [$FeBr_2$]:[Me_6TREN] = 0.05:0.09 was used for **P36a**, full conversion for the second block was obtained after 24 hours. However, the appearance of the trace in the region of 17 to 20 minutes indicates not full initiation of all chains from the first block (black trace). Additionally, a small high molecular weight shoulder appears at 14 minutes (**Figure 5.25a**).

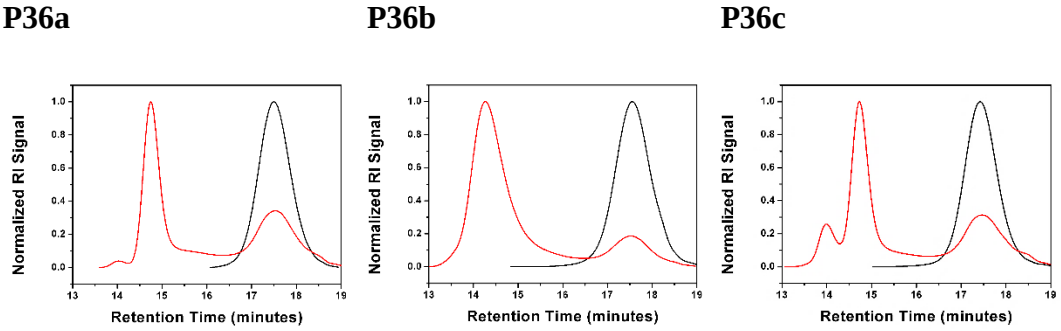

Figure 5.25: Overlay of the GPC traces for **a) P35a** and **P36a, b) P35b** and **P36b,** and **c) P35c** and **P36c.**

Standard conditions of [$FeBr_2$]:[Me_6TREN] = 0.10:0.19 yielded a broader peak after the chain extension and a lower conversion (88%) for the second block. Interestingly, no shoulder in the high molecular weight region was visible for **P36b** in **Figure 5.25b,** which was not the case for **P36b**, when a higher concentration was used with [$FeBr_2$]:[Me_6TREN] = 0.20:0.38. The increase of $FeBr_2$ and ligand resulted in an additional and significantly visible peak at 14 minutes in the higher molecular weight region, concluding the occurrence of coupling reactions (**Figure 5.25c**). Nevertheless, ^{1}H NMR spectroscopy revealed full conversion for the second block after 24 hours.

5.2.3 Synthesis of *"all-acrylic"* polymer *via* amidation (P38)

Chain extension of **P30** was repeated in a next experiment to yield a polymer for further modification. Initially, $FeBr_2$ was employed to chain extend P(MA) with ETA to poly(MA_{20}-*b*-ETA_{10}) (**P37,** $M_{n,GPC}$ = 2390 g/mol, PDI = 1.20). Block copolymer **P37** was used further for amidation to allow for detailed characterisation, with conditions that were previously optimised on a sequence controlled oligomer (**Scheme 5.13**).[21] For this purpose, **P37** was first purified by dialysis. To the pure polymers, 25.0 eq. of benzylamine was added. The relatively mild conditions allow for modification with only a thiol as side product.

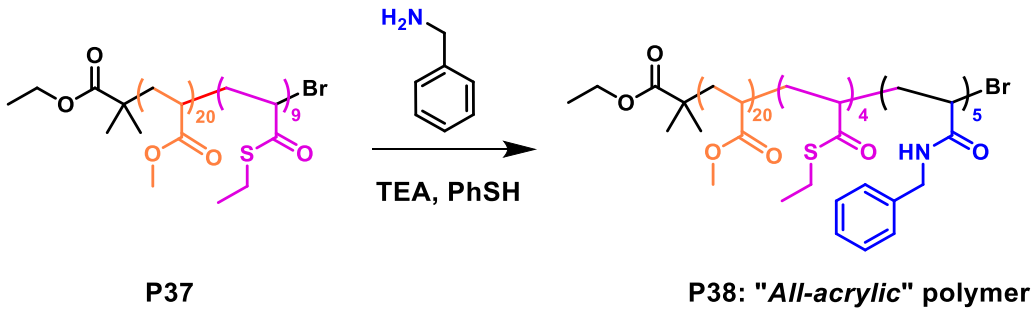

Scheme 5.13: General scheme for amidation of poly(MA_{20}-b-ETA_9) **P37** with benzyl amine resulting in an all-acrylic polymer (**P38**).

The addition of ETA to P(MA) by *in situ* addition resulted in a clear shift of the molecular weight distribution by GPC analysis (**Figure 5.26a**). Furthermore, 97% conversion was obtained for the second block calculated from the ^{1}H NMR spectrum.

a) **b)**

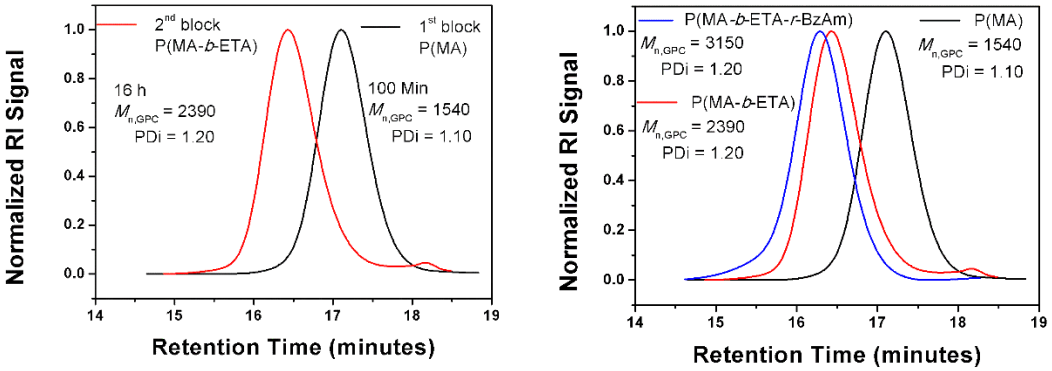

Figure 5.26: Overlay of the obtained GPC traces for the synthesis of **a) P37** and **b) "***all-acrylic"* polymer **P38.**

Table 5.5: Overview of the obtained GPC results for the synthesis of **P37** and its amidation product **P38.**

Entry	$M_{n,theo}$ **(g/mol)**	$M_{n,GPC}$[b] **(g/mol)**	**PDI**[b]	**Composition**
P37 1st block	1920	1540	1.10	$P(MA)_{20}$
P37 2nd block	2960	2390	1.20	$P(MA_{20}$-*b*-$ETA_9)$
P38	3190	3150	1.20	$P(MA_{20}$-*b*-ETA_4-*r*-$BzAm_5)$

[a] Conversion measured by ^{1}H NMR spectroscopy. [b] THF eluent, linear PMMA standard.

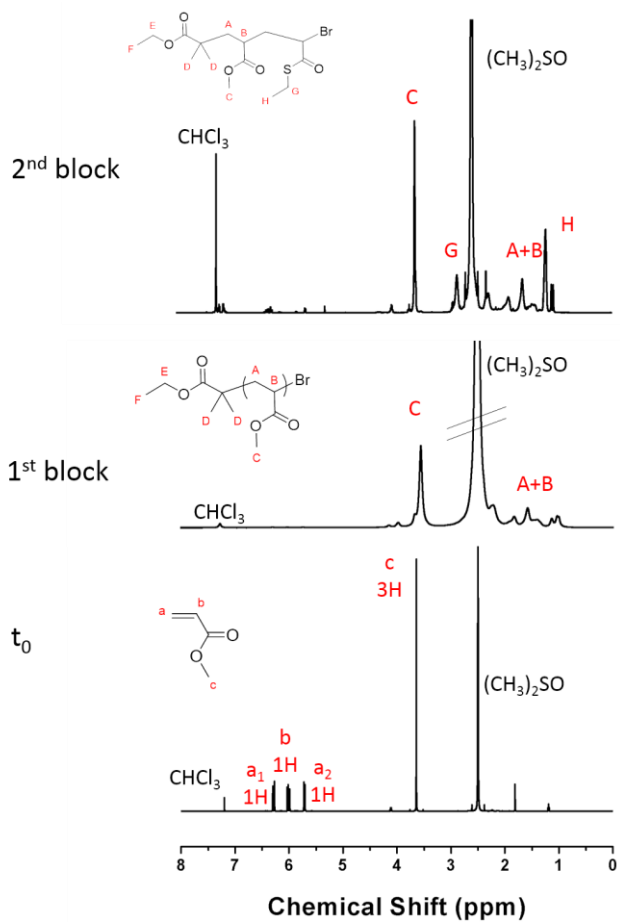

Figure 5.27: ^{1}H NMR spectra obtained, before and after the polymerisation of MA (bottom and middle spectra, respectively) and after the completion of the chain extension with ETA (top spectrum). Monomer conversion for the chain extension was calculated to be 97% **P37**.

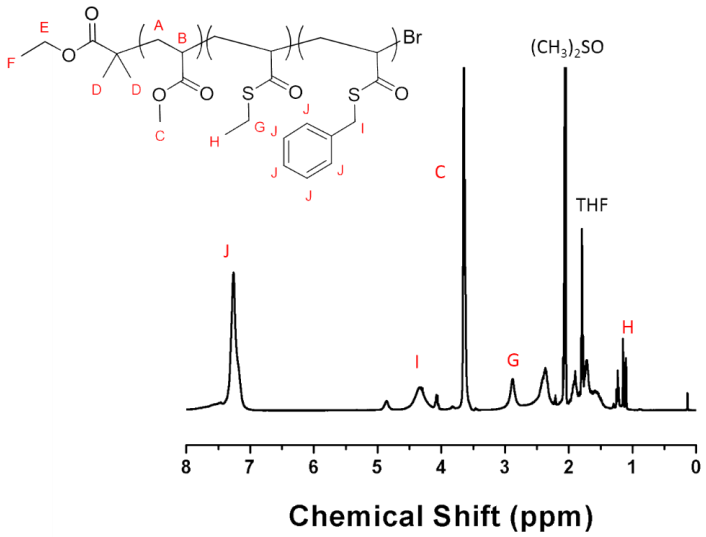

Figure 5.28: ^{1}H NMR spectrum obtained for **P38** after purification.

5.2.4 Comparison of thioester initiators with an ester and amide initiator

Initially, due to the commercial availability, a series of phenylic initiators were prepared, which allowed the direct comparison of their polymerisation kinetics under identical reaction conditions. For this purpose, phenol, thiophenol and aniline were transformed into initiators using α-Bromoisobutyryl bromide (**Scheme 5.14**). The successful synthesis thereof was confirmed *via* ^{1}H NMR (*i.e.* shift of the corresponding phenyl -C*H* signal) and mass spectrometry (see 5.4 Experimental section for detailed description for their synthesis and full product characterisation). The obtained initiators were used to polymerise ethyl acrylate (DP=10) at 25 °C using a preactivated Cu(0)-wire and [M]:[I]:[$CuBr_2$]:[Me_6TREN] = 10:1:0.1:0.19.

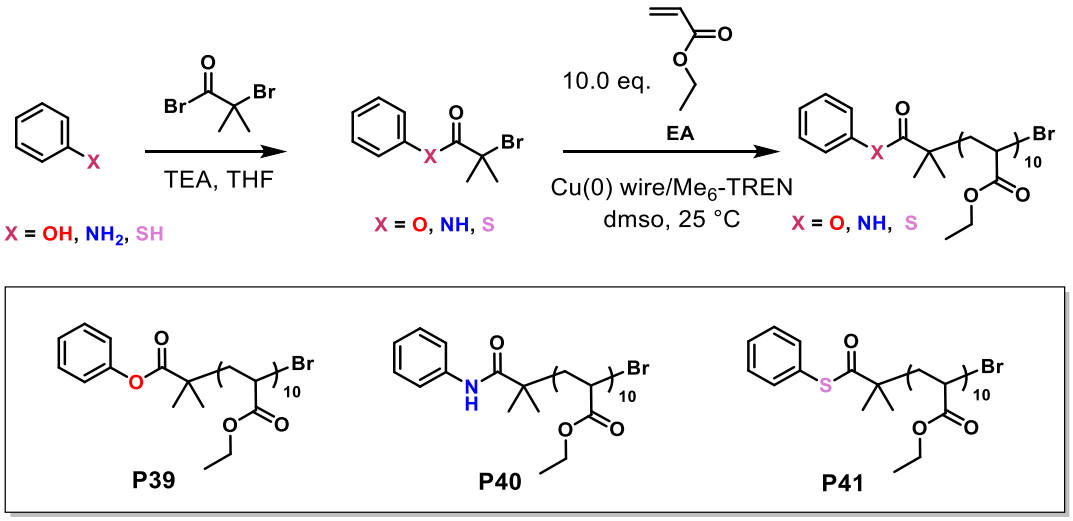

Scheme 5.14: General synthesis route for the three initiators and their polymerisation of ethyl acrylate (**P39-P41**).

The polymerisation was followed for 150 minutes and samples were taken periodically for conversion and GPC. For the first 40 minutes of the polymerisation, the conversion for all polymers were calculated to be below 10%, indicative of the presence of an induction period (**Figure 5.29**). The reasoning of the induction period can be found throughout the literature and will therefore not be discussed in this report.[22, 23] While the conversion for the amide based initiator (PhNHBIB) remains low, conversions obtained for the ester- and thioester based initiators after 150 minutes were similar. The apparent kinetic rate constants (k_p^{app}) calculated after the induction period were also indicative of almost identical monomer consumptions (**P31:** PhBIB=0.032 min^{-1}, **P32:** PhNHBIB=0.002 min^{-1}, while for **P33:** PhSBIB=0.031 min^{-1}).

a) **b)**

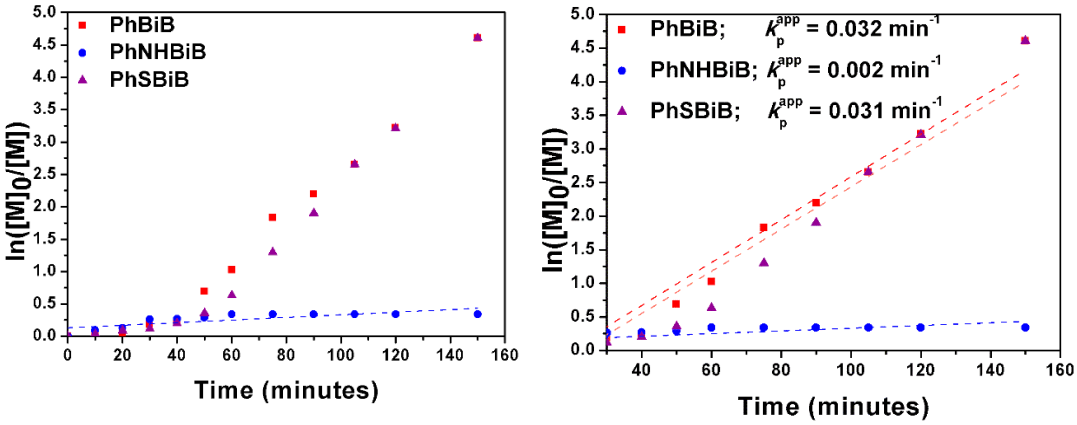

Figure 5.29: a) First order kinetic plots for all three different initiators obtained from periodic sampling during polymerisation with [EA]:[I]:[$CuBr_2$]:[Me_6TREN] = 10:1:0.1:0.19. **b)** Calculated apparent kinetic rate constants (k_p^{app}) after the induction period.

To be able to exclude an effect of the aromatic ring, a comparison of EBiB (**P43**) with its thioester counterpart (*S*-EBiB, **P44**) was carried out, yielding almost identical results for the first linear region of the kinetic plot (**Figure 5.30**). However, after 90 minutes of polymerisation, both reactions start to level off, resulting in full monomer conversion in 120 minutes (**P43**) and 240 minutes (**P44**). Thus the above obtained results for the different initiators show that where an amide based initiator is not sufficient to polymerise ethyl acrylate, an ester and a thioester initiator can be used interchangeably. A prolonged reaction time for *S*-EBiB should be noted.

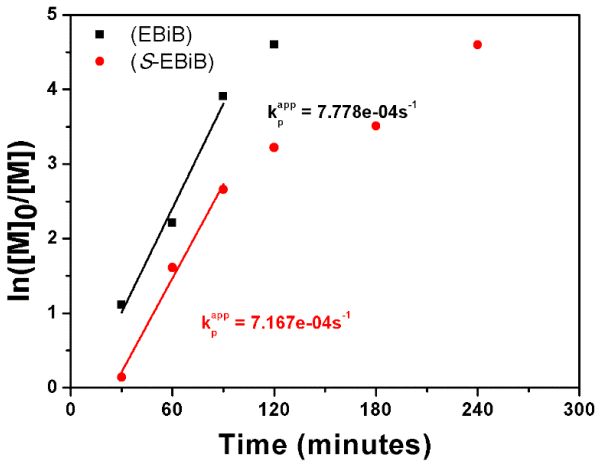

Figure 5.30: Comparison of EBiB and *S*-EBiB used for polymerisations of EA. [EA]:[I]:[Me_6TREN]:[$CuBr_2$] = 60:1:0.19:0.1 in DMSO.

In order to investigate, whether the Cu(0)-wire/$FeBr_2$ system can be used as well, EA_{10} was polymerised with $CuBr_2$ (**P45**) and $FeBr_2$ (**P46**) and thioester initiator. This simple comparison in a pair of kinetic experiments has revealed that the mixed system could be applied, as only very small differences were visible. This is particularly useful, for block copolymerisations of thioacrylates, using a thioester based initiator, as this would allow molecular weights to be targeted, owing to quantitative monomer conversion.

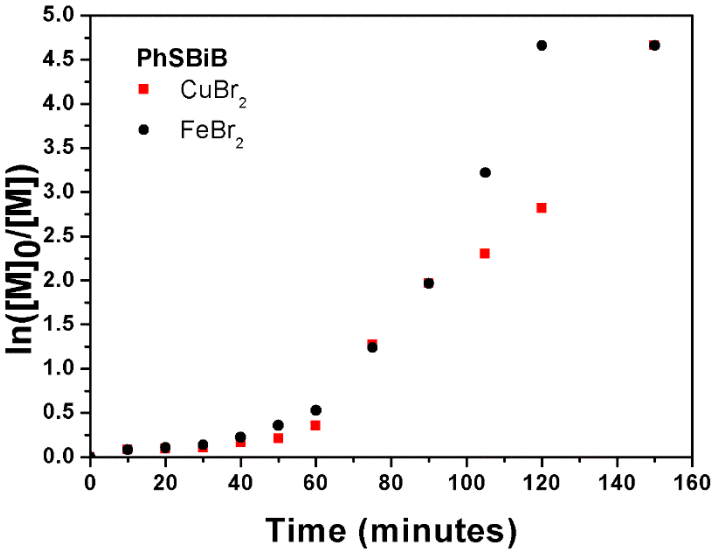

Figure 5.31: Comparison of $CuBr_2$ and $FeBr_2$ used for polymerisations using PhSBiB.

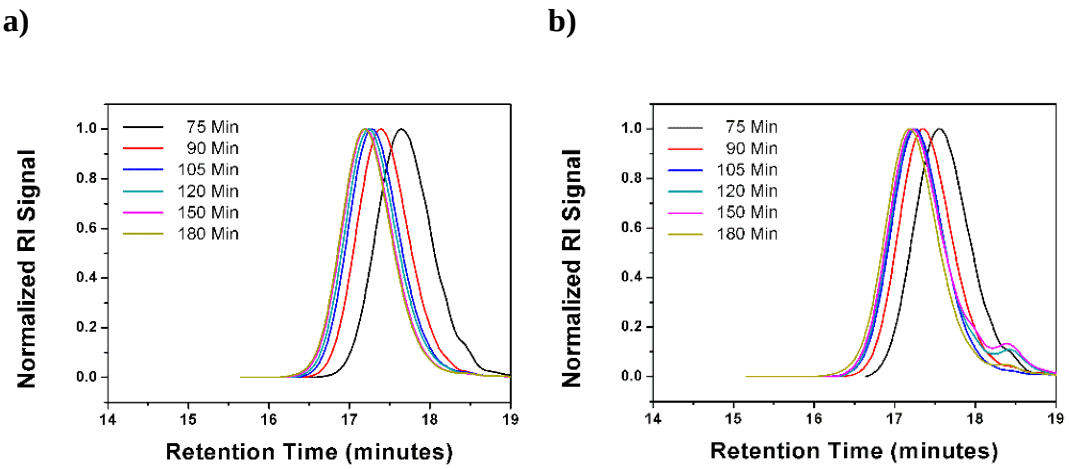

Figure 5.32: Obtained GPC traces for polymers using **a) P45**: $CuBr_2$ and **b) P46:** $FeBr_2$.

5.2.5 Star-shaped thioester polymer and its dissociation into linear polymers *via* native chemical ligation

Parallel to the investigation of the amidation of the ETA polymers mentioned earlier, a tetrathiol functional molecule was converted into a tetra functional star initiator, giving four thioester groups. Initially, di(ethylene glycol) ethyl ether acrylate (eDEGA) was polymerised using [M]:[I]:[$CuBr_2$]:[Me_6TREN]=200:1:0.1:0.19 (**Scheme 5.15**).

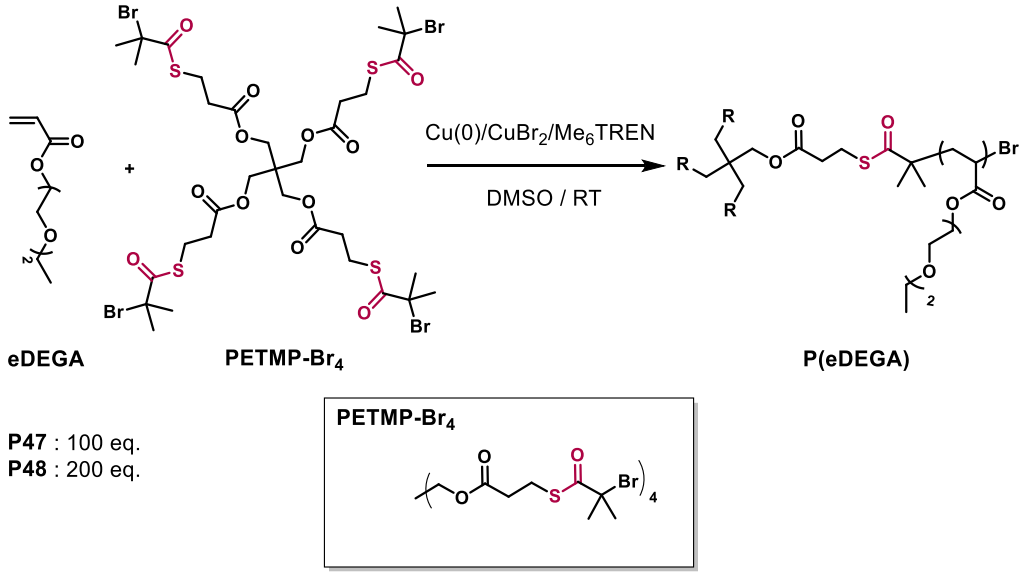

Scheme 5.15: General overview of the polymerisation of eDEGA using a 4-arm thioester star initiator to obtain star polymers **P47** and **P48.**

The obtained GPC traces show a rapid increase in molecular weight, especially after 60 minutes into the polymerisation (**Figure 5.33)**. However, at higher reaction times, the formation of star-star coupling was visible. Nevertheless, near quantitative monomer conversions were reached for both star polymers.

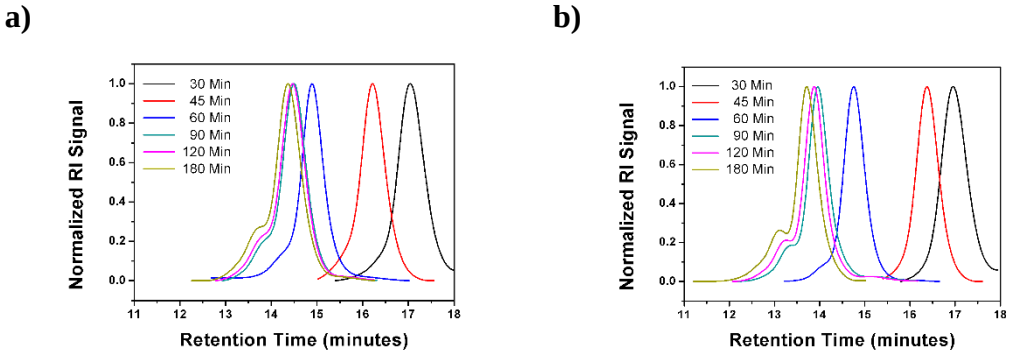

Figure 5.33: Overlay of the GPC traces obtained from kinetic sampling for **a) P47** and **b) P48.**

The obtained results during the polymerisation of **P47** and **P48** are summarised below in **Table 5.6** and **Table 5.7**.

Table 5.6: Overview of the GPC results obtained during the polymerisation of **P47.**

Time (min)	$M_{n,theo}$ **(g/mol)**	$M_{n,GPC}$[b] **(g/mol)**	**PDI**[b]	**Conv.**[a] **(%)**
15	2210	N/A	N/A	6
30	4470	1740	1.14	18
45	5220	3550	1.24	22
60	12560	11040	1.37	61
90	17840	15660	1.33	89
120	18590	16310	1.21	93
180	19340	18100	1.10	97

Polymerisation condition: [ETA]:[I]:[$CuBr_2$]:[Me_6TREN] = 100:1:0.1:0.19. [a]Conversion measured by ^{1}H NMR spectroscopy. [b] THF eluent, linear PMMA standard.

Table 5.7: Overview of the GPC results obtained during the polymerisation of **P48.**

Time (min)	$M_{n,theo}$ **(g/mol)**	$M_{n,GPC}$[b] **(g/mol)**	**PDI**[b]	**Conv.**[a] **(%)**
15	4090	N/A	N/A	8
30	6350	1860	1.08	14
45	7480	3080	1.08	17
60	17270	12100	1.12	43
90	31580	24060	1.78	81
120	34970	26570	1.19	90
180	36100	47450	1.40	93

Polymerisation condition: [ETA]:[I]:[$CuBr_2$]:[Me_6TREN] = 200:1:0.1:0.19. [a]Conversion measured by ^{1}H NMR spectroscopy. [b] THF eluent, linear PMMA standard.

Reducing star-star coupling in a polymerisation with a multifunctional initiator is known to be difficult and exhaustive, as next to the catalyst system, initiator concentration and factors such as temperature and monomer concentration *etc.* can have a big impact on the rate of polymerisation. Ideally, the rate of polymerisation should be low enough to avoid star-star coupling, yet fast enough to result in a well-defined polymer and full monomer conversion. Due to this, further optimisation

of the polymerisation system was avoided and the polymerisation was repeated and stopped after 60 minutes, to result in a well-defined thioester based star polymer (**Scheme 5.16**).

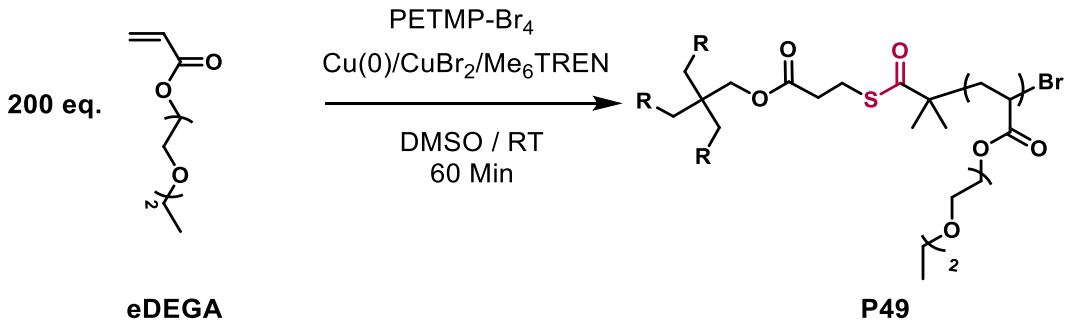

Scheme 5.16: General overview of the polymerisation of eDEGA with [M]:[I]=200. Note that the polymerisation was stopped after 60 minutes to yield **P49**.

As per the kinetic investigation of the polymerisation, the new polymerisation was intentionally terminated after 60 minutes. Assigned ^{1}H NMR spectra from the polymerisation and process and the purified product is displayed below in **Figure 5.34.**

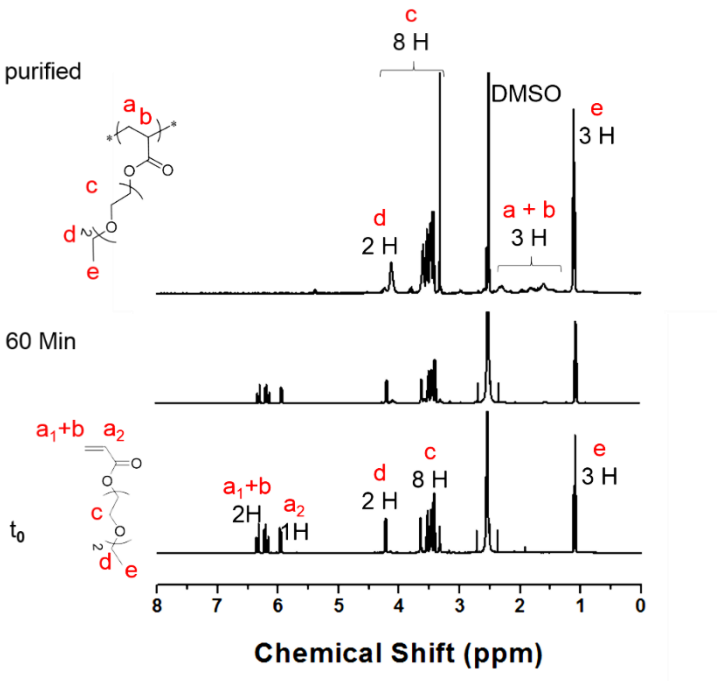

Figure 5.34: Overlay of the obtained ^{1}H NMR spectra for the polymerisation of eDEGA at time zero (**bottom**), after 60 minutes (**middle**) and after purification by dialysis (**P49, top**).

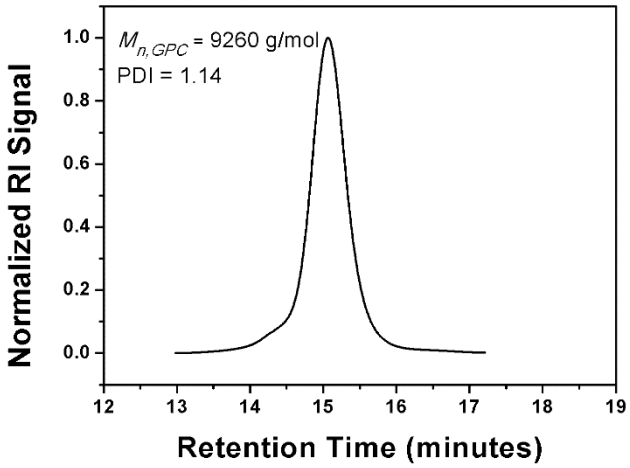

Figure 5.35: Obtained GPC trace for the purified polymer of **P49.**

The obtained star polymer was well defined proving that thioester initiated star polymerisations remain well controlled (**P49**, $M_{n,GPC}$ = 9300 g/mol, PDI = 1.14, **Figure 5.35**). Thioesters are functional precursors for chemoselective amidation reactions in nature, typically *via* native chemical ligation. The transfer reaction with cysteine is well explored and understood.[24] With this knowledge, it was hypothesised that a thioester containing polymer could be conjugated to a peptide containing cysteine or its derivative. Carrying out such ligation chemistry on **P49**, would allow a transition from star to a linear polymer. To demonstrate this, L-cysteine methyl ester hydrochloride was introduced to the star polymer, which slowly started to dissociate into its linear arms over a native chemical ligation mechanism.

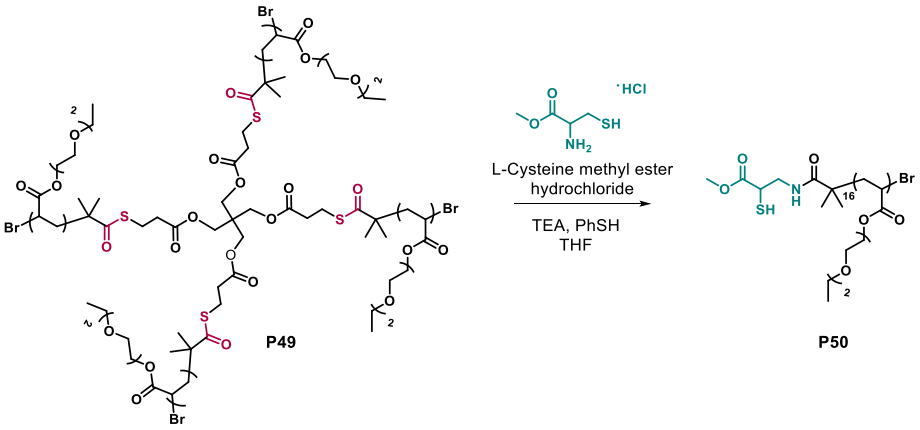

Scheme 5.17: General dissociation route of the thioester star polymer **P49**, into its linear arms **P50** *via* native chemical ligation with L-cysteine methyl ester hydrochloride.

The dissociation reaction was followed *via* GPC over a period of 19 hours, displaying a reduction in hydrodynamic volume (**Figure 5.36**). Full dissociation was observed after 19h, confirmed by the disappearance of the initial signal between 14 and 16 minutes.

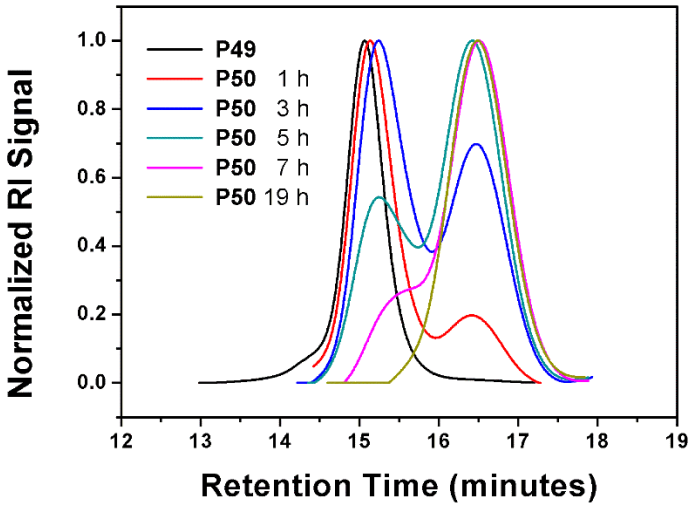

Figure 5.36: Overlay of the GPC traces obtained during the dissociation of the star polymer **P49**, displaying a shift towards lower retention times.

The end polymer obtained (**P50,** $M_{n,GPC}$ = 2800 g/mol, PDI = 1.10) was additionally analysed *via* MALDI-ToF-MS. The obtained MALDI-ToF-MS spectrum, not only is in accordance with the identification of the linear species, but also shows that no incomplete dissociation remained (**Figure 5.37**). The mass spectrum displayed two main distributions, which arise primarily from the main product (red denoted A in **Figure 5.38**) and a side product, that is calculated to be the oxidised sulfur (*i.e.* L-cysteine sulfinic acid methyl ester, blue and denoted B in **Figure 5.38**), as the reaction was carried out under air. The peaks showed a difference of m/z = 188.20, in agreement with the molecular weight of the monomer. Both products also displayed additional distributions, which corresponded to the –Br chain terminus (labelled –Br) and the chain end hydrolysed –H terminus (labelled –H) (Se**e Table 5.8** for full peak assignment).

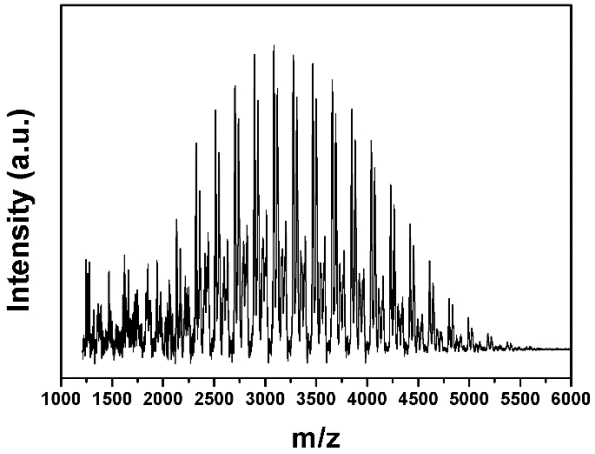

Figure 5.37: Obtained MALDI-ToF-MS spectrum, indicating full dissociation of **P49** into **P50.** See next figure for a zoom in.

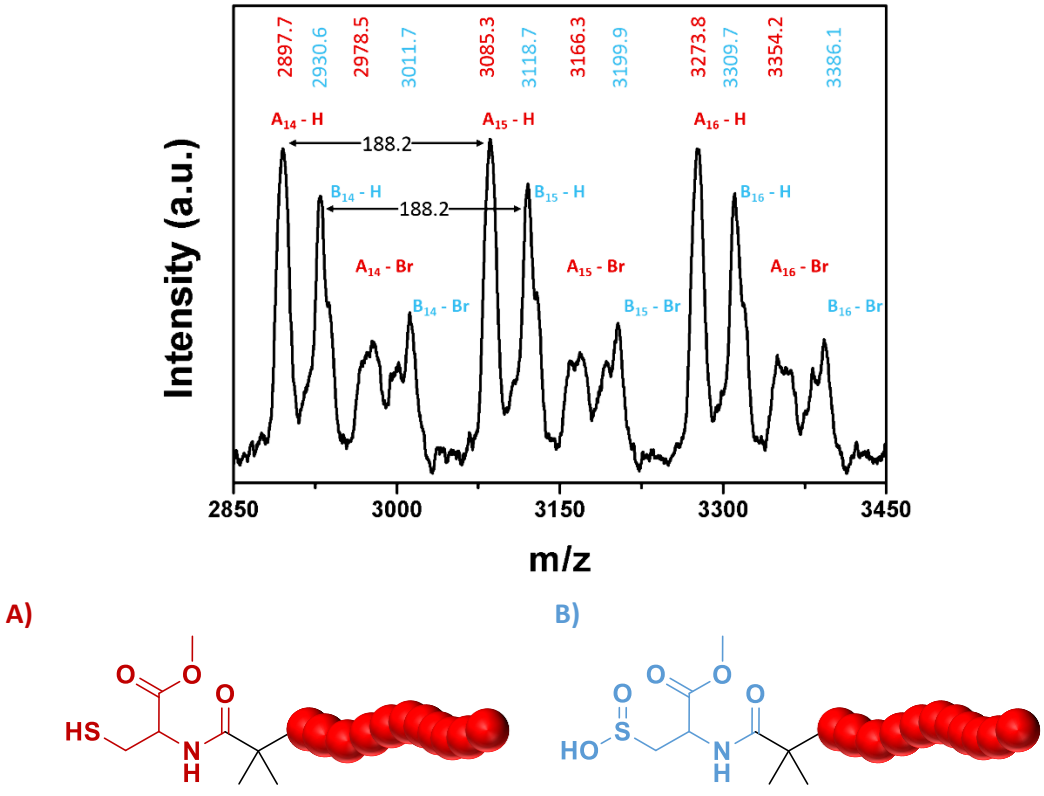

Figure 5.38: MALDI-ToF-MS spectrum obtained from the reaction of **P49** after 19 hours, displaying the product **P50**. Two main distributions are evident, which are calculated to be linear chains with their initiator end bearing **A)** free thiol end group and **B)** sulfinic acid end group. Additionally, different chain ends are denoted as –H and –Br in the spectra, whereas subscript denotes the number of repeating units.

Table 5.8: Overview of the assigned MALDI-ToF-MS peaks and their corresponding calculated *m/z* values

Peak$_{(DP)}$ – Chain end	**Formula**	**Calculated *m/z***	**Observed *m/z***
A_{14} – H	$C_{133}H_{237}NO_{57}SAg^+$	2900.45	2897.7
A_{15} – H	$C_{142}H_{253}NO_{61}SAg^+$	3087.55	3085.3
A_{16} – H	$C_{151}H_{269}NO_{65}SAg^+$	3275.65	3273.8
B_{14} – H	$C_{133}H_{237}NO_{59}SAg^+$	2931.43	2930.6
B_{15} – H	$C_{142}H_{253}NO_{63}SAg^+$	3119.54	3118.7
B_{16} – H	$C_{151}H_{269}NO_{67}SAg^+$	3307.64	3309.7
A_{14} – Br	$C_{133}H_{236}NO_{57}BrSAg^+$	2977.36	2978.5
A_{15} – Br	$C_{142}H_{252}NO_{61}BrSAg^+$	3165.46	3166.3
A_{16} – Br	$C_{151}H_{268}NO_{65}BrSAg^+$	3353.56	3354.2
B_{14} – Br	$C_{133}H_{236}NO_{59}BrSAg^+$	3009.35	3011.7
B_{15} – Br	$C_{142}H_{252}NO_{63}BrSAg^+$	3197.45	3199.9
B_{16} – Br	$C_{151}H_{268}NO_{67}BrSAg^+$	3385.66	3386.1

5.3 Conclusion

In conclusion, this work reports the first polymerisation of a thioacrylate *via* SET-LRP after a series of optimisation reactions. It was found that using $FeBr_2$ instead of $CuBr_2$ as deactivator, gives similarly good control, while allowing full monomer conversion of thioacrylates. Furthermore, it was shown that both deactivators can be used for the polymerisations of acrylates. The results obtained from this, allowed the synthesis of an acrylate-*block*-thioacrylate copolymer, that was used for partial amidation resulting in a novel "all acrylic" block copolymer that is reported for the first time. Physical and thermal properties of such a polymer is currently under investigation.

In parallel, the very first use of a thioester based initiator for SET-LRP is described. Adapting the conditions to a star shaped thioester initiator allowed the synthesis of a star polymer, bearing four thioester groups in the core, which could easily be followed *via* GPC and MALDI-ToF-MS. The dissociation of this star polymer with L-cysteine methyl ester *via* NCL has been shown to be an efficient way to initiate a structural transition of star polymers into linear polymers, that could also allow the conjugation with cysteine or cysteine derivatives containing peptides.

5.4 Experimental

5.4.1 General Consideration:

All reactions involving air- and/or moisture-sensitive substances were carried out under an inert atmosphere (argon or nitrogen) using standard Schlenk techniques. Solvents were dried and degassed using standard laboratory techniques.

Molecular weight averages and polymer dispersity of obtained polymers were determined by GPC in THF. Measurements were performed on an Agilent 390-LC system equipped with a PL-AS RT autosampler, 2PLgel 5 μm mixed-C columns (300×7.5 mm), a PLgel 5 mm guard column (50×7.5 mm), and a differential refractive index (DRI). The system was eluted with THF containing 2% trimethylamine (TEA) at a flow rate of 1 mL min^{-1} and the DRI was calibrated with linear narrow poly(methyl methacrylate) standards in range of 1010 to 2136000 g/mol. All samples were passed through neutral aluminium oxide to remove any catalyst residues and filtered using 0.2 μm PTFE filters before analysis.

^{1}H NMR spectra were recorded on a Bruker AV-400 or Bruker Avance 600 spectrometer at 303K. The resonance signal at 7.26 ppm (1H) was used as residual $CDCl_3$ or for $(CD_3)_2CO$ at 2.05 ppm peak for the chemical shift (δ). For ^{13}C NMR spectra were referenced relative to the solvent signal (77.16 ppm).

High-resolution mass spectra (HRMS) were recorded on a Waters SYNAPT G2-Si High Definition Mass Spectrometry system using a solvent gradient (0->100% Acetonitrile in Water + 0.1% Formic acid) in positive electrospray ionisation (ESI+) mode equipped with an Acquity UPLC BEH C18 column (2.1 x 50 mm; 130Å). The instrument was tuned using a Leucin Enkephalin mix to optimum resolution and signal intensity and was calibrated using a Waters Major Mix IMS/ToF in a range of m/z 50-1200.

5.4.2 General Procedures:

5.4.2.1 Synthesis of Pentaerythritol tetrakis(2-bromoisobutyrate) (PEP-Br4)

Was synthesised according to literature procedure.[25]

5.4.2.2 Synthesis of *S*-phenyl 2-bromo-2-methylpropanethioate (*S*-EBiB)

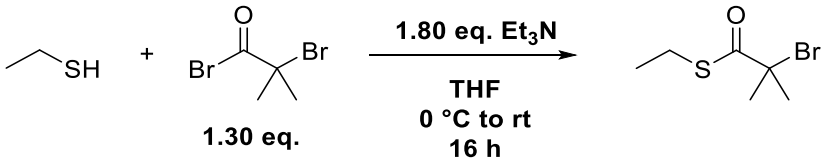

In a 500 mL 2-neckround bottom flask, ethanethiol (3.60 mL, 48.65 mmol) and NEt_3 (12.17 mL, 87.31 mmol) were stirred in dry THF (100 mL) and cooled down to 0°C in an ice-bath. A mixture of BIBB (8.99 mL, 72.99 mmol) and THF (50 mL) were added dropwise over a period of 1 hour under argon. The mixture was then allowed to warm up to ambient temperature and stirred overnight. The precipitated salt was removed *via* filtration and washed with 60 mL of THF. The filtrate was collected an concentrated in *vacuo*, dissolved in DCM, washed with 10% HCl (3 x 30 mL), 5% NaOH (3 x 30 mL), brine (3 x 30 mL) and passed over a column of basic aluminium oxide to remove any impurities to yield a viscous pale yellow oil. (**Yield**=4.90 g, 48%)

^{1}H NMR ($CDCl_3$, 400 MHz) δ: 2.89 (q, 3H), 194 (s, 6H), 1.27 ppm (t, 2H).

^{13}C NMR ($CDCl_3$, 400 MHz) δ: 200.02, 64.25, 31.23, 24.59, 14.24 ppm.

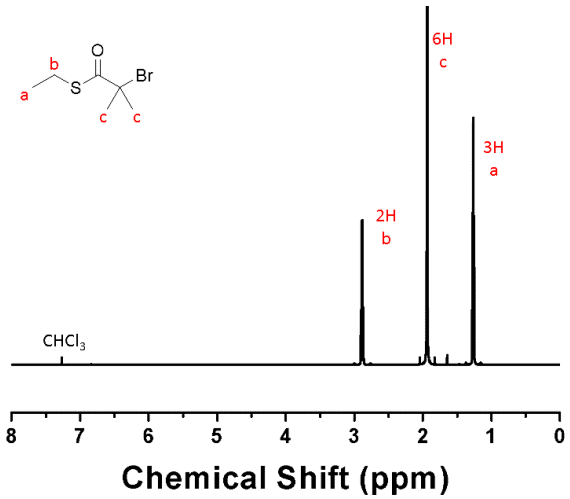

Figure 5.39: ^{1}H NMR spectrum obtained for *S*-EBiB.

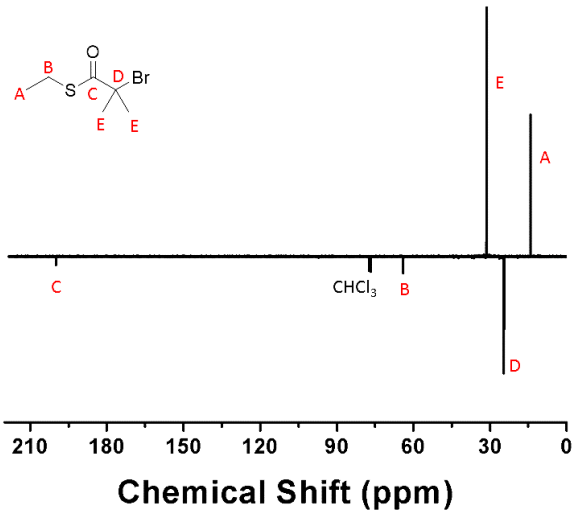

Figure 5.40: ^{13}C NMR spectrum obtained for *S*-EBiB.

5.4.2.3 Synthesis of S-phenyl 2-bromo-2-methylpropanetioate (PhSBiB)

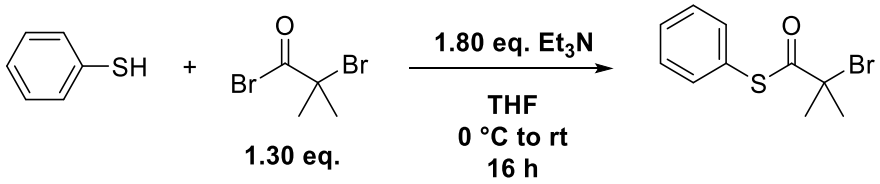

In a 500 mL 2-neckround bottom flask, thiophenol (10 mL, 97.39 mmol) and NEt_3 (24.34 mL, 174.62 mmol) were stirred in dry THF (100 mL) and cooled down to 0°C in an ice-bath. A mixture of BIBB (17.98 mL, 145.98 mmol) and THF (50 mL) were added dropwise over a period of 1 hour under argon. The mixture was then allowed to warm up to ambient temperature and stirred for 15 h. The precipitated salt was removed *via* filtration and washed with 60 mL of THF. The filtrate was collected an concentrated in *vacuo*, dissolved in DCM, washed with 10% HCl (3 x 100 mL), 5% NaOH (3 x 100 mL), brine (3 x 100 mL) and passed over a column of basic aluminium oxide to remove any impurities to yield a viscous pale yellow oil. (**Yield**=14.88 g, 59%).

^{1}H NMR ($CDCl_3$, 400 MHz) δ: 1.86 (s, H_d, 6H), 7.06-7.35 ppm (H_a, H_b, H_c, 5H).

^{13}C NMR ($CDCl_3$, 400 MHz) δ: 30.79, 64.96, 127.36, 130.12, 135.22, 197.04.

HRMS (m/z): $C_{10}H_{11}BrOS$, calc.: 257.97, found: 258.96 $[MH]^+$

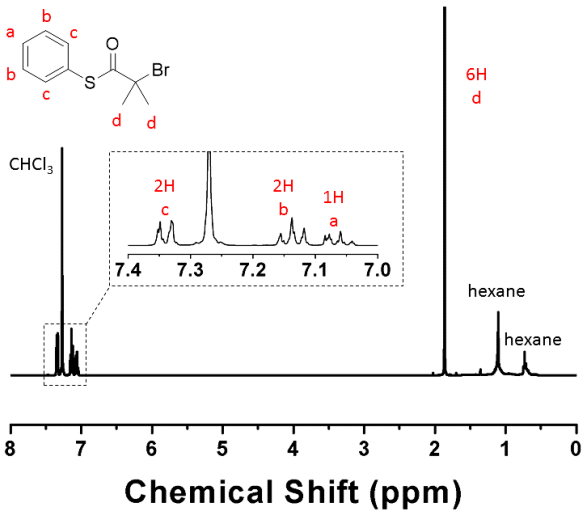

Figure 5.41: ^{1}H NMR spectrum obtained for PhSBiB.

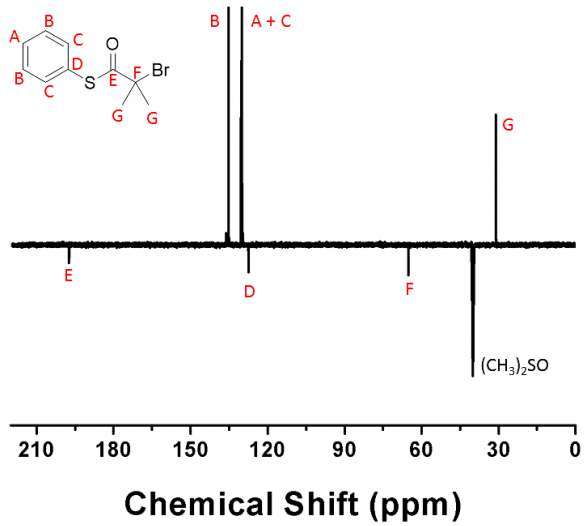

Figure 5.42: ^{13}C NMR spectrum obtained for PhBSiB.

5.4.2.4 Synthesis of Phenyl 2-bromo-2-methylpropanoate (PhBiB)

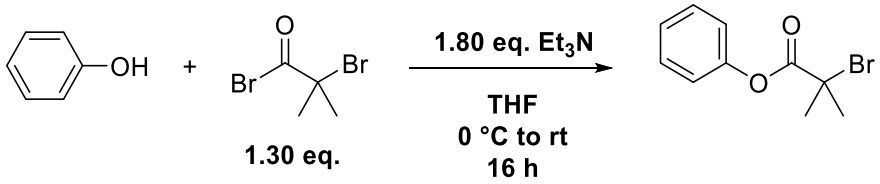

In a 500 mL 2-neckround bottom flask, phenol 5.00 g, 53.13 mmol) and NEt_3 (13.00 mL, 92.68 mmol) were stirred in dry THF (100 mL) and cooled down to 0°C in an ice-bath. A mixture of BIBB (8.50 mL, 69.06 mmol) and THF (50 mL) were

added dropwise over a period of 1 hour under argon. The mixture was then allowed to warm up to ambient temperature and stirred for 15 h. The precipitated salt was removed *via* filtration and washed with 60 mL of THF. The filtrate was collected an concentrated in *vacuo*, dissolved in DCM, washed with 10% HCl (3 x 100 mL), 5% NaOH (3 x 100 mL), brine (3 x 100 mL) and passed over a column of basic aluminium oxide to remove any impurities to yield a pale brown solid. (**Yield**=10.61 g, 82%).

^{1}H NMR ($(CH_3)_2SO$, 400 MHz) δ = 2.05 (s, H_d, 6H), 7.18 – 7.47 (m, H_a, H_b, H_c, 5H)

^{13}C NMR ($(CH_3)_2SO$, 400 MHz) δ: 30.22, 57.28, 121.28, 126.44, 129.83, 150.57, 169.68 ppm.

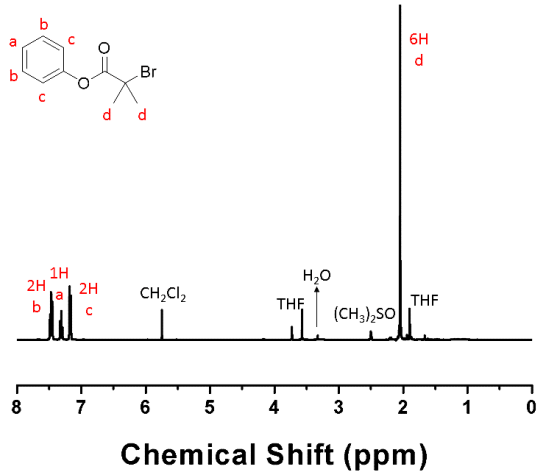

Figure 5.43: ^{1}H NMR spectrum obtained for PhBiB.

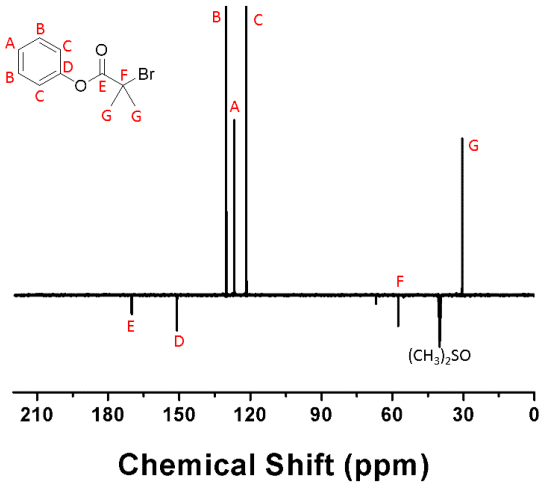

Figure 5.44: ^{13}C NMR spectrum obtained for PhBiB.

5.4.2.5 Synthesis of Phenyl 2-bromo-2-methylpropanoate (PhNHBiB)

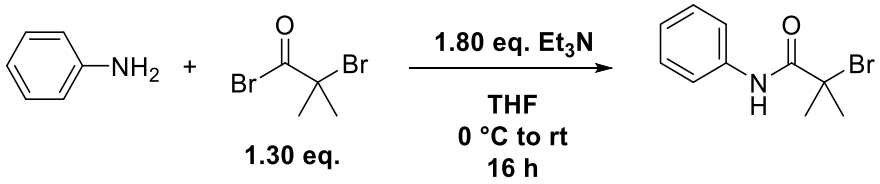

In a 500 mL 2-neckround bottom flask, aniline 10.2 g, 109 mmol) and NEt_3 (24.3 mL, 174 mmol) were stirred in dry THF (150 mL) and cooled down to 0°C in an ice-bath. A mixture of BIBB (30.4 mL, 247 mmol) and THF (50 mL) were added dropwise over a period of 1 hour under argon. The mixture was then allowed to warm up to ambient temperature and stirred for 15 h. The precipitated salt was removed *via* filtration and washed with 200 mL of THF. The filtrate was collected an concentrated in *vacuo*, dissolved in DCM, washed with 10% HCl (3 x 150 mL), 5% NaOH (3 x 150 mL), brine (3 x 150 mL) and passed over a column of basic aluminium oxide to remove any impurities to yield a pale brown solid. (**Yield** = 23.9 g, 90%).

^{1}H NMR ($(CH_3)_2SO$, 400 MHz) δ = 2.00 (s, H_e, 6H), 7.11 – 7.64 (m, H_a, H_b, H_c, 5H), 9.77 ppm (s, H_d, 1H).

^{13}C NMR ($(CH_3)_2SO$, 400 MHz) δ: 30.79, 60.56, 120.31, 123.68, 128.54, 138.54, 169.35 ppm.

HRMS (m/z): $C_{10}H_{12}BrNO$, calc.: 241.01, found: 242.00 $[MH]^+$

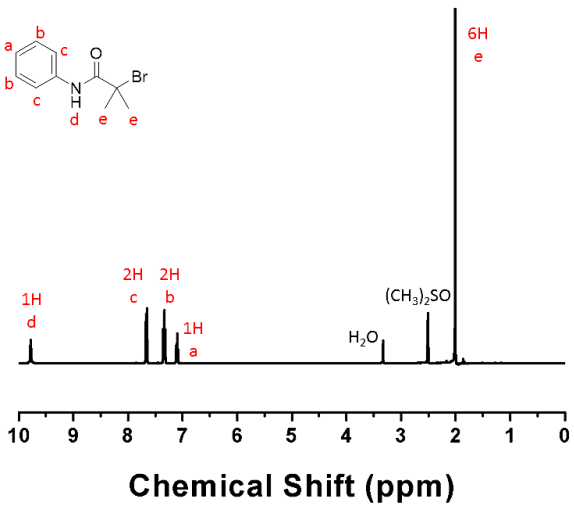

Figure 5.45: ^{1}H NMR spectrum obtained for PhNHBiB.

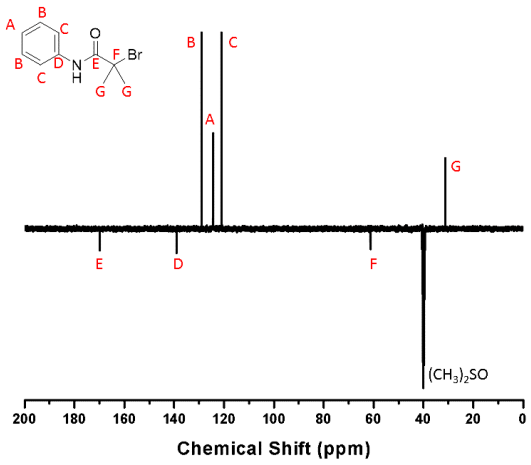

Figure 5.46: ^{13}C NMR spectrum obtained for PhNHBiB.

5.4.2.6 Synthesis of Pentaerythritol tetrakis 3-mercaptoprionate-2-bromoisobutyrate (PETMP-Br$_4$)

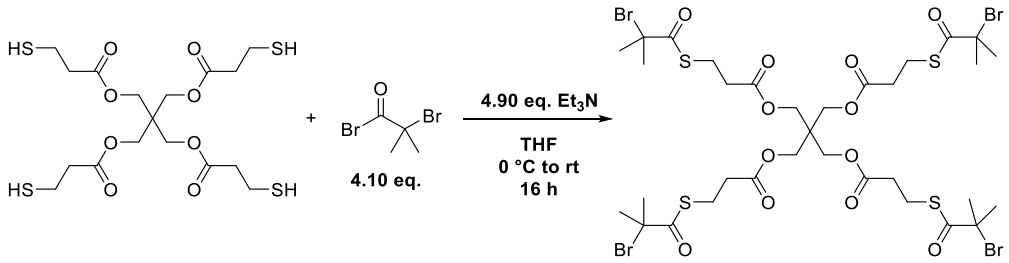

In a 500 mL 2-neckround bottom flask, Pentaerythritol tetrakis(3-mercaptopropionate) (7.00 mL, 17.74 mmol) and Et_3N (12.17 mL, 87.85 mmol) were stirred in dry THF (100 mL) and cooled down to 0°C in an ice-bath. A mixture of BIBB (8.99 mL, 72.93 mmol) and THF (50 mL) were added dropwise over a period of 1 hour under argon. The mixture was then allowed to warm up to ambient temperature and stirredfor 15 h. The precipitated salt was removed *via* filtration and washed with 60 mL of THF. The filtrate was collected an concentrated in *vacuo*, dissolved in DCM, washed with 10% HCl (3 x 100 mL), 5% NaOH (3 x 100 mL), brine (3 x 100 mL) and passed over a column of basic aluminium oxide to remove any impurities to yield a viscous pale yellow oil. (**Yield** = 9.60 g, 50%).

$\boldsymbol{M}_{\mathbf{n,GPC}}$ = 1020 gmol^{-1} , (PDi = 1.03).

^{1}H NMR ($CDCl_3$, 400 MHz) δ: 4.17 (s, 8H), 3.14 (t, 8H), 2.68 (t, 8H), 1.96 (s, 24H) ppm.

^{13}C NMR ($CDCl_3$, 400 MHz) δ: 24.67, 30.79, 33.46, 41.77, 77.04-76.70, 170.97, 199.43 ppm.

HRMS (m/z): $C_{33}H_{48}Br_4O_{12}S_4$, calc.: 1083.87, found: 1084.89 $[MH]^+$

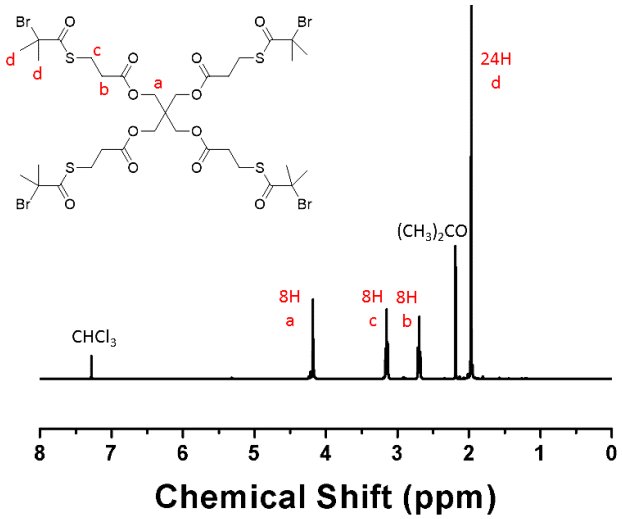

Figure 5.47: ^{1}H NMR spectrum obtained for PETMP-Br_4.

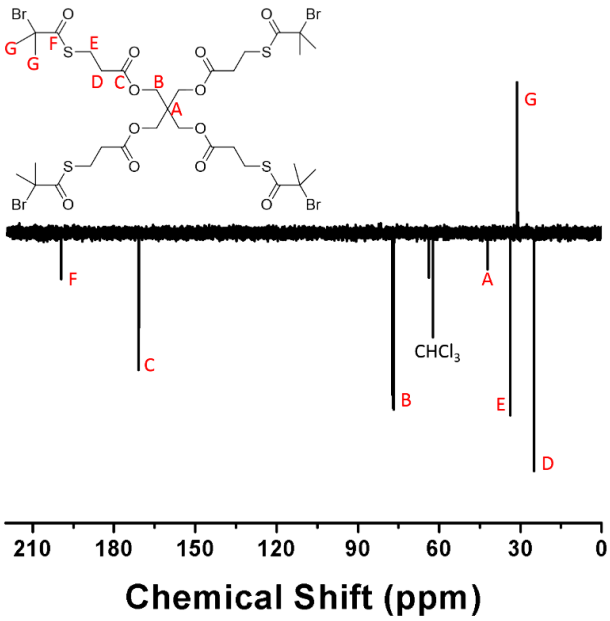

Figure 5.48: ^{13}C NMR spectrum obtained for PETMP-Br_4.

5.4.2.7 General Polymerisation Procedure for Homopolymerisation of ETA with EBiB (P1, P3–P16)

General polymerisation procedure will be exemplified on **P3**. For a typical polymerisation, $CuBr_2$ (0.10 eq., 4.23mg, 18.9 μmol), DMSO (0.88 mL), Me_6TREN (0.19 eq., 9.60 μL, 36.0 μmol), ETA (20.0 eq., 0.44 g, 3.79 mmol) and initiator (1 eq., 27.8 μL, 189 μmol) were added to a Schlenk tube containing a stirrer bar. The Schlenk tube was subsequently sealed with a rubber septum, lowered into an oil bath set to 25 °C and degassed with argon for 30 minutes. At the same time, the copper wire was preactivated in 10 mL HCl (conc. 37%) for 15 minutes, then washed with deionised water and acetone and dried under argon. The activated copper wire was then transferred to the Schlenk tube containing the polymerisation mixture to start the reaction (the addition of the copper wire defines t = 0).

5.4.2.8 Synthesis of star P(ETA) with PEB-Br_4 (P2)

For a typical polymerisation, $CuBr_2$ (0.4 eq.,12.8 mg, 0.04 mmol), DMSO (4.00 mL), Me_6TREN (29.1 μL, 0.11 mmol), ETA (60 eq., 1.00 g, 8.61 mmol), mesitylene (2.5%, *v/v*) and PEB-Br_4 (1.0 eq., 105 mg, 0.14 mmol) were added to a Schlenk tube containing a stirrer bar. The Schlenk tube was subsequently sealed with a rubber septum, lowered into an oil bath set to 25 °C and degassed with argon for 30 minutes. At the same time, the copper wire was preactivated in 10 mL HCl (conc. 37%) for 20 minutes, then washed with deionised water and acetone and dried under argon. The activated copper wire was then transferred to the Schlenk tube containing the polymerisation mixture to start the reaction (the addition of the copper wire defines t=0).

5.4.2.9 General Polymerisation Procedure for Homopolymerisation of EA, DP=10 (P17-P20)

Table 5.9: Overview of the amounts used for the polymerisation of **P17-P20**.

Polymer	EA (g)	EBiB (µL)	Me_6TREN (µL)	Metal halide (mg)	DMSO (mL)
P21	1.00	147	50.7	$CuBr_2$: 22.3	2.00
P22	1.00	147	50.7	$FeBr_2$: 21.5	2.00
P23	1.00	147	50.7	$FeBr_3$: 29.5	2.00
P24	1.00	147	50.7	CuBr: 14.2	2.00

Polymerisation condition: [EA] : [EBiB] : [metal halide]:[Me_6TREN] = 10 : 1 : 0.1 : 0.19.

For a typical polymerisation, metal halide (0.4 eq.), DMSO (1:2 *v*/*v*), Me_6TREN (0.19 eq.), EA (10 eq.), mesitylene (2.5%, *v*/*v*) and EBiB (1.0 eq.) were added to a Schlenk tube containing a stirrer bar. The Schlenk tube was subsequently sealed with a rubber septum, lowered into an oil bath set to 25 °C and degassed with argon for 30 minutes. At the same time, the copper wire was preactivated in 10 mL HCl (conc. 37%) for 20 minutes, then washed with deionised water and acetone and dried under argon. The activated copper wire was then transferred to the Schlenk tube containing the polymerisation mixture to start the reaction (the addition of the copper wire defines t=0).

5.4.2.10 General Polymerisation Procedure for Homopolymerisation of ETA, DP=10 (P21-P24)

Table 5.10: Overview of the amounts used for the polymerisation of **P21-P24**.

Polymer	ETA (g)	EBiB (µL)	Me_6TREN (µL)	Metal halide (mg)	DMSO (mL)
P21	0.44	55.6	19.0	$CuBr_2$: 8.40	0.88
P22	0.88	111	38.0	$FeBr_2$: 16.3	1.76
P23	0.88	111	38.0	$FeBr_3$: 22.3	1.76
P24	0.58	73.3	25.0	CuBr: 7.15	1.16

Polymerisation condition: [ETA]:[EBiB]:[metal halide]:[Me_6TREN] = 10:1:0.1:0.19.

For a typical polymerisation, metal halide (0.4 eq.), DMSO (1:2 *v*/*v*), Me_6TREN (0.19 eq.), ETA (10 eq.), mesitylene (2.5%, *v*/*v*) and EBiB (1.0 eq.) were added to a Schlenk tube containing a stirrer bar. The Schlenk tube was subsequently sealed with a rubber septum, lowered into an oil bath set to 25 °C and degassed with argon for 30 minutes. At the same time, the copper wire was preactivated in 10 mL HCl (conc. 37%) for 20 minutes, then washed with deionised water and acetone and dried under argon. The activated copper wire was then transferred to the Schlenk tube containing the polymerisation mixture to start the reaction (the addition of the copper wire defines t=0).

5.4.2.11 General Polymerisation Procedure for Homopolymerisation of DMA, DP = 10 (P25-P27)

Table 5.11: Overview of the amounts used for the polymerisation of **P25-P27**.

Polymer	DMA (g)	EBiB (µL)	Me_6TREN (µL)	Metal halide (mg)	DMSO (mL)
P25	0.375	55.6	19.0	$CuBr_2$: 8.40	0.74
P26	0.375	55.6	19.0	$FeBr_2$: 8.13	0.74
P27	0.375	55.6	19.0	$FeBr_3$: 11.2	0.74

Polymerisation condition: [DMA]:[EBiB]:[metal halide]:[Me_6TREN] = 10:1:0.1:0.19.

For a typical polymerisation, metal halide (0.4 eq.), DMSO (1:2 *v*/*v*), Me_6TREN (0.19 eq.), DMA (10 eq.), mesitylene (2.5%, *v*/*v*) and EBiB (1.0 eq.) were added to a Schlenk tube containing a stirrer bar. The Schlenk tube was subsequently sealed with a rubber septum, lowered into an oil bath set to 25 °C and degassed with argon for 30 minutes. At the same time, the copper wire was preactivated in 10 mL HCl (conc. 37%) for 20 minutes, then washed with deionised water and acetone and dried under argon. The activated copper wire was then transferred to the Schlenk tube containing the polymerisation mixture to start the reaction (the addition of the copper wire defines t = 0).

5.4.2.12 Chain extension of P(MA) with ETA (P29)

The general procedure for MA homopolymerisation was followed (P48). Upon detection of >99% conversion a 1 : 2 mixture of degassed ETA and DMSO was added to the reaction mixture *via* degassed syringe. Sample was taken after 16 hours and conversions was measured using ^{1}H NMR and GPC analysis.

5.4.2.13 Chain extension of P(MA) with ETA (P30)

The general procedure for MA homopolymerisation was followed (**P48**). Upon detection of >99% conversion a 1 : 2 mixture of degassed ETA and DMSO was added to the reaction mixture *via* degassed syringe. Additional ligand (0.19 eq) and $FeBr_2$ (0.10 eq.) were added to Sample was taken after 16 hours and conversions was measured using ^{1}H NMR and GPC analysis.

5.4.2.14 Chain extension of P(MA) with ETA (P32)

The general procedure for MA (20.0 eq.) homopolymerisation was followed (**P48**). Upon detection of >99% conversion at 140 minutes, a 1 : 2 mixture of degassed ETA (5.00 eq.) and DMSO was added to the reaction mixture *via* degassed syringe. Sample was taken after 16 hours and conversions was measured using ^{1}H NMR and GPC analysis.

5.4.2.15 Chain extension of P(MA) with ETA (P34)

The general procedure for MA (10.0 eq.) homopolymerisation was followed (**P48**). Upon detection of >99% conversion at 100 minutes, a 1 : 2 mixture of degassed ETA (6000 eq.) and DMSO was added to the reaction mixture *via* degassed syringe. Sample was taken after 24 hours and conversions was measured using ^{1}H NMR and GPC analysis.

5.4.2.16 Chain extension of P(ETA) with MA (P36)

The general procedure for ETA (10.0 eq.) homopolymerisation was followed (**P22**). Upon detection of >99% conversion at 360 minutes, a 1 : 2 mixture of degassed MA (60.0 eq.) and DMSO was added to the reaction mixture *via* degassed syringe. Sample was taken after 24 hours and conversions was measured using ^{1}H NMR and GPC analysis.

5.4.2.17 Synthesis of all-acrylic block copolymer (P38)

The general procedure for P(MA_{20}-*b*-ETA_{10}) chain extension was followed (**P30**). Sample was taken after 24 hours and conversions was measured using ^{1}H NMR and GPC analysis. Polymer was purified by dialysis. 475 mg of purified **P37** was added to a vial, 2.00 mL of THF was added. $BzNH_2$, PhSH and TEA were subsequently added and the reaction was stirred for 24 h. The polymer was precipitated in cold H_20/MeOH (1:2). Degree of amidation was measured using ^{1}H NMR and GPC analysis.

Table 5.12: Amidation conditions used to obtain the all acrylic block copolymer **P38**.

	P37	**PhSH**	**$BzNH_2$**	**TEA**	**Solvent**
eq.	1.00	2.00	2.50	2.00	
used	475 mg	270 μL	360 μL	370 μL	2.00 mL

Amidation condition: room temperature.

5.4.2.18 General Polymerisation Procedure for Homopolymerisation of EA, DP=10 (P39-P41)

For a typical polymerisation, $CuBr_2$ (0.1 eq.), DMSO (1:2 *v*/*v*), Me_6TREN (0.19 eq.), EA (10 eq.), mesitylene (2.5%, *v*/*v*) and EBiB (1.0 eq.) were added to a Schlenk tube containing a stirrer bar. The Schlenk tube was subsequently sealed with a rubber septum, lowered into an oil bath set to 25 °C and degassed with argon for 30 minutes. At the same time, the copper wire was preactivated in 10 mL HCl (conc. 37%) for 20 minutes, then washed with deionised water and acetone and dried under argon. The activated copper wire was then transferred to the Schlenk tube containing the polymerisation mixture to start the reaction (the addition of the copper wire defines t=0).

Table 5.13: Overview of the amounts used for the polymerisation of **P39-P41**.

Polymer	EA (g)	Initiator	Initiator (mg)	Me_6TREN (µL)	$CuBr_2$ (mg)	DMSO (mL)
P39	1.00	PhBiB	242	50.7	22.3	2.00
P40	1.00	PhNHBiB	241	50.7	22.3	2.00
P41	1.00	PhS-BiB	259	50.7	22.3	2.00

Polymerisation condition: [EA] : [I] : [$CuBr_2$]:[Me_6TREN] = 10 : 1 : 0.1 : 0.19 with 4 cm Cu(0)wire at 25 °C.

5.4.2.19 Homopolymerisation of MA (P51)

For a typical polymerisation, $CuBr_2$ (0.1 eq.,16.8 mg, 0.07 mmol), DMSO (1.30 mL), Me_6TREN (0.19 eq., 38.4 µL, 16.1 mmol), DMA (20 eq., 0.652 g, 7.58 mmol), mesitylene (2.5%, *v/v*) and EBiB (1.0 eq., 111 µL, 0.38 mmol) were added to a Schlenk tube containing a stirrer bar. The Schlenk tube was subsequently sealed with a rubber septum, lowered into an oil bath set to 25 °C and degassed with argon for 30 minutes. At the same time, the copper wire was preactivated in 10 mL HCl (conc. 37%) for 20 minutes, then washed with deionised water and acetone and dried under argon. The activated copper wire was then transferred to the Schlenk tube containing the polymerisation mixture to start the reaction (the addition of the copper wire defines t = 0).

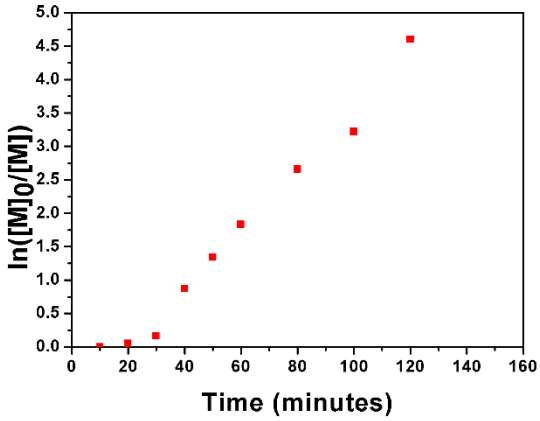

Figure 5.49: First order kinetic plot for the polymerisation of MA **(P51).**

5.4.2.20 Homopolymerisation of MA (P52)

For a typical polymerisation, $FeBr_2$ (0.1 eq.,16.3 mg, 0.07 mmol), DMSO (1.30 mL), Me_6TREN (0.19 eq., 38.4 µL, 16.1 mmol), MA (20 eq., 0.652 g, 7.58 mmol), mesitylene (2.5%, v/v) and EBiB (1.0 eq., 111 µL, 0.38 mmol) were added to a Schlenk tube containing a stirrer bar. The Schlenk tube was subsequently sealed with a rubber septum, lowered into an oil bath set to 25 °C and degassed with argon for 30 minutes. At the same time, the copper wire was preactivated in 10 mL HCl (conc. 37%) for 20 minutes, then washed with deionised water and acetone and dried under argon. The activated copper wire was then transferred to the Schlenk tube containing the polymerisation mixture to start the reaction (the addition of the copper wire defines t = 0).

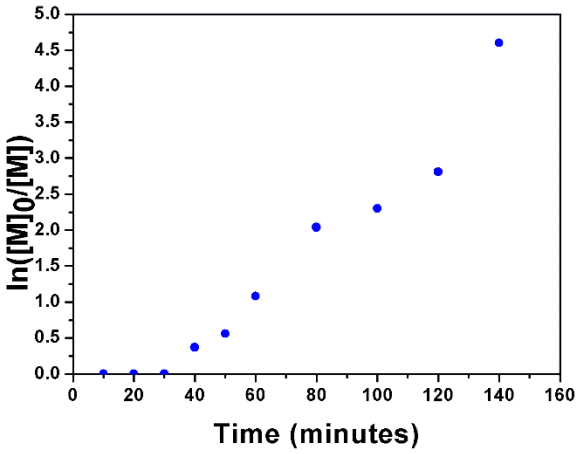

Figure 5.50: First order kinetic plot for the polymerisation of MA **(P52).**

5.5 References

1. V. Percec, T. Guliashvili, J. S. Ladislaw, A. Wistrand, A. Stjerndahl, M. J. Sienkowska, M. J. Monteiro and S. Sahoo, *J. Am. Chem. Soc.*, 2006, **128**, 14156-14165.
2. Q. Zhang, P. Wilson, Z. Li, R. McHale, J. Godfrey, A. Anastasaki, C. Waldron and D. M. Haddleton, *J. Am. Chem. Soc.*, 2013, **135**, 7355.
3. A. Anastasaki, V. Nikolaou, G. Nurumbetov, P. Wilson, K. Kempe, J. F. Quinn, T. P. Davis, M. R. Whittaker and D. M. Haddleton, *Chem. Rev.*, 2016, **116**, 835-877.
4. R. Aksakal, M. Resmini and C. R. Becer, *Polym. Chem.*, 2016, **7**, 171-175.
5. S. Aksakal and C. Remzi Becer, *Polym. Chem.*, 2016, **7**, 7011-7018.
6. J. Mosnáček and M. Ilčíková, *Macromolecules*, 2012, **45**, 5859-5865.
7. V. Darcos, S. Monge and D. M. Haddleton, *J. Polym. Sci. A.*, 2004, **42**, 4933-4940.
8. C. A. Bell, M. R. Whittaker, L. R. Gahan and M. J. Monteiro, *J. Polym. Sci. A.*, 2008, **46**, 146-154.
9. S. R. Samanta, M. E. Levere and V. Percec, *Polym. Chem.*, 2013, **4**, 3212-3224.
10. S. R. Samanta, R. Cai and V. Percec, *Polym. Chem.*, 2014, **5**, 5479-5491.
11. N. Bensabeh, J. C. Ronda, M. Galià, V. Cádiz, G. Lligadas and V. Percec, *Biomacromolecules*, 2018, **19**, 1256-1268.
12. R. Aksakal, M. Resmini and C. R. Becer, *Polym. Chem.*, 2016, **7**, 6564.
13. K. Matyjaszewski, H.-j. Paik, P. Zhou and S. J. Diamanti, *Macromolecules*, 2001, **34**, 5125-5131.
14. G. Singh, S. Rani, A. Saroa, S. Girdhar, J. Singh, A. Arora, D. Aulakh and M. Wriedt, *RSC Advances*, 2015, **5**, 65963-65974.
15. A. H. R. Al-Daraji and I. H. R. Tomi, *Polymer-Plastics Technology and Engineering*, 2012, **51**, 1327-1333.
16. G. Gody, T. Maschmeyer, P. B. Zetterlund and S. Perrier, *Macromolecules*, 2014, **47**, 3451-3460.
17. J. T. Rademacher, M. Baum, M. E. Pallack, W. J. Brittain and W. J. Simonsick, *Macromolecules*, 2000, **33**, 284-288.
18. K. Matyjaszewski, *Macromolecules*, 2012, **45**, 4015-4039.
19. S. Aksakal, R. Aksakal and C. R. Becer, *Polym. Chem.*, 2018, **9**, 4507-4516.
20. T. R. Barlow, J. C. Brendel and S. Perrier, *Macromolecules*, 2016, **49**, 6203-6212.
21. J. O. Holloway, S. Aksakal, F. E. Du Prez and C. R. Becer, *Macromol. Rapid Commun.*, 2017, **38**, 1700500.
22. Y. Gao, T. Zhao, D. Zhou, U. Greiser and W. Wang, *Chem. Commun.*, 2015, **51**, 14435-14438.
23. S. Harrisson, P. Couvreur and J. Nicolas, *Macromolecules*, 2012, **45**, 7388-7396.
24. H. M. Burke, L. McSweeney and E. M. Scanlan, *Nat. Commun.*, 2017, **8**, 15655.
25. R. Aksakal, M. Resmini and C. R. Becer, *Polym. Chem.*, 2016, **7**, 6564-6569.

Chapter 6

6 Tailored modification of thioacrylates in a versatile, sequence-defined procedure

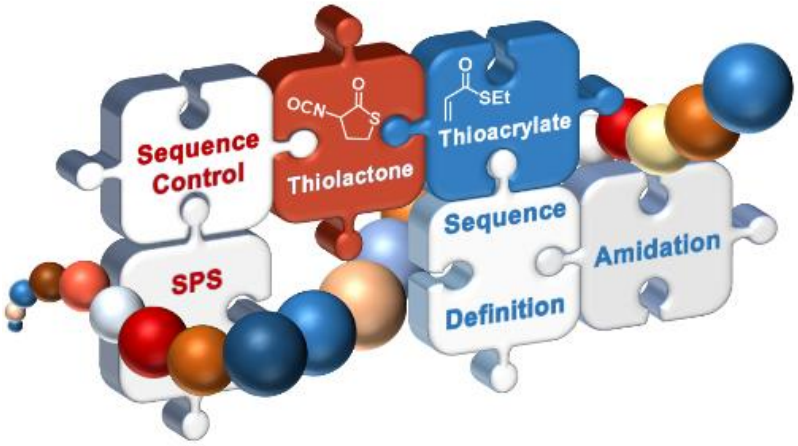

We herein report a strategy for the synthesis of sequence-defined oligomers using a selective side group insertion approach making use of thiophenol catalysed amidation reactions. In this context, a new thiolactone-based, multi-step, iterative protocol was designed utilising thioacrylates in combination with solid-phase synthesis for step-by-step growth, resulting in sequence-defined oligomers. Sequence definition and structure variation was introduced by substituting the thioacrylate side groups with a wide variety of amines. The step-by-step growth of the oligomers was followed closely by Liquid Chromatography Mass Spectroscopy (LCMS) and High Resolution Mass Spectroscopy (HRMS) to determine both conversion and purity.

Parts of this chapter have been published;

J. O. Holloway, S. Aksakal, F. E. Du Prez, C.R. Becer, *Macromol. Rapid Commun*., 2017, **38**, 1700500

6.1 Introduction

The field of polymer chemistry has grown exponentially in recent decades, yielding macromolecules of unprecedented structure and design for wide-ranging applications, most notably through recent advances in controlled polymerisations and click chemistry approaches.[1-4] However, when it comes to complete structural control over the sequenced order in which the monomers are placed, Nature is way ahead of current synthetic materials.[5, 6] However, scientists are now experiencing an evolution in synthetic macromolecules that takes inspiration from Nature, resulting in tailor-made, complex architectures, with precise control over the monomeric sequence, as was previously only witnessed in bio-polymers such as DNA.[7-12] This has led to the development of the field of sequence-defined macromolecular synthesis. This tailoring of macromolecules on a molecular level is enabled through a series of highly efficient and selective reactions,[12] mostly based on unique, biologically relevant, organic chemical reactions such as amide bond formation[13], thiol-thioester exchange[14] and disulfide formation[15]. There are numerous recent examples of biomimetic, synthetic approaches such as molecular knots, which can be found in DNA strands or the synthesis of molecular machines, which resulted in the 2016 Nobel Prize in chemistry, that mimic ribosome.[16, 17]

Since its introduction in 2001,[18] "click" chemistry has become a powerful tool across many branches of synthetic chemistry and whilst it has become one of the most established reactions in polymer science,[4, 5, 19, 20] it is through this technique that many sequence-defined, synthetic approaches have arisen.[9-11, 21-26] One of the methods towards sequence-defined synthesis and tailored functionalisation of monodisperse oligomers is a thiolactone-based chemical approach[10, 21] using a solid-phase, Merrifield-inspired synthesis.[27] The promising versatility of the aforementioned method is achieved by introduction of highly efficient, iterative reactions to create a multi-step, protecting group-free, synthetic cycle.

First, aminolysis of the thiolactone moiety and a subsequent *Michael* addition of the in-situ generated thiol to the double bond of an acrylic compound occurs in a one-pot fashion. Then, re-introduction of the thiolactone group was, after a series of observations, the most effective and precise method to continue the synthetic cycle.

Previously reported approaches resulted in an elegant incorporation of a diverse range of side-groups with impressive oligomeric length and purity of structures.[10]
However, the previous use of acrylics in this synthetic cycle was limited to acrylates and a small number of acrylamides, so the aim was the expansion of the monomeric toolbox with the use of promising sulfur analogues, also known as thioacrylates (TA), to unleash new potential applications.[28] This class of acrylics has already been described as a useful candidate for reversible-deactivation radical polymerisations, which enables various post-polymerisation functionalisations, while these reactions were previously restricted to only specific acrylates (e.g. activated esters).

Within this chapter, a redesigned synthesis strategy of a thiolactone-based protocol which includes a thioacrylate for further side chain functionalisation is presented. The functionalisation was studied for different primary amines resulting in the corresponding amide structures in the side chain, thus mimicking an acrylamide which could not be used before.

6.2 Results and Discussion

6.2.1 Initial attempts for the incorporation of ethyl thioacrylate in a protocol from literature (1)

The substitution of ethyl acrylate (EA) with ethyl thioacrylate (ETA) in a thiolactone-based protocol for the synthesis of multifunctional sequence-defined oligomers from the literature[10] was investigated. Thioacrylate was necessary in order to modify the thioester with a range of amines *via* an amidation reaction. A polystyrene resin, funcionalised with thiolactone (TLa) was reacted with ethanolamine and ETA, to open the thiolactone and the released thiol subsequently react with the thioacrylate through a nucleophilic thiol-ene reaction. This was carried out two times for 15 minutes (**Scheme 6.1**).

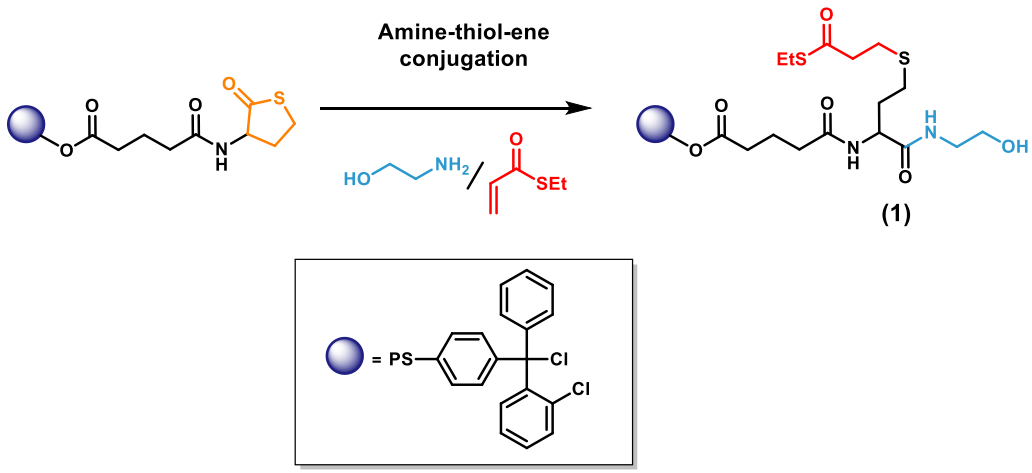

Scheme 6.1: Amine-thiol-ene conjugation of the thiolactone with ethanolamine and ETA in a one-pot reaction.

LC –ESI-MS was recorded to verify sample purity and a successful incorporation of the ETA. However, the LC chromatogram of the reaction mixture (**Scheme 6.1**) displayed five peaks instead of one peak; peak (**III**) with a retention time of 3.7 minutes corresponds with the expected product **1**. A small impurity peak (**V**) is also be observable at 4.8 minutes in the present LCMS but also appears in most LCMS chromatograms below. This is the result of an impurity from the column, with a mass of 278 g/mol (shown in **Figure 6.51**). The peak **I** with a retention time of 1.1 minutes can be attributed to the injection peak itself. When a LCMS of acetonitrile with no compound dissolved inside was measured at a wavelength of 214 nm, this peak was

already observed (**Figure 6.50**). The peak **II** with a retention time of 2.7 minutes agrees with the mass of the starting material. Peak **VI** could not further identified but probably represents the product from a side reaction. While the first reaction indicated unreacted starting material, the protocol was further modified for this to react for 18 hours. However, no better results were obtained with this adjustment as unreacted thiolactone was still very evident in the LCMS.

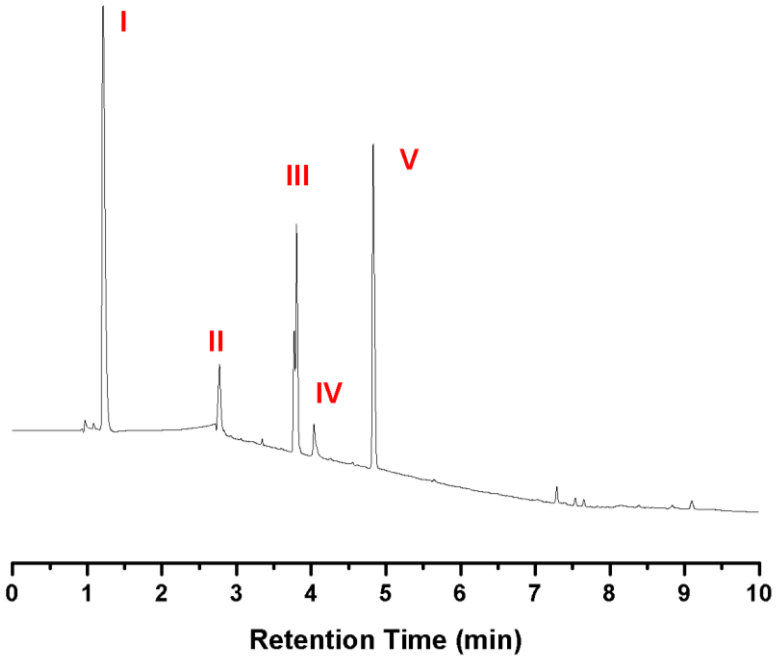

Figure 6.1: LCMS chromatogram at λ = 214 nm showing the progress of the one-pot reaction of **1**.

A closer investigation was necessary to identify the interference factor for this reaction. The two parameters that have been changed to the previously reported procedure was the monomer itself and instead of the hydroxyl-functionalised thiolactone linker, a carboxylic acid-functionalised linker was used.

In order to identify any interference of the ETA with the ethanolamine, the compatibility of ethylthioacrylate and ethanolamine was studied and followed by ^{1}H NMR.

For this analysis a nonfunctional amine and ETA were diluted in chloroform and transferred to a NMR tube and a spectrum was recorded every 6 mins for 2 hours, while spinning in the instrument. The same reaction was followed but using ethyl acrylate and is depicted below in **Figure 6.2**.

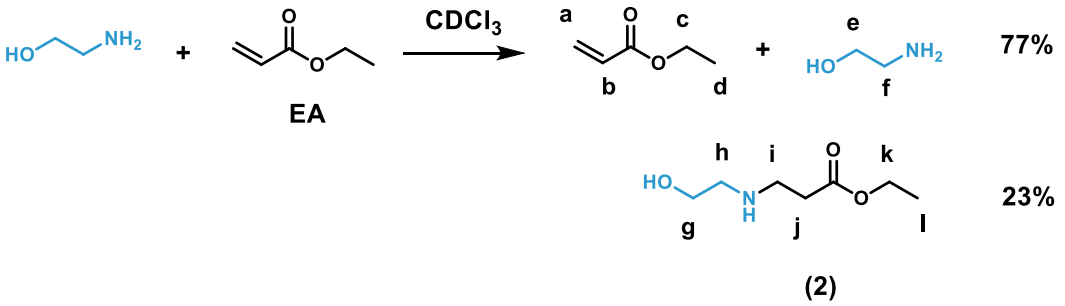

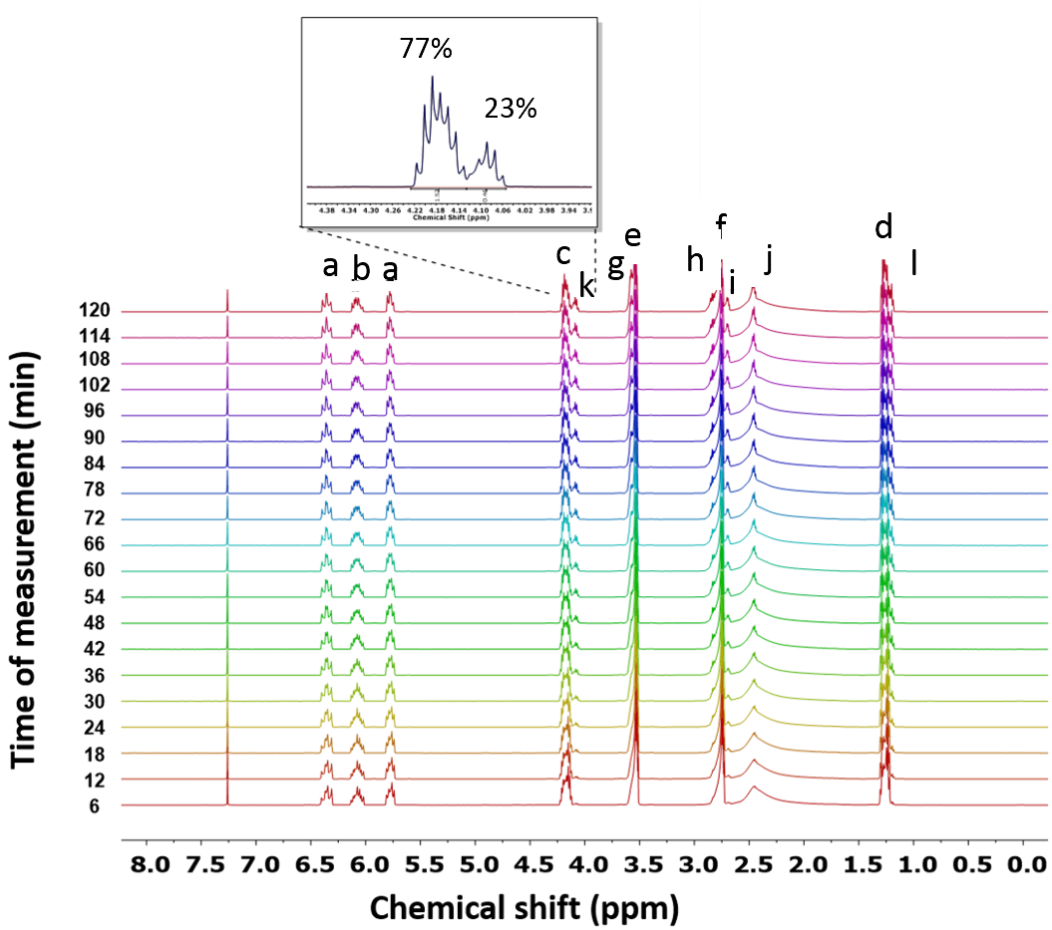

Figure 6.2: ^{1}H NMR spectra recorded every 6 minutes to compare the reactivity of ethanolamine with EA.

Whereas the reaction with EA showed little interaction of the acrylate functionality with the primary amine, the reaction with ETA revealed an aza-*Michael* reaction of the double bond and the primary amine **3**. Additionally, reaction between the ethanolamine and ethyl thioacrylate was very rapid and was complete within 18 minutes (as demonstrated by the rapid disappearance of the acrylic protons in **Figure 6.3**, thus illustrating why thiolactone aminolysis was ineffective when both molecules were present.

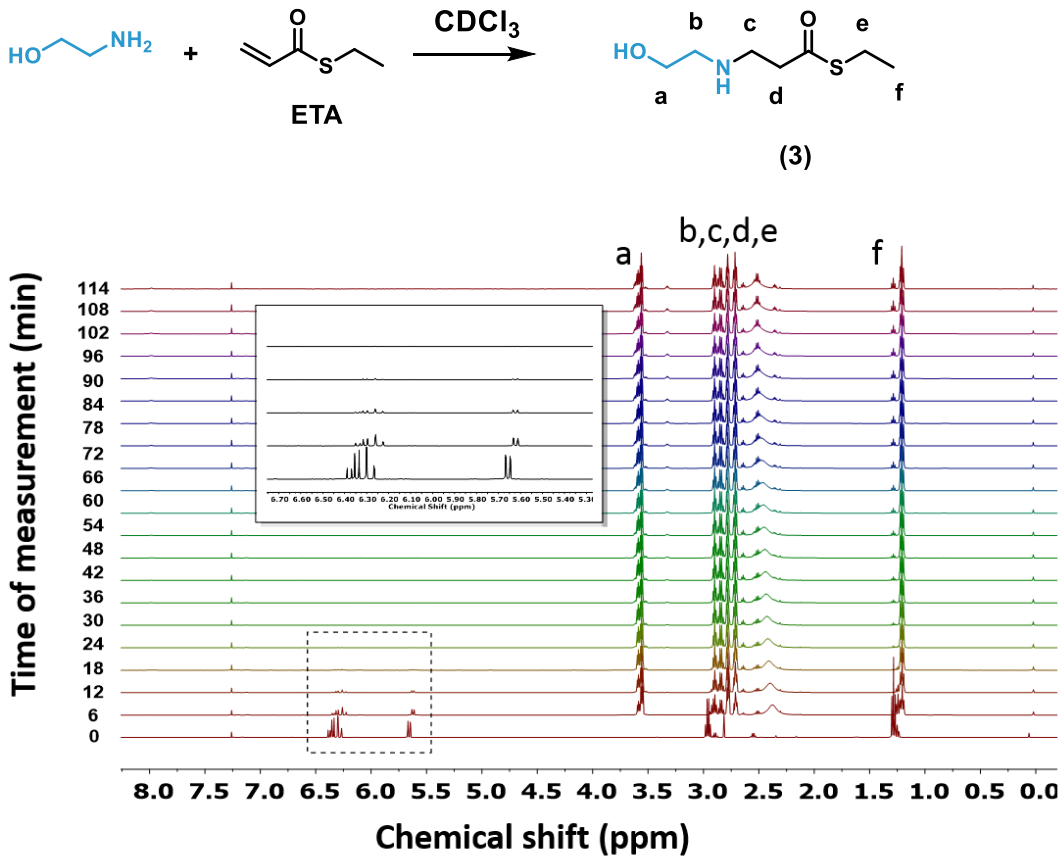

Figure 6.3: ^{1}H NMR spectra recorded every 6 minutes to compare the reactivity of ethanolamine with ETA.

6.2.2 Thioacrylate based iterative protocol: Aminolysis (4)

Therefore,the use of thioacrylates required a new protocol to be designed, somewhat combining previously reported approaches to enable us to harness the advantages of using these acrylics as a *Michael* acceptor in a thiolactone based, sequence-defined protocol. The first step of the four-step protocol consists of the reaction between the thiolactone group, attached to a solid phase, with ethanolamine. While the amine function is known to react in a chemoselective way with a thiolactone unit,[29] the alcohol function serves in the last, (*i.e.*, fourth step) as a functional handle to react with α-thiolactone-γ-isocyanate at the end of the cycle.

The side reaction was overcome by carrying out the aminolysis and *Michael* addition steps separately. In order to prevent disulfide bond formation from the newly released thiol moieties of thiolactone aminolysis, two equivalents of dimethylphenylphosphine (DMPP) were added to reduce the disulfide bonds as they formed (**Scheme 6.1**).

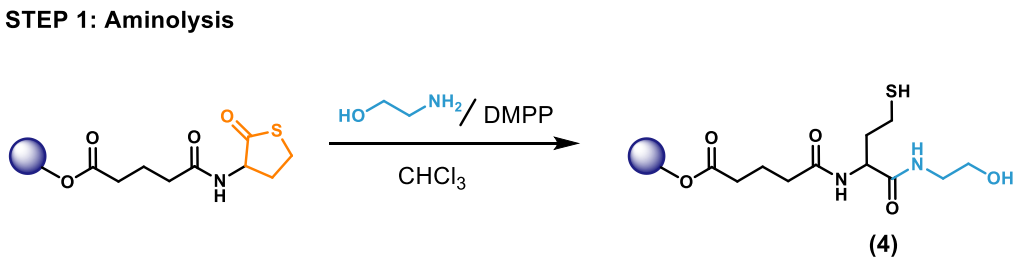

Scheme 6.2: Reaction scheme of the investigated nucleophilic opening of the thiolactone (aminolysis) while DMPP was present to prevent disulfide formation.

As it was observed that DMPP also catalysed the reaction between the ETA and alcohol group of the applied ethanolamine, it was not possible to first carry out aminolysis, followed by addition of ETA and DMPP to both reduce the disulfide bonds and catalyse the thiol-*Michael* addition. On the other hand, the addition of DMPP with the aminolysis caused no further problems, in terms of undesired side products or side reactions, which were a concern when compared with another previously reported approach.[21] The process was followed every hour by LCMS for a period of three hours. However, no observable change was seen by LCMS in this experiment (**Figure 6.48**). It was difficult to quantitatively follow the kinetics because the retention time of the thiol-containing product, or possible unwanted disulphide side-product, have retention times which coincide with the solvent injection peak, present in all LC chromatograms measure on this instrument (see **Figure 6.50**).

The MS spectra of the main peak in **Figure 6.4** indicated the presence of the desired thiol product along with disulfide side-product, but the quantity present, in percentage terms, was unclear as MS itself is not a quantitative technique, and a small presence can still ionise very easily and thus be visible in the ESI-MS spectra despite being barely present in reality.

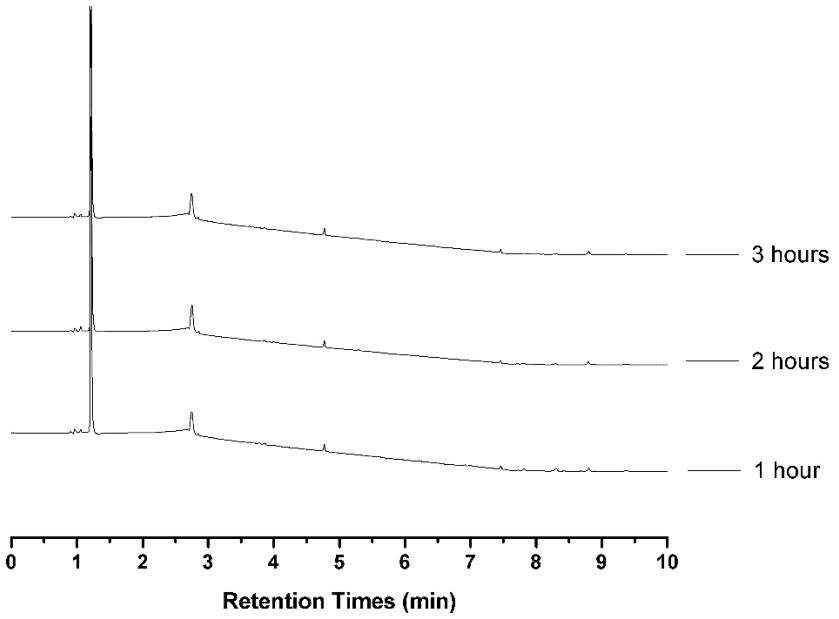

Figure 6.4: LCMS chromatogram at $\lambda = 214$ nm showing the progress of the aminolysis of thiolactone with ethanolamine (in the presence of DMPP to prevent disulphide bond formation) over 3 hours.

Nonetheless, subsequent reactions to synthesise functional monomers and oligomers, showed no obvious side reaction or unwanted by-product from this step. The LCMS showed no change over 3 hours (see **Figure 6.4**), so 4 hours was selected as the suitable reaction duration to be sure of completion.

6.2.3 Thioacrylate based iterative protocol: Thiol-*Michael* addition (5)

As such, the free thiol was able to undergo subsequent *Michael* addition in the following step with ETA. *N,N'*-dimethylformamide (DMF) was selected as the reaction solvent as it provided a perfect combination of being a good swelling solvent for the solid phase resin[30] and is also a highly polar solvent, which can assist the speed of the *Michael* addition.[31]

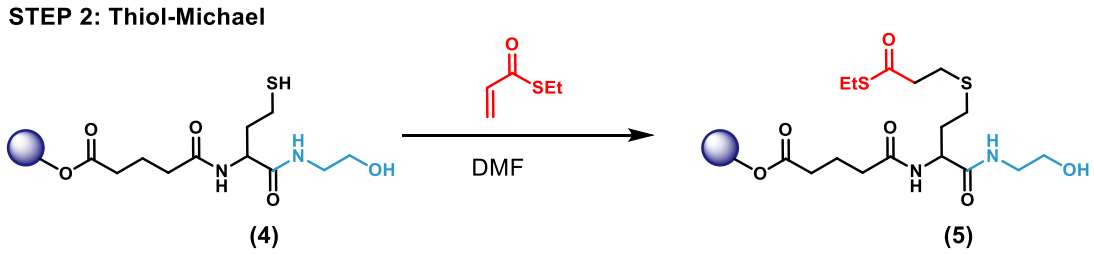

Scheme 6.3: General concept of the investigated Thiol-*Michael* reaction of **4** with ETA.

Ring opening of the thiolactone by aminolysis and subsequent thiol-ene reaction with ethyl thioacrylate (ETA) allowed the introduction of the thioacrylate moieties. Again, the kinetics shown in **Figure 6.5** display no apparent change in the reaction over the period of 4 hours. The double peak at retention time of 3.75 minutes is that of the desired product, initially indicating that it is formed within the first hour.

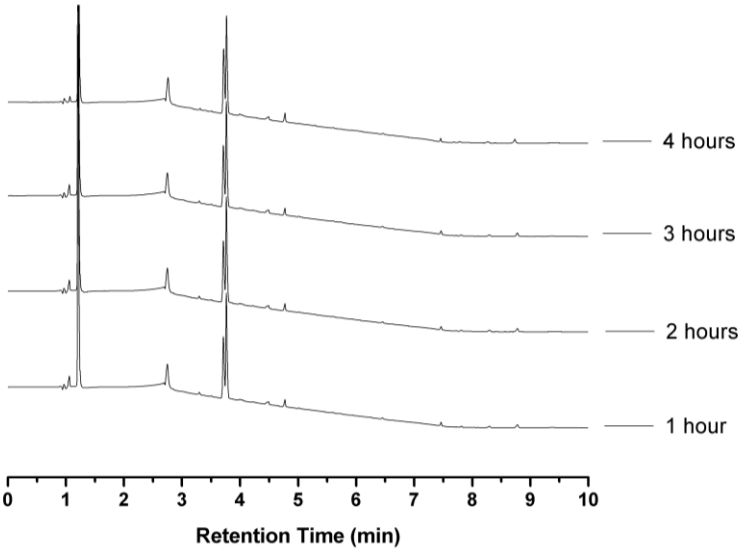

Figure 6.5: LCMS chromatogram at λ = 214 nm following the kinetics of the thiol *Michael* addition of ethyl thioacrylate over 4 hours.

However, the thiol containing precursor or the possible disulfide side-product from Step 1 are, as described above, difficult to distinguish from the injection peak as a result of similar retention times, thus making it difficult to be sure of when complete reaction of the thiol-*Michael* addition occurs. However, leaving this reaction for 4 hours, seemed to yield no obvious side reactions or problems as sequences were synthesised. Thus indicating that the *Michael* addition reaction is complete within this time frame.

6.2.4 Thioacrylate based iterative protocol: Model study for amidation (7)

To confirm the occurrence of the amidation reaction between a thioester containing moiety and a primary amine, NMR and GC measurements of both starting material (thiol) and amidation products were carried out before and after amidation with butylamine, both in the absence of and presence of thiophenol as a catalyst.

The use of ethyl thioacrylate (step 2, **Scheme 6.3**) enabled us to introduce side groups, as desired, from primary amines using a thiophenol catalysed amidation reaction of the thioester functional group.[32] **Figure 6.6** demonstrates how the addition of thiophenol rapidly increased the kinetics of the amidation of a thioester moiety in the side chain of the sequence, thus allowing for this tailored modification of the side chain. It should be noted that the ^{1}H NMR model study between *S*-ethyl thioacetate (**6**) and butylamine was performed at 20 Hz continual spinning within the NMR instrument and results in a faster reaction in comparison to a non-spinning reaction.

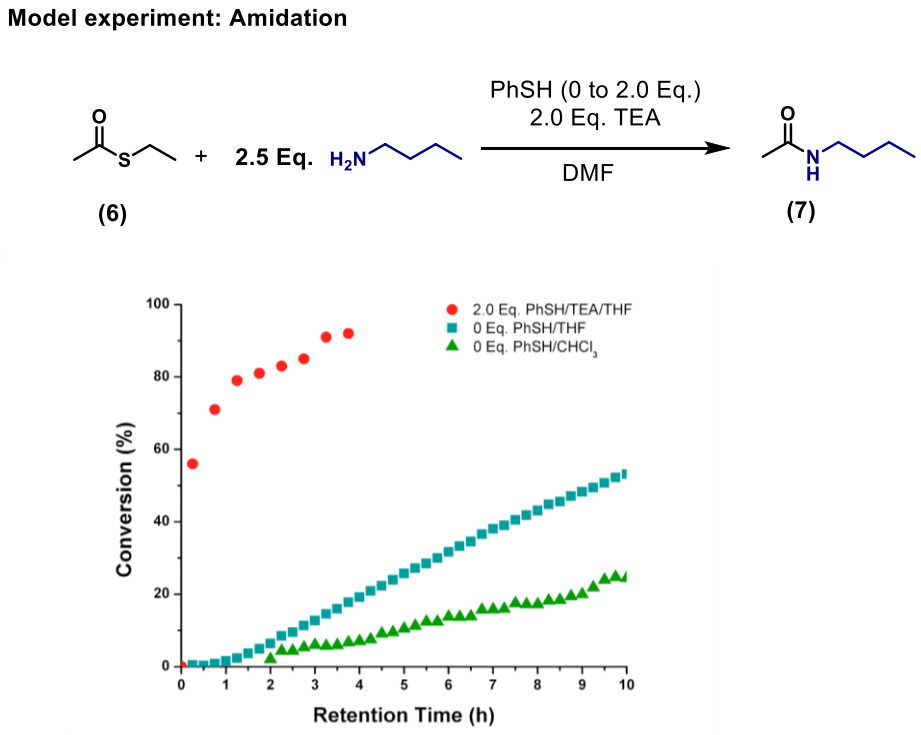

Figure 6.6: Graph showing the influence of thiophenol on catalysing the amidation reaction between a primary amine (butylamine) and a thioester containing moiety (**6**). The non-catalysed reaction was followed by ^{1}H NMR every six minutes with a sample spin of 20 Hz, whereas the thiophenol catalysed reaction was carried out in a Schlenk tube, equipped with a magnetic stirring bar. In this case, the chemical process was followed by recording ^{1}H NMR, GC and GC-MS every 30 minutes.

Therefore, through a thiophenol-catalysed amidation reaction, it was possible to substitute the thioacrylate side group with any chosen primary amine, resulting in the corresponding amide structure (**7**). The amidation reaction of the thioester moiety has opened the possibility to introduce many side-chain functionalities. The limited acrylamide library that can be utilised to also result in such amide structure can, therefore, be overcome and mimicked by using the respective primary amine, which are already commercially available in a broad variety and mostly at relatively low cost, to achieve complete sequence-control of the monomeric order.

6.2.5 Thioacrylate based iterative protocol: Amidation on Solid Phase (8)

Encouraged by the successful model studies, the thiophenol catalysed amidation was applied on solid phase (**Scheme 6.4**) with a ten-fold excess of all compounds and the reaction kinetics were better followed by LCMS as shown below in **Figure 6.7**. Benzylamine was used as it gives agreeable slow rates of reaction with thiolactone aminolysis compared to, for example, aliphatic amines.[33]

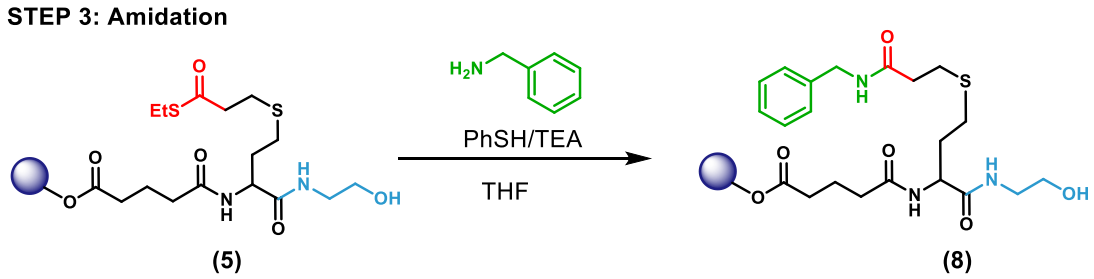

Scheme 6.4: General concept of the investigated thiophenol-catalysed amidation of **5** with benzylamine.

Benzylamine also reacted within a reasonable time frame in this kinetic study (within 6 hours), and therefore it was assumed (correctly) that other amines, with similar or faster reaction rates would fit this kinetic profile too as the primary amine chosen will determine the rate of reaction. For the kinetic study, a sample was analysed from the solid-phase reaction every 2 hours by LCMS analysis.

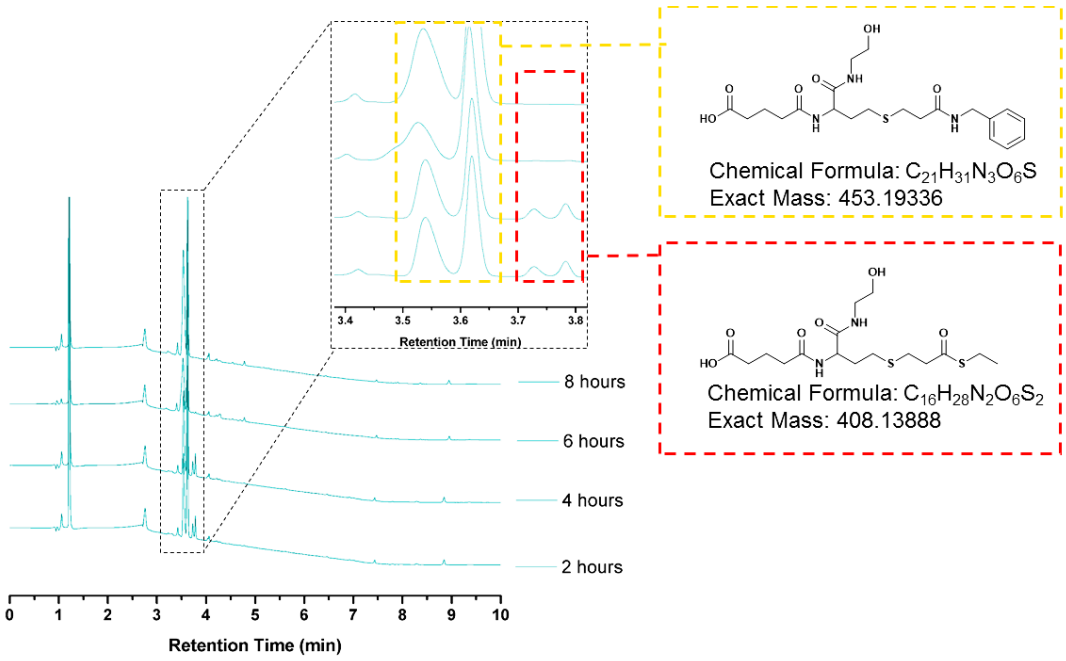

Figure 6.7: LCMS chromatogram at $\lambda = 214$ nm showing the kinetics of the thiophenol catalysed amidation reaction with benzylamine over 8 hours. The thioether moiety can be seen to be fully amidated after 6 hours.

LCMS analysis revealed two peaks, corresponding with masses of 408 g/mol and 453 g/mol of the starting material (**5**) and the forming amide product (**8**) respectively. The process of the thiophenol-catalysed amidation was followed by comparing the peak of **5** with product **8** every two hours for a period of 8 hours. From the analysis, it was clear that, when using 25.0 equivalents of amine and 20.0 equivalents of ETA, the reaction was finished within 6 hours, evident by the decrease and disappearance of the peak with the mass of 408 g/mol. The conditions were applied to further reactions with different amines, where the reaction was also shaken for at least 6 hours.

6.2.6 Thioacrylate based iterative protocol: Chain Extension (9)

In the next step, chain extension was performed *via* the reaction of α-thiolactone-γ-isocyanate (**Scheme 6.11**, **Figure 6.47**) with the remaining alcohol function (STEP 4, **Scheme 6.5**) with a catalytic amount of dibutyltin dilaurate (DBTL) and was shaken vigorously at room temperature for at least 1 hour. The kinetics were previously reported[34] and therefore the same conditions were applied and the resulting product **9** was analysed *via* LCMS, ^{1}H NMR and ^{13}C NMR.

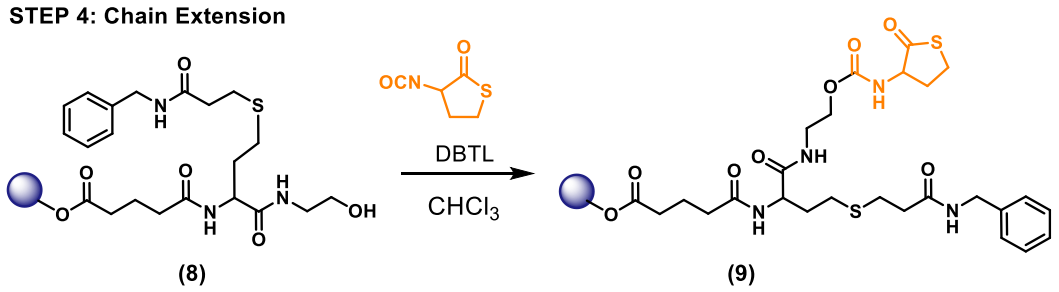

Scheme 6.5: General concept of the investigated chain extension of **8** with α-thiolactone-γ-isocyanate.

Only one peak was visible in the LCMS (**Figure 6.8**) with a mass of 596 /mol, corresponding to the successful chain extension products of **8**. It is worth noting that the molecules synthesised on the resin were cleaved from this support using 1% TFA solution. It is thought that this can lead to a slight oxidation of one of the thioether bonds in the structure, resulting in a small side peak to the left of the main peak in the LCMS spectrum, as seen below in **Figure 6.8** on the left with a mass of 612 g/mol.

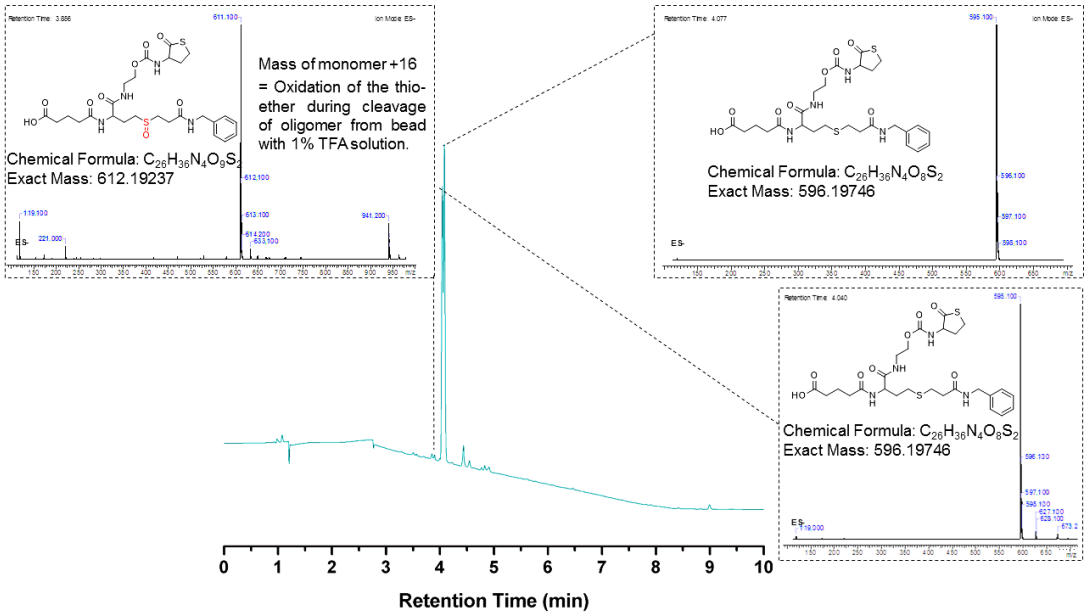

Figure 6.8: LCMS chromatogram at λ = 214 nm of the chain extension (**9**). HRMS (ESI) *m/z*: $[M + H]^+$ calculated for $C_{26}H_{36}N_4O_8S_2$, 597.1975; found, 597.2058.

Figure 6.9 shows the ^{1}H NMR spectrum of compound 9. Spectral assignment for all proton and carbon peaks are presented in **Section 6.4.3.10.1**.

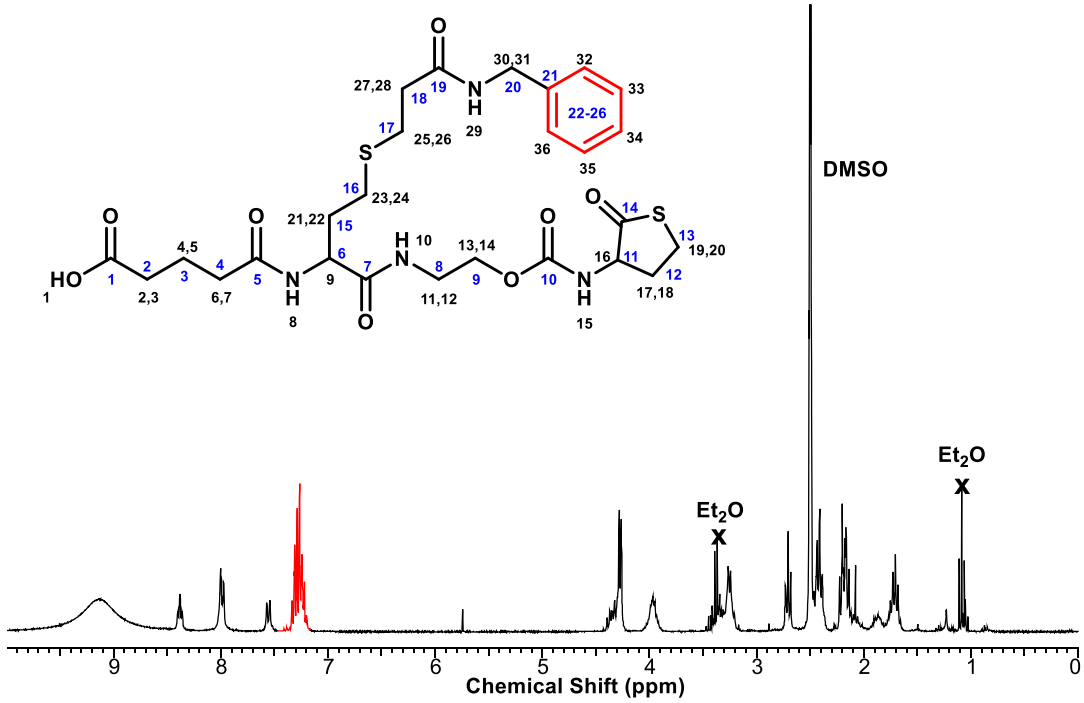

Figure 6.9: ^{1}H NMR of benzylamine containing monomer highlighting the functional side group.

In the downfield region (7-7.5 ppm) of the proton spectrum, six H-resonances corresponding to the aromatic protons of the phenyl ($H_{32\text{-}36}$) were found, highlighted in red. The aromatic group was also found in the ^{13}C NMR in the typical region at 126.76 ppm for C22-26. A full assignment can be found in **Section 6.4.3.10.1.**

6.2.7 Thioacrylate based iterative protocol: Different Amines

As the amidation with benzylamine proved to be successful in the synthesis for a monomer, a range of amines with other functional groups (*e.g.* furan, naphtyl and morpholino) were introduced to allow further extension of the scope of the methodology (**Figure 6.10**). All purified monomers were analysed by LCMS (ESI), NMR (^{1}H and ^{13}C) and a few are discussed below in more detail in **Section 6.4.3.10**. The first two peaks in each LCMS chromatogram, with retention times 1.2 minutes and 2.8 minutes are a result of the solvent injection into the column and so can be considered artifacts of the LCMS and not an impurity, as shown below in **Figure 6.50**. They can be seen more clearly on the LC-chromatograms of higher wavelengths. A small impurity peak is also observable at 4.8 minutes in most LCMS chromatograms.

This is the result of an impurity from the column, with a mass of 278 g/mol, as shown below in **Figure 6.51**

It can be seen in the LCMS chromatograms mentioned below that, along with the principle desired product peak in the LC-chromatogram (214 nm), a smaller side peak is visible with the mass of the product +16 g/mol. It is believed that this is a result of an oxidation of one of the thioether bonds as a result of the mildly acidic resin cleavage conditions of 1 % TFA. As this occurs when the molecule is cleaved from the solid-phase resin, it can be seen as a side-effect of the cleavage and not an impurity within the synthesis. It could be controlled, in principle, by further reducing the cleavage time or concentration of TFA or by cleaving in inert conditions.[35]

All products were also fully characterised by ^{1}H and ^{13}C NMR techniques, aided with COSY, HSQC and HMBC. It can be noted that there is a large, broad, shifting resonance in the ^{1}H NMR spectra below, most probably a result of exchange between the carboxylic acid proton and the water in the DMSO-d_6 and some residual TFA.

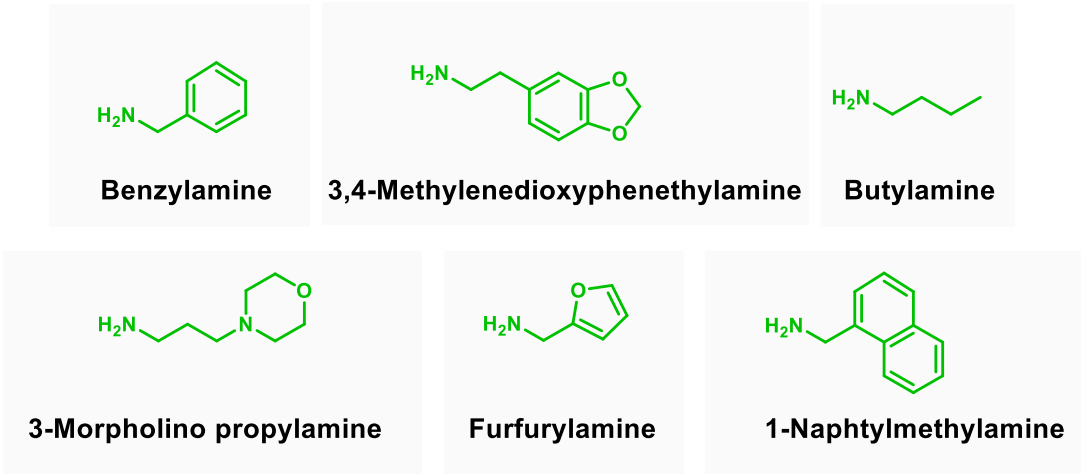

Figure 6.10: Overview of different amines used in this chapter, illustrating the diversity of structures that have been used in this protocol.

6.2.7.1 Thioacrylate based iterative protocol: Butylamine (10)

An aliphatic amine was also been used for the amidation step (**Scheme 6.6**) and results of the LCMS and ^{1}H NMR analysis can be found below in **Figure 6.11** and **Figure 6.12**. In the same manner, **5** was reacted with butylamine, washed and then reacted with α-thiolactone-γ-isocyanate to complete the first cycle.

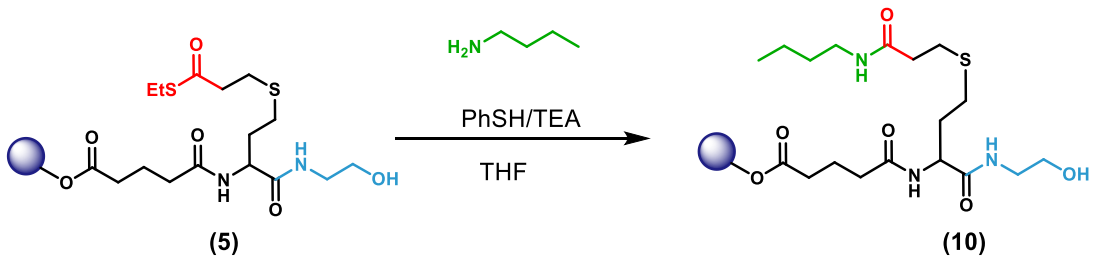

Scheme 6.6: The thiophenol-catalysed amidation of (**5**) with butylamine.

A major peak with the mass of 562 g/mol is present in the LCMS, corresponding to **10**. The oxidation product of this compound can also be found, due to the TFA cleavage.

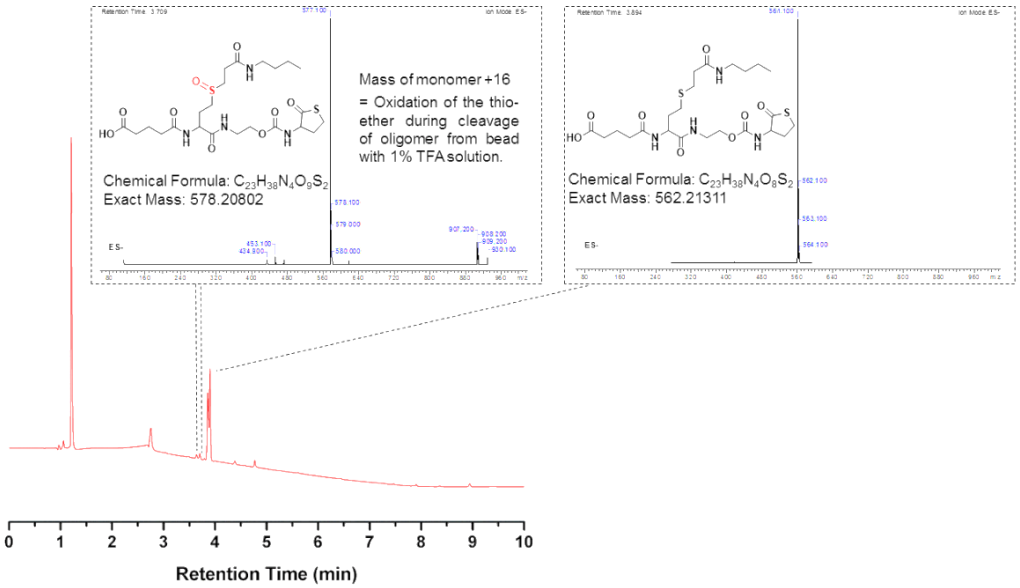

Figure 6.11: LCMS chromatogram at λ = 214 nm of monomer, with butylamine used in the amidation step. HRMS (ESI) *m/z*: $[M + H]^+$ calculated for $C_{23}H_{38}N_4O_8S_2$, 563.2131; found, 563.2220 of 10 after chain extension.

In the ^1H NMR below (**Figure 6.12**), the methylene resonance for $H_{36\text{-}38}$ were found as triplet signals at 0.86 ppm with a coupling constant of 7.1 Hz, supporting the assignment next to an ethylene group from the aliphatic group. Additionally, in the ^{13}C NMR the carbon of the methyl group C_{23} appears in a typical range for methyl groups between 10-15 ppm, at 13.96 ppm.

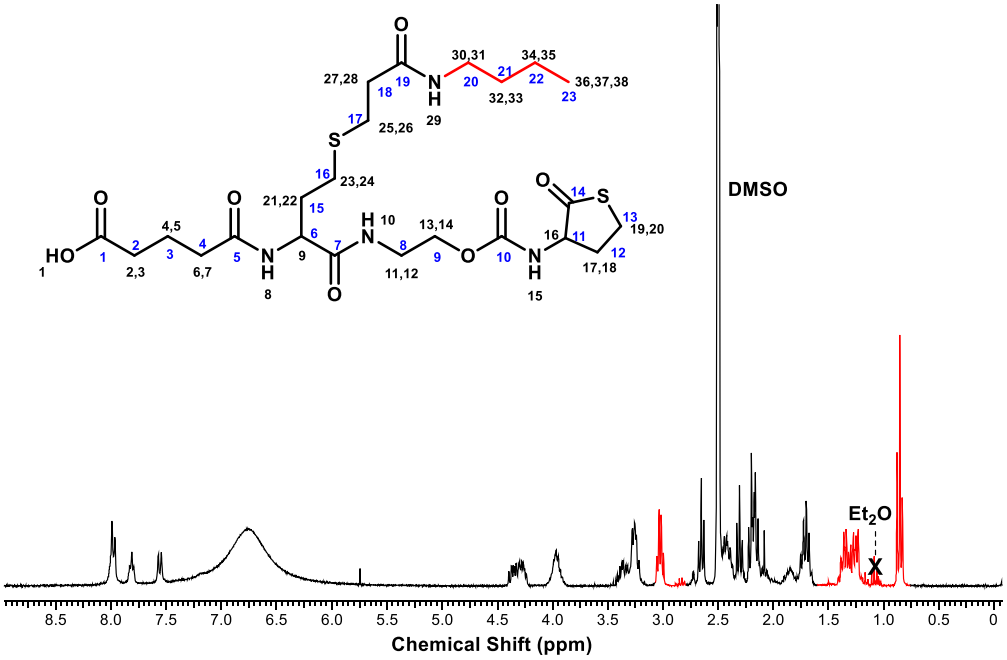

Figure 6.12: ^{1}H NMR of butylamine containing monomer highlighting the functional side group after chain extension of **10**.

The full ^{13}C and ^{1}H assignment for monomer **10** can be found in the **Section 6.4.3.10.2.**

6.2.7.2 Thioacrylate based iterative protocol: Furfurylamine (11)

As an example of an oxygen-containing heterocycle, furfurylamine was used to modify the thioester in an amidation reaction (**Scheme 6.7**).

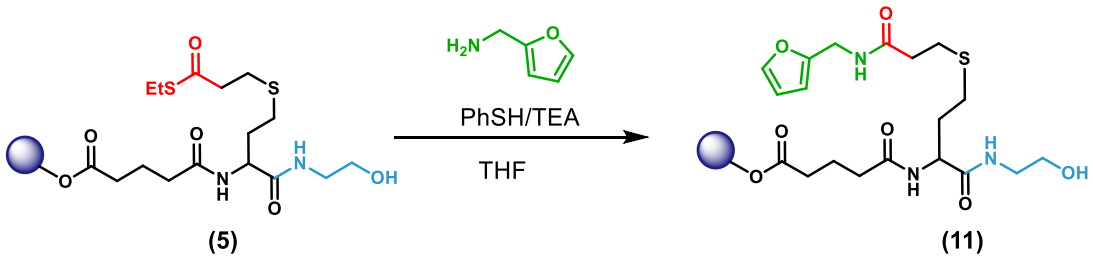

Scheme 6.7: The thiophenol-catalysed amidation of **5** with furfurylamine.

LC–MS analysis of the sample after acidic cleavage, revealed full amidation of the thioester **5**, corresponding to the mass of 586 g/mol of the furfuryl-functionalised monomer **11** below (**Figure 6.13**).

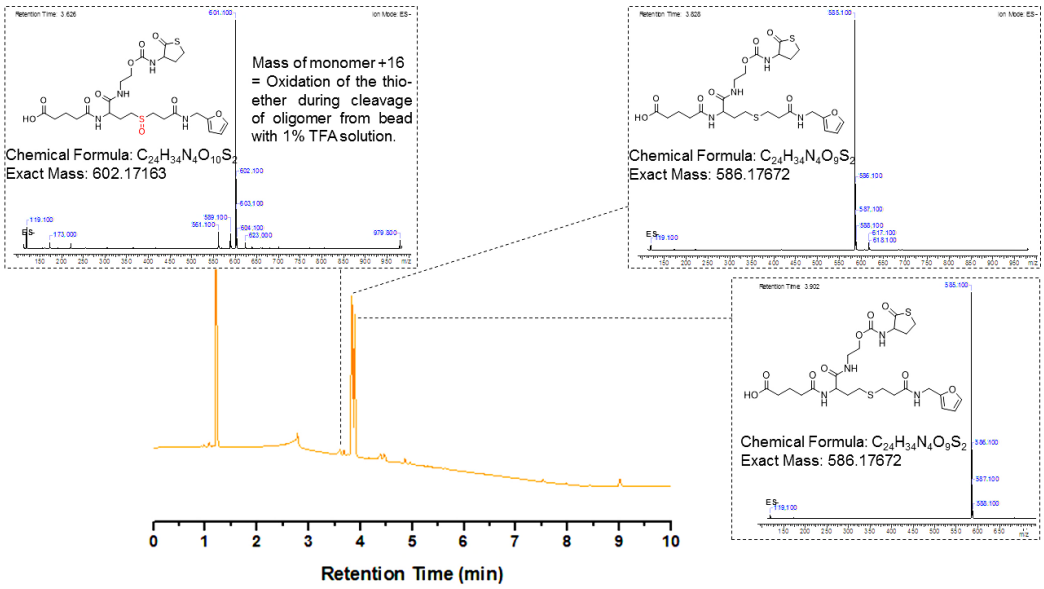

Figure 6.13: LCMS chromatogram at λ = 214 nm of a monomer, with furfurylamine used in the amidation step. HRMS (ESI) *m/z*: $[M + H]^+$ calcd for $C_{24}H_{34}N_4O_9S_2$, 587.1767; found, 587.1852 after chain extension of **11**.

The ^{1}H NMR spectrum of the furfuryl-functionalised monomer is depicted below in **Figure 6.14** and fully assigned in **Section 6.4.3.10.4**. The furfuryl-group is highlighted in red, H_{32} and H_{33} are directly attached to a C=C double bond, the resonance signal of both protons are shifted to low field, due to the inductive effect. The correct order of resonances of H_{32}, H_{33} and H_{34} can be determined by analyzing the signal splitting; H_{33} has two vicinal neighboring protons H_{32} and H_{34}. H_{33} will couple to these protons and resonate as a doublet of doublets at 6.24 ppm. As a result of the coupling to both neighbouring protons, two different vicinal coupling constants can be found: $J_{32,33}$ = 3.2 Hz and $J_{33,34}$ = 0.9 Hz and are in agreement with furan and the signal group at 6.38 ppm can be assigned to proton H_{33}.

Another doublet of doublets was observed at low field (6.38 ppm). The analysis revealed the following coupling constants: 3.2 and 1.9 Hz. The coupling constant J = 3.2 Hz has been already determined by the analysis of the signal group resonating at high field and arises from an interaction of proton H_{32} and H_{33}. Owing to the same coupling constant, the low-field resonance signal was assigned to proton H_{32}. The second coupling constant of 1.9 Hz, arose from the long-distance coupling with proton H_{34}.

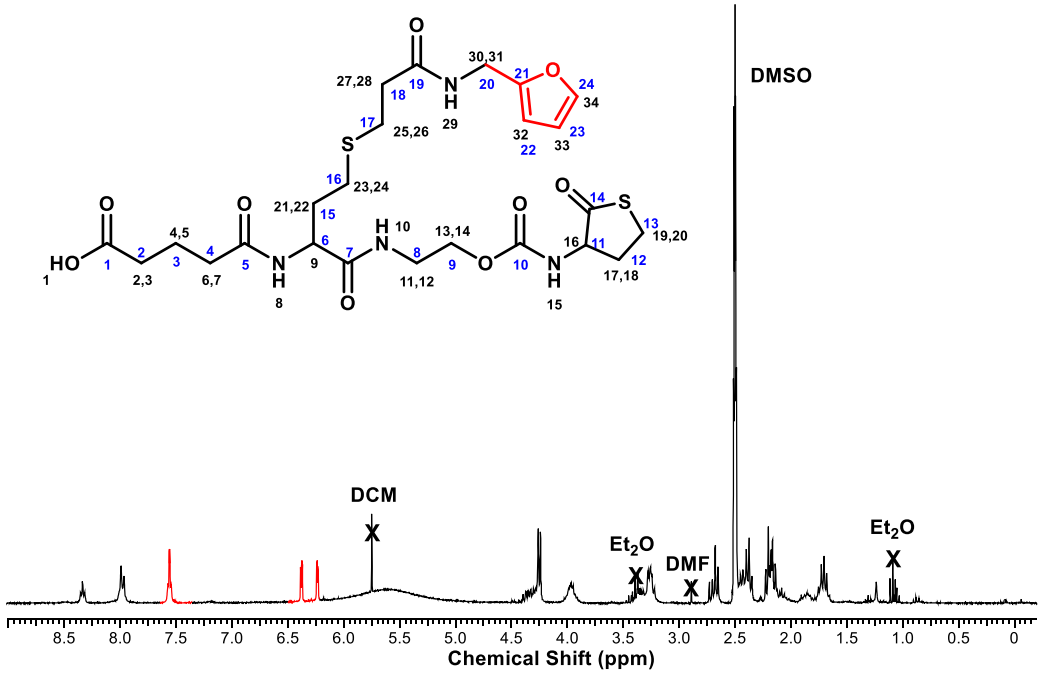

Figure 6.14: ^{1}H NMR of furfurylamine containing monomer highlighting the functional side group.

The remaining signal group at 7.62 to 7.51 ppm belongs to proton H_{34}. As the coupling between H_{33} –H_{34} was already determined by 2D analysis, the same coupling in the resonance signal of proton H_{34} should be present. However, in this case, the coupling constant could not be calculated as the proton resonance of H_{15} was overlapping, but is assumed to resonate as a doublet of doublets. But the fact, that proton H_{34} was in the proximity of an oxygen atom and also directly attached to a C=C double bond, the resonance for this proton was be shifted downfield, further than H_{32} and H_{33}, due to the inductive effect and therefore reducing the electron density of the hydrogen atom. A full assignment for all proton and carbon atoms can be found in **Section 6.4.3.10.4**.

6.2.7.3 Thioacrylate based iterative protocol: 1-Naphtylmethylamine (12) 3,4-Methylendioxyphenethylamine1 (13)and 3-Morpholino propylamine (14)

To investigate if the protocol was applicable to systems that are more complex in terms of aromatic polycyclic compounds, 1-Naphtylmethylamine (**12**) and 3,4-Methylendioxy-phenethylamine (**13**) were used. Additionally, a heterocycle which not only contains one heteroatom (such as the furfurylamine), a heterocycle featuring both an amine and an ether functional group was used and represented by

3-Morpholino propylamine (**14**). The structures of the resulting amidation reaction with these three amines are depicted in the **Scheme 6.8** below.

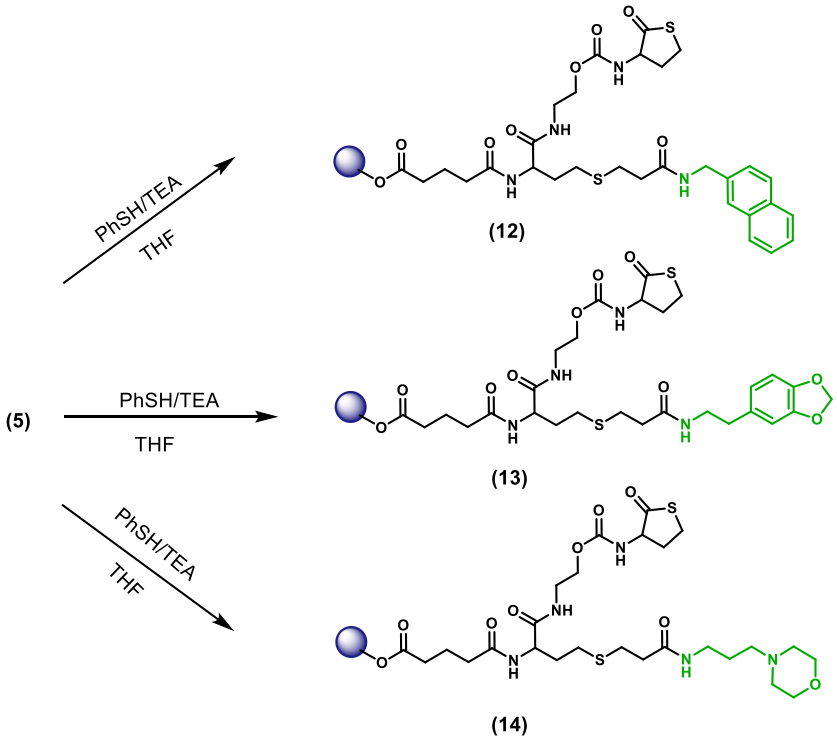

Scheme 6.8: Amidation reaction of thioester compound **5** with a range of functional amines.

In all three cases, only one peak with the mass corresponding the product, was obtained in the LCMS, providing further efficient pathway of the amidation reaction. Furthermore, full NMR analysis was carried out and also displayed the spectra of expected products, along with some impurities, attributed to the washing process with different solvents. (**Sections 6.4.3.10.6, 6.4.3.10.5 and 6.4.3.10.3**). As a result of the aforementioned investigations,the four-step protocol could be then used for more monomeric addition to the sequenced chain, thus resulting in a sequence defined oligomer, this approach is illustrated in **Scheme 6.9** below.

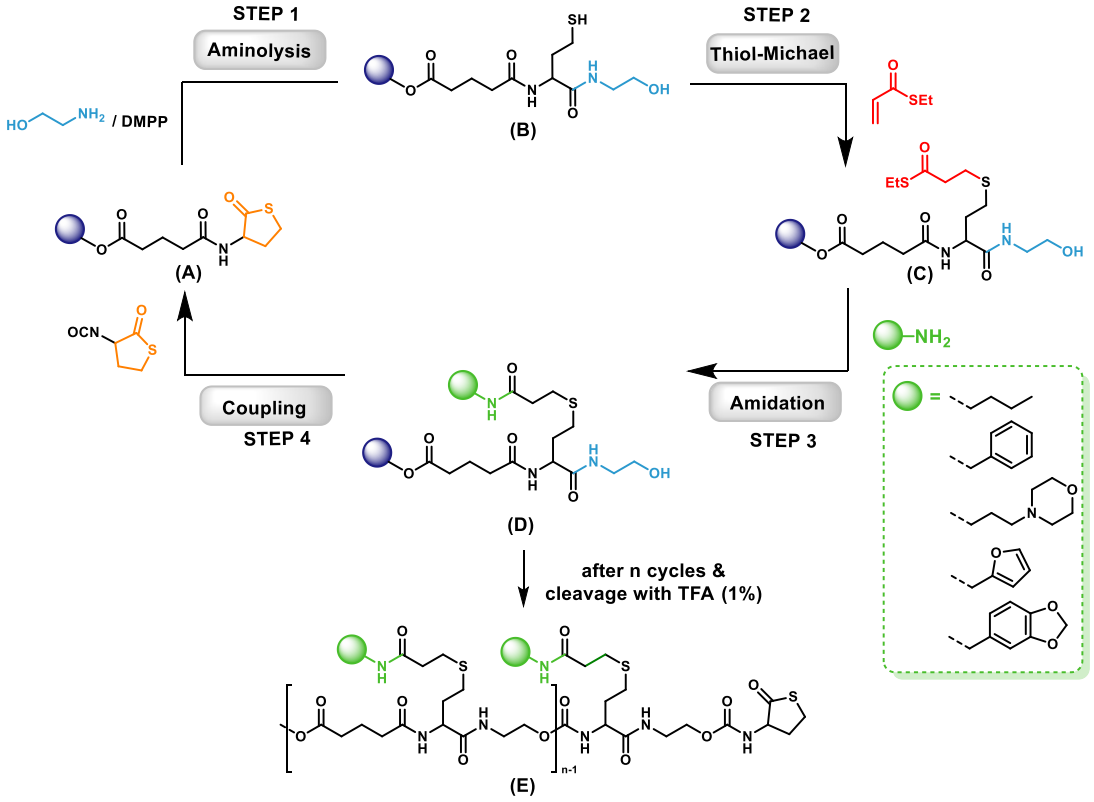

Scheme 6.9: Solid-phase-based synthetic protocol for the preparation of multi-functional, sequence-defined oligomers, including a post-modification (**C**) step by making use of thioacrylates and subsequent amidation. Experimental details of the general synthetic procedure outlined in **Section 6.4.3.5** for all steps.

6.2.8 Preparation of a multi-functional hexamer (15)

An oligomer was then prepared, incorporating all of these amines into one, multifunctional, sequence-defined hexamer (**Figure 6.15**). LCMS and HRMS were again measured after each complete cycle and the final oligomer was also analysed by NMR spectroscopy. It should be emphasised here that, despite the wide variety of functional groups and reactions used, they are all compatible in such a way that this method is completely protecting group-free. By following this herein reported protocol, three different, sequenced oligomers were prepared, which were subsequently analysed after each iterative cycle, principally by LCMS, to check conversion and purity, demonstrating the viability and versatility of this protocol.

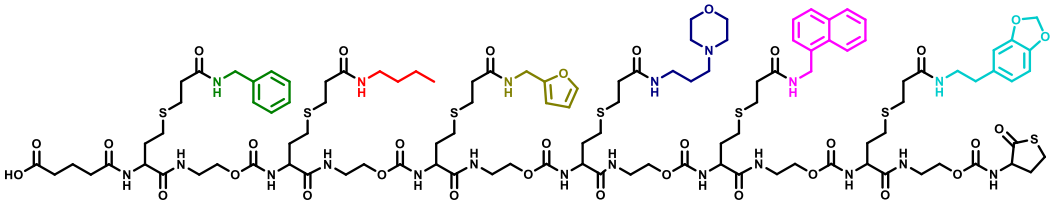

(15)

Figure 6.15: Structural representation of multifunctional hexamer structure **15**.

6.2.8.1 Synthesis of a multifunctional hexamer: Monomer

For the synthesis of a multifunctional hexamer, benzylamine was used for the first cycle (**Figure 6.15**). The amidation with benzylamine and subsequent chain extension with the α-thiolactone-γ-isocyanate was followed by LCMS.

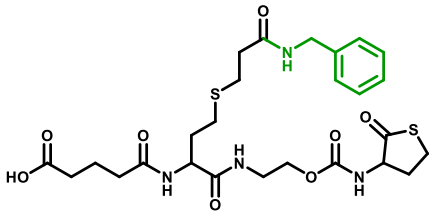

(15a)

Figure 6.16: Structural representation of monomer structure **15a** for the multifunctional hexamer **15**.

A small amount of the product was analysed to confirm the amidation was complete and also to confirm the purity. In the LCMS analysis, a main peak was detected after of 4.0 minutes retention time, corresponding to a mass of 596 g/mol and represents the desired product (**Figure 6.17**).

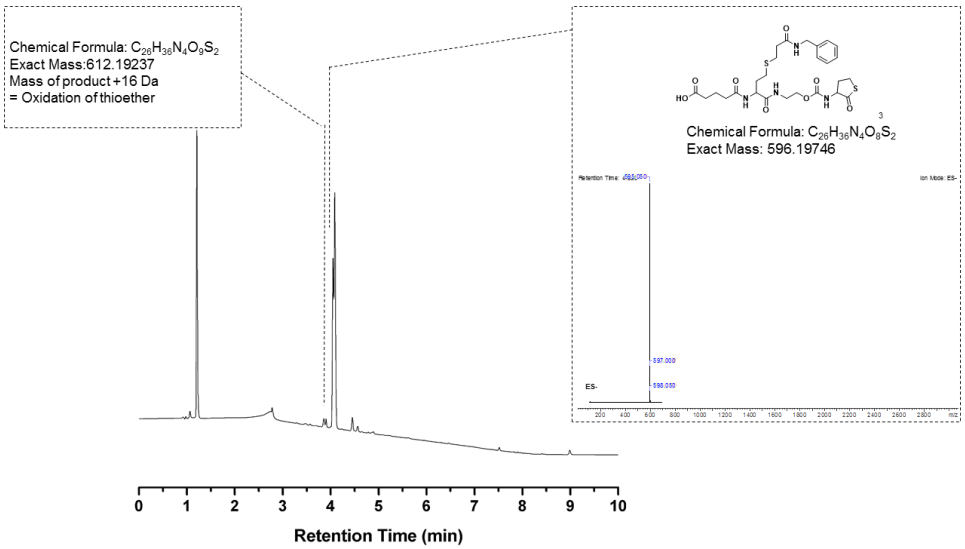

Figure 6.17: LCMS chromatogram of monomer step of multifunctional hexamer synthesis.

6.2.8.2 Synthesis of a multifunctional hexamer: Dimer

As the monomer appeared to be pure, a second cycle of the remaining product was performed. For this, the thiolactone was opened again, addition of ETA and subsequent amidation with butylamine resulting in a dimer with the benzylamine und butylamine containing functional groups (**15b**).

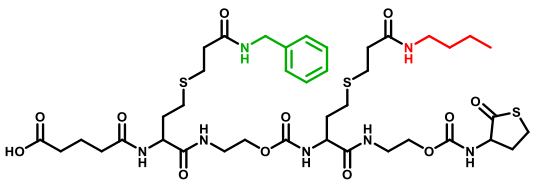

(15b)

Figure 6.18: Structural representation of dimer structure **15b** of the multifunctional hexamer **15.**

Again, a small amount (~2 mg) of the product was analysed, confirming that the amidation reaction took place. In the LCMS analysis, a main peak was detected with

the retention time changing from 4.0 to 4.5 minutes, as expected for a higher molecular weight structure. A higher mass of 928 g/mol was found and matched the calculated mass well (**Figure 6.19**).

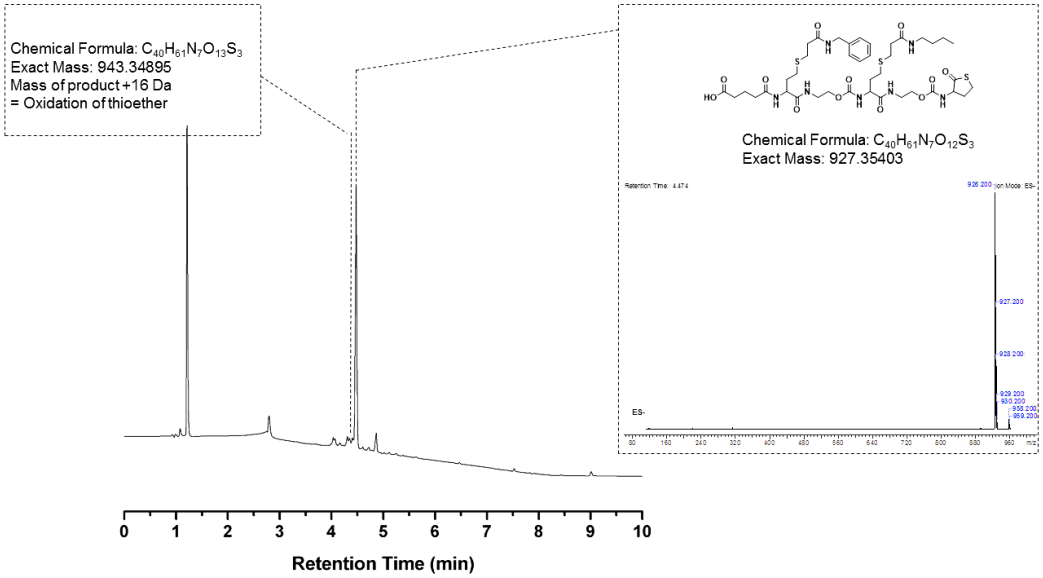

Figure 6.19: LCMS chromatogram at λ = 214 nm of dimer step of multifunctional hexamer synthesis.

6.2.8.3 Synthesis of a multifunctional hexamer: Trimer

Subsequently, the protocol was continued, resulting in a trimer with the addition of a furfuryl amine (**Figure 6.20**).

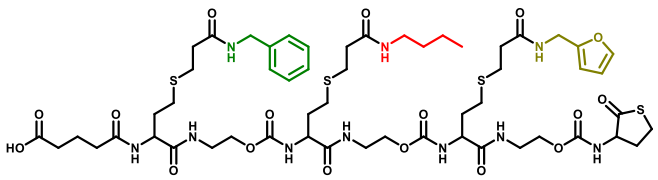

(15c)

Figure 6.20: Structural representation of trimer structure **15c** of the multifunctional hexamer **15.**

LCMS was recorded to verify sample purity and successful incorporation of furfurylamine in the backbone. The LC chromatogram of **15c** displayed one major peak at 4.7 minutes which corresponded with the expected product (**Figure 6.21**). However, a minor peak at 4.9 minutes was found in the chromatogram as well. This was already present as a very small peak in **Figure 6.19** for **15b**. The LCMS shown

below in **Figure 6.21**, confirms the presence of the mass of 1282 g/mol found in the ESI-MS spectrum for the peak at 4.7 minutes.

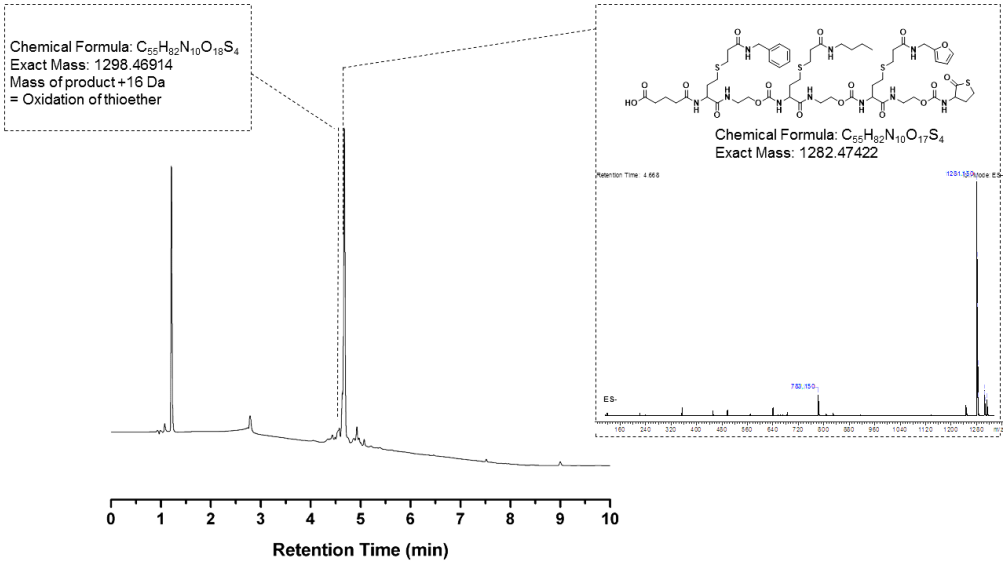

Figure 6.21: LCMS thermogram at $\lambda = 214$ nm of trimer step of multifunctional hexamer synthesis.

6.2.8.4 Synthesis of a multifunctional hexamer: Tetramer

To further investigate the influence of the small impurity from the previous step, a next cycle was performed, to see if it appeared again in the LCMS. In the following step for a tetramer, 3-morpholinopropylamine was used in the next cycle to yield a tetramer. The structure is depicted in **Figure 6.22**, where each colour represents a functional group for the respective primary amines used.

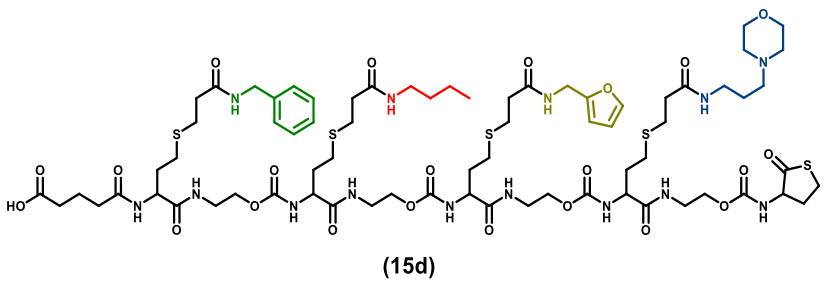

Figure 6.22: Structural representation of tetramer structure **15d** of the multifunctional hexamer **15.**

Interestingly, the impurity from the previous step disappeared and only one peak at 4.6 minutes was detectable. The mass of this peak was found to be 1685 g/mol and is

in agreement with the expected value. The disappearance of the impurity in the LCMS suggest that the present impurities did not directly affect the subsequent step and was probably present due to inefficient washing. The LCMS of tetramer **15d** is depicted in **Figure 6.23** below.

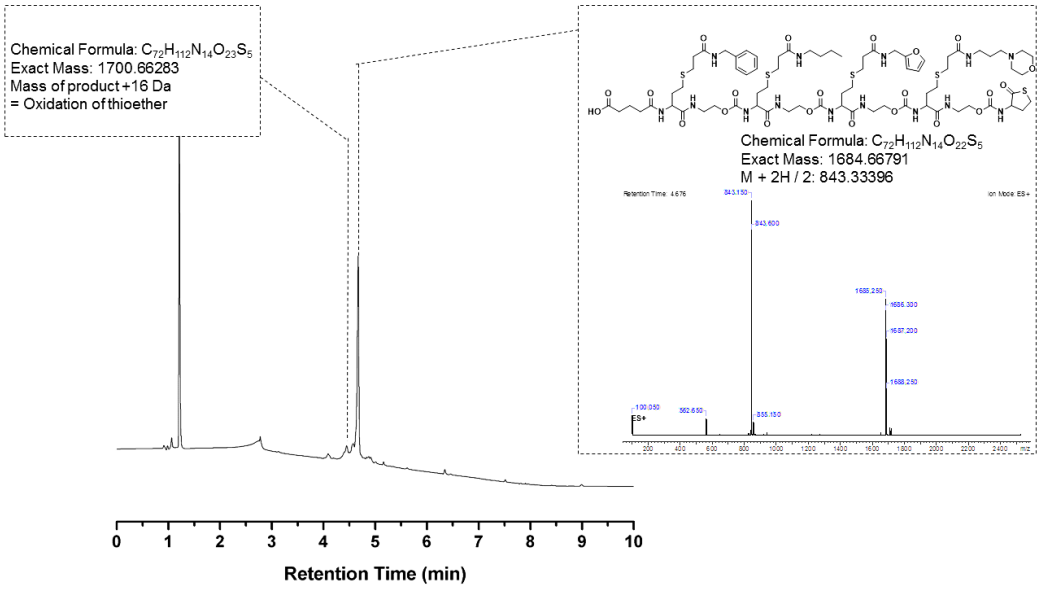

Figure 6.23: LCMS chromatogram of tetramer step of multifunctional hexamer synthesis.

6.2.8.5 Synthesis of a multifunctional hexamer: Pentamer

So far, aromatics, aliphatic and cyclic functionalised amines have been successfully incorporated. In the next step, a first polycyclic amine was chosen for the pentamer structure. The general structure of the pentamer, where the naphthyl-group is highlighted in pink, is depicted in **Figure 6.24** below.

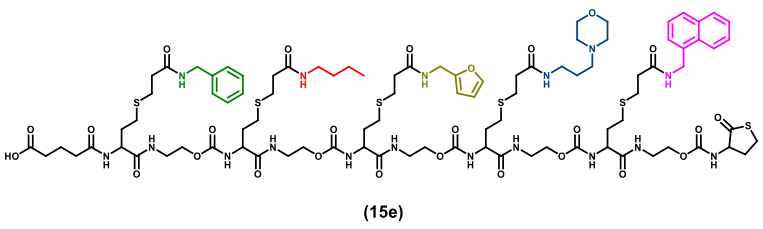

Figure 6.24: Structural representation of pentamer structure **15e** for the multifunctional hexamer **15.**

The LCMS revealed a new, small peak in addition to the principle product peak. The product peak from the tetramer at 4.7 minutes in the previous step, disappeared completely and instead the major peak of the spectrum shifted to 5.0 minutes. The shift in retention time and the fact that it gave a mass of 2099 g/mol in the ESI-MS spectrum, is in good agreement with the expected value of 2099 g/mol (**Figure 6.25**) for the pentamer product of this reaction.

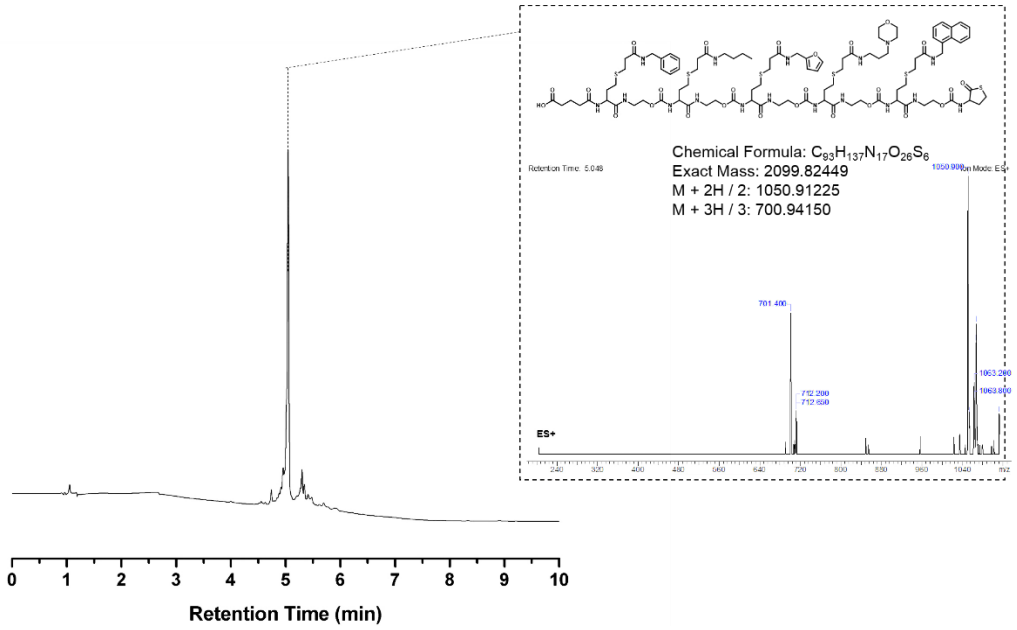

Figure 6.25: LCMS chromatogram of pentamer step of multifunctional hexamer synthesis.

6.2.8.6 Synthesis of a multifunctional hexamer: Hexamer

In the final cycle, a second polycyclic amine was chosen for the ultimate side group. The general structure of the hexamer, where the protected dopamine in the 3-morpholino propylamine is highlighted in turquoise is depicted in **Figure 6.26**.

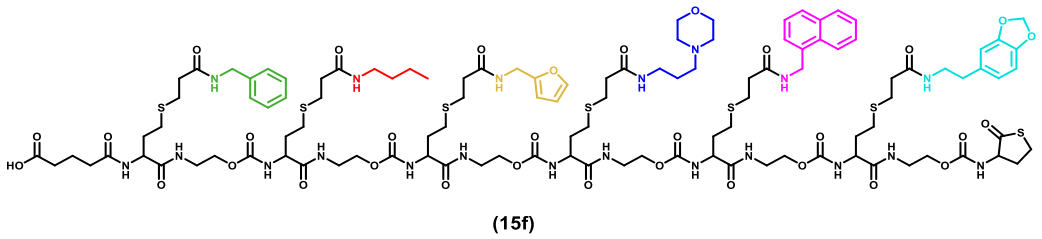

Figure 6.26: Structural representation of hexamer structure **15f** of the multifunctional hexamer **15.**

The LCMS chromatogram of the hexamer step of the multifunctional hexamer synthesis revealed a larger impurity this time (**Figure 6.27**). However, the shift in retention time to 5.3 minutes, of the principal peak and the found expected mass of 2522 g/mol which could be attributed to a successful introduction of the protected dopamine, confirmed the success of the reaction.

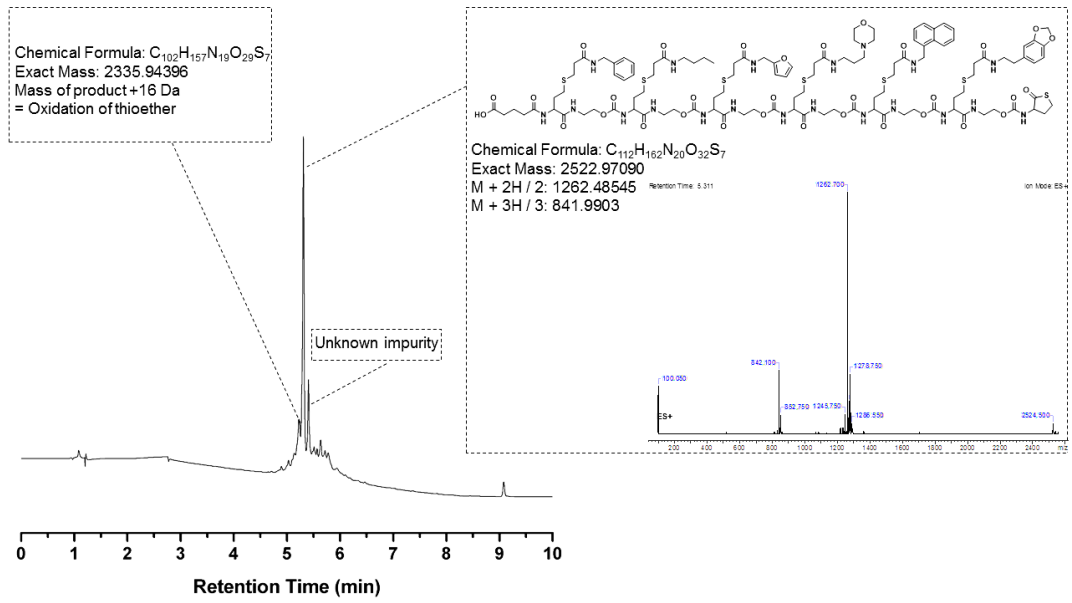

Figure 6.27: LCMS chromatogram of hexamer step of multifunctional hexamer synthesis.

In order to be able to visualise the overall progress of the reaction, LCMS chromatograms from the monomer to hexamer are stacked and are shown below in **Figure 6.28**, where each colour represents the chosen amine.

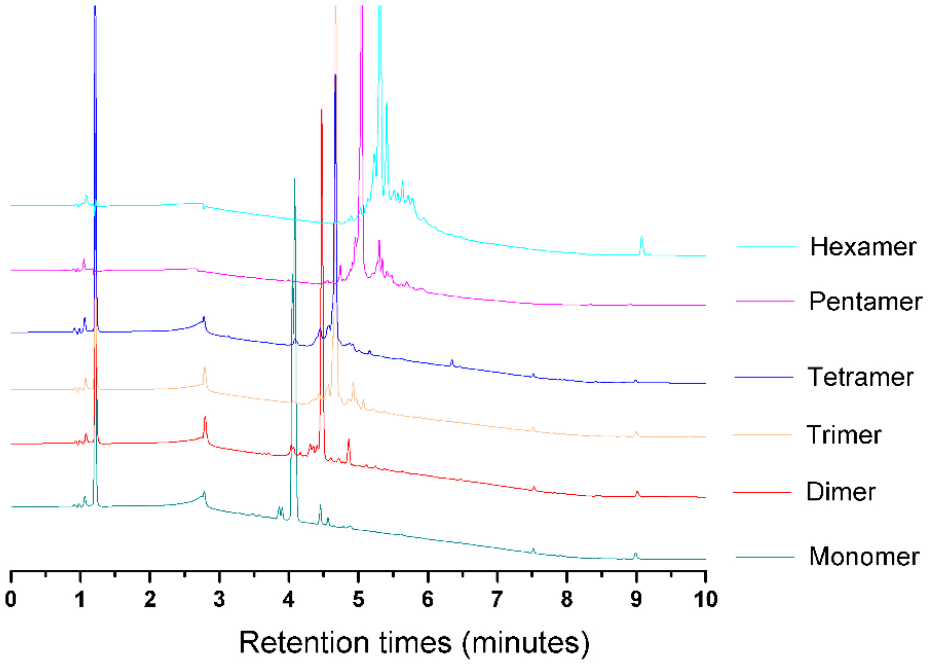

Figure 6.28: LCMS stack of multifunctional oligomer from monomer through to hexamer.

^{1}H NMR spectrum was recorded to verify sample purity and the successful incorporation of various side chain residues of respective amines. The full analysis details and spectrum is given in **Figure 6.66**. The structure was fully resolved by NMR spectroscopy **(Section 6.4.3.11.3**).

Whilst the LCMS chromatogram of each cycle in the multifunctional hexamer clearly shows that the protocol works (**Figure 6.28**), indeed the purity of this oligomer in the last step appeared not to be as high, as expected and evidenced by their LCMS chromatograms in the same figure. Although it is not yet known why this is the case, it could be that the combination of these varying functional groups into one oligomer introduces unforeseen folding interactions that effect the synthesis. Folding and structural arrangement is an area that needs more investigation in this field as it is not currently clear how precise sequence control can effect this. Individually the primary amines used reacted completely, resulting in pure monomers using this protocol as reported in the supporting information. The tetramer step in **Figure 6.20**, for example, appears very pure in comparison to the trimer and pentamer, suggesting that the present impurities do not directly affect the subsequent step.

To improve reproducibility and scientific accuracy in such a repetitive, synthetic process, further optimisation of this protocol, including automation, would most likely further improve the purity of the resulting oligomers. However, it is worth noting that for further use within potential applications, purification by preparative HPLC, as typically performed in peptide solid phase chemistry, would anyway be required in a similar way as an organic compound would be purified by, for example, column chromatography before further use.

6.2.9 Preparation of a bifunctional octamer a (22)

Two alternating bifunctionalised octamer with alternating benzyl- and butyl- side groups was synthesised. LCMS was used again as the primary analysis technique, confirming both the effectiveness of the protocol and the purity of the oligomers synthesised, as it requires only a few mg of loaded resin whereas NMR characterisation was only possible with the final oligomers, as all of the remaining resin has to be cleaved from the oligomer to yield enough compound to be fully analysed by NMR spectroscopy.

6.2.9.1 Preparation of a bifunctional octamer: Dimer (16)

In the following an aliphatic and aromatic amine containing alternating structure was synthesised *via* the validated protocol (**Scheme 6.9**). The butylamine functionalised monomer **10** was used for further reaction, in a second cycle with a second amine, the benzylamine to give the A-B dimer structure. The resulting octamer had a monomer sequence of A-B-A-B-A-B-A-B, where A represents the butylamine and B the employed benzylamine (**Figure 6.29**).

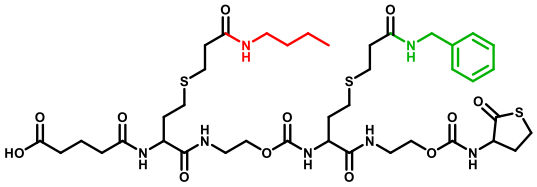

(16)

Figure 6.29: Structural representation of dimer structure **16** of the bifunctional octamer.

The LCMS of **16** is depicted below in **Figure 6.30** and illustrates the purity of the dimer; the primary peak can be found at 4.5 minutes with a mass of 928 g/mol observed with a detector set to wavelength of 240 nm. The observed mass is equal to the calculated mass.

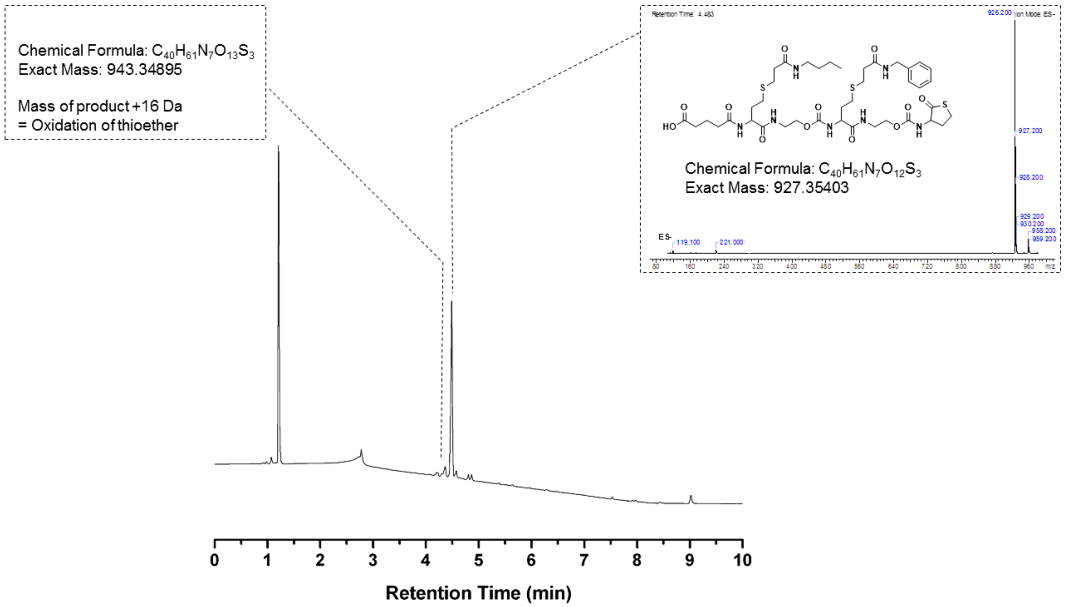

Figure 6.30: LCMS chromatogram of dimer step in octameric sequence.

6.2.9.2 Preparation of a bifunctional octamer: Trimer (17)

The thiolactone function in **16** was then opened with ethanolamine, the released thiol was exposed to ETA, followed by an amidation reaction with butylamine to yield a trimer with an alternating A-B-A order (**Figure 6.31**).

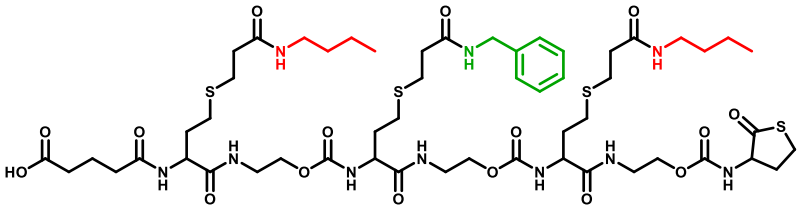

(17)

Figure 6.31: Structural representation of trimer structure for the bifunctional octamer.

The LCMS in **Figure 6.32** shows the disappearance of the peak at 4.5 minutes, belonging to the previous designated product **16** and the full conversion of **16** to **17**. A new peak at 4.7 minutes, with a mass of 1259 g/mol is in perfect agreement with the expected value of 1259.

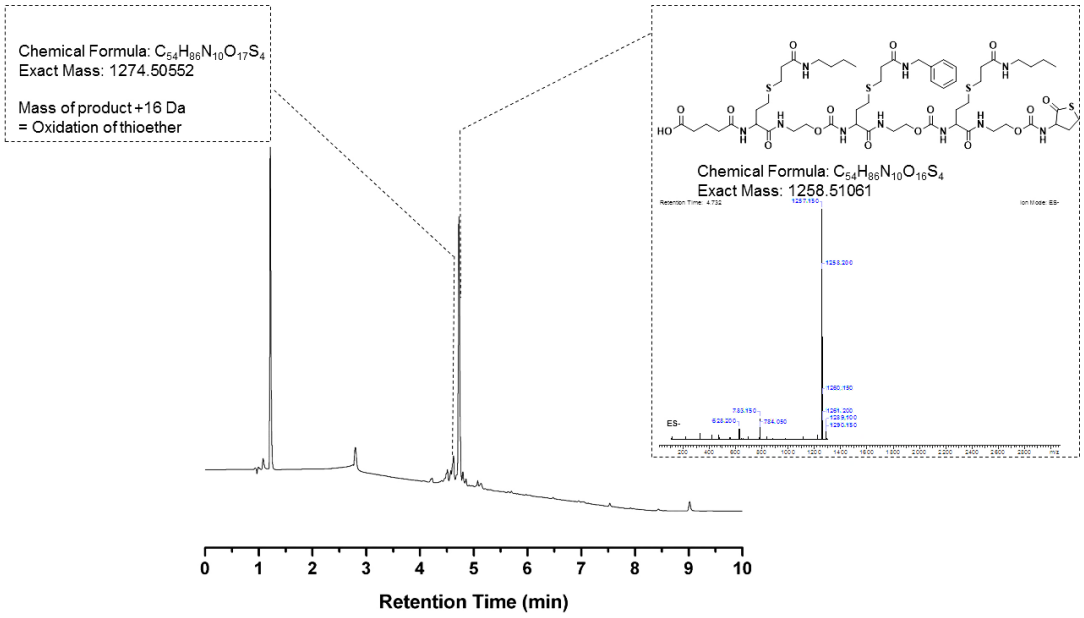

Figure 6.32: LCMS chromatogram of trimer step in octameric sequence.

6.2.9.3 Preparation of a bifunctional octamer: Tetramer (18)

According to the protocol in **Scheme 6.9**, trimer **17** was subjected to ring-opening, thiol was subsequently reacted with the ETA and followed by a thiophenol-catalysed amidation with butylamine to yield a tetramer. The general structure is depicted in **Figure 6.33** below and shows the butylamine units in red, whereas the benzylamines are highlighted in green.

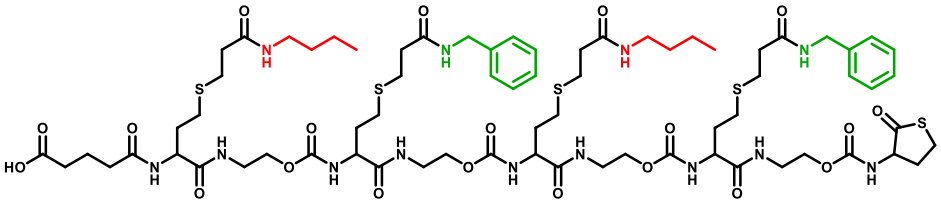

(18)

Figure 6.33: Structural representation of tetramer structure of the bifunctional octamer.

The LCMS in **Figure 6.34** shows the appearance of a new peak at 4.9 minutes, with a mass of 1624 g/mol and represents the protonated mass of the tetramer **18**. Additionally, no impurities by means of the detection of another peak could be found.

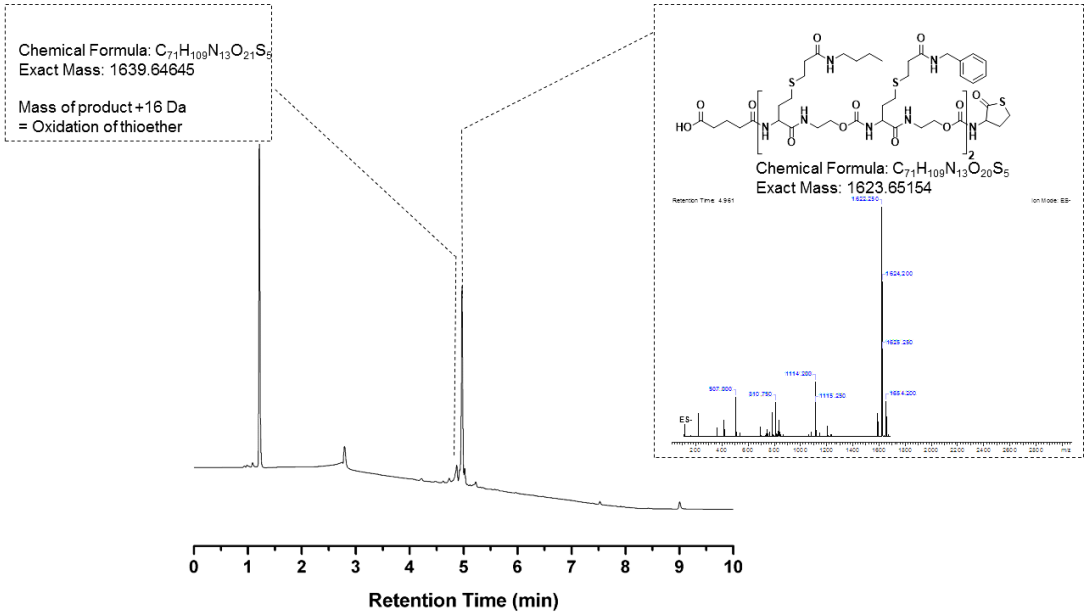

Figure 6.34: LCMS chromatogram of tetramer step in octameric sequence.

6.2.9.4 Preparation of a bifunctional octamer: Pentamer (19)

Tetramer **18**, underwent a further cycle, followed by amidation with butylamine. The general structure of the bifunctional pentamer is depicted in **Figure 6.35** below.

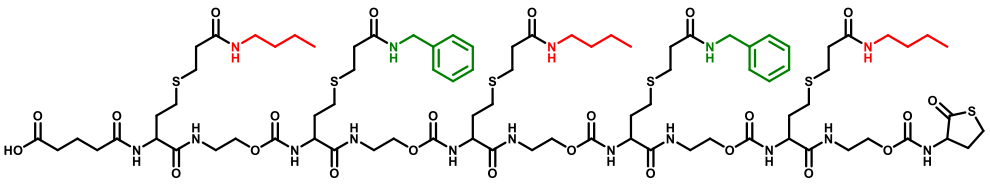

(19)

Figure 6.35: Structural representation of pentamer structure of the bifunctional octamer.

Again, LCMS was recorded for the obtained product, to confirm sample purity and the incorporation of the butyl side chain residues. In the LCMS, a compound with MW = 1955 g/mol was detected as a major peak at 5.1 minutes, corresponding to the protonated products. However, a second peak was detected at a higher retention time of 5.2 minutes and could not be identified (see in **Figure 6.36**).

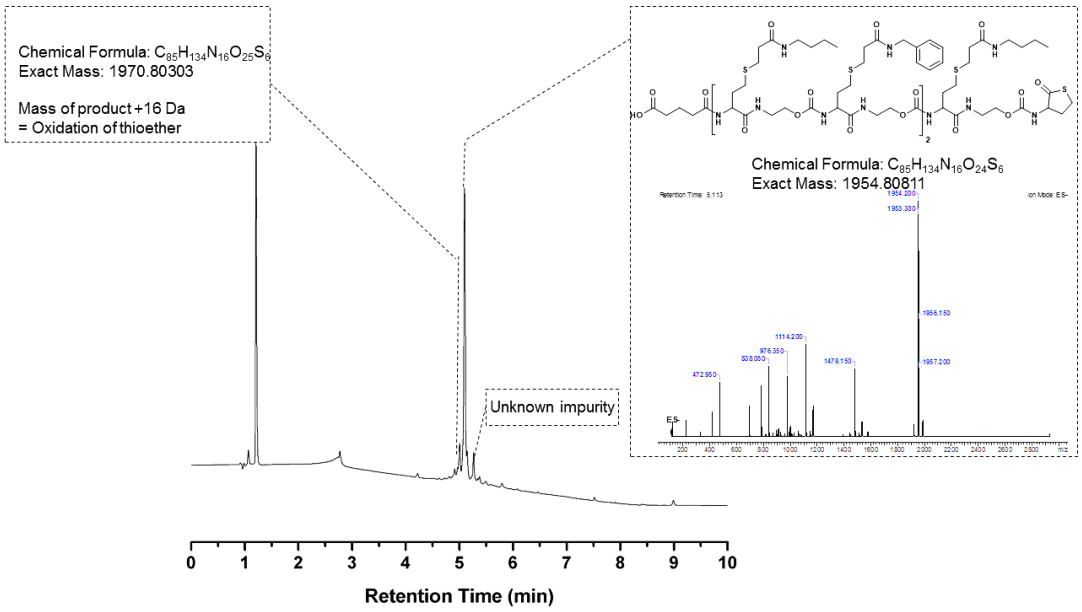

Figure 6.36: LCMS chromatogram of pentamer step in octameric sequence.

6.2.9.5 Preparation of a bifunctional octamer: Hexamer (20)

The thiolactone moiety in the pentamer (**19**) was reacted with ethanolamine, thus releasing the thiol during the ring opening reaction, which was further reacted with ETA in a thiol-*Michael* reaction. Amidation was performed with benzylamine and chain extension of this product with a thiolactone-isocyanate to yield the functional

group for a next cycle. The structure of the obtained hexamer is depicted in (**Figure** 6.37).

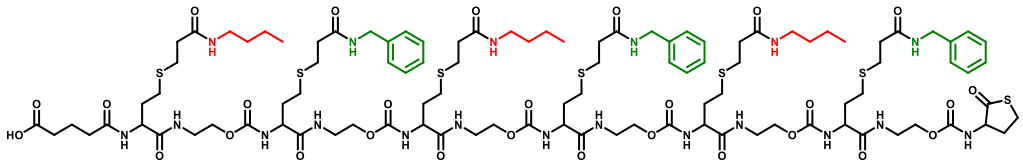

(20)

Figure 6.37: Structural representation of hexamer structure of the bifunctional octamer.

The fragmentation of this product, overserved in the MS spectrum is exemplified in **Figure 6.38** below.

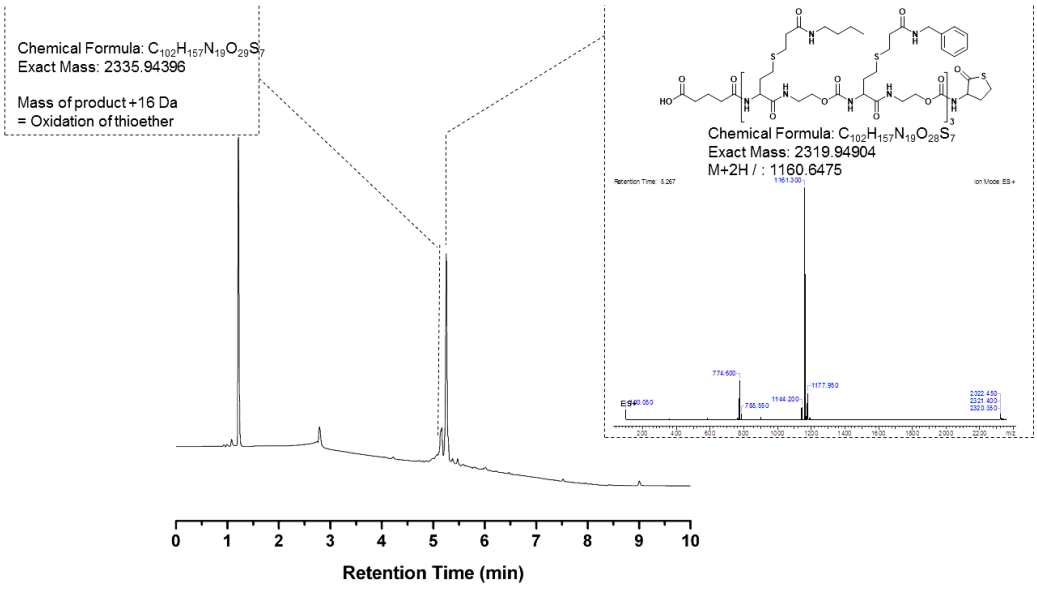

Figure 6.38: LCMS chromatogram of hexamer step in octameric sequence.

Interestingly, the impurity observed in the previous step for the pentamer 20 disappeared completely. One peak at 5.3 minutes with a mass of 1160 g/mol can be detected and matches well the twice protonated calculated mass for the hexamer **20**.

6.2.9.6 Preparation of a bifunctional octamer: Octamer (22)

Hexamer **20** underwent two more reaction cycles. The first cycle resulting in a heptamer **21** was carried out with butylamine. However, no analysis of this step was performed as confident of the robustness of the protocol with benzylamine, and instead, a final cycle using octamer **22** was carried out, which depicted below in **Figure 6.39.**

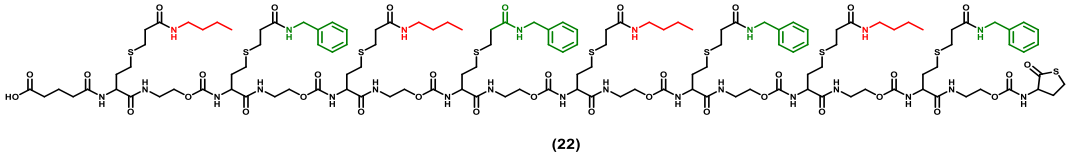

(22)

Figure 6.39: Structural representation of octamer **22**.

In the LCMS spectrum below in **Figure 6.40**, one peak with the retention time of 5.4 minutes could be detected in positive mode. The change in retention time as a result of the increase of molecular weight to 3016 g/mol displays the efficient progress of the reaction from a monomer through to the final octamer **22**.

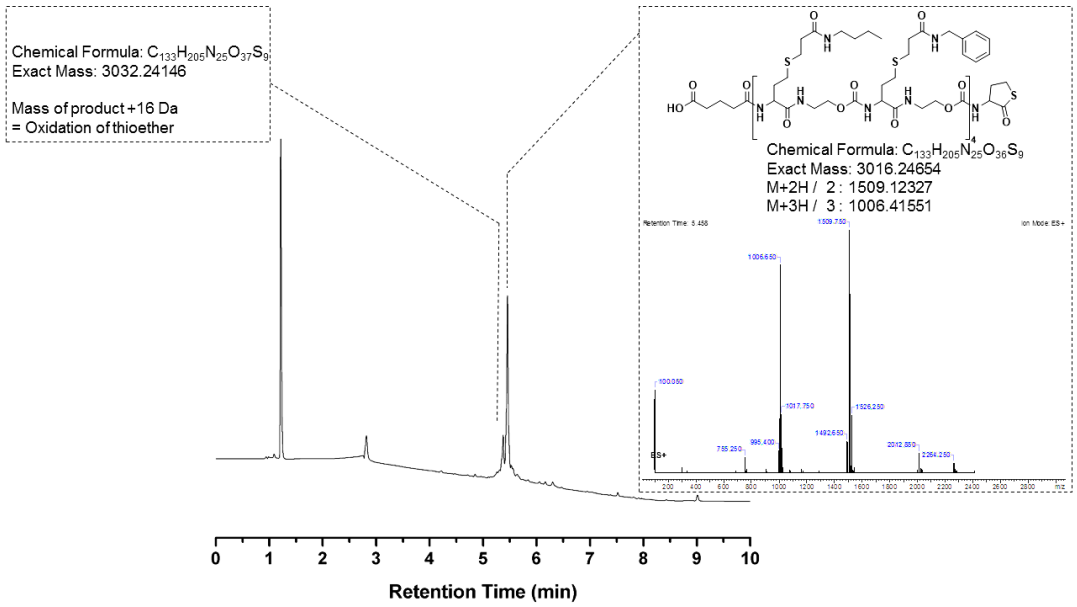

Figure 6.40: LCMS chromatogram of the final octamer step in the octameric sequence, spectrum recorded in positive mode.

In order to be able to visualise the overall progress of the reaction, LCMS chromatograms from the monomer to octamer are stacked and are shown below in **Figure 6.41**, where each colour represents the chosen amine. Starting with a butyl-functionalised monomer in red, as the sequence grows in length an overall increase in the retention times as well as the detected molecular mass. Interestingly, the impurity recognised in the LCMS (**Figure 6.36**) of the pentamer **19**, disappeared in the LCMS (**Figure 6.38**), measured for the hexamer **20.**

Through the iterative approach depicted in **Scheme 6.9**, the synthesis of a multi-functionalised hexamer could be further extended to a bifunctional, oligomeric macromolecule, beginning from a thiolactone moiety that was immobilised on a 2-chlorotrityl chloride functionalised solid-phase resin. Even though the sequence was longer, compared to the multi-functionalised hexamer **15**, the overall purity was higher.

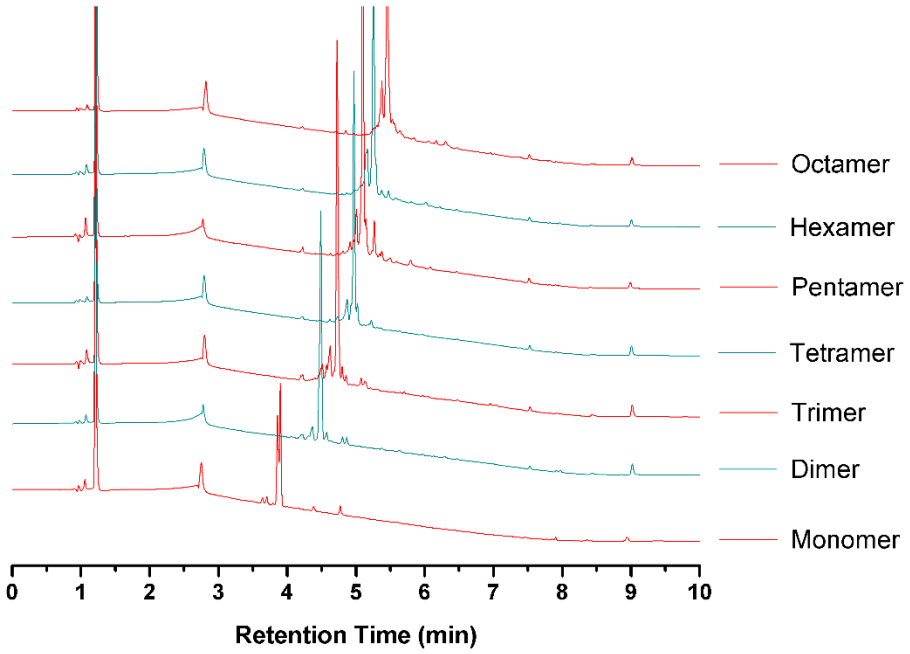

Figure 6.41: Stack of LCMS chromatograms of bifunctionalised octamer from monomer through to octamer synthesised with alternating butyl- and benzyl- side groups.

Proton and carbon NMR spectra were recorded in DMSO; the aromatic protons of the benzylamine appear in the downfield region (7-7.5 ppm) of the proton spectrum, and highlighted in green in the spectrum below (**Figure 6.42**).

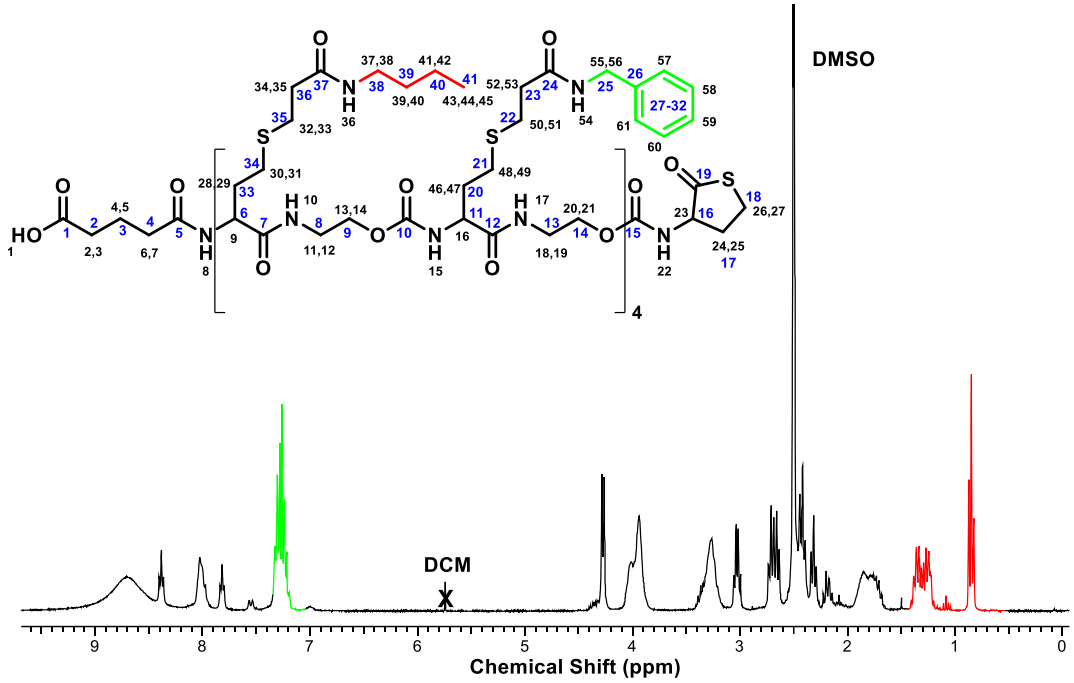

Figure 6.42: ^{1}H NMR of octamer **20**.

The methylene resonance for $H_{57\text{-}61}$ of the butyl side chain were found as a triplet at 0.85 ppm with a coupling constant of 7.0 Hz, supporting the assignment next to an ethylene group from the aliphatic chain. Additionally, in the ^{13}C NMR the carbon of the methyl group C_{41} appears in a typical range for methyl groups between 10-15 ppm, at 13.69 ppm. Besides the DCM present in the NMR spectrum, from the cleavage solution, no other impurity could be found, full assignment for all proton and carbon NMRs can be found in (**Section 6.4.3.11.1**).

6.2.10 Preparation of a bifunctional octamer b (30)

A second octamer was synthesised with alternating benzyl- and butyl- side groups, sequenced in the opposite order on each oligomer to demonstrate that this had no effect on the synthesis or purity (**Figure 6.43**).

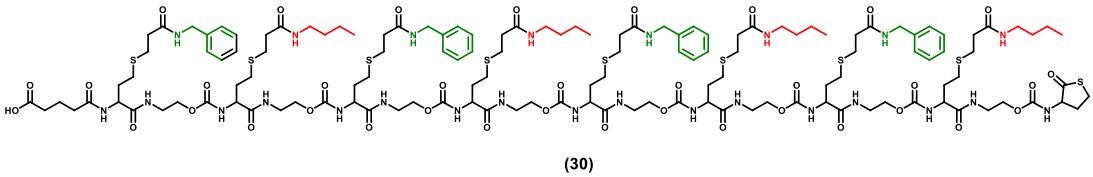

(30)

Figure 6.43: Structural representation of octamer **30**.

LCMS was again used as the primary analysis technique, confirming both the effectiveness of the protocol and the purity of the oligomers synthesised, because it requires only a few mg of loaded resin whereas NMR characterisation was only possible with the final oligomers, as all of the remaining resin has to be cleaved from the oligomer to yield enough compound to be fully analysed by NMR spectroscopy. The LCMS spectrum of the final product **30** is depicted below in **Figure 6.44**. As nothing unusual could be detected in the LCMS from all cycles, only the octamer is be discussed below. The analysis of all other steps are depicted separately below (**Section 6.4.3.11.2**). In **Figure 6.44** the LCMS demonstrates the purity of the product as a major peak at 5.4 minutes, which is the same time found for the octamer **22** in reverse order (**Figure 6.40**).

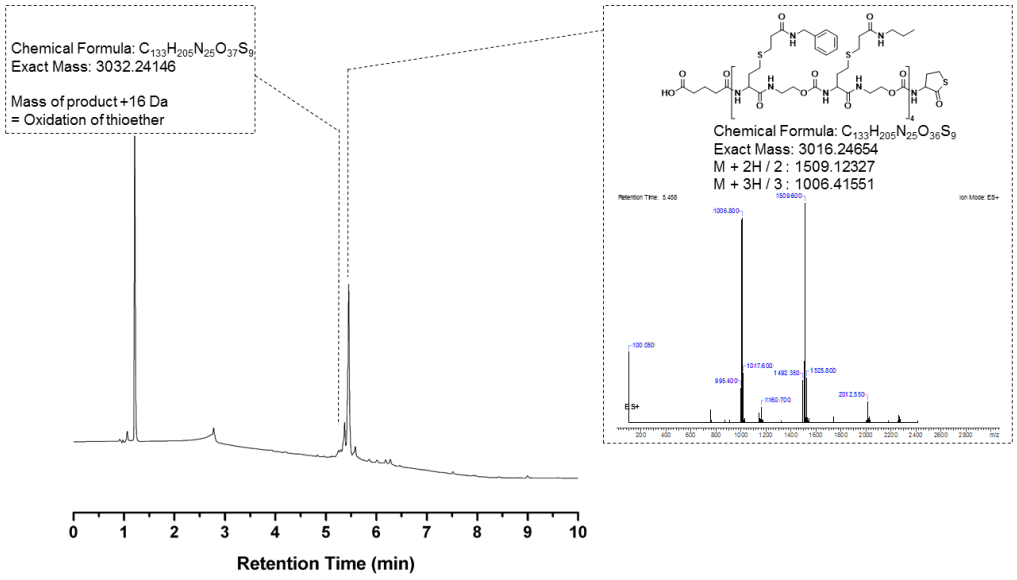

Figure 6.44: LCMS chromatogram of final octamer step in octameric sequence. Spectrum recorded in positive mode.

The LCMS chromatograms of all steps consistently displayed one major peak, corresponding with the expected product. Two functionalities were incorporated, by using benzyl and butylamine in the amidation step, yielding a pure octamer (**30**). The

overlay of the LCMS chromatograms of all steps in the sequence from a monomer to an octamer **8** is depicted below in **Figure 6.45**, where the green colour represents the use of benzylamine and the red chromatograms amidation with butylamine.

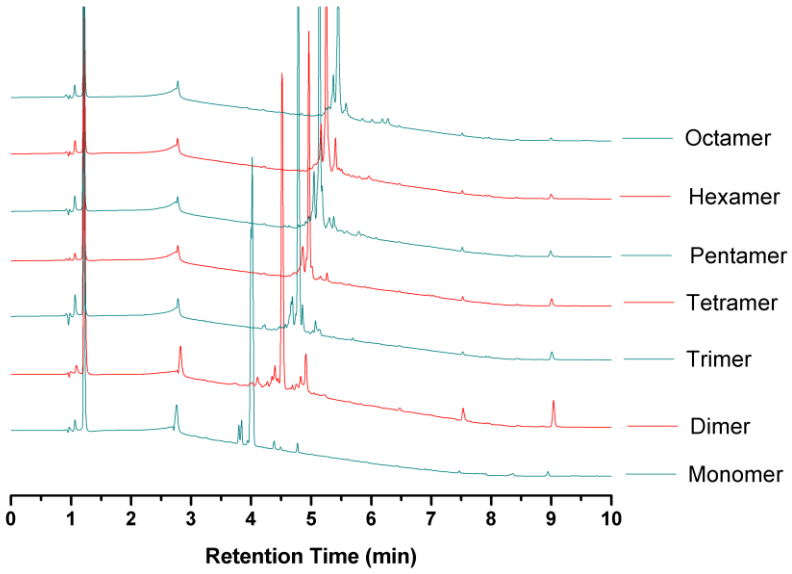

Figure 6.45: Stack of LCMS chromatograms of benzyl-butyl functionalised octamer from monomer through to an octamer.

Again, a small impurity visible as a second minor peak can be seen in the LCMS chromatogram, obtained for the dimer and hexamer, when butylamine was used. The same presence of an impurity in the LCMS could be observed in octamer **22** when butylamine was used (**Figure 6.41)** and the multifunctional hexamer **15f** when butylamine was used for the synthesis of the dimer **(Figure 6.28**). However, as mentioned earlier the detected small impurity vanishes by the next cycle and was not visible anymore after the step and thus was potentially an impurity from the burylamine that was washed away.

6.3 Conclusions

Here, a new chemical protocol for the synthesis of multi-functional and post-modified sequence-defined oligomers was successfully demonstrated. The protocol was constructed following ^{1}H NMR model studies and careful study of the kinetics and the compatibility of certain steps and reagents to ensure efficient and orthogonal reaction and to eliminate the need for protecting groups. Through this, it was possible to synthesise several sequence-defined oligomers, to demonstrate the versatility of this approach and its potential in terms of side chain functionalisation. It was also shown how advantageous solid-phase chemistry is in such iterative protocols as used in the synthesis of sequence-defined oligomers, as they allow for small-scale reactions, easy handling and facile purification by extensive washing. In future studies, it is hoped that this protocol will allow for the incorporation of more specific functional groups, thus resulting in unique applications for such sequence-defined oligomers, further confirming the need for the advancement of this specific branch of polymer chemistry. Finally, the successful coupling of thiolactone and thioacrylate chemistry was shown, thus demonstrating the compatibility of these two classes of molecules in click-inspired reactions and within sequence-defined chemistry.

6.4 Experimental

6.4.1 Instrumentation

6.4.1.1 Nuclear Magnetic Resonance (NMR)

^{1}H- and ^{13}C-NMR APT (Attached Proton Test) spectra were recorded on a Bruker Avance 300 at 300 MHz, a Bruker Avance 400 at 400 MHz and Bruker Avance 500 at 500 MHz. Chemical shifts are presented in parts per million (δ) relative to DMSO-*d*$_6$ or $CHCl_3$-*d* (2.50 ppm or 7.26 ppm in ^{1}H- and 39.51 ppm or 77.24 ppm in ^{13}C-NMR respectively) as internal standard. Coupling constants (J) are reported in Hertz (Hz). All measurements were performed at 25 °C and MestReNova NMR Processor or ACD/NMR Processor Academic Edition was used for the processing of all data. Full assignment of monomers and oligomer structures was aided by use of 2D NMR techniques (COSY, HSQC and HMBC).

Nuclear magnetic resonance (NMR) spectra were also recorded on a Bruker AV-III 400 for ^{1}H- and at 101 MHz for ^{13}C NMR measurements. $CDCl_3$ was used as solvent and the resonance signal at 7.26 ppm (^{1}H) and 77.16 ppm (^{13}C) served as reference for the chemical shift δ. All measurements were performed at 25 °C and MestReNova NMR Processor was used for the processing of all data.

6.4.1.2 Liquid Chromatography-Mass Spectrometry (LCMS)

An Agilent technologies 1100 series LC/MSD system equipped with a diode array detector and single quad MS detector (VL) with an electrospray source (ESI-MS) was used for classic reversed phase LCMS and MS analysis. All results were recorded in negative mode unless otherwise stated. Analytic reversed phase HPLC (high-performance liquid chromatography) was performed with a Phenomenex C18 (2) column (5 μ, 250 x 4.6 mm) using a solvent gradient (0 → 100 % acetonitrile in H_2O in 15 min) and the eluting compounds were detected *via* UV-detection (λ = 214 nm).

6.4.1.3 High Resolution Mass Spectroscopy (HRMS)

HRMS spectra were collected using an Agilent 6220 Accurate-Mass time-of-flight (TOF) equipped with a multimode ionisation (MMI) source.

6.4.1.4 UV-Vis Spectroscopy

UV-Vis spectroscopy was recorded on an Analytikjena Specord 200 at λ=254 nm using 1 cm quartz cuvettes.

6.4.1.5 Gas chromatography (GC)

Gas chromatography – flame ionisation detection (GC-FID) analysis was performed using Agilent Technologies 7820A. An Agilent J&W HP-5 capillary column of 30 m x 0.320 mm, film thickness 0.25 μm was used. The oven temperature was programmed as follows: 40 °C (hold for 1 minute) increase at 30 °C min^{-1} to 300 °C (hold for 2.5 minutes). The injector was operated at 250 °C and the FID was operated at 320 °C. Nitrogen was used as carrier gas at a flow rate of 6.5 mL min^{-1} and a split ratio of 1:1 was applied. Chromatographic data was processed using OpenLab CDS ChemStation Edition, version C.01.05. Conversions were obtained by the comparing the integral of starting material (*S*-Ethyl thioacetate) or primary amine with integral of solvent or internal standard.

6.4.2 Materials

All chemicals were used as supplied, unless otherwise stated. THF-d_8 ≥ 99.5 %, DMSO-d_6, ≥ 99.8 %) and $CDCl_3$-d, ≥ 99.8 % were purchased from Euriso-top. D,L-Homocysteine thiolactone hydrochloride, 99 % was purchased from Haihang Industry (Jinan City, China). Magnesium sulfate, dried, ≥ 99 %, sodium hydrogen carbonate, ≥ 99 % and sodium chloride, ≥ 99 % were purchased from Carl Roth. Hydrochloric acid, 36 % was purchased from Chem Lab NV. Trifluoroacetic acid, peptide grade and 2-chlorotrityl chloride resin (100-200 mesh, 1 % DVB, 1.6 mmol/g) were purchased from Iris Biotech GmbH. Anhydrous dichloromethane, *N,N'*-dimethylformamide, 99.8 % and anhydrous tetrahydrofuran, 99.5 %, extra dry, over molecular sieves were purchased from Acros Organics. Calcium hydride, ca. 93 %, extra pure, 0.20 mm grain size, 1,4-dioxane, 99 %+, dichloromethane, pyridine, 99 %+ extra pure and *N,N'*-dimethylformamide, extra pure were also purchased from Acros Organics. Anhydrous diisopropylethylamine (DIPEA), 99.5 %, purified by redistillation. Ethyl acrylate, 99.5 % stabilised with 10 - 20 ppm 4-Methoxyphenol, *S*-

Ethyl thioacetate, ≥ 98 %, thiophenol, 97 %, ethanolamine, ACS Reagent grade > 99.0 %, benzylamine, ReagentPlus®, 99 %, 3-morpholinopropylamine, dimethylphenylphosphine (DMPP), 99 % and furfurylamine, ≥ 99 % were purchased from Sigma Aldrich. Chloroform, HPLC grade and Methanol, HPLC grade, 99.9 % were also purchased from Sigma Aldrich. Butylamine > 99.0 %, Triphosgene, 98.0 % and dibutyltin dilaurate (DBTL) were purchased from the Tokyo Chemical Industry. 1-Naphthylmethylamine, 98 % was purchased from Alfar Aesar. 3,4-Methylene-dioxyphenethylamine, 95 % was purchased from Fluorochem Ltd. Acetonitrile, HPLC grade, was purchased from Fischer Scientific. Diethyl ether, HPLC grade, HiPerSolv CHROMANORM and Acetone, HPLC grade, HiPerSolv CHROMANORM were purchased from VWR. When anhydrous chloroform was required, HPLC grade chloroform, from Sigma Aldrich was dried over calcium hydride. Water, when used in the synthesis, was de-ionised.

Silicagel (60 Å, 40-63 μm) was supplied by ROCC and used for purification of compounds by column chromatography. Thin Layer Chromatography (TLC) was performed using Merck Kieselgel 60 F_{254} coated aluminium plates.

6.4.3 Procedures

6.4.3.1 Synthesis of functional thiolactone compounds: Synthesis of thiolactone-carboxylic acid (31)

Thiolactone-carboxylic acid was prepared by a modified version of the previously reported procedure.[36]

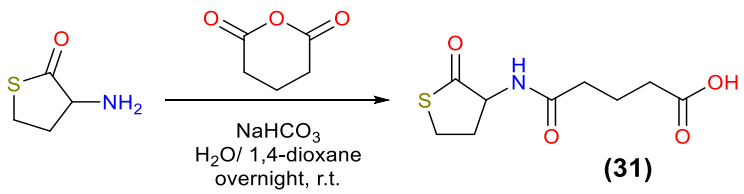

Scheme 6.10: Synthesis of thiolactone-carboxylic acid **31**.

D,L-homocysteine thiolactone hydrochloride (7.013 g, 45.6 mmol) was dissolved in an ice-cooled solution of H_2O/1,4-dioxane (1:1 100 mL). $NaHCO_3$ (19.15 g, 0.2279 mol) was added and the reaction was stirred for 30 minutes at 0 °C. Glutaric anhydride (10.41 g, 91.2 mmols) was added in several portions to the reaction mixture and the

reaction was allowed to reach room temperature and left to stir overnight. To adjust the pH to 1, 12 M HCl solution was added dropwise. Brine solution (100 mL) was added and the reaction mixture extracted with ethyl acetate (3 x 200 mL). The combined organic fractions were dried over $MgSO_4$, filtered and evaporated *in vacuo*. The crude was a white, crystalline solid, and analysis by LCMS spectroscopy. This indicated good purity, with only a small presence of the di-acid of glutaric anhydride as a side-product. The crude was purified by recrystallisation in minimum volume of acetone, yielding a white, crystalline solid (8.404 g, 79.7 %).

^{1}H NMR (300 MHz, DMSO-d_6, δ): 12.04 (s, 1H, H_1), 8.16 (d, J = 8.3 Hz, 1H, H_8), 4.59 (ddd, J = 12.6, 8.4, 7.0 Hz, 1H, H_9), 3.55-3.13 (m, 2H, $H_{12,13}$), 2.46-2.33 (m, 1H, H_{10}) 2.27-1.97 (m, 5H, $H_{2,3,6,7,11}$), 1.71 (p, J = 7.5 Hz, 2H, $H_{4,5}$); ^{13}C NMR (75 MHz, DMSO-d_6, δ): 206.51 (C), 174.18 (C), 171.85, (C), 58.11 (CH), 34.29 (CH_2), 32.82 (CH_2), 30.13 (CH_2), 26.73 (CH_2), 20.57(CH_2). HRMS (ESI) *m/z*: $[M + H]^+$ calcd for $C_9H_{13}NO_4S$, 232.0565; found, 232.0644.

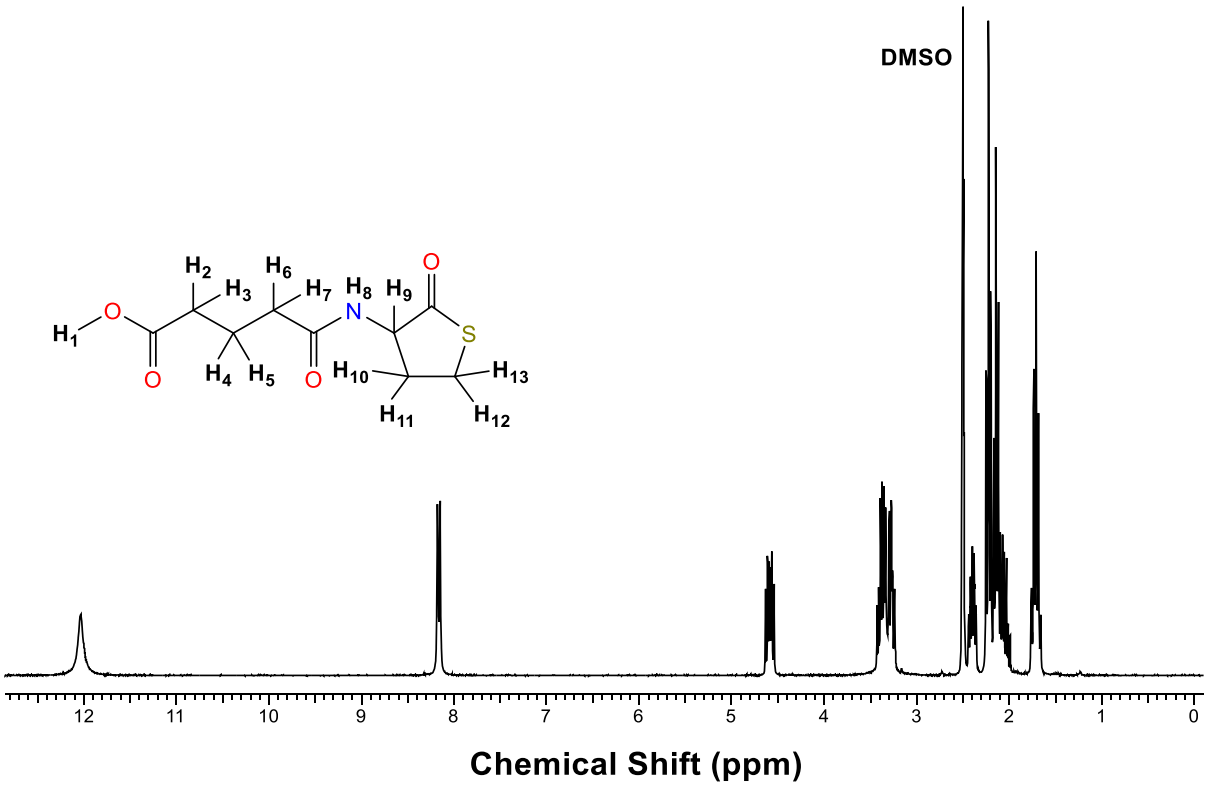

Figure 6.46: ^{1}H NMR of thiolactone-carboxylic acid **31**.

6.4.3.2 Synthesis of α-thiolactone-γ-isocyanate

Thiolactone-isocyanate was prepared according to the procedure previously reported.[34]

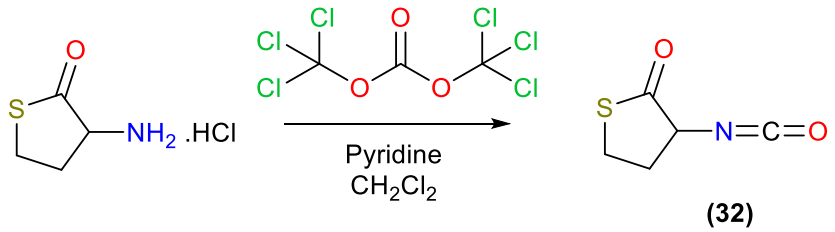

(32)

Scheme 6.11: Synthesis of α-thiolactone-γ-isocyanate **32**.

Triphosgene (50.0 g, 0.168 mol) was dissolved in ice-cooled CH_2Cl_2 (500 mL) and then a further 400 mL of CH_2Cl_2 was added. DL-homocysteine thiolactone hydrochloride (74.0 g, 0.480 mol), dried by azeotropic evaporation 3 times with toluene and then under vacuum for at least 3 hours, was added gently to the reaction mixture. Anhydrous pyridine (128.22 mL, 1.584 mol) was added dropwise to the cooled reaction mixture. After 1 hour, the ice-bath was removed and the reaction stirred for a further 4 hours at room temperature. The aqueous work-up was performed quickly to avoid degradation of the isocyanate formed. The pyridinium hydrochloride salt formed during the reaction was filtered directly into a separating funnel. The salt was rinsed with CH_2Cl_2 (300 mL) and washed with cooled 2M $HCl_{(aq)}$ (500 mL), ice-water (500 mL) and brine solution (500 mL). The aqueous phase was extracted with CH_2Cl_2 (200 mL) The organic phases were collected and dried over $MgSO_4$, filtered and the solvent removed *in vacuo*. The product was purified by vacuum distillation (85-95 °C, 0.08 mbar), yielding a colourless liquid.

^{1}H NMR (300 MHz, $CDCl_3$, δ): 4.22 (dd, J = 12.7, 6.8 Hz, 1H, H_1), 3.40-3.13 (m, 2H, $H_{4,5}$), 2.74-2.52 (m, 1H, H_2), 2.21-1.90 (m, 1H, H_3); ^{13}C NMR (75 MHz, $CDCl_3$, δ): 203.33 (C), 127.56 (C), 62.62 (CH), 30.13 (CH_2), 27.03 (CH_2)

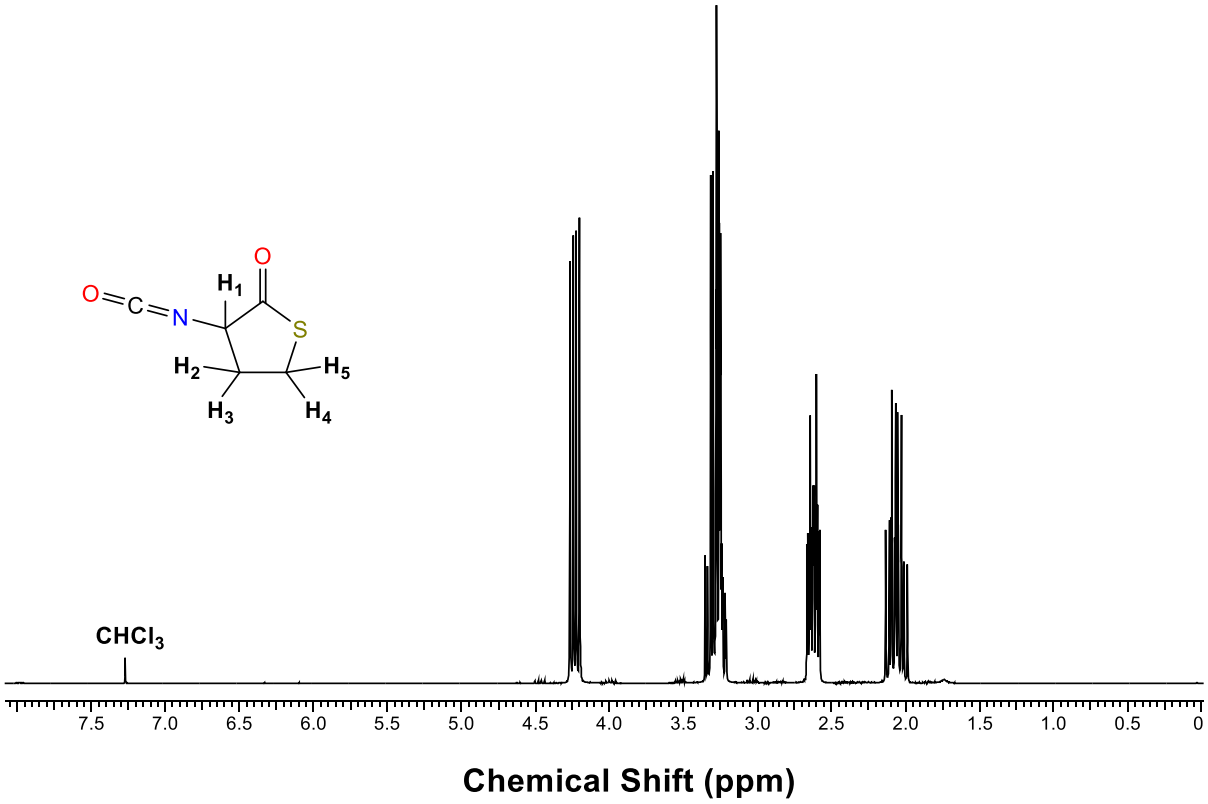

Figure 6.47: ^{1}H NMR of thiolactone isocyanate **32**, purified by vacuum distillation.

6.4.3.3 Synthesis of ethyl thioacrylate

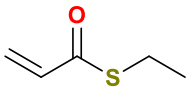

(33)

Ethyl thioacrylate was prepared according to the procedure previously reported.[37]

^{1}H NMR (400 MHz, $CDCl_3$, δ): 6.32 (dd, J = 17.2, 9.7 Hz, C$\underline{H_2}$-CH), 6.28 (dd, J = 17.2, 1.6 Hz, C$\underline{H_2}$-CH), 5.59 (dd, J = 9.8, 1.6 Hz, CH_2-C$\underline{H}$), 2.89 (q, J = 7.4 Hz, C$\underline{H_2}$-CH_3), 1.21 (t, J = 7.4 Hz, CH_2-C$\underline{H_3}$); ^{13}C-NMR (101 MHz, $CDCl_3$, δ): 190.1, 135.1, 125.9, 23.1, 14.6.

6.4.3.4 *Manipulation of the solid support and general synthetic procedure:* Loading of the 2-chlorotrityl chloride polystyrene solid-phase resin[38]

2-chlorotrityl chloride resin (2.999g, 1.6 mmol g^{-1}, 1.0 equiv.) and thiolactone carboxylic acid **1** (862 mg, 0.8 equiv.) were dissolved in anhydrous-DCM (30 mL), anhydrous-DMF (3 mL) and anhydrous-DIPEA (5 mL) in a solid-phase reactor. The reaction was left to shake vigorously at room temperature for 3 hours. The reaction was then filtered and washed with 17:2:1 DCM : MeOH : DIPEA (3 x 30 mL), shaking for 15 mins each time, to cap unreacted 2-chlorotrityl chloride groups on the resin. The reaction was then washed with DCM (3 x 30 mL), DMF (2 x 30 mL), DCM (2 x 30 mL) and Et_2O (3 x 30 mL). The product was then dried under vacuum for 3 hours. A 2 mg sample of the resin was suspended for 5 mins in 0.5 mL 1% TFA in DCM solution, concentrated by evaporation and diluted in acetonitrile. This sample was analysed by ESI-LCMS (**Figure 6.48**).

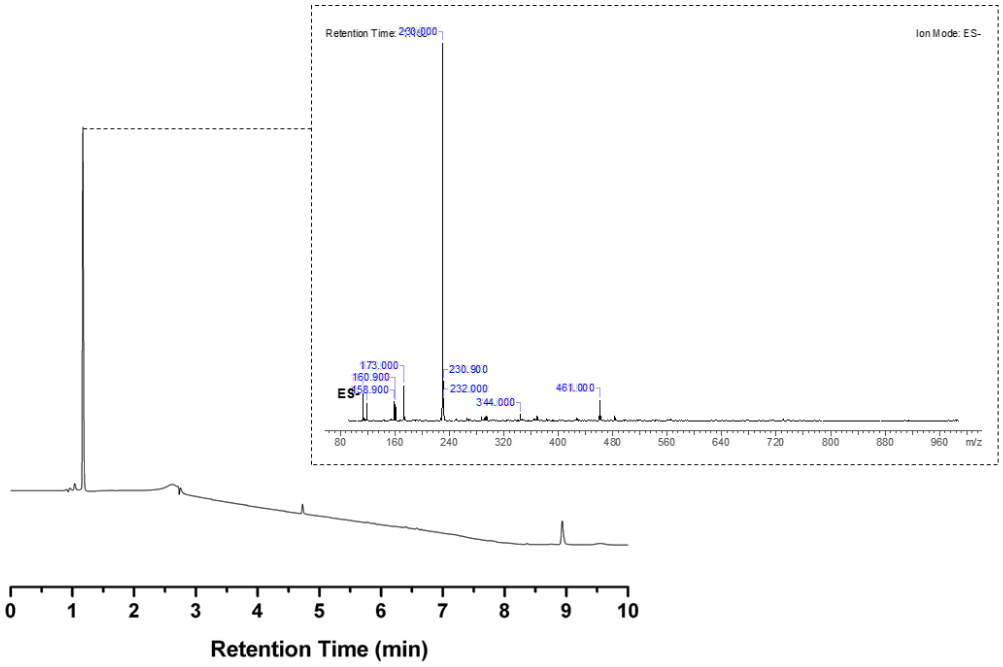

Figure 6.48: LCMS chromatogram of thiolactone carboxylic acid 1 cleaved from resin.

The loading efficiency was determined by UV-Vis spectroscopy at 254 nm with a calibration curve prepared (**Figure 6.49)** for the thiolactone carboxylic acid **31** as previously described.[36] The loading was determined to be 0.705 mmol of thiolactone carboxylic acid per gram of resin, giving a loading efficiency of 44%.

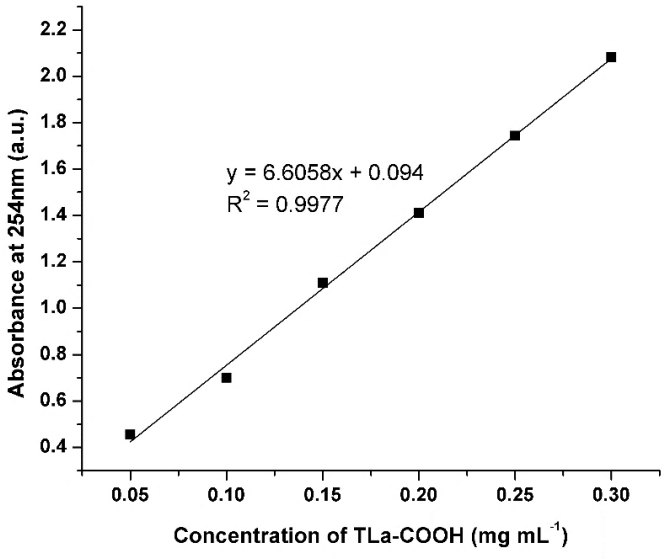

Figure 6.49: UV-calibration curve of the thiolactone carboxylic acid linker 1.

6.4.3.5 General procedure for oligomers

1. Swelling

The resin for each reaction was swollen for at least 10 minutes in the reaction solvent (1 mL of solvent per 100 mg of resin).

2. Washing

The solid phase resin was extensively washed, under filtration, after each reaction to ensure removal of remaining unreacted starting chemicals or unwanted side-products formed such as precipitates. Washing was done sequentially with DMF (x4), MeOH (x4), $CHCl_3$ (x4) and Et_2O (x4).

3. Cleavage

For analysis, the sequence was cleaved from the resin. This was done by suspension in 1% TFA (trifluoroacetic acid) in DCM (dichloromethane) solution for 5 minutes before filtration of the sample and then concentration by evaporation. During cleavage, a colour change of the beads could be observed from yellow to red as a result of the trityl cation formed on the resin.

4. Step 1: Aminolysis with ethanolamine

Thiolactone carboxylic acid, **1**, prepared as previously reported[36], was immobilised on a 2-chlorotrityl chloride functionalised polystyrene resin (as described above) with a loading of 0.705 mmols/g. The resin (40.00 mg, 1.0 equiv.) was swollen in chloroform

(1 mL/100 mg of resin) for at least 10 minutes. Then, ethanolamine (86.1 µL, 50.0 equiv.), DMPP (8.0 µL, 2.0 equiv.) and 1 drop of water were added. The reaction was shaken vigorously for at least 4 hours at room temperature, although for convenience, this was sometimes left to shake overnight. The reaction was filtered and the resin washed with DMF (x4), MeOH (x4), $CHCl_3$ (x4) and Et_2O (x4).

5. **Step 2: Thiol-*Michael* Addition with ethyl thioacrylate**

The resin was then swollen in anhydrous-DMF (1 mL/100 mg of resin) for at least 10 minutes. Ethyl thioacrylate, **3**, (32.8 mg, 10.0 equiv.) was added and the reaction was shaken vigorously for at least 4 hours at room temperature, although for convenience, this was sometimes left to shake overnight. The resin was filtered and washed with DMF (x4), MeOH (x4), $CHCl_3$ (x4) and Et_2O (x4).

6. **Step 3:Thiophenol catalysed amidation**

The resin was then swollen in anhydrous-THF (tetrahydrofuran) (1 mL/100 mg of resin) for at least 10 minutes. The desired primary amine (**Table 6.1**) (25.0 equiv.) and thiophenol (57.5 µL, 20.0 equiv.) were added and the reaction shaken vigorously for at least 6 hours at room temperature (see kinetics in **Figure 6.7** although for convenience, this was sometimes left to shake overnight. Usually, addition of the primary amine resulted in the immediate formation of a white precipitate, but with some amines, this took longer during the reaction time to form. The resin was filtered and washed with DMF (x4), MeOH (x4), $CHCl_3$ (x4) and Et_2O (x4).

Table 6.1: Table of different amines used for thiophenol catalysed amidation step.

Primary Amine	M_w **(g/mol)**	**V (*µL*)**	**ρ (g/mL)**
Benzylamine	107.16	77.00	0.981
Butylamine	73.14	69.70	0.740
3-morpholino propylamine	144.21	103.00	0.987
Furfurylamine	97.12	62.30	1.099
1-naphtylmethylamine	157.21	103.10	1.073
3,4-methylenedioxyphenethylamine	165.19	116.46	N/A

7. **Step 4: Chain extension**

The resin was then swollen in anhydrous-$CHCl_3$ (1 mL/100 mg of resin) for at least 10 minutes. Then, α-thiolactone-γ-isocyanate, **2**, (61.2 µL, 20.0 equiv.) was added followed by a catalytic amount of dibutyltin dilaurate (~3 drops). The reaction was shaken vigorously at room temperature for at least 1 hour (the kinetics were previously reported[34] and commented on below), although for convenience, this was sometimes left to shake overnight. The resin was filtered and washed with DMF (x4), MeOH (x4), $CHCl_3$ (x4) and Et_2O (x4).

6.4.3.6 Analysis of monomers/oligomers

2 mg of the solid-phase resin was suspended in a 1% TFA (in DCM) solution (~1 mL) for 5 minutes to cleave and recover the immobilised monomer/oligomer, before filtration, concentration by evaporation and then dilution in acetonitrile. This was then analysed by LCMS and HRMS. After the final synthetic step in the synthesis of oligomers, in addition to LCMS and HRMS analysis, the remainder of the synthesised compound was recovered by cleavage from the remaining resin for and diluted in DMSO-d_6 for ^{1}H NMR analysis.

6.4.3.7 Kinetics and ^{1}H NMR Studies

6.4.3.7.1 Amidation of model molecule ^{1}H NMR study

In a typical NMR experiment, an NMR tube was charged with 0.75 mL of solvent (THF-d_8 or $CDCl_3$) and *S*-Ethyl thioacetate (16.00 µL, 0.15 mmol). NMR was measured as t_0. Next, Butylamine (37.00 µL, 0.37 mmol, 2.5-fold molar excess) was added and NMR spectra were measured every 6 minutes to follow the reaction while constantly spinning inside the NMR instrument (sample spin rate = 20Hz).

For a typical thiophenol catalysed amidation, *S*-Ethyl thioacetate (160.00 µL, 1.5 mmol) was added to a 25 mL round bottom flask and 7.5 mL of THF-d_8 was added. 2.5 equiv. of butylamine (370.00 µL, 3.70 mmol), triethylamine (420.00 µL, 3.00 mmol) and thiophenol (306 µL, 3.00 mmol) were added to the solution sequentially. The mixture was stirred at room temperature and NMR spectra were recorded at 30

minute times intervals to follow the reaction. The results are displayed graphically in **Figure 6.2**.

6.4.3.7.2 Compatibility of ethylthioacrylate and ethanolamine ^{1}H NMR study

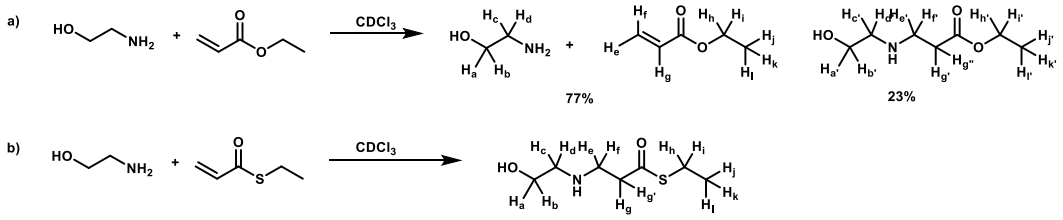

a) To an NMR tube, ethanolamine (21.34 μL, 0.3443 mmols) was added to ethyl acrylate (18.3 μL, 0.1721 mmols). 0.75 mL of $CDCl_3$ was added and a ^{1}H NMR measurement was taken every 6 mins at 500 MHz during the reaction for a period of 2 hours.

b) To an NMR tube, ethyl thioacrylate (20.0 mg, 0.1721 mmols) was added along with 0.75 mL of $CDCl_3$ and a ^{1}H NMR measurement was taken. Ethanolamine (21.34 μL, 0.3433 mmols) was added and a ^{1}H NMR measurement was taken every 6 mins at 500 MHz during the reaction for a period of 2 hours.

The results can be seen graphically in **Figure 6.3**. The ^{1}H NMR spectra after 2 hours are assigned below:

a) ^{1}H NMR (400 MHz, $CDCl_3$, δ): 6.35 (td, J = 17.1, 16.7, 3.9 Hz, 1H, H_f), 6.17-5.99 (m, 1H, H_g), 5.77 (td, J = 10.7, 3.4 Hz, 1H, H_e), 4.27-4.04 (m, 4H, $H_{h,i}$, $H_{h',i'}$), 3.64-3.49 (m, 4H, $H_{a,b}$, $H_{a',b'}$), 2.91-2.67 (m, 6HH, $H_{c,d}$, $H_{c',d'}$, $H_{e',f'}$), 2.50-2.43 (m, 4H, $H_{g',g''}$) 1.33-1.16 (m, 6H, $H_{j,k,l}$, $H_{j',k',l'}$).

b) ^{1}H NMR (400 MHz, $CDCl_3$, δ): 3.67-3.54 (m, 2H, $H_{a,b}$), 2.90 (t, J = 6.5 Hz, 2H, $H_{h,i}$), 2.88-2.81 (m, 2H, $H_{e,f}$), 2.80-2.76 (m, 2H, $H_{c,d}$), 2.74-2.69 (m, 2H, $H_{g,g'}$), 1.25-1.18 (m, 3H, $H_{j,k,l}$).

6.4.3.8 LCMS kinetics

The reaction kinetics were followed by LCMS. A small sample of the solid-phase resin (ca. 2 mg) could be easily taken from the reaction at periodic points, washed and the molecule could be cleaved from the resin for LCMS analysis to observe the reaction conversion. An NMR study, as described above would not easily provide accurate, quantitative results regarding reaction conversion, as solid-phase and solution-phase chemistry kinetics are not always comparable. Conversion is not always so clear by NMR as the spectra can be highly complex.

Step 1: Aminolysis of thiolactone by ethanolamine

A sample (ca. 2 mg) was analysed from the solid-phase reaction after 1, 2 and 3 hours by LCMS analysis.

Step 2: Thiol-*Michael* Addition

A sample (ca. 2 mg) was analysed from the solid-phase reaction after 1, 2, 3 and 4 hours by LCMS analysis.

Step 3: Thiophenol catalysed amidation

A sample (ca. 2 mg) was analysed from the solid-phase reaction after 2, 4, 6 and 8 hours by LCMS analysis.

Step 4: Thiolactone-isocyanate addition

The reaction kinetics of the addition of α-thiolactone-γ-isocyanate, **2**, to the free alcohol moetiy has been previously reported. In chloroform, the reaction is complete within 30 minutes.[34]

6.4.3.9 LCMS characterisation

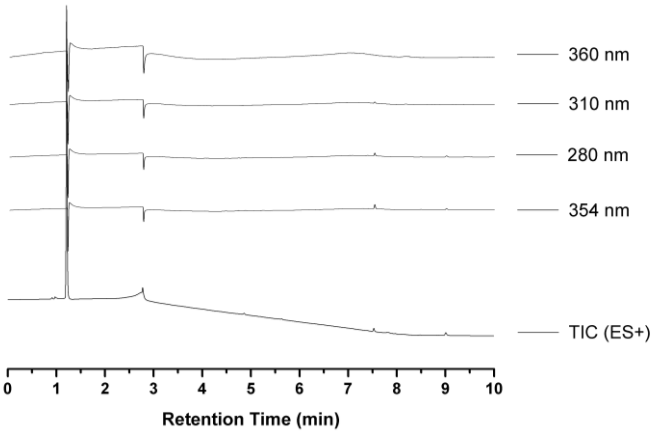

Figure 6.50: LCMS chromatogram to show the peaks resulting from the injection solvent.

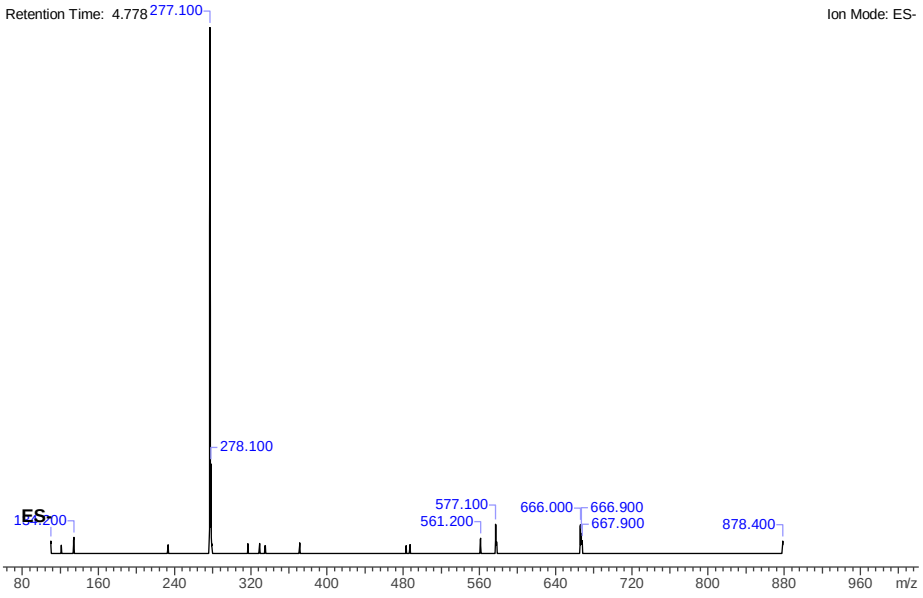

Figure 6.51: MS spectra of LCMS impurity artifact measured in negative mode. Retention time = 4.8 minute.

6.4.3.10 Monomers

6.4.3.10.1 Benzylamine

^{1}H NMR (300 MHz, DMSO-d_6, δ): 8.38 (t, J = 5.9 Hz, 1H, H_{29}), 7.99 (d, J = 8.0 Hz, $H_{8,10}$), 7.55 (d, J = 8.6 Hz, 1H, H_{15}), 7.39-7.15 (m, 5H, $H_{32\text{-}36}$), 4.46-4.19 (m, 4H, $H_{9,16,30,31}$), 4.10-3.86 (m, 2H, $H_{13,14}$), 3.50-3.14 (m, 4H, $H_{11,12,19,20}$), 2.71 (t, J = 7.3 Hz, 2H, $H_{25,26}$), 2.49-2.31 (m, 5H, $H_{17,23,24,27,28}$), 2.26-2.00 (m, 5H, $H_{2,3,6,7,18}$) 1.97-1.81(m, 1H, H_{21}) 1.79-1.63 (m, 3H, $H_{4,5,22}$).

^{13}C NMR (100 MHz, DMSO-d_6, δ): 205.61 (C_{14}, C), 174.17 (C_1, C), 171.90 (C_7, C), 171.66 (C_5, C), 170.56 (C_{19}, C), 155.96 (C_{10}, C), 139.44 (C_{21}, C), 128.29, 127.25, 126.76 ($C_{22\text{-}26}$, C_{ar}), 64.96 (C_9, CH_2), 59.90 (C_{11}, CH), 51.87 (C_6, CH), 42.14 (C_{20}, CH_2), 38.26 (C_8, CH_2), 35.73 (C_{12}, CH_2), 34.28, 33.08 ($C_{2,4}$, CH_2), 32.30 (C_{15}, CH_2), 29.87 (C_{18}, CH_2), 27.69 (C_{16}, CH_2), 27.06 (C_{17}, CH_2), 26.42 (C_{13}, CH_2), 20.65 (C_3, CH_2).

6.4.3.10.2 Butylamine

HRMS (ESI) *m/z*: $[M + H]^+$ calcd for $C_{23}H_{38}N_4O_8S_2$, 563.2131; found, 563.2220.

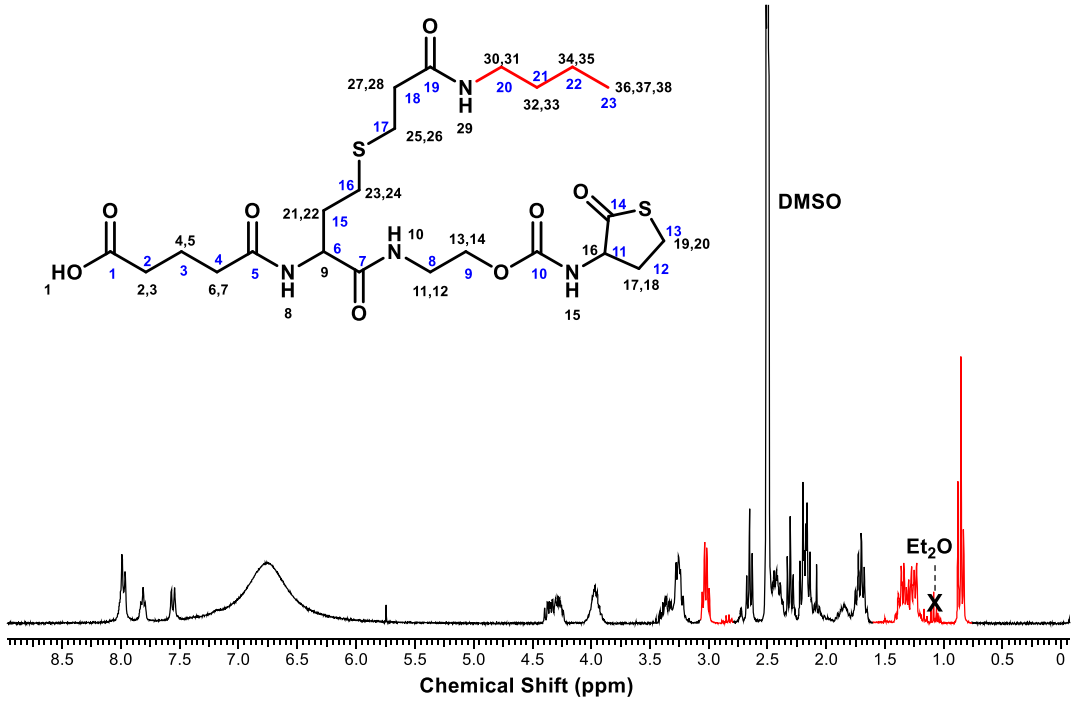

Figure 6.52: ^{1}H NMR of butylamine containing monomer highlighting the functional side group.

^{1}H NMR (300 MHz, DMSO-d_6, δ): 7.98 (d, J = 8.0 Hz, 2H, $H_{8,10}$), 7.81 (t, J = 5.6 Hz, 1H, H_{29}), 7.56 (d, J = 8.7 Hz, 1H, H_{15}), 4.44-4.21 (m, 2H, $H_{9,16}$), 4.06-3.87 (m, 2H, $H_{13,14}$), 3.48-3.16 (m, 4H, $H_{11,12,19,20}$) 3.03 (q, J = 6.9, 6.6 Hz, 2H, $H_{30,31}$), 2.65 (t, J = 7.3 Hz, 2H, $H_{25,26}$), 2.48-2.36 (m, 3H, $H_{17,23,24}$), 2.31 (t, J = 7.4 Hz, 2H, $H_{27,28}$), 2.25-2.06 (m, 5H, $H_{2,3,6,7,18}$), 1.95-1.80 (m, 1H, H_{21}), 1.70 (p, J = 7.5, 7.3 Hz, 3H, $H_{4,5,22}$), 1.43-1.20 (m, 4H, H_{32-35}), 0.86 (t, J = 7.1 Hz, 3H, H_{36-38}).

^{13}C NMR (100 MHz, DMSO-d_6, δ): 205.59 (C_{14}, C), 174.26 (C_1, C), 171.88 (C_7, C), 171.64 (C_5, C), 170.28 (C_{19}, C), 155.94 (C_{10}, C), 62.57 (C_9, CH_2), 59.89 (C_{11}, CH), 51.85 (C_6, CH), 38.22 ($C_{8,20}$, CH_2), 35.80 (C_{12}, CH_2), 34.26, 33.06 ($C_{2,4}$, CH_2), 32.26 (C_{15}, CH_2), 31.23 (C_{21}, CH_2), 29.86 (C_{18}, CH_2), 27.66 (C_{16}, CH_2), 27.08 (C_{17}, CH_2), 26.41 (C_{13}, CH_2), 20.63 (C_3, CH_2), 19.59 (C_{22}, CH_2), 13.96 (C_{23}, CH_3).

6.4.3.10.3 3-morpholino propylamine

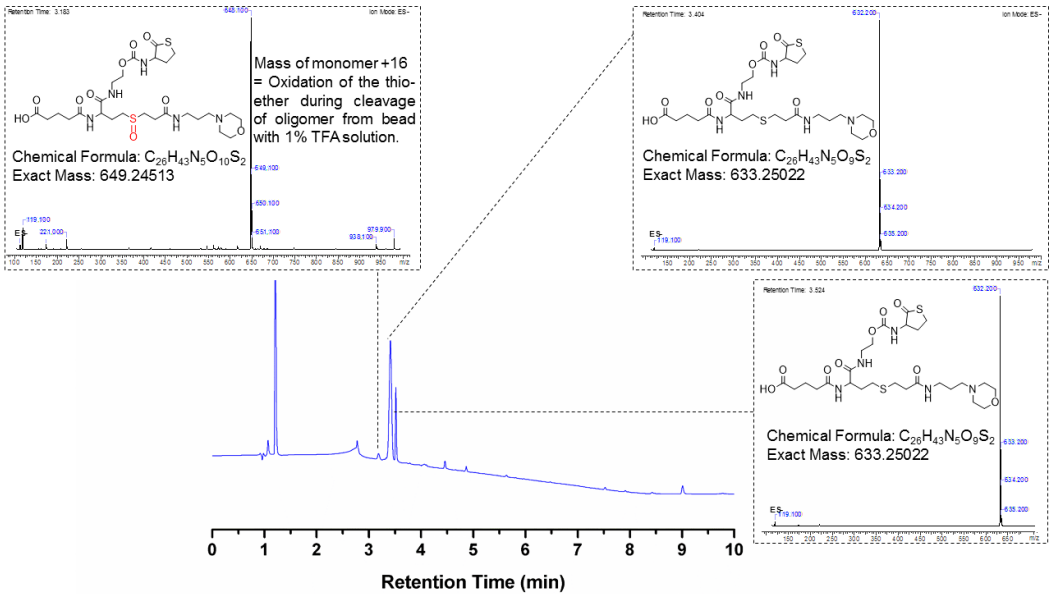

Figure 6.53: LCMS chromatogram of a monomer, with 3-moropholino propylamine used in the amidation step.

HRMS (ESI) *m/z*: $[M + H]^+$ calcd for $C_{26}H_{43}N_5O_9S_2$, 634.2502; found, 634.2595.

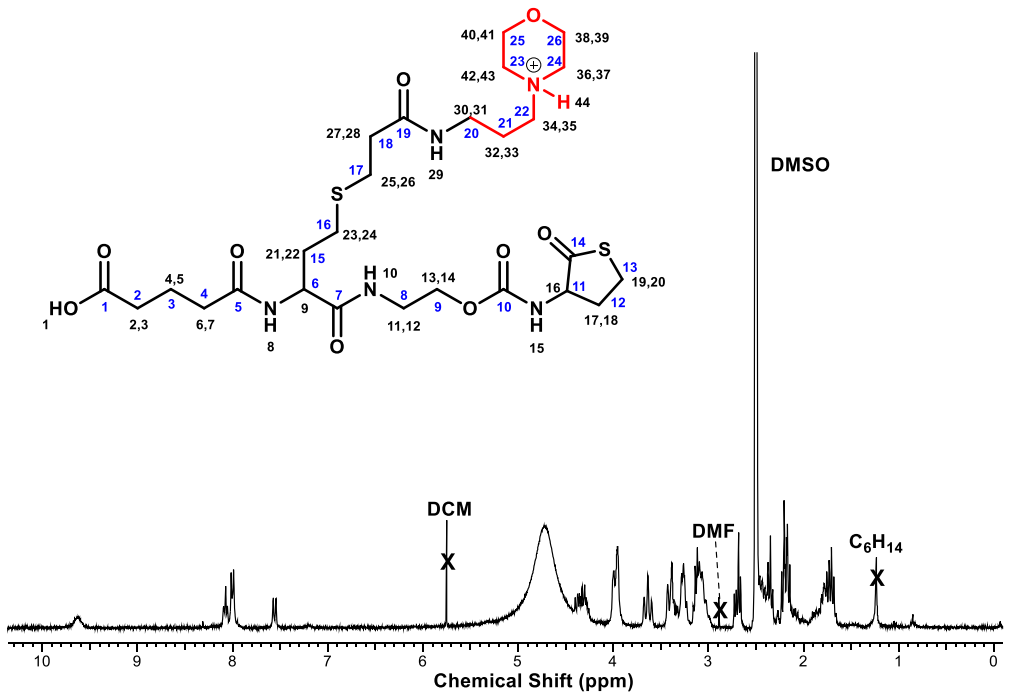

Figure 6.54: ^{1}H NMR of 3-morpholino propylamine containing monomer highlighting the functional side group.
^{1}H NMR (300 MHz, DMSO-d_6, δ): *9.63 (s, 1H, H_{44}), 8.08 (t, J = 5.9 Hz, 1H, H_{29}), 8.00 (d, J = 7.7 Hz, 2H, $H_{8,10}$), 7.56, (d, J = 8.6 Hz, 1H, H_{15}), 4.44-4.18 (m, 2H, $H_{9,16}$), 3.98 (d, J = 11.6 Hz, 4H, $H_{13,14,39,40}$), 3.64 (t, J = 12.2 Hz, 2H, $H_{38,41}$), 3.48-2.93 (m, 12H, $H_{11,12,19,20,30,31,34,35,36,37,42,43}$), 2.75-2.62 (m, 2H, $H_{25,26}$), 2.47-2.29 (m, 5H, $H_{17,23,24,27,28}$), 2.25-2.03 (m, 5H, $H_{2,3,6,7,18}$), 1.95-1.61 (m, 6H, $H_{4,5,21,22,32,33}$).

*The cleavage from the resin, using TFA causes the protonation of the nitrogen atom of the 3-morpholino side-group.

^{13}C NMR (100 MHz, DMSO-d_6, δ): 205.62 (C_{14}, C), 174.24 (C_1, C), 171.92 (C_7, C), 171.64 (C_5, C), 171.04 (C_{19}, C), 155.92 (C_{10}, C), 63.42 ($C_{25,26}$, CH_2), 62.52 (C_9, CH_2), 59.87 (C_{11}, CH), 54.04 (C_{22}, CH_2), 51.73 (C_6, CH), 51.21 ($C_{23,24}$, CH_2), 138.17 (C_8, CH_2), 35.65 (C_{12}, CH_2), 34.25, 33.04 ($C_{2,4}$, CH_2), 32.15 (C_{15}, CH_2), 29.83 (C_{18}, CH_2), 27.66 (C_{16}, CH_2), 26.98 (C_{17}, CH_2), 26.40 (C_{13}, CH_2), 23.68 (C_{21}, CH_2), 20.60 (C_3, CH_2). * Not visible as a result of DMSO peak (C_8, CH_2).

6.4.3.10.4 Furfurylamine

^{1}H NMR (300 MHz, DMSO-d_6, δ): 8.34 (t, J = 5.7 Hz, 1H, H29), 7.98 (d, J = 8.0 Hz, 2H, $H_{8,10)}$, 7.62-7.51 (m, 2H, $H_{15,34}$), 6.38 (dd, J = 3.2, 1.9 Hz, 1H, H_{33}), 6.24 (dd, J – 3.2, 0.9 Hz, 1H, H_{32}), 4.44-4.19 (m, 4H, $H_{9,16,30,31}$), 4.07-3.86 (m, 2H, $H_{13,14}$), 3.49-

3.16 (m, 4H, $H_{11,12,19,20}$), 2.70 (dd, *J* = Hz, 8.2, 7.3 Hz, 2H, $H_{25,26}$), 2.49-2.31 (m, 5H, $H_{17,23,24,27,28}$), 2.27-1.99 (m, 5H, $H_{2,3,6,7,18}$), 1.95-1.80 (m, 1H, H_{21}), 1.71 (q, *J* = 7.7, 7.4 Hz, 3H, $H_{4,5,22}$).

^{13}C NMR (100 MHz, DMSO-d_6, δ): 205.59 (C_{14}, C), 174.24 (C_1, C), 171.85 (C_7, C), 171.61 (C_5, C), 170.38 (C_{19}, C), 152.24 (C_{10}, C),142.08 (C_{24}, CH), 110.45 (C_{23}, CH), 106.81 (C_{22}, CH) 62.55 (C_9, CH_2), 59.87 (C_{11}, CH), 51.83 (C_6, CH), 38.23 (C_8, CH_2), 35.57 (C_{12}, CH_2), 35.50 (C_{20}, CH_2), 34.24, 33.04 ($C_{2,4}$, CH_2), 32.24 (C_{15}, CH_2), 29.84 (C_{18}, CH_2), 27.63 (C_{16}, CH_2), 26.88 (C_{17}, CH_2), 26.39 (C_{13}, CH_2), 20.63 (C_3, CH_2). C_{21}, C is not visible.

6.4.3.10.5 3,4-methylenedioxyphenethylamine

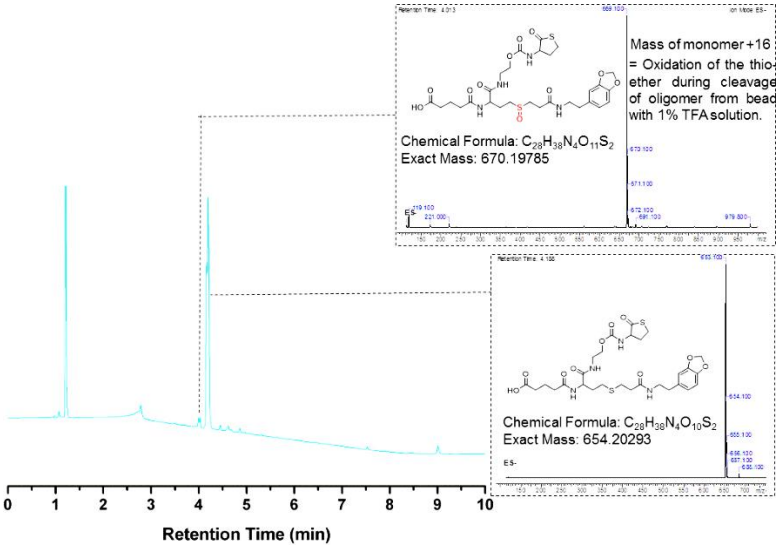

Figure 6.55: LCMS chromatogram of a monomer, with 3,4-methylenedioxyphenethylamine used in the amidation step.

HRMS (ESI) *m/z*: $[M + H]^+$ calcd for $C_{28}H_{38}N_4O_{10}S_2$, 655.2029; found, 655.2096.

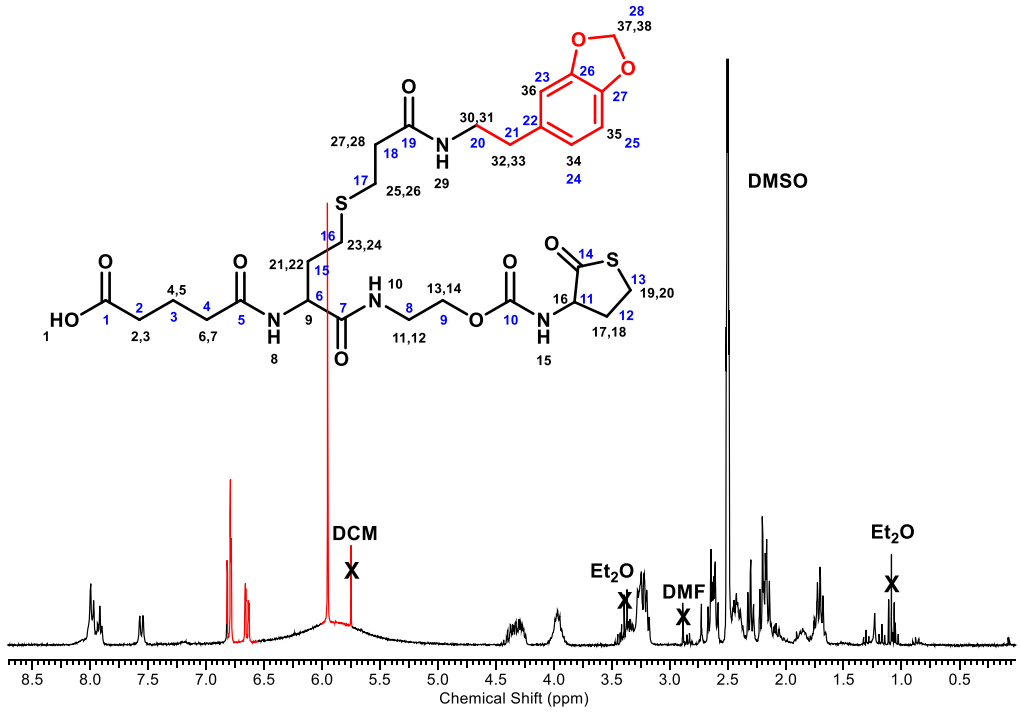

Figure 6.56: ^{1}H NMR of protected dopamine containing monomer highlighting the functional side group.

^{1}H NMR (300 MHz, DMSO-d_6, δ): 7.98 (d, J = 8.2 Hz, 1H, $H_{8,10}$), 7.92 (t, J = 5.6 Hz, 1H, H_{29}), 7.56 (d, J = 8.7 Hz, 1H, H_{15}), 6.85-6.75 (m, 2H, $H_{35,36}$), 6.65 (dd, J = 7.9, 1.7 Hz, 1H, H_{34}), 5.95 (s, 2H, $H_{37,38}$), 4.46-4.22 (m, 2H, $H_{9,16}$), 4.07-3.87 (m, 2H, $H_{13,14}$), 3.45-3.13 (m, 6H, $H_{11,12,19,20,30,31}$), 2.63 (dt, J = 11.2, 7.3 Hz, 4H, $H_{25,26,32,33}$), 2.47-2.35 (m, 3H, $H_{17,23,24}$), 2.30 (t, J = 7.3 Hz, 2H, $H_{27,28}$), 2.26-2.01 (m, 5H, $H_{2,3,6,7,18}$), 1.95-1.79 (m, 1H, H_{21}), 1.80-1.62 (m, 3H, $H_{4,5,22}$).

^{13}C NMR (100 MHz, DMSO-d_6, δ): 205.59 (C_{14}, C), 174.25 (C_1, C), 171.86 (C_7, C), 171.63 (C_5, C), 170.39 (C_{19}, C), 155.92 (C_{10}, C), 147.16 (C_{26}, C), 145.49 (C_{27}, C), 133.28 (C_{22}, C), 121.54 (C_{24}, CH), 109.08 (C_{25}, CH), 108.09 (C_{23}, CH), 100.64 (C_{28}, CH_2), 62.56 (C_9, CH_2), 59.87 (C_{11}, CH), 51.83 (C_6, CH), 40.46 (C_{20}, CH_2), 38.23 (C_8, CH_2), 35.71 (C_{18}, CH_2), 34.83, (C_{21}, CH_2), 34.25, 33.05 ($C_{2,4}$, CH_2), 32.28 (C_{15}, CH_2), 29.85 (C_{12}, CH_2), 27.62 (C_{16}, CH_2), 27.00 (C_{17}, CH_2), 26.40 (C_{13}, CH_2), 20.61 (C_3, CH_2).

6.4.3.10.6 1-naphthylmethylamine

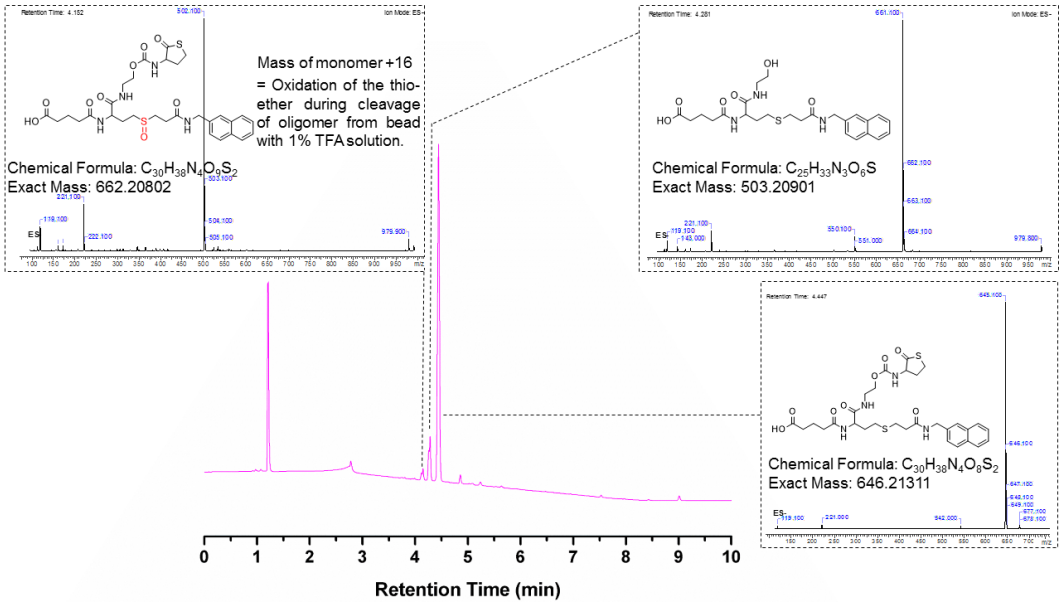

Figure 6.57: LCMS chromatogram of a monomer, with 1-napthylmethylamine used in the amidation step. HRMS (ESI) *m/z*: $[M + H]^+$ calcd for $C_{30}H_{38}N_4O_8S_2$, 647.2131; found, 647.2227.

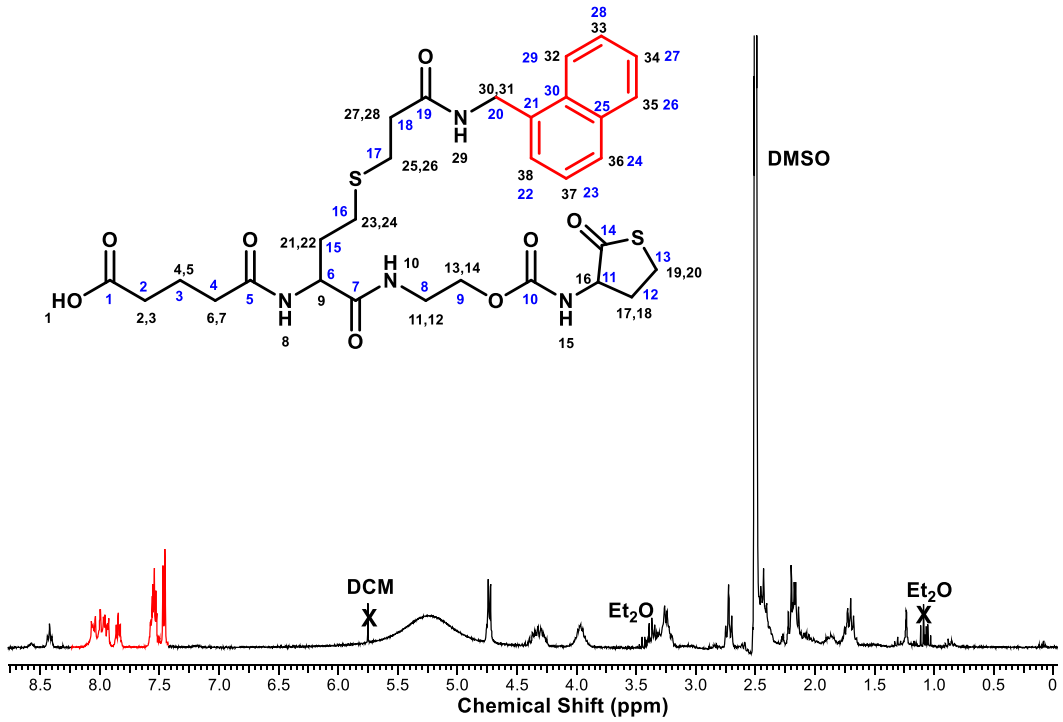

Figure 6.58: ^{1}H NMR of 1-naphthylemthylamine containing monomer highlighting the functional side group.

^{1}H NMR (300 MHz, DMSO-d_6, δ): 8.42 (t, J = 5.7 Hz, 1H, H_{29}), 8.14-7.91 (m, 4H, $H_{8,10,32,35}$), 7.85 (t, J = 4.8 Hz 1H, H_{37}), 7.64-7.49 (m, 3H, $H_{15,33,34}$), 7.47 (d, J = 5.5 Hz, 2H, $H_{36,38}$), 4.73 (d, J = 5.4 Hz, 2H, $H_{30,31}$), 4.42-4.23 (m, 2H, $H_{9,16}$), 4.05-3.86 (m, 2H, $H_{13,14}$), 3.48-3.17 (m, 4H, $H_{11,12,19,20}$), 2.72 (t, J = 7.2 Hz, 2H, $H_{25,26}$), 2.48-2.32 (m, 5H, $H_{17,23,24,27,28}$), 2.26-1.99 (m, 5H, $H_{2,3,6,7,18}$), 1.96-1.79 (m, 1H, H_{21}), 1.79-1.63 (m, 3H, $H_{4,5,22}$).

^{13}C NMR (100 MHz, DMSO-d_6, δ): 205.58 (C_{14}, C), 174.25 (C_1, C), 171.86 (C_7, C), 171.62 (C_5, C), 170.43 (C_{19}, C), 155.51 (C_{10}, C), 134.50, 133.30 ($C_{25,30}$, C), 130.89 (C_{21}, C), 128.49, 127.58, 126.24, 125.82, 125.54, 125.42, 123.55 ($C_{22\text{-}24,26\text{-}29}$ CH_{ar}), 62.56 (C_9, CH_2), 59.87 (C_{11}, CH), 51.84 (C_6, CH), 40.30 (C_{20}, CH_2), 38.22 (C_8, CH_2), 35.66 (C_{12}, CH_2), 34.24, 33.04 ($C_{2,4}$, CH_2), 32.27 (C_{15}, CH_2), 29.83 (C_{18}, CH_2), 27.65 (C_{16}, CH_2), 27.05 (C_{17}, CH_2), 26.39 (C_{13}, CH_2), 20.61 (C_3, CH_2).

6.4.3.11 Oligomeric sequence structures and characterisation

6.4.3.11.1 Alternating benzyl and butyl functionalised octamers a

^{1}H NMR (300 MHz, DMSO-d_6, δ): 8.38 (t, J = 5.9 Hz, 4H, H_{54}), 8.09-7.93 (m, 9H, $H_{8,10,17}$), 7.82 (t, J = 5.6 Hz, 4H, H_{36}), 7.55 (d, J = 8.6 Hz, 1H, H_{22}), 7.37-7.17 (m, 24H, $H_{15,57\text{-}61}$), 4.35-4.22 (m, 9H, $H_{23,55,56}$), 4.10-3.84 (m, 24H, $H_{9,13,14,16,20,21}$), 3.43-3.17 (m, 18H, $H_{11,12,18,19,26,27}$), 3.03 (q, J = 6.5, 6.4 Hz, 8H, $H_{37,38}$), 2.68 (dt, J = 15.5, 7.2 Hz, 16H, $H_{32,33,50,51}$), 2.48-2.36 (m, 25H, H $_{24,30,31,48,49,52,53}$), 2.31 (t, J = 7.3 Hz, 8H, $H_{34,35}$), 2.23-2.06 (m, 5H, $H_{2,3,6,7,25}$), 1.95-1.63 (m, 18H, $H_{4,5,28,29,46,47}$), 1.41-1.19 (m, 16H, $H_{39\text{-}42}$), 0.85 (t, J = 7.0 Hz, 12H, $H_{43\text{-}45}$).

^{13}C NMR (100 MHz, DMSO-d_6, δ): 205.60 (C_{19}, C), 174.28 (C_1, C), 171.85 (C_5, C), 170.62, 170.38, 170.33 ($C_{7,12,24,37}$, C), 155.96 ($C_{10,15}$, C), 139.42 (C_{26}, C), 128.29, 127.25, 126.77 ($C_{27\text{-}32}$, CH_{ar}), 62.54 ($C_{14,9}$, CH_2), 59.91 (C_{16}, CH), 53.95 ($C_{6,11}$, CH), 42.16 (C_{25}, CH_2), 38.25 ($C_{8,13,38}$, CH_2), 35.84 (C_{17}, CH_2), 34.29, 33.07 ($C_{2,4}$, CH_2), 32.13 ($C_{20,33}$, CH_2), 31.24 (C_{39}, CH_2), 29.87 ($C_{23,36}$, CH_2), 27.72 ($C_{21,34}$, CH_2), 27.07 ($C_{22,35}$, CH_2), 26.43 (C_{18}, CH_2), 20.65 (C_3, CH_2), 19.65 (C_{40}, CH_2), 13.69 (C_{41}, CH_3).

6.4.3.11.2 Alternating benzyl and butyl functionalised octamers b

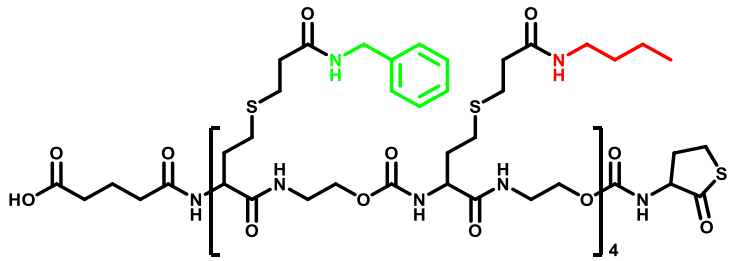

Figure 6.59: Structural representation of benzyl- and butyl- functionalised alternating octamer.

Dimer

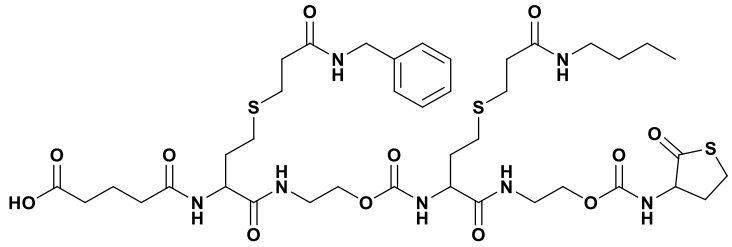

HRMS (ESI) *m/z*: $[M + H]^+$ calcd for $C_{40}H_{61}N_7O_{12}S_3$, 928.3540; found, 928.3647.

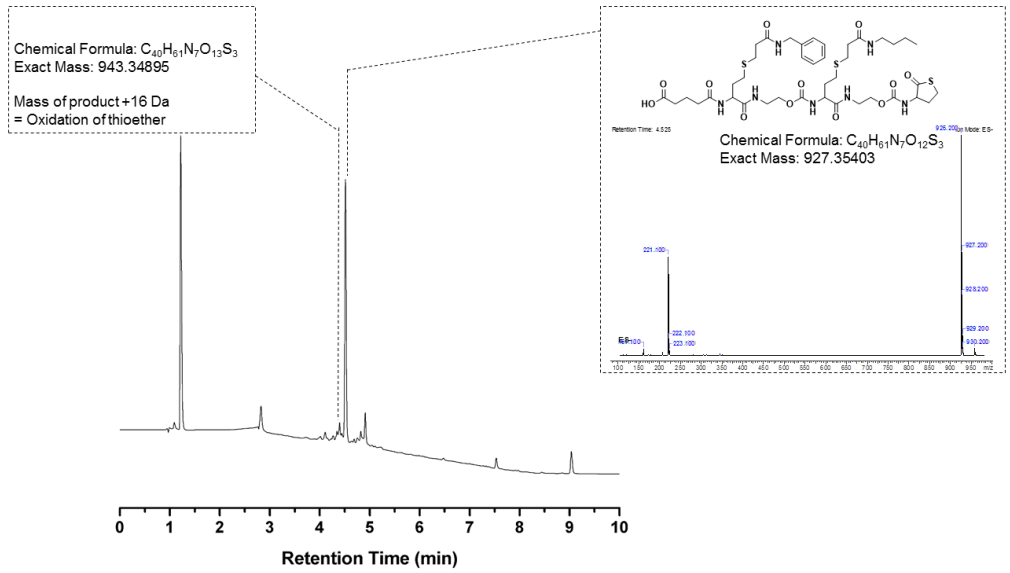

Figure 6.60: LCMS chromatogram of dimer step in octameric sequence.

Trimer

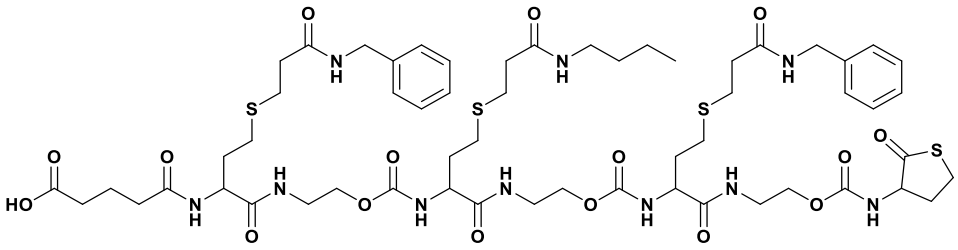

HRMS (ESI) *m/z*: $[M + H]^+$ calcd for $C_{57}H_{84}N_{10}O_{16}S_4$, 1293.4950; found, 1293.5077.

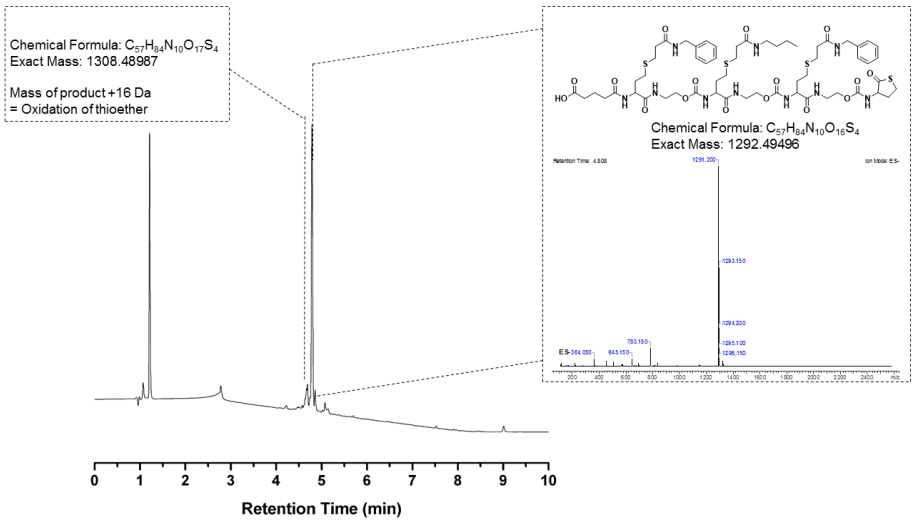

Figure 6.61: LCMS chromatogram of trimer step in octameric sequence.

Tetramer

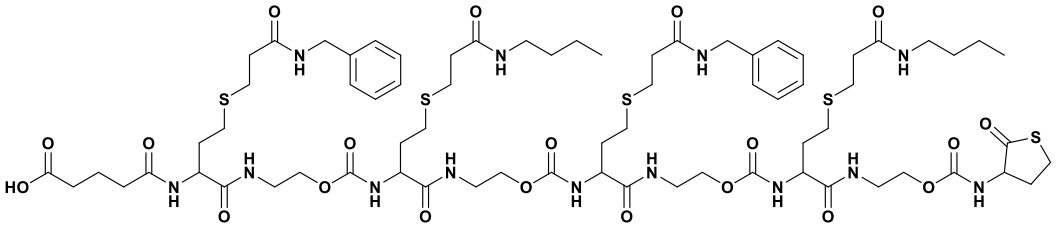

HRMS (ESI) *m/z*: $[M + H]^+$ calcd for $C_{71}H_{109}N_{13}O_{20}S_5$, 1624.6515; found, 1624.6573.

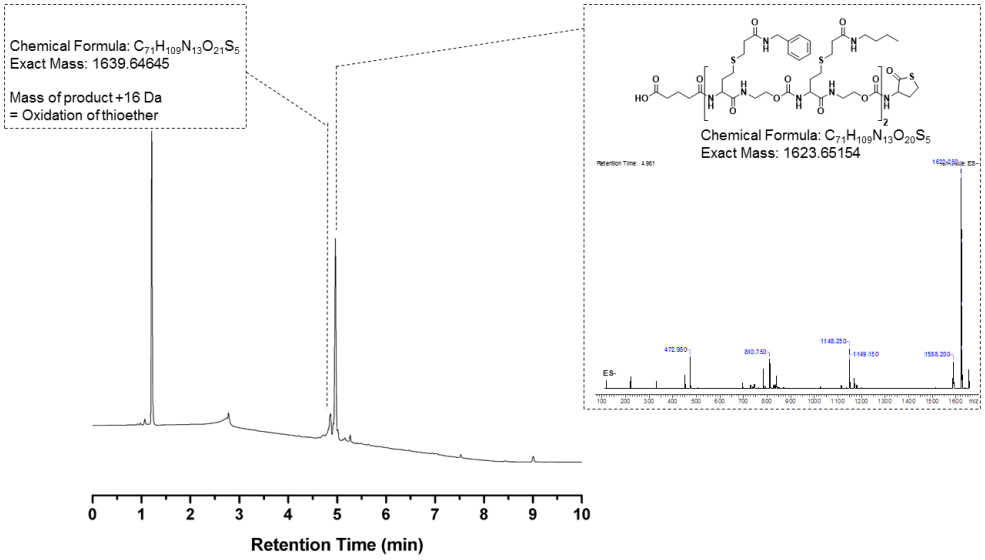

Figure 6.62: LCMS chromatogram of tetramer step in octameric sequence.

Pentamer

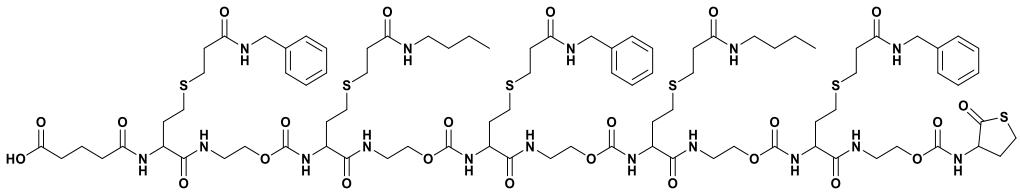

HRMS (ESI) *m/z*: $[M + H]^+$ calcd for $C_{88}H_{132}N_{16}O_{24}S_6$, 1989.7925; found, 1989.8078.

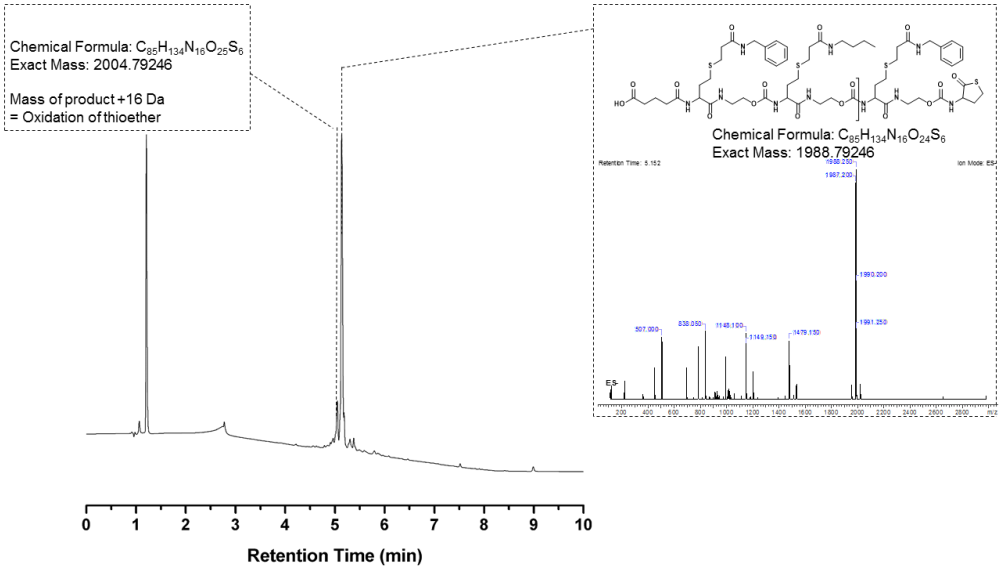

Figure 6.63: LCMS chromatogram of pentamer step in octameric sequence.

Hexamer

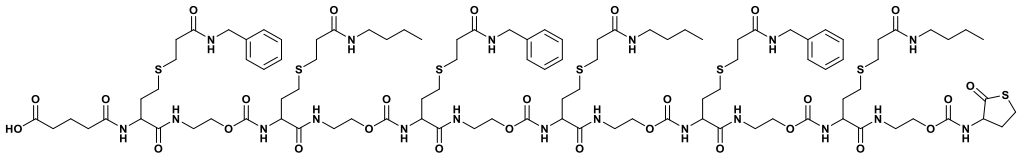

HRMS (ESI) *m/z*: $[\frac{M+2H}{2}]^+$ calcd for $C_{102}H_{157}N_{19}O_{28}S_8$, 1160.6475; found, 1160.9827.

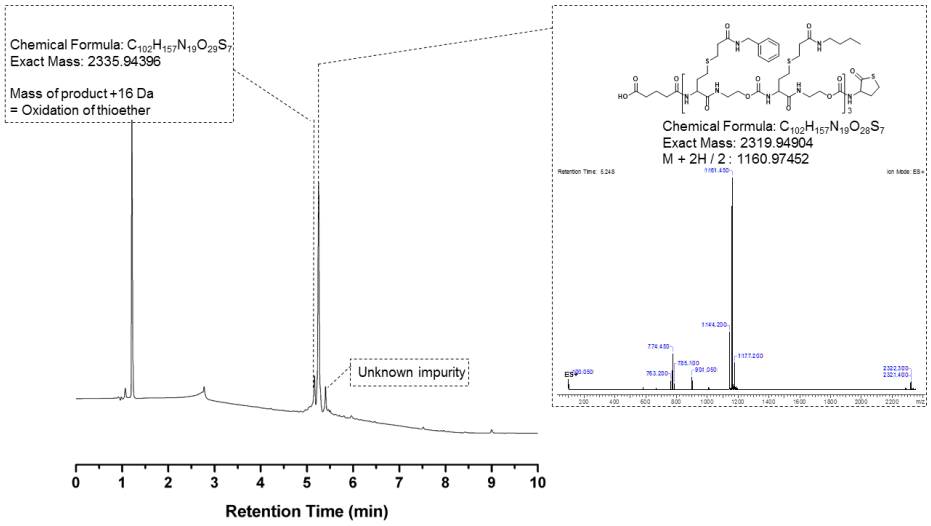

Figure 6.64: LCMS chromatogram of hexamer step in octameric sequence. Spectum recorded in positive mode.

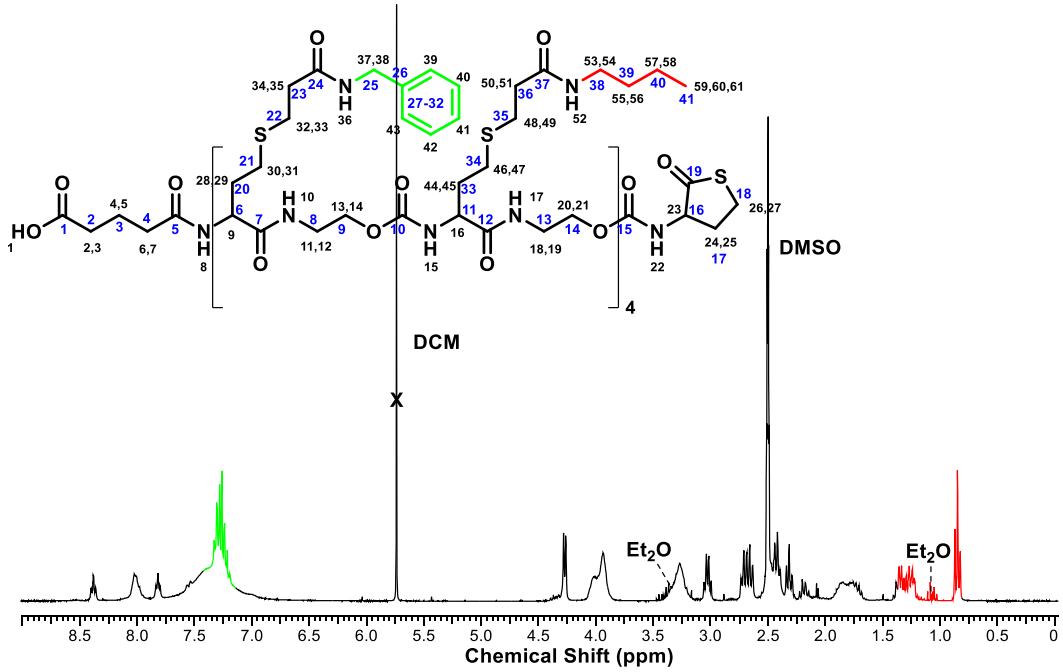

Figure 6.65: ^{1}H NMR of octamer.

^{1}H NMR (300 MHz, DMSO-d_6, δ): 8.38 (t, J = 5.9 Hz, 4H, H_{36}), 8.09-7.91 (m, 9H, $H_{8,10,17}$), 7.82 (t, J = 5.6 Hz, 4H, H_{52}), 7.58-7.49 (m, 1H, H_{22}), 7.35-7.18 (m, 24H, $H_{15,39-43}$), 4.37-4.22 (m, 9H, $H_{23,37,38}$), 4.13-3.80 (m, 24H, $H_{9,13,14,16,20,21}$), 3.40-3.13 (m, 18H, $H_{11,12,18,19,26,27}$), 3.03 (q, J = 6.5, 6.4 Hz, 8H, $H_{53,54}$), 2.68 (dt, J = 15.3, 7.1 Hz, 16H, $H_{32,33,48,49}$), 2.49-2.36 (m, 25H, H $_{24,30,31,34,35,46,47}$), 2.31 (t, J = 7.3 Hz, 8H, $H_{50,51}$), 2.24-2.10 (m, 5H, $H_{2,3,6,7,25}$), 1.97-1.63 (m, 18H, $H_{4,5,28,29,44,45}$), 1.43-1.20 (m, 16H, H_{53-58}), 0.85 (t, J = 7.2, 6.9 Hz, 12H, H_{59-61}).

^{13}C NMR (100 MHz, DMSO-d_6, δ): 205.63 (C_{19}, C), 174.31 (C_1, C), 172.00 (C_5, C), 170.65, 170.61, 170.342 ($C_{7,12,24,37}$, C), 155.98 ($C_{10,15}$, C), 139.43 (C_{26}, C), 128.31, 127.27, 126.79 (C_{27-32}, CH_{ar}), 62.57 ($C_{14,9}$, CH_2), 59.93 (C_{16}, CH), 53.96 ($C_{6,11}$, CH), 42.18 (C_{25}, CH_2), 38.27 ($C_{8,13,38}$, CH_2), 35.86 (C_{17}, CH_2), 34.31, 33.09 ($C_{2,4}$, CH_2), 32.13 ($C_{20,33}$, CH_2), 31.26 (C_{39}, CH_2), 29.89 ($C_{23,36}$, CH_2), 27.73 ($C_{21,34}$, CH_2), 27.09 ($C_{22,35}$, CH_2), 26.46 (C_{18}, CH_2), 20.67 (C_3, CH_2), 19.62 (C_{40}, CH_2), 13.70 (C_{41}, CH_3).

6.4.3.11.3 Multifunctional Hexamer

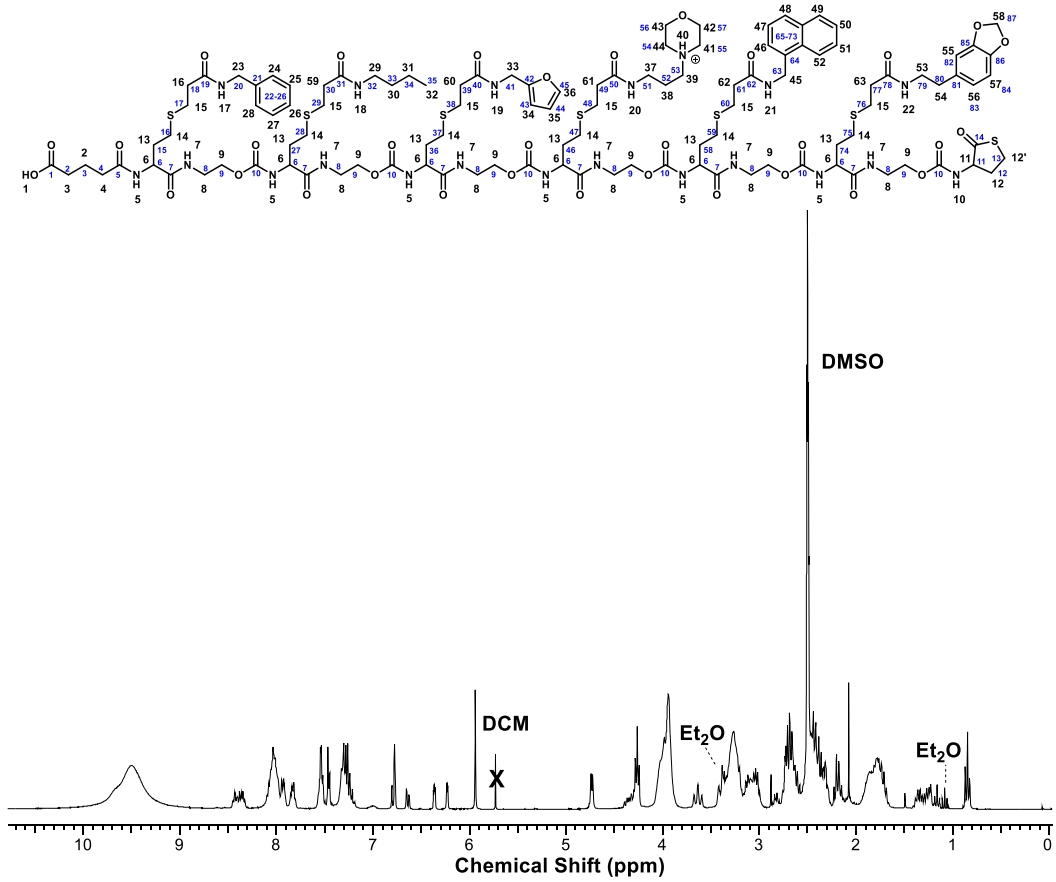

Figure 6.66: ^{1}H NMR of multifunctional oligomer.

^{1}H NMR (300 MHz, DMSO-d_6, δ): 8.49-8.29 (m, 3H, $H_{17,19,21}$), 8.15-7.76 (m, 15H, $H_{5,7,47,49,52}$), 7.61-7.36 (m, 6H, $H_{10,36,46,48,50,51}$), 7.38-7.17 (m, 8H, $H_{18,20,22,24\text{-}28,}$), 6.87-6.72 (m, 2H, $H_{55,57}$), 6.64 (dd, J = 7.9, 1.7 Hz, 1H, H_{56}), 6.37 (dd, J = 3.2, 1.8 Hz, 1H, H_{35}), 6.23 (d, J = 3.1 Hz, 1H, H_{34}), 5.94 (s, 1H, H_{58}), 4.73 (d, J = 5.5 Hz, 2H H_{45}), 4.38-4.19 (m, 5H, $H_{11,23,33}$), 4.10-3.82 (m, 20H, $H_{6,9,42,43}$), 3.64 (t, J = 11.8 Hz, 2H, $H_{42',43'}$), 3.45-2.95 (m, 26H, $H_{8,16,29,37,39,41,44,54,}$), 2.78-2.58 (m, 14H, $H_{15,53}$), 2.48-2.27 (m, 22H, $H_{14,59\text{-}63}$), 2.25-2.10 (m, 5H, $H_{3,4,12}$), 1.9-1.63 (m, 15H, $H_{12',13,38}$), 1.42-1.14 (m, 6H, $H_{30,31,2}$), 0.85 (t, J = 7.1 Hz, H_{32}).

^{13}C NMR (100 MHz, DMSO-d_6, δ): 205.66 (C_{14}, C), 174.33 (C_1, C), 172.02 (C_5, C), 171.92, 171.81, 171.22, 170.63, 170.59, 170.56, 170.44 ($C_{7,19,31,40,50,62,78}$, C), 156.01 (C_{10}, C), 152.30 (C_{42}, C), 147.24 (C_{85}, C), 145.57 (C_{86}, C), 142.12 (C_{45}, CH), 139.47 (C_{21}, C), 134.55, 133.38 ($C_{65\text{-}74}$, C) 133.34 (C_{81}, C), 130.97 (C_{64}, C), 128.32, 127.29, 126.80 ($C_{22\text{-}26}$, CH_{ar}), 128.56, 127.66, 126.30, 125.88, 125.63, 125.47, 123.61 ($C_{65\text{-}73}$, CH_{ar}), 121.60 (C_{83}, CH), 110.50 (C_{44}, CH), 109.14 (C_{82}, CH), 108.14 (C_{84}, CH), 106.89 (C_{43}, CH), 100.71 (C_{87}, CH_2), 63.49 ($C_{56,57}$, CH_2), 62.59 (C_9, CH_2), 59.96 (C_{11}, CH), 54.14 (C_{53}, CH_2), 53.96 (C_6, CH), 51.30 ($C_{54,55}$, CH_2), 43.67 (C_{20}, CH_2), 38.29

($C_{8,32}$, CH_2), 35.88, 35.77 ($C_{41,80}$, CH_2), 34.90 (C_{12}, CH_2), 34.34, 33.11 ($C_{2,4}$, CH_2), 32.13 ($C_{15,27,36,46,58,74}$, CH_2), 31.27 ($C_{33,63}$, CH_2), 29.91 ($C_{18,30,39,49,61,77}$, CH_2), 27.75 ($C_{16,28,37,47,59,75}$, CH_2), 27.11 ($C_{17,29,38,48,60,76}$, CH_2), 26.47 (C_{13}, CH_2), 23.76 (C_{52}, CH_2), 20.69 (C_3, CH_2), 19.64 (C_{34}, CH_2), 13.71 (C_{35}, CH_3). * Not visible as a result of DMSO peak ($C_{15,27,36,46,58,74,79,}$ CH_2).

^{1}H NMR (300 MHz, DMSO-d_6, δ): 8.49-8.29 (m, 3H, $H_{17,19,21}$), 8.15-7.76 (m, 15H, $H_{5,7,47,49,52}$), 7.61-7.36 (m, 6H, $H_{10,36,46,48,50,51}$), 7.38-7.17 (m, 8H, $H_{18,20,22,24\text{-}28,}$), 6.87-6.72 (m, 2H, $H_{55,57}$), 6.64 (dd, J = 7.9, 1.7 Hz, 1H, H_{56}), 6.37 (dd, J = 3.2, 1.8 Hz, 1H, H_{35}), 6.23 (d, J = 3.1 Hz, 1H, H_{34}), 5.94 (s, 1H, H_{58}), 4.73 (d, J = 5.5 Hz, 2H H_{45}), 4.38-4.19 (m, 5H, $H_{11,23,33}$), 4.10-3.82 (m, 20H, $H_{6,9,42,43}$), 3.64 (t, J = 11.8 Hz, 2H, $H_{42',43'}$), 3.45-2.95 (m, 26H, $H_{8,16,29,37,39,41,44,54,}$), 2.78-2.58 (m, 14H, $H_{15,53}$), 2.48-2.27 (m, 22H, $H_{14,59\text{-}63}$), 2.25-2.10 (m, 5H, $H_{3,4,12}$), 1.9-1.63 (m, 15H, $H_{12',13,38}$), 1.42-1.14 (m, 6H, $H_{30,31,2}$), 0.85 (t, J = 7.1 Hz, H_{32}).

6.4.4 References

1. J. Chiefari, Y. K. Chong, F. Ercole, J. Krstina, J. Jeffery, T. P. T. Le, R. T. A. Mayadunne, G. F. Meijs, C. L. Moad, G. Moad, E. Rizzardo and S. H. Thang, *Macromolecules*, 1998, **31**, 5559-5562.
2. M. Kato, M. Kamigaito, M. Sawamoto and T. Higashimura, *Macromolecules*, 1995, **28**, 1721-1723.
3. J. S. Wang and K. Matyjaszewski, *J. Am. Chem. Soc.*, 1995, **117**, 5614-5615.
4. C. Barner-Kowollik, F. E. Du Prez, P. Espeel, C. J. Hawker, T. Junkers, H. Schlaad and W. Van Camp, *Angew. Chem. Int. Ed.*, 2011, **50**, 60-62.
5. P. Espeel and F. E. Du Prez, *Macromolecules*, 2015, **48**, 2-14.
6. N. Badi and J.-F. Lutz, *Soc. Rev.*, 2009, **38**, 3383-3390.
7. L. Charles, C. Laure, J.-F. Lutz and R. K. Roy, *Macromolecules*, 2015, **48**, 4319-4328.
8. S. C. Solleder, K. S. Wetzel and M. A. R. Meier, *Polym. Chem.*, 2015, **6**, 3201-3204.
9. S. C. Solleder and M. A. R. Meier, *Angew. Chem. Int. Ed.*, 2014, **53**, 711-714.
10. S. Martens, J. Van den Begin, A. Madder, F. E. Du Prez and P. Espeel, *J. Am. Chem. Soc.*, 2016, **138**, 14182-14185.
11. N. Zydziak, F. Feist, B. Huber, J. O. Mueller and C. Barner-Kowollik, *Chemical Communications*, 2015, **51**, 1799-1802.
12. S. Martens, J. O. Holloway and F. E. Du Prez, *Macromol. Rapid. Comm.*, 2017, **38**, 1700469.
13. V. R. Pattabiraman and J. W. Bode, *Nature*, 2011, **480**, 471-479.
14. P. J. Bracher, P. W. Snyder, B. R. Bohall and G. M. Whitesides, *Orig Life Evol Biosph*, 2011, **41**, 399-412.
15. S. N. Semenov, L. J. Kraft, A. Ainla, M. Zhao, M. Baghbanzadeh, V. E. Campbell, K. Kang, J. M. Fox and G. M. Whitesides, *Nature*, 2016, **537**, 656-660.
16. E. R. Kay and D. A. Leigh, *Angew. Chem. Int. Ed.*, 2015, **54**, 10080-10088.
17. J.-F. Ayme, J. E. Beves, D. A. Leigh, R. T. McBurney, K. Rissanen and D. Schultz, *Nat Chem*, 2012, **4**, 15-20.
18. H. C. Kolb, M. G. Finn and K. B. Sharpless, *Angew. Chem.*, 2001, **113**, 2056-2075.
19. S. Slavin, J. Burns, D. M. Haddleton and C. R. Becer, *Eur. Polym. J.*, 2011, **47**, 435-446.
20. C. R. Becer, R. Hoogenboom and U. S. Schubert, *Angew. Chem. Int. Ed.*, 2009, **48**, 4900-4908.
21. E. Pieter, C. L. L. G., B. Katarzyna, C. Sven, M. J. C., D. P. F. E. and M. Annemieke, *Angew. Chem. Int. Ed.*, 2013, **52**, 13261-13264.
22. S. Binauld, D. Damiron, L. A. Connal, C. J. Hawker and E. Drockenmuller, *Macromol. Rapid. Comm.*, 2011, **32**, 147-168.
23. H.-F. Chow, K.-N. Lau, Z. Ke, Y. Liang and C.-M. Lo, *Chemical Communications*, 2010, **46**, 3437-3453.
24. T. T. Trinh, L. Oswald, D. Chan-Seng and J.-F. Lutz, *Macromol. Rapid. Comm.*, 2014, **35**, 141-145.
25. Z. Zhang, Y.-Z. You, D.-C. Wu and C.-Y. Hong, *Polymer*, 2015, **64**, 221-226.

26. L. Yang, Z. Zhang, B. Cheng, Y. You, D. Wu and C. Hong, *Science China Chemistry*, 2015, **58**, 1734-1740.
27. R. B. Merrifield, *J. Am. Chem. Soc.*, 1963, **85**, 2149-2154.
28. S. Aksakal and C. Remzi Becer, *Polym. Chem.*, 2016, **7**, 7011-7018.
29. P. Espeel and F. E. Du Prez, *Eur. Polym. J.*, 2015, **62**, 247-272.
30. , Rapp Polymere, http://www.rapp-polymere.com/index.php?id=1218, accessed: April 2017.
31. G.-Z. Li, R. K. Randev, A. H. Soeriyadi, G. Rees, C. Boyer, Z. Tong, T. P. Davis, C. R. Becer and D. M. Haddleton, *Polym. Chem.*, 2010, **1**, 1196-1204.
32. M. Le Neindre, B. Magny and R. Nicolaÿ, *Polym. Chem.*, 2013, **4**, 5577-5584.
33. P. Espeel, F. Goethals, F. Driessen, L.-T. T. Nguyen and F. E. Du Prez, *Polym. Chem.*, 2013, **4**, 2449-2456.
34. S. Martens, J. Van den Begin, A. Madder, F. E. Du Prez and P. Espeel, *J. Am. Chem. Soc.*, 2016, **138**, 14182-14185.
35. S. Celasun, F. E. Du Prez and H. G. Börner, *Macromol. Rapid. Comm.*, 2017, **38**, 1700688.
36. P. Espeel, L. L. G. Carrette, K. Bury, S. Capenberghs, J. C. Martins, F. E. Duprez and A. Madder, *Angewandte Chemie International Edition*, 2013, **52**, 13261-13264.
37. S. Aksakal and C. R. Becer, *Polym. Chem.*, 2016, **7**, 7011-7018.
38. B. B. Shankar, D. Y. Yang, S. Girton and A. K. Ganguly, *Tetrahedron Lett.*, 1998, **39**, 2447.

7 Outlook

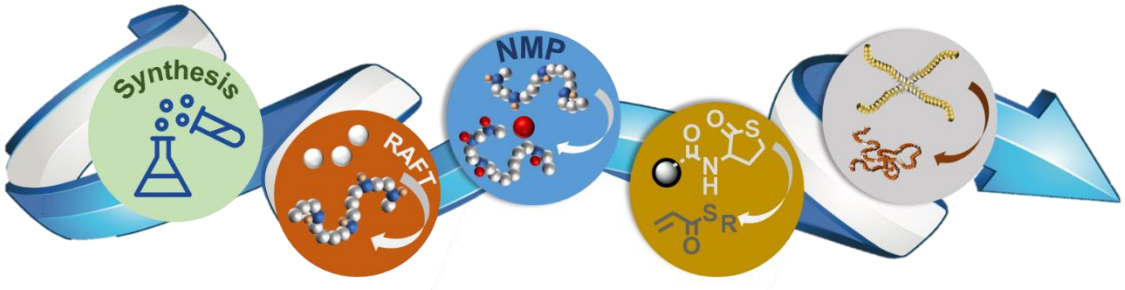

7.1 Summary

In the world of synthetic polymers, scientists are more and more looking for polymers that perform new functions. The basis of every polymer is their smallest units, called monomers. Up to date, many techniques have been reported on the synthesis of polymers and more useful ways are just about to develop with more sophisticated features. For example, CRP evolved after anionic living polymerisation was reported back in 1950s, resulting in the development of NMP 30 years later. Ten years later, ATRP was discovered, which was followed shortly after by RAFT and SET-LRP. The establishment of new ways to polymerise a monomer has since then witnessed a significant uprise in the synthesis of a broad range of functional (soft)materials. With regards to monomers, acrylics also recorded a pleasant and positive continued development in the past 50 years. Publications on (meth)acrylates and (meth)acrylamides have increased steadily **Figure 7.1**, while it is not surprising that the industry has started with their distribution and resulted in a commercial accessibility of the monomers. Around 150 different (meth)acrylates and 30 of (meth)acrylamides are available, ranging from short to long alkyl chains, aromatic side groups, functional groups to the introduction of heteroatoms in the side group.

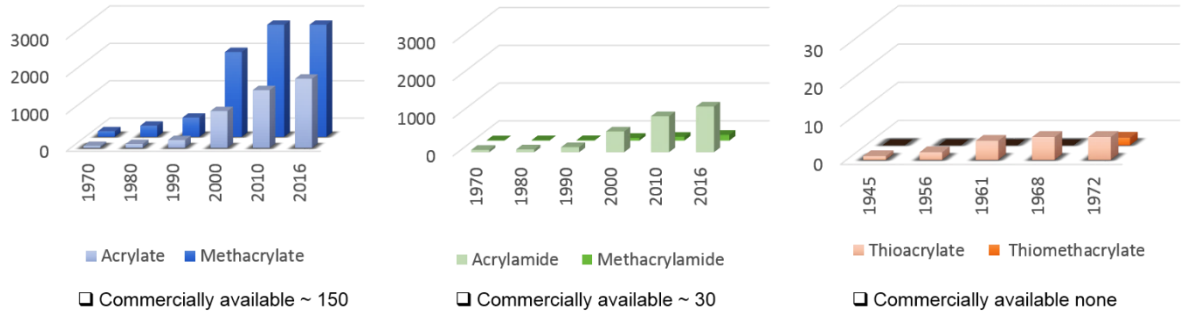

Figure 7.1: Number of publications on (meth)acrylates, (meth)acrylamides and thio (meth)acrylates in the past 50 years with their commercial availability, based on numbers from the Sigma-Aldrich catalogue and webofknowledge.com (accessed December 2018).

Interestingly, while thio(meth)acrylates have been reported as early as 1945 and a small number of publications are found, no thio(meth)acrylate monomer has been commercialised. In addition, thioester containing compounds for the polymer synthesis, such as initiators are also not available, whereas a broad variety of nitroxides, CTAs and ATRP initiators exist. With regards to the incorporation of a thioester, the literature provides interesting examples and proves that the inclusion of a thioester functional group provides advantages over their counterparts. Many reports display that the position of the thioester can be specific and easily

incorporated in any region and position on the polymer, giving materials with tailored thermal and structural properties. Exchange reactions, amidation on the thioester and NCL are main functionalisation pathways and are well established in incorporating further functionalities. Many reports also contain the synthesis of complex structures, whereas the thioester bond can be transformed into different linkages. Although thioesters on polymers are well understood, future research in mimicking the thioester chemistry on the macromolecular scale and implementing it to polymers with thioesters will open new avenues to materials with unique properties and tailor-made functionalities. However, no recent example of a thioester containing acrylic or thioester initiators for common radical polymerisation techniques was found and has led to the investigation of the potential of thioesters in monomers and initiators in polymerisation processes and push the employed techniques to its limits in order to show the versatility of this new starting material. Therefore, the class of thio(meth)acrylates, have been synthesised from various thiols as starting material as shown in **Figure 7.2** and discussed in **Chapter 2**.

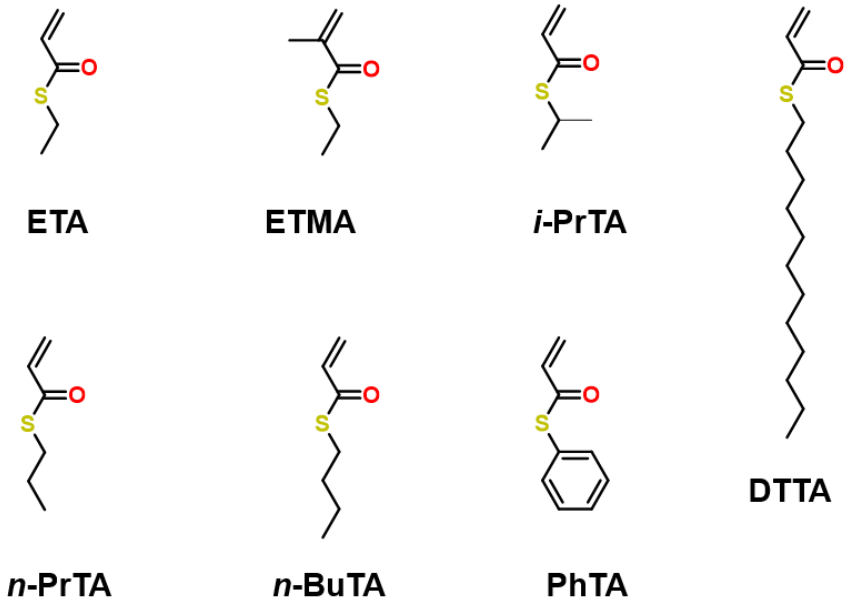

Figure 7.2: Overview of thioacrylate and thio methacrylate monomers synthesised in the present study.

Based on the series of thio(meth)acrylates, chemical intermediates and final monomers were analysed in detail by ^{1}H NMR and ^{13}C NMR. Monomers obtained from the synthesis *via* a *Wittig* reaction generated monomers with high purity grades (>99%).

The reports of *Hadjichristidis et al.* from the 1980s on the synthesis of thio methacrylates *via* FRP using AIBN, inspired this work to investigate CRP of thioacrylates. For this, RAFT

polymerisation was used for a range of thioacrylates and excellent control over the polymerisation (PDI 1.11–1.19) were obtained with quantitative conversions (**Scheme 7.1**).

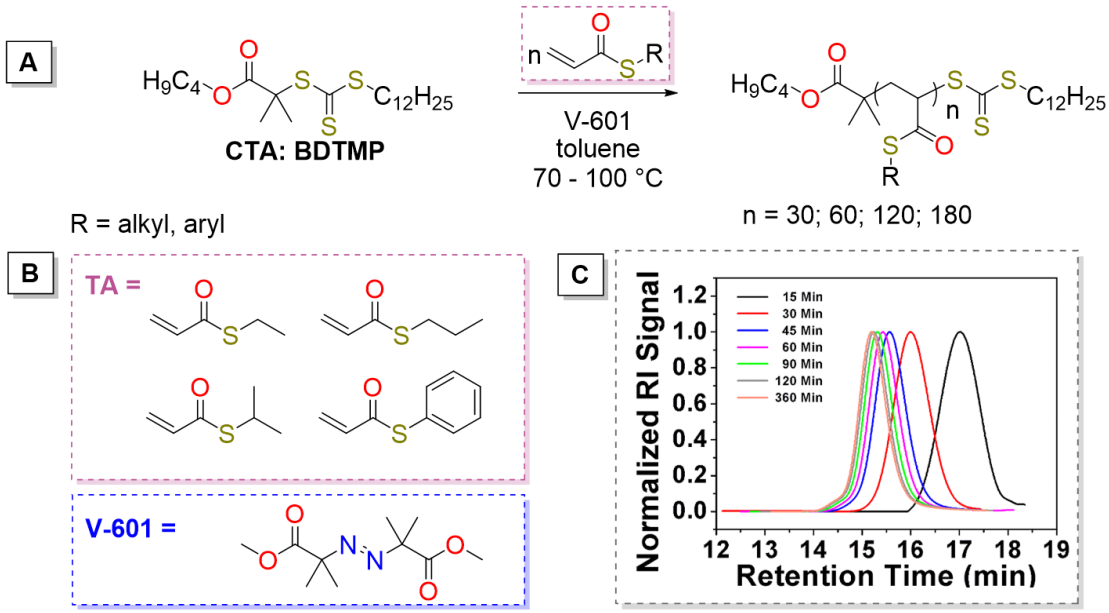

Scheme 7.1: Synthesis and homopolymerization conditions of thioacrylates via RAFT, **(B)** Structure of monomomers used in this thesis, **(C)** GPC traces of poly(isopropyl thioacrylate) with DP = 60 in toluene at 70 °C and [I] = 0.1 mol%.

Ethyl thioacrylate (ETA) was found to polymerise at a similar rate compared to its oxoester acrylic counterpart ethyl acrylate (EA), whereas dispersities remained low and observed molecular weight was close to the theoretical. It was shown that this new monomer class can be polymerised *via* more modern controlled radical polymerisation techniques, allowing better control over the architecture. Finally, both the water contact angel and the T_g for P(ETA) was observed to be significantly higher than for P(EA), which provides evidence that thioacrylates give access to new materials with different properties. Obtained results of the polymerisation and DSC, TGA and WCA analysis of the polymers are outlined in **Chapter 3**.

Moreover, DSC analysis was used on post modified P(ETA) to investigate the degree of amidation with benzylamine, resulting in higher T_g values described in **Chapter 4**. For this, NMP has been used for the polymerisation of ETA. Obtained polymers displayed moderate dispersity values (~1.46) and good agreement with theoretical ($M_{n,theo}$) and experimental number-average molecular weight ($M_{n,GPC}$) for P(ETA) as well as for P(BuTA). While acrylates have been copolymerised *via* RAFT with ETA in **Chapter 3**, a styrenic derivative (PFS) was used in **Chapter 4** to copolymerise with BuTA, obtained *via* NMP. A lower

polymerisation rate was observed by substituting the BuTA with BuA at high and low temperatures. Furthermore, full amidation was achieved with benzylamine and isopropylamine for P(ETA) in a microwave reaction, whereas an incomplete substitution was observed with benzylalcohol.

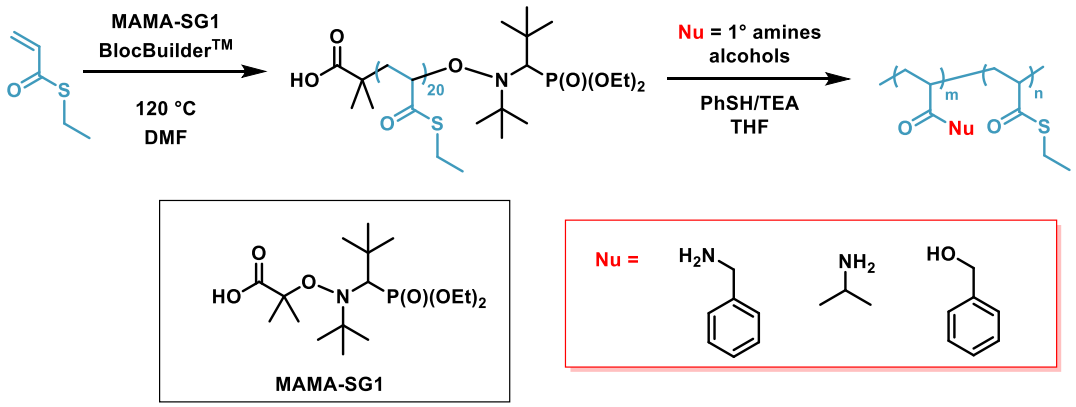

Scheme 7.2: Nitroxide mediated polymerisation of ETA, yielding Poly(ETA) and subsequent substitution of Poly(ETA) with generic nucleophile Nu.

The *T*g of P(ETA) with different degrees of amidation was analysed *via* DSC, where polymers with a higher incorporated amide group resulted in a overall raise in *Tg* from -32.2 °C for a poly(thioacrylate) to 49.2 °C.

SET-LRP could also be used for the synthesis of P(ETA), after careful optimisation, where $FeBr_2$ was used instead of $CuBr_2$ and is discussed in **Chapter 5**. The polymerisation gave similarly good control, while allowing full monomer conversion of thioacrylates. Furthermore, a way to generate block copolymers with ester, thioester and amide functionality was developed. In addition to a thioester containing monomer, two linear thioester containing ATRP initiators were synthesised and compared to structural identical amide and ester counterparts. A 4-arm thioester containing initiator was synthesised and used for the synthesis of a watersoluble P(eDEGA), which was exposed to cysteine in a NCL reaction. The reaction was followed *via* GPC and MALDI-ToF-MS and showed a dissociation of this star polymer with L-cysteine methyl ester into linear polymers.

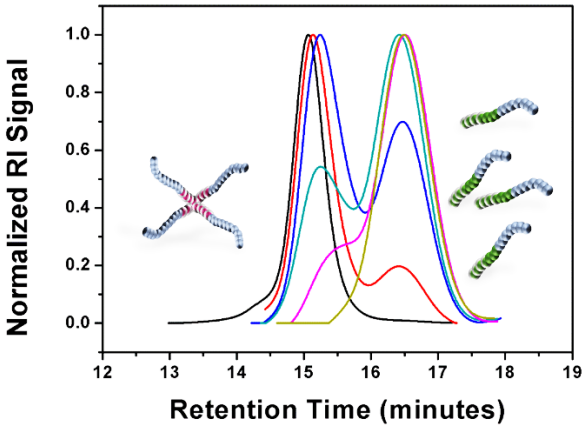

Figure 7.3: Overlay of the GPC traces obtained during the dissociation of the star polymer **P49** in **Chapter 5**, displaying a shift towards lower retention times.

The double bond of a thioacrylate monomer was found to be more reactive towards nucleophiles compared to its oxoester analogue, this feature was used in a protocol on solid phase in combination with thiolactone chemistry.

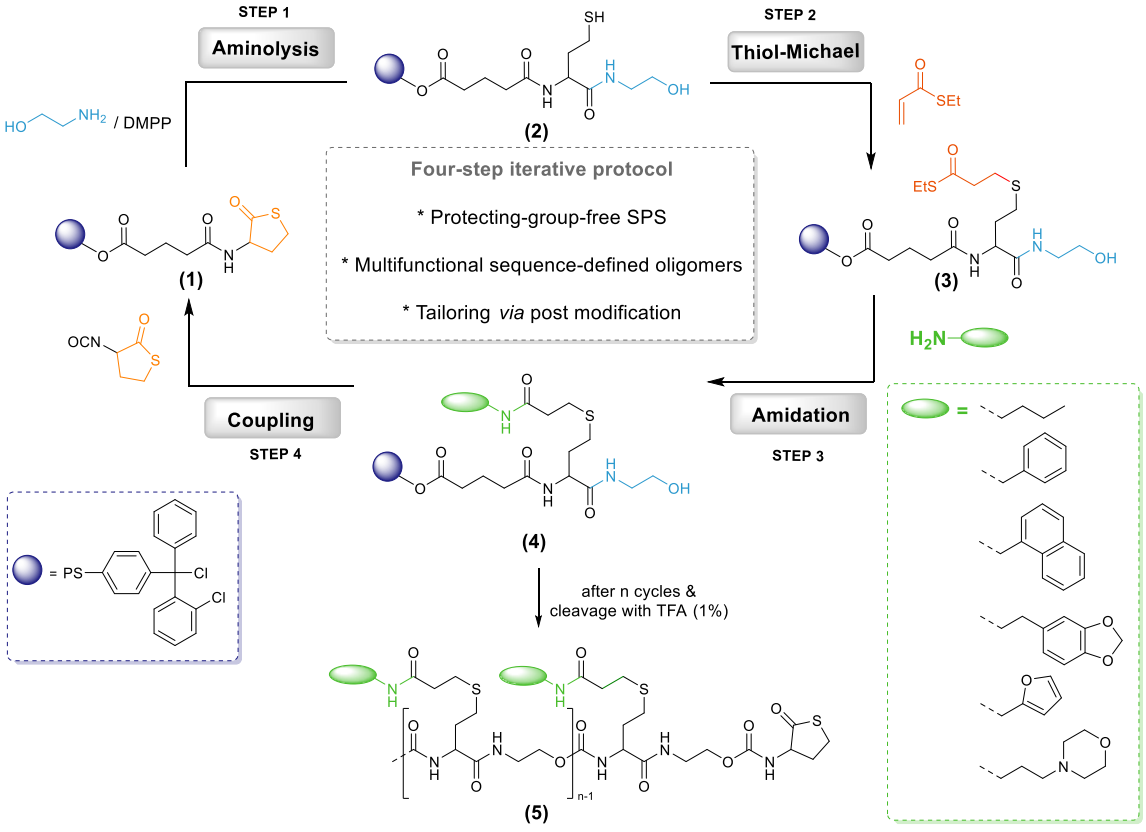

Scheme 7.3: Solid phase protocol with incorporated thioacrylates *via* Thiol-*Michael* reaction and subsequent amidation with various primary amines.

For this, a new synthetic protocol for the synthesis of sequence-defined oligomers was developed, using an iterative protocol based on thiolactone chemistry (**Chapter 6**). Test

reactions between the *in situ* liberated free thiol and acrylamides to form a side chain were proven to be unsuccessful. By incorporating thioacrylates into the side chain over a thiol-ene chemistry however, it was possible to introduce different amines over an amidation reaction of the thioester. This overcame the inefficiency of the reactions between the thiol and acrylamides, yielding in sequences of high purity.

The current status of thioesters in starting materials for polymerisation processes enables the design and synthesis of functional materials in various architectures and compositions with the herein described thioacrylates and thioester initiators. The thioester can be easily incorporated in the side group of a polymer as a thioacrylate, or the polymer end functionalised using a respective thioester initiator. Thioacrylates have been shown to be compatible with acrylates and styrenics, but can also be transformed to acrylamides on the polymer. Moreover, copolymers could also be realised by conducting amidation or esterification on a poly thioacrylate at the same time, overcoming the necessity of employing acrylates and acrylamides.

Given that NCL of a thioester containing polymer with an amino acid could be easily performed under neat conditions, emphasis on the future work will be on applying this reaction to more biologically relevant systems to generate bioconjugates with peptides or carbohydrates. Alternatively, a direct synthesis of a thioacrylate bearing a sugar or amino acid on the side group can be envisaged for the direct incorporation of sugars into the polymer to study targeted delivery of molecules. Furthermore, thioacrylates can be modified with azides in a *Staudinger* ligation to yield amide structures, or can be transformed in a Pd or Ni catalysed reaction to respective thioethers. The possibilities are endless and by exploring the reactivity of the novel functional monomer/initiators towards other compounds, more reaction pathways can be realised. The thioester handle on a polymer opens new avenues to new chemical reactions to be carried out on polymer chains. This in turn, will help polymer chemists with the investigation and understanding of structurally more diverse, sequence defined polymers with more complex and purpose tailored architectures and properties.